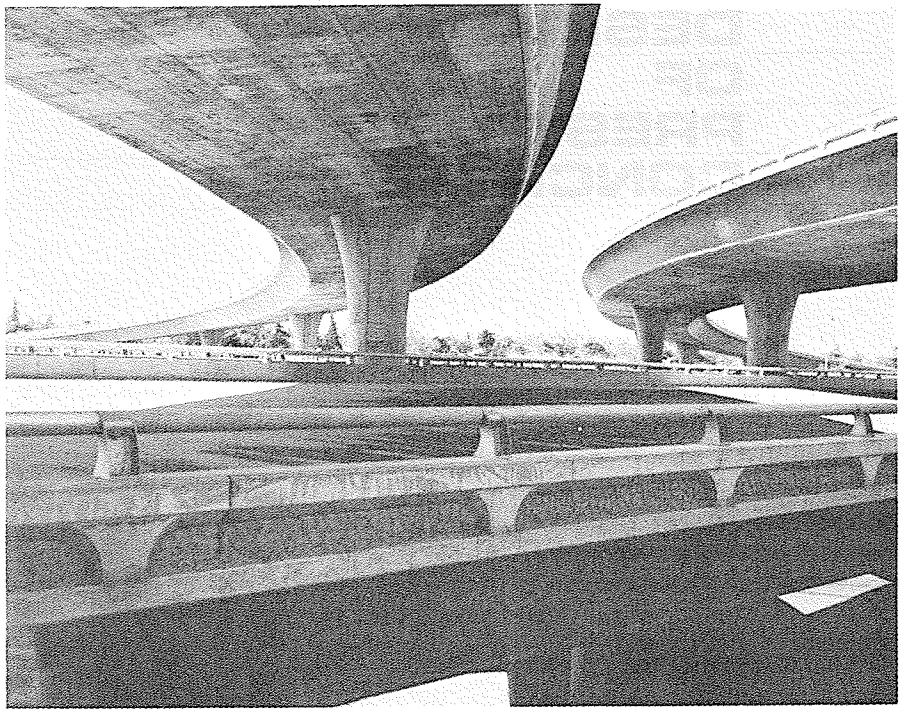

Curved prestressed concrete bridge girders used . r highway grade separation. Courtesy of State of California, Department of Public Works.

DESIGN OF PRESTRESSED CONCRETE

SECOND EDITION

ARTHUR H. NILSON
Professor of Structural Engineering
Cornell University

JOHN WILEY & SONS
New York • Chichester • Brisbane • Toronto • Singapore

Library of Congress Cataloging in Publication Data:

Nilson, Arthur H.
Design of prestressed concrete.
Includes bibliographical references and index.
1. Prestressed concrete construction. I. Title.
TA683.9.N54 1987 624.1'83412 86-26792

Printed in the Republic of Singapore

10 9 8 7 6 5 4 3 2 1

PREFACE

Although the first proposal to apply prestressing to concrete was made as early as 1886, in the United States, it was only as a result of the studies of the renowned French engineer Eugene Freyssinet in the 1930s that prestressed concrete became a practical reality. In Europe, in the period of acute material shortages following World War II, Freyssinet and other pioneers demonstrated the remarkable possibilities of this new concept of design, and set the stage for the development that was to take place in the following years.

Largely for economic rather than technical reasons, the evolution of prestressed concrete in the United States has been along somewhat different lines than in Europe. Until just a few years ago, interest was mainly in standardized precast and pretensioned units of relatively short span, which could be mass-produced with great saving in labor cost. Hollowcore slabs and single and double-T beams were, and are, widely used for floors, roofs, and walls of buildings. For highway bridges, standard I-beams, T-beams, and box section beams evolved. Precast members of these types have accounted for a significant fraction of all new construction and undoubtedly will continue to do so.

However, changing economic conditions and a rapidly evolving technology are producing important changes in U. S. practice. Construction labor is not in such short supply. The cost of materials is constantly increasing. There is a serious concern about conservation of resources. Improved materials and more powerful methods of analysis are generally available. Under these circumstances, it is natural that engineers should turn to more sophisticated designs, such as those developed meanwhile in Europe, which more fully exploit the potential of prestressed concrete. Cast-in-place flat plate floors, post-tensioned for full continuity, are now common in buildings. Short to medium span highway bridges, often combining vertical grade with horizontal curvature and superelevation (see frontispiece, for example) are used to ensure smooth traffic flow. Segmentally cast continuous-beam bridges and cable-stayed girders of prestressed concrete have dramatically extended previous span limits.

The continued evolution of both conventional and more innovative types of prestressed concrete construction has created the need for engineers who have a firm understanding of fundamental principles, on the one hand, and the ability to create efficient and practical designs, on the other. Familiarity with governing codes and specifications is necessary but is not sufficient for present-day practice. Engineers are needed who can not only be effective in optimizing existing forms of construction but also can apply fundamental concepts with confidence in new and unusual situations.

I hope that this book will be an effective aid in the educaton of such persons. The initial emphasis is placed on fundamentals of behavior. This is followed by presentation and explanation of important code provisions and design office procedures, illustrated by practical examples.

Although intended mainly as a college textbook for use at the fourth- or fifth-year level, a special effort has been made to develop a clear, self-contained presentation, so that the book may also be used by engineers in practice who wish to improve their knowledge of this relatively new field. The material has been carefully coordinated with codes governing U. S. practice, particularly the latest edition of *Building Code Requirements for Reinforced Concrete*, published by the American Concrete Institute. ACI Code notation is used as far as possible. Frequent reference is made to the publications of the Prestressed Concrete Institute and the Post-Tensioning Institute, providing an insight into actual design practice for the student, and suggesting sources of practical information. Extensive reference lists at the end of each chapter provide a guide to the literature for those whose needs go beyond the coverage of this text.

The book has grown from a set of lecture notes that I developed while teaching prestressed concrete to civil engineering students at Cornell University over a 30-year period. The arrangement of the material follows that of my lectures. After an introduction to the basic concepts in Chapter 1, and a summary of concrete and steel material properties in Chapter 2, the analysis and design of beams is presented in Chapters 3 to 5. Losses of prestress are considered in Chapter 6. It may be argued that analysis of losses should precede beam analysis and design, but I have concluded that, from a pedagogical viewpoint, there is greater advantage to getting on with the business of design early. In many practical cases, losses need be considered in no more detail than in Chapters 3 and 4.

The study of deflections (Chapter 9) and the design of slabs (Chapter 10) are fundamental and should be included in a first course of study. However, the teacher may not find time to cover composite beams or continuous members (Chapters 7 and 8, respectively). These topics, as well as treatment of axially loaded members (Chapter 11), may be deferred until a later course or taken up through self-study.

Chapters 12 and 13, which deal respectively with precast construction and applications, have been written to permit their assignment as outside reading.

Appendix A contains a variety of design aids. These are useful in connection with examples and assigned problems, and may increase the usefulness of the book to the practicing engineer. Appendix B contains engineering data for certain post-tensioning systems. No attempt was made to be encyclopedic, but only to present sufficient detail to permit realistic proportioning of members in problem assignments. Finally, Appendix C provides SI conversion factors and metric equivalents.

The present edition of this text is an update and an expansion of the first, and includes changes in design philosophy and methodology corresponding to changes in current practice. New information is presented on materials, particularly relating to high-strength concrete, now in common use, and newly available types of prestressing steel. In the chapters on flexural analysis and design, additional emphasis has been placed on partial prestressing, combining prestressed and non-prestressed reinforcement. These changes, among other things, have resulted in modification of design equations for flexural strength and more elaborate methods for calculating beam deflections. The reader will find much new material pertaining to prestressed slabs, particularly one-way banded slab construction.

Many new design aids have been added. Section properties are given for standard hollowcore slabs, and for single- and double-T beams, used for floors and roofs. For bridges, section property tables have been included for standard AASHTO I-beams, and for other sections now used by a number of state highway departments. Section properties are also given for voided slabs, box section beams, and single-T beams, such as are widely used for shorter span highway bridges.

Finally, it will be noted that many new problems have been added at the end of each chapter for home assignment.

A word is in order relating to units of measurement. Nationwide, there is a movement toward adoption of the International System (SI) of metric units, although progress in that direction has been slow. In many cases, basic science and engineering science courses are taught using SI units. Certain manufacturing industries have converted, but in the construction industry, the familiar "English" or "customary" units are still almost universal. Although a metric version of the ACI Code is available, the ACI Code in customary units is the one found in most design offices. Recognizing that users of this text may have become familiar with SI units in preparatory studies, but will soon enter design offices in which customary units prevail, I have proceeded as follows: (1) all graphs and tabulated information of a fundamental nature (e.g., the tables of Chapter 2) are given in dual units;

(2) examples are worked in customary units, but SI equivalents are provided in parentheses for input data and key answers; (3) design aids in Appendix A are given in customary units only. This appears to be a reasonable compromise between encouragement to adopt the superior SI system, and recognition of the probable facts of professional life over the next 10 to 20 years.

Many individuals and several organizations have contributed to this volume. Particular thanks are due to Professors Dan Branson, David Darwin, and Maher Tadros for their careful review of the entire manuscript and their many constructive suggestions. Illustrations and design aids were obtained, in many cases, with the cooperation of Dan Jenny and George Nasser, of the Prestressed Concrete Institute, and Cliff Freyermuth, of the Post-Tensioning Institute. Additional photographs were obtained through Charles Dolan of ABAM Engineers and David Goodyear of Arvid Grant and Associations. Finally, I would like to acknowledge a special debt to my former students, who have not only worked through all of the examples and problems found in the text, but have contributed materially through classroom interaction to the evolution of the lecture notes on which this book is based.

Ithaca, New York
February 1987

Arthur H. Nilson

CONTENTS

ONE

BASIC CONCEPTS

1.1 INTRODUCTION

Prestressing can be defined in general terms as the preloading of a structure, before application of the service loads, so as to improve its performance in specific ways. Although the principles and techniques of prestressing have been applied to structures of many types and materials, the most common application is in the design of structural concrete.

Concrete is essentially a compression material. Its strength in tension is much lower than that in compression, and in many cases, in design, the tensile resistance is discounted altogether. The prestressing of concrete, therefore, naturally involves application of a compressive loading, prior to applying the anticipated service loads, so that tensile stresses that otherwise would occur are reduced or eliminated.

In fact, the original concept of prestressing concrete was to introduce sufficient axial precompression in beams so that all tension in the concrete was eliminated in the member at service load. However, as knowledge of this relatively new form of construction has developed, it has become clear that this view is unnecessarily restrictive, and in present design practice tensile stress in the concrete, even some limited cracking, is permitted. By varying the amount of compressive prestress, the number and width of cracks can be limited to the

desired degree. Of equal importance, the deflection of the member may be controlled. Beams may even be designed to have zero deflection at a specific combination of prestress and external loading. In the sense of improved serviceability, such partial prestressing represents a substantial improvement, not only over conventional reinforced concrete construction, but also over the original form of full prestressing that, while eliminating service-load cracking, often produced troublesome upward camber.

But it is not only through improved serviceability that prestressing has achieved its position of importance. By crack and deflection control at service loads, prestressing makes it possible to employ economical and efficient high tensile strength steel reinforcement and high strength concrete.

Crack widths in conventional reinforced concrete beams are roughly proportional to the stress in the tensile reinforcement, and for this reason steel stresses must be limited to values far less than could otherwise be used. In prestressed beams, high steel stress is not accompanied by wide concrete cracks, because much of the strain is applied to the steel before it is anchored to the concrete and before the member is loaded.

Deflection of ordinary reinforced concrete beams is also linked directly to stresses. If very high stresses were permitted, the accompanying high strains in the concrete and steel would inevitably produce large rotations of the cross

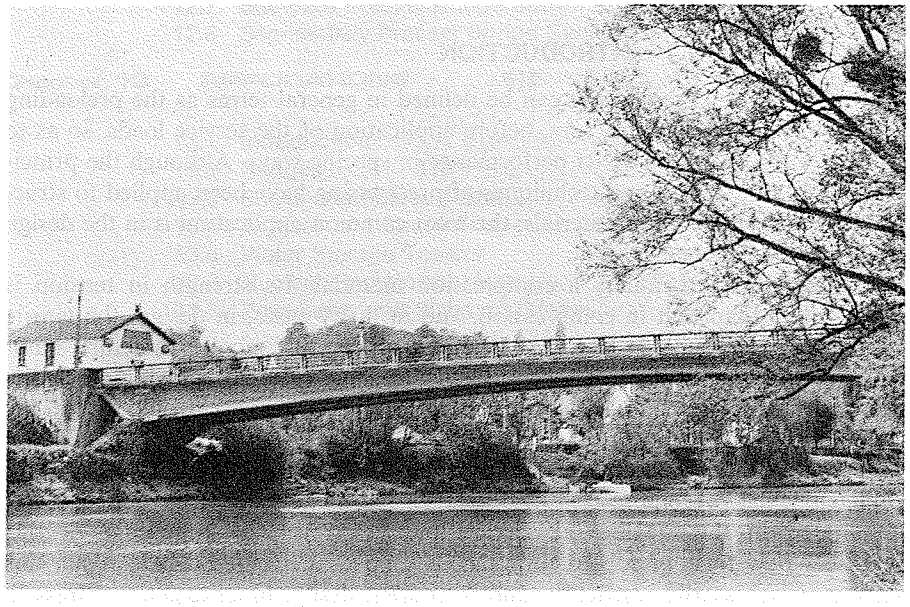

FIGURE 1.1 Bridge of 180-ft span over the river Marne at Luzancy designed by Freyssinet and built in 1941.

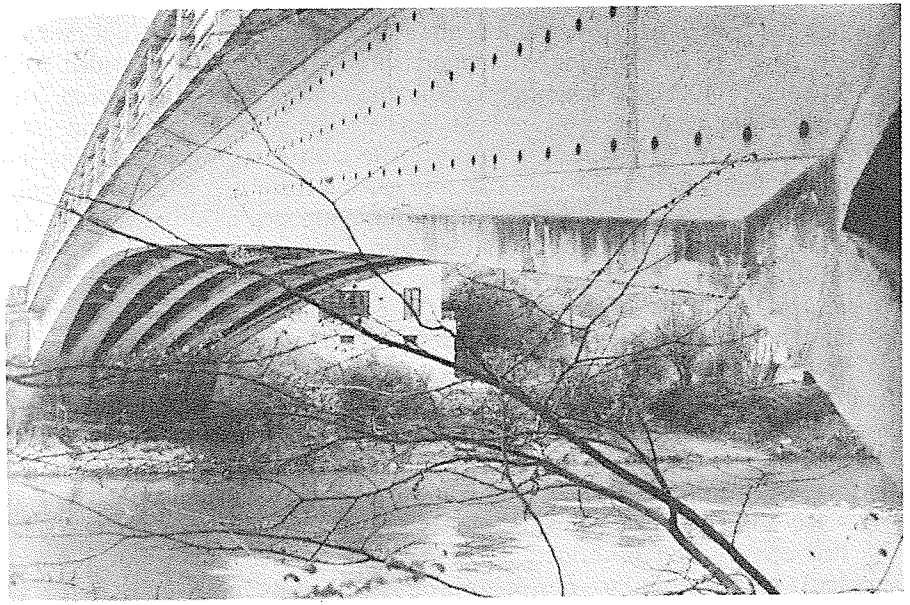

FIGURE 1.2 View of the Luzancy bridge.

sections along the member, which translate directly into large deflections. By prestraining the high strength reinforcement of prestressed beams, the large rotations and deflections that would otherwise occur are avoided. In addition, the essentially uncracked concrete member is stiffer, for given section dimensions, than it would be if cracking were permitted to the extent typical of reinforced concrete construction.

Thus, it is not only because of improvement of service load behavior, by controlling cracking and deflection, that prestressed concrete is attractive, but also because it permits utilization of efficient high strength materials. Smaller and lighter members may be used. The ratio of dead to live load is reduced, spans increased, and the range of application of structural concrete is greatly extended.

The dramatic improvements in the performance of concrete structures that could be obtained by prestressing were first recognized by the renowned French engineer Eugene Freyssinet. His studies of the time-dependent effects of shrinkage and creep of concrete, which began as early as 1911, led him to realize the importance of using steel at a high initial stress to prestress concrete members. In 1940 he introduced a system for prestressing using wedge-anchored high strength steel cables, a practical arrangement that is still in wide use.

The remarkable bridge over the river Marne at Luzancy, France, shown in Figs. 1.1 and 1.2, illustrates the innovation and daring that was to be typical of Freyssinet's later designs. Built in 1941, this very flat, two-hinged portal frame

structure has a span of 180 ft and a depth at midspan of only 4.17 ft, a ratio of span to depth of 43. The hinged supports of the bridge were provided with adjustments in order to compensate for the effects of shrinkage and creep. The I-shaped bridge segments were precast. The flanges were cast first and were connected by wires that were tensioned prior to casting the web by jacking the flanges apart. After the webs were cast, the jacking force was released, precompressing the webs to counteract diagonal tensile stresses resulting from loads. Individual segments were then assembled into larger components, which were placed in final position by cableways, and the entire structure then post-tensioned. This structure, and five other nearly identical spans in the same region, provide the model for segmentally precast bridges now widely used.

Prestressing has been applied to great advantage in a wide variety of situations, a few of which are illustrated by the following photographs. Figure 1.3 shows the use of precast "double-T" beams carrying a floor with clear span of about 20 ft. End support is provided by the precast L-section beam over the window, also prestressed. Such precast prestressed construction has been used extensively throughout the United States.

The construction of bridges by the cantilever method, in which newly completed segments are prestressed to completed construction, is illustrated by Fig. 1.4. The twin spans shown under construction, near Paris, carry four lanes of traffic.

FIGURE 1.3 Precast prestressed double-T floor beams.

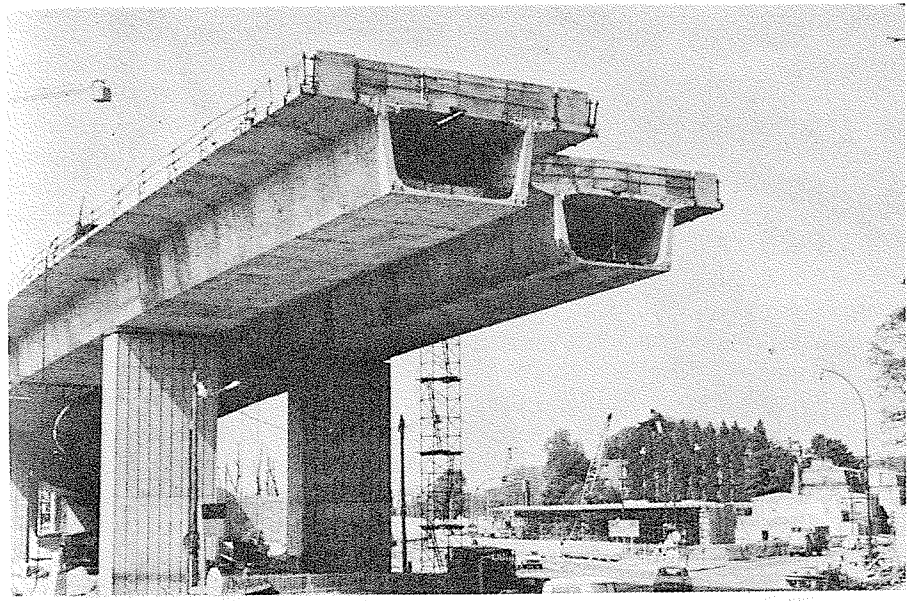

FIGURE 1.4 Twin box-girder bridge under construction using the segmentally cast cantilever method.

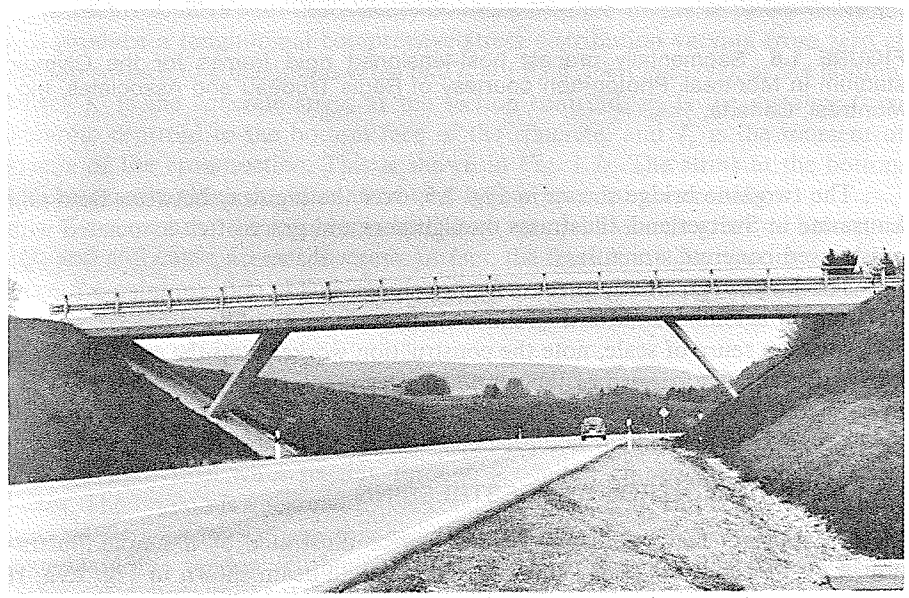

FIGURE 1.5 Highway crossing in Switzerland, continuous over three spans.

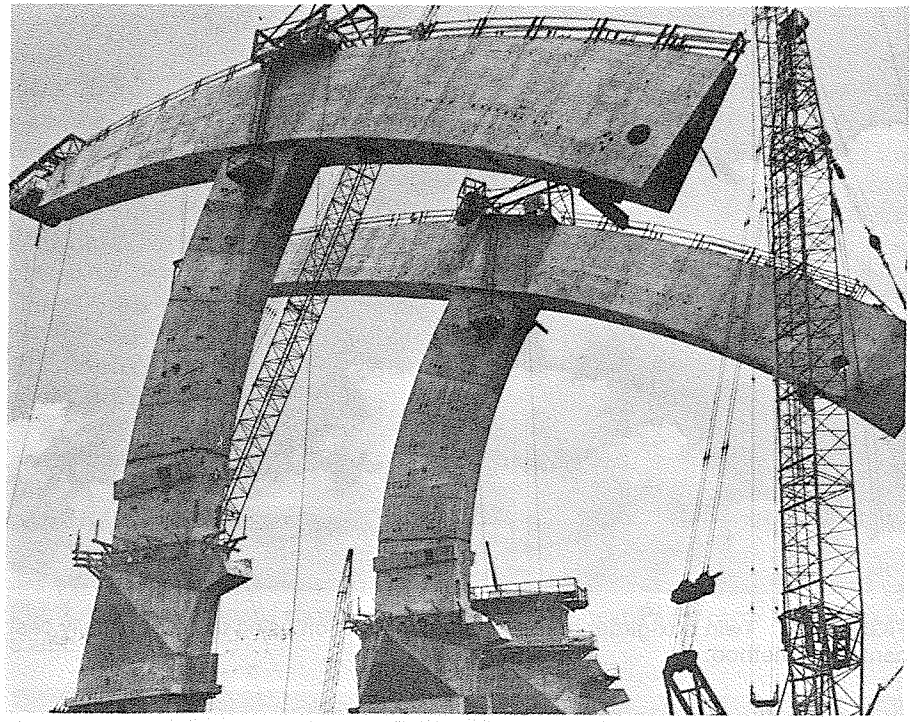

FIGURE 1.6 Segmentally precast post-tensioned rigid frames for the Olympic stadium in Montreal. Photograph courtesy of Regis Trudeau and Associates, Inc., Montreal, Canada.

The two-lane bridge shown in Fig. 1.5, over the highway between Bern and Lausanne in Switzerland, illustrates the lightness and grace often associated with prestressed concrete structures.

The huge, segmentally precast frames shown in Fig. 1.6, completed for the 1976 Olympic Games in Montreal illustrate the versatility of prestressed concrete. To provide a sense of scale, note the construction worker atop the catwalk of the farther frame, just forward of the supporting leg.

1.2 STRESS CONTROL BY PRESTRESSING

Many important features of prestressing can be illustrated by a simple illustration. Consider first the plain, unreinforced concrete beam shown in Fig. 1.7*a*. It carries a single concentrated load at the center of its span. (The self-weight of the member will be neglected here.) As the load W is gradually applied, longitudinal flexural stresses are induced. Assuming that the concrete is stressed only within its elastic range, the flexural stress distribution at midspan will be linear, as shown.

At a relatively low load, the tensile stress in the concrete at the bottom of the member will reach the tensile strength of the material, f_r, and a crack will form. Since no restraint is provided against upward extension of the crack, the member will collapse without further increase of load.

Now consider an otherwise identical beam, as in Fig. 1.7*b*, in which a longitudinal axial force P is introduced prior to the vertical loading. The longitudinal prestressing force will produce a uniform axial compressive stress $f_c = P/A_c$, where A_c is the cross-sectional area of the concrete. The force can be adjusted in magnitude, so that, when the transverse load Q is applied, the superposition of stresses due to P and Q will result in zero tensile stress at the bottom of the beam, as shown. Tensile stress in the concrete may be eliminated in this way or reduced to a specified amount.

But it would be more logical to apply the prestressing force near the bottom of the beam, so as to compensate more effectively for the load-induced tension. A possible design specification, for example, might be to introduce the maximum compression at the bottom of the member without causing tension at the top, when only the prestressing force acts. It is easily shown that, for a rectangular cross-section beam, the corresponding point of application of the force is at the lower third point of the section depth. The force P, with the same value as before, but applied with eccentricity $e = h/6$ relative to the concrete centroid, will produce a longitudinal compressive stress distribution varying from zero at the top surface to a maximum value of $2f_c = (P/A_c) + (Pec_2/I_c)$, at the bottom, where f_c is the concrete stress at the section centroid, c_2 is the distance from concrete centroid to the bottom face of the concrete, and I_c is the moment of inertia of the cross section. This is shown in Fig. 1.7*c*. The stress at the bottom will be exactly twice the value produced before by axial prestressing.

Consequently, the transverse load may now be twice as great as before, or $2Q$, and still cause no tensile stress. In fact, the final stress distribution resulting from the superposition of load and prestressing force in Fig. 1.7*c* is identical to that of Fig. 1.7*b*, although the load is twice as great. The advantage of eccentric prestressing is obvious.

The methods by which concrete members are prestressed will be discussed in some detail in Section 1.6 with further details given in Appendix B. For present purposes, it is sufficient to know that one common method of prestressing uses high strength steel wires passing through a conduit embedded in the concrete beam. The tendon is anchored to the concrete at one end, and is stretched at the far end by a hydraulic jack that reacts against the concrete. When the desired tension in the tendon is obtained, it is anchored against the concrete at the jacking end as well, and the jack is removed. The result is a self-contained system by which the force P of Fig. 1.7 may be applied.

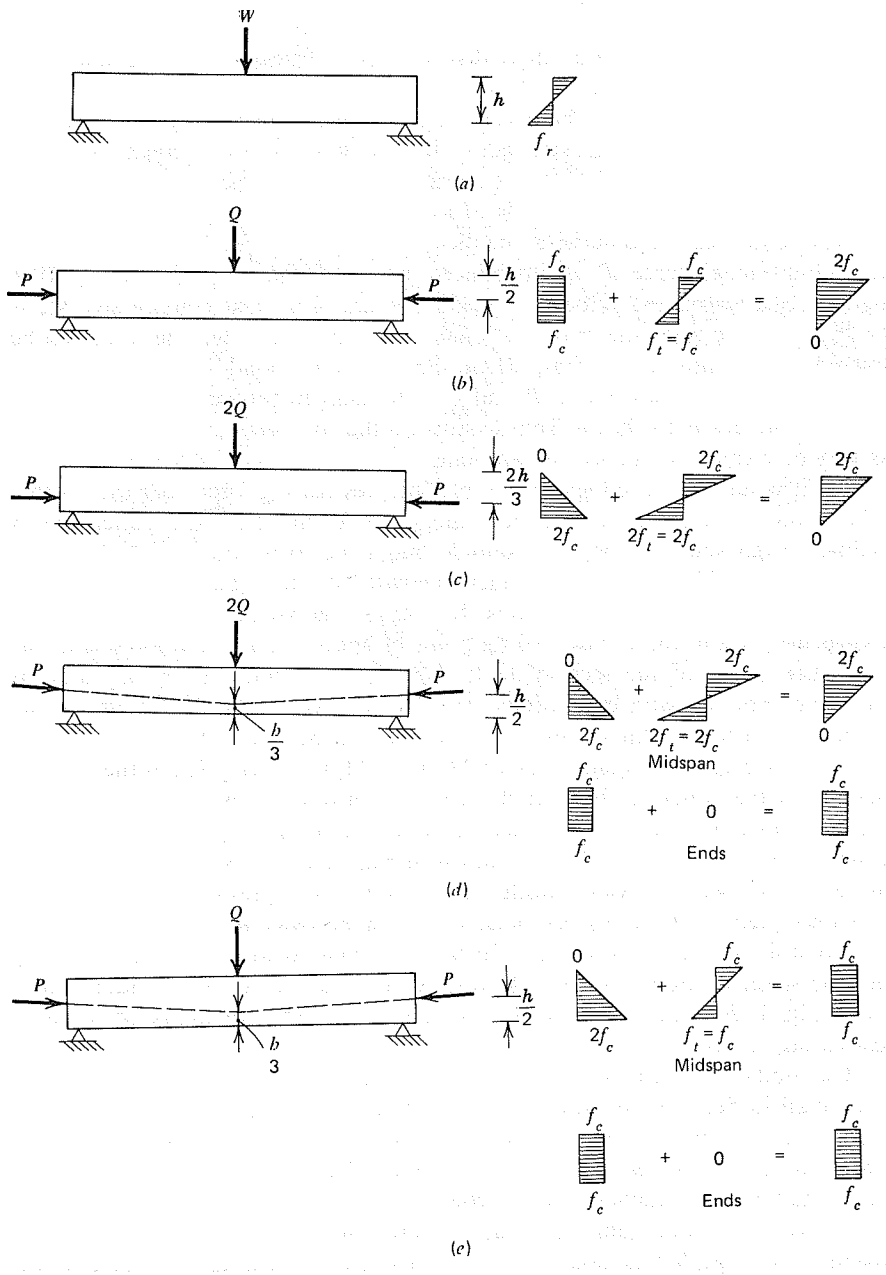

FIGURE 1.7 Alternative schemes for prestressing a rectangular concrete beam. (*a*) Plain concrete beam. (*b*) Axially prestressed beam. (*c*) Eccentrically prestressed beam. (*d*) Beam prestressed with variable eccentricity. (*e*) Balanced load stage for a beam with variable eccentricity.

If such a system is used, a significant improvement over the arrangement of Figs. 1.7*b* or 1.7*c* can be made by using a variable eccentricity of prestress force with respect to the centroid of the concrete section along the length of the member. The load $2Q$ produces a bending moment that varies linearly along the span from zero at the supports to maximum at the center. Intuitively, one suspects that the best arrangement of prestressing would produce a countermoment, acting in the opposite sense, that would vary in the same way. This is easily done, because the prestress moment is directly proportional to the eccentricity of the tendon, measured from the steel centroid to the concrete centroid. Accordingly, the tendon is now given an eccentricity that varies linearly from zero at the supports to maximum at the center of the span. Such an arrangement is shown in Fig. 1.7*d*. The stresses at midspan are the same as before, both when the load $2Q$ acts and when it does not. At the supports, where only the prestress force acts, with zero eccentricity, a uniform compressive stress f_c is obtained as shown.

It should be clear that, for each characteristic load arrangement, there is a "best" tendon profile in the sense that it produces a prestress moment diagram that corresponds to that of the applied load. It is of further interest to note that, if the prestress countermoment should be made exactly equal and opposite to the moment from the loads all along the span, the result is a beam that is subject only to uniform axial compressive stress throughout for that particular loading. The beam would not only be free of cracking but also (neglecting the influence of concrete shrinkage and creep) would deflect neither up nor down when that load is in place, compared to its unstressed position. Such a situation would be obtained for a load of $\frac{1}{2} \times (2Q) = Q$, as in Fig. 1.7*e*, for example. This condition is referred to as the balanced load stage.

Although this brief discussion has been presented with reference to the elimination of flexural tension and control of cracking and deflection in concrete beams, it should be recognized that prestressing may be used effectively for many other reasons, such as to reduce or eliminate diagonal tensile stresses in beams, hoop tension in liquid storage vessels or pipes, tensile stresses due to loading or shrinkage in pavements, or tension from the eccentric loading of columns. The fundamental principles are broadly applicable and provide design engineers with a powerful means to improve the performance of structures of many types.

1.3 EQUIVALENT LOADS

The effect of a change in the vertical alignment of a prestressing tendon is to produce a transverse vertical force on the concrete member. That force, together with the prestressing forces acting at the ends of the member through the tendon anchorages, may be looked upon as a system of external forces in studying the effect of prestressing.

In Fig. 1.8*a*, for example, a tendon that applies force P at the centroid of the concrete section at the ends of a beam and that has a uniform slope at angle θ

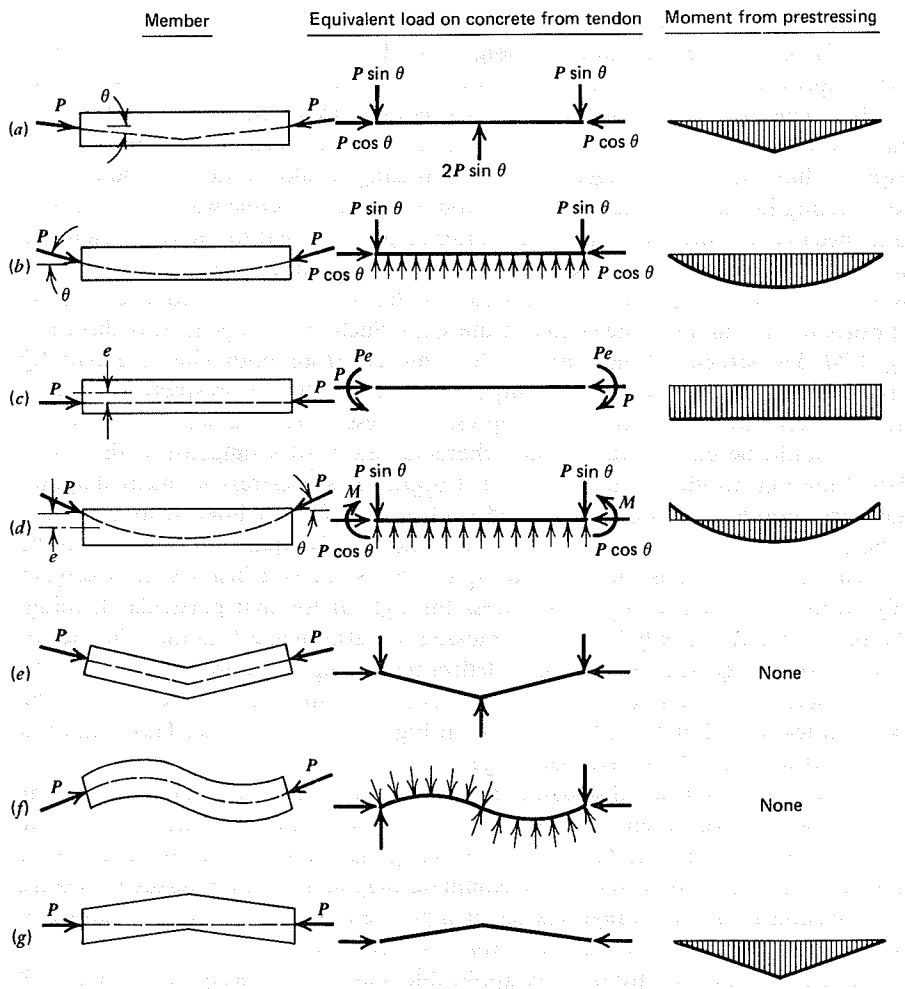

FIGURE 1.8 Equivalent loads and moments produced by prestressing tendons.

between the ends and midspan introduces the transverse force $2P \sin \theta$ at the point of change in tendon alignment at midspan. At the anchorages, the vertical component of the prestressing force is $P \sin \theta$ and the horizontal component is $P \cos \theta$. The horizontal component is very nearly equal to the force P for the usual small slope angles. The moment diagram for the beam of Fig. 1.8*a* is seen to have the same form as that for any center-loaded simple span.

The beam of Fig. 1.8*b*, with a curved tendon, is subject to a transverse distributed load from the tendon, as well as the forces P at each end. The exact distribution of the load depends on the alignment of the tendon. A tendon with a parabolic profile, for example, will produce a uniformly distributed transverse load. In this case, the moment diagram will have a parabolic shape, as for a uniformly loaded simple span beam.

If a straight tendon is used with constant eccentricity e, as in Fig. 1.8*c*, there are no transverse forces on the concrete. But the member is subject to a moment Pe at each end, as well as the axial force P, and a diagram of constant moment results.

The end moment must also be accounted for in considering the beam of Fig. 1.8*d*, in which a parabolic tendon is used that does not pass through the concrete centroid at the ends of the span. In this case, a uniformly distributed transverse load and end anchorage forces are produced, just as in Fig. 1.8*b*. But, in addition, the end moments $M = Pe \cos \theta$ must be considered.

The concept of equivalent transverse loading is a useful one, but it must be applied with care. In all of the cases considered thus far, the profile of the concrete centroid was straight. The concrete thrust was horizontal, consequently, and any change in alignment of the tendon produced an unbalanced force acting on the concrete at that section. If the beam axis is curved, as in Figs. 1.8*e* and 1.8*f*, and if the tendon and concrete centroid coincide at all sections, then the lateral force produced by the steel at any section is balanced by a resultant force in the opposite direction produced by the thrust from the adjacent concrete, and no bending moment results.

On the other hand, if the tendon is straight but the concrete centroidal axis has some other alignment, as in Fig. 1.8*g*, then the lateral force produced by the concrete thrust is not balanced by the lateral forces from the steel, and bending moment is produced as shown.

It may be evident that, for any arrangement of applied loads, a tendon profile can be selected such that the equivalent loads acting on the beam from the tendon are just equal and opposite to the applied loads. The result would be a state of pure compression in the beam, as discussed in somewhat different terms at the end of the preceding section. An advantage of the equivalent loading concept is that it leads the designer to select what is probably the best tendon profile for any given load configuration.

It is worth emphasizing that *all* of the systems shown in Fig. 1.8 are self-equilibrating, and that the application of prestressing forces produce no external reactions. This is always true for statistically determinate beams, but is not generally true for indeterminate spans, as will be discussed in Chapter 8.

1.4 OVERLOAD BEHAVIOR AND STRENGTH IN FLEXURE

In describing the effect of prestressing in Section 1.2, it was implied that the beam responded in a linear elastic way and that the principle of superposition was valid. This requires that the beam remain uncracked and that both the concrete and steel be stressed only within their elastic ranges. This may be the

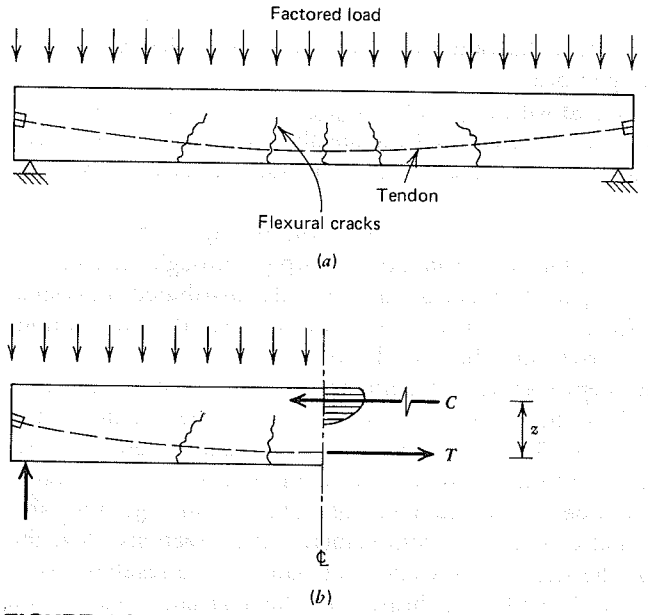

FIGURE 1.9 Prestressed concrete beam at ultimate flexural load. (*a*) Beam with factored load. (*b*) Equilibrium of forces on left half of beam.

case up to approximately the level of *service load*, that is, the actual self-weight of the member plus those superimposed loads that may reasonably be expected to act during the life of the member. But should the loads be increased further, tensile stresses resulting from flexure will eventually exceed the tensile strength of the concrete, and cracks will form. These cracks do not cause failure, because of the presence of the steel, and the loads generally can be increased well beyond the cracking load without producing distress.

Eventually, with loads increased still further, either the steel or the concrete, or both, will be stressed into their nonlinear range. The condition at incipient failure is represented by Fig. 1.9, which shows a beam carrying a *factored load*, equal to some multiple of the expected service load. In designing a member, the magnitude of the load factor can be selected to provide the desired degree of safety.

For the overloaded condition, the beam undoubtedly would be in a partially cracked state; a possible pattern of cracking is shown in Fig. 1.9. Only the concrete in compression is considered to be effective, just as in the analysis of ordinary reinforced concrete. The steel in tension works with the concrete in compression to form an internal force couple, which resists the moment from the applied load.

The concrete stress distribution in the compression zone at failure can be found by methods presented in Chapter 3, as can the magnitude of the compressive resultant C, the tensile force T in the steel, and the distance between the two. If the internal lever arm is z then the ultimate resisting moment is

$$M_n = Cz = Tz \tag{1.1}$$

It will be recognized that, at the ultimate load stage, when the beam is at the point of incipient failure in flexure, it behaves very much as an ordinary reinforced concrete beam. The main difference is that the steel used has very high strength and requires a very large strain to achieve a high stress level. If it were to be used without being prestressed (and prestrained) in tension, unacceptably large deformation and cracking of the beam would result.

Through review of this section and the two preceding sections, it will be clear that the effects of prestressing have been considered from three points of view: providing concrete stress control (Section 1.2), creating equivalent transverse loads (Section 1.3), and providing overload strength through creating an internal force couple, just as in ordinary reinforced concrete (Section 1.4). Each of these approaches is useful in the analysis and design of prestressed concrete, and each will be used in the work that follows. It should be emphasized that analysis based on elastic stresses provides no information about member strength. Strength prediction requires development of equations that account for both cracking and nonlinear material behavior. On the other hand, strength analysis reveals nothing about stresses under normal service loads, nor does it provide information about cracking or deflections, whereas elastic stress analysis and equivalent load analysis will do so. In most cases, prestress effects must be considered at different load states, and from different points of view, in the total prestressed concrete design process.

1.5 PARTIAL PRESTRESSING

Early designers of prestressed concrete focused on the complete elimination of tensile stresses in members at normal service load. This is defined as *full prestressing*. As experience has been gained with prestressed concrete construction, it has become evident that a solution intermediate between fully prestressed concrete and ordinary reinforced concrete offers many advantages. Such an intermediate solution, in which concrete tension, and usually some flexural cracking, is permitted at full service load, is termed *partial prestressing*.

Although full prestressing offers the possibility of complete elimination of cracks at full service load, it may at the same time produce members with objectionably large camber, or negative deflection, at more typical loads less than the full value. A smaller amount of prestress force may produce improved

deflection characteristics at load stages of interest. While cracks will usually form in partially prestressed beams should the specified full service load be applied, these cracks are small and will close completely when the load is reduced.

In addition to improved deflection characteristics, partial prestressing may result in significant economy by reducing the amount of prestressed reinforcement and by permitting the use of cross-section configurations with certain practical advantages compared with those required by full prestressing.

Even though the amount of prestress force may be reduced through use of partial prestressing, a beam must still have an adequate factor of safety against failure. This will often require the addition of ordinary reinforcing bars in the tension zone. Alternatives are to provide the total steel area needed for strength by high strength tendons, but to stress those tendons to less than their full permitted value, or to leave some of the strands unstressed.

Partial prestressing is looked upon with increasing favor in the United States, as it offers the combined advantages of reinforced and prestressed concrete.

1.6 PRESTRESSING METHODS

Although many methods have been used to produce the desired state of precompression in concrete members, all prestressed concrete members can be placed in one of two categories: *pretensioned* or *post-tensioned*. Pretensioned prestressed concrete members are produced by stretching the tendons between external anchorages *before* the concrete is placed. As the fresh concrete hardens, it bonds to the steel. When the concrete has reached the required strength, the jacking force is released, and the force is transferred by bond from steel to concrete. In the case of post-tensioned prestressed concrete members, the tendons are stressed *after* the concrete has hardened and achieved sufficient strength, by jacking against the concrete member itself.

A. PRETENSIONING

The greater part of prestressed concrete construction in the United States is pretensioned. The tendons, usually in the form of multiple-wire stranded cables, are stretched between abutments that are a permanent part of the plant facility, as shown in Fig. 1.10*a*. The extension of the strands is measured, as well as the jacking force.

With the forms in place, the concrete is cast around the stressed tendon. High early strength concrete is often used, together with steam curing to accelerate the hardening of the concrete. After sufficient strength is attained, the jacking pressure is released. The strands tend to shorten, but are prevented from doing so because they are bonded to the concrete. In this way, the prestress force is transferred to the concrete by bond, mostly near the ends of the beam, and no

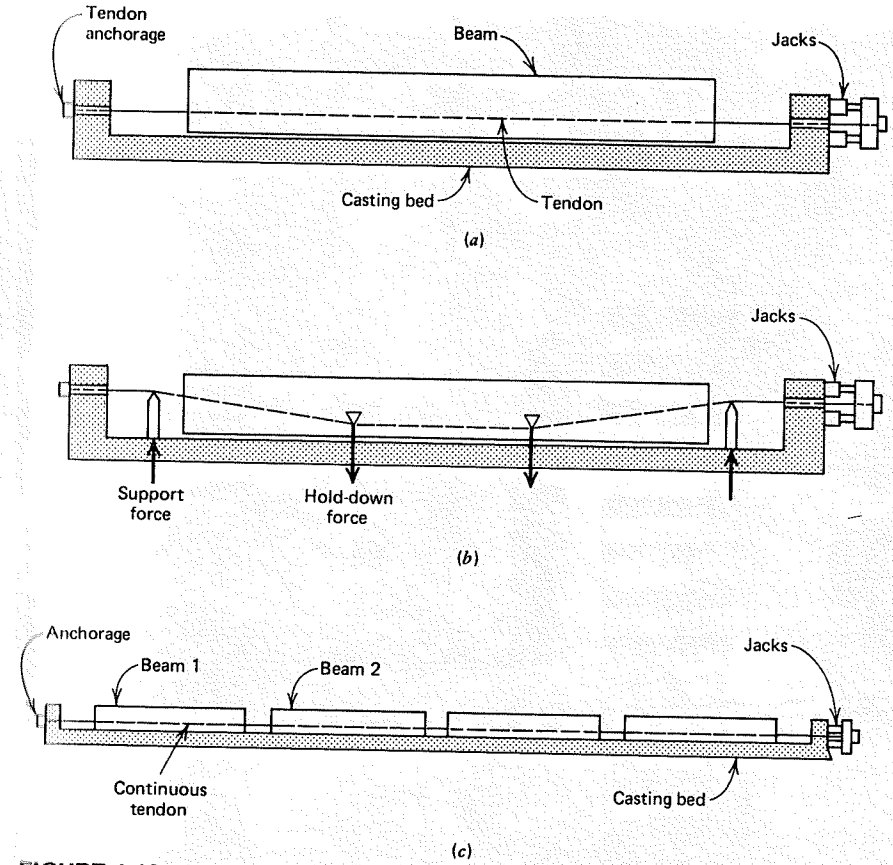

FIGURE 1.10 Methods of pretensioning. (*a*) Beam with straight tendon. (*b*) Beam with variable tendon eccentricity. (*c*) Long-line stressing and casting.

special anchorage is needed. Figure 1.11 shows the jacking frame at the end of a casting bed being used to pretension many steel cables simultaneously.

It was noted in Section 1.2 that it is often advantageous to vary the tendon eccentricity along a beam span. This can be done when pretensioning by holding down the strands at intermediate points and holding them up at the ends of the span, as shown in Fig. 1.10*b*. One, two, or three intermediate cable depressors are often used to obtain the desired profile. These hold-down devices remain embedded in the member. To minimize frictional loss of tension, it is common practice to stretch the straight cable, then to depress it to the final profile by using auxiliary jacks. Allowance must be made, in this case, for the increase in tension as the cable is forced out of straight alignment.

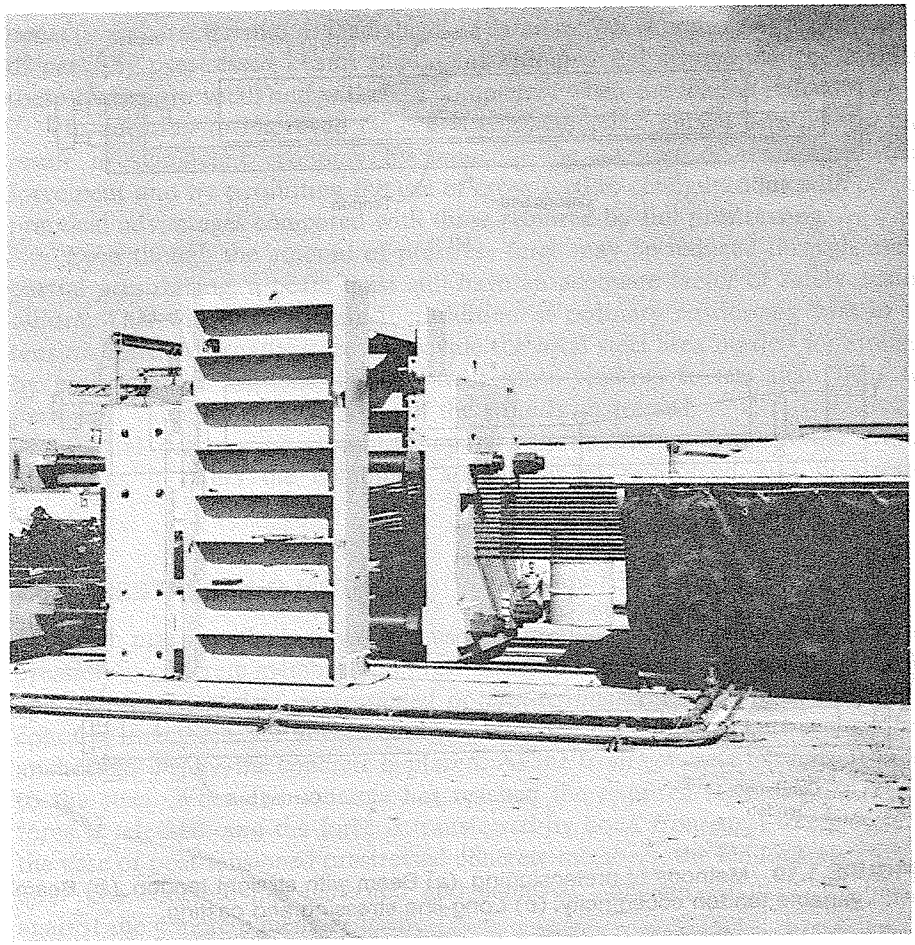

FIGURE 1.11 Jacking frame at end of casting bed used for pretensioning many strands simultaneously.

Pretensioning is well suited to the mass production of beams using the *long-line method* of prestressing as suggested by Fig. 1.10*c*. In present practice anchorage and jacking abutments may be as much as 800 ft apart. The strands are tensioned over the full length of the casting bed at one time, after which a number of individual members are cast along the stressed tendon. When the jacking force is released, the prestress force is transferred to each member by bond, and the strands are cut free between members. Although a straight tendon is shown in the sketch, cable depressors are often used with long-line prestressing,

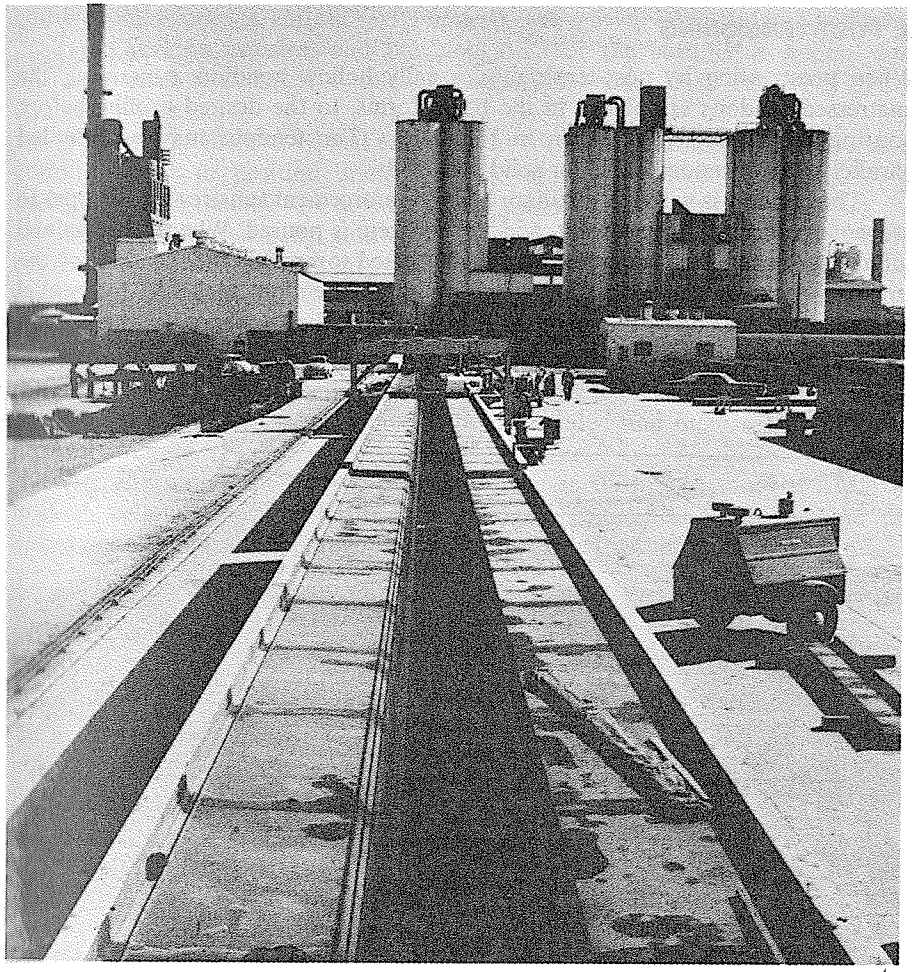

FIGURE 1.12 View of long-line prestressing bed showing metal forms and tensioned strands.

just as with individual members. Figure 1.12 is a view of a long-line pretensioning operation, showing the stressed tendons in place in the metal forms. Note the hold-down frame in the middle distance; the tendons have not yet been depressed.

Pretensioning is a particularly economical method of prestressing, not only because the standardization of design permits reusable steel or fiberglass forms, but also because the simultaneous prestressing of many members at once results in great saving of labor. In addition, expensive end-anchorage hardware is eliminated.

B. POST-TENSIONING

When prestressing by post-tensioning, usually hollow conduits containing the unstressed tendons are placed in the beam forms, to the desired profile, before pouring the concrete, as shown in Fig. 1.13*a*. The tendons may be bundled parallel wires, stranded cable, or solid steel rods.

The conduit is wired to auxiliary beam reinforcement (unstressed stirrups) to prevent accidental displacement, and the concrete is poured. When it has gained sufficient strength, the concrete beam itself is used to provide the reaction for the stressing jack, as shown in the sketch. With the tendon anchored by special fittings at the far end of the member, it is stretched, then anchored at the jacking

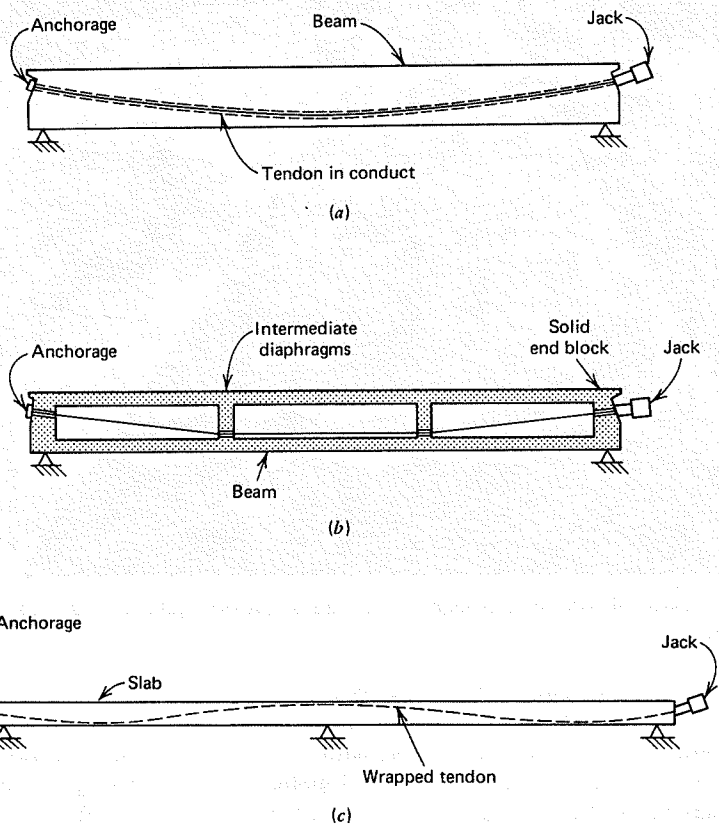

FIGURE 1.13 Methods of post-tensioning. (*a*) Beam with hollow conduit embedded in concrete. (*b*) Hollow cellular beam with intermediate diaphragms. (*c*) Continuous slab with plastic-sheathed tendons.

end by similar fittings, and the jack removed. The tension is gauged by measuring both the jacking pressure and the elongation of the steel. The tendons are normally tensioned one at a time, although each tendon may consist of many strands or wires.

Figure 1.14 shows a typical arrangement for post-tensioning with the tendon conduit wired in position and anchorage fittings in place. In Fig. 1.15, a multiple-strand tendon, one of three in the beam, is being stressed.

Tendons are normally grouted in their conduits after they are stressed. A cement paste grout is forced into the conduit at one end under high pressure, and pumping is continued until the grout appears at the far end of the tube. When it hardens, the grout bonds to the tendon and to the inner wall of the conduit, permitting transfer of force. Although the anchorage fittings remain in place to transfer the main prestressing force to the concrete, grouting improves the performance of the member should it be overloaded and increases its ultimate flexural strength.

An alternative method of post-tensioning is illustrated in Fig. 1.13*b*. A hollow, cellular concrete beam with solid end blocks and intermediate diaphragms is shown. Anchorage fittings are provided as before, but the tendons

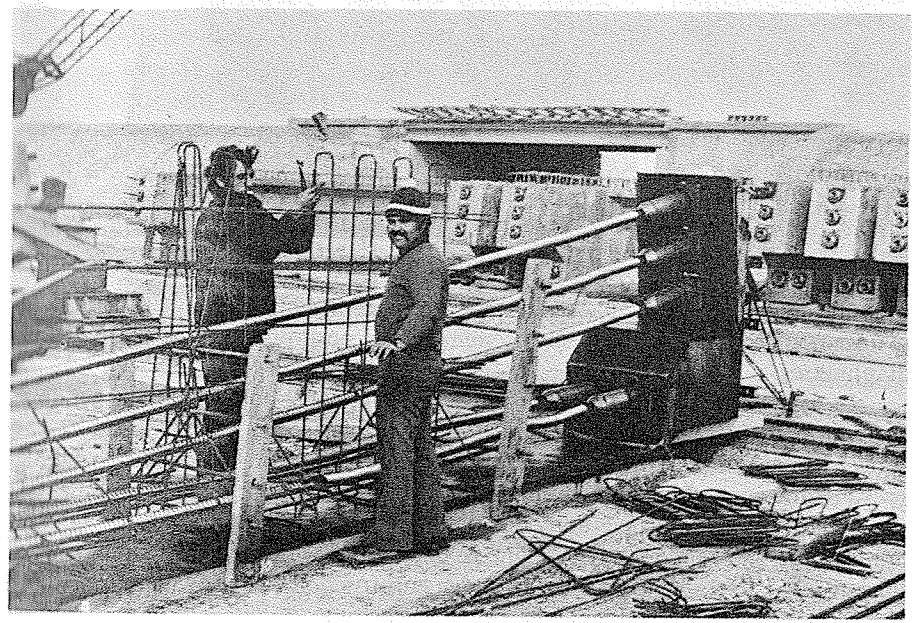

FIGURE 1.14 Post-tensioned beam under construction, showing draped tendon conduits and anchorages in position prior to placing side forms and pouring concrete.

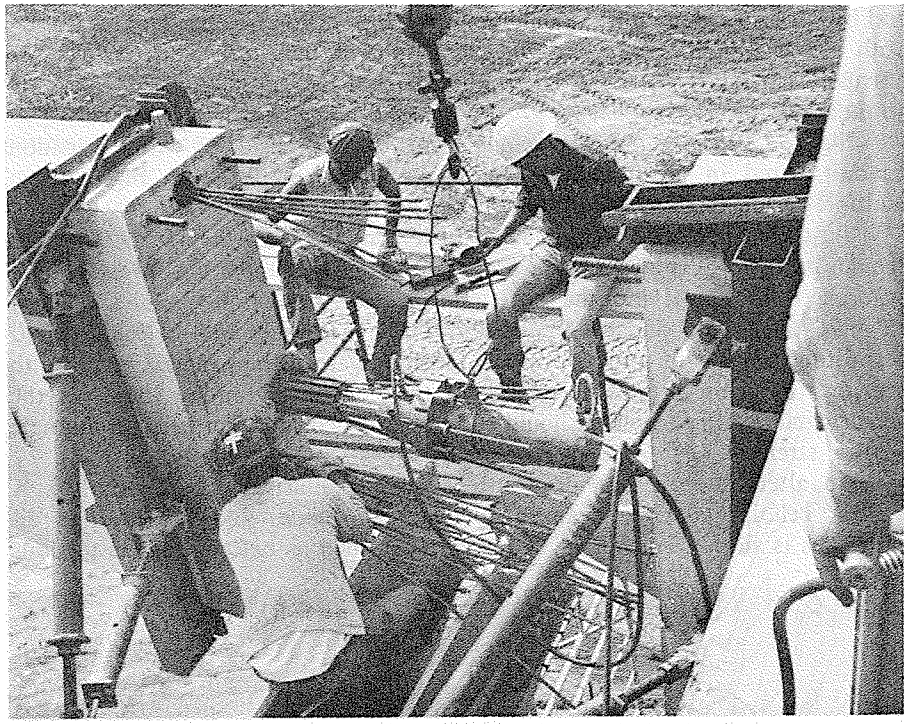

FIGURE 1.15 Post-tensioning a beam using multiple-strand tendons.

pass through the void spaces in the member. The desired cable profile is maintained by passing the steel through sleeves positioned in the intermediate diaphragms.

In many cases, particularly in relatively thin slabs, post-tensioning tendons are wrapped with asphalt-impregnated paper or encased in plastic sheathing, as shown in Fig. 1.13*c*. Anchorage and jacking hardware is provided. The wrapping prevents the concrete from bonding to the steel. When the concrete has hardened, the tendons are stretched and anchored, and the jack removed. Obviously, bonding of the tendon by grouting is impossible with such an arrangement. Figure 1.16 shows a two-way slab under construction, which will be post-tensioned using the sheathed tendons shown in position.

Countless patented systems of post-tensioning are available, along with all necessary hardware. Explicit details of representative systems are found in Appendix B. A significant advantage of all post-tensioning schemes is the ease

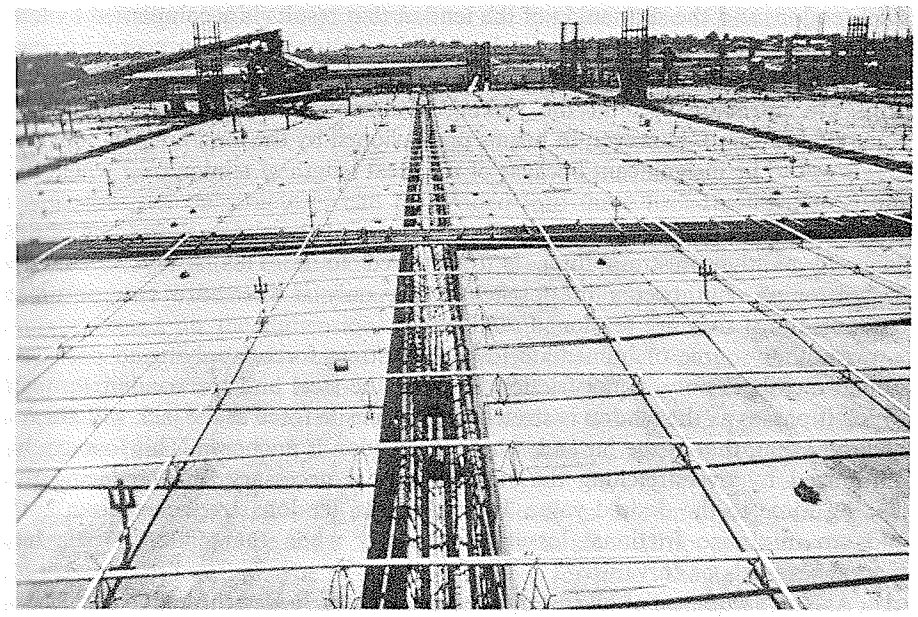

FIGURE 1.16 Two-way prestressed slab, using unbonded wrapped tendons, under construction. Courtesy of the Post-Tensioning Institute.

with which the tendon eccentricity can be varied along the span to provide the desired countermoment.

1.7 CHANGES IN PRESTRESS FORCE

The magnitude of prestressing force in a concrete member is not constant, but assumes different values during the life of the member. Some of the changes are instantaneous or nearly so, some are time-dependent, and some are a function of the superimposed loading. All such changes must be accounted for in the design. Neglect of time-dependent losses, in particular, accounts for the lack of success of all early attempts to prestress concrete.

With the exception of conditions at severe overloading, the greatest force that acts is during the jacking operation. The *jacking force* will be referred to subsequently as P_j. For a post-tensioned member, this force is applied as a reaction directly upon the concrete member, while with pretensioning, the jacking force reacts against external anchorages and does not act on the concrete at all.

At the moment of transfer of prestress force from the jack to the anchorage fittings that grip the tendon, there is an immediate reduction in force. There is inevitably a small amount of slip as the wedges or grips seat themselves into the

steel tendon, and the shortening of the tendon that results is accompanied by loss in tensile strain and stress. This is always a factor to consider in post-tensioned beams. Corresponding slip loss occurs in pretensioning too, because temporary grips are normally used at the jacking abutment to hold the strand as the concrete is poured. However, in beams pretensioned by the long-line method, slip loss is apt to be insignificant because of the great length of tendon over which the slip is distributed.

There is an instantaneous stress loss because of the elastic shortening of the concrete as the prestress force is transferred to it. This always occurs in pretensioning, but occurs in post-tensioning only if there are two or more tendons and if they are tensioned sequentially.

Another source of immediate loss of prestress force, applying to post-tensioned members only, is the friction between the steel and the conduit through which it passes as the tendon is stretched. The tensile force at the jack will always be larger than that at the far end, where the tendon is anchored. This loss can be minimized by overstretching the steel slightly if necessary, then reducing the jacking force to the desired value. In some cases, tendons are jacked from both ends to minimize frictional losses, particularly when the tendon profile has several reversals of curvature.

As a consequence of all instantaneous losses, including those due to anchorage slip, elastic shortening, and friction, the jacking force P_j is reduced to a lower value P_i, defined as the *initial prestress force*.

With the passage of time, the steel stress is further reduced. The changes that cause this reduction occur rather rapidly at first, but the rate of change of stress soon decreases. A nearly constant stress level is approached, but only after many months, or even several years.

The main causes of time-dependent loss are shrinkage of the concrete and concrete creep under sustained compressive stress. Both of these produce shortening of the member, which results in a reduction in steel strain and stress. In addition, the steel experiences a gradual relaxation of stress, as it is held at nearly constant strain. The result of all time-dependent effects, including concrete shrinkage and creep and steel relaxation, is that the initial prestress force is gradually reduced to what will be termed the *effective prestress force* P_e.

The sum of all losses, immediate and time-dependent, may be of the order of 20 to 35 percent of the original jacking force. All losses must be accounted for in the design of prestressed concrete. They will be examined in detail in Chapter 6.

Loading of a prestressed beam will generally produce an *increase* in stress in the tendon. As long as the member remains uncracked, the increase is so small that it is usually neglected in design. However, cracking of the concrete is accompanied by an instantaneous increase in steel stress, as the tensile force formerly carried by the concrete is transferred to the steel. If the load is increased further, the member behaves much as ordinary reinforced concrete, and the steel stress increases roughly in proportion to the load until the nonlinear range of material behavior is reached, followed by eventual failure. The steel may reach its ultimate tensile strength at failure, although this is not generally so.

1.8 LOADS

Loads that act on structures can be divided into three broad categories: *dead loads*, *live loads*, and *environmental loads*. Dead loads are fixed in location and constant in magnitude throughout the life of the structure. Usually the *self-weight* of a structure is the most important part of the dead load. This can be calculated closely, based on the dimensions of the structure and the unit weight of the material. Concrete density varies from about 90 to 120 pcf (14 to 19 kN/m^3) for lightweight concrete and is about 145 pcf (23 kN/m^3) for normal concrete. In calculating the dead load of structural concrete, usually a 5 pcf (1 kN/m^3) increment is included with the weight of the concrete to account for the presence of the reinforcement.

Live loads consist chiefly of occupancy loads in buildings and traffic loads on bridges. They may be either fully or partially in place or not present at all and may change in location. The minimum live loads for which the floors and roof of a building should be designed are usually specified in the building code that governs at the site of construction. Representative values of minimum live loads to be used in a wide variety of buildings are found in *Minimum Design Loads for Buildings and Other Structures* (Ref. 1.1), a portion of which is reprinted in Table 1.1. The table gives uniformly distributed live loads for various types of occupancies; these include impact provisions where necessary. These loads are expected maxima and considerably exceed average values. In addition to these uniformly distributed loads, it is recommended that, as an alternative to the uniform load, floors be designed to support safely certain concentrated loads if these loads produce a greater stress. Certain reductions are permitted in live load for members supporting large areas on the premise that it is not likely that the entire area would be fully loaded at one time.

Service live loads for highway bridges are specified by the American Association of State Highway and Transportation Officials (AASHTO) in its *Standard Specifications for Highway Bridges* (Ref. 1.2). For railway bridges, the American Railway Engineering Association (AREA) has published the *Manual of Railway Engineering* (Ref. 1.3).

Environmental loads consist mainly of snow loads, wind pressure and suction, earthquake loads (i.e., inertia forces caused by earthquake motions), soil pressures on subsurface portions of structures, loads from possible ponding of rainwater on flat surfaces, and forces caused by temperature differentials. Like live loads, environmental loads at any given time are uncertain both in magnitude and distribution. Reference 1.1 contains much information on environmental

Table 1.1 Minimum uniformly distributed live loads

Occupancy or Use	Live Load (psf)	Occupancy or Use	Live Load (psf)
Apartments (see residential)		Manufacturing:	
Armories and drill rooms	150	Light	125
		Heavy	250
Assembly areas and theaters:			
Fixed seats (fastened to floor)	60	Marquees and canopies	75
Lobbies	100	Office buildings:	
Movable seats	100	File and computer rooms shall	
Platforms (assembly)	100	be designed for heavier loads	
Stage floors	150	based on anticipated occupancy	
Balconies (exterior)	100	Lobbies	100
On one- and two-family residences		Offices	50
only, and not exceeding 100 ft^2	60	Penal Institutions:	
Bowling alleys, poolrooms, and		Cell blocks	40
similar recreational areas	75	Corridors	100
Corridors:		Residential:	
First floor	100	Dwellings (one- and two-family)	
Other floors, same as occupancy		Uninhabitable attics	
served except as indicated		without storage	10
Dance halls and ballrooms	100	Uninhabitable attics	
		with storage	20
Decks (patio and roof)		Habitable attics and sleeping	
Same as area served, or for the		areas	30
type of occupancy accommodated		All other areas	40
Dining rooms and restaurants	100	Hotels and multifamily houses	
		Private rooms and corridors	
Dwellings (see residential)		serving them	40
Fire escapes	100	Public rooms and corridors	
On single-family dwellings only	40	serving them	100
Garages (passenger cars only)	50	Schools:	
For trucks and buses use AASHTO[a]		Classrooms	40
lane loads		Corridors above first floor	80
		Sidewalks, vehicular driveways,	
Grandstands (see stadium and arena		and yards, subject to trucking[b]	250
bleachers)		Stadium and arena bleachers[c]	100
Gymnasiums, main floors and		Stairs and exitways	100
balconies	100		
		Storage warehouses:	
Hospitals:		Light	125
Operating rooms, laboratories	60	Heavy	250
Private rooms	40		
Wards	40	Stores:	
Corridors above first floor	80	Retail	
		First floor	100
Hotels (see residential)		Upper floors	75
Libraries:		Wholesale, all floors	125
Reading rooms	60	Walkways and elevated platforms	
Stack rooms—not less than [d]	150	(other than exitways)	60
Corridors above first floor	80	Yards and terraces (pedestrians)	100

Source: From Ref. 1.1. Courtesy of the American National Standards Institute.
[a]American Association of State Highway and Transportation Officials.
[b]AASHTO lane loads should also be considered where appropriate.
[c]For detailed recommendations, see American National Standard for Assembly Seating, Tents, and Air-Supported Structures, ANSI / NFPA 102-1978.
[d]The weight of books and shelving shall be computed using an assumed density of 65 lb / ft^3 (pounds per cubic foot, sometimes abbreviated pcf) and converted to a uniformly distributed load; this load shall be used if it exceeds 150 psf.

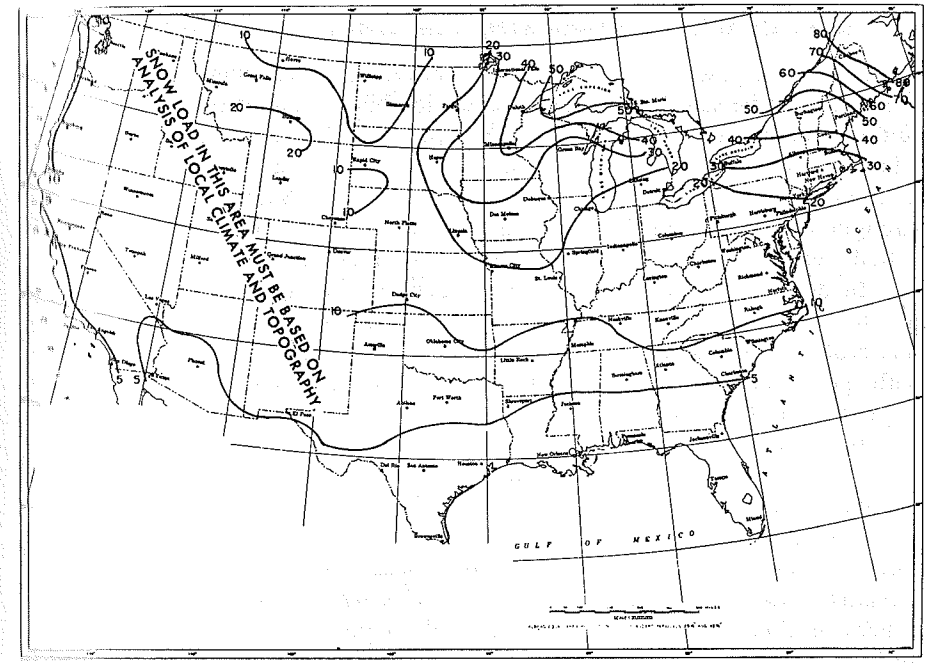

FIGURE 1.17 Estimated weight of seasonal snowpack (psf) equaled or exceeded one year in ten. From Ref. 1.1, courtesy of American National Standards Institute, New York.

loads, which is often modified locally depending, for instance, on local climatic or seismic conditions.

Figure 1.17, from the 1972 edition of Ref. 1.1, gives snow loads for the continental United States and is included here for illustration. The 1982 edition of Ref. 1.1 gives much more detailed information.

Much progress has been made in recent years in developing rational methods for predicting horizontal forces on structures due to wind and seismic action. Reference 1.1 summarizes current thinking regarding wind forces and has much information pertaining to earthquake loads as well. Reference 1.4 presents detailed recommendations for lateral forces from earthquakes.

The sum of the calculated dead load and the specified or calculated live and environmental loads is called the *service load*, because this is the best estimate of the maximum load that can be expected to act during the service life of the structure. The *factored load*, or failure load, that a structure must be capable of resisting to ensure an adequate margin of safety against collapse, is a multiple of the service load, as explained in the following section.

1.9 SERVICEABILITY, STRENGTH, AND STRUCTURAL SAFETY

To serve its purpose, a structure must be serviceable under ordinary conditions of use and must be safe against collapse. Serviceability requires that deflections be suitably small, that crack widths be kept to within acceptable limits, that vibrations be minimized, and so on. In addition, most specifications impose limitations on the stresses in the concrete and steel. Safety requires that the strength of the structure be adequate to resist overloading should the loads actually expected to act be increased by a certain amount.

In designing prestressed concrete structures, the engineer must consider a number of load stages and must impose certain limiting conditions defining serviceability and safety. This process is sometimes known as *limit states design*, with specific consideration of cracking limit state, deflection limit state, strength limit state, and the like.

In the United States, the design of a prestressed concrete member usually starts with the consideration of limit stresses in the concrete and steel when the member is in the unloaded stage (member self-weight plus prestress) and the full service load stage. Tentative member dimensions, and prestressing steel area and force are selected based on stress limits imposed by specifications such as the *Building Code Requirements for Reinforced Concrete* (Refs. 1.5 and 1.6) of the American Concrete Institute.[1] For the trial member, crack widths, deflections, and other serviceability limit conditions are checked and the design modified if necessary. The ultimate strength of the member is then calculated and compared with strength required to resist hypothetical overloads. Section dimensions, prestressing, and other reinforcement may be further modified to produce the required margin of safety.

The strength of a structure depends on the strength of the materials from which it is made. Minimum material strengths are specified in certain, standardized ways. The properties of concrete and its components, the methods of mixing, placing, and curing to obtain the required quality, and the methods for testing are specified in documents such as Ref. 1.5, for example. Included by reference in that document are standards of the American Society for Testing Materials (ASTM) pertaining to reinforcing and prestressing steels and concrete.

[1]Throughout this text repeated reference will be made to the American Concrete Institute and its recommendations. As one part of its activity, the American Concrete Institute has published the *Building Code Requirements for Reinforced Concrete* (ACI 318-83), which serves as a guide in the design and construction of reinforced and prestressed concrete buildings. The Code has no official status in itself. However, it is generally regarded as an authoritative statement of current good practice. As a result it has been incorporated by law into countless municipal and regional building codes that do have legal status, and its provisions thereby attain, in effect, legal significance. Most structural concrete in the United States and in many other countries is designed in accordance with the ACI Building Code and its current amendments. A second publication, *Commentary on Building Code Requirements for Reinforced Concrete* (ACI 318R-83) provides background material and rationale for the Code provisions (Ref. 1.6).

Strength also depends on the care with which the structure is built, that is, the accuracy with which the drawings and specifications of the engineer are followed. Member sizes may differ from specified dimensions, reinforcement may be out of position, prestressing force may be improperly applied, or poor placement of the concrete may result in voids. An important part of the engineer's job is to provide proper supervision of construction, and slighting of this responsibility has had disastrous consequences in more than one instance.

If strength could be predicted accurately and if loads were known with equal certainty, then safety could be assured by providing strength just barely in excess of the requirements of the loads. But there are many sources of uncertainty in the estimation of loads, as well as in analysis and design of the structure and in construction. These uncertainties require a larger margin of safety. The selection of an appropriate safety margin is not a simple matter, but much progress has been made in recent years toward rational safety provisions in design codes (Refs. 1.7 to 1.10).

The approach to safety that is found in the ACI Code (Ref. 1.5) is as follows. Separate consideration is given to loads and strength. *Load factors*, larger than unity, are applied to the calculated dead loads and calculated or specified service live and environmental loads to obtain *factored loads* that the member must just be capable of sustaining at incipient failure. Load factors pertaining to different types of loads vary, depending on the degree of uncertainty associated with loads of various types, and with the likelihood of simultaneous occurrence of different loads.

The load factors specified in the ACI Code are summarized in Table 1.2. The *required strength* U is calculated by applying individual load factors to the respective service loads: dead load D, live load L, wind load W, earthquake load E, earth pressure H, fluid pressure F, impact allowance I, and environmental effects T that may include settlement, creep, shrinkage, and temperature change. Lower factors are used for loads known with greater certainty, for example, dead loads, compared with loads of greater variability, for example, live loads. Furthermore, for load combinations such as dead plus live loads plus wind forces, a reduction coefficient is introduced that reflects the improbability that an excessively large live load coincides with an unusually high windstorm. The factors also reflect, in a general way, uncertainties with which internal load effects are calculated from external loads in systems as complex as are highly indeterminate, inelastic, reinforced or prestressed concrete structures. Finally, the load factors distinguish between two situations: (1) where the effects of all simultaneous forces are additive, or (2) where the various load effects tend to counteract each other, such as when horizontal forces are present in addition to gravity forces. In all cases in Table 1.2, the controlling equation is the one that gives the largest factored load effect U.

The required strength, should the member be overloaded, must not exceed a conservative estimate of the actual strength. To obtain that estimate, the *nominal*

Table 1.2 Factored load combinations for determining required strength U in the ACI Code

Condition	Factored load or load effect U
Basic	$U = 1.4D + 1.7L$
Winds	$U = 0.75(1.4D + 1.7L + 1.7W)$ and include consideration of $L = 0$ $U = 0.9D + 1.3W$ $U = 1.4D + 1.7L$
Earthquake	$U = 0.75(1.4D + 1.7L + 1.87E)$ and include consideration of $L = 0$ $U = 0.9D + 1.43E$ $U = 1.4D + 1.7L$
Earth pressure	$U = 1.4D + 1.7L + 1.7H$ $U = 0.9D + 1.7H$ $U = 1.4D + 1.7L$
Fluids	Add $1.4F$ to all loads that include L
Impact	Substitute $(L + I)$ for L
Settlement, creep, shrinkage, or temperature change effects	$U = 0.75(1.4D + 1.4T + 1.7L)$ $U = 1.4(D + T)$

strength S_n is calculated according to the best available information concerning materials and member behavior. That nominal strength is reduced by applying a *strength reduction factor* ϕ to obtain what is called the *design strength* of the member. The design strength must be at least equal to the required strength calculated from the factored loads, that is,

$$\phi S_n \geq U \tag{1.2}$$

Equation (1.2) is stated in general terms. It can be interpreted as applying either to loads acting on a member or to the related internal effects such as moment, shear, and thrust. Thus, in specific terms for a member subjected, say, to moment, shear, and thrust:

$$\phi M_n \geq M_u \tag{1.3a}$$

$$\phi V_n \geq V_u \tag{1.3b}$$

$$\phi P_n \geq P_u \tag{1.3c}$$

where terms with the subscript n are the nominal strengths in flexure, shear, and thrust, respectively, and terms with the subscript u are the factored load moment, shear, and thrust.

The strength reduction factors ϕ found in the ACI Code are summarized in Table 1.3. These are given different values depending on the state of knowledge

Table 1.3 Strength reduction factors in the ACI Code

Kind of strength	Strength reduction factor (ϕ)
Flexure, without axial load	0.90
Axial load, and axial load with flexure:	
Axial tension, and axial tension with flexure	0.90
Axial compression, and axial compression with flexure:	
Members with spiral reinforcement	0.75
Other members	0.70
except that for low values of axial load, ϕ may be increased in accordance with the following:[a]	
For members in which f_y does not exceed 60,000 psi, with symmetrical reinforcement, and with $(h - d' - d_s)/h$ not less than 0.70 ϕ may be increased linearly to 0.90 as ϕP_n decreases from $0.10 f'_c A_g$ to zero.	
For other reinforced members, ϕ may be increased linearly to 0.90 as ϕP_n decreases from $0.10 f'_c A_g$ or ϕP_{nb}, whichever is smaller, to zero.	
Shear and torsion	0.85
Bearing on concrete	0.70

[a] The details of, and reasons for, these permissible increases are discussed in Chapter 11.

of particular kinds of member behavior, that is, the confidence with which various strengths can be calculated. Thus, the ϕ value for bending is higher than that for shear or bearing. Also, ϕ values reflect the probable importance, for survival of the structure, of the particular member, as well as the probable quality control achievable. For both these reasons, a lower ϕ value is used for columns than for beams.

Provisions in the ACI Code and other specifications for strength reduction factors and load factors are based to some extent on statistical information and analysis such as summarized in Refs. 1.7 to 1.10, but currently are based to a much larger degree on engineering experience, intuition, and judgment.

REFERENCES

1.1 *Minimum Design Loads for Buildings and Other Structures*, ANSI A58.1-1982, American National Standards Institute, New York, 1982.

1.2 *Standard Specifications for Highway Bridges*, 13th ed., American Association of State Highway and Transportation Officials (AASHTO), Washington, D.C., 1983.

1.3 *Manual of Railway Engineering*, American Railway Engineering Association (AREA), Washington, D.C., 1973.

1.4 *Recommended Lateral Force Requirements and Commentary*, Report by Seismology Committee, Structural Engineers Association of California, 1980.

1.5 *Building Code Requirements for Reinforced Concrete*, ACI 318-83, American Concrete Institute, Detroit, 1983.

1.6 *Commentary on Building Code Requirements for Reinforced Concrete*, ACI 318R-83, American Concrete Institute, Detroit, 1983.

1.7 MacGregor, J. G., Mirza, S. A., and Ellingwood B., "Statistical Analysis of Resistance of Reinforced and Prestressed Concrete Members," *J. ACI*, Vol. 80, No. 3, May–June 1983, pp. 167–176.

1.8 MacGregor, J. G., "Load and Resistance Factors for Concrete Design," *J. ACI*, Vol. 80, No. 4, July–August 1983, pp. 279–287.

1.9 MacGregor, J. G., "Safety and Limit States Design for Reinforced Concrete," *Can. J. Civ. Eng.*, Vol. 3, No. 4, 1976, pp. 484–513.

1.10 Winter, G., Safety and Serviceability Provisions in the ACI Building Code, ACI-CEB-FIP-PCI Symp., ACI Spec. Publ. SP-59, 1979.

PROBLEMS

1.1 For cases (*a*) through (*e*) of Fig. P1.1, indicate the equivalent loads and moment diagram resulting from application of a prestress force P with tendon eccentricity as shown. Plot the moment diagram on the compression side of the beam in each case. Disregard member self-weight and disregard the effect of losses of prestress force.

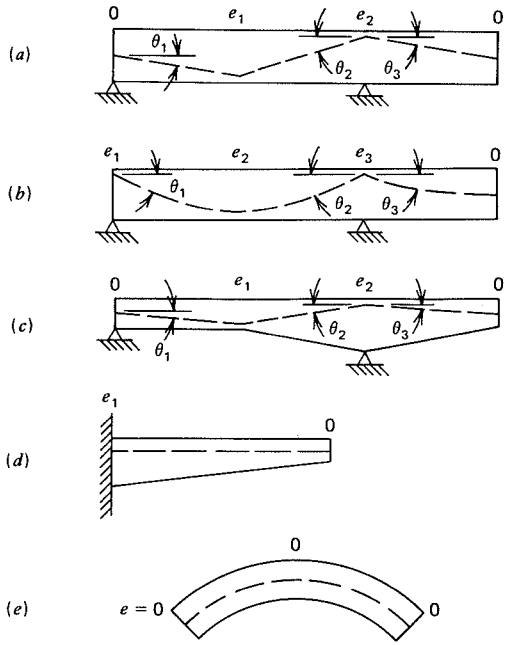

FIGURE P1.1

1.2 For cases (*a*) through (*e*) of Fig. P1.2, sketch the tendon profile that is "best" in the sense of balancing the indicated loads. Disregard member self-weight and disregard the effect of prestress losses.

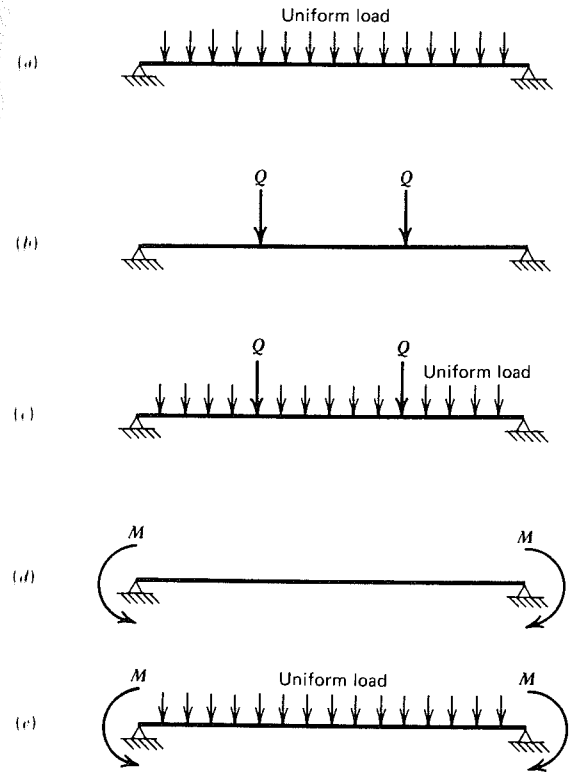

FIGURE P1.2

1.3 The simple span beam shown in Fig. P1.3 is prestressed with a force of 150 kips and tendon eccentricities as shown. (Eccentricity is considered to be positive if measured

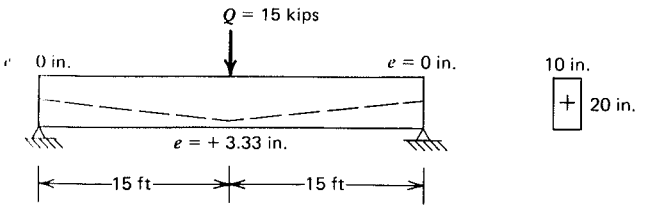

FIGURE P1.3

downward from the concrete centroid.) (a) What are the concrete stresses at midspan and supports, at the top and bottom of the beam, resulting from prestress force if acting alone? Find these stresses based first on prestress force and eccentricity, and second using the equivalent load approach. (b) What stresses result from the superposition of prestress and self-weight of 208 plf? (c) What concrete stresses are obtained when the live load $Q = 15$ kips is introduced? (d) Could a level (zero deflection everywhere) member be attained for some value of Q for the loading and tendon profile shown?

TWO

MATERIALS

2.1 INTRODUCTION

The structures and component members to be considered are composed of concrete, prestressed with steel tendons. Supplemental non-prestressed reinforcement is also used for various purposes. Although the general characteristics of the materials are well known to students of structural engineering and practicing engineers, certain special properties are of profound significance in the design of prestressed concrete. Indeed, it was the failure to consider some of these special properties that accounted for lack of success of all early efforts to prestress concrete. For example, it was only after Freyssinet established the significance of time-dependent shrinkage and creep of concrete that prestressed structures could be built successfully.

The use of high strength steel for prestressing is necessary for basic physical reasons. The mechanical properties of this steel, as disclosed by stress–strain curves, are quite different from those of the steel used for ordinary reinforced concrete. In addition to the higher strength, the designer must account for differences in ductility, lack of a well-defined yield point, and other characteristics of great engineering significance.

Ordinary bar reinforcement, of the same type used for ordinary reinforced concrete structures, also plays an important role in prestressed construction. It is used for web reinforcement, supplementary longitudinal reinforcement, and other purposes.

The concrete used in prestressed members is characteristically of higher strength than that used for reinforced concrete. Differences in elastic modulus,

strain capacity, and strength must be accounted for in design, and time-dependent characteristics assume crucial importance.

The increasing use of lightweight concrete in recent years has permitted reduction of dead loads, a matter of special significance in concrete structures, and has facilitated handling of large precast structural components. Advances in concrete technology have resulted in the development of lightweight aggregate concrete of strength comparable to normal density material. Its deformational characteristics, including time-dependent effects, must be fully understood before it can be used with confidence.

2.2 IMPORTANCE OF HIGH STRENGTH STEEL

The reason for the lack of success of most early attempts to prestress concrete was the failure to employ steel at a sufficiently high stress and strain. The time-dependent length changes permitted by shrinkage and creep of the concrete completely relieved the steel of stress. The importance of high initial strain and the corresponding high initial stress in the steel can be shown by a simple example.

Shown in Fig. 2.1(a) is a short concrete member that is to be axially prestressed using a steel tendon. In the unstressed state, the concrete has length l_c and the unstressed steel has length l_s. After tensioning of the steel and transfer of force to the concrete through the end anchorages, the length of the concrete is shortened to l'_c and the length of the stretched steel is l'_s. These values must, of course, be identical, as indicated by the figure.

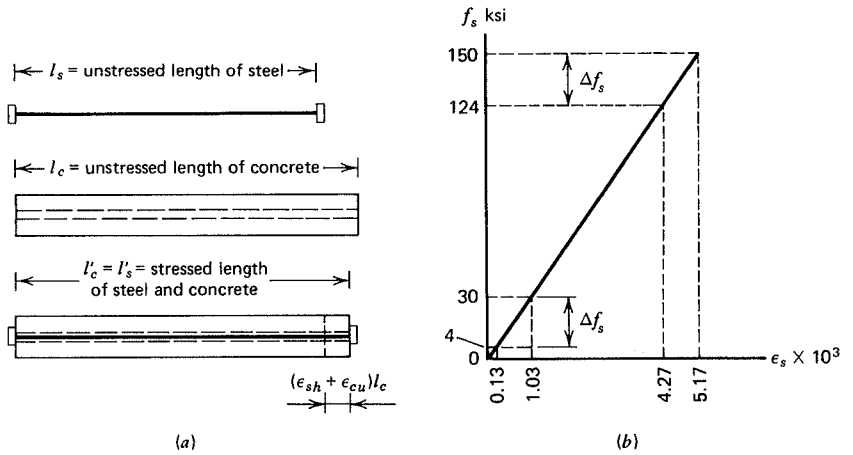

FIGURE 2.1 Effect of shrinkage and creep of concrete in reducing prestress force. (a) Axially prestressed concrete member. (b) Stress in steel.

But the concrete experiences a shrinkage strain ϵ_{sh} with the passage of time and, in addition, if held under compression will suffer a creep strain ϵ_{cu}. The total length change in the member

$$\Delta l_c = (\epsilon_{sh} + \epsilon_{cu})l_c \tag{a}$$

may be such that it exceeds the stretch in the steel that produced the initial stress, and complete loss of prestress force will result.

The importance of shrinkage and creep strain can be minimized by using a very high initial strain and a high initial stress in the steel. The reduction in steel stress from these causes depends only on the unit strains in the concrete associated with shrinkage and creep, and the elastic modulus E_s of the steel:

$$\Delta f_s = (\epsilon_{sh} + \epsilon_{cu})E_s \tag{b}$$

It is independent of the initial steel stress.

It is informative to study the results of calculations for representative values of the various parameters. Suppose first that the member is prestressed using ordinary reinforcing steel at an initial stress f_{si} of 30 ksi. The modulus of elasticity E_s for all steels is about the same and will be taken here as 29,000 ksi. The initial strain in the steel is

$$\epsilon_{si} = \frac{f_{si}}{E_s} = \frac{30}{29{,}000} = 1.03 \times 10^{-3}$$

and the total steel elongation is

$$\epsilon_s l_s = 1.03 \times 10^{-3} l_s \tag{c}$$

But a conservative estimate of the sum of shrinkage and creep strain in the concrete is about 0.90×10^{-3}, and the corresponding length change is

$$(\epsilon_{sh} + \epsilon_{cu})l_c = 0.90 \times 10^{-3} l_c \tag{d}$$

Since l_s and l_c are nearly the same, it is clear by comparing (c) and (d) that the combined effects of shrinkage and creep of the concrete is almost a complete loss of stress in the steel. The effective steel stress remaining after time-dependent effects would be

$$f_{se} = (1.03 - 0.90) \times 10^{-3} \times 29 \times 10^3 = 4 \text{ ksi}$$

Alternatively, suppose that the prestress were applied using high strength steel at an initial stress of 150 ksi. In this case, the initial strain would be

$$\epsilon_{si} = \frac{150}{29{,}000} = 5.17 \times 10^{-3} \tag{e}$$

and the total elongation

$$\varepsilon_s l_s = 5.17 \times 10^{-3} l_s \tag{f}$$

The length change resulting from the shrinkage and creep effects would be the same as before

$$(\varepsilon_{sh} + \varepsilon_{cu}) l_c = 0.90 \times 10^{-3} l_c$$

and the effective steel stress f_{se} after losses due to shrinkage and creep would be

$$f_{se} = (5.17 - 0.90)10^{-3} \times 29 \times 10^3 = 124 \text{ ksi}$$

The loss is about 17 percent of the initial steel stress in this case compared with 87 percent loss when mild steel was used.

The results of these calculations are shown graphically by Fig. 2.1*b* and illustrate clearly the need in prestressing for using steel that is capable of a very high initial stress.

2.3 TYPES OF PRESTRESSING STEEL

There are three common forms in which steel is used for prestressed concrete tendons: cold-drawn round wires, stranded cable, and alloy steel bars. Grade designations for strand and bars, correspond to the minimum tensile strength in ksi units. For the widely used seven-wire strand, two grades are available: Grade 250 (f_{pu} = 250 ksi) and Grade 270. The higher strength Grade 270 strand is now more widely used than the lower strength strand. For alloy steel bars, two grades are used: the regular Grade 145 is most common, but special Grade 160 bars can be ordered. The minimum tensile strength for cold-drawn wires varies from 235 to 250 ksi, depending on diameter and type.

A. ROUND WIRES

The round wires used for post-tensioned prestressed concrete construction and occasionally for pretensioned work are manufactured to meet the requirements of ASTM Specification A 421, "Uncoated Stress-Relieved Wire for Prestressed Concrete." The individual wires are manufactured by hot-rolling steel billets into round rods. After cooling, the rods are passed through dies to reduce their diameter to the required size. In the process of this drawing operation, cold work is done on the steel, greatly modifying its mechanical properties and increasing its strength. The wires are stress-relieved after cold drawing by a continuous heat treatment to produce the prescribed mechanical properties.

Table 2.1 Properties of uncoated stress-relieved wire (ASTM A 421)

Nominal diameter in. (mm)	Minimum tensile strength psi (MPa)		Minimum stress at 1% extension psi (MPa)	
	Type BA	Type WA	Type BA	Type WA
0.192 (4.88)	[a]	250,000 (1725)	[a]	200,000 (1380)
0.196 (4.98)	240,000 (1655)	250,000 (1725)	192,000 (1325)	200,000 (1380)
0.250 (6.35)	240,000 (1655)	240,000 (1655)	192,000 (1325)	192,000 (1325)
0.276 (7.01)	[a]	235,000 (1622)	[a]	188,000 (1295)

[a] These sizes are not commonly furnished in Type BA wire.

Wires are available in four diameters as shown in Table 2.1 and in two types. Type BA wire is used for applications in which cold-end deformation is used for anchoring purposes (button anchorage). Type WA is used for applications in which the ends are anchored by wedges and no cold-end deformation of the wire is involved (wedge anchorage). Examples of tendons with button anchorages, more common in United States practice, are shown in Appendix B.

Low-relaxation wire, sometimes known as stabilized wire, is also available. It is used when it is desirable to reduce loss of prestress to the minimum (see Section 2.6).

Tendons are normally composed of groups of wires, the number of wires in each group depending on the particular system used and the magnitude of prestress force required. Typical prefabricated post-tensioning tendons may consist of 8 to 52 individual wires. Multiple tendons, each composed of groups of wires, may be used to meet requirements.

B. STRANDED CABLE

Stranded cable is almost always used for pretensioned members, and is often used for post-tensioned construction as well. Strand is manufactured to ASTM Specification A 416, "Uncoated Seven-Wire Stress-Relieved Strand for Prestressed Concrete." It is fabricated with six wires wound tightly around a seventh of slightly larger diameter. The pitch of the spiral winding is between 12 and 16 times the nominal diameter of the strand.

The same type of cold-drawn stress-relieved wire is used in making stranded cable as is used for individual prestressing wires. However, the apparent mechanical properties are slightly different because of the tendency for the stranded wires to straighten when subjected to tension because the axis of the wires does not coincide with the direction of tension. Cable is stress-relieved by heat treatment after stranding. Low-relaxation or stabilized strand is widely available (see Section 2.6).

Strands may be obtained in a range of sizes from 0.250 in. to 0.600 in. diameter, as shown in Table 2.2. Two grades are manufactured: Grade 250 and

Table 2.2 Properties of uncoated seven-wire stress-relieved strand (ASTM A 416)

Nominal diameter in. (mm)	Breaking strength lb (kN)	Nominal area of strand in.^{2} (mm^2)	Minimum load at 1% extension lb (kN)
		Grade 250	
0.250 (6.35)	9,000 (40.0)	0.036 (23.22)	7,650 (34.0)
0.313 (7.94)	14,500 (64.5)	0.058 (37.42)	12,300 (54.7)
0.375 (9.53)	20,000 (89.0)	0.080 (51.61)	17,000 (75.6)
0.438 (11.11)	27,000 (120.1)	0.108 (69.68)	23,000 (102.3)
0.500 (12.70)	36,000 (160.1)	0.144 (92.90)	30,600 (136.2)
0.600 (15.24)	54,000 (240.2)	0.216 (139.35)	45,900 (204.2)
		Grade 270	
0.375 (9.53)	23,000 (102.3)	0.085 (54.84)	19,550 (87.0)
0.438 (11.11)	31,000 (137.9)	0.115 (74.19)	26,350 (117.2)
0.500 (12.70)	41,300 (183.7)	0.153 (98.71)	35,100 (156.1)
0.600 (15.24)	58,600 (260.7)	0.217 (140.00)	49,800 (221.5)

Grade 270 have minimum ultimate strengths of 250,000 and 270,000 psi (1720 and 1860 MPa), respectively, based on the nominal area of the strand.

C. ALLOY STEEL BARS

In the case of alloy steel bars, the required high strength is obtained by introducing certain alloying elements, mainly manganese, silicon, and chromium, during the manufacture of the steel. In addition, cold work is done in making the bars, further increasing the strength. After cold-stretching, the bars are stress-relieved to obtain the required properties. Bars are manufactured to meet the requirements of ASTM Specification A 722, "Uncoated High-Strength Steel Bar for Prestressing Concrete."

Alloy steel bars are available in diameters ranging from $\frac{5}{8}$ in. to $1\frac{3}{8}$ in., as shown in Table 2.3, and in two grades, Grade 145 and Grade 160, corresponding to the minimum ultimate strengths of 145,000 and 160,000 psi (1000 and 1100 MPa), respectively.

2.4 NON-PRESTRESSED REINFORCEMENT

Non-prestressed steel has several important applications in prestressed concrete construction. Although web reinforcement for diagonal tensile stress (see Chapter 5) may be prestressed, ordinarily it is non-prestressed bar steel. Supplementary non-prestressed reinforcement is commonly used in the region of high local

Table 2.3 Properties of alloy steel bars

Nominal diameter in. (mm)	Nominal area of bar in.^{2} (mm^2)	Breaking strength lb (kN)	Minimum load at 0.7% extension lb (kN)
		Grade 145	
0.625 (15.88)	0.307 (198)	45,000 (200)	40,000 (178)
0.750 (19.05)	0.442 (285)	64,000 (285)	58,000 (258)
0.875 (22.23)	0.601 (388)	87,000 (387)	78,000 (347)
1.000 (25.40)	0.785 (507)	114,000 (507)	102,000 (454)
1.125 (28.58)	0.994 (642)	144,000 (641)	129,000 (574)
1.250 (31.75)	1.227 (792)	178,000 (792)	160,000 (712)
1.375 (34.93)	1.485 (958)	215,000 (957)	193,000 (859)
		Grade 160	
0.625 (15.88)	0.307 (198)	49,000 (218)	43,000 (191)
0.750 (19.05)	0.442 (285)	71,000 (316)	62,000 (276)
0.875 (22.23)	0.601 (388)	96,000 (427)	84,000 (374)
1.000 (25.40)	0.785 (507)	126,000 (561)	110,000 (490)
1.125 (28.58)	0.994 (642)	159,000 (708)	139,000 (619)
1.250 (31.75)	1.227 (792)	196,000 (872)	172,000 (765)
1.375 (34.93)	1.485 (958)	238,000 (1059)	208,000 (926)

compressive stress at the anchorages of post-tensioned beams. For both pretensioned and post-tensioned members, it is common to provide longitudinal bar steel to control shrinkage and temperature cracking. Overhanging flanges of T- and I-shaped cross sections are normally reinforced in both the transverse and longitudinal directions with nontensioned bars. Finally, it is often convenient to increase the flexural strength of prestressed beams using supplementary longitudinal bar reinforcement.

Such non-prestressed reinforcing bars, which are identical to those used for ordinary reinforced concrete construction, are manufactured to meet the requirements of ASTM Specification A 615, "Deformed and Plain Billet-Steel Bars for Concrete Reinforcement," A 616, "Rail Steel Deformed and Plain Bars for Concrete Reinforcement, or A 617, "Axle Steel Deformed and Plain Bars for Concrete Reinforcement." For applications where bending or welding are important, the provisions of Specification A 706, "Low-Alloy Steel Deformed Bars for Concrete Reinforcement," must be met. Bars are available in nominal diameters from $\frac{3}{8}$ to $1\frac{3}{8}$ in., in $\frac{1}{8}$ in. increments, and in two larger sizes of about $1\frac{3}{4}$ and $2\frac{1}{4}$ in. diameter. They are generally referred to by number, the number corresponding to the number of eighth inches in the nominal bar diameter; for example, a No. 7 bar has nominal diameter of $\frac{7}{8}$ in.

To identify bars that meet the requirements of the ASTM Specifications, distinguishing marks are rolled into the surface of one side of the bar to denote:

(a) the point of origin (the producer's mill designation), (b) the size designation by number, (c) the type of steel (N for billet steel, a rail symbol for rail steel, or A for axle steel), and (d) in the case of Grade 60 bars either the number 60 or a single continuous longitudinal line through at least five spaces offset from the center of the bar side.

In the case of bar reinforcement, it is important that steel and concrete deform together, that is, that there be a sufficiently strong bond between the two materials so that little or no relative movement can occur. This bond is provided by the relatively large chemical adhesion that develops at the steel–concrete interface, by the natural roughness of the mill scale on hot-rolled reinforcement, and by closely spaced rib-shaped surface deformations with which bars are furnished to provide a high degree of interlocking of the two materials. Minimum requirements for these deformations have been developed in experimental research and are described in the ASTM specifications. Different bar producers use different patterns to satisfy these requirements.

Bars are produced in different strengths. Grades 40, 50, and 60 have specified minimum yields strengths of 40,000, 50,000, and 60,000 psi, respectively (276, 345, and 414 MPa). The present trend is toward the use of Grade 60 bars; the bars of lower yield strength may not be commonly available. Large-diameter bars with 75,000 and 90,000 psi (517 and 621 MPa) yield are available on special order, although they find little application in prestressed concrete members.

Apart from single reinforcing bars, welded wire mesh is often used for reinforcing slabs, beam flanges, and other surfaces such as shells. The mesh consists of longitudinal and transverse cold-drawn steel wires, at right angles, welded at all points of intersection. Mesh is available with wire spacings from 2 in. to 12 in. and wire diameters from 0.080 in. to 0.628 in., although all

Table 2.4 Non-prestressed reinforcement

Type	Grade or size	Specified minimum yield strength psi (MPa)	Tensile strength psi (MPa)
Billet steel and axle steel bars	40	40,000 (276)	70,000 (483)
	60	60,000 (414)	90,000 (621)
Rail steel bars	50	50,000 (345)	80,000 (552)
	60	60,000 (414)	90,000 (621)
Cold-drawn wire		70,000 (483)	80,000 (552)
Welded wire mesh	W1.2 and larger	65,000 (448)	75,000 (517)
	Smaller than W1.2	56,000 (386)	70,000 (483)

combinations are not readily available. The size and spacing of the wires may be the same in both directions or different as needed. The steel wire and the wire mesh must meet the requirements of ASTM Specifications A 82, "Cold-Drawn Steel Wire for Concrete Reinforcement," and A 185, "Welded Steel Wire Fabric for Concrete Reinforcement."

Table 2.4 lists all commonly available reinforcing steels, including wire mesh, with information on yield stress and tensile strength. Further information pertaining to bar steel and mesh will be found in Appendix A.

2.5 STRESS–STRAIN PROPERTIES OF STEEL

Most of the mechanical properties for steels of interest to the design engineer can be read directly from their stress–strain curves. Such important characteristics as proportional elastic limit, yield point, strength, ductility, and strain hardening properties are immediately evident.

It is instructive to compare, in general terms, the tensile stress–strain curves for ordinary bar reinforcement and typical prestressing steels, as in Fig. 2.2. The

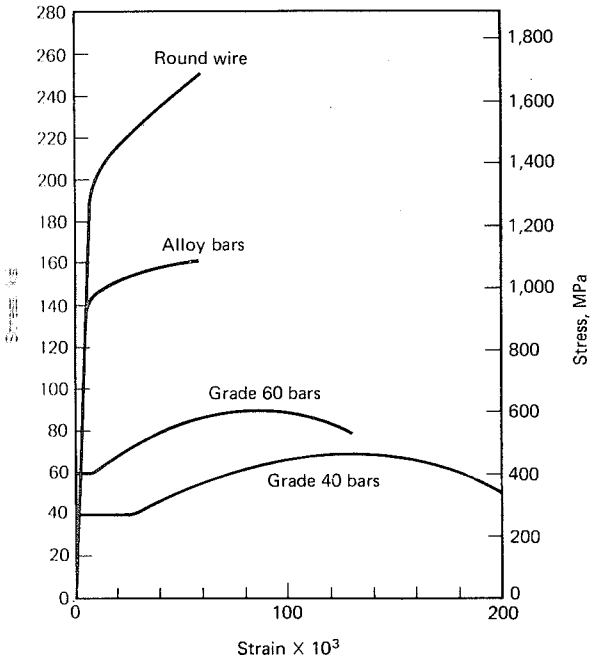

FIGURE 2.2 Comparative stress–strain curves for reinforcing steel and prestressing steel.

most striking differences are the much higher proportional elastic limit and strength available in the round wires and alloy bars used for prestressing, and the substantially lower ductility.

For ordinary reinforcing steel, typified here by Grades 40 and 60, there is an initial elastic response up to a sharply defined yield point, beyond which there is a substantial increase in strain without an accompanying increase in stress. If the load is increased, this yield plateau is followed by a region of strain hardening, during which a very nonlinear relation between stress and strain is obtained. Eventually, rupture of the material will occur at a rather large tensile strain of about 13 percent for Grade 60 bars and 20 percent for Grade 40 bars.

The contrast provided by prestressing steels is striking. They show no well-defined yield stress. The proportional limit for round wires (and for strand made up of such wires) is about 200 ksi, five times the yield point for Grade 40 bars. With further loading, the wires show gradual yielding, but the curve continues to rise monotonically until the steel fractures. The failure stress for the wire shown is 250 ksi (1720 MPa), almost four times that for Grade 40 bars, but the strain at failure is only one-third as great. Alloy bars have characteristics similar to those of round wire or strand, but the proportional limit and strength are 30 to 40 percent less.

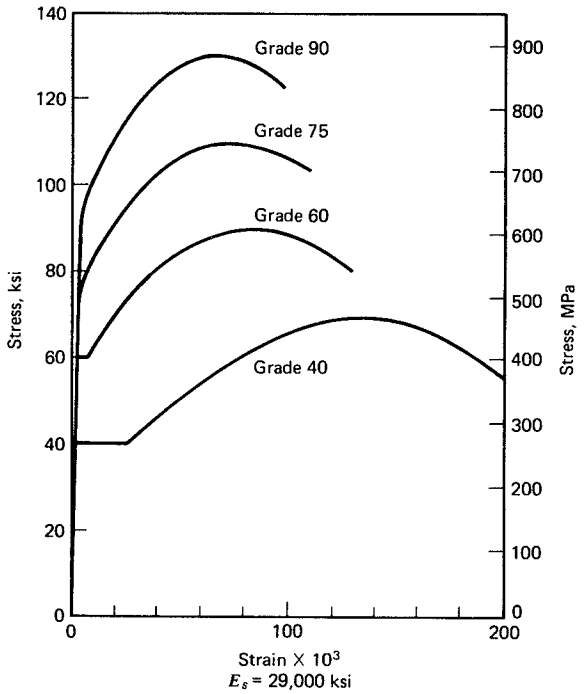

FIGURE 2.3 Typical stress–strain curves for nontensioned reinforcing bars.

More detailed stress–strain curves for reinforcing bar steel are shown in Fig. 2.3. The elastic modulus for all such steels is about the same: 29,000 ksi (200,000 MPa). Although Grades 40 and 60 steels usually show a well-defined yield point, this is not so for the higher strength steels. For such cases, an equivalent yield point is defined as that stress at which the total strain is 0.35 percent, according to ACI Code. All grades show extensive strain hardening after the yield stress is reached. Ductility, as measured by the total strain at failure, is significantly less for the higher grades.

Detailed stress–strain curves for typical prestressing wires, strand, and alloy bars are given in Fig. 2.4. For smooth, round wires, the elastic modulus is about the same as for ordinary reinforcement, that is, about 29,000 ksi (200,000 MPa). For stranded cable, the apparent modulus is somewhat less, about 27,000 ksi (186,000 MPa), although the strand is manufactured from the same wire. This happens because the spiral-wound strand tends to straighten slightly as the cable is loaded in tension. The modulus for cables embedded in concrete may be closer to that for round wires. The elastic modulus for alloy bars is also about 27,000 ksi

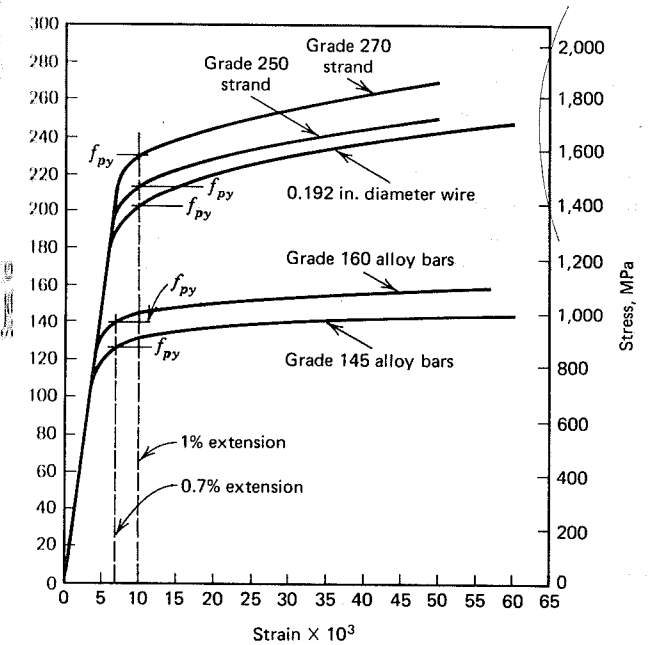

$E_p \approx 29{,}000$ ksi = 200 kN/mm² for wires
$E_p \approx 27{,}000$ ksi = 186 kN/mm² for strand
$E_p \approx 27{,}000$ ksi = 186 kN/mm² for bars

FIGURE 2.4 Typical stress–strain curves for prestressing steels.

(186,000 MPa), the reduction in this case occurring because of the presence of alloying elements.

In the absence of a well-defined yield stress for prestressing steels of all types, it is necessary to adopt arbitrary definitions of yielding. For wire and strand, the yield stress is defined as the stress at which a total extension of 1 percent is attained. For alloy bars, the yield stress is taken as equal to the stress producing an extension of 0.7 percent. These values are shown in Fig. 2.4.

2.6 STEEL RELAXATION

When prestressing steel is stressed to the levels that are customary during initial tensioning and at service loads, it exhibits a property known as *relaxation*. Relaxation is defined as the loss of stress in a stressed material held at constant length. (The same basic phenomenon is known as *creep* when defined in terms of change in length of a material under constant stress.) In prestressed concrete members, creep and shrinkage of the concrete as well as fluctuations in superimposed load cause changes in tendon length. However, in evaluating loss of steel stress as a result of relaxation, the length may be considered constant.

Relaxation is not a short-lived phenomenon. From available evidence it appears to continue almost indefinitely, although at a diminishing rate. It must be accounted for in design because it produces significant loss of prestress force.

The amount of relaxation varies depending on the type and grade of steel, but the most significant parameters are time and intensity of the initial stress. Analysis of the results of many experimental investigations, some exceeding nine years duration, has produced the information presented graphically in Fig. 2.5, in which f_p is the final stress after t hours, f_{pi} is the initial stress, and f_{py} is the yield stress. The yield stress may be taken equal to the effective yield stress as defined in Section 2.5.

The information shown in Fig. 2.5 may be approximated with satisfactory accuracy by the following expression.

$$\frac{f_p}{f_{pi}} = 1 - \frac{\log t}{10}\left(\frac{f_{pi}}{f_{py}} - 0.55\right) \tag{2.1}$$

where $\log t$ is to the base 10, and f_{pi}/f_{py} is not less than 0.55 (Ref. 2.1).

The tests on which Fig. 2.5 and Eq. (2.1) are based were all carried out on round stress-relieved wires. The results are equally applicable to stress-relieved strand, and in the absence of other information, may also be applied to alloy steel bars.

In the case of pretensioned members, the relaxation loss occurring before release (transfer of force to the concrete) should be subtracted from the total relaxation loss predicted for the effective stress at release. For example, if the stress is to be estimated at time t_n, the wire tensioned at time zero, and released

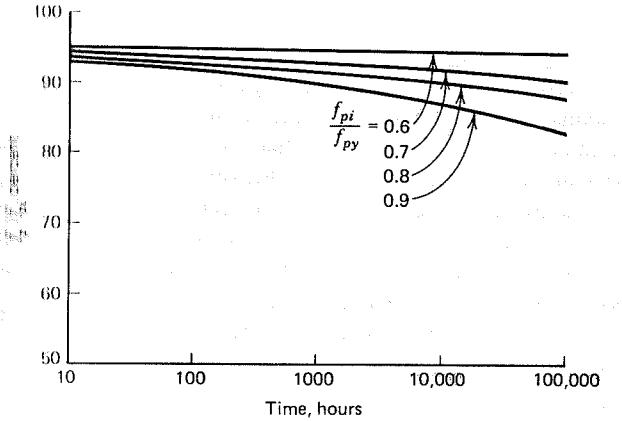

FIGURE 2.5 Steel relaxation curves for ordinary stress-relieved wire and strand. After Ref. 2.1.

at time t_r, then Eq. (2.1) may be modified as follows:

$$\frac{f_p}{f_{pi}} = 1 - \left(\frac{\log t_n - \log t_r}{10}\right)\left(\frac{f_{pi}}{f_{py}} - 0.55\right) \tag{2.2}$$

The term f_{pi} may be taken as the steel stress at release.

In some cases, relaxation losses have been reduced by prestretching, a technique by which the stress in the steel is increased to a level higher than the intended initial stress, held at that level for a short period of time, and then reduced to the intended initial stress. Since the practical level of initial stress is about 70 percent of the strength of the steel, it is not feasible to overstress by more than about 15 percent. On the basis of available evidence (Ref. 2.1) it appears that prestretching is of little consequence if the prestretching period is limited to only a few minutes.

Special low-relaxation wire and strand are available, and their use is becoming common. According to ASTM Specifications A 416 and A 421, such steel will exhibit relaxation after 1,000 hours not more than 2.5 percent when initially loaded to 70 percent of the specified tensile strength, and not more than 3.5 percent when loaded to 80 percent of the specified tensile strength. Relaxation loss for low-relaxation wire and strand can be taken to be about 25 percent of the loss for normal wire and strand.

2.7 TYPES OF CONCRETE

For several reasons the concrete used for prestressed construction is characterized by a higher strength than that used for ordinary reinforced concrete. It is usually

subjected to higher forces, and an increase in quality generally leads to more economical results. Use of high strength concrete permits the dimensions of member cross sections to be reduced to the minimum. Significant saving in dead load results and longer spans become technically and economically possible. Objectionable deflection and cracking, which would otherwise be associated with the use of slender members at high stress, are easily controlled by prestressing.

There are other advantages. High strength concrete has a higher elastic modulus than low strength concrete, so that loss of prestress force resulting from elastic shortening of the concrete is reduced. Creep losses, which are roughly proportional to elastic losses, are lower also. High bearing stresses in the vicinity of tendon anchorages for post-tensioned members are more easily accommodated, and the size of expensive anchorage hardware can be reduced. In the case of pretensioned elements, higher bond strength results in a reduction in the development length required to transfer prestress force from the cables to the concrete. Finally, concrete of higher compressive strength also has a higher tensile strength, so that the formation of flexural and diagonal tension cracks is delayed.

The greater part of prestressed concrete construction in the United States is precast under carefully controlled plant conditions. With external form vibration as well as internal vibration of the fresh concrete, very stiff high strength mixes, with low water–cement ratios, can be placed without danger of voids. Careful control of mix proportions is more easily achieved. Steam curing is often used, which provides a more complete hydration of the cement. Also, for prestressed concrete members cast on the job site, higher strength concrete is generally specified and more easily obtained, because of the more precisely engineered natured of the construction. Workability of the mix can be maintained, even with the very low water–cement ratios needed for high strength, through the use of superplasticizers.

In present practice, compressive strength between 4,000 and 8,000 psi (28 and 55 MPa) is commonly specified for prestressed concrete members, although strengths as high as 12,000 psi (83 MPa) have been used. It should be emphasized, however, that the concrete strength assumed in the design calculations and specified must be attained with certainty, because the calculated high stresses resulting from prestress force really do occur.

Special mention should be made of lightweight concrete, attained through use of lightweight aggregate in the mix. The aggregates used may be shale, clay, slate, slag, or pelletized fly ash. They are light in weight because of the porous, cellular structure of the individual aggregate particles, achieved in most cases by gas or steam formation in processing the aggregates in rotary kilns at high temperatures. Concrete can be produced, using these aggregates, with careful mix design, having unit weight between 90 and 120 pcf (14 and 19 kN/m^3) compared with about 145 pcf (23 kN/m^3) for normal density concrete. The strength of lightweight concrete can be made comparable to that of stone aggregate concrete through proper selection and proportioning of components and control of the water–cement ratio.

The design and control of concrete mixes and the development of proper procedures for placing and curing are a highly specialized field of study and not within the scope of this book. Attention here will be focused on the engineering properties of the resulting material. For information on what is generally known as *concrete material technology*, the reader is referred to the comprehensive treatments contained in Refs. 2.2 and 2.3. Practical information of great value is contained in publications by the Portland Cement Association (Ref. 2.4) and the American Concrete Institute (Refs. 2.5 to 2.8).

2.8 CONCRETE IN UNIAXIAL COMPRESSION

Concrete is useful mainly in compression and, at controlling sections of members, is often subject to a state of stress that is approximately uniaxial. Accordingly, the uniaxial compressive stress–strain curve is of primary interest. Such a curve is obtained by loading standard cylinders parallel to their axis at prescribed rates of loading.[1] Figure 2.6 shows a typical set of such curves for normal weight concrete with w_c of about 145 pcf obtained from uniaxial compressive tests performed at normal, moderate testing speeds on concrete 28 days old. Figure 2.7 shows corresponding curves for lightweight concretes with a density of 100 pcf.

All the curves have a similar character. They consist of an initial relatively straight elastic portion in which stress and strain are closely proportional, then begin to curve to the horizontal, reaching the maximum stress, that is, the compressive strength, at a strain that ranges from about 0.002 to 0.003 for normal weight concretes and 0.003 to 0.0035 for lightweight concretes (Ref. 2.9 and 2.10), the larger values in each case corresponding to the higher strengths. All curves show a descending branch after the peak stress is reached; however, the characteristics of the curves after peak stress are highly dependent on the method of testing. If special procedures are followed in testing to insure constant strain rate while cylinder strength is decreasing, long stable descending branches can be obtained (Ref. 2.11). In the absence of special devices, unloading past the point of peak stress may be rapid, particularly for the higher strength concretes, which are generally more brittle than low strength concrete. According to present design practice, the limiting strain in uniaxial compression is taken as 0.003.

It should be emphasized that the exact shape of the stress–strain curve for any concrete is highly dependent on such variables as rate of loading, the particular testing equipment, the method of testing, and the size and shape of the specimen. The relations shown in Figs. 2.6 and 2.7 are typical only of test results obtained by present standard procedures. In the actual structure, quite different conditions may be obtained. Fortunately, design procedures have evolved that are not particularly sensitive to the shape of the stress–strain curve.

[1] See ASTM Specification C 192, "Standard Method of Making and Curing Concrete Test Specimens in the Laboratory," and C 39, "Standard Test Method for Compressive Strength of Cylindrical Concrete Specimens."

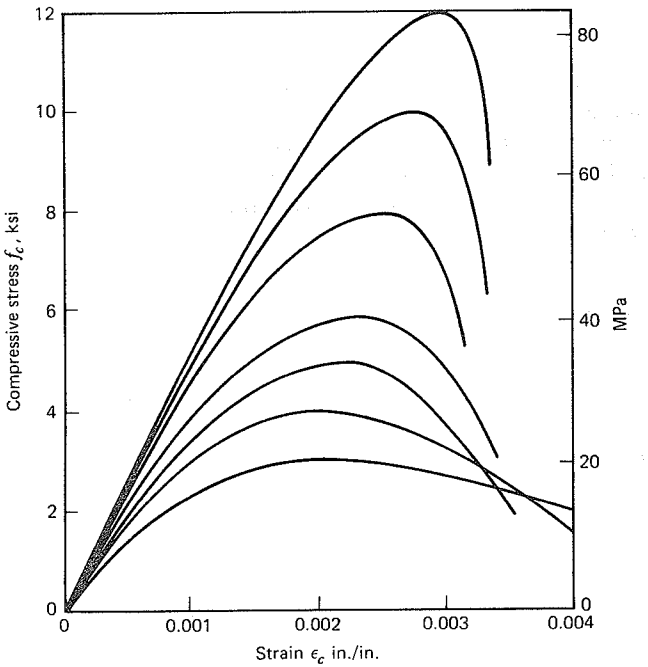

FIGURE 2.6 Typical compressive stress–strain curves for normal density concrete with w_c = 145 pcf. Adapted from Ref. 2.9.

The *modulus of elasticity* E_c (in psi units), that is, the slope of the initial straight part of the stress–strain curve, is larger the higher the strength of the concrete. For concretes in the strength range to about 6,000 psi, E_c can be computed with reasonable accuracy from the empirical equation found in the ACI Code:

$$E_c = 33w_c^{1.5}\sqrt{f'_c} \tag{2.3}$$

where w_c is the unit weight of the hardened concrete in pcf and f'_c its strength in psi.[2] Equation (2.3) was obtained by testing structural concretes with values of w_c from 90 to 155 pcf. For normal sand-and-stone concretes with w_c = 145 pcf, E_c may be taken as

$$E_c = 57{,}000\sqrt{f'_c} \tag{2.4}$$

For compressive strengths in the range from 6,000 to 12,000 psi, the ACI Code

[2]See Appendix C for the SI equivalent of this and other dimensionally inconsistent equations.

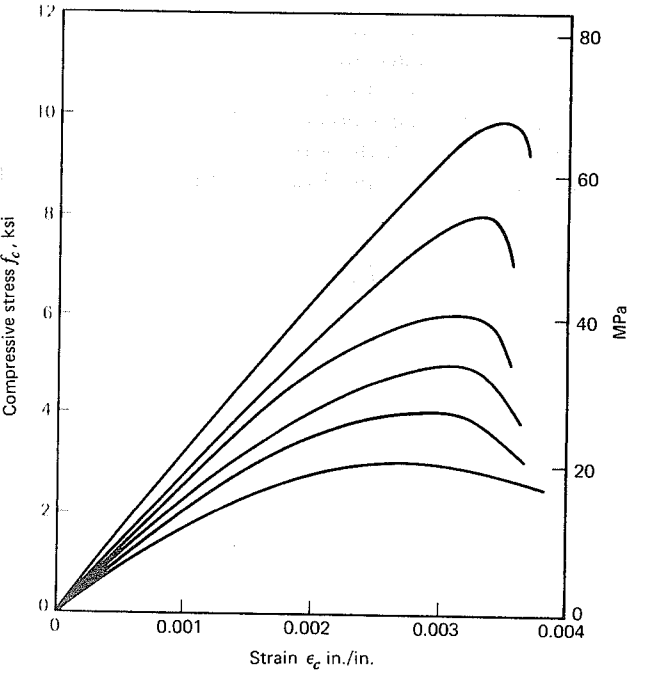

FIGURE 2.7 Typical compressive stress–strain curves for lightweight concrete with w_c = 100 pcf. Adapted from Ref. 2.10.

equation overestimates E_c for both normal weight and lightweight material by as much as 20 percent. Based on recent research at Cornell University (Refs. 2.9 and 2.10), the following equation is recommended for normal weight concretes with f'_c in the range from 3,000 to 12,000 psi, and for lightweight concretes from 3,000 to 9,000 psi.

$$E_c = \left(40{,}000\sqrt{f'_c} + 1{,}000{,}000\right)\left(\frac{w_c}{145}\right)^{1.5} \tag{2.5}$$

where terms and units are as defined previously for the ACI Code equations.

When compressed in one direction, concrete, like all other materials, expands in the direction transverse to the direction of the applied stress. The ratio of the transverse strain to the longitudinal strain is known as *Poisson's ratio*. It is meaningful only in the elastic range, at stresses less than about half the concrete strength. In this range, Poisson's ratio for concrete varies between about 0.15 and 0.20.

The strength of concrete varies with age, the gain in strength being rapid at first, then much slower. This variation of strength is specially important in the

design and fabrication of prestressed concrete members, because heavy loads may be caused at quite an early age by the tensioned steel. In prestressed construction of all types, but particularly for pretensioned plant-produced members, special methods are often followed to insure rapid development of compressive strength. These include the use in the concrete mix of high-early-strength Portland cement (Type III) rather than ordinary Portland Cement (Type I), and the use of steam curing.

A study of extensive experimental data indicates that the following expressions are suitable for predicting the strength of concrete at any time (Refs. 2.12 and 2.15).

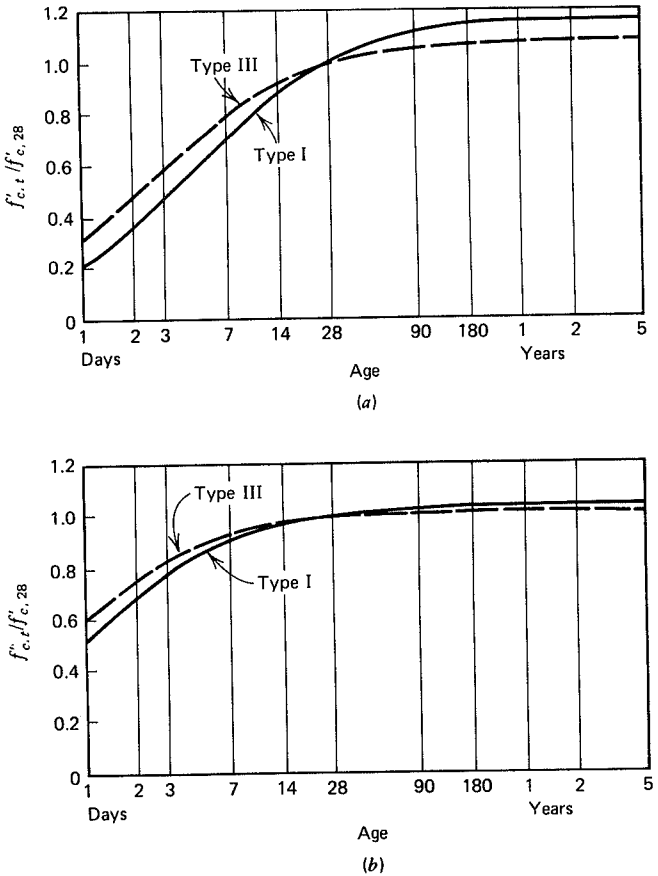

FIGURE 2.8 Effect of age on uniaxial compressive strength of concrete. (*a*) Moist cured. (*b*) Steam cured. Adapted from Ref. 2.15.

For moist-cured concrete using Type I cement:

$$f'_{c,t} = \frac{t}{4.00 + 0.85t} f'_{c,28} \tag{2.6a}$$

For moist-cured concrete using Type III cement:

$$f'_{c,t} = \frac{t}{2.30 + 0.92t} f'_{c,28} \tag{2.6b}$$

For steam-cured concrete using Type I cement:

$$f'_{c,t} = \frac{t}{1.00 + 0.95t} f'_{c,28} \tag{2.6c}$$

For steam-cured concrete using Type III cement:

$$f'_{c,t} = \frac{t}{0.70 + 0.98t} f'_{c,28} \tag{2.6d}$$

In these equations, $f'_{c,t}$ is the compressive strength at time t, $f'_{c,28}$ is the compressive strength at 28 days, and t is the age of the concrete in days. Figure 2.8 presents these strength-time functions graphically, with time plotted to a logarithmic scale. Test evidence indicates that Eqs. (2.6*a*) through (2.6*d*) are equally applicable for normal weight, sand-lightweight, and all-lightweight aggregate concretes.

2.9 CONCRETE IN UNIAXIAL TENSION

Cracks in prestressed concrete members may be caused by direct tension, flexure, combined shear and flexure in beams webs, torsion, and other actions. The behavior of members often changes abruptly when tensile cracks form. Accordingly, it is important to know the tensile strength of the material.

There are several ways to measure the tensile strength of concrete, none of them entirely satisfactory. *Direct tensile tests* have been made using dumbbell-shaped specimens held in special grips. Results show great scatter because of the effects of minor misalignments, stress concentrations in the grips, and random effects associated with the location of aggregate, and for this reason, direct tension tests are seldom used. For many years, tensile strength has been measured using either the *modulus of rupture test* or the *split cylinder test.*

The modulus of rupture is the computed flexural tensile stress at which a test beam of plain concrete fractures. The test arrangement, shown in Figure 2.9, is

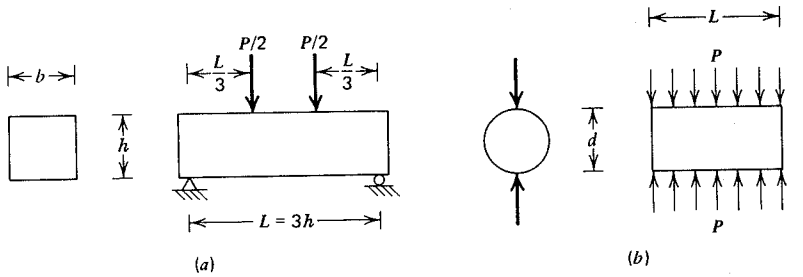

FIGURE 2.9 Tests to determine the tensile strength of concrete. (*a*) Modulus of rupture test. (*b*) Split cylinder test.

standardized by ASTM specifications. It employs a small block of unreinforced concrete, supported at its ends and loaded at the third points. Usually a 6 × 6 in. beam is used, with 18 inches between supports. The modulus of rupture is

$$f_r = \frac{PL}{bh^2} \tag{2.7}$$

where P is the total load at fracture, L is the span, and b and h, respectively, the width and depth of the cross section. For normal density concrete the modulus of rupture is usually between $8\sqrt{f_c'}$ and $12\sqrt{f_c'}$, whereas for lightweight aggregate concrete it may range from $6\sqrt{f_c'}$ to $8\sqrt{f_c'}$. In each case, the smaller values apply to higher strength concretes. Because the modulus of rupture is computed on the assumption that concrete is an elastic material, and because the critical stress occurs only at the outer surface, it is apt to be larger than the strength of concrete in uniform axial tension, which is often taken between $3\sqrt{f_c'}$ and $5\sqrt{f_c'}$ for normal density concrete and $2\sqrt{f_c'}$ and $3\sqrt{f_c'}$ for lightweight material.

In recent years, the split cylinder test has come into favor because of good reproducibility of results. The standard arrangement is shown in Figure 2.9*b*. A 6 × 12 in. concrete cylinder (the same as used for the standard uniaxial compressive test) is inserted in a compression testing machine in the horizontal position, so that compression is applied along two diametrically opposite generators. It can be shown that, in an elastic cylinder loaded this way, a nearly uniform tensile stress exists at right angles to the plane of the load. The cylinder splits at a stress that is computed from the equation:

$$f_{ct} = \frac{2P}{\pi Ld} \tag{2.8}$$

where P is the rupture load, d is the diameter of the cylinder, and L is its length. For normal aggregate concrete, the split cylinder strength is usually between $6\sqrt{f_c'}$ and $8\sqrt{f_c'}$, whereas for lightweight concrete it is generally between $4\sqrt{f_c'}$ and $6\sqrt{f_c'}$. As before, the lower values correspond to higher strength concretes.

Concrete subject to uniaxial tension responds nearly elastically up to the fracture load. The modulus of elasticity and Poisson's ratio in tension can be taken equal to the corresponding values in uniaxial compression for design purposes.

2.10 BIAXIALLY STRESSED CONCRETE

In many locations in structures, concrete is subjected to a complex state of stress. For example, beam webs carry shear, combined with flexural tension or compression. Torsional shearing stresses in members generally act concurrently with transverse shears and longitudinal normal stresses. Other examples are easily found. It is clearly of some importance to be able to predict the strength as well as the behavior before failure of concrete subject to various states of combined stress.

Such complex stress states can always be reduced to three equivalent principal stresses, acting at right angles to each other, by appropriate coordinate transformation. Any of the principal stresses can be tension or compression. If one of them is zero, a state of *biaxial stress* is said to exist. If two of them are zero, the state of stress is *uniaxial*.

In spite of extensive research in recent years, no general theory of the strength of concrete under combined stress has yet emerged. Progress has been made toward establishing experimentally the effect of multi-axial stresses, notably for cases of biaxial stress (Refs. 2.13 and 2.14). Figure 2.10 shows the influence of the lateral principal stress f_y on the failure stress f_x in the perpendicular direction. All stresses are expressed nondimensionally in terms of the uniaxial compressive strength f_c'. It is seen that, in the biaxial compression quadrant, lateral compression in the amount of 20 percent or more of the compression in the longitudinal direction is sufficient to increase the strength in the longitudinal direction by about 20 percent. In the biaxial tension quadrant the strength is almost independent of lateral stress. In the tension-compression stress state, an approximately linear interaction is obtained. A relatively small value of lateral tension results in significant loss of longitudinal compressive strength.

It has also been found that lateral compression or tension modifies the apparent stress–strain curve obtained for a uniaxial state of stress (Ref. 2.14). This is due partially to the Poisson effect, but also results from the increased confinement of internal microcracks in the case of lateral compression. Such information has been useful in the refined analysis, using finite element methods, of concrete members such as deep beams and shear walls where the stress state can be considered biaxial.

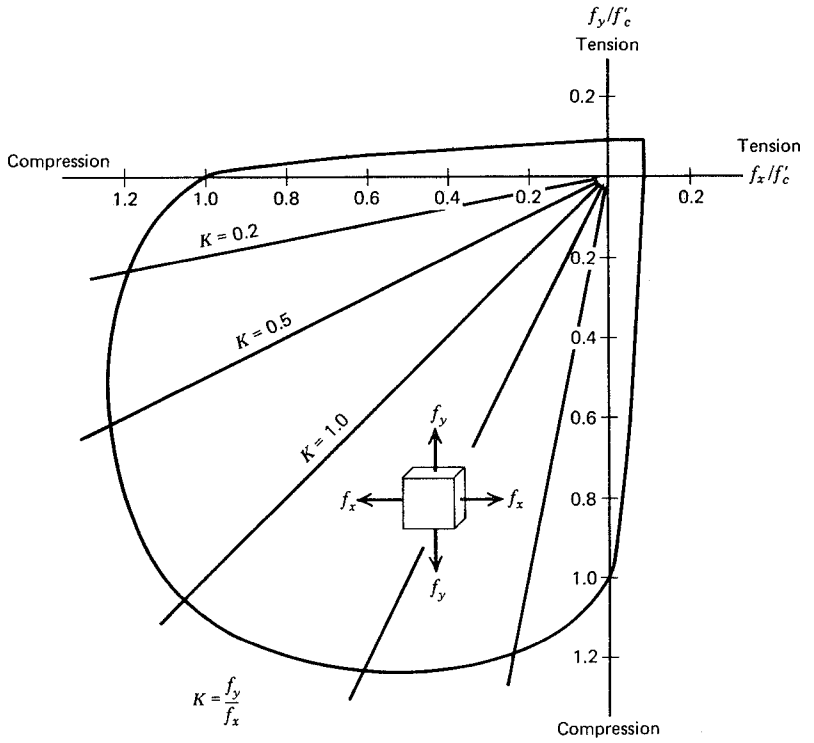

FIGURE 2.10 Strength envelope for concrete subject to biaxial stress. Adapted from Ref. 2.14.

Although some progress has been made in studying the behavior and strength of concrete in triaxial stress, information has not yet been developed that would be useful in design. Fortunately, in most practical cases, the stress state can be idealized as uniaxial or biaxial; in other cases, empirical methods of design continue to serve.

2.11 TIME-DEPENDENT DEFORMATION OF CONCRETE

Time-dependent deformation of concrete resulting from creep and shrinkage is of crucial importance in the design of prestressed concrete structures, because these volumetric changes result in a partial loss of prestress force, and they produce significant changes in deflection. A careful estimate of the effects of creep and shrinkage requires quantitative engineering information relating such volume changes to time, stress intensity, humidity, and other factors. Because of their importance, both creep and shrinkage have been the subject of intensive research over a long period of time. The most productive studies have been experimental,

and from such investigations the necessary functional relationships have been derived.

A. CREEP

Creep is the property of many materials by which they continue deforming over considerable lengths of time at constant stress or load. The rate of strain increase is rapid at first, but decreases with time until, after many months, a constant value is approached asymptotically.

Creep strain for concrete has been found experimentally to depend not only on time, but on the mix proportions, humidity, curing conditions, and the age of the concrete when it is first loaded. Creep strain is nearly linearly related to stress intensity, to a stress of at least $\frac{1}{2}f'_c$. It is therefore possible to relate the creep strain to the inital elastic strain by a *creep coefficient* defined as

$$C_u = \frac{\varepsilon_{cu}}{\varepsilon_{ci}} \tag{2.9}$$

where ε_{ci} is the initial elastic strain and ε_{cu} is the *additional* strain in the concrete, after a long period of time, resulting from creep.

The same phenomenon is sometimes described in terms of unit creep strain, or creep per unit stress, such that

$$\varepsilon_{cu} = \delta_u f_{ci} \tag{2.10}$$

where δ_u is the unit creep coefficient, sometimes called the specific creep, and f_{ci} is the stress intensity. Since the additional strain ε_{cu} can be written either as $C_u\varepsilon_{ci}$ or $\delta_u f_{ci}$, it is easily seen that

$$C_u = \delta_u E_c \tag{2.11}$$

The values of Table 2.5, quoted from Ref. 2.2 and extended for high strength concrete based on recent research at Cornell University, are typical values for average humidity conditions for concretes loaded at the age of seven days.

Table 2.5 Typical creep parameters

Compressive strength		Specific creep δ_u		Creep coefficient
psi	MPa	10^{-6} per psi	10^{-6} per MPa	C_u
3,000	21	1.00	145	3.1
4,000	28	0.80	116	2.9
6,000	41	0.55	80	2.4
8,000	55	0.40	58	2.0
10,000	69	0.28	41	1.6

A comprehensive study was made by Branson and Kripanarayanan of existing and original data pertaining to both shrinkage and creep (Refs. 2.12, and 2.15). Basic equations describing the functional relationships between both creep and shrinkage strains and time were recommended, together with modification factors that permit accounting for the other variables of greatest significance. These recommendations were endorsed by ACI Committee 209, charged with the study of creep and shrinkage in concrete, and provide information in a useful form for design (Ref. 2.16).

The creep coefficient at any time C_t can be related to the ultimate creep coefficient C_u by the equation:

$$C_t = \frac{t^{0.60}}{10 + t^{0.60}} C_u \qquad (2.12a)$$

or alternatively

$$\delta_t = \frac{t^{0.60}}{10 + t^{0.60}} \delta_u \qquad (2.12b)$$

where t is time in days after loading. This relation is shown graphically in Fig. 2.11.

Equation (2.12) applies for "standard" conditions, defined by Branson and Kripanarayanan as concrete with 4 in. slump or less, 40 percent relative humidity, minimum thickness of member of 6 in. or less, and loading age of seven days for moist-cured concrete or loading age of one to three days for steam-cured concrete. For other than standard conditions, correction factors are recommended as follows, to be applied either to C_t or δ_t:

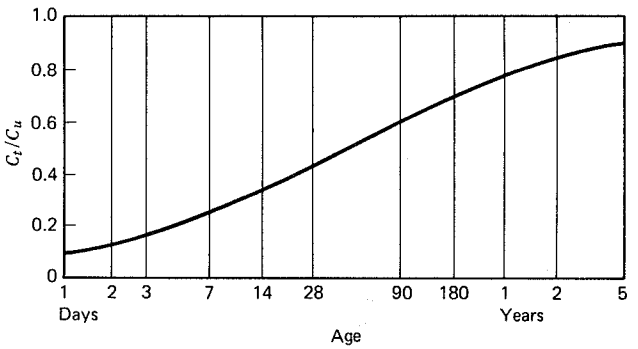

FIGURE 2.11 Variation of creep coefficient with time. Adapted from Ref. 2.15.

Table 2.6 Creep correction factors for nonstandard loading ages

Age at loading t_{la} days	Creep correction factor $F_{c,la}$	
	Moist-cured, loaded later than 7 days	Steam-cured, loaded later than 1 to 3 days
10	0.95	0.90
20	0.87	0.85
30	0.83	0.82
60	0.77	0.76
90	0.74	0.74

For loading ages later than seven days for moist-cured concrete:

$$F_{c,la} = 1.25 t_{la}^{-0.118} \qquad (2.13a)$$

where t_{la} is the loading age in days.

For loading ages later than one to three days for steam-cured concrete:

$$F_{c,la} = 1.13 t_{la}^{-0.095} \qquad (2.13b)$$

For greater than 40 percent relative humidity:

$$F_{c,h} = 1.27 - 0.0067H \qquad (2.14)$$

where H is the relative humidity in percent. Some specific values for the correction factors $F_{c,la}$ and $F_{c,h}$ are given in Tables 2.6 and 2.7, respectively. In most cases corrections associated with member size, higher slump concrete, and other variables can be neglected.

Table 2.7 Creep and shrinkage correction factors for nonstandard relative humidity

Relative humidity H (percent)	Creep correction factor $F_{c,h}$	Shrinkage correction factor $F_{sh,h}$
40 or less	1.00	1.00
50	0.94	0.90
60	0.87	0.80
70	0.80	0.70
80	0.73	0.60
90	0.67	0.30
100	0.60	0.00

B. SHRINKAGE

Normal concrete mixes contain more water than is required for hydration of the cement. This free water evaporates in time, the rate and completeness of drying depending on the humidity, ambient temperature, and the size and shape of the concrete specimen. Drying of the concrete is accompanied by a reduction in volume, the change occurring at a higher rate initially than later, when limiting dimensions are approached asymptotically.

Branson and Kripanarayanan suggest "standard" equations relating shrinkage to time as follows:

For moist-cured concrete at any time t after age seven days:

$$\varepsilon_{sh,t} = \frac{t}{35 + t}\varepsilon_{sh,u} \tag{2.15a}$$

where $\varepsilon_{sh,t}$ is the shrinkage strain at time t in days and $\varepsilon_{sh,u}$ is the ultimate shrinkage strain. The value of $\varepsilon_{sh,u}$ may be taken as 800×10^{-6} if local data are not available. For steam-cured concrete at any time after age one to three days:

$$\varepsilon_{sh,t} = \frac{t}{55 + t}\varepsilon_{sh,u} \tag{2.15b}$$

An average value for $\varepsilon_{sh,u}$ of 730×10^{-6} is suggested for steam-cured concrete.

The relation between shrinkage strain and time, plotted to semilogarithmic scale, is shown in Fig. 2.12 for both moist-cured and steam-cured concrete.

For other than standard conditions of humidity. Eqs. (2.15a) and (2.15b) must be modified by a correction factor:

$$\text{For } 40 < H \leq 80\% \qquad F_{sh,h} = 1.40 - 0.010H \tag{2.16a}$$

$$\text{For } 80 < H \leq 100\% \qquad F_{sh,h} = 3.00 - 0.030H \tag{2.16b}$$

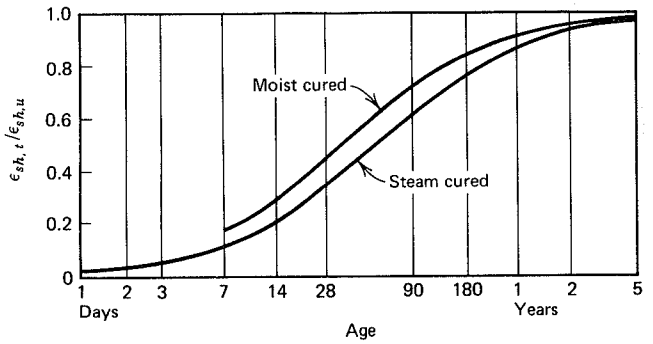

FIGURE 2.12 Variation of shrinkage coefficient with time. Adapted from Ref. 2.15.

Representative values of the shrinkage correction for various humidity levels are presented in Table 2.7. For most prestressed concrete members, the effect of member size on creep and shrinkage is relatively small.

Test evidence shows no consistent variation between normal weight, sand-lightweight, and all-lightweight concrete, and no consistent difference between concretes using Type I or Type III cement (Refs. 2.12, 2.15, and 2.16). In the absence of other information, the equations and correction factors given previously may be used for all cases.

REFERENCES

2.1 Magura, D. D., Sozen, M. A., and Siess, C. P., "A Study of Stress Relaxation in Prestressing Reinforcement," *J. PCI*, Vol. 9, No. 2, April 1964, pp. 13–57.

2.2 Neville, A. M., *Properties of Concrete*, 3rd ed., Wiley, New York, 1981.

2.3 Troxell, G. E., Davis, H. E., and Kelly, J. W., *Composition and Properties of Concrete*, 2nd ed., McGraw-Hill, New York, 1968.

2.4 *Design and Control of Concrete Mixtures*, 12th ed., Portland Cement Association, Skokie, Illinois, 1979.

2.5 "Standard Practice for Selecting Proportions for Normal, Heavyweight, and Mass Concrete," ACI Committee 211, *ACI Manual of Concrete Practice*, Part 1, 1983.

2.6 "Recommended Practice for Measuring, Mixing, Transporting, and Placing Concrete," ACI Committee 304, *ACI Manual of Standard Practice*, Part 2, 1983.

2.7 "Guide for Structural Lightweight Aggregate Concrete," ACI Committee 213, *ACI Manual of Concrete Practice*, Part 1, 1983.

2.8 "Standard Practice for Selecting Proportions for Structural Lightweight Concrete," ACI Committee 211, *ACI Manual of Concrete Practice*, Part 1, 1983.

2.9 Carrasquillo, R. L., Nilson, A. H., and Slate, F. O., "Properties of High Strength Concrete Subject to Short Term Loads," *J. ACI*, Vol. 78, No. 3, May–June 1981, pp. 171–178.

2.10 Martinez, S., Nilson, A. H., and Slate, F. O., "Short Term Mechanical Properties of High Strength Lightweight Concrete," *Research Report No.* 82-9, Dept. of Structural Engineering, Cornell University, August 1982.

2.11 Wang, P. T., Shah, S. P., and Naaman, A. E., "Stress-Strain Curves of Normal and Lightweight Concrete in Compression," *J. ACI*, Vol. 75, No. 11, November 1978, pp. 603–611.

2.12 Branson, D. E., *Deformation of Concrete Structures*, McGraw-Hill, New York, 1977.

2.13 Kupfer, H., Hillsdorf, H. K., and Rusch, H., "Behavior of Concrete Under Biaxial Stresses," *J. ACI*, Vol. 66, No. 8, August 1969, pp. 656–666.

2.14 Tasuji, M. E., Slate, F. O., and Nilson, A. H., "Stress–Strain Response and Fracture of Concrete in Biaxial Loading," *J. ACI*, Vol. 75, No. 7, July 1978, pp. 306–312.

2.15 Branson, D. E. and Kripanarayanan, K. M., "Loss of Prestress, Camber and Deflection of Non-Composite and Composite Prestressed Concrete Structures," *J. PCI*, Vol. 16, No. 5, September 1971, pp. 22–52.

2.16 "Prediction of Creep, Shrinkage, and Temperature Effects in Concrete Structures," Report by ACI Committee 209, *Designing for Effects of Creep, Shrinkage, Temperature in Concrete Structures*, ACI Special Publication SP-27, 1971, pp. 51–93.

THREE

FLEXURAL ANALYSIS

3.1 INTRODUCTION

Beams may require analysis or design. In the case of *flexural analysis*, the concrete and steel dimensions, as well as the magnitude and line of action of the effective prestress force, are usually known. If the loads are given, one may wish to find the resulting stresses and compare these against a set of permissible values. Alternately, if permissible stresses are known, then one may calculate maximum loads that could be carried without exceeding those stresses. For known material strengths, the member capacity can be calculated and safety against collapse determined for any loading.

In contrast, in *flexural design*, permissible stresses and material strengths are known, the loads to be resisted are specified, and the engineer must determine concrete and steel dimensions as well as the magnitude and line of action of the prestressing force.

The analysis of prestressed flexural members is by far the simpler task. Design is complicated by the interdependence of the many variables. Changes in one variable generally will affect many, if not all, of the others, and often the best path to the final design is an iterative one. A trial member chosen on the basis of approximate calculation is analyzed to check its adequacy and then refined. In this way, the designer converges on the solution that is "best" in some sense.

Both analysis and design of prestressed concrete may require the consideration of several load stages as follows:

1. Initial prestress, immediately after transfer, when P_i alone may act on the concrete.
2. Initial prestress plus self-weight of the member.
3. Initial prestress plus full dead load.
4. Effective prestress, P_e, after losses, plus service loads consisting of full dead and expected live loads.
5. Ultimate load, when the expected service loads are increased by load factors, and the member is at incipient failure.

At and below the service load level, both concrete and steel stresses are usually within the elastic range. Should the member be overloaded, however, one or both materials are likely to be stressed into the inelastic range, in which case predictions of ultimate strength must be based on actual, nonlinear stress–strain relations.

Only simple-span, statically determinate beams will be treated in this chapter. Study of such members permits the establishment of basic principles in the clearest possible way. In addition, these members are of great practical importance, because a large percentage of prestressed concrete construction in the United States is presently precast and erected in the form of simple spans.

The study of indeterminate beams, used increasingly for buildings as well as bridges and other structures, will be deferred until Chapter 8.

3.2 NOTATION

The study and design of prestressed concrete structures is greatly facilitated by adoption of a logical and self-consistent set of symbols to describe dimensions, stresses, forces, loads, and other important quantities. The ACI Code notation provides the basis for the notation used in this text. A few minor changes have been made in the interest of clarity or consistency. In these instances, the reader should have little difficulty adapting to Code notation, if he or she prefers. All symbols are defined when they first appear.

Consistent with the general practice in structural engineering, tensile strains and stresses are taken to be positive (since they are associated with length increase) and compressive strains and stresses as negative. Strains or stresses referring to the top surface of a flexural member are given the subscript 1 and those referring to the bottom the subscript 2.

3.3 PARTIAL LOSS OF PRESTRESS FORCE

It is not possible to proceed very far with the analysis or design of prestressed concrete members without considering that the prestressing force is not constant. As already discussed briefly in Chapter 1, the jacking tension P_j, initially applied to the tendon, is reduced at once to what is termed the initial prestress force P_i. A part of this loss in jacking tension, that due to friction between a post-tensioned tendon and its encasing duct, actually occurs before the transfer of prestress force to the concrete. The remainder due to elastic shortening of the concrete and due to slip at post-tensioning anchorages as the wedges take hold, occurs immediately upon transfer.

Additional losses occur over an extended period, because of concrete shrinkage and creep, and because of relaxation of stress in the steel tendon. As a result the prestress force is reduced from P_i to its final or effective value, P_e after all significant time-dependent losses have taken place.

The values of greatest interest to the designer are the initial prestress P_i and the effective prestress P_e. It is convenient to express the relation between these values in terms of an *effectiveness ratio* R, defined such that

$$P_e = RP_i \tag{3.1}$$

Put another way, the ratio of time-dependent losses to initial prestress force is

$$\frac{P_i - P_e}{P_i} = 1 - R \tag{3.2}$$

In works of major importance, it is always advisable to make a careful estimate of each component of loss of prestress force, making use of the best available knowledge of the material properties and the construction sequence. In routine design or in cases of lesser importance, it is adequate to assume a value for the effectiveness ratio R based on published information or past experience with similar construction. Detailed information to assist in the calculation of individual loss components will be presented in Chapter 6. In all of the present chapter's examples, a reasonable value for losses will be assumed, so that the fundamental principles will not be obscured by detailed loss calculation.

3.4 ELASTIC FLEXURAL STRESSES IN UNCRACKED BEAMS

A. BEHAVIOR OF PRESTRESSED BEAMS IN THE ELASTIC RANGE

A simple-span prestressed beam with a curved tendon is shown in Fig. 3.1*a*. The concrete centroid is that of the entire, uncracked cross section, and the steel will be represented by its centroidal axis, whether there is one tendon or many. The eccentricity of the steel centroid, positive if measured downward from the concrete centroid, is e. The distances from the concrete centroid to the top and bottom surfaces of the member are c_1 and c_2, respectively.

Figure 3.1*b* shows the force resultants acting on the concrete after the steel is tensioned. The force F acts on the concrete at the tendon anchorages near the

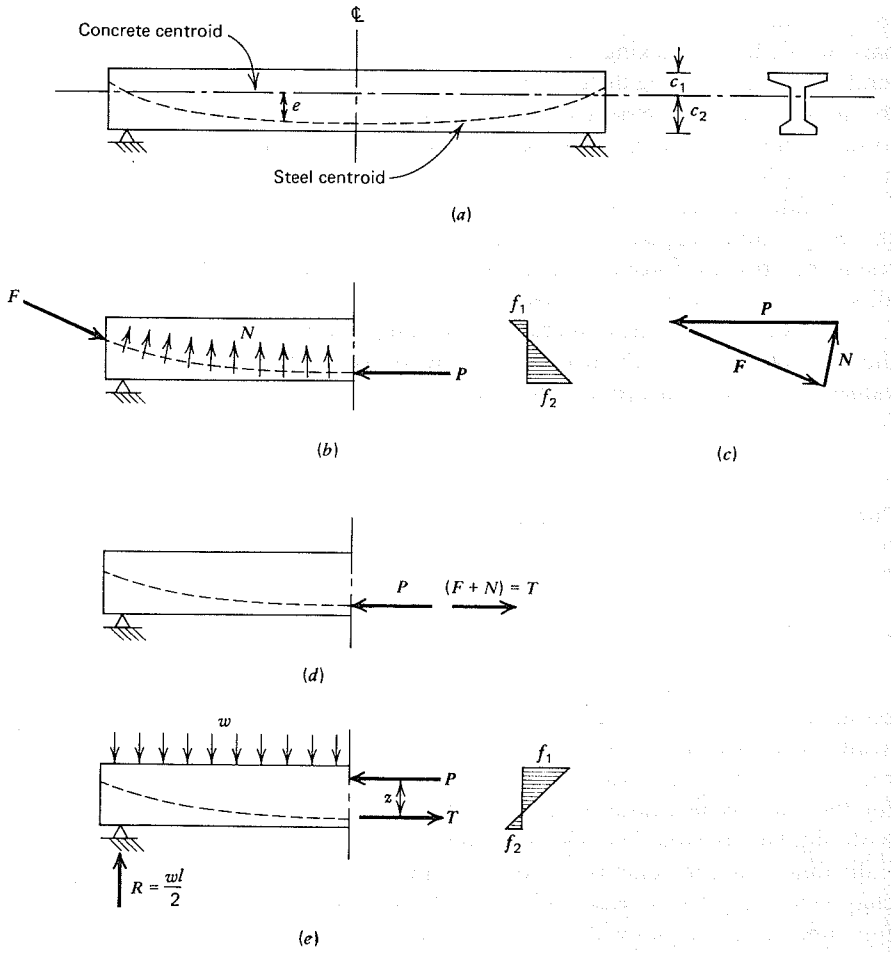

FIGURE 3.1 Forces acting on typical prestressed beam. (*a*) Beam profile and section. (*b*) Forces acting on concrete. (*c*) Force equilibrium polygon. (*d*) Anchorage and curvature forces replaced by resultant. (*e*) Beam with transverse loads.

ends of the member. The force P at midspan is the resultant of all the normal compressive stresses in the concrete at that section. These normal stresses vary from a value f_1 at the top surface to f_2 at the bottom surface. The forces N are exerted on the concrete by the tendon because of its curvature, and the exact distribution of these forces depends on the particular tendon profile used.

The three forces F, N, and P form a self-equilibrating system, as illustrated by the closing force polygon of Fig. 3.1*c*. Note that when prestress forces act alone on a statically determinate beam, the external reactions on the beam are zero.

Figure 3.1*d* shows an alternative representation of the forces of Fig. 3.1*b*, in which the forces F and N are replaced by their vector sum T. The compressive resultant P acts as before. Note that P and T are equal and opposite forces, acting at the same point on the cross section. It is concluded that, for a statically determinate beam, the consequence of prestressing is a compressive resultant force that acts at the location of the steel centroid at any section.

The direction of the compressive resultant is always tangent to the tendon profile at any section. For the midspan section of the symmetrical beam just considered, the compressive resultant was horizontal. If the section had been taken at another location, say, at the quarter point of the span, the compressive resultant would have both a horizontal and vertical component. In such case, the horizontal component would represent the summation of all the normal forces acting on the concrete, and the vertical component the summation of all the shearing forces.

Next, a uniformly distributed load of intensity w is applied as shown in Fig. 3.1*e*. There is an associated reaction force $R = wl/2$ at each support. As the load w is gradually applied, the magnitude of the prestressing force stays essentially constant (the actual, slight increase will be discussed in Section 3.6), and T maintains both its magnitude and position. As flexural stresses due to the applied load are superimposed on axial and flexural stresses due to prestressing, the compressive resultant P moves upward. An internal resisting couple is generated, with equal forces P and T and lever arm z. This couple exactly equilibrates the external moment.

The difference between the behavior of a prestressed concrete beam and a reinforced concrete beam should be noted carefully. In the case of the reinforced concrete beam, the internal lever arm remains essentially constant as the load is increased, and the increasing moment is accompanied by an almost proportionate increase in the internal forces. For the prestressed beam, the forces stay essentially constant as the load is increased, and the increasing moment is accompanied by an increase in the internal lever arm.

B. ELASTIC STRESSES

As long as the beam remains uncracked, and both steel and concrete are stressed only within their elastic ranges, then concrete stresses can be found using the familiar equations of mechanics, based on linear elastic behavior. In present practice, these conditions are often satisfied up to, and including, the level of service loading. Stresses may be found using linear elastic methods, even though the *nominal* tension is somewhat in excess of the probable value of the modulus of rupture. The rationale for this is that a certain amount of bonded reinforcement, prestressed or otherwise, must be provided in the tension zone. This serves the purpose of controlling both cracking and deflection, and permits the member to respond essentially as if it were uncracked.

If the member is subjected only to the initial prestressing force P_i, it has just been shown that the compressive resultant acts at the steel centroid. The concrete stress f_1 at the top face of the member and f_2 at the bottom face can be found by superimposing axial and bending effects:

$$f_1 = -\frac{P_i}{A_c} + \frac{P_i e c_1}{I_c} \tag{3.3a}$$

$$f_2 = -\frac{P_i}{A_c} - \frac{P_i e c_2}{I_c} \tag{3.3b}$$

where e is the tendon eccentricity measured downward from the concrete centroid, A_c is the area of the concrete cross section, and I_c is the moment of inertia of the concrete cross section. Other terms are as already defined. Substituting the radius of gyration $r^2 = I_c/A_c$, these equations can be written in the more convenient form:

$$f_1 = -\frac{P_i}{A_c}\left(1 - \frac{e c_1}{r^2}\right) \tag{3.4a}$$

$$f_2 = -\frac{P_i}{A_c}\left(1 + \frac{e c_2}{r^2}\right) \tag{3.4b}$$

The resulting stress distribution is shown in Fig. 3.2*a*.

Almost never would the initial prestress P_i act alone. In most practical cases, with the tendon below the concrete centroid, the beam will deflect upward because of the bending moment caused by prestressing. It will then be supported by the formwork or casting bed essentially at its ends, and the dead load of the beam itself will cause moments M_o to be superimposed immediately. Consequently, at the initial stage, immediately after transfer of prestress force, the stresses in the concrete at the top and bottom surfaces are

$$f_1 = -\frac{P_i}{A_c}\left(1 - \frac{e c_1}{r^2}\right) - \frac{M_o}{S_1} \tag{3.5a}$$

$$f_2 = -\frac{P_i}{A_c}\left(1 + \frac{e c_2}{r^2}\right) + \frac{M_o}{S_2} \tag{3.5b}$$

where M_o is the bending moment resulting from the self-weight of the member, and $S_1 = I_c/c_1$ and $S_2 = I_c/c_2$ are the section moduli with respect to the top and bottom surfaces of the beam. The stress distribution at this load stage is shown in Fig. 3.2*b*.

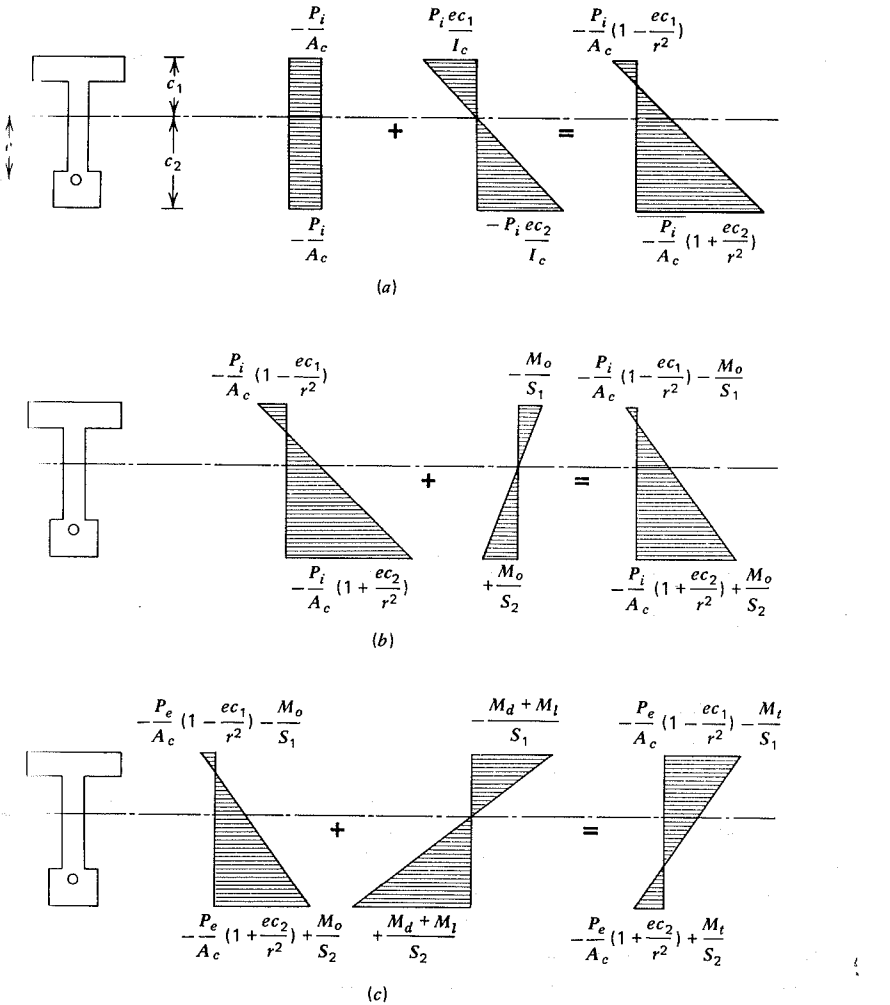

FIGURE 3.2 Elastic stresses in an uncracked prestressed beam. (*a*) Effect of initial prestress. (*b*) Effect of initial prestress plus self-weight. (*c*) Effect of final prestress plus full service load.

Superimposed dead loads (in addition to the self-weight) may be placed when the prestress force is still close to its initial value, that is, before time-dependent losses have occurred. However, this load stage would seldom, if ever, control the design, as can be confirmed by study of Fig. 3.2.

Superimposed live loads are generally applied sufficiently late for the greatest part of the loss of prestress to have occurred. Consequently, the next

load stage of interest is the full service load stage, when the effective prestress P_e acts with the moments resulting from self-weight (M_o), superimposed dead load (M_d), and superimposed live load (M_l). The resulting stresses are

$$f_1 = -\frac{P_e}{A_c}\left(1 - \frac{ec_1}{r^2}\right) - \frac{M_t}{S_1} \tag{3.6a}$$

$$f_2 = -\frac{P_e}{A_c}\left(1 + \frac{ec_2}{r^2}\right) + \frac{M_t}{S_2} \tag{3.6b}$$

where the total moment M_t is

$$M_t = M_o + M_d + M_l \tag{3.7}$$

These *service-load stresses* are shown in Fig. 3.2*c*.

C. CALCULATION OF SECTION PROPERTIES

In calculating the properties of the concrete cross section to be used in the previous equations, it should be noted that in post-tensioned construction tendons may pass through ducts of considerable size. Before the tendons are grouted, stresses in the concrete should be calculated using the net section, with holes deducted. After grouting, the transformed section should be used. Holes may be considered filled with concrete and the steel replaced with its transformed area of equivalent concrete equal to $(n_p - 1)A_p$, where n_p is the modular ratio E_p/E_c and A_p is the area of the prestressing steel (see Ref. 3.1). In practical cases, although the hole deduction may be significant, use of the gross concrete section after grouting rather than the transformed section will normally be satisfactory. In many cases, the hole deduction is small and the gross concrete section can provide the basis for all calculations. This will almost always be the case when unbonded wrapped tendons without ducts are used.

In pretensioned construction, the transformed cross section should, in theory, be used for all calculations. However the difference in properties of the gross and transformed sections is usually small, permitting calculations to be based on the gross cross section.

D. CROSS SECTION KERN OR CORE

When the prestressing force, acting alone, causes no tension in the cross section, it is said to be acting within the *kern* or the *core* of the cross section. In the limiting cases, triangular stress distributions will result from application of the prestress force, with zero concrete stress at the top or the bottom of the member.

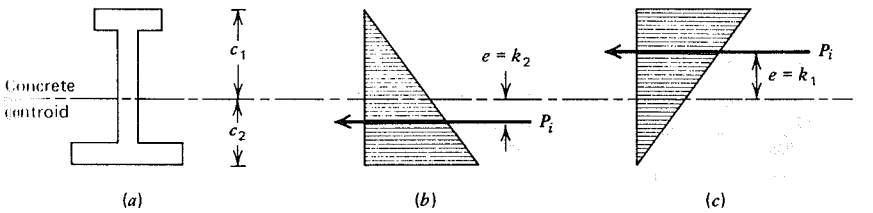

FIGURE 3.3 Stress distributions for prestress force applied at kern limits. (*a*) Cross section. (*b*) Lower kern limit. (*c*) Upper kern limit.

The kern limit dimensions can be found from Eqs. (3.4*a*) and (3.4*b*). To find the lower kern dimension, the concrete stress at the top surface is set equal to zero as illustrated in Fig. 3.3. Thus

$$f_1 = -\frac{P_i}{A_c}\left(1 - \frac{ec_1}{r^2}\right) = 0$$

indicating that the quantity in parentheses must equal zero. Solving for that particular eccentricity, defined as $e = k_2$, the lower kern limit is

$$1 - \frac{k_2 c_1}{r^2} = 0$$

$$k_2 = \frac{r^2}{c_1} \tag{3.8a}$$

Similarly, the upper kern limit is found by setting the expression for the concrete stress at the bottom surface equal to zero, from which

$$k_1 = -\frac{r^2}{c_2} \tag{3.8b}$$

the minus sign confirming that the limit dimension is measured upward from the concrete centroid.

It would be unwise to place great emphasis on these limit dimensions. It should not be implied that the steel centroid must remain within the kern. However, the kern limits often serve as convenient reference points in the design of beams.

EXAMPLE: Flexural Stresses for Given Beam and Loads

The simply supported I-beam shown in cross section and elevation in Fig. 3.4 is to carry a uniformly distributed service dead and live load totaling 0.55 kips/ft over

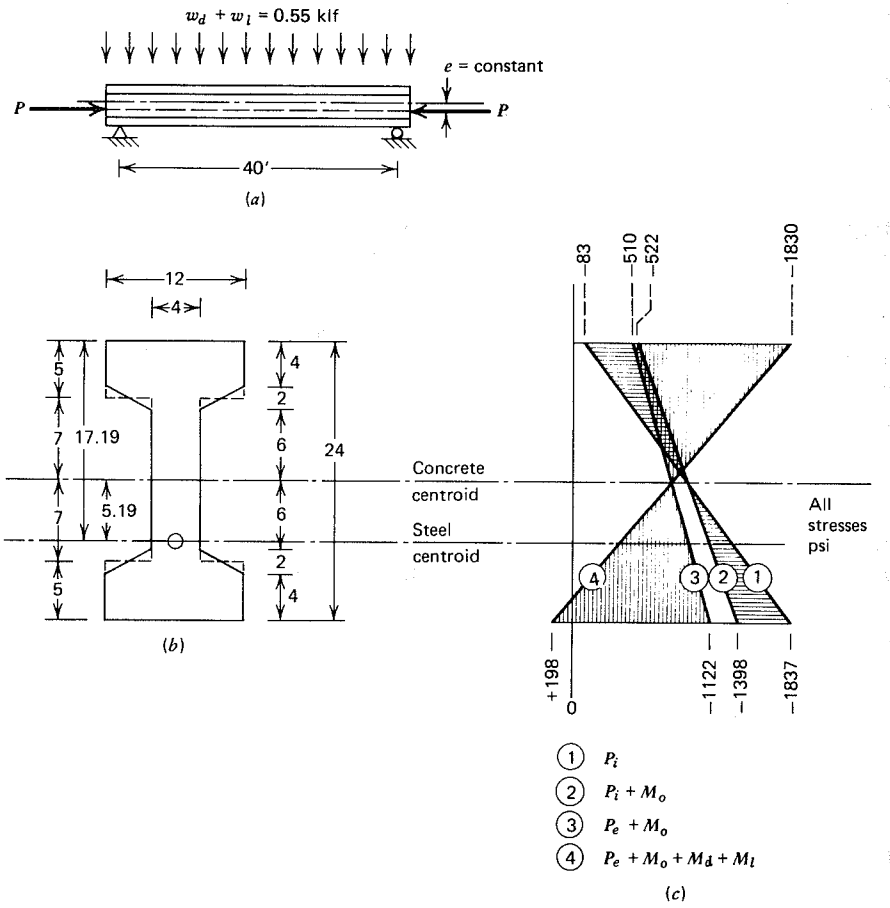

FIGURE 3.4 I-beam with constant eccentricity. (*a*) Elevation. (*b*) Cross section. (*c*) Concrete stresses at midspan.

the 40-ft span, in addition to its own weight. Normal concrete having density of 150 lb/ft^3 will be used. The beam will be pretensioned using multiple seven-wire strands; eccentricity is constant and equal to 5.19 in. The prestress force P_i immediately after transfer (after elastic shortening loss) is 169 kips. Time-dependent losses due to shrinkage, creep, and relaxation total 15 percent of the initial prestress force. Find the concrete flexural stresses at midspan and support sections under initial and final conditions. (Load = 8.02 kN/m, span = 12.19 m, density = 24 kN/m^3, e = 132 mm, P_i = 752 kN.)

For pretensioned beams using stranded cables, the difference between section properties based on the gross and transformed section is usually small. Accordingly, all calculations will be based on properties of the gross concrete section. Average flange thickness will be used, as shown in Fig. 3.4*b*. For that section

Moment of inertia	I_c = 12,000 in.^{4} (4.99 × 10^9 mm^4)
Concrete area	A_c = 176 in.^{2} (114 × 10^3 mm^2)
Section modulus	$S_1 = S_2$ = 1,000 in.^{3} (16.4 × 10^6 mm^3)
Radius of gyration	$r^2 = I_c/A_c$ = 68.2 in.^{2} (44 × 10^3 mm^3)

Stresses in the concrete resulting from the initial prestress force of 169 kips may be found by Eq. (3.4). At the top and bottom surfaces, respectively, these stresses are

$$f_1 = -\frac{P_i}{A_c}\left(1 - \frac{ec_1}{r^2}\right) = -\frac{169{,}000}{176}\left(1 - \frac{5.19 \times 12}{68.2}\right) = -83 \text{ psi}$$

$$f_2 = -\frac{P_i}{A_c}\left(1 + \frac{ec_2}{r^2}\right) = -\frac{169{,}000}{176}\left(1 + \frac{5.19 \times 12}{68.2}\right) = -1837 \text{ psi}$$

as shown by distribution (1) in Fig. 3.4*c*. These stresses exist throughout the length of the member. However, as the prestress force is applied, the beam will camber off the casting bed, and stresses due to the beam-load bending moment will act. The member dead load is

$$w_o = \frac{176}{144} \times 0.150 = 0.183 \text{ kips/ft}$$

At midspan the corresponding moment is

$$M_o = \frac{1}{8} \times 0.183 \times 40^2 = 36.6 \text{ ft-kips}$$

This moment produces top and bottom concrete stresses at midspan of

$$f_1 = -\frac{M_o}{S_1} = -\frac{36.6 \times 12{,}000}{1{,}000} = -439 \text{ psi}$$

$$f_2 = +\frac{M_o}{S_2} = +\frac{36.6 \times 12{,}000}{1{,}000} = +439 \text{ psi}$$

The combined effect of initial prestress and self-weight is found by superposition.

$$f_1 = -83 \quad - 439 = -522 \text{ psi } (-3.6 \text{ MPa})$$

$$f_2 = -1{,}837 + 439 = -1398 \text{ psi } (-9.6 \text{ MPa})$$

as shown by distribution (2).

Time-dependent losses are 15 percent of P_i. Accordingly, the effectiveness ratio

$$R = \frac{P_e}{P_i} = 0.85$$

and the effective prestress force after all losses is

$$P_e = 0.85 \times 169 = 144 \text{ kips}$$

Top and bottom concrete stresses due to P_e are

$$f_1 = 0.85 \times (-83) \quad = -71 \text{ psi}$$

$$f_2 = 0.85 \times (-1{,}837) = -1{,}561 \text{ psi}$$

Flexural stresses due to self-weight must be superimposed as before. The resulting midspan stresses due to P_e and self-weight are

$$f_1 = -71 \quad -439 = -510 \text{ psi } (-3.5 \text{ MPa})$$

$$f_2 = -1{,}561 + 439 = -1{,}122 \text{ psi } (-7.7 \text{ MPa})$$

as given by distribution (3) in Fig. 3.4*c*.

The midspan moment due to superimposed dead and live load is

$$M_d + M_l = \frac{1}{8} \times 0.55 \times 40^2 = 110 \text{ ft-kips}$$

and the corresponding concrete stresses are

$$f_1 = -\frac{110 \times 12{,}000}{1{,}000} = -1320 \text{ psi}$$

$$f_2 = +\frac{110 \times 12{,}000}{1{,}000} = +1320 \text{ psi}$$

Then, combining effective prestress force with moments due to self-weight and superimposed load, the stresses produced are

$$f_1 = -510 \quad -1{,}320 = -1{,}830 \text{ psi } (-12.6 \text{ MPa})$$

$$f_2 = -1{,}122 + 1{,}320 = +198 \text{ psi } (+1.4 \text{ MPa})$$

as shown by distribution (4). In Fig. 3.4*c*, the stress change resulting from the member self-weight is shown by horizontal shading, and that resulting from superimposed dead and live loads is shown by vertical shading.

At the support sections, the transverse loads cause no flexural stresses, and concrete stresses are those resulting from prestress alone. The initial values of -83 and $-1{,}837$ psi at the top and bottom surfaces gradually reduce to -71 and $-1{,}561$ psi, respectively, as time-dependent losses occur.

Additional Comments

1. The stress at the concrete centroid due to initial prestress is

$$f_{cc} = -\frac{169{,}000}{176} = -960 \text{ psi}$$

   and this stress does not change as the member self-weight is introduced. Nor does the concrete centroidal stress, after losses, of $0.85 \times (-960) = -816$ psi change as the superimposed dead and live loads are applied.
2. The stress change in the prestressing steel resulting from application of loads can easily be calculated. Assuming that the bond between concrete and steel remains intact, the change in steel stress will be n_p times the change in concrete stress at that level in the member, where $n_p = E_p/E_c$. A value of $n_p = 8$ will be assumed here. Referring to Fig. 3.4*c*, as the self-weight is applied, the stress increase in the steel is

$$\Delta f_p = 8(-1{,}398 + 1{,}837) \times \frac{5.19}{12} = 1{,}519 \text{ psi}$$

   and the further increase associated with the superimposed dead and live load is

$$\Delta f_p = 8(198 + 1{,}122) \times \frac{5.19}{12} = 4{,}567 \text{ psi}$$

   The total increase is about 3 percent of the probable initial stress in the steel. This change is generally disregarded.
3. The magnitude of tensile stress at the bottom concrete surface of 198 psi tension is well below the probable modulus of rupture of the concrete, confirming that the concrete has not cracked and that the stress calculations based on the entire cross section are valid.
4. Note that in the unloaded stage, represented by stress distribution (2), substantial precompression exists in the upper part of the beam, which will later be further compressed by application of a superimposed load. This suggests that a more efficient design would result from the use of increased tendon eccentricity, or reduced prestress force, or both. However, for a member with straight tendons, such changes may result in undesirably large tensile stresses at the top of the member at the supports, where beam dead load causes no flexural stress. For this and other reasons, tendon eccentricity is often reduced toward the supports.

3.5 ALLOWABLE FLEXURAL STRESSES

Most specifications for prestressed concrete construction impose certain limitations on stresses in the concrete and steel at particular stages, such as while tensioning the steel, immediately after transfer of prestress force to the concrete, and at full service load. These stress limits are intended to avoid damage to the member during construction, and to insure serviceability by indirectly limiting crack width and deflection. In present practice, stress limit specifications often provide the starting point in selecting the dimensions for prestressed concrete members. The resulting design must, of course, be checked for strength to insure adequate safety against failure. Often deflections must also be calculated explicitly at particular load stages of importance.

A. CONCRETE

Concrete stress limits imposed by the ACI Code are summarized in Table 3.1. Here f'_{ci} is the compressive strength of the concrete at the time of initial prestress, and f'_c is the specified compressive strength of the concrete. Both are expressed in psi units, as are the resulting stresses.

The allowable stresses of Part 1 of Table 3.1 apply immediately after transfer of prestress force to the concrete, after losses due to friction, anchorage slip, and

Table 3.1 Permissible Stresses in Concrete in Prestressed Flexural Members[a]

1. Stresses immediately after prestress transfer (before time-dependent prestress losses) shall not exceed the following:	
a. Extreme fiber stress in compression	$0.60f'_{ci}$
b. Extreme fiber stress in tension except as permitted in *c*	$3\sqrt{f'_{ci}}$
c. Extreme fiber stress in tension at ends of simply supported members Where computed tensile stresses exceed these values, bonded auxiliary reinforcement (non-prestressed or prestressed) shall be provided in the tensile zone to resist the total tensile force in the concrete computed with the assumption of an uncracked section.	$6\sqrt{f'_{ci}}$
2. Stresses at service loads (after allowance for all prestress losses) shall not exceed the following:	
a. Extreme fiber stress in compression	$0.45f'_c$
b. Extreme fiber stress in tension in precompressed tensile zone	$6\sqrt{f'_c}$
c. Extreme fiber stress in tension in precompressed tensile zone of members (except two-way slab systems) where analysis based on transformed cracked sections and on bilinear moment-deflection relationships shows that immediate and long-time deflections comply with requirements stated elsewhere in the Code, and where special cover requirements are met.	$12\sqrt{f'_c}$
3. The permissible stresses of Sections 1 and 2 may be exceeded if shown by test or analysis that performance will not be impaired.	

[a]Adapted with permission of the American Concrete Institute from ACI Building Code 318-83.

elastic shortening of the concrete have been deducted, but before time-dependent losses due to shrinkage, creep, and relaxation are taken into account. The tension stress limits of $3\sqrt{f'_{ci}}$ and $6\sqrt{f'_{ci}}$ refer to tensile stress at locations other than the precompressed tensile zone.[1] If the tensile stress exceeds the applicable limiting value, the total force in the tension zone should be calculated, and bonded auxiliary reinforcement provided to resist this force. For design purposes, such steel is assumed to act at a stress of 60 percent of its yield stress, but not at a stress greater than 30 ksi.

The service load stress limits of Part 2 of Table 3.1 apply after all losses have occurred and when the full service load acts. The allowable concrete tensile stress of $6\sqrt{f'_c}$ has been established mostly on the basis of experience with test members and actual structures. Use of this stress limit, rather than a lower value or zero,

[1]The precompressed tension zone is defined in the ACI Code Commentary as that portion of the member in which flexural tension occurs under dead and live loads.

requires that there be a sufficient amount of bonded reinforcement in the precompressed tension zone to control cracking, that the amount of concrete cover for the reinforcement is sufficient to avoid corrosion, and that unusually corrosive conditions will not be encountered. Bonded reinforcement may consist of bonded prestressed or non-prestressed tendons, or of bonded reinforcing bars, well distributed over the tension zone.

The use of a tensile stress limit of $12\sqrt{f'_c}$ is permitted to obtain improved service load deflection characteristics, particularly when a substantial part of the live load is of a transient nature. It should be emphasized that an allowable tensile stress of $12\sqrt{f'_c}$, calculated on the basis of an uncracked cross section, is a nominal stress only, since its value is well above that of the modulus of rupture of the concrete. If this stress limit is used, the concrete protection for the reinforcement must be increased 50 percent above its usual value, according to the Code, and an explicit check made of service load deflection.

The "escape clause" of Part 3 of Table 3.1, permits higher stress limits to be used when tests or analysis indicate that satisfactory performance can be expected.

B. STEEL

The permissible tensile stresses in prestressing steel given in Table 3.2 are expressed in terms of f_{pu}, the ultimate strength of the steel, and f_{py}, the specified yield strength. It is seen that the stress permitted by the Code depends on the stage of loading. When the jacking force is first applied, a stress of $0.85f_{pu}$ or $0.94f_{py}$ is allowed, whichever is lower. The justification for these high stress limits is that the steel stress is known rather precisely during the stretching operation, since hydraulic pressure and total steel strain can easily be measured.

Table 3.2 Permissible Stresses in Prestressing Steel[a]

Tensile stress in prestressing tendons shall not exceed the following:	
1. Due to tendon jacking force but not greater than $0.85f_{pu}$ or maximum value recommended by manufacturer of prestressing tendons or anchorages.[b]	$0.94f_{py}$
2. Immediately after prestress transfer but not greater than $0.74f_{pu}$.	$0.82f_{py}$
3. Post-tensioning tendons, at anchorages and couplers, immediately after tendon anchorage	$0.70f_{pu}$

[a]Adapted with permission of the American Concrete Institute from ACI Building Code 318-83.

[b]The limit of $0.85f_{pu}$ may be reduced to $0.80f_{pu}$ with publication of the 1989 edition of the ACI Building Code. This change would affect only low-relaxation steel tendons with $f_{py} = 0.90f_{pu}$. For ordinary stress-relieved strands with $f_{py} = 0.85f_{pu}$, the jacking tension is controlled by $0.94f_{py} = 0.80f_{pu}$ regardless.

The values of $0.74f_{pu}$ and $0.82f_{py}$ apply after elastic shortening and anchorage slip losses have taken place, but before time-dependent losses due to shrinkage, creep, and relaxation. No limit need be placed on final steel stress after all losses, because that stress will always be less than the steel stress under initial conditions, when an adequate factor of safety must be obtained.

The allowable steel stresses of Table 3.2, quoted from the 1983 ACI Code, have been modified compared with earlier editions of the ACI Code to reflect the properties of low-relaxation wire and strand, which are now in general use and typically have a higher ratio of f_{py}/f_{pu} than ordinary tensions. With the higher allowable initial stresses now permitted, final steel stresses after losses may prove to be higher. The Code Commentary warns that designers should be concerned with setting a limit on final stress when the structure is subject to corrosive conditions or repeated loadings.

3.6 CRACKING LOAD

The relation between applied load and steel stress in a typical well-bonded pretensioned beam is shown in a qualitative way in Fig. 3.5. Performance of a grouted post-tensioned beam is similar. When the jacking force is first applied

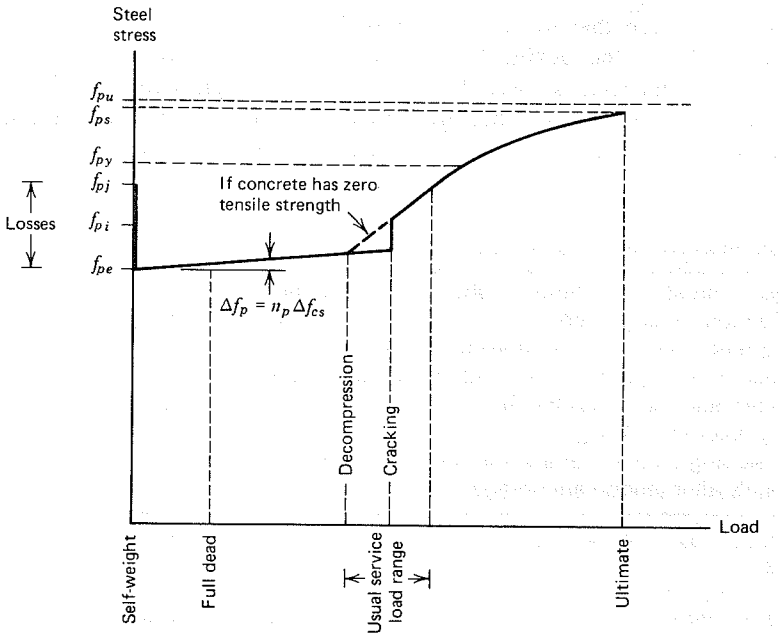

FIGURE 3.5 Variation of steel stress with load in bonded pretensioned beam.

and the strand is stretched between abutments, the steel stress is f_{pj}. Upon transfer of force to the concrete member, there is an immediate reduction of stress to the initial stress level f_{pi}, due to elastic shortening of the concrete. At the same time, the self-weight of the member is caused to act as the beam cambers upward. It will be assumed here that all time-dependent losses occur prior to superimposed loading, so that the stress is further reduced to the effective prestress level f_{pe}, as shown in Fig. 3.5.

As the superimposed dead and live loads are added, there is a slight increase in steel stress. Assuming that perfect bond is maintained between steel and concrete, this increase must be n_p times the increase in stress in the concrete at the level of the steel. The change is no more than about 3 or 4 percent of the initial stress, and is usually ignored in the calculations.

Unless the beam has cracked prior to loading due to shrinkage or other causes, there is no significant modification in behavior at the *decompression load*, when the compression at the bottom of the member is reduced to zero. The steel stress continues to increase only slightly and linearly, until the cracking load is reached. At that load, there is a sudden increase in steel stress, as the tension that was formerly carried by the concrete is transferred to the steel. In a beam with prior cracks or in a segmentally cast beam, the curve changes slope at the decompression load as shown.

After cracking, the steel stress increases much more rapidly than before. After the yield stress f_{py} is reached, the steel elongates disproportionately, but carries increasing stress due to the shape of its stress–strain curve, and the stress vs. load curve continues upward at a gradually reducing slope. The steel stress when the beam fails f_{ps} may be equal to the tensile strength f_{pu}, but is usually somewhat below it, depending on the geometry of the beam, the steel ratio, the properties of the materials, and the initial prestress in the steel.

The cracking load represents the limit of validity of those equations for elastic stresses in the concrete that are based on the homogeneous cross section (although that section may provide the basis of *nominal* stress calculations above that load, as indicated in Section 3.5). Although the importance of cracking has been overemphasized in the past, it may be necessary to predict the cracking load for any of the following reasons:

1. Deflection is influenced by the reduction in flexural rigidity that accompanies cracking.
2. After the beam cracks, the prestressing steel is more vulnerable to corrosion.
3. The fatigue resistance of beams is reduced by cracking because of the greater stress range experienced by the prestressing steel near the cracks.
4. Cracks may be visually objectionable in some cases.
5. In the case of liquid containment vessels, leaks are more likely after cracking.

The moment causing cracking may easily be found for a typical beam by writing the equation for the concrete stress at the bottom face, based on the

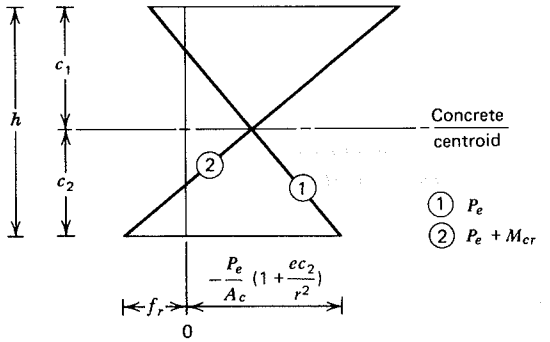

FIGURE 3.6 Change in concrete stresses as cracking moment is applied.

homogeneous section, and setting it equal to the modulus of rupture:

$$f_2 = -\frac{P_e}{A_c}\left(1 + \frac{ec_2}{r^2}\right) + \frac{M_{cr}}{S_2} = f_r \tag{a}$$

in which M_{cr} is the total moment at cracking (including moment due to self-weight and superimposed dead and partial live loads) and f_r is the modulus of rupture (see Section 2.9). Rearranging, we obtain

$$\frac{M_{cr}}{S_2} = f_r + \frac{P_e}{A_c}\left(1 + \frac{ec_2}{r^2}\right) \tag{b}$$

This simply states that the change in bottom face stress as the full cracking moment is applied must be such as to overcome the initial precompression due to prestress, and to introduce a tensile stress just equal to the modulus of rupture. This is shown in Fig. 3.6. If we rearrange terms and note that $S_2 = I_c/c_2$, the equation for cracking moment is

$$M_{cr} = f_r S_2 + P_e\left(\frac{r^2}{c_2} + e\right) \tag{3.9}$$

It may be observed that the first term in the parentheses in Eq. (3.9) is the dimension to the upper kern limit and, consequently, the entire second term represents the moment necessary to move the compressive resultant from the level of the steel centroid to the upper kern where, by definition, it will produce zero stress at the bottom of the beam. The additional moment corresponding to the first term, when superimposed, results in flexural cracking.

It is sometimes useful to state the safety factor relative to cracking. This may be defined in several ways but is usually stated with respect to the live-load bending moment such that

$$M_o + M_d + F_{cr}M_l = M_{cr} \tag{c}$$

in which the factor F_{cr} may be less than, equal to, or larger than unity. Then

$$F_{cr} = \frac{M_{cr} - M_o - M_d}{M_l} \tag{3.10}$$

EXAMPLE: Calculation of Cracking Moment for Given Beam and Loads

Calculate the cracking moment and find the factor of safety against cracking for the I-beam considered in the example in Section 3.4 and shown in Fig. 3.4. The modulus of rupture of the concrete is f_r = 350 psi (2.4 MPa).

The cracking moment can be found by direct substitution into Eq. (3.9):

$$M_{cr} = f_r S_2 + P_e\left(\frac{r^2}{c_2} + e\right)$$

$$= 350 \times 1{,}000 + 144{,}000\left(\frac{68.2}{12} + 5.19\right)$$

$$= 1{,}916{,}000 \text{ in.-lb}$$

$$= 160 \text{ ft-kips (217 kN-m)}$$

Assuming for present purposes that the entire superimposed load is a live load, then the safety factor against cracking, expressed with respect to an increase in the live load is, from Eq. (3.10):

$$F_{cr} = \frac{M_{cr} - M_o - M_d}{M_l}$$

$$= \frac{160 - 37 - 0}{110} = 1.12$$

3.7 FLEXURAL STRENGTH ANALYSIS

The most important single property of a structure is its strength, because a member's strength relates directly to its safety. Adequate strength of a prestressed concrete member is *not* automatically insured by limiting stresses at service load. Should the member be overloaded, significant changes in behavior result from cracking, and because one or both of the materials will be stressed into the inelastic range before failure. The true factor of safety can be established only by calculating the strength of the member, with full recognition of these effects, and comparing the load that would cause the member to fail with the load that is actually expected to act.

It has already been shown that prestressed concrete beams differ in their behavior from reinforced concrete beams. As the load is increased up to about

the service load stage, the forces composing the internal resisting couple stay nearly constant, the increase in applied moment being resisted through an increase in the internal lever arm.

Obviously, this cannot continue indefinitely. Upon cracking, there is a sudden increase in the steel stress, accompanied by an increase in the concrete compressive stress resultant. As the load is further increased, a prestressed beam behaves more like an ordinary reinforced concrete beam. The internal lever arm remains about constant, and both concrete and steel stresses increase with load. As for a reinforced concrete beam, the flexural capacity is reached when the steel is stressed to its ultimate strength, or when the compressive strain capacity of the concrete is reached.

Even at loads near the ultimate, there are important differences between prestressed and reinforced concrete beams, as a result of the following: (1) In reinforced concrete, under zero load, the strain in the reinforcement is zero. In prestressed concrete, the strain in the tendons at zero load is not zero, but corresponds to the effective prestress after losses. Any further strain in the steel caused by applied loads adds to this preexisting strain. (2) The stress–strain characteristics of prestressing steel are quite different from those of reinforcing bars, as shown by Fig. 2.2. Prestressing steels do not show a definite yield plateau. Yielding develops gradually and, in the inelastic range, the stress–strain curve continues to rise smoothly until the tensile strength is reached. The spread between the nominal yield strength f_{py} and the ultimate tensile strength f_{pu} is much smaller for prestressing steels than is the spread between the corresponding values for reinforcing steel. Also, the strain ε_{pu} at rupture is much smaller.

A. STRESS – STRAIN CURVES

Representative stress–strain curves for prestressing steel and concrete are shown in Fig. 3.7 for reference. For steel, Fig. 3.7*a*, a convenient and easily remembered notation, is:

f_{pe}, ε_{pe} = stress and strain in the steel due to effective prestress force P_e after all losses[2]

f_{py}, ε_{py} = yield stress and yield strain for the steel, defined as in Section 2.5

f_{pu}, ε_{pu} = ultimate tensile strength and ultimate strain of the steel

f_{ps}, ε_{ps} = stress and strain in the steel when the beam fails

[2]This stress is termed f_{se} in the ACI Code.

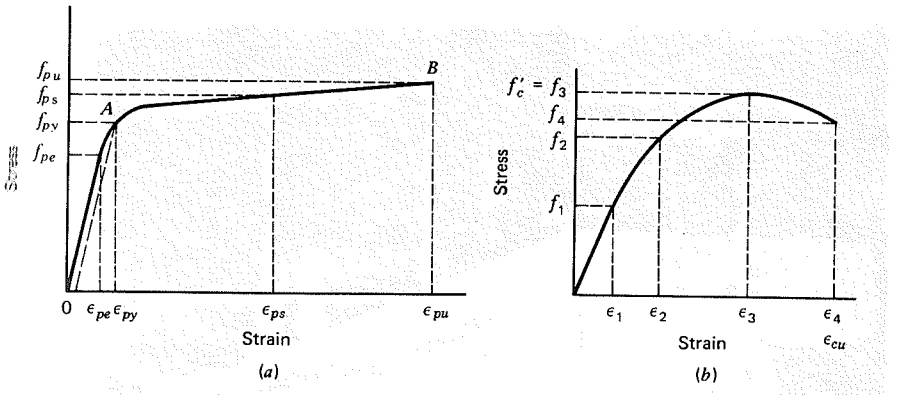

FIGURE 3.7 Representative stress – strain curves. (*a*) Prestressing steel. (*b*) Concrete.

For the concrete, the ultimate compressive strength is termed f'_c as usual, and the failure strain is ε_{cu}, shown in Fig. 3.7*b*. Measurements of concrete strain at failure in beam tests indicate that values of ε_{cu} between 0.003 and 0.004 are attained. Consistent with the ACI Code, a limiting strain of 0.003 for the concrete will be assumed.

B. SUCCESSIVE CONCRETE STRESS DISTRIBUTIONS AS BEAM IS OVERLOADED

As for ordinary reinforced concrete beams, prestressed beams may be divided into two types, based on mode of flexural failure. For under-reinforced beams, failure is initiated by yielding of the tensile steel. The associated large tensile strains permit widening of flexural cracks and upward migration of the neutral axis. The increased concrete stresses acting on the reduced compressive area result in a "secondary" compression failure of the concrete, even though the failure is initiated by yielding. The stress in the steel at failure will be between points *A* and *B* of Fig. 3.7*a*. The large steel strains produce visible cracking and considerable deflection of the member before the failure load is reached, as illustrated by the test beam of Fig. 3.8. This is an important safety consideration.

Over-reinforced beams, on the other hand, fail when the compressive strain limit of the concrete is reached, at a load when the steel is still below its yield stress, between points *O* and *A* of Fig. 3.7*a*. This second type of failure is accompanied by a *downward* movement of the neutral axis, because the concrete is stressed into its nonlinear range although the steel response is still linear. This type of failure occurs suddenly with little warning.

The concrete compressive stress distributions in under- and over-reinforced prestressed beams, at successive loading stages, are shown in Fig. 3.9. For either

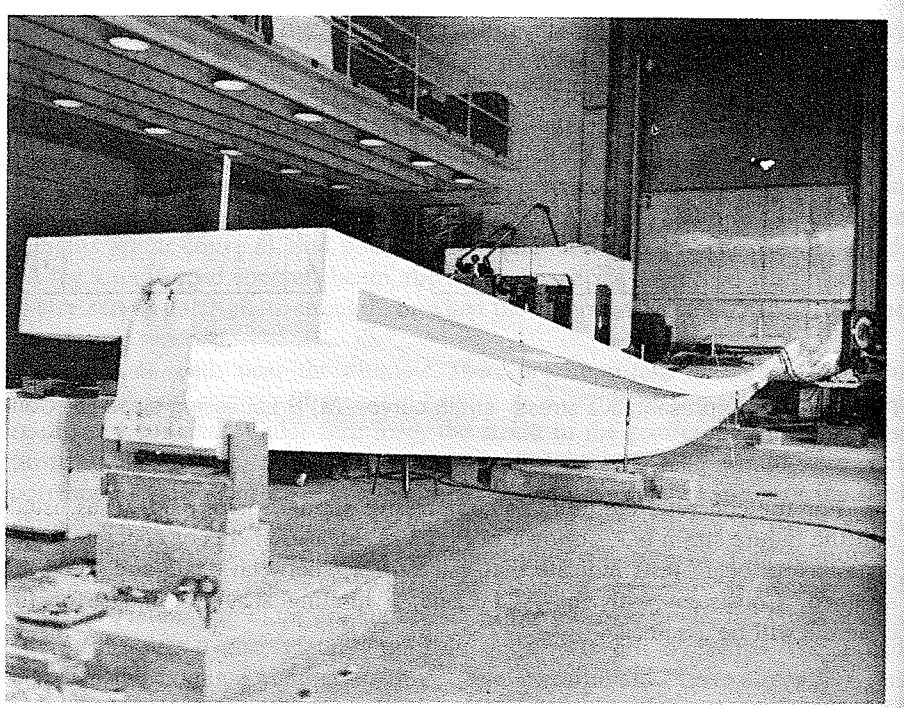

FIGURE 3.8 Flexural failure of bonded pretensioned beam. Courtesy of Portland Cement Association.

under- or over-reinforced members, the stress distribution at any stage can be found from the concrete stress–strain curve as follows.

Based on the usual assumption that plane cross sections of a beam remain plane as bending moment is applied, the concrete strains at any load stage vary linearly from zero at the neutral axis to a maximum at the top face. Consequently, the variation of compressive stress with distance from the neutral axis is identically the same as the variation of stress with strain indicated by the stress–strain curve, up to that strain corresponding to the maximum value, at the top face of the beam.

Accordingly, the stress distribution at stage (1) (Figs 3.9*a* or 3.9*b*) is approximately linear, whereas that at stage (2) shows a slight curvature near the top of the beam. At stage (3), the stress–strain curve up to the maximum stress f'_c is reproduced, but failure is not obtained until stage (4), when the maximum strain is equal to ε_{cu} and the entire stress–strain curve is reproduced.

Except in unusual cases, prestressed concrete beams are under-reinforced. When the concrete reaches its limiting strain, the steel stress f_{ps} will be between f_{py} and f_{pu}, as shown in Fig. 3.7*a*.

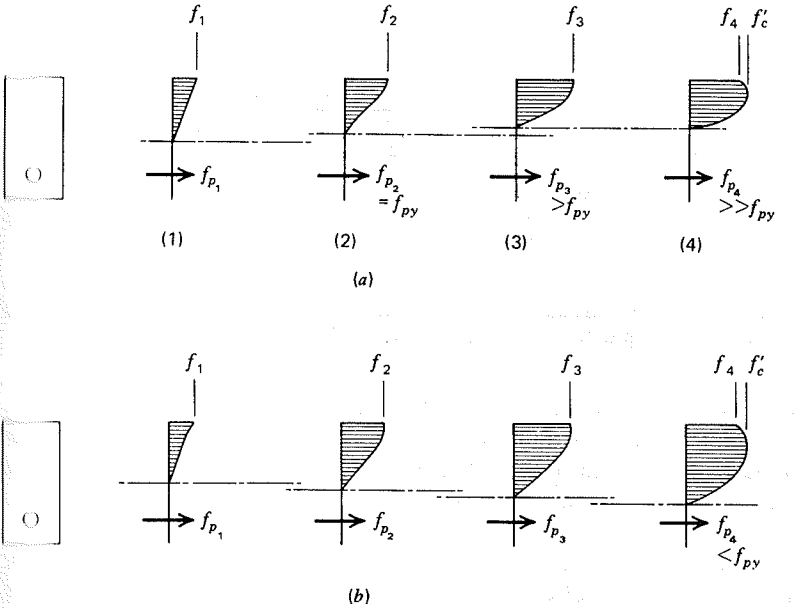

FIGURE 3.9 Successive flexural stress distributions as load is increased from cracking to ultimate loads. (*a*) Under-reinforced prestressed beam. (*b*) Over-reinforced prestressed beam.

It is interesting to observe that an over-reinforced prestressed beam, in which the steel stress is below yield at failure, can be transformed into an under-reinforced prestressed beam by increasing the intensity of prestress in the steel. Thus, it is evident that the distinction between an under- and over-reinforced prestressed beam depends, not only on the steel ratio and properties of the materials, as for a reinforced concrete beam, but on the intensity of prestress in the steel as well. But it must also be noted that, if the intensity of stress in the steel is to be increased, yet the same prestress force applied to the beam as before, a decrease in the steel area is required. It is actually this change that causes the beam to be under-reinforced, according to the definition given.

C. EQUIVALENT RECTANGULAR STRESS BLOCK

All that is needed to calculate the ultimate resisting moment of a prestressed concrete beam is the value of the compressive resultant C (which must equal the tensile force T) and the internal lever arm at failure.

If the concrete had a stress–strain curve that could be defined mathematically, it would be a simple matter to establish explicit relations for both the magnitude and location of C. However, as was discussed in Section 2.8, the shape

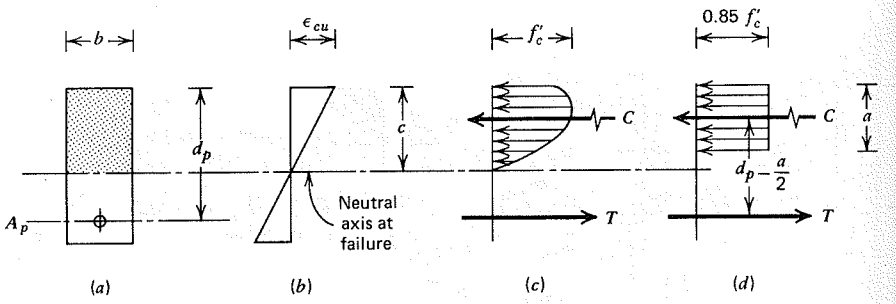

FIGURE 3.10 Strain and stress distributions at failure load. (*a*) Cross section. (*b*) Strains. (*c*) Actual stress distribution. (*d*) Equivalent rectangular distribution.

of the stress–strain curve for concrete varies greatly. For this reason, such explicit equations cannot be written. But the actual unknown distribution of concrete stress can be replaced with a simplified representation chosen so that (a) the correct value of C is obtained and (b) the force C acts at the correct level in the beam.

It has been found, using an approach combining analysis and experiment, that the actual distribution of compressive stress in the beam can be replaced by an equivalent rectangular stress distribution having a uniform stress intensity of $0.85f'_c$ and a depth a, as shown in Fig. 3.10. The relation between the equivalent and actual stress-block depths is

$$a = \beta_1 c \tag{3.11}$$

The value of β_1 has been established experimentally as given by the relation $\beta_1 = 0.85 - 0.05(f'_c - 4{,}000)/1{,}000$, where β_1 is not to exceed 0.85 and is not to be less than 0.65. Values for common concrete strengths are shown in Table 3.3.

A complete explanation of the equivalent rectangular stress block and its development is to be found in Ref. 3.1. It must be emphasized that the depth a is *not* the distance to the true neutral axis, nor are the concrete stresses actually distributed in the highly unlikely way suggested by Fig. 3.10*d*. The rectangular stress block is merely a computational device invented to give the correct answers, even though the actual distribution of concrete stress is not known in a particular case.

Table 3.3 Values of β_1 = Stress-Block Depth/Neutral Axis Depth

Concrete compressive strength f'_c	psi	3,000	4,000	5,000	6,000	7,000	≥ 8,000
	MPa	21	28	34	41	48	≥ 55
$\beta_1 = a/c$		0.85	0.85	0.80	0.75	0.70	0.65

D. EFFECTIVE FLANGE WIDTH

If the compression flange of a prestressed concrete beam is but little wider than the web, the entire flange can be considered effective in resisting the compressive force. However, for very wide flanges, the compressive stress in the flange is not uniform, but decreases with lateral distance from the web. This is so because of shearing deformation of the flange, which relieves the more remote elements of some compressive stress.

Although the actual longitudinal compression varies because of this effect, it is convenient in design to make use of an *effective flange width* that may be smaller than the actual flange width, but that is considered to be uniformly stressed. This effective width has been found to depend primarily on the beam span and on the relative thickness of the slab.

The recommendations for effective flange width for reinforced concrete that appear in the ACI Code are as follows:[3]

1. For symmetrical T beams the effective width b shall not exceed one-fourth the span length of the beam. The overhanging width $(b - b_w)/2$ on either side of the beam web shall not exceed 8 times the thickness of the slab, nor one-half the clear distance to the next beam.
2. For beams having a flange on one side only, the effective overhanging flange width shall not exceed one-twelfth the span length of the beam, nor 6 times the slab thickness, nor one-half the clear distance to the next beam.
3. For isolated beams in which the T form is used only for the purpose of providing additional compressive area, the flange thickness shall not be less than one-half the width of the web, and the total flange width shall not be more than 4 times the web width.

E. FLEXURAL STRENGTH BY STRAIN-COMPATIBILITY ANALYSIS

Strains and stresses in the concrete and steel at loading stages presently of interest are shown in Fig. 3.11. Strain distribution (1) of Fig. 3.11*a* results from application of effective prestress force P_e, acting alone, after all losses. At this stage, the stress in the steel and the associated strain, are respectively,

$$f_{pe} = \frac{P_e}{A_p} \tag{3.12}$$

$$\varepsilon_1 = \varepsilon_{pe} = \frac{f_{pe}}{E_p} \tag{3.13}$$

Steel strain, in Fig. 3.11*a*, is shown with respect to its own separate origin.

[3]Although these provisions "shall not apply to prestressed concrete," according to the ACI Code, no alternative recommendations are included; they are commonly used for prestressed concrete members, both in calculating stresses and strength. The Code Commentary notes that successful experience may provide the basis for variation in specific cases.

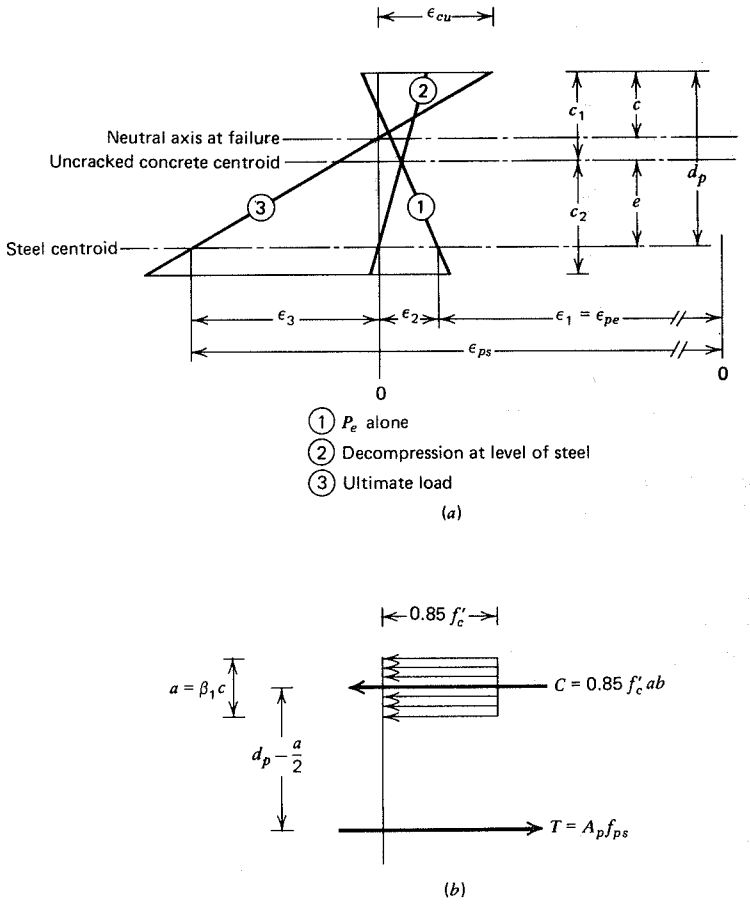

FIGURE 3.11 Strains and stresses as beam load is increased to failure. (*a*) Strains in concrete and steel. (*b*) Equivalent concrete stress distribution at failure.

Next, it is useful to consider an intermediate load stage (2) corresponding to decompression of the concrete at the level of the steel centroid. Assuming that bond remains intact between the concrete and steel, the increase in steel strain produced as loads pass from stage (1) to stage (2) is the same as the decrease in concrete strain at that level in the beam. It is given by the expression

$$\varepsilon_2 = \frac{P_e}{A_c E_c}\left(1 + \frac{e^2}{r^2}\right) \tag{3.14}$$

All terms are as defined earlier in this chapter.

When the member is overloaded to the failure stage (3), the neutral axis is at a distance c below the top of the beam. The increment of strain is

$$\varepsilon_3 = \varepsilon_{cu}\left(\frac{d_p - c}{c}\right) \tag{3.15}$$

The total steel strain at failure ε_{ps} is the sum of the three components just found from Eqs. (3.13), (3.14), and (3.15):

$$\varepsilon_{ps} = \varepsilon_1 + \varepsilon_2 + \varepsilon_3 \tag{3.16}$$

and the corresponding steel stress at failure is f_{ps}.

The depth of the compressive stress block at failure can be found from the equilibrium requirement that $C = T$. For a beam in which the compression zone is of constant width b

$$0.85f'_c\, ab = A_p f_{ps} \tag{3.17}$$

Solving this equation for the stress-block depth

$$a = \frac{A_p f_{ps}}{0.85f'_c b} = \beta_1 c \tag{3.18}$$

The resisting moment at failure is the product of the tensile (or compressive) force and the internal lever arm. For a member with constant width compression zone, referring to Fig. 3.11*b*, the nominal flexural strength is

$$M_n = A_p f_{ps}\left(d_p - \frac{a}{2}\right) \tag{3.19}$$

Equations (3.18) and (3.19) cannot be used directly to calculate the failure moment for a beam, because the steel stress f_{ps} at failure is unknown. An iterative solution can be devised, along the following lines:

1. Assume a reasonable value for the steel stress f_{ps} at failure, and note from the steel stress–strain curve the corresponding failure strain ε_{ps}.
2. Calculate the depth c to the actual neutral axis for that steel stress, using Eq. (3.18) based on horizontal equilibrium.
3. Calculate the incremental strain ε_3 from Eq. (3.15) and add this to the prior strains as indicated by Eq. (3.16).
4. If the failure strain ε_{ps} so obtained differs significantly from that assumed in step (1), revise that assumption and repeat steps (1) through (3) until satisfactory agreement is obtained.
5. With both $a = \beta_1 c$ and f_{ps} now known, calculate the ultimate flexural moment using Eq. (3.19).

It will be found that in most cases the iterative solution proposed converges quite rapidly and that often only two cycles are sufficient. An example of the calculation of ultimate flexural strength by the strain-compatibility method and iteration will be found following Section 3.8.

The method just described pertains to beams for which the width of the compression zone at failure is constant. Thus, it applies to rectangular section beams, and to T- and I-section beams for which the stress-block depth a is less than, or at the most equal to, the compression flange thickness. This is often the case.

For beams having a T or I-section and for which the stress-block depth is greater than the flange thickness, Eqs. (3.18) and (3.19) are not correct because of the irregular shape of the compression zone. However, the depth a can easily be found on the basis that the compression zone, when stressed uniformly to $0.85f_c'$, must provide a force equal to the tensile force $A_p f_{ps}$. The ultimate resisting moment is found taking the internal lever arm equal to the distance from the steel centroid to the centroid of the irregularly shaped compression zone.

The suitability of the equivalent rectangular stress block, with uniform stress of $0.85f_c'$, for determining the resisting moment of I- and T-sections may reasonably be questioned. Its experimental basis was developed with reference to rectangular section beams. However, comparison with results of extensive calculations based on stress distributions from actual compressive stress–strain curves (Ref. 3.2) indicates that use of the rectangular stress block for T- and I-section beams, as well as for beams of circular or triangular section, introduces only minor error and is fully justified.

The method for finding f_{ps} and M_n based on strain compatibility, using the iterative method just described, converges rapidly to satisfactory agreement between assumed and calculated values of ε_{ps}, after which M_n is easily found. If desired, iteration can be avoided using a graphical method to determine ε_{ps} and f_{ps} as follows.

From the *equilibrium* relation of Eq. (3.17),

$$f_{ps} = \frac{0.85f_c'ab}{A_p} \tag{a}$$

Substituting $A_p = \rho_p bd_p$ and $a = \beta_1 c$, this can be written

$$f_{ps} = \frac{0.85\beta_1 f_c'}{\rho_p} \times \frac{c}{d_p} \tag{b}$$

Then, combining the *geometric* relations of Eqs. (3.15) and (3.16),

$$\varepsilon_{ps} = \varepsilon_{pe} + \varepsilon_2 + \varepsilon_{cu}\frac{d_p - c}{c} \tag{c}$$

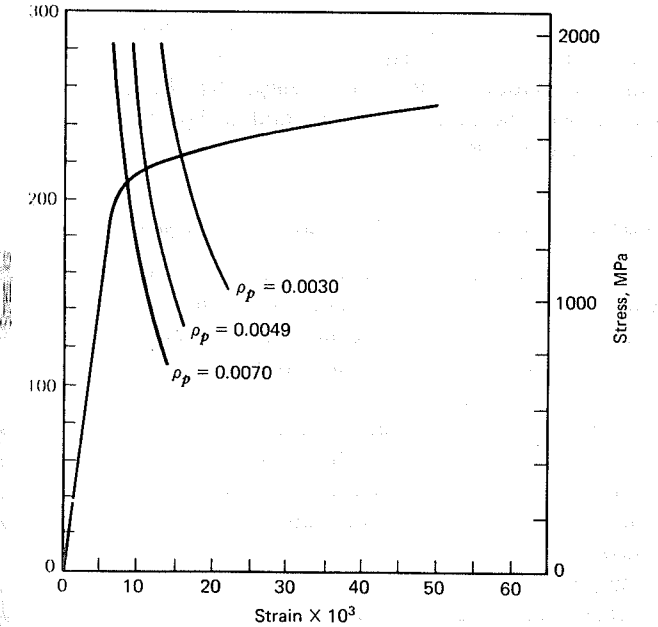

FIGURE 3.12 Stress in prestressed reinforcement at flexural failure by curve intersection.

from which

$$\frac{c}{d_p} = \frac{\varepsilon_{cu}}{\varepsilon_{cu} + \varepsilon_{ps} - \varepsilon_{pe} - \varepsilon_2} \tag{d}$$

Substituting (d) into (b), one obtains

$$f_{ps} = \frac{0.85\beta_1 f_c'}{\rho_p} \times \frac{\varepsilon_{cu}}{\varepsilon_{cu} + \varepsilon_{ps} - \varepsilon_{pe} - \varepsilon_2} \tag{3.20}$$

In Eq. (3.20), for a given concrete with known f_c', β_1, and ε_{cu}, with ε_{pe} and ε_2 also known, and for particular values of ρ_p, the steel stress at failure f_{ps} is a function of only one unknown, the steel strain at failure ε_{ps}. The relation between f_{ps} and ε_{ps}, for particular values of prestressing steel ratio ρ_p, can be plotted as in Fig. 3.12 to produce the family of curves shown. This set of curves defines points that satisfy the requirements of strain geometry and equilibrium at failure, for each specific steel ratio. The *stress–strain curve* for the prestressing steel is then superimposed. Stress and strain at failure must also fall on that curve. The intersection of the stress–strain curve with the applicable plot of Eq. (3.20) gives

the values f_{ps} and ε_{ps} that satisfy all conditions. The nominal flexural strength can then be found without difficulty using Eqs. (3.18) and (3.19).

An example of the calculation of flexural strength by the method just described will be found following Section 3.8. The method also provides the basis for design aids such as are found in Ref. 3.3.

F. FLEXURAL STRENGTH OF MEMBERS WITH UNBONDED TENDONS

The preceding analysis is applicable if the steel tendons are bonded to the concrete, so that no relative movement (slip) occurs between the two components. This is naturally the case for pretensioned beams, and is normally true for post-tensioned members in which the tendons are grouted after they are tensioned.

However, with some types of post-tensioned construction, such as when greased, plastic-sheathed tendons are used, or when tendons are located in the hollow cells of box girders, grouting is not possible. In the resulting members, where the steel is not bonded to the concrete, slip can occur between the two as flexural loading is applied.

The result is that the elongation of the steel is distributed over the entire length of the tendon, rather than being concentrated at the cracks as for bonded construction. The increase in steel strain and stress at the critical moment section is less than for a bonded beam, and the stress may be only slightly more than the effective prestress f_{pe} when the member fails. Failure in such case is characterized by a small number of rather wide cracks. The growth of such cracks causes a concentration of compression in the reduced area of concrete above the cracks, exceeding the capacity of the concrete to resist.

Tests indicate that the failure load of an unbonded beam may be only 75 to 80 percent of that for an otherwise identical bonded member (Ref. 3.4).

G. CONTRIBUTION OF NON-PRESTRESSED REINFORCEMENT

Prestressed concrete beams almost always contain a significant amount of non-prestressed reinforcing bars, as indicated in Fig. 3.13. Stirrups (a) are provided to resist shear and diagonal tensile stresses, as in ordinary reinforced concrete construction. Transverse bars (b) insure the integrity of thin projecting flanges or may be included (c) as an aid in positioning other steel during construction. Small diameter longitudinal bars (d) and (e) are included in post-tensioned members to control shrinkage cracking prior to tensioning the main steel and to aid in crack control in partially prestressed beams; the contribution to flexural resistance of these small longitudinal bars is usually not significant.

However, other non-prestressed bars (f) of larger diameter are often included in partially prestressed beams (see Section 3.9) to provide the required ultimate flexural strength, supplementing the contribution of the prestressed

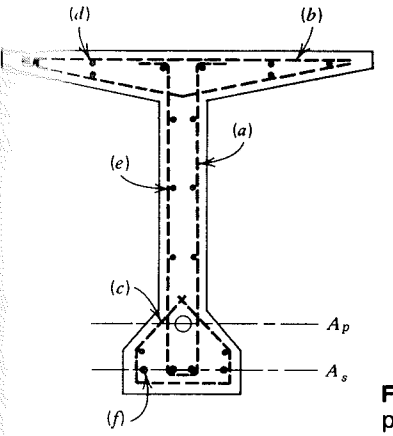

FIGURE 3.13 Cross section of post-tensioned beam.

tendons. Although the eccentricity of the prestressing tendons must be limited to avoid excessive tensile stresses at the top of the unloaded beam, the unstressed bars (f) can be placed as close to the tension face of the beam as permitted by requirements of concrete protection for the bars. In this way their contribution to flexural strength is maximized. Members in which substantial amounts of non-prestressed flexural reinforcement are present are sometimes referred to as *prestressed reinforced concrete beams* (Refs. 3.5 and 3.6).

The non-prestressed bars of area A_s (Fig. 3.13) will usually be stressed at or above their yield strength when the member is loaded to failure. The reason for this is evident from Fig. 3.14, in which the stress–strain curves for the non-prestressed and prestressed reinforcement are superimposed. When the tendon is at its effective stress f_{pe}, the reinforcing bars carry a compressive stress equal to n_s times the concrete compressive stress at the level of the steel, where $n_s = E_s/E_c$. (Effects of concrete shrinkage and creep are neglected here. See Ref. 3.16 for full discussion.) As the beam is overloaded to failure, both the tendon and the bar reinforcement experience the same strain increment $\Delta\varepsilon$ if they are at the same level in the member. If, as is often the case, the bars are at a greater depth than the tendon, they will experience a strain increment greater than that of the tendon. In either case, the strain increment $\Delta\varepsilon$ is sufficient to stress the bars past the tensile yield point except in unusual cases.

The inclusion of non-prestressed bars in a strain-compatibility analysis presents no serious complications. The modifications to be made will be discussed and illustrated by an example in Section 3.10 in connection with the treatment of partially prestressed beams, which usually contain a significant amount of tension bar reinforcement. In the ACI Code approximate approach to the calculation of ultimate flexural strength described in Section 3.8, such bars are assumed to act at their tensile yield stress.

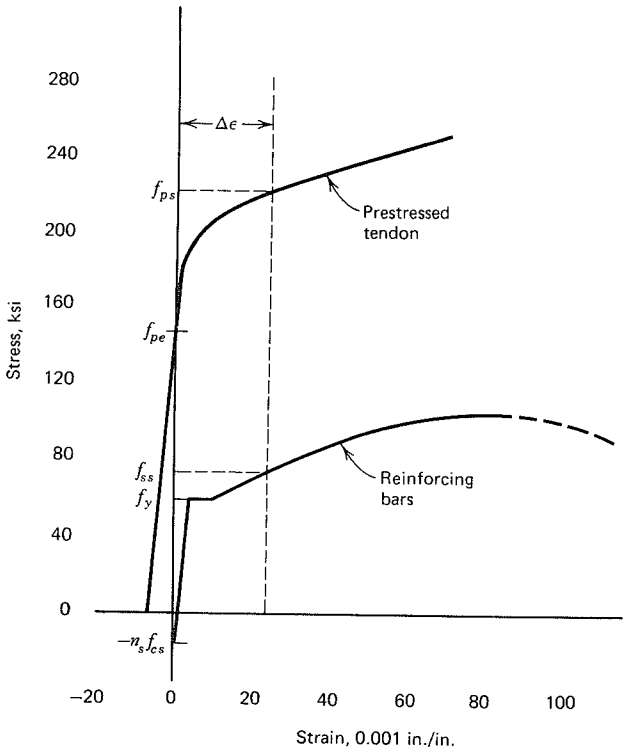

FIGURE 3.14 Superimposed stress – strain curves for reinforcing bars and tendons.

3.8 FLEXURAL STRENGTH BY ACI CODE EQUATIONS

According to the ACI Code, the flexural strength of prestressed concrete beams can be calculated using a strain-compatibility analysis such as described in Section 3.7. Alternatively, within certain limits, approximate equations for f_{ps} may be used to compute flexural strength. In practice, a strain-compatibility analysis is seldom required, and the ACI Code approximate approach or its equivalent is used.

A. STEEL STRESS f_{ps} AT FLEXURAL FAILURE

The ACI Code contains approximate equations for f_{ps}, the stress in the prestressed steel when the beam fails, based on a combination of test evidence and analysis. Code equations for f_{ps} can be applied only if f_{pe} is not less than $0.5f_{pu}$. In their general form, they apply to prestressed members that may also contain non-prestressed tension reinforcement, compression reinforcement, or both.

1. Members with Bonded Tendons but without Tension or Compression Rebars

For prestressed beams that do not contain supplementary bar reinforcement, or for cases where the contribution of such reinforcement to flexural strength can be neglected, the stress in the tendons at beam failure can be found from the following:

$$f_{ps} = f_{pu}\left(1 - \frac{\gamma_p}{\beta_1}\frac{\rho_p f_{pu}}{f'_c}\right) \tag{3.21}$$

In this equation, the prestressed reinforcement ratio is $\rho_p = A_p/bd_p$, in which d_p is the effective depth to the centroid of the prestressing steel. Differences in the stress–strain properties of low-relaxation wire and strand compared with ordinary steel require the introduction of the coefficient γ_p. Based on calculations using strain-compatibility analysis (see Ref. 3.7),

$\gamma_p = 0.40$ for f_{py}/f_{pu} not less than 0.85 (ordinary stress-relieved tendons)

$\gamma_p = 0.28$ for f_{py}/f_{pu} not less than 0.90 (low-relaxation wire and strands)

All other terms in Eq. (3.21) are as already defined.

2. Members With Bonded Tendons, Plus Tension or Compression Rebars

The influence of supplementary tension or compression bar reinforcement on the flexural strength of prestressed beams is accounted for in the ACI Code method, first by modifying the equation for f_{ps} (which will generally be lower for beams with tension rebars than for those without because of increase in depth to the neutral axis as A_s is added) and second, by including the forces in the rebars in computation of nominal flexural strength M_n. For beams containing supplementary bar reinforcement, the stress in the tendons can be calculated from:

$$f_{ps} = f_{pu}\left(1 - \frac{\gamma_p}{\beta_1}\left[\frac{\rho_p f_{pu}}{f'_c} + \frac{d}{d_p}(\omega - \omega')\right]\right) \tag{3.22}$$

In Eq. (3.22),

d = effective depth to non-prestressed tension steel

d_p = effective depth to prestressing steel

$\omega = \rho f_y/f'_c$

$\omega' = \rho' f_y/f'_c$

where $\rho = A_s/bd$ and $\rho' = A'_s/bd$ as usual for reinforced concrete beams. Other terms in Eq. (3.22) have already been defined. If compression steel has been taken into account when calculating f_{ps} by Eq. (3.22), the term in square brackets is not to be taken less than 0.17, and depth d' to the compression bars must not be greater than 0.15 d_p, according to Code.

3. Members With Unbonded Tendons and a Span-to-Depth Ratio of 35 or Less

It was pointed out in Section 3.7F that for members in which the tendons are not bonded to the concrete along their length, the increase in tendon stress as the beam is loaded to failure is much less than otherwise. The beam span-to-depth ratio has been found by tests to be a significant parameter also (Refs. 3.8 and 3.9). According to ACI Code, for unbonded beams with span-to-depth ratio of 35 or less (this is typical of most ordinary beams):

$$f_{ps} = f_{pe} + 10{,}000 + \frac{f'_c}{100\rho_p} \tag{3.23}$$

with the restriction that f_{ps} in Eq. (3.23) shall not be greater than f_{py}, nor greater than $(f_{pe} + 60{,}000)$.

4. Members With Unbonded Tendons and a Span-to-Depth Ratio Greater than 35.

For slabs, the span-to-depth ratio is usually greater than 35, and often as high as 50. It has been found that for such cases, the increase in stress in the tendons is less than that for less slender members. Accordingly, the ACI Code provides that for such cases,

$$f_{ps} = f_{pe} + 10{,}000 + \frac{f'_c}{300\rho_p} \tag{3.24}$$

with the restrictions that f_{ps} in Eq. (3.24) shall not be greater than f_{py}, nor greater than $(f_{pe} + 30{,}000)$.

B. FLEXURAL STRENGTH

The flexural strength of prestressed beams is computed, according to ACI Code, by the same methods as are used for ordinary reinforced concrete members, with appropriate changes in detail. The stress f_{ps} in the tendons at failure is determined by the applicable equation from Section 3.8A. Non-prestressed bar reinforcement, if present on the tension side of the beam, is assumed to contribute to flexural strength acting at its yield stress f_y.

1. Rectangular Cross Sections

For beams with rectangular cross sections (or for T- or I-beams in which the stress-block depth falls within the thickness of the compression flange) and containing no supplementary reinforcing bars on the tension side, according to the ACI Code Commentary, the nominal flexural strength is

$$M_n = A_p f_{ps}\left(d_p - \frac{a}{2}\right) \tag{3.25}$$

where

$$a = \frac{A_p f_{ps}}{0.85 f'_c b} \tag{3.26}$$

Equations (3.25) and (3.26) are identical to Eqs. (3.19) and (3.18), respectively. For design purposes, according to the Code, the nominal strength is to be multiplied by the strength reduction factor ϕ to obtain the design strength

$$\phi M_n = \phi A_p f_{ps}\left(d_p - \frac{a}{2}\right) \tag{3.27}$$

where $\phi = 0.90$ for flexure.

If non-prestressed reinforcing bars are included on the tension side of the beam, the nominal flexural strength is

$$M_n = A_p f_{ps}\left(d_p - \frac{a}{2}\right) + A_s f_y\left(d - \frac{a}{2}\right) \tag{3.28}$$

where

$$a = \frac{A_p f_{ps} + A_s f_y}{0.85 f'_c b} \tag{3.29}$$

If, in addition to prestressed and non-prestressed tension reinforcement, the beam contains reinforcing bars in the compression zone, the influence of those bars on flexural strength can be found using a strain-compatibility analysis to find the steel stress in all reinforcement at failure. Alternatively, the ACI Code Commentary includes additional provisions for such a case. In most cases, the contribution of those bars to flexural strength can be neglected.

2. Flanged Sections with Stress-Block Depth Greater Than Flange Thickness

For flanged sections, the depth of the stress block may be greater than the thickness of the flange. If so, the equations for flexural strength must be modified

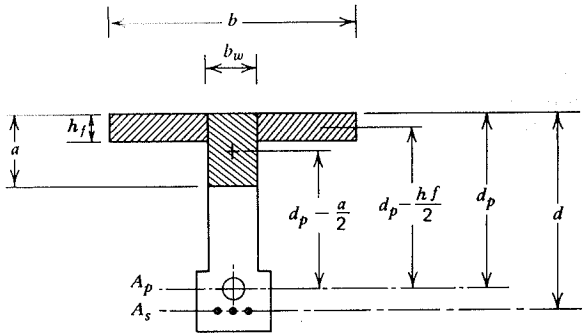

FIGURE 3.15 Division of compression zone of flanged beam for computation of ultimate resisting moment.

to account for the nonrectangular shape of the compression zone. Whether or not this must be considered can easily be determined by calculating the stress-block depth a, assuming that rectangular beam analysis applies, using either Eq. (3.26) or Eq. (3.29), whichever is applicable. Depth a is then compared with the flange thickness h_f. If a is greater than h_f, the calculation is invalid and the flanged section equations for flexural strength must be used. They are developed as follows.

The total compression force in the beam section is divided for computational purposes into two parts. The first, the compression in the overhanging portion of the flange, is equilibrated by a part of the total tension force. This partial tension is defined as $A_{pf}f_{ps}$. Accordingly,

$$A_{pf}f_{ps} = 0.85f_c'(b - b_w)h_f \tag{3.30}$$

where all geometric terms are defined in Fig. 3.15. This flange force provides a resisting moment, with the internal lever arm measured to the centroid of the prestressing steel, of $(d_p - h_f/2)$. The remaining part of the total tension force $(A_pf_{ps} + A_sf_y)$ is equilibrated by the compression in the beam web, and is defined as $A_{pw}f_{ps}$. Thus, we define

$$A_{pw}f_{ps} = A_pf_{ps} + A_sf_y - A_{pf}f_{ps} \tag{3.31}$$

The compression force in the web, which is equal to this partial tension, has internal lever arm, measured to the centroid of the prestressing steel, of $(d_p - a/2)$, where

$$a = \frac{A_{pw}f_{ps}}{0.85f_c'b_w} \tag{3.32}$$

The final contribution to the resisting moment is provided by the non-prestressed tension reinforcement, if any, contributing a force A_sf_y acting at a distance $(d - d_p)$ from the center of moments at the prestressing steel centroid.

The total resisting moment at failure is found by summing the contributions of the three parts:

$$M_n = A_{pw}f_{ps}\left(d_p - \frac{a}{2}\right) + A_sf_y(d - d_p) + A_{pf}f_{ps}\left(d_p - \frac{h_f}{2}\right) \tag{3.33}$$

For design purposes, as usual, the flexural resistance is assumed equal to ϕM_n with $\phi = 0.90$.

C. LIMITS FOR REINFORCEMENT

To ensure that prestressed concrete beams, if overloaded, shall have a ductile response before failure, it is desirable to place an upper limit on the tensile steel ratio, thereby ensuring that the steel will be stressed at least to its yield stress when the beam fails. Such a requirement is analogous to that imposed in the design of ordinary reinforced concrete beams, for which the tensile steel ratio must not exceed three-fourths of the balanced value, according to Code.

For prestressed concrete beams, based on an effective prestress f_{pe} of $0.60f_{pu}$, reasonably typical of beams in practice, it is shown in Ref. 3.7 that upper limits should be placed on the reinforcement indices as follows.

For rectangular sections with prestressing steel only:

$$\omega_p = 0.36\beta_1 \tag{3.34a}$$

where

$$\omega_p = \rho_p f_{ps}/f_c'$$

For rectangular sections with prestressing steel and non-prestressed reinforcement:

$$\omega_p + \frac{d}{d_p}(\omega - \omega') = 0.36\beta_1 \tag{3.34b}$$

where

$$\omega = \rho f_y/f_c'$$

$$\omega' = \rho' f_y/f_c'$$

For flanged sections:

$$\omega_{pw} + \frac{d}{d_p}(\omega_w - \omega'_w) = 0.36\beta_1 \qquad (3.34c)$$

In Eq. (3.34c), the reinforcement indices for flanged sections are calculated using steel ratios ρ based on the web width b_w, rather than beam width b as for rectangular sections. In all of the equations above, flanged sections with stress-block depth equal to or less than flange thickness are treated as rectangular sections.

If a reinforcement index greater than that determined by these equations is used, the nominal flexural strength is calculated based on the compression portion of the moment couple. It is shown in Ref. 3.7 (see ACI Code Commentary also) that this nominal flexural strength is:

For rectangular sections or flanged sections in which a does not exceed h_f:

$$M_n = f'_c b d_p^2 (0.36\beta_1 - 0.08\beta_1^2) \qquad (3.35a)$$

For flanged sections in which a exceeds h_f:

$$M_n = f'_c b_w d_p^2 (0.36\beta_1 - 0.08\beta_1^2) + 0.85 f'_c (b - b_w) h_f \left(d_p - \frac{h_f}{2}\right) \qquad (3.35b)$$

Nominal flexural strengths are to be multiplied by ϕ to obtain design strengths. Although the usual value of $\phi = 0.90$ for flexure is often applied, for prestressed beams in which compression controls, it appears more rational to use $\phi = 0.70$ as used elsewhere for axial load plus flexure.

As a precaution against abrupt flexural failure resulting from rupture of the prestressing steel immediately on flexural cracking of the beam, the ACI Code requires that the ultimate resisting moment be at least 1.2 times the cracking moment, calculated using a modulus of rupture of $7.5\sqrt{f'_c}$ (see Section 3.6). An exception to this requirement is permitted if the flexural and shear strengths of the member are at least twice that required.

EXAMPLE: Ultimate Flexural Capacity by Strain-Compatibility Analysis with Iteration

Using the strain-compatibility method of Section 3.7E, find the ultimate moment capacity for the I-beam example of Section 3.4, shown in Figs. 3.4 and 3.16. Normal density concrete is to be used, with compressive strength $f'_c = 4{,}000$ psi and elastic modulus $E_c = 3.61 \times 10^6$ psi. The ultimate strain-capacity of the concrete is $\varepsilon_{cu} = 0.0030$, and $\beta_1 = 0.85$. The beam is pretensioned, using seven ordinary Grade 250

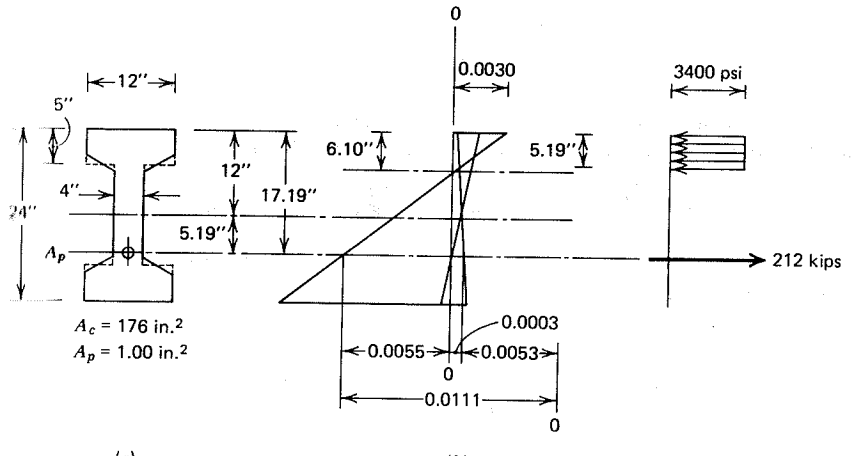

FIGURE 3.16 Flexural strength analysis of I-beam. (*a*) Cross section. (*b*) Strains in concrete and steel. (*c*) Stress and steel force.

$\frac{1}{2}$-in. diameter seven-wire strands, for which the stress–strain curve is as shown in Fig. 2.4. The effective prestress force $P_e = 144$ kips as for the previous example ($f'_c = 28$ MPa, $E_c = 24{,}890$ MPa, and $P_e = 641$ kN).

From Table 2.2 the cross-sectional area of one $\frac{1}{2}$-in. strand is 0.144 in.^{2}; hence

$$A_p = 7 \times 0.144 = 1.008 \text{ in.}^2$$

The stress and strain in the tendons resulting from the effective prestress force are, respectively,

$$f_{pe} = \frac{P_e}{A_p} = \frac{144}{1.008} = 143 \text{ ksi}$$

$$\varepsilon_{pe} = \frac{f_{pe}}{E_p} = \frac{143}{27{,}000} = 0.0053 = \varepsilon_1$$

The increase in steel strain as the concrete at its level is decompressed is found from Eq. (3.14)

$$\varepsilon_2 = \frac{P_e}{A_c E_c}\left(1 + \frac{e^2}{r^2}\right) = \frac{144}{176 \times 3.61 \times 10^3}\left(1 + \frac{5.19^2}{68.2}\right) = 0.0003$$

The steel stress at failure will initially be assumed to be 200 ksi. From Fig. 2.4 the corresponding strain is $\varepsilon_{ps} = 0.0070$. Assuming that the stress-block depth is less than the average flange thickness of 5 in., its depth is calculated using Eq. (3.18):

$$a = \frac{A_p f_{ps}}{0.85 f'_c b} = \frac{1.008 \times 200}{0.85 \times 4 \times 12} = 4.94 \text{ in.}$$

and the actual neutral axis location is

$$c = \frac{4.94}{0.85} = 5.81$$

below the top surface. Next, the increment of steel strain as the beam passes from the decompression stage to failure is found, using Eq. (3.15):

$$\varepsilon_3 = \varepsilon_{cu}\frac{d_p - c}{c} = 0.0030 \times \frac{17.19 - 5.81}{5.81} = 0.0059$$

and the total steel strain at failure, found from the sum of the three parts, as indicated by Eq. (3.16) is

$$\begin{aligned}\varepsilon_{ps} &= \varepsilon_1 + \varepsilon_2 + \varepsilon_3 \\ &= 0.0053 + 0.0003 + 0.0059 \\ &= 0.0115\end{aligned}$$

which must be compared with the strain of 0.0070 assumed at the start. Clearly, a revised estimate is required.

For the second trial, a steel failure stress of 210 ksi is assumed, with corresponding strain of 0.0095. The stress-block depth in this case is

$$a = 4.94 \times \frac{210}{200} = 5.19$$

$$c = \frac{5.19}{0.85} = 6.10$$

and the incremental strain in the tendon

$$\varepsilon_3 = 0.0030 \times \frac{17.19 - 6.10}{6.10} = 0.0055$$

as shown in Fig. 3.16*b*. The total steel strain at failure is thus

$$\begin{aligned}\varepsilon_{ps} &= 0.0053 + 0.0003 + 0.0055 \\ &= 0.0111\end{aligned}$$

compared with the assumed value of 0.0095. It is clear from inspection of the stress–strain curve that further refinement would result in negligible change in the failure stress in the steel. The stress at failure is very close to 210 ksi (1,450 MPa) and the nominal strength, from Eq. (3.19) is

$$\begin{aligned}M_n &= A_p f_{ps}\left(d_p - \frac{a}{2}\right) \\ &= 1.008 \times 210\left(17.19 - \frac{5.19}{2}\right) \\ &= 3{,}089 \text{ in.-kips} \\ &= 257 \text{ ft-kips (348 kN-m)}\end{aligned}$$

Additional Comments

1. Although the stress-block depth exceeds the thickness of the outer portions of the flange, it is about equal to the average thickness; refinement to account for the actual shape of the compression zone would have little effect on results in this case.
2. The steel strain increment ε_2 caused by decompression of the concrete is very small compared with ε_1 and ε_3. Neglect of this quantity would have little influence on results.
3. The steel strain at failure is close to that corresponding to the yield stress. Consequently, very little elongation of the steel would occur, should the beam be overloaded, prior to abrupt crushing of the concrete. From the viewpoint of safety, the design could be improved if a more ductile failure mode could be insured. Such modifications will be explored in Chapter 4.

EXAMPLE: Ultimate Flexural Capacity by Strain Compatibility Analysis Using Graphical Solution for Steel Stress

Find the ultimate moment capacity of the beam just considered, determining the stress in the prestressed reinforcement at failure by graphical rather than iterative means.

From Eq. (3.20), with $\rho_p = 1.008/(12 \times 17.19) = 0.0049$, one obtains

$$f_{ps} = \frac{0.85 \times 0.85 \times 4{,}000}{0.0049} \times \frac{0.003}{0.003 + \varepsilon_{ps} - 0.0053 - 0.0003}$$

or

$$f_{ps} = \frac{1{,}770}{\varepsilon_{ps} - 0.0026}$$

This relationship, combining the requirements of equilibrium and strain compatibility, is plotted in Fig. 3.12 for the strain range of interest, and is labelled $\rho_p = 0.0049$. Also shown in Fig. 3.12 is the stress–strain curve for the prestressing strand, reproduced exactly from Fig. 2.4. The single stress that satisfies all requirements is found from the intersection of the stress–strain curve with the curve plotted for Eq. (3.20), and has a value $f_{ps} = 216$ ksi, compared with the approximate value of 210 ksi found by iteration in the previous example. The true depth of the compressive stress block is

$$a = \frac{1.008 \times 216}{0.85 \times 4 \times 12} = 5.34 \text{ in.}$$

The nominal flexural strength of the beam can then be found from Eq. (3.19) to be

$$\begin{aligned}M_n &= 1.008 \times 216\left(17.19 - \frac{5.34}{2}\right) \\ &= 3{,}160 \text{ in.-kips} \\ &= 263 \text{ ft-kips (357 kN-m)}\end{aligned}$$

The approximate value of 257 ft-kips found in the preceding example by iteration agrees within 2 percent.

EXAMPLE: Ultimate Flexural Capacity by ACI Equations

Find the ultimate moment capacity of the beam just considered by using the approximate ACI equations.

The ratio of effective prestress to ultimate strength of the steel is

$$\frac{f_{pe}}{f_{pu}} = \frac{143}{250} = 0.57 > 0.50$$

Consequently, Eq. (3.21) may be used to obtain the approximate value of steel stress at failure. With steel ratio

$$\rho_p = \frac{A_p}{bd_p} = \frac{1.008}{12 \times 17.19} = 0.0049$$

the failure stress, by Eq. (3.21) is

$$f_{ps} = f_{pu}\left(1 - \frac{\gamma_p}{\beta_1}\frac{\rho_p f_{pu}}{f'_c}\right)$$

$$= 250\left(1 - \frac{0.40}{0.85}\frac{0.0049 \times 250}{4}\right) = 214 \text{ ksi}$$

The prestressed reinforcement index for this beam is

$$\omega_p = \frac{\rho_p f_{ps}}{f'_c} = 0.0049 \times \frac{214}{4} = 0.26$$

This does not exceed the limit value of $0.36\beta_1 = 0.36 \times 0.85 = 0.31$, so the beam is classed as under-reinforced, according to the Code, and either Eq. (3.25) or Eq. (3.33) is applicable. To determine which equation to use, one calculates the depth of the stress block using Eq. (3.26), which is based on stress-block depth less than or equal to flange thickness.

$$a = \frac{1.008 \times 214}{0.85 \times 4 \times 12} = 5.29 \text{ in.}$$

Because this exceeds the average flange thickness, Eq. (3.33) for flanged sections must be used to calculate M_n, according to Code. From Eq. (3.30)

$$A_{pf} f_{ps} = 0.85 \times 4(12 - 4) \times 5 = 136 \text{ kips}$$

and from Eq. (3.31)

$$A_{pw} f_{ps} = 1.008 \times 214 - 136 = 80 \text{ ksi}$$

The stress-block depth within the web is found from Eq. (3.32):

$$a = \frac{80}{0.85 \times 4 \times 4} = 5.88 \text{ in.}$$

after which the nominal flexural strength is easily found from Eq. (3.33):

$$M_n = 80\left(17.19 - \frac{5.88}{2}\right) + 136\left(17.19 - \frac{5}{2}\right)$$

$$= 3{,}140 \text{ in.-kips}$$

$$= 262 \text{ ft-kips (355 kN-m)}$$

Additional Comments

1. The predicted failure moment of 262 ft-kips according to the ACI approximate method is very close to the value of 263 ft-kips obtained by the more exact strain-compatibility analysis. Agreement will not always be so good, particularly for beams with high steel ratios.
2. Although a flanged-beam analysis is indicated by the Code equation, the depth of the stress block in the web, when calculated, is actually nearly equal to the flange thickness of 5 in. This indicates that an analysis based on a constant width compression zone would have been suitable, as was used for the strain-compatibility analysis.
3. Whichever method is used to calculate the nominal flexural strength M_n, that value must be reduced by the factor ϕ to obtain the design strength ϕM_n.

3.9 PARTIAL PRESTRESSING

Early in the development of prestressed concrete, the goal of prestressing was the complete elimination of concrete tensile stress at service loads. The concept was that of an entirely new, homogeneous material that would remain uncracked and respond elastically up to the maximum anticipated loading. This kind of design, where the limiting tensile stress in the concrete at full service load is zero, is generally known as *full prestressing*, whereas an alternative approach, in which flexural tension, and usually some cracking, are permitted in the concrete at normal service load, is called *partial prestressing*.[4]

There are cases in which it is necessary to avoid all risk of cracking and in which full prestressing is required. Such cases include tanks or reservoirs where leaks must be avoided, submerged structures or those subject to a highly corrosive environment where maximum protection of reinforcement must be insured, and structures subject to high frequency repetition of load where fatigue of the reinforcement may be a consideration.

However, there are many cases where substantially improved performance, reduced cost, or both may be obtained through the use of a lesser amount of prestress. Fully prestressed beams may exhibit an undesirable amount of upward camber because of the eccentric prestressing force, a displacement that is only partially counteracted by the gravity loads producing downward deflection. This tendency is aggravated by creep in the concrete, which magnifies the upward displacement due to the prestress force, but has little influence on the downward deflection due to live loads, which may be only intermittently applied. Also, should heavily prestressed members be overloaded and fail, they may do so in a

[4]The pioneer designer Freyssinet was originally a strong advocate of full prestressing, although in later years he modified his position, indicating that concrete tensile stress somewhat in excess of the modulus of rupture was quite appropriate for bridge structures, for example, where the maximum load occurred only rarely.

brittle way, rather than gradually as do beams with a smaller amount of prestress. This is important from the point of view of safety, because sudden failure without warning is dangerous, and gives no opportunity for corrective measures. Furthermore, fully prestressed beams may show other undesirable side effects, such as severe longitudinal shortening and substantial loss of prestress.

Although concrete cracking may be allowed at full service load, it is also recognized that such full service load may be infrequently applied. The more typical load acting is likely to be the dead load plus a small fraction of the specified live load. Thus, a partially prestressed beam may not be subject to tensile stress under the usual conditions of loading. Cracks may form occasionally, when full service load is applied, but these will close completely when that load is removed. They may be no more objectionable in prestressed structures than in ordinary reinforced concrete, in which flexural cracks always form. They may be considered a small price to pay for the improvements in performance and economy that are obtained.

Partial prestressing was pioneered in Europe by Abeles (Refs. 3.10 to 3.12; see also Ref. 3.4 to 3.6). There is increasing use of partial prestressing in the United States. It has been observed that reinforced concrete, on the one hand, and fully prestressed concrete, on the other hand, are merely the two extreme cases of the broad class of steel-reinforced concrete systems. Partially prestressed concrete represents everything between these limit cases (Ref. 3.13).

Load-deflection relations for beams with a varying amount of prestress force are presented in a qualitative way in Fig. 3.17. Both reinforced concrete and prestressed concrete beams may be *under-reinforced* with a relatively small steel area such that failure is preceeded by yielding of the steel, or *over-reinforced*, with a relatively large steel area so that failure is initiated by crushing of the concrete on the compression side of the member before the steel reaches its yield stress. In each case, the amount of prestress force introduced by the given steel area may vary from zero (reinforced concrete) to a very large value (over-prestressing).

Figure 3.17*a* shows load-deflection curves for under-reinforced beams, all with the same steel area and concrete dimensions but varying amounts of prestress. The dotted lines represent load-deflection curves calculated using the flexural rigidity of the uncracked transformed cross section (E_cI_{ut}) and that of the cracked transformed cross section (E_cI_{ct}). The load causing failure is about the same in all cases. Beam (a), with zero prestress, responds linearly up to its cracking load, after which its load-deflection curve is approximately linear and parallel to the E_cI_{ct} line. Obviously for the beams (b), (c), and (d) that are prestressed, the load causing cracking is higher because initial compression stresses are superimposed in the tension zone. The location of the point of departure from the line E_cI_{ut} depends on the degree of prestress. Beam (b) represents a partially prestressed beam, in which cracking may occur below full service load, whereas beam (c) is fully prestressed, with zero tensile stress at service load, cracking only when a higher load is reached. Beam (d) is over-

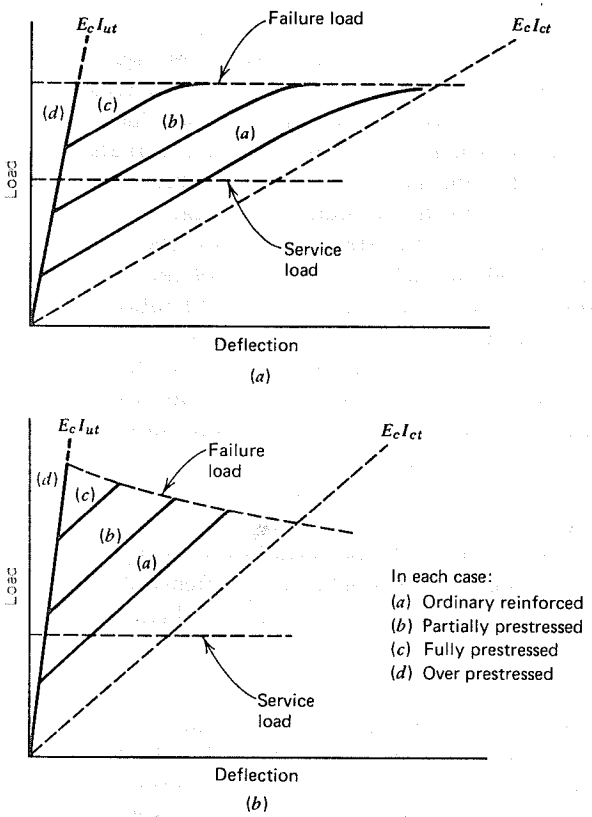

FIGURE 3.17 Idealized load-deflection curves for beams with varying amounts of prestress force. Adapted from Ref. 3.10. (*a*) Under-reinforced beams. (*b*) Over-reinforced beams.

prestressed, and will fail suddenly in a brittle fashion. As shown in the figure, for under-reinforced beams there is normally a further change in slope of the load-deflection curve before failure, as the steel is stressed to its inelastic range, and as extensive cracking occurs.

The corresponding curves for over-reinforced beams are given by Fig. 3.17*b*. Such beams may also have zero prestress or may be partially, fully, or overprestressed, the degree of prestressing determining the cracking load as before. However, after cracking, the curves follow more or less parallel to the E_cI_{ct} line all the way to failure. They fail suddenly and with much less warning than before. The effect of varying the prestress is similar to that for under-reinforced beams, except that the load that causes failure increases to some extent as the prestress force is increased (Refs. 3.10 and 3.11).

One may speak of the *ductility* of a prestressed concrete beam when referring to its capacity to deflect extensively before failure. It is clear from Fig. 3.17 that, as a class, under-reinforced beams are more ductile than over-reinforced beams, and that in either case, partially prestressed beams exhibit more ductility than fully or over-prestressed beams. The capacity of flexural members to absorb the energy of impact is directly related to the area under its load-deflection diagram. The advantage of partial prestressing, in this respect, is also clear.

The choice of a suitable amount of prestress, as Abeles has observed, is governed by a variety of factors. These include the nature of the loading (for example, highway or railroad bridges, storage, and so on), the ratio of live to dead load, the frequency of occurrence of the full load, and the presence of corrosive agents. With structures in which the direction of loading may be reversed, such as in transmission poles (see Chapter 13), a high uniform prestress would result in reduced ultimate strength and in brittle failure. In such a case, partial prestressing provides the only satisfactory solution.

Regardless of the amount of prestress force selected, the tensile steel must provide a total tension force, on overloading of the beam, that will develop the needed flexural strength. A member designed for partial prestressing, using the full allowable initial stress to determine the tendon area A_p, often will not satisfy strength requirements without modification. There are at least three alternatives in modifying the design:

1. Increase the tendon area to that required by conditions at ultimate, using initial tension less than the allowed limit to give the desired initial prestress.
2. Increase the tendon area according to requirements at ultimate, but stress only a part of the tendons to the allowed initial value, leaving the remainder unstressed.
3. Provide the needed tension force at ultimate by a combination of tendons, stressed initially to the full allowable value, and non-prestressed bar reinforcement.

Alternatives 1 or 2 are generally favored for pretensioned, precast beams. Strands are much stronger than rebars, so a smaller area can be used, requiring less space in the forms. If unstressed strand is used (Alternative 2), short pieces of strand can be utilized that would otherwise be wasted. Strands tensioned below their full allowable value (Alternative 1) will experience lower relaxation loss. The third alternative is usually more economical for post-tensioned beams, because it reduces the number of tendon anchorages and field jacking operations. It will be shown in Section 3.10 (see Fig. 3.14 also) that, when non-prestressed bars are used in this way, they will almost always be stressed to their full yield strength when the beam fails.

The ACI Code permits concrete tension of $6\sqrt{f_c'}$ at full service load, slightly less than the usual modulus of rupture, and requires the inclusion of sufficient bonded reinforcement in the tension zone to control cracking. If explicit calculation of deflection due to immediate and sustained loads indicates that those deflections are within allowable limits, and if the concrete protection for the reinforcement is increased above the usual limit, the Code permits an allowable tensile stress of $12\sqrt{f_c'}$ (see Table 3.1). Both stresses are equivalent to partial prestressing, according to the definition given earlier.

In each case, according to present United States practice, the stresses are calculated on the basis of properties of the uncracked cross section. It is clear, then, that the higher stress limit represents only a *nominal stress*, since it is well above the modulus of rupture. The justification for basing calculations on the uncracked section, in such a case, is that sufficient bonded steel is present to confine and control cracking, and that the overall performance of the member at that load is approximately what it would be if the concrete could, in fact, develop the nominal tensile stress.

After the member has cracked, if both concrete and steel stresses remain in the elastic range, stresses may be computed using properties of the cracked transformed cross section (Ref. 3.14). Such calculations are described in the following section.

3.10 ELASTIC FLEXURAL STRESSES AFTER CRACKING AND STRENGTH OF PARTIALLY PRESTRESSED BEAMS

At the full service load stage, partially prestressed beams are usually cracked, although generally both concrete and steel stresses remain within the elastic range. Although service load stresses at a cracked cross section may properly be considered of secondary importance, compared with the strength and safety of the member should it be overloaded, calculation of stresses may be required for several reasons:

1. For prestressed members, crack widths at service load are related to the increase in steel stress past the stage of concrete decompression; consequently, the service load steel stress must be known as well as the stress at decompression.
2. An accurate calculation of both elastic and creep deflection at service load requires that curvatures be based on actual, not nominal, stress and strain distributions.
3. If fatigue is a factor in design, it is necessary to determine actual stress ranges in both concrete and steel.
4. It may be necessary to compute stresses in the cracked section to demonstrate compliance with design codes. (The ACI Code does not require this.)

For an ordinary reinforced concrete beam, calculation of stresses at a cracked section is a simple matter. The transformed section concept permits use of the familiar equations of mechanics for homogeneous elastic beams to locate neutral axis, determine section properties, and calculate stresses. Alternately, explicit equations may be derived for nonhomogeneous reinforced concrete sections (Ref. 3.1).

For cracked prestressed concrete beams, matters are more complicated. The neutral axis location and effective section properties depend not only on the

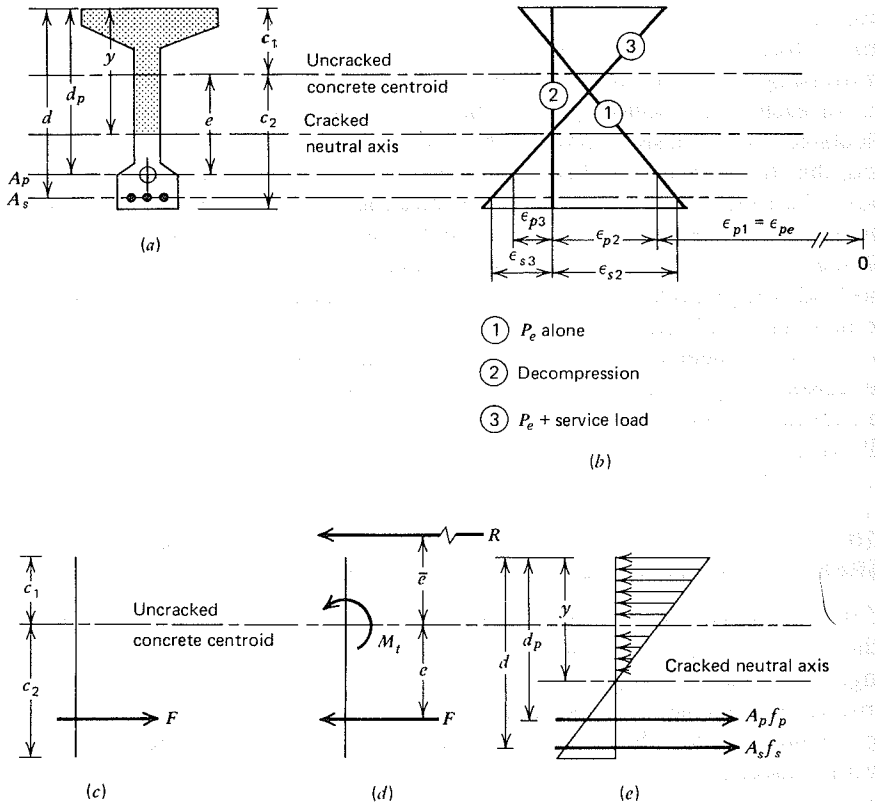

FIGURE 3.18 Basis for analysis of cracked cross section. (*a*) Cracked cross section. (*b*) Concrete and steel strains. (*c*) Decompression force. (*d*) Forces on cracked section. (*e*) Resulting stresses.

geometry of the cross section and the material properties, as for reinforced concrete beams, but also on the axial prestressing force and the loading. The axial prestressing force and the loading. The axial force is not constant after cracking, but depends on the loading and the section properties.

The effective cross section of a typical partially prestressed beam at service load is shown in Fig. 3.18*a*. The member shown includes both prestressed steel of area A_p and non-prestressed bar reinforcement of area A_s, as is commonly the case. It is assumed that the member has cracked, that both concrete and steel are stressed only within their elastic ranges, and that the contribution of the tensile concrete can be disregarded.

The strains and stresses in the concrete and steel will be considered at several load stages, certain of which are not actually experienced by the member, but are considered only as a computational convenience (Refs. 3.14 and 3.15).

Load stage (1) (Fig. 3.18*b*) corresponds to application of effective prestress P_e alone. At this stage, the stress in the tendon is

$$f_{p1} = f_{pe} = \frac{P_e}{A_p} \tag{3.36}$$

The compressive strain in the bar reinforcement at this stage, assuming perfect bond between the two materials, is the same as that in the concrete at the same level. Consequently, the reinforcement is initially subjected to a compressive stress

$$f_{s1} = -E_s\varepsilon_{s2} \tag{3.37}$$

Next, it is useful to consider a fictitious load stage (2) corresponding to complete decompression of the concrete, at which there is zero concrete strain through the entire depth, as shown in Fig. 3.18*b*. Compatibility of deformation of the concrete and steel requires that the changes of stress in the tendon and the bar reinforcement as the beam passes from stage (1) to stage (2) are, respectively,

$$f_{p2} = E_p\varepsilon_{p2} \tag{3.38}$$

$$f_{s2} = E_s\varepsilon_{s2} \tag{3.39}$$

At this hypothetical load stage, the stress in the bar reinforcement, neglecting the effects of shrinkage and creep, is

$$f_s = E_s(-\varepsilon_{s2} + \varepsilon_{s2}) = 0 \tag{3.40}$$

The change in strain in the tendon is the same as that in the concrete at that level, and can be calculated on the basis of the uncracked concrete section properties:

$$\varepsilon_{p2} = \frac{P_e}{A_cE_c}\left(1 + \frac{e^2}{r^2}\right) \tag{3.41}$$

after which f_{p2} can be found from Eq. (3.38).

The bar reinforcement is unstressed at stage (2), as noted, but to produce the zero stress state in the concrete, the tendon must be pulled with a *fictitious external force*

$$F = A_p(f_{p1} + f_{p2}) \tag{3.42}$$

as shown in Fig. 3.18*c*.

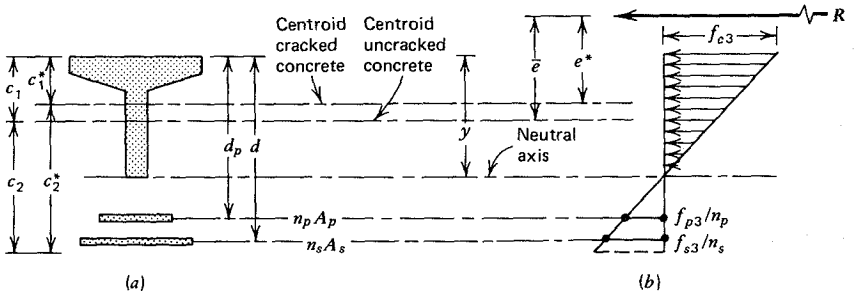

FIGURE 3.19 Transformed cracked cross section of partially prestressed beam. (*a*) Transformed cracked cross section. (*b*) Stresses.

The effect of this fictitious decompressing force is now cancelled by applying an equal and opposite force F, as shown in Fig. 3.18*d*. This force, together with the external moment M_t due to self-weight and superimposed loads, can be represented by a resultant force R applied with eccentricity $\bar{e}$ above the uncracked concrete centroid, where $R = F$ and

$$\bar{e} = \frac{M_t - Fe}{R} \tag{3.43}$$

The beam can now be analyzed as an ordinary reinforced concrete member subjected to an eccentric compression force. The resultant strain distribution (3) in the concrete is shown in Fig. 3.18*b*. The incremental strains in the tendon and bar reinforcement, ε_{p3} and ε_{s3}, respectively, together with their corresponding stresses f_{p3} and f_{s3}, are superimposed on the strains and stresses already present in the tendon and bar.

These incremental steel stresses, as well as the stress in the concrete, can be found using the transformed section concept (Ref. 3.1). The tendon is replaced by an equivalent area of tensile concrete n_pA_p and the bar reinforcement is replaced by the area n_sA_s, where $n_p = E_p/E_c$ and $n_s = E_s/E_c$, as shown in Fig. 3.19*a*.

The neutral axis for the equivalent homogeneous transformed section, a distance y from the top surface, can be found from the equilibrium condition that the moment of all internal forces about the line of action of R must be zero. These internal forces are based on the concrete stresses and the stresses acting on the transformed steel areas, as shown in Fig. 3.19*b*.

The moment equation for the internal forces about the external resultant R results in a cubic equation for y that can be solved by successive trials. Once y is known, the effective transformed area A_{ct} and moment of inertia I_{ct} of the cracked section, *about its own centroid* c_1^* from the top surface, can be found. The

incremental stresses sought, as loading passes from stage (2) to stage (3), are

$$f_{c3} = -\frac{R}{A_{ct}} - \frac{Re^*c_1^*}{I_{ct}} \tag{3.44}$$

$$f_{p3} = n_p\left[-\frac{R}{A_{ct}} + \frac{Re^*(d_p - c_1^*)}{I_{ct}}\right] \tag{3.45}$$

$$f_{s3} = n_s\left[-\frac{R}{A_{ct}} + \frac{Re^*(d_s - c_1^*)}{I_{ct}}\right] \tag{3.46}$$

where geometric terms are as defined in Fig. 3.19.

The final stress in the tendon is now found by superimposing the stresses of Eqs. (3.36), (3.38), and (3.45). The stress in the bar reinforcement is given by Eq. (3.46). The concrete stress at the top surface of the beam is given by Eq. (3.44). Specifically,

$$f_p = f_{p1} + f_{p2} + f_{p3} \tag{3.47}$$

$$f_s = f_{s3} \tag{3.48}$$

$$f_c = f_{c3} \tag{3.49}$$

The calculations described are greatly facilitated by design tables presented in Ref. 3.16. (See also Ref. 3.17.)

EXAMPLE: Elastic Flexural Stresses in Partially Prestressed Beam after Cracking

The partially prestressed T beam shown in cross section in Fig. 3.20*a* is subjected to superimposed dead and service live load moments of 38 and 191 ft-kips, in addition to a moment of 83 ft-kips resulting from its own weight. An effective prestress force of 123 kips is applied using six Grade 250 $\frac{1}{2}$-in. diameter strands. Two non-prestressed Grade 60 no. 8 bars are located close to the tension face of the beam. The elastic moduli for the concrete, tendon steel, and bar steel are, respectively, 3.61×10^6 psi, 27×10^6 psi, and 29×10^6 psi. The modulus of rupture of the concrete is 500 psi. Find the stresses in the concrete, prestressed steel, and bar reinforcement at the full service load. (M_o = 113 kN-m, M_d = 52 kN-m, M_l = 259 kN-m, P_e = 547 kN, E_c = 24,900 MPa, E_p = 186,000 MPa, E_s = 200,000 MPa, and f_r = 3.4 MPa.)

First, the tensile stress in the concrete at the bottom of the beam will be checked, assuming the member is uncracked. Properties of the uncracked cross

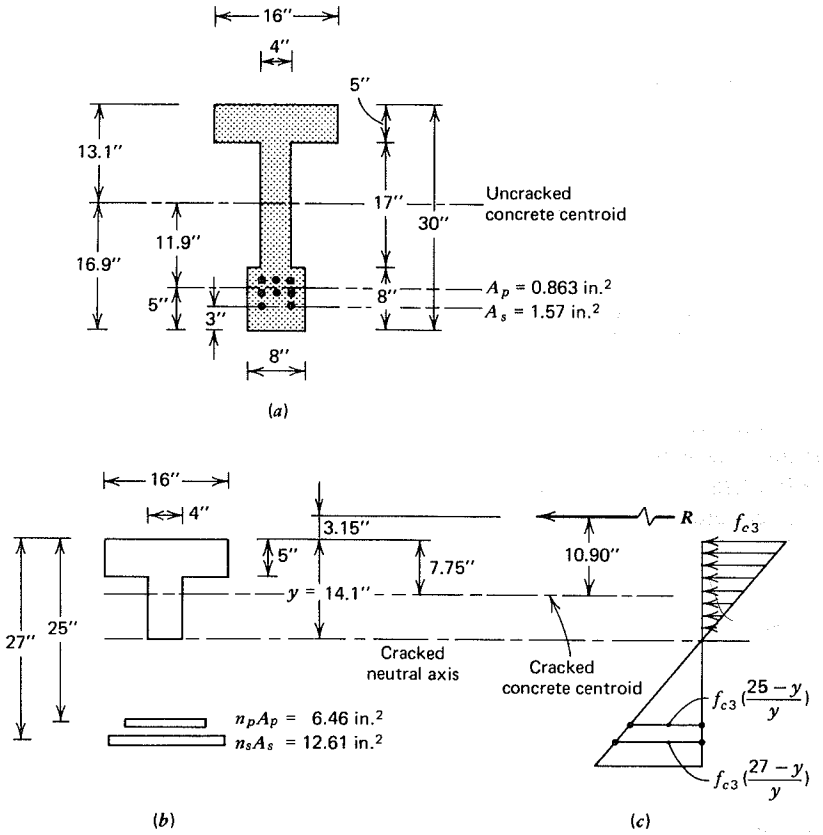

FIGURE 3.20 Cracked section analysis of T-beam. (*a*) Member cross section. (*b*) Transformed cracked cross section. (*c*) Concrete stresses.

section are

$$A_c = 212 \text{ in.}^2 \ (137 \times 10^3 \text{ mm}^2)$$

$$S_1 = 1{,}664 \text{ in.}^3 \ (27.3 \times 10^6 \text{ mm}^3)$$

$$S_2 = 1{,}290 \text{ in.}^3 \ (21.1 \times 10^6 \text{ mm}^3)$$

$$c_1 = 13.1 \text{ in. (333 mm)}$$

$$c_2 = 16.9 \text{ in. (429 mm)}$$

$$r^2 = 103 \text{ in.}^2 \ (66.5 \times 10^3 \text{ mm}^3)$$

Then, using Eq. (3.6).

$$f_2 = -\frac{P_e}{A_c}\left(1 + \frac{ec_2}{r^2}\right) + \frac{M_t}{S_2}$$

$$= -\frac{123{,}000}{212}\left(1 + \frac{11.9 \times 16.9}{103}\right) + \frac{312{,}000 \times 12}{1{,}290}$$

$$= +1{,}186 \text{ psi (8.2 MPa)}$$

This stress greatly exceeds the modulus of rupture, indicating that the section has, in fact, cracked. Analysis will proceed according to the method described earlier.

From Eq. (3.36), the effective stress in the tendon when P_e acts alone is

$$f_{p1} = f_{pe} = \frac{P_e}{A_p} = \frac{123{,}000}{0.863} = 143{,}000 \text{ psi (986 MPa)}$$

Then, with reference to Fig. 3.18*b* and using Eq. (3.41) the change in strain in the tendon as the section is decompressed is

$$\varepsilon_{p2} = \frac{P_e}{A_c E_c}\left(1 + \frac{e^2}{r^2}\right) = \frac{123{,}000}{212 \times 3.61 \times 10^6}\left(1 + \frac{11.9^2}{103}\right) = 0.0004$$

Thus, the corresponding increase in stress in the tendon is found from Eq. (3.38) to be

$$f_{p2} = E_p \varepsilon_{p2} = 27 \times 10^6 \times 0.0004 = 10{,}800 \text{ psi (74 MPa)}$$

To obtain decompression of the concrete, the fictitious external tension

$$F = A_p(f_{p1} + f_{p2}) = 0.863(143 + 10.8) = 133 \text{ kips}$$

must have been applied to the tendon. This is now cancelled by applying an equal and opposite force F. This force, acting together with the total moment of 312 ft-kips, is equivalent to a compressive force $R = 133$ kips applied with eccentricity

$$\bar{e} = \frac{M_t - Fe}{R} = \frac{312 \times 12 - 133 \times 11.9}{133} = 16.25 \text{ in.}$$

above the centroid of the uncracked concrete, or 3.15 in. above the top surface of the member as shown in Fig. 3.20. With $n_p = 27 / 3.61 = 7.48$ and $n_s = 29 / 3.61 = 8.03$, the transformed areas of the tendon and the bars are, respectively, 6.46 in.² and 12.61 in.² The effective cross section of the cracked beam, with neutral axis dimension y still unknown, is shown in Fig. 3.20*b*.

The stresses in the concrete and transformed steel, as the loads pass from stage (2) to stage (3), are shown in Fig. 3.20*c*. Taking moments of the resulting forces about the force R gives a cubic equation in y that is solved by successive trial to obtain $y = 14.1$ in. as shown.

With y known, the location of the centroid of the cracked transformed section is a routine matter. Taking moments of the partial areas about the top surface locates the centroid $c_1^* = 7.75$ in. from the top of the section. Section properties are

$$A_{ct} = 135 \text{ in.}^2$$

$$I_{ct} = 9{,}347 \text{ in.}^4$$

The eccentricity of the force R with respect to the centroid of the cracked transformed section is

$$e^* = 16.25 - 13.1 + 7.75 = 10.90 \text{ in.}$$

Now the incremental stresses in the concrete and steel can be found from Eqs. (3.44), (3.45), and (3.46):

$$f_{c3} = -\frac{R}{A_{ct}} - \frac{Re^* c_1^*}{I_{ct}}$$

$$= -\frac{133{,}000}{135} - \frac{133{,}000 \times 10.90 \times 7.75}{9{,}347} = -2{,}190 \text{ psi } (-15.1 \text{ MPa})$$

$$f_{p3} = n_p\left[-\frac{R}{A_{ct}} + \frac{Re^*(d_p - c_1^*)}{I_{ct}}\right]$$

$$= 7.48\left[-\frac{133{,}000}{135} + \frac{133{,}000 \times 10.90 \times 17.25}{9{,}347}\right] = 12{,}600 \text{ psi (87 MPa)}$$

$$f_{s3} = n_s\left[-\frac{R}{A_{ct}} + \frac{Re^*(d_s - c_1^*)}{I_{ct}}\right]$$

$$= 8.03\left[-\frac{133{,}000}{135} + \frac{133{,}000 \times 10.90 \times 19.25}{9{,}347}\right] = 16{,}100 \text{ psi (111 MPa)}$$

The final stress in the tendon at full service load is found by summing the three parts:

$$f_p = f_{p1} + f_{p2} + f_{p3}$$

$$= 143{,}000 + 10{,}800 + 12{,}600 = 166{,}400 \text{ psi (1147 MPa)}$$

while the stress in the bar reinforcement is

$$f_s = f_{s3} = 16{,}100 \text{ psi (111 MPa)}$$

and that at the top surface of the concrete is

$$f_c = f_{c3} = -2{,}190 \text{ psi } (-15.1 \text{ MPa})$$

Additional Comments

1. The stress increase in the tendon as the beam is brought to full service load is about 17 percent of the effective prestress. In calculating service load stresses in partially prestressed beams, such increase clearly cannot be neglected.
2. The service load stress of only 16,100 psi in the bar reinforcement indicates that requirements of strength, not service load stress, probably controlled the choice of bar area.
3. Although the allowable concrete stress was not given, the stress of 2,190 psi appears reasonable for concrete having a compressive strength of about 5 ski.
4. The strain and stress information developed provides a rational basis for judging the serviceability of the beam. For example, an estimate of crack width could be made based on the stress in the bar reinforcement, using standard methods, or could be based on the increase in stress in the tendon as the member passes from the decompression stage to the full service load stage.

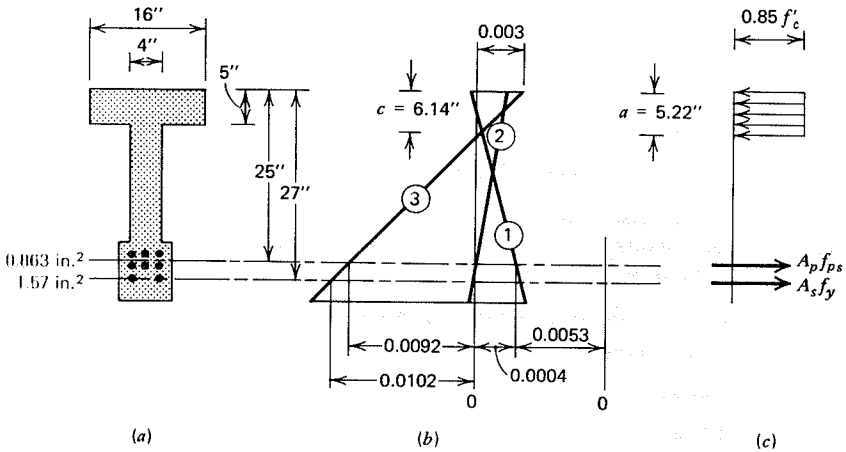

FIGURE 3.21 Flexural strength analysis of partially prestressed T-beam. (*a*) Cross section. (*b*) Concrete and steel strains. (*c*) Stresses at failure.

EXAMPLE: Ultimate Flexural Strength of Beam with Prestressed and Non-Prestressed Reinforcement

Using the strain-compatibility method, find the ultimate moment capacity of the T-beam of the preceding example. Normal density concrete having strength f'_c = 4,000 psi is to be used; its elastic modulus is $57{,}000\sqrt{4{,}000} = 3.61 \times 10^6$ psi, and its strain limit $\varepsilon_{cu} = 0.003$. It may be assumed that the stress–strain curve for the strands is as shown by Fig. 2.4, and that for the bars is as shown by Fig. 2.3. (f'_c = 28 MPa and E_c = 24,900 MPa).

The strain in the tendon at effective prestress is

$$\varepsilon_{p1} = \varepsilon_{pe} = \frac{f_{pe}}{E_p} = \frac{143{,}000}{27 \times 10^6} = 0.0053$$

and the increment of strain as the concrete at the level of the tendon is decompressed is $\varepsilon_{p2} = 0.0004$ as before (see Fig. 3.21).

The stress in the tendon will first be assumed at 200,000 psi at failure, and from the stress–strain curve the corresponding strain is $\varepsilon_{ps} = 0.0070$. The non-prestressed bars are assumed to act at their yield stress of 60,000 psi. In this case, the stress-block depth at failure is

$$a = \frac{A_p f_{ps} + A_s f_y}{0.85 f'_c b}$$

$$= \frac{0.863 \times 200 + 1.57 \times 60}{0.85 \times 4 \times 16} = 4.90 \text{ in.}$$

and $c = 4.90 / 0.85 = 5.77$ in. Then, the increment of strain in the tendon as the

loads pass from stage (2) to stage (3) is

$$\varepsilon_{p3} = \varepsilon_{cu}\frac{d-c}{c} = 0.003\left(\frac{25-5.77}{5.77}\right) = 0.0100$$

and the total steel strain at failure is

$$\varepsilon_{ps} = 0.0053 + 0.0004 + 0.0100 = 0.0157$$

rather than 0.0070 as assumed.

Revised calculations for an assumed stress at failure of 220,000 psi and attendant strain of 0.0130 give

$a = 5.22$ in. (133 mm) (essentially equal to the flange thickness)

$c = 6.14$ in. (156 mm)

$\varepsilon_{p3} = 0.0092$

$\varepsilon_{ps} = 0.0149$

as shown in Fig. 3.21*b*. It is clear from the stress–strain curve for the strand that no further refinement is necessary.

The strain in the bar reinforcement at failure is

$$\varepsilon_{s3} = 0.003\left(\frac{27-6.14}{6.14}\right) = 0.0102 > \varepsilon_y$$

confirming that the bars have yielded as assumed previously.

The resisting moment at failure is found taking moments of the steel forces about the compressive resultant (which may be assumed to act at the middepth of the flange in the present case):

$$M_n = A_p f_{ps}\left(d_p - \frac{a}{2}\right) + A_s f_y\left(d_s - \frac{a}{2}\right)$$

$$= 0.863 \times 220\left(25 - \frac{5}{2}\right) + 1.57 \times 60\left(27 - \frac{5}{2}\right)$$

$$= 6{,}580 \text{ in.-kips} = 548 \text{ ft-kips (743 kN-m)}$$

If we apply the usual strength reduction factor, the design strength of the beam is

$$\phi M_n = 0.90 \times 548 = 493 \text{ ft-kips (669 kN-m)}$$

REFERENCES

3.1 Nilson, A. H. and Winter, G., *Design of Concrete Structures*, 10th ed., McGraw-Hill, New York, 1986.

3.2 Dolan, C. W., *Ultimate Capacity of Reinforced Concrete Sections Using a Continuous Stress–Strain Function*, M.S. thesis, Cornell University, Ithaca, N.Y., 1967.

3.3 *PCI Design Handbook*, 3rd ed., Prestressed Concrete Institute, Chicago, 1985.

3.4 Leonhardt, F., *Prestressed Concrete Design and Construction*, 2nd ed., Wilhelm Ernst and Son, Berlin, 1964.

3.5 Guyon, Y., *Limit State Design of Prestressed Concrete*, Vol. 1, John Wiley and Sons, New York, 1972.

3.6 Guyon, Y., *Limit State Design of Prestressed Concrete*, Vol. 2, John Wiley and Sons, New York, 1974.

3.7 Mattock, A. H., "Modification of ACI Code Equation for Stress in Bonded Prestressed Reinforcement at Flexural Failure," *J. ACI*, Vol. 81, No. 4, July–August 1984, pp. 331–339.

3.8 Yamazaki, J., Kattula, B. T., and Mattock, A. H., "A Comparison of the Behavior of Post-Tensioned Prestressed Concrete Beams With and Without Bond," Report SM69-3, University of Washington, College of Engineering, Structures and Mechanics, Seattle, Washington, December 1969.

3.9 Mojtahedi, S. and Gamble, W. L., "Ultimate Steel Stresses in Unbonded Prestressed Concrete," *J. Structural Division*, ASCE, Vol. 104, No. ST7, July 1978, pp. 1159–1165.

3.10 Abeles, P. W., *Introduction to Prestressed Concrete*, Vol. 1, Concrete Publications Ltd., London, 1964.

3.11 Abeles, P. W., *Introduction to Prestressed Concrete*, Vol. 2, Concrete Publications Ltd., London, 1966.

3.12 Abeles, P. W. and Bardhan-Roy, B. K., *Prestressed Concrete Designer's Handbook*, 3rd ed., Cement and Concrete Association, Wexham Springs, Slough, 1981.

3.13 Naaman, A. E., "A Proposal to Extend Some Code Provisions on Reinforcement to Partial Prestressing," *J. PCI*, Vol. 26, No. 2, March–April 1981, pp. 74–91.

3.14 Nilson, A. H., "Flexural Stresses After Cracking in Partially Prestressed Beams," *J. PCI*, Vol. 21, No. 4, July–August 1976, pp. 72–81.

3.15 Thurlimann, B., "A Case for Partial Prestressing," *Structural Concrete Symposium Proceedings*, University of Toronto, May 1971, pp. 253–301.

3.16 Tadros, M. K., "Expedient Service Load Analysis of Cracked Prestressed Concrete Sections," *J. PCI*, Vol. 27, No. 6, November–December 1982, pp. 86–111.

3.17 Nilson, A. H., Discussion of Ref. 3.16, *J. PCI*, Vol. 28, No. 6, November–December 1983, pp. 145–147.

PROBLEMS

3.1 A rectangular concrete beam of width $b = 11$ in. and total depth $h = 28$ in. is post-tensioned using a single parabolic tendon having eccentricity $e = 7.8$ in. at midspan and 0 in. at the simple supports. The initial prestress force $P_i = 334$ kips and the effectiveness ratio $R = 0.84$. The member is to carry superimposed dead and live loads of 300 lb/ft and 1,000 lb/ft, respectively, uniformly distributed over the 40-ft span. Specified concrete strength is $f'_c = 5000$ psi, and at the time of transfer, $f'_{ci} = 4{,}000$ psi. Determine the flexural stress distributions in the concrete at midspan

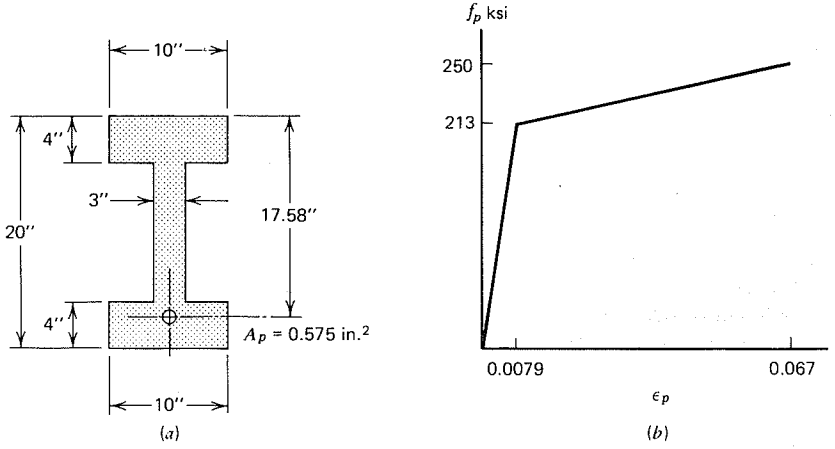

FIGURE P3.2

(a) for initial conditions before application of superimposed load, and (b) at full service load. Compare with ACI limit stresses.

3.2 The concrete I-beam of Fig. P3.2*a* is prestressed with four stranded cables having total area $A_p = 0.575$ in.^{2}. Eccentricity of the steel varies parabolically from 0 at the supports to 7.58 in. at the center of the 30-ft span. The effective stress in the steel after losses is 132,000 psi. (a) What uniformly distributed superimposed load will produce cracking of the beam, given that the modulus of rupture $f_r = 475$ psi? (b) What superimposed load will produce a balanced condition of external and equivalent prestress load, such that uniform axial compression will be obtained in the concrete? (c) For the balanced load just computed, would the midspan deflection be downward, upward, or zero? Explain.

3.3 Given that the prestressing steel for the beam of Problem 3.2 has a stress–strain curve as idealized in Fig. P3.2*b*, and that the concrete has ultimate strain capacity of 0.003, determine the nominal flexural strength M_n of the member, based (a) on a strain-compatibility analysis finding f_{ps} by iteration, (b) based on a strain-compatibility analysis finding f_{ps} by curve intersection, and (c) based on the ACI equation for f_{ps}. Concrete strength $f'_c = 4{,}000$ psi. Compare and comment on your results.

3.4 An AASHTO Type II bridge girder (see Appendix A, Table A11) is used on a 50-ft simple span. The beam is pretensioned using stranded cables that apply a compressive force P_i of 432 kips at transfer. After all time-dependent losses, an effective prestress P_e of 367 kips is attained. The steel consists of 29 $\frac{3}{8}$-in. diameter Grade 270 strands and the centroid has a constant eccentricity of 12.5 in. (a) Given that the girder cambers upward immediately upon release of prestress force to the beam, what concrete stresses are obtained at midspan at that loading stage? (b) What stresses are obtained for the unloaded member (prestress plus self-weight only) after all important losses have occurred? (c) What stresses result upon application of full service load (sum of superimposed dead and live load) of 1.630 kips/ft? (d) What is the safety factor against cracking (defined with respect to the superimposed load increase) given that the modulus of rupture is 530 psi? (e) If the concrete strength $f'_c = 5{,}000$ psi and the steel has a stress–strain curve as shown by Fig. 2.4, what total load will produce failure of the member? (Use the ACI equation for f_{ps} and apply the usual strength reduction factor to the nominal member strength.)

3.5 Recalculate the nominal flexural strength for the AASHTO girder of Problem 3.4 based on a strain-compatibility analysis, using iteration or curve intersection, and compare with the previous results. Comment.

3.6 For the I-beam shown in Fig. 3.16 and described in the accompanying example, study the effect on flexural strength and ultimate rotation capacity of (a) reducing the number of $\frac{1}{2}$-in. diameter strands from seven to five, while keeping the effective prestress force at 144 kips, (b) reducing the effective prestress force to 72 kips while keeping the number of strands unchanged at seven, and (c) reducing the effective prestress force to 72 kips to be provided by five $\frac{7}{16}$-in. diameter strands, and providing sufficient non-prestressed reinforcing bars with $f_y = 60$ ksi to restore the original flexural capacity. Rotation capacity in each case may be computed from the strain diagram at flexural failure. Comment on your results.

3.7 The I-beam shown in Fig. P3.7 is to be used in a roof support system spanning 45 ft between simple supports. It will carry a superimposed dead load of 400 lb/ft and service live load of 425 lb/ft in addition to its own weight. The member will be post-tensioned with a force $P_i = 190$ kips. At midspan the eccentricity is 11.5 in. Time-dependent losses of 20 percent will be assumed. Normal weight concrete is specified with $f'_c = 5{,}000$ psi, and at time of stressing, $f'_{ci} = 3{,}750$ psi. (a) Find concrete flexural stresses at midspan at the time of initial tensioning and compare with ACI limits. (b) Find concrete stresses at full service load and compare with ACI

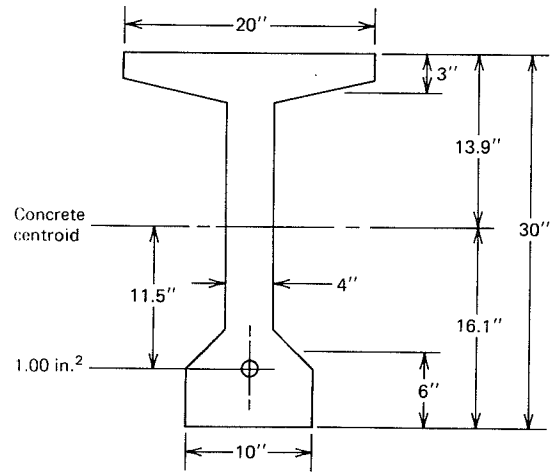

FIGURE P3.7

limits. (c) Find the safety factor against cracking, expressed as percentage increase of service live load. (d) Using ACI approximate equations, find the nominal and design flexural strength. Assume the prestress force is applied by Grade 270 strands having total area $A_p = 1.00$ in.^{2}, with properties as given by Fig. 2.4. A limiting concrete strain of 0.003 may be used. (e) Does the member meet ACI requirements with respect to cracking vs. flexural strength? With respect to safety against flexural failure?

FOUR

FLEXURAL DESIGN

4.1 BASIS OF DESIGN

It is helpful in discussing beam design to summarize the performance of a typical concrete beam in terms of its load-deflection curve, shown in Fig. 4.1. When the initial prestress force is applied, there will be an immediate upward camber δ_{pi} resulting from the bending moment associated with prestress eccentricity. With the beam supported mainly at its ends, the self-weight is immediately brought into effect, superimposing a downward component of deflection δ_o on the upward camber due to prestressing. This is referred to as the *unloaded stage*, with initial prestress and self-weight acting.

It will be assumed here, for simplicity, that all losses occur at once, such that the net deflection at the start is $\delta_{pe} - \delta_o$, resulting from the combination of effective prestress force P_e and self-weight w_o. At this stage, the concrete flexural stress distribution at midspan is generally as shown by the small shaded sketch superimposed on the load-deflection curve, varying linearly from a low value of tensile stress at the top face of the beam to maximum compression at the bottom.

When the superimposed dead load is added, the deflection increases in the positive, downward sense by the amount δ_d. The net deflection is often upward at this stage, as suggested by Fig. 4.1, but this is not always so.

At some particular loading, a *balanced load stage* will be reached, such that the upward equivalent load from prestressing is exactly equal to the downward

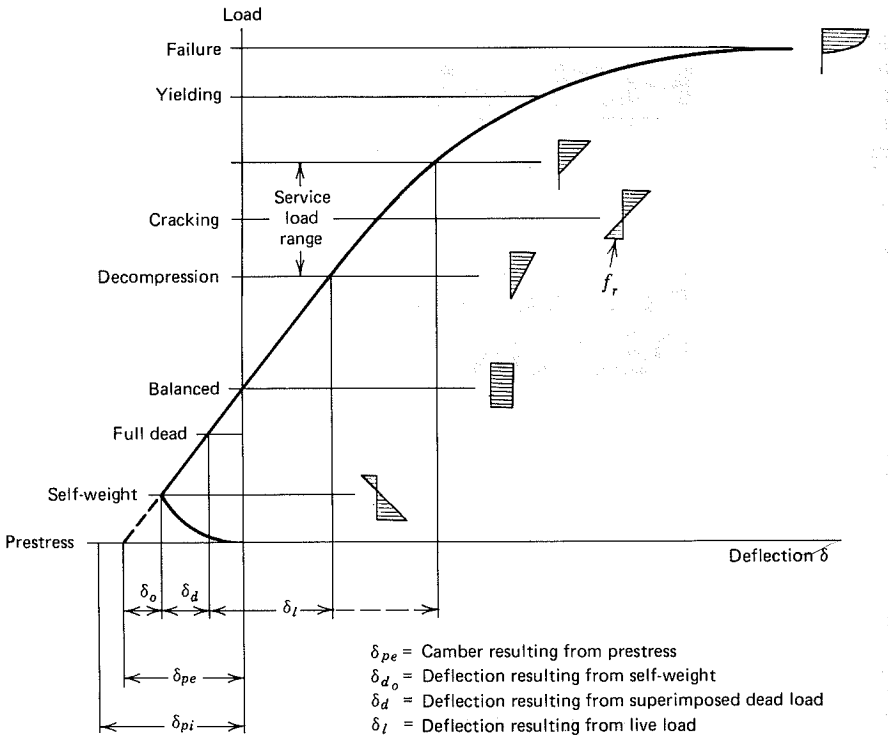

FIGURE 4.1 Load-deflection curve for typical beam.

external load. The result is a uniform compressive stress in the member, as shown in Fig. 4.1, and, neglecting the time-dependent effects, zero deflection.

With the further addition of live load, the *decompression stage* is reached, at which the concrete stress at the bottom face of the beam is zero. The beam response is linear up to, and somewhat beyond, this stage until the *cracking load* is reached, when the concrete tensile stress equals the modulus of rupture.

The usual range of service load falls between the decompression stage and the partially cracked stage, as indicated in the figure. Cracking initiates nonlinear response, although both concrete and steel stresses usually remain in the elastic ranges until somewhat beyond the cracking load.

Eventually, as loads are further increased, either the steel will commence yielding, or the concrete will enter the nonlinear range, in the *overload stage*. Near failure, the beam response is very nonlinear, as indicated. The concrete stress distribution in the cracked member, when failure is imminent, is approximately as shown by the last stress sketch.

Any of the load stages described may serve as the starting point in proportioning a prestressed concrete beam, but the member must be checked at all other significant stages to insure that it will be satisfactory over the full range.

According to current practice in the United States, prestressed concrete members are proportioned using the *allowable stress design* method.[1] Cross-section dimensions, prestress force, and prestress eccentricity are selected to keep concrete stresses within specified limits as the member ranges from the unloaded stage to the full service load stage. When the member is unloaded, with initial prestress force P_i and self-weight acting, concrete stress limits are imposed that relate to the concrete strength f'_{ci} at the time the prestress force is transferred to the concrete. At full service load, with effective prestress force P_e acting, plus the actual dead loads and specified service live loads, other concrete stress limits are imposed that relate to the full specified concrete strength f'_c. The prestress tendon area is chosen, usually based on the required initial prestress force P_i and certain allowable stresses for the steel, related to the yield strength and ultimate strength of the steel.

Concrete stress limits imposed by the provisions of the ACI Code are summarized in Table 3.1, and allowable steel stresses are shown in Table 3.2.

Beams proportioned based on stress limits as just described must also satisfy other requirements. Deflections at full service load, under sustained load, and possibly other load combinations must be calculated, and the results compared against limit values. For partially prestressed beams, in which cracking at full service loads is normal, control of crack width is important to insure that cracks will not be visually objectionable and will not permit corrosion of the highly stressed tendons. Most important, an adequate margin of safety against collapse must be assured. This requires that the flexural strength be calculated and compared against the strength required to resist factored loads. Load factors specified in the ACI Code are given in Table 1.2, and are used in conjunction with the strength reduction factors shown in Table 1.3. If the strength of the trial section is found to be inadequate, the design must be modified.

Another basis for beam design is known as *strength design*.[2] By this method, the concrete section dimensions, steel area, and steel centroid location are selected to provide the required strength at factored loads. This approach is similar to that generally used for reinforced concrete. It is more difficult to employ for prestressed beams, mainly because the stress in the tendon at flexural failure f_{ps} is unknown at the start of the design procedure. For typically under-reinforced concrete beams, the steel stress is equal to the yield stress f_y. This difficulty can be avoided in several ways that are described later.

A member designed by strength methods must be checked to ensure that immediate deflections at normal service load, as well as sustained load deflections, are not excessive. Cracking must be investigated, and, in most cases, it is also necessary to check that steel and concrete stress limits imposed by the Code for the initial unloaded stage and the full service load stage are satisfied. All of

[1]Also known as working stress design, service load design, or elastic design.
[2]Also known as ultimate strength design or load-and-resistance factor design.

the load stages considered in allowable stress design must usually be investigated when using strength design, although in a different order.

A third alternative in designing prestressed beams is to start with *load balancing* (see Section 1.3). Trial dimensions are selected for the concrete section, and prestress force and eccentricity are chosen to provide an upward equivalent load that is equal and opposite to a certain downward load (often the full dead load). The factored load stage is then investigated, and if the flexural strength is less than that required, the strength is increased, usually by adding non-prestressed bar reinforcement to supplement the tensile force in the prestressing tendons. The resulting design is often a combination of reinforced concrete and prestressed concrete. (See the discussion of partially prestressed concrete in Section 1.5.) Flexural tensile cracks are generally present at normal service load, and a check of crack widths is important. Deflections must be calculated, accounting for the partially cracked state of the beam, using methods similar to those for ordinary reinforced concrete.

4.2 FLEXURAL DESIGN BASED ON ALLOWABLE STRESSES

The emphasis in this chapter will be on the allowable stress design approach, because this is most common presently. Alternative approaches will be considered in Sections 4.6 and 4.7.

According to the allowable stress design method, the concrete cross-section dimensions, prestress force, and prestress eccentricity are selected to ensure that specified limiting concrete stresses are not exceeded as the beam passes from the unloaded stage to the full service load stage. Both concrete and steel may be considered elastic in this range, and the member is usually assumed to be uncracked. In a complete design, after member proportions have been found, deflections, cracking, and strength must be investigated and the tentative design modified, if necessary.

Many designers adopt a trial-and-error approach. A cross section is assumed, and the prestress force and profile determined. The trial member is then checked to ensure that stresses are within allowable limits. A more systematic approach is possible, however, based on attaining limit stresses, as nearly as possible, at the controlling load stages (Ref. 4.1). This approach will be followed here.

Notation is established pertaining to the concrete stresses at limiting stages as follows:

f_{ci} = allowable compressive stress immediately after transfer
f_{ti} = allowable tensile stress immediately after transfer
f_{cs} = allowable compressive stress at service load, after all losses
f_{ts} = allowable tensile stress at service load, after all losses

The values of these limit stresses are normally set by specification (see Table 3.1).

A. BEAMS IN WHICH PRESTRESS ECCENTRICITY VARIES ALONG THE SPAN

For a typical beam in which the tendon eccentricity is permitted to vary along the span, flexural stress distributions in the concrete at the maximum moment section are shown in Fig. 4.2*a*. The eccentric prestress force, having an initial value of P_i, produces the linear distribution (1). Because of the upward camber of the beam as that force is applied, the self-weight of the member is immediately introduced, the flexural stresses resulting from the moment M_o are superimposed, and the distribution (2) is the first that is actually attained. At this stage, the tension at the top surface is not to exceed f_{ti} and the compression at the bottom surface is not to exceed f_{ci}, as suggested by Fig. 4.2*a*.

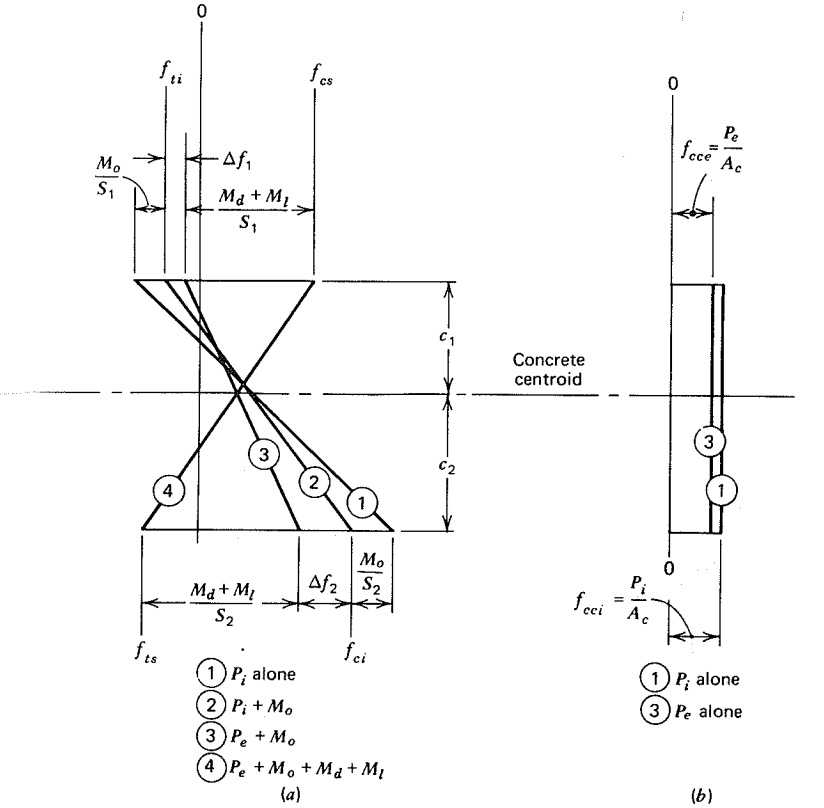

FIGURE 4.2 Flexural stress distributions for beams with variable eccentricity. (*a*) Maximum moment section. (*b*) Support section.

It will be assumed that all the losses occur at this stage, and that the stress distribution gradually changes to distribution (3). The losses produce a reduction of tension in the amount Δf_1 at the top surface, and a reduction of compression in the amount Δf_2 at the bottom surface.

As the superimposed dead load moment M_d and the service live load moment M_l are introduced, the associated flexural stresses, when superimposed on stresses already present, produce distribution (4). At this stage, the tension at the bottom surface must not be greater than f_{ts}, and the compression at the top of the section must not exceed f_{cs} as shown.

The requirements for the sections moduli S_1 and S_2 with respect to the top and bottom surfaces, respectively, are

$$S_1 \geq \frac{M_d + M_l}{f_{1r}} \tag{a}$$

$$S_2 \geq \frac{M_d + M_l}{f_{2r}} \tag{b}$$

where the available stress ranges f_{1r} and f_{2r} at the top and bottom face can be calculated from the specified stress limits f_{ti}, f_{cs}, f_{ts}, and f_{ci}, once the stress changes Δf_1 and Δf_2, associated with prestress loss, are known.

The effectiveness ratio R has been defined in Section 3.3 as

$$R = \frac{P_e}{P_i} \tag{3.1}$$

Thus, the loss in prestress force is

$$P_i - P_e = (1 - R)P_i \tag{3.2}$$

The changes in stress at the top and bottom faces, Δf_1 and Δf_2, as losses occur, are equal to $(1 - R)$ times the corresponding stresses due to the initial prestress force P_i *acting alone*:

$$\Delta f_1 = (1 - R)\left(f_{ti} + \frac{M_o}{S_1}\right) \tag{c}$$

$$\Delta f_2 = (1 - R)\left(-f_{ci} + \frac{M_o}{S_2}\right) \tag{d}$$

where Δf_1 is a reduction of tension at the top surface and Δf_2 is a reduction of compression at the bottom surface.[3] Thus, the stress ranges available as the superimposed load moments $M_d + M_l$ are applied are

$$f_{1r} = f_{ti} - \Delta f_1 - f_{cs}$$

$$= Rf_{ti} - (1 - R)\frac{M_o}{S_1} - f_{cs} \tag{e}$$

and

$$f_{2r} = f_{ts} - f_{ci} - \Delta f_2$$

$$= f_{ts} - Rf_{ci} - (1 - R)\frac{M_o}{S_2} \tag{f}$$

The minimum acceptable value of S_1 is thus established:

$$S_1 \geq \frac{M_d + M_l}{Rf_{ti} - (1 - R)\dfrac{M_o}{S_1} - f_{cs}}$$

or

$$S_1 \geq \frac{(1 - R)M_o + M_d + M_l}{Rf_{ti} - f_{cs}} \tag{4.1}$$

Similarly, the minimum value of S_2 is

$$S_2 \geq \frac{(1 - R)M_o + M_d + M_l}{f_{ts} - Rf_{ci}} \tag{4.2}$$

The cross section must be selected to provide at least these values of S_1 and S_2. Furthermore, since $I_c = S_1c_1 = S_2c_2$, the centroidal axis must be located such that

$$\frac{c_1}{c_2} = \frac{S_2}{S_1} \tag{g}$$

[3]Note that the stress limits such as f_{ti} and other specific points along the stress axis are considered signed quantities, whereas stress changes such as M_o/S_1 and Δf_2 are taken as absolute values.

or in terms of the total section depth $h = c_1 + c_2$

$$\frac{c_1}{h} = \frac{S_2}{S_1 + S_2} \tag{4.3}$$

From Fig. 4.2*a*, the concrete centroidal stress under initial conditions is given by

$$f_{cci} = f_{ti} - \frac{c_1}{h}(f_{ti} - f_{ci}) \tag{4.4}$$

The initial prestress force is easily obtained by multiplying the value of the concrete centroidal stress by the concrete cross-sectional area A_c:

$$P_i = A_c f_{cci} \tag{4.5}$$

The eccentricity of the prestress force may be found by considering the flexural stresses that must be imparted by the bending moment $P_i e$. With reference to Fig. 4.2, the flexural stress at the top surface of the beam resulting from the eccentric prestress force alone is

$$\frac{P_i e}{S_1} = (f_{ti} - f_{cci}) + \frac{M_o}{S_1} \tag{h}$$

from which the required eccentricity is

$$e = (f_{ti} - f_{cci})\frac{S_1}{P_i} + \frac{M_o}{P_i} \tag{4.6}$$

To summarize the design process in determining the best cross section, and the required prestress force and eccentricity based on stress limitations: the required section moduli with respect to the top and bottom surfaces of the member are found from Eqs. (4.1) and (4.2), with the centroidal axis located by Eq. (4.3). Concrete dimensions are chosen to satisfy these requirements as nearly as possible. The concrete centroidal stress for this ideal section is given by Eq. (4.4), the desired initial prestress force is found by Eq. (4.5), and its eccentricity by Eq. (4.6).

In practical cases, although the inequalities of Eqs. (4.1) and (4.2) will be satisfied, concrete dimensions will exceed those producing the minimum acceptable values of S_1 and S_2. Further discussion of this situation, where the concrete section is larger than the minimum, will be found in Section 4.2F.

It will be observed that an estimate of the dead weight of the member must be made at the outset of the calculations since M_o is required. This estimate may be made on the basis of typical span-to-depth ratios or past experience. If the estimate of member self-weight is substantially in error, the calculations should be revised.

The stress distributions of Fig. 4.2*a*, on which the design equations are based, apply at the maximum moment section of the member. Elsewhere, M_o is less and, consequently, the prestress eccentricity or the force must be reduced if the stress limits f_{ti} and f_{ci} are not to be exceeded. In Section 4.2C expressions are developed that establish the limits of tendon eccentricity elsewhere in the span. In many cases, tendon eccentricity is reduced to zero at the support sections, where all moments due to transverse load are zero. In this case, the stress distributions of Fig. 4.2*b* are obtained. The stress in the concrete is uniformly equal to the centroidal value f_{cci} under conditions of initial prestress and f_{cce} after losses.

EXAMPLE: Design of Beam with Variable Eccentricity Tendons

A post-tensioned prestressed concrete beam is to carry a live load of 1,000 plf and superimposed dead load of 500 plf, in addition to its own weight, on a 40-ft simple span. Normal density concrete will be used with design strength $f'_c = 6{,}000$ psi. It is estimated that, at the time of transfer, the concrete will have attained 70 percent of its ultimate strength, or 4,200 psi. Time-dependent losses may be assumed at 15 percent of the initial prestress, giving an effectiveness ratio of 0.85. Determine the required concrete dimensions, magnitude of prestress force, and eccentricity of the steel centroid based on ACI stress limitations as given in Tables 3.1 and 3.2. ($w_l = 14.6$ kN/m, $w_d = 7.3$ kN/m, span = 12.2 m, $f'_c = 41$ MPa, and $f'_{ci} = 29$ MPa.)

Referring to Table 3.1, we obtain the following stress limits:

$$f_{ci} = -0.60 \times 4{,}200 = -2{,}520 \text{ psi}$$

$$f_{ti} = 3\sqrt{4{,}200} = +195 \text{ psi}$$

$$f_{cs} = -0.45 \times 6{,}000 = -2{,}700 \text{ psi}$$

$$f_{ts} = 6\sqrt{6{,}000} = +465 \text{ psi}$$

The self-weight of the girder will be estimated at 250 plf. The moments due to transverse loading are

$$M_o = \frac{1}{8} \times 0.250 \times 40^2 = 50 \text{ ft-kips}$$

$$M_d + M_l = \frac{1}{8} \times 1.500 \times 40^2 = 300 \text{ ft-kips}$$

The required section moduli with respect to the top and bottom surfaces of the concrete beam are found from Eqs. (4.1) and (4.2):

$$S_1 \geq \frac{(1 - R)M_o + M_d + M_l}{Rf_{ti} - f_{cs}} = \frac{(0.15 \times 50 + 300)12{,}000}{0.85 \times 195 + 2{,}700} = 1{,}288 \text{ in.}^3$$

$$S_2 \geq \frac{(1 - R)M_o + M_d + M_l}{f_{ts} - Rf_{ci}} = \frac{(0.15 \times 50 + 300)12{,}000}{465 + 0.85 \times 2{,}520} = 1{,}415 \text{ in.}^3$$

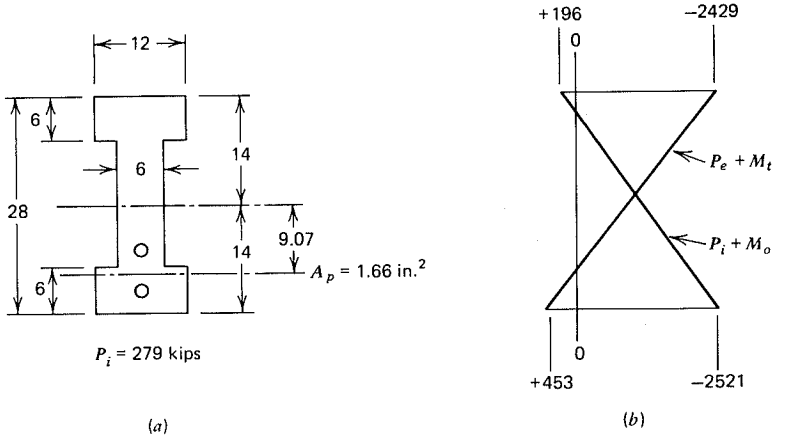

FIGURE 4.3 Beam with variable eccentricity of tendons. (*a*) Cross section dimensions. (*b*) Stresses at midspan.

These values are so nearly the same that a symmetrical beam will be adopted. The 28-in. depth I-section shown in Fig. 4.3*a* will meet the requirements, and has the following properties:

$$I_c = 19{,}904 \text{ in.}^4 \ (8.28 \times 10^9 \text{ mm}^4)$$

$$S = 1{,}422 \text{ in.}^3 \ (23.3 \times 10^6 \text{ mm}^3)$$

$$A_c = 240 \text{ in.}^2 \ (155 \times 10^3 \text{ mm}^2)$$

$$r^2 = 82.9 \text{ in.}^2$$

$$w_o = 250 \text{ plf (as assumed)}$$

Next, the concrete centroidal stress is found from Eq. (4.4):

$$f_{cci} = f_{ti} - \frac{c_1}{h}(f_{ti} - f_{ci}) = 195 - \frac{1}{2}(195 + 2{,}520) = -1{,}163 \text{ psi}$$

and from Eq. (4.5) the initial prestress force is

$$P_i = A_c f_{cci} = 240 \times 1.163 = 279 \text{ kips (1241 kN)}$$

From Eq. (4.6) the required tendon eccentricity at the maximum moment section of the beam is

$$e = (f_{ti} - f_{cci})\frac{S_1}{P_i} + \frac{M_o}{P_i} = (195 + 1{,}163)\frac{1{,}422}{279{,}000} + \frac{50 \times 12{,}000}{279{,}000}$$

$$= 9.07 \text{ in. (230 mm)}$$

Elsewhere along the span the eccentricity will be reduced in order that the concrete stress limits not be violated.

The required initial prestress force of 279 kips will be provided using tendons consisting of 1/4-in. diameter stress-relieved wires. The minimum tensile strength, according to Table 2.1, is f_{pu} = 240 ksi, and for normal prestressing wire, the yield strength may be taken as $f_{py} = 0.85 \times f_{pu}$ = 204 ksi. According to the ACI Code (Table 3.2), the permissible stress in the wire immediately after transfer must not exceed $0.82f_{py}$ = 168 ksi or $0.74f_{pu}$ = 178 ksi. The first criterion controls. The required area of prestressed steel is

$$A_p = \frac{279}{168} = 1.66 \text{ in.}^2 \ (1{,}071 \text{ mm}^2)$$

The cross-sectional area of one 1/4-in. diameter wire is 0.0491 in.^{2}; hence, the number of wires required is

$$\text{Number of wires} = \frac{1.66}{0.0491} = 34$$

Two 17-wire tendons will be used, as shown in Fig. 4.3*a*.

It is good practice to check the calculations by confirming that stress limits are not exceeded at critical load stages. The top and bottom surface concrete stresses produced, in this case, by the separate loadings are:

$$P_i\text{: } f_1 = -\frac{279{,}000}{240}\left(1 - \frac{9.07 \times 14}{82.9}\right) = +618 \text{ psi}$$

$$f_2 = -\frac{279{,}000}{240}\left(1 + \frac{9.07 \times 14}{82.9}\right) = -2{,}943 \text{ psi}$$

$$P_e\text{: } f_1 = 0.85 \times 618 = 525 \text{ psi}$$

$$f_2 = 0.85(-2{,}943) = -2{,}501 \text{ psi}$$

$$M_o\text{: } f_1 = -\frac{50 \times 12{,}000}{1{,}422} = -422 \text{ psi}$$

$$f_2 = +422 \text{ psi}$$

$$M_d + M_l\text{: } f_1 = -\frac{300 \times 12{,}000}{1{,}422} = -2{,}532 \text{ psi}$$

$$f_2 = +2{,}532 \text{ psi}$$

Thus, when the initial prestress force of 279 kips is applied and the beam self-weight acts, the top and bottom stresses in the concrete at midspan are, respectively:

$$f_1 = +618 - 422 = +196 \text{ psi}$$

$$f_2 = -2{,}943 + 422 = -2{,}521 \text{ psi}$$

When the prestress force has reduced to its effective value of 237 kips and the full service load is applied, the concrete stresses are:

$$f_1 = +525 - 422 - 2532 = -2{,}429 \text{ psi}$$

$$f_2 = -2501 + 422 + 2532 = +453 \text{ psi}$$

These limiting stress distributions are shown in Fig. 4.3*b*. Comparison with the specified limit stresses confirms that the design is satisfactory.

Additional Comments

1. From the resulting stresses shown in Fig. 4.3*b*, it is clear that the specified stress limits are satisfied almost exactly at the top and bottom surface for the initial condition (slight differences appear because of rounding errors and

selecting practical dimensions). In the fully loaded condition, the tension at the bottom surface of 453 psi is close to the limit of 465 psi; however, the compression at the top of the beam, 2,429 psi, is well below the allowable 2,700 psi. This result is because of the use of a symmetrical member, the section modulus of which is larger than the required S_1.

2. For cases such as this, in which one or both of the section moduli exceed the minimum requirement, some flexibility exists regarding the selection of prestress force and eccentricity. This point will be developed in Section 4.2F.
3. The cross section shown in Fig. 4.3*a* is idealized for computational purposes. The member actually used would probably have tapered inner flange surfaces, filets, and other features to facilitate construction.
4. The final design should also include non-prestressed longitudinal reinforcement to control possible cracking resulting from shrinkage before the beam is post-tensioned, and would undoubtedly include web reinforcement to provide the required resistance to shear forces.

B. BEAMS WITH CONSTANT ECCENTRICITY

The design method presented in the previous section was based on stress conditions at the maximum moment section of a beam, with the maximum value of moment M_o resulting from self-weight immediately superimposed. If P_i and e were to be held constant along the span, as is often convenient in pretensioned prestressed construction, then the stress limits f_{ti} and f_{ci} would be exceeded elsewhere along the span, where M_o is less than its maximum value. To avoid this condition, the constant eccentricity must be less than that given by Eq. (4.6). Its maximum value is given by conditions at the support of a simple span, where M_o is zero.

Figure 4.4 shows the flexural stress distributions at the support and midspan sections for a beam with constant eccentricity. In this case, the stress limits f_{ti} and f_{ci} are not to be violated when the eccentric prestress moment acts alone, as at the supports. The stress changes Δf_1 and Δf_2 as losses occur are equal to $(1 - R)$ times the top and bottom surface stresses, respectively, due to initial prestress alone:

$$\Delta f_1 = (1 - R)(f_{ti}) \tag{a}$$

$$\Delta f_2 = (1 - R)(-f_{ci}) \tag{b}$$

In this case, the available stress ranges between limit stresses must provide for the effect of M_o as well as M_d and M_l, as seen from Fig. 4.4*a*, and are

$$f_{1r} = f_{ti} - \Delta f_1 - f_{cs} = Rf_{ti} - f_{cs} \tag{c}$$

$$f_{2r} = f_{ts} - f_{ci} - \Delta f_2 = f_{ts} - Rf_{ci} \tag{d}$$

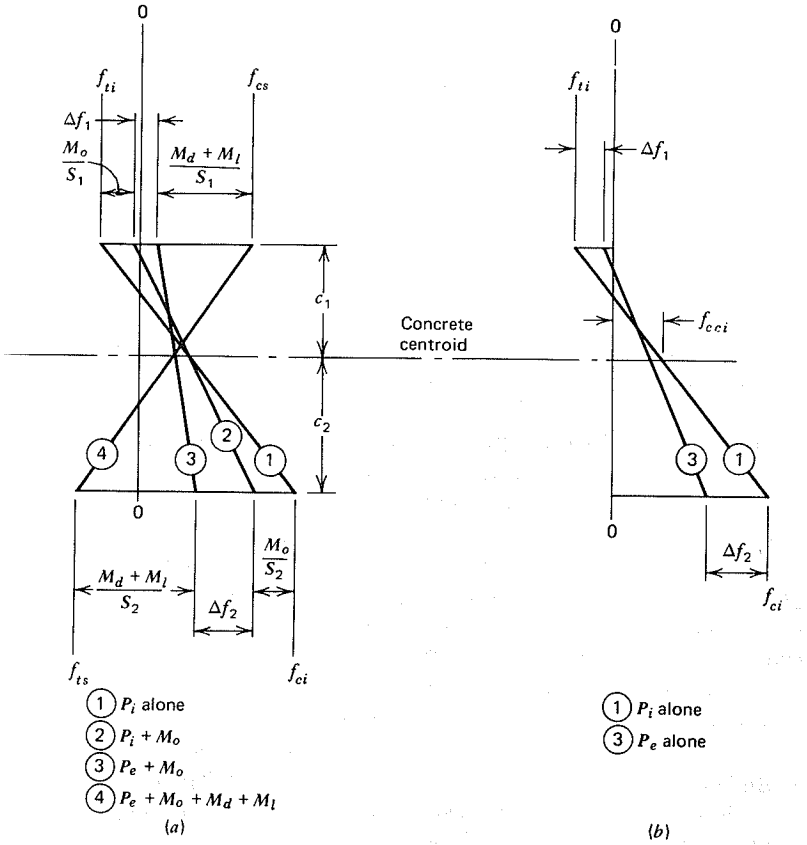

FIGURE 4.4 Flexural stress distributions for beam with constant eccentricity. (*a*) Maximum moment section. (*b*) Support section.

and the requirements on the section moduli are that

$$S_1 \geq \frac{M_o + M_d + M_l}{Rf_{ti} - f_{cs}} \tag{4.7}$$

$$S_2 \geq \frac{M_o + M_d + M_l}{f_{ts} - Rf_{ci}} \tag{4.8}$$

The concrete centroidal stress may be found by Eq. (4.4) and the initial prestress force by Eq. (4.5) as before. However, the expression for required eccentricity

differs. In this case, referring to Fig. 4.4*b*,

$$\frac{P_i e}{S_1} = f_{ti} - f_{cci} \tag{e}$$

from which the required eccentricity is

$$e = (f_{ti} - f_{cci})\frac{S_1}{P_i} \tag{4.9}$$

A significant difference between beams with variable eccentricity and those with constant eccentricity will be noted by comparing Eqs. (4.1) and (4.2) with the corresponding Eqs. (4.7) and (4.8). In the first case, the section modulus requirement is governed mainly by the superimposed load moments M_d and M_l. Almost all of the self-weight is carried "free," that is, without increasing section modulus or prestress force, by the simple expedient of increasing the eccentricity along the span by the amount M_o/P_i. In the second case, the eccentricity is controlled by conditions at the supports, where M_o is zero, and the full moment M_o due to self-weight must be included in determining section moduli. Nevertheless, beams with constant eccentricity are often used for practical reasons.

Certain alternative means are available for coping with the problem of excessive concrete stresses resulting from prestress at the ends of members with constant eccentricity. The prestress force may be reduced near the ends of the span by encasing some of the tendons in plastic sheathing, effectively moving the point of application of prestress force inward toward midspan for a part of the strands. Or supplementary non-prestressed bar reinforcement may be used in the end regions to accommodate the local high stresses.

The ACI Code includes a special provision that the concrete tensile stress immediately after transfer, before time-dependent losses, at the ends of simply supported members, may be as high as $6\sqrt{f'_{ci}}$, twice the limit of $3\sqrt{f'_{ci}}$ that applies elsewhere (see Table 3.1). Conditions at the supports will generally control for beams with constant eccentricity, and f_{ti} may be taken equal to $6\sqrt{f'_{ci}}$ in preceding equations. Superposition of M_o at midspan will generally result in tension at the top surface in that region less than the allowed $3\sqrt{f'_{ci}}$.

EXAMPLE: Design of Beam with Constant Eccentricity Tendons

The beam of the preceding examples is to be redesigned using straight tendons with constant eccentricity. All other design criteria are the same as before. At the supports, a temporary concrete tensile stress of $6\sqrt{f'_{ci}} = 390$ psi is permitted.

Anticipating a somewhat less efficient beam, the dead load estimate will be increased to 270 plf in this case. The resulting moment M_o is 54 ft-kips. The moment due to superimposed dead load and live load is 300 ft-kips as before.

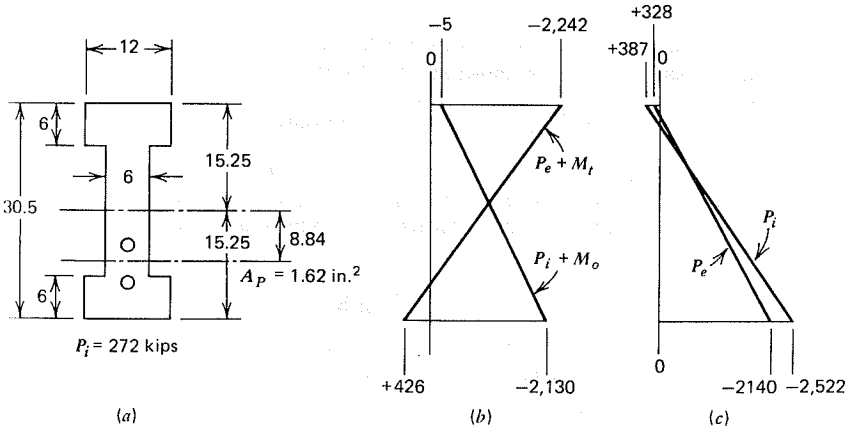

FIGURE 4.5 Beam with constant eccentricity of tendons. (*a*) Cross section dimensions. (*b*) Stresses at midspan. (*c*) Stresses at supports.

Using Eqs. (4.7) and (4.8), the requirements for section moduli are

$$S_1 \geq \frac{M_o + M_d + M_l}{Rf_{ti} - f_{cs}} = \frac{(54 + 300)12{,}000}{0.85 \times 390 + 2{,}700} = 1{,}401 \text{ in.}^3$$

$$S_2 \geq \frac{M_o + M_d + M_l}{f_{ts} - Rf_{ci}} = \frac{(54 + 300)12{,}000}{465 + 0.85 \times 2{,}520} = 1{,}629 \text{ in.}^3$$

Once again, a symmetrical section will be chosen. Flange dimensions and web width will be kept unchanged compared with the previous example, but in this case a beam depth of 30.5 in. is required. The dimensions of the cross section are shown in Fig. 4.5*a*. The following properties are obtained:

$I_c = 25{,}207 \text{ in.}^4 \ (10.49 \times 10^9 \text{ mm}^4)$

$S = 1{,}653 \text{ in.}^3 \ (27.1 \times 10^6 \text{ mm}^3)$

$A_c = 255 \text{ in.}^2 \ (165 \times 10^3 \text{ mm}^2)$

$r^2 = 98.9 \text{ in.}^2$

$w_o = 266$ plf (close to the assumed value)

The concrete centroidal stress, from Eq. (4.4), is

$$f_{cci} = f_{ti} - \frac{c_1}{h}(f_{ti} - f_{ci}) = 390 - \frac{1}{2}(390 + 2{,}520) = -1{,}065 \text{ psi}$$

and, from Eq. (4.5), the initial prestress force is

$$P_i = A_c f_{cci} = 255 \times 1.065 = 272 \text{ kips } (1{,}210 \text{ kN})$$

From Eq. (4.9), the required constant eccentricity is

$$e = (f_{ti} - f_{cci})\frac{S_1}{P_i} = (390 + 1{,}065)\frac{1{,}653}{272{,}000} = 8.84 \text{ in. } (224 \text{ mm})$$

Again, two tendons will be used to provide the required force P_i, each composed of multiple 1/4-in. diameter wires. With the maximum permissible stress in the wires of 168 ksi, the total required steel area is

$$A_p = \frac{272}{168} = 1.62 \text{ in.}^2 \ (1{,}045 \text{ mm}^2)$$

A total of 34 wires is required as before, 17 in each tendon.

The calculations will be checked by verifying concrete stresses at the top and bottom of the beam for the critical load stages. The component stress contributions are

$$P_i\text{: } f_1 = -\frac{272{,}000}{255}\left(1 - \frac{8.84 \times 15.25}{98.9}\right) = +387 \text{ psi}$$

$$f_2 = -\frac{272{,}000}{255}\left(1 + \frac{8.84 \times 15.25}{98.9}\right) = -2{,}522 \text{ psi}$$

$$P_e\text{: } f_1 = 0.85 \times 387 = +328 \text{ psi}$$

$$f_2 = 0.85(-2{,}522) = -2{,}144 \text{ psi}$$

$$M_o\text{: } f_1 = -\frac{54 \times 12{,}000}{1{,}653} = -392 \text{ psi}$$

$$f_2 = +392 \text{ psi}$$

$$M_d + M_l\text{: } f_1 = -\frac{300 \times 12{,}000}{1{,}653} = -2{,}178 \text{ psi}$$

$$f_2 = +2{,}178 \text{ psi}$$

Superimposing the appropriate stress contributions, the stress distributions in the concrete at midspan and at the supports are obtained, as shown in Figs. 4.5*b* and 4.5*c*, respectively. When the initial prestress force of 272 kips acts alone, as at the supports, the stresses at the top and bottom surfaces are

$$f_1 = +387 \text{ psi}$$

$$f_2 = -2{,}522 \text{ psi}$$

After losses, the prestress force is reduced to 231 kips and the support stresses are reduced accordingly. At midspan the beam weight is immediately superimposed, and stresses resulting from P_i plus M_o are

$$f_1 = +387 - 392 = -5 \text{ psi}$$

$$f_2 = -2{,}522 + 392 = -2{,}130 \text{ psi}$$

When the full service load acts, together with P_e, the midspan stresses are

$$f_1 = +328 - 392 - 2{,}178 = -2{,}242 \text{ psi}$$

$$f_2 = -2{,}144 + 392 + 2{,}178 = +426 \text{ psi}$$

If we check against the specified limiting stresses, it is evident that the design is satisfactory in this respect at the critical load stages and locations.

Additional Comments

1. Once again, it is found that the stress specification is satisfied almost exactly at the supports under conditions of initial prestress, and closely satisfied at midspan at the bottom surface for the loaded condition. Because of the choice of a symmetrical section, the compressive stress at the top of the member at midspan in the fully loaded stage is well below the permitted value.
2. At midspan in the unloaded stage, with only P_i and self-weight acting, compressive stresses of 5 psi and 2,130 psi are present at the top and bottom surfaces, respectively. The stress ranges that were available in the previous example to resist superimposed dead and live loads are reduced. This may be thought of as a penalty that is often paid in the case of pretensioned members to obtain the practical advantages of straight tendons. In post-tensioned members, it is easy to provide for variable eccentricity, and it is likely that the design of the previous example would be chosen.
3. Comparing the designs with variable and constant eccentricity, the increase in concrete section in the second case is about six percent. For longer span beams, in which the self-weight is proportionately larger, the penalty would be larger than this.

C. LIMIT ZONE FOR TENDON CENTROID

The equations developed in Section 4.2A for members with variable tendon eccentricity establish the requirements for section modulus, prestress force, and eccentricity at the maximum moment section of the member. Elsewhere along the span, the eccentricity of the steel must be reduced if the concrete stress limits for the unloaded stage are not to be exceeded. (Alternatively, the section must be increased, as in Section 4.2B.) Conversely, there is a minimum eccentricity, or upper limit for the steel centroid, such that the limiting concrete stresses are not exceeded when the beam is in the full service load stage.

Limiting locations for the prestress steel centroid at any point along the span can be established using Eqs. (3.5) and (3.6), which give the values of concrete stress at the top and bottom of the beam in the unloaded and service load stages, respectively. The stresses produced for those load stages should be compared with the limiting stresses applicable in a particular case, such as the ACI stress limits of Table 3.1. This permits a solution for tendon eccentricity e as a function of distance x along the span.

To indicate that both eccentricity e and moments M_o or M_t are functions of distance x from the support, they will be written as $e(x)$ and $M_o(x)$ or $M_t(x)$, respectively. In writing statements of inequality, it is convenient to designate tensile stress as larger than zero and compressive stress as smaller than zero. Thus, $+450 > -1{,}350$, and $-600 > -1{,}140$, for example.

Considering first the unloaded stage, we find the tensile stress at the top of the beam must not exceed f_{ti}. From Eq. (3.5*a*)

$$f_{ti} \geq -\frac{P_i}{A_c}\left(1 - \frac{e(x)c_1}{r^2}\right) - \frac{M_o(x)}{S_1} \qquad \text{(a)}$$

Solving for the maximum eccentricity, we obtain

$$e(x) \le \frac{f_{ti}S_1}{P_i} + \frac{S_1}{A_c} + \frac{M_o(x)}{P_i} \tag{4.10}$$

At the bottom of the unloaded beam, the stress must not exceed the limiting initial compression. From Eq. (3.5*b*)

$$f_{ci} \le -\frac{P_i}{A_c}\left(1 + \frac{e(x)c_2}{r^2}\right) + \frac{M_o(x)}{S_2} \tag{b}$$

hence, the second lower limit for the steel centroid is

$$e(x) \le -\frac{f_{ci}S_2}{P_i} - \frac{S_2}{A_c} + \frac{M_o(x)}{P_i} \tag{4.11}$$

Now considering the member in the fully loaded stage, the upper limit values for the eccentricity may be found. From Eq. (3.6*a*)

$$f_{cs} \le -\frac{P_e}{A_c}\left(1 - \frac{e(x)c_1}{r^2}\right) - \frac{M_t(x)}{S_1} \tag{c}$$

from which

$$e(x) \ge \frac{f_{cs}S_1}{P_e} + \frac{S_1}{A_c} + \frac{M_t(x)}{P_e} \tag{4.12}$$

and using Eq. (3.6*b*)

$$f_{ts} \ge -\frac{P_e}{A_c}\left(1 + \frac{e(x)c_2}{r^2}\right) + \frac{M_t(x)}{S_2} \tag{d}$$

from which

$$e(x) \ge -\frac{f_{ts}S_2}{P_e} - \frac{S_2}{A_c} + \frac{M_t(x)}{P_e} \tag{4.13}$$

Using Eqs. (4.10) and (4.11), the lower limit of tendon eccentricity is established at successive points along the span. Then, using Eqs. (4.12) and

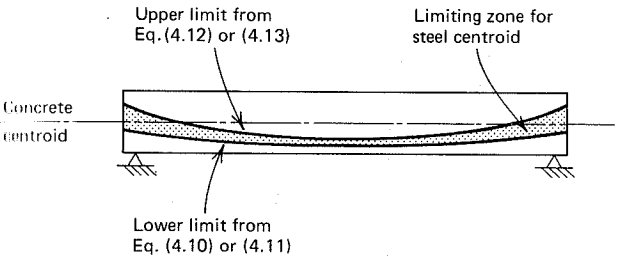

FIGURE 4.6 Typical limiting zone for centroid of prestressing steel.

(4.13), the corresponding upper limit is established. This upper limit may well be negative, indicating that the tendon centroid may be above the concrete centroid at that location.

It is often convenient to plot the envelope of acceptable tendon profiles, as has been done in Fig. 4.6, for a typical case in which both dead and live loads are uniformly distributed. Any tendon centroid falling completely within the shaded zone would be satisfactory from the point of view of concrete stress limits. It should be emphasized that it is only the tendon centroid that must be within the shaded zone; individual cables are often outside of it.

The tendon profile actually used is often a parabolic curve or a catenary in the case of post-tensioned beams. The duct containing the prestressing steel is draped to the desired shape and held in that position by wiring it to the transverse web reinforcement, after which the concrete may be poured. In pretensioned beams, *deflected tendons* are often used. The cables are held down at midspan, at the third points, or at the quarter points of the span and held up at the ends, so that a smooth curve is approximated to a greater or lesser degree.

For simple spans designed by load-balancing methods (see Section 4.5), the tendon centroid must pass through the concrete centroid at the supports, because the moments due to external loads are zero at the supports. It is seen from Fig. 4.6 that this special case is included in the range of acceptable tendon profiles.

In practical cases, it is often not necessary to make a centroid zone diagram, such as is shown in Fig. 4.6. By placing the centroid at its known location at midspan, at or close to the concrete centroid at the supports, and with a near-parabolic shape between those control points, satisfaction of the limiting stress requirements is assured. With nonprismatic beams, beams in which a curved concrete centroidal axis is employed, or with continuous beams, diagrams such as Fig. 4.6 are a great aid.

EXAMPLE: Determination of Tendon Centroid Limit Zone

Determine the limiting tendon zone for the 40-ft span post-tensioned beam of 28-in. depth designed in the example of Section 4.2A. (Span is 12.2 m and depth 711

mm.) Results of that design are summarized as follows:

$f_{ci} = -2{,}520$ psi (-17.4 MPa)	$M_o = 50$ ft-kips (6 kN-m)	$S_1 = 1{,}422$ in.^{3} (23.3×10^6 mm^3)
$f_{ti} = +195$ psi ($+1.3$ MPa)	$M_t = 350$ ft-kips (475 kN-m)	$S_2 = 1{,}422$ in.^{3} (23.3×10^6 mm^3)
$f_{cs} = -2{,}700$ psi (-18.6 MPa)	$P_i = 279$ kips (1241 kN)	$A_c = 240$ in.^{2} (155×10^3 mm^2)
$f_{ts} = +465$ psi ($+3.2$ MPa)	$P_e = 237$ kips (1,054 kN)	$r^2 = 82.9$ in.^{2} (53.5×10^3 mm^2)

Since the member self-weight and all superimposed loads are uniformly distributed, the variation of all moments is parabolic, from maximum at midspan to zero at the supports. Accordingly, the moment ordinates may be established:

	Midspan	*Quarter Span*	*Support*
M_o	50 ft-kips	37.5 ft-kips	0
M_t	350 ft-kips	262.5 ft-kips	0

The lower limit of the steel centroid will be found first from Eq. (4.10):

At support:

$$e(x) = \frac{195 \times 1{,}422}{279{,}000} + \frac{1{,}422}{240} = 6.92 \text{ in. (176 mm)}$$

At quarter span:

$$e(x) = 6.92 + \frac{37.5 \times 12{,}000}{279{,}000} = 8.53 \text{ in. (217 mm)}$$

At midspan:

$$e(x) = 6.92 + \frac{50 \times 12{,}000}{279{,}000} = 9.07 \text{ in. (230 mm)}$$

and the lower limits from Eq. (4.11) are:

At support:

$$e(x) = \frac{2{,}520 \times 1{,}422}{279{,}000} - \frac{1{,}422}{240} = 6.92 \text{ in. (176 mm)}$$

At quarter point:

$$e(x) = 8.53 \text{ in. (217 mm)}$$

At midspan:

$$e(x) = 9.07 \text{ in. (230 mm)}$$

That identical results are obtained from Eqs. (4.10) and (4.11) simply confirms that the prestress force has been chosen to exactly satisfy the stress limits f_{ti} and f_{ci}.

Next, the upper limit curve will be established using Eqs. (4.12) and (4.13). From Eq. (4.12):

At support:

$$e(x) = \frac{-2{,}700 \times 1{,}422}{237{,}000} + \frac{1{,}422}{240} = -10.28 \text{ in. (261 mm)}$$

At quarter point:

$$e(x) = -10.28 + \frac{263 \times 12{,}000}{237{,}000} = 3.04 \text{ in. (77 mm)}$$

At midspan:

$$e(x) = -10.28 + \frac{350 \times 12{,}000}{237{,}000} = 7.44 \text{ in. (189 mm)}$$

and from Eq. (4.13):

At support:

$$e(x) = \frac{-465 \times 1{,}422}{237{,}000} - \frac{1{,}422}{240} = -8.72 \text{ in. } (-221 \text{ mm})$$

At quarter span:

$$e(x) = -8.72 + \frac{263 \times 12{,}000}{237{,}000} = 4.60 \text{ in. (117 mm)}$$

At midspan:

$$e(x) = -8.72 + \frac{350 \times 12{,}000}{237{,}000} = 9.00 \text{ in. (229 mm)}$$

It is clear that Eq. (4.13), based on limiting tension, controls in the loaded stage. This could be anticipated by study of Fig. 4.3*b*, which indicates that in the loaded stage, for the value of effective prestress used, top surface compression is well below the allowed value.

The results of the calculations are summarized in Fig. 4.7*a*, which shows the upper and lower limit curves for the tendon centroid. The small range between the upper and lower limits of the prestress force at midspan is typical of closely designed beams in which the concrete cross section meets, but does not greatly exceed, the requirements of flexure. The actual centerline profiles of the two tendons is shown in Fig. 4.7*b*. The ducts are spaced 4 in. apart at midspan with the steel centroid 9 in. below the concrete centroid. Steel and concrete centroids are made to coincide at the supports, but the individual tendons are flared apart to provide clearance for the end anchorage hardware. A parabolic variation of eccentricity along the span is used for each tendon.

D. BEAMS WITH DEFLECTED TENDONS

In pretensioned prestressed beams, the are often practical advantages in using a tendon profile that is *segmentally linear*, that is, a tendon profile that only

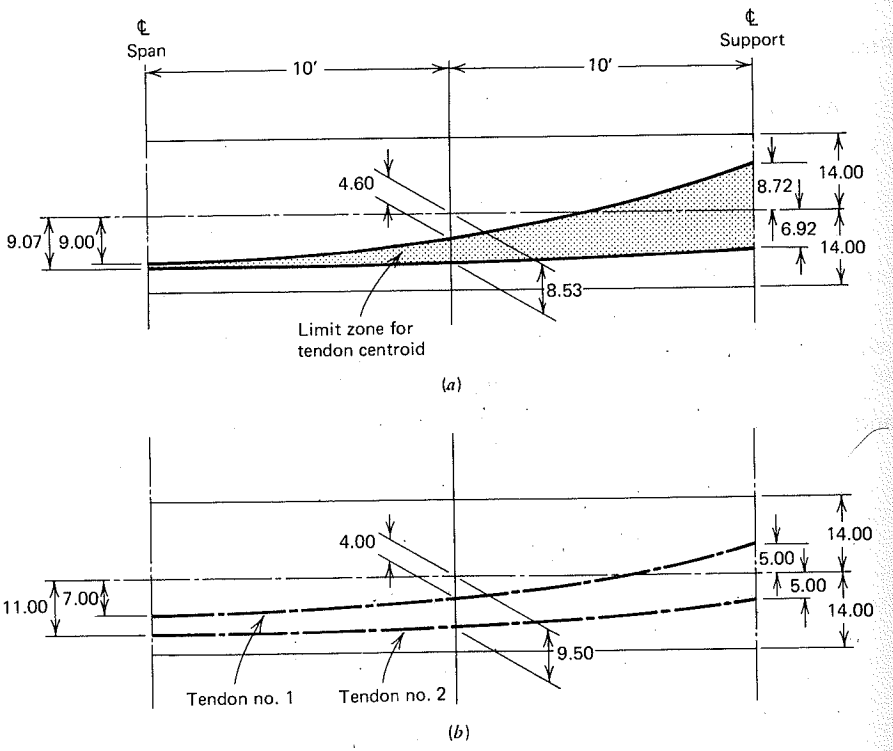

FIGURE 4.7 Location of tendons for example beam. (*a*) Upper and lower steel centroid limits. (*b*) Actual tendon locations.

approximates the parabolic variation of eccentricity that could be considered ideal if loads are uniformly distributed. The tendon centroid profile in a typical pretensioned beam with *deflected tendons* appears as shown in Fig. 4.8*a*. Tendon deflectors hold the tendons down at points *a* and *b* before the concrete is cast, and end forms, with holes through which the tendons pass, hold them up at the supports. The deflection points are often at the one-third points or one-quarter points of the span, and the support eccentricity is often zero, as shown. The result is a tendon eccentricity that varies linearly from supports to the hold-down points and is constant throughout the central region.

For such cases, certain modifications must be made in the design equations developed in Sections 4.2A and 4.2B (Ref. 4.2). The critical section for the beam when in the unloaded stage immediately after transfer will be at the hold-down points *a* and *b*, rather than at midspan as for the beam with variable eccentricity, or at the supports as for the beam with constant eccentricity.

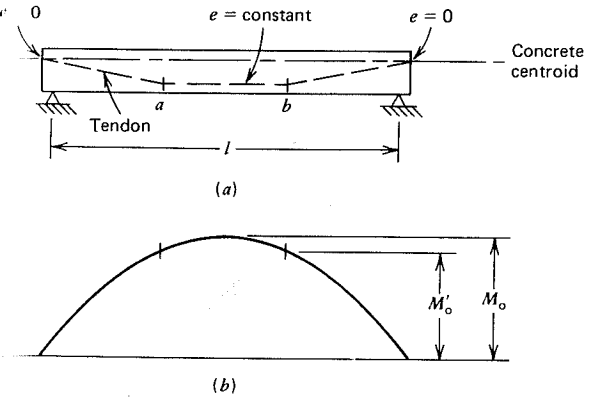

FIGURE 4.8 Pretensioned beam with deflected tendons. (*a*) Tendon profile. (*b*) Moment variation resulting from self-weight.

The self-weight moment variation along the span for a typical prismatic beam is shown in Fig. 4.8*b*. The maximum self-weight moment is at midspan as before and has value M_o. At the hold-down points, it has a lower value M'_o.

The flexural stress distributions in the concrete for the various load stages are shown in Fig. 4.9*a* for the midspan section, and in Fig. 4.9*b* for the critical section at the hold-down location. Immediately after transfer, the stress limits f_{ti} and f_{ci} are imposed as usual. In the central region with constant eccentricity, the self-weight moment is never less than M'_o, its value at the hold-down locations. With reference to Fig. 4.9*b*, stress distribution (2) is the first that is actually attained. The limits f_{ti} and f_{ci} are imposed at this stage, so the initial prestress force P_i can be applied, with appropriate eccentricity, to produce distribution (1) if it were acting alone. The stress distribution at the support (not shown in Fig. 4.9) would be uniform compression with a value P_i/A_c, if zero eccentricity is specified there, and would not control.

The concrete flexural stress distributions at the maximum moment section, generally at midspan, are shown in Fig. 4.9*a*. Distribution (1), which is the result of P_i acting alone, is identical to distribution (1) in Fig. 4.9*b*, and would never actually be attained, because the self-weight comes into effect at once. Distribution (2) at midspan would produce tension less than f_{ti} at the top, and compression less than f_{ci} at the bottom, because the stress changes M_o/S_1 and M_o/S_2 are larger than M'_o/S_1 and M'_o/S_2, respectively. This confirms that the hold-down section controls at the initial stage, not the maximum moment section.

As losses take place, concrete stresses pass from distribution (2) to distribution (3) at midspan, and as the external dead load and live load is introduced, they will then have distribution (4). At this stage, the service load stress limits f_{cs} and f_{ts} are imposed.

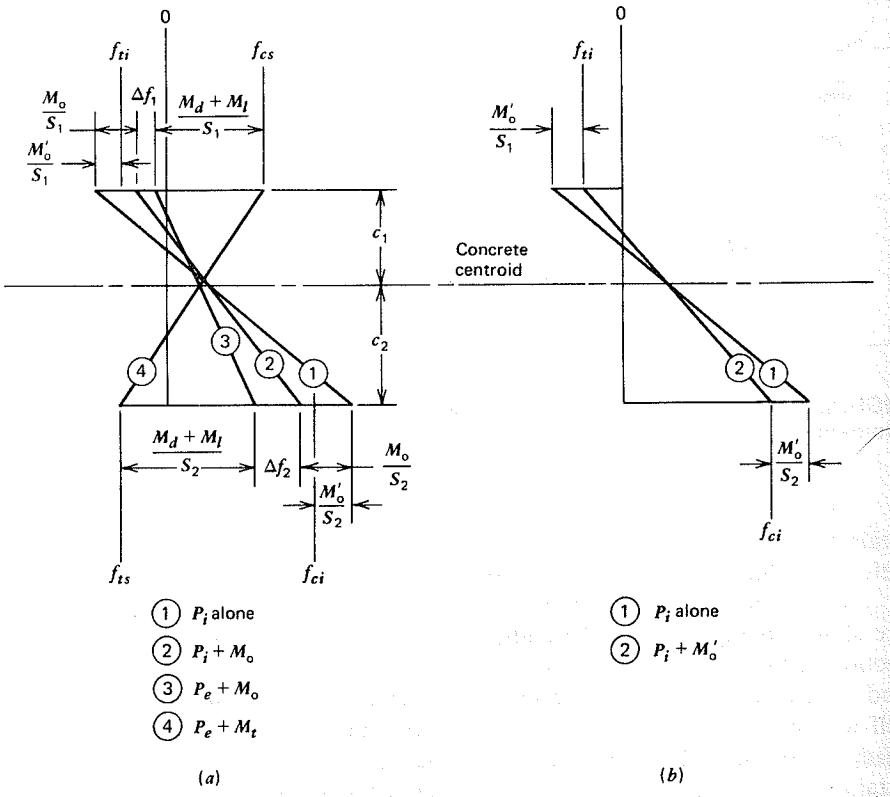

FIGURE 4.9 Flexural stress distributions for beam with deflected tendons. (*a*) Maximum moment section. (*b*) Deflection point of tendons.

It is seen from Fig. 4.9*a* that the requirements for the section moduli S_1 and S_2 at the top and bottom face are

$$S_1 \geq \frac{(M_o - M'_o) + M_d + M_l}{f_{1r}} \tag{a}$$

$$S_2 \geq \frac{(M_o - M'_o) + M_d + M_l}{f_{2r}} \tag{b}$$

where the available stress ranges f_{1r} and f_{2r} can be calculated from the specified limit stresses once the stress changes resulting from loss of prestress force are known. These are equal to $(1 - R)$ times the corresponding stresses due to initial prestress force P_i acting alone:

$$\Delta f_1 = (1 - R)\left(f_{ti} + \frac{M'_o}{S_1}\right) \tag{c}$$

$$\Delta f_2 = (1 - R)\left(-f_{ci} + \frac{M'_o}{S_2}\right) \tag{d}$$

Then, it is easily shown that

$$f_{1r} = Rf_{ti} - (1 - R)\frac{M'_o}{S_1} - f_{cs} \tag{e}$$

$$f_{2r} = f_{ts} - Rf_{ci} - (1 - R)\frac{M'_o}{S_2} \tag{f}$$

from which the minimum requirements for section modulus for a beam with deflected tendons are

$$S_1 \geq \frac{(1 - R)M'_o + (M_o - M'_o) + M_d + M_l}{Rf_{ti} - f_{cs}} \tag{4.14}$$

$$S_2 \geq \frac{(1 - R)M'_o + (M_o - M'_o) + M_d + M_l}{f_{ts} - Rf_{ci}} \tag{4.15}$$

The concrete centroidal axis will be located by Eq. (4.3) as before. The concrete centroidal stress under initial conditions of loading is calculated from Eq. (4.4), and the initial prestress force is calculated from Eq. (4.5) without change. But the prestress eccentricity, constant through the central region, will now be given by

$$e = (f_{ti} - f_{cci})\frac{S_1}{P_i} + \frac{M'_o}{P_i} \tag{4.16}$$

Equations (4.14), (4.15), and (4.16) replace Eqs. (4.1), (4.2), and (4.6) of Section 4.2A, and permit selection of the ideal section, prestress force, and eccentricity for a beam that will use deflected tendons.

E. REDUCTION OF PRESTRESS FORCE ALONG THE SPAN

It has already been shown that a particular combination of prestress force and eccentricity that may prove satisfactory at the maximum moment section of a beam may result in excessive stresses elsewhere, where the moment due to

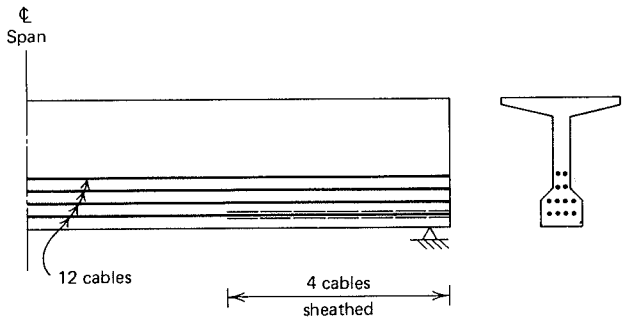

FIGURE 4.10 Use of sheathed tendons to reduce prestress force near supports.

self-weight is less. This can be avoided by reducing the eccentricity of the steel near the supports. An alternative with distinct practical advantages for pretensioned beams is to keep the eccentricity constant or nearly so, but to reduce the magnitude of the prestress force.

This is easily achieved by preventing certain of the cables from bonding to the concrete near the ends of the span. The most common way to accomplish this is to enclose those cables in tightly fitting split plastic tubes, as suggested by Fig. 4.10, or to wrap the cables with heavy paper or cloth tape through the desired length. In such a case, there is no prestress force transmitted to the concrete from the sheathed strands near the ends of the span, and the effective prestress force is provided by the remainder of the steel area. It may be evident that there will usually be some reduction in the effective eccentricity as well, even if straight cables are used, because of the upward shift of the steel centroid when a part of the steel area becomes ineffective.

With such an arrangement, consideration should be given to the required transfer length for the sheathed tendons, measured toward the center of the span from the end of the sheathing, to insure that the total prestress force is developed where needed (See Section 4.9).

In post-tensioned beams of long span, particularly in bridges, it is often advantageous to stop off certain of the tendons where they are no longer needed to resist flexural stress. Normally, they are swept upward and anchored at the top face of the beam, as shown in Fig. 4.11. Apart from an appreciable saving in the quantity of high tensile steel, the main advantage of this arrangement is that it is usually possible to raise the tendons one by one without thickening the web, as will often prove necessary if several tendons are raised at one location. In addition, anchoring part of the tendons in the top face of the beam reduces the number of anchorages that must be accommodated in the end sections and avoids excessive stresses there. Furthermore, the inclined component of compression due to prestress produces a shear of sign opposite to that resulting from applied loads, reducing the net shear force acting.

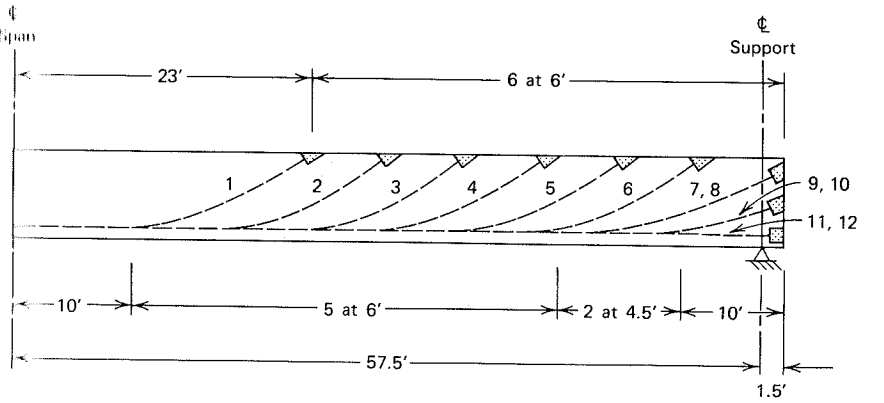

FIGURE 4.11 Bridge girder with raised tendons. Adapted from Ref. 4.3.

Frictional losses may be large for cables that are stopped short of the supports because of the curvature of the ducts. Such losses can be minimized by keeping the inclination of the raised ends as small as possible and by using a large radius of curvature. If the number of through cables is equal to or greater than the number of raised cables, it is possible to raise only one end of each tendon, and to have the other half of the same cable run straight through to the far end of the beam. In this case, the cables are arranged in pairs so that there are two symmetrically placed raised anchorages for each pair (Refs. 4.3 and 4.4).

In post-tensioned continuous beams, an arrangement similar to that of Fig. 4.11 is used, except that in this case it is usually the cables needed for negative bending at the supports that are swept down and anchored at the bottom face of the member.

F. SECTIONS HAVING EXCESS CAPACITY

In practical situations, very seldom will the concrete section chosen have exactly the required values of S_1 and S_2, as found by the methods of Sections 4.2A through 4.2D, nor will the concrete centroid be exactly at the theoretically ideal level. Rounding upward of concrete dimensions, provision of broad flanges for functional reasons, or the use of standardized cross-sectional shapes will normally result in a member whose section properties will exceed the minimum requirements. In such a case, the stresses in the concrete as the member passes from the unloaded stage to the full service load stage will stay within the allowable limits, but the limit stresses will not be obtained exactly. An infinite number of combinations of prestress force and eccentricity will satisfy requirements. Usually the design requiring the lowest value of prestress force, and the largest practical eccentricity, will be the most economical.

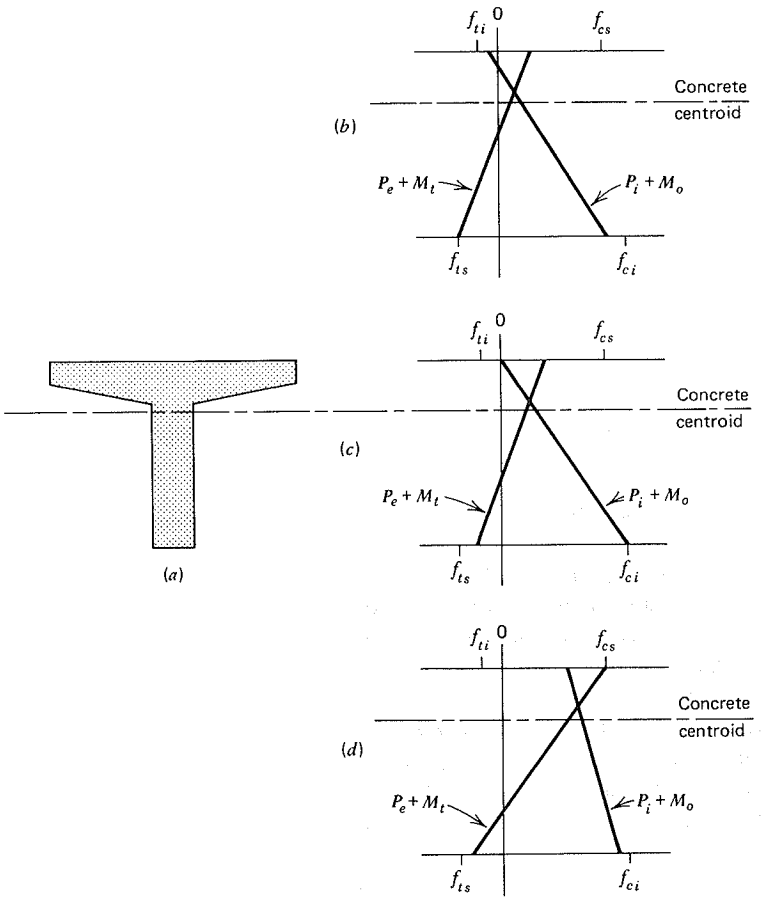

FIGURE 4.12 Alternate concrete stress distributions for a section with excess capacity.

A typical situation is illustrated in Fig. 4.12. For functional reasons, a beam having a T-shaped cross section with a broad top flange has been selected. The section moduli S_1 and S_2 exceed the minimum requirements. At the bottom face, as the beam passes from the unloaded to the service load stage, the concrete stresses are within, and come close to, the allowable limits f_{ts} and f_{ci} as shown by Fig. 4.12*c*, for example. At the top face, because of the high location of the concrete centroid, the stress change is much smaller and the concrete stresses are easily contained within the range from f_{ti} to f_{cs}.

Three of the many possible solutions for such a case are illustrated by Figs. 4.12*b*, *c*, and *d*, corresponding to different combinations of prestress force and eccentricity. In Fig. 4.12*b*, a relatively low value of P_i has been used (as confirmed by the low concrete centroidal stress compared with the other cases) combined with a high eccentricity (indicated by the slope of the stress distribution labeled $P_i + M_o$). In Fig. 4.12*c*, a higher value of P_i has been selected. Since the stress distribution $P_i + M_o$ has about the same slope as before, the eccentricity must have been somewhat less than that for Fig. 4.12*b*. In the final case, shown in Fig. 4.12*d*, a substantially larger prestress force has been used combined with a very small eccentricity.

All three cases illustrated by Fig. 4.12 meet the requirement that the stresses stay within the indicated limits in all stages between unloaded and full service load. However, the first choice would no doubt be the best, because it requires the smallest value of prestress force. In addition, the large eccentricity would be advantageous in maximizing the ultimate flexural strength of the member, since it would offer the largest internal lever arm between tension and compression resultants should the beam be overloaded.

In cases such as that just illustrated, where the concrete section has excess capacity, the previous equations for concrete centroidal stress and required eccentricity do not apply, because the stress limits f_{ti} and f_{ci} are not realized exactly. However, those equations may easily be modified to suit the circumstances. If the desired values of concrete stress in the initial stage, at the top and bottom faces of the member, are, respectively, f_{1i} and f_{2i}, then the concrete centroidal stress in the initial condition is

$$f_{cci} = f_{1i} - \frac{c_1}{h}(f_{1i} - f_{2i}) \tag{4.17}$$

The initial prestress force P_i is calculated by Eq. (4.5) as before. However, the eccentricity is found based on attaining the selected concrete stresses f_{1i} and f_{2i} under the combined effects of initial prestress force plus whatever self-weight moment acts at the controlling section. Thus, f_{1i} is substituted for f_{ti}, and f_{cci} from Eq. (4.17) is used in Eq. (4.6), (4.9), or (4.16) for beams with variable eccentricity, constant eccentricity, or deflected tendons, respectively.

Often the best combination of prestress force and eccentricity will be that which produces concrete stress f_{ti} in the initial stage with P_i and M_o acting and results in concrete tension f_{ts} at the full service load stage. In this case, some iteration normally will be required to arrive at the correct value of f_{2i} for use in Eq. (4.17), because the concrete stress change Δf_2 due to losses, which reduces the stress range available for moments due to external loads, is not known until P_i is calculated.

A graphical solution indicating all acceptable combinations of prestress force and eccentricity is helpful in making the best choice for a given concrete cross section (Ref. 4.5). There are four limit stresses to be satisfied: two at the initial unloaded stage and two at the full service load stage. The requirements

may be restated as follows for a beam with variable eccentricity, for example:

$$f_{ti} \geq -\frac{P_i}{A_c}\left(1 - \frac{ec_1}{r^2}\right) - \frac{M_o}{S_1} \tag{a}$$

$$f_{ci} \leq -\frac{P_i}{A_c}\left(1 + \frac{ec_2}{r^2}\right) + \frac{M_o}{S_2} \tag{b}$$

$$f_{ts} \geq -\frac{RP_i}{A_c}\left(1 + \frac{ec_2}{r^2}\right) + \frac{M_t}{S_2} \tag{c}$$

$$f_{cs} \leq -\frac{RP_i}{A_c}\left(1 - \frac{ec_1}{r^2}\right) - \frac{M_t}{S_1} \tag{d}$$

These equations may be rearranged to give the inverse of the initial prestress force as a linear function of eccentricity. For the initial stage, from Eqs. (a) and (b), respectively:

$$\frac{1}{P_i} \geq \frac{(-1 + ec_1/r^2)}{(f_{ti} + M_o/S_1)A_c} \tag{4.18}$$

$$\frac{1}{P_i} \geq \frac{(1 + ec_2/r^2)}{(-f_{ci} + M_o/S_2)A_c} \tag{4.19}$$

and for the service load stage, from Eqs. (c) and (d), respectively:

$$\frac{1}{P_i} \leq \frac{R(1 + ec_2/r^2)}{(-f_{ts} + M_t/S_2)A_c} \tag{4.20}$$

$$\frac{1}{P_i} \leq \frac{R(-1 + ec_1/r^2)}{(f_{cs} + M_t/S_1)A_c} \tag{4.21}$$

These functional relationships are plotted in Fig. 4.13 for a typical case. Equation (4.18) establishes a lower bound on $1/P_i$ (i.e., an upper bound on P_i) such that the tensile stress limit f_{ti} is not exceeded in the initial stage. Any value of $1/P_i$ above the line established by Eq. (4.18) is acceptable, as indicated by the shading. Similarly, Eq. (4.19) establishes another lower bound on $1/P_i$ such that the compressive stress limit f_{ci} is not violated. Upper limits on $1/P_i$ are established by Eq. (4.20), based on the service load tensile stress limit f_{ts}, and by Eq. (4.21), based on the service load compressive stress limit f_{cs}. The zone

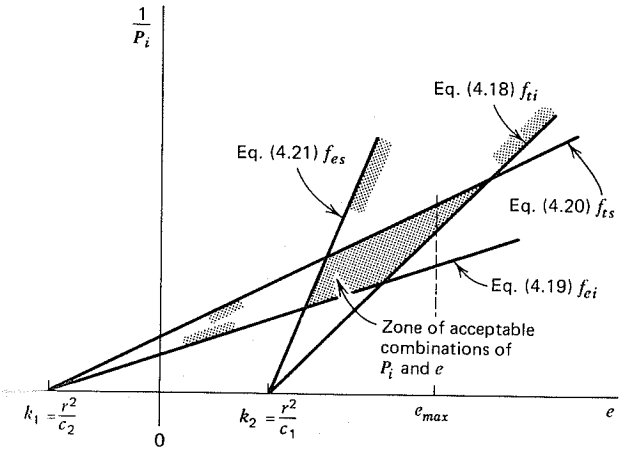

FIGURE 4.13 Variation of prestress force with eccentricity for beam section with excess capacity.

indicating acceptable combinations of P_i and e that meet all four requirements is shown shaded on the graph.

It is interesting to note the results of setting $1/P_i$ equal to zero for each of Eqs. (4.18) through (4.21). Equations (4.18) and (4.21) indicate that $e = r^2/c_1$, that is, $e = k_2$, the lower kern dimension. In physical terms, an infinite value of P_i can be applied at the lower kern without violating stress limits at the top of the member, since that concrete stress would be zero for any value of P_i. Similarly, Eqs. (4.19) and (4.20), when set equal to zero, indicate that $e = -r^2/c_2$, that is, $e = k_1$, the upper kern dimension. An infinite value of P_i can be applied at the upper kern without violating stress limits at the bottom of the member. The eccentricities corresponding to k_1 and k_2 are shown in Fig. 4.13.

The maximum eccentricity that can be used without violating any of the four stress limits is found at the intersection of Eqs. (4.18) and (4.20) in Fig. 4.13. This also corresponds to the minimum acceptable value of P_i (i.e., maximum $1/P_i$), and probably represents the most desirable solution.[4] In many practical cases, a maximum value e_{max} would be established by physical limitations, based on the available distance c_2 reduced by the necessary concrete cover for the tendons, measured from the steel centroid. Given that condition, in the example of Fig. 4.13, the best value of $1/P_i$ is that at the intersection of e_{max} with Eq. (4.20).

Note that in Fig. 4.13 all lines have been shown with positive slope. This is not always true and, for some cases, the lines may have infinite slope or a

[4] This confirms the earlier observation that the best combination of prestress force and eccentricity will be that which produces concrete stress f_{ti} in the initial stage and f_{ts} in the full service load stage.

negative slope. This is typically the case for T-beams, in which the top flange is often sufficiently large that the loads can be carried without exceeding f_{cs}, even if no prestress force were used. In this case, a negative slope is obtained for Eq. (4.21), and it does not control in the calculations.

The actual plotting of a diagram such as Fig. 4.13 is unnecessary in many practical cases if its general features are recognized. For example, for the widely used single-T and double-T beam sections, the eccentricity will often be controlled by the maximum depth available from the concrete centroid to the bottom face, less an allowance for concrete cover for the tendons. For that maximum eccentricity, as seen from Fig. 4.13, the minimum prestress force P_i will be governed by Eq. (4.20), based on the allowable service load tensile stress f_{ts}. The required prestress force can be calculated directly from Eq. (4.20), setting $e = e_{max}$. The concrete stresses in the initial stage and service load stage should then be checked, and if stress limits are not satisfied, the design can be modified after plotting all four equations, as in Fig. 4.13, to determine the best combination of P_i and e. However, this will seldom prove necessary.

The equations just developed, which pertain to beams with eccentricity varying along the span, are easily modified to apply to beams with constant eccentricity by setting $M_o = 0$, its value at the controlling support section, or to beams with deflected tendons by substituting M'_o for M_o.

EXAMPLE: Design of Beam Using Standard Cross Section Having Capacity Above That Required

A post-tensioned prestressed concrete roof deck is to be designed using 8-ft width single-T beams (see Section 12.2 and Appendix A) spanning 70 ft between simple supports. Service loads include live load of 88 psf, superimposed dead load of 10 psf, and estimated self-weight of 75 psf. Normal weight concrete is used with specified compressive strength $f'_c = 5{,}000$ psi and strength at time of prestressing $f'_{ci} = 3{,}500$ psi. The prestressing force will be provided using 1/2-in. diameter Grade 270 low-relaxation strands with $f_{pu} = 270$ ksi and $f_{py} = 243$ ksi. The effectiveness ratio can be assumed to be $R = 0.85$. Select an appropriate standard single-T section beam, and determine the required magnitude and eccentricity of prestress force based on ACI Code stress limitations. ($w_o = 8.75$ kN/m, $w_d = 1.17$ kN/m, $w_l = 10.27$ kN/m, span = 21.3 m, $f'_c = 34$ MPa, $f'_{ci} = 24$ MPa, $f_{pu} = 1{,}860$ MPa, $f_{py} = 1{,}680$ MPa.)

Referring to Table 3.1, the permissible stresses in the concrete immediately after transfer and at service load are:

$$f_{ci} = 0.60 \times 3{,}500 = -2{,}100 \text{ psi}$$

$$f_{ti} = 3\sqrt{3{,}500} = +177 \text{ psi}$$

$$f_{cs} = 0.45 \times 5{,}000 = -2{,}250 \text{ psi}$$

$$f_{ts} = 12\sqrt{5{,}000} = +849 \text{ psi}^5$$

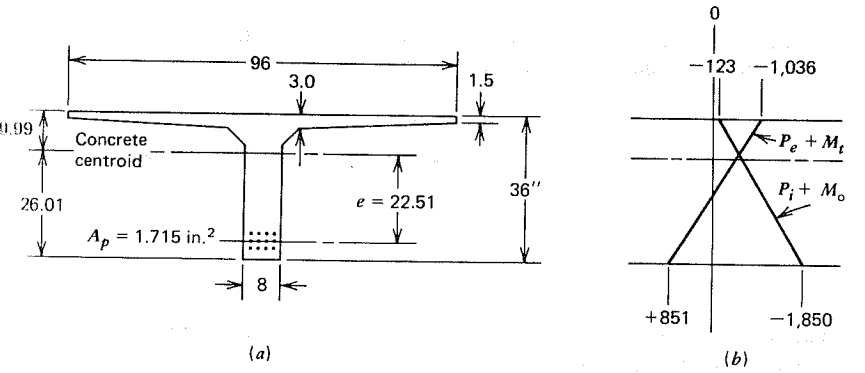

FIGURE 4.14 Example of design using standard single-T section beam. (*a*) Beam cross section. (*b*) Stresses at midspan.

The beam loads per foot and maximum moment values are found as follows:

$w_o = 75 \times 8 = 600$ plf	$M_o = 0.600 \times 70^2/8 = 368$ ft-kips	
$w_d = 10 \times 8 = 80$ plf	$M_d = 0.080 \times 70^2/8 = 49$ ft-kips	
$w_l = 88 \times 8 = 704$ plf	$M_l = 0.704 \times 70^2/8 = 431$ ft-kips	
Total	M_t	$= 848$ ft-kips

The minimum acceptable section moduli with respect to the top and bottom faces of the beam are found from Eqs. (4.1) and (4.2):

$$S_1 \geq \frac{(1-R)M_o + M_d + M_l}{Rf_{ti} - f_{cs}} = \frac{(0.15 \times 368 + 49 + 431)12{,}000}{0.85 \times 177 + 2{,}250} = 2{,}675 \text{ in.}^3$$

$$S_2 \geq \frac{(1-R)M_o + M_d + M_l}{f_{ts} - Rf_{ci}} = \frac{(0.15 \times 368 + 49 + 431)12{,}000}{849 + 0.85 \times 2{,}100} = 2{,}438 \text{ in.}^3$$

Consulting tables of section properties of standard single-T sections found in Ref. 4.6, it is found that the smallest section that can be used is a 36-in. depth member with the dimensions shown in Fig. 4.14*a*. For that cross-section, the section modulus $S_2 = 2{,}650$ in.^{3} is somewhat above the requirement, and $S_1 = 6{,}899$ in.^{3} is greatly above the required value. Complete section properties of the selected cross-section are:

$A_c = 570$ in.^{2}	$S_1 = 6{,}899$ in.^{3}
$I_c = 68{,}917$ in.^{4}	$S_2 = 2{,}650$ in.^{3}
$c_1 = 9.99$ in.	$r^2 = 120.9$ in.^{2}
$c_2 = 26.01$ in.	$w_o = 594$ plf (approximately as assumed)

For members of this type, it is probable that the eccentricity will be controlled by

[5] This will require a special check of deflections in the final design, based on a bilinear moment-deflection relationship.

the maximum available depth. Allowing for 3.5 in. from the tendon centroid to the bottom face of the beam, $e_{max} = 26.01 - 3.50 = 22.51$ in. Referring to Fig. 4.13, it is seen that the prestress force can be calculated from Eq. (4.20):

$$\frac{1}{P_i} = \frac{R(1 + ec_2/r^2)}{(-f_{ts} + M_t/S_2)A_c} = \frac{0.85(1 + 22.51 \times 26.01/120.9)}{(-849 + 848 \times 12{,}000/2{,}650)570}$$

from which

$$P_i = 343{,}000 \text{ lb}$$

According to ACI Code (see Table 3.2), the permissible tension in the steel immediately after transfer should not exceed $0.82f_{py} = 0.82 \times 243 = 200$ ksi, and must not exceed $0.74f_{pu} = 0.74 \times 270 = 200$ ksi, identical in this case. Thus, the required steel area is

$$A_p = \frac{343}{200} = 1.715 \text{ in.}^2$$

Each 1/2-in. diameter strand provides an area of 0.153 in.^{2} (see Table A.1 of Appendix A). Thus, the number of strands required is

$$\text{Number of strands} = \frac{1.715}{0.153} = 11.21$$

Twelve strands will be used, in a single tendon having eccentricity $e = 22.51$ in at midspan, decreasing parabolically to zero at the supports. Stresses in the concrete at midspan will now be checked, first calculating the separate effects, then superimposing.

$$P_i\text{: } f_1 = -\frac{343{,}000}{570}\left(1 - \frac{22.51 \times 9.99}{120.9}\right) = +517 \text{ psi}$$

$$f_2 = -\frac{343{,}000}{570}\left(1 + \frac{22.51 \times 26.01}{120.9}\right) = -3{,}516 \text{ psi}$$

$$P_e\text{: } f_1 = +517 \times 0.85 = +439 \text{ psi}$$

$$f_2 = -3{,}516 \times 0.85 = -2{,}989$$

$$M_o\text{: } f_1 = \frac{368 \times 12{,}000}{6{,}899} = -640 \text{ psi}$$

$$f_2 = \frac{368 \times 12{,}000}{2{,}650} = +1{,}666 \text{ psi}$$

$$M_t\text{: } f_1 = \frac{848 \times 12{,}000}{6{,}899} = -1{,}475 \text{ psi}$$

$$f_2 = \frac{848 \times 12{,}000}{2{,}650} = +3{,}840 \text{ psi}$$

Then, under initial conditions, immediately after transfer, the concrete stresses at the top and bottom faces are:

$$P_i + M_o\text{: } f_1 = +517 - 640 = -123 \text{ psi}$$

$$f_2 = -3{,}516 + 1{,}666 = -1{,}850 \text{ psi}$$

and at full service load, after all losses, they are:

$$P_e + M_t\text{: } f_1 = +439 - 1{,}475 = -1{,}036 \text{ psi}$$

$$f_2 = -2{,}989 + 3{,}840 = +851 \text{ psi}$$

These stress distributions are shown in Fig. 4.14*b*. Comparison with specified limit stresses confirms that the design is satisfactory.

Additional Comments

1. The selection of a single-T section beam, with broad top flange, was dictated by the functional requirements of providing a flat roof surface using identical beams at 8-ft lateral spacing. As a consequence of the section shape, the section modulus S_1 was greatly in excess of that required, although S_2 was quite close to that required. Correspondingly, the stresses of +851 psi and −1,850 psi at the bottom of the beam are close to the limit values $f_{ts} = +849$ psi and $f_{ci} = -2{,}100$ psi. (Except for rounding errors, f_{ts} would be satisfied exactly.) At the top of the section, stresses do not approach the limit values, but satisfy those limits.
2. Use of f_{ts} of $12\sqrt{f'_c}$ rather than $6\sqrt{f'_c}$ requires a deflection calculation that accounts for cracking at service loads, using a bilinear moment-deflection relationship, according to ACI Code.
3. Satisfaction of ACI Code stress limits does not guarantee an adequate safety margin against flexural failure. Adequate flexural strength must be provided to resist moments at factored loads. For sections of this type, it is often necessary to add non-prestressed bar reinforcement to work with the prestressed tendon steel in developing the required M_n.
4. Other bar reinforcement to be calculated in a complete design includes both longitudinal and transverse steel in the thin flange, web reinforcement in the girder web, and probably additional longitudinal rebars distributed through the depth of the web to control cracking. Special reinforcement is also required at the anchorage zone at the ends of the girder.

6. BEAMS OF LIMITED DEPTH

In deriving Eqs. (4.1) and (4.2) for required section moduli, the stress limits f_{ti} and f_{ci} were matched against the stresses at the top and bottom faces of the beam that resulted from the combined effects of the eccentric prestress force P_i and the full moment M_o due to self-weight, as shown by Fig. 4.2*a*. The moment

due to the beam's own weight was compensated by increasing the tendon eccentricity by the amount M_o/P_i below the eccentricity that would produce the limiting stresses, were P_i to be acting alone. The entire stress range $f_{ti} - f_{cs}$ at the top surface, and the full stress range $f_{ts} - f_{ci}$ at the bottom surface, reduced only by the effect of loss of prestress force, were available to resist the superimposed load moment $M_d + M_l$.

Full compensation for member self-weight may not be possible if the beam depth is limited for architectural reasons, or clearance requirements, or if there is a high ratio of self-weight to superimposed loads, as would be the case for long spans. The problem will become evident when the required tendon eccentricity is calculated from Eq. (4.6). The calculated eccentricity may provide insufficient concrete cover for the tendon, and in extreme cases, may indicate that the tendon be placed outside of the concrete section, obviously not a practical arrangement. It is possible to calculate the "critical span" for a member of given cross section, up to which the self-weight can be compensated for by tendon eccentricity, and beyond which it cannot (Refs. 4.3 and 4.3).

If the calculations indicate that for the concrete section chosen, the desired tendon eccentricity cannot be achieved, the section proportions should be modified if possible, providing the same section moduli with a section that is deeper and narrower and that can accommodate the desired tendons. If it is not possible to make the section deeper, then the section moduli must be increased for the member of restricted depth, since the stress ranges available to accommodate the superimposed loads are reduced.

The modified equations for required section moduli are developed with reference to Fig. 4.15. If the eccentric prestress force P_i were acting alone, distribution (1) would result. The moment M_o due to self-weight is immediately superimposed, however, and distribution (2) is obtained. It is noted that the stress limits f_{ti} and f_{ci} are satisfied, but not equaled. Since the bending moment due to prestress force P_i cannot be increased because of the restriction on depth and eccentricity, this condition must be accepted.

The effect of this is that the partial stress distribution shown shaded must be accounted for in writing the equations for the required section moduli. At the top surface, the additional compressive stress to be included within the available stress range between f_{ti} and f_{cs} is $\mu M_o/S_1$, and at the bottom, the tensile stress to be included between f_{ts} and f_{ci} is $\mu M_o/S_2$, where μ is a number, less than unity, defining the fractional part of the stresses due to the self-weight to be accounted for in this way. Thus,

$$S_1 \geq \frac{\mu M_o + M_d + M_l}{f_{1r}} \tag{a}$$

$$S_2 \geq \frac{\mu M_o + M_d + M_l}{f_{2r}} \tag{b}$$

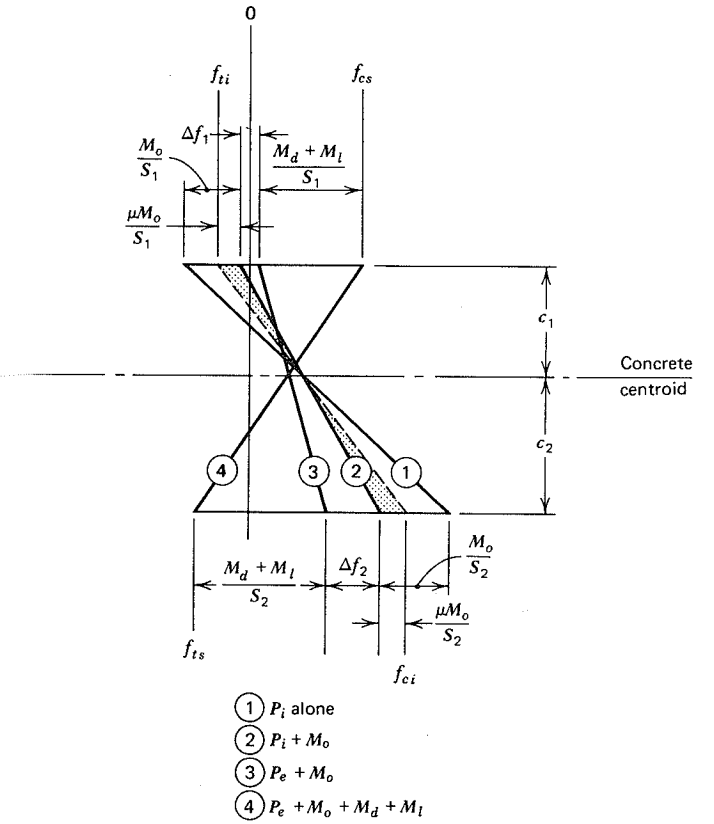

FIGURE 4.15 Flexural stress distributions when member self-weight cannot be fully compensated.

The change in top and bottom surface stresses as losses in prestress force take place are, respectively

$$\Delta f_1 = (1 - R)\left(f_{ti} + \frac{(1 - \mu)M_o}{S_1}\right) \tag{c}$$

$$\Delta f_2 = (1 - R)\left(-f_{ci} + \frac{(1 - \mu)M_o}{S_2}\right) \tag{d}$$

Then the stress ranges available to carry the moments included in Eqs. (a) and (b)

are:

$$f_{1r} = f_{ti} - \Delta f_1 - f_{cs}$$

$$= Rf_{ti} - (1 - R)\frac{(1 - \mu)M_o}{S_1} - f_{cs} \tag{e}$$

$$f_{2r} = f_{ts} - f_{ci} - \Delta f_2$$

$$= f_{ts} - Rf_{ci} - (1 - R)\frac{(1 - \mu)M_o}{S_2} \tag{f}$$

The equations for required section moduli are found by substituting the stress ranges of Eqs. (e) and (f) into Eqs. (a) and (b). The results are as follows:

$$S_1 \geq \frac{(1 - R + \mu R)M_o + M_d + M_l}{Rf_{ti} - f_{cs}} \tag{4.22}$$

$$S_2 \geq \frac{(1 - R + \mu R)M_o + M_d + M_l}{f_{ts} - Rf_{ci}} \tag{4.23}$$

Comparing Eqs. (4.1) and (4.2) with Eqs. (4.22) and (4.23), it is seen that they differ only by the inclusion of the factor μR in the last two equations. Since μ is not known at the outset of a design, it must be assumed; a good initial guess is zero.

The concrete centroidal stress and the initial prestress force can be found by using the equations of Section 4.2A without change:

$$f_{cci} = f_{ti} - \frac{c_1}{h}(f_{ti} - f_{ci}) \tag{4.4}$$

$$P_i = A_c f_{cci} \tag{4.5}$$

as is easily confirmed by Fig. 4.15. The maximum eccentricity e_{max} is determined on the basis of the minimum distance from the steel centroid to the bottom face of the beam, based on requirements of tendon spacing and concrete cover. With e_{max} known, the ratio μ can be determined for the beam chosen, and this value compared with that originally assumed. With reference to Fig. 4.15:

$$\frac{P_i e}{S_1} = (f_{ti} - f_{cci}) + (1 - \mu)\frac{M_o}{S_1} \tag{g}$$

from which

$$e = (f_{ti} - f_{cci})\frac{S_1}{P_i} + (1 - \mu)\frac{M_o}{P_i} \tag{4.24}$$

This eccentricity is now set equal to the available e_{max} and Eq. (4.24) is solved for μ, the only unknown. If this value differs appreciably from that assumed in calculating the section moduli, a revised value of μ is adopted and the calculations repeated.

It is clear from Eqs. (4.22) and (4.23) that the calculations are not sensitive to changes in μ, and as a result, the iterative design process converges to a satisfactory degree very quickly, often in only one cycle.

4.3 SHAPE SELECTION AND FLEXURAL EFFICIENCY

One of the unique features of prestressed concrete design is the freedom to select cross-sectional proportions and dimensions to suit the special requirements of the job at hand. The steel designer is limited to choosing from a number of readily available, usually symmetrical, cross-sectional shapes. In timber design, rectangular sections are used almost without exception. But in the case of prestressed concrete, not only can the member depth be changed, but the web thickness modified and the flange widths and thicknesses varied independently to produce a beam with nearly ideal proportions for a given case. Particularly for post-tensioned beams of medium or long span, the careful design of the cross section is an important part of the total design process.

For short span beams, in which the dead load of the beam is likely to be only a small fraction of the total load to be carried, rectangular members such as in Fig. 4.16*a* may provide the most economical solution, because forming costs are minimized. But for rectangular sections the kern distances are small, and the distance through which the compressive resultant may pass as load is applied is limited. For medium and long spans, the more efficient flanged shapes of Figs. 4.16*b* through 4.16*e* are preferred. The steel centroid may be kept lower, for such sections, without exceeding stress limits in the unloaded stage. The internal lever arm between tension and compression resultant forces at the service load and ultimate load stages is maximized.

In choosing a section, often the most expedient procedure is to start with a trial section, the properties of which match very closely the desired values of S_1 and S_2. The tabulated section constants of Appendix A will prove helpful in this connection. The trial section is then modified as required. With only two conditions to be satisfied (provision of the required S_1 and S_2) and six independent section dimensions to be chosen in general (Fig. 4.16), it is clear that there are many possible solutions. The designer must choose the best.

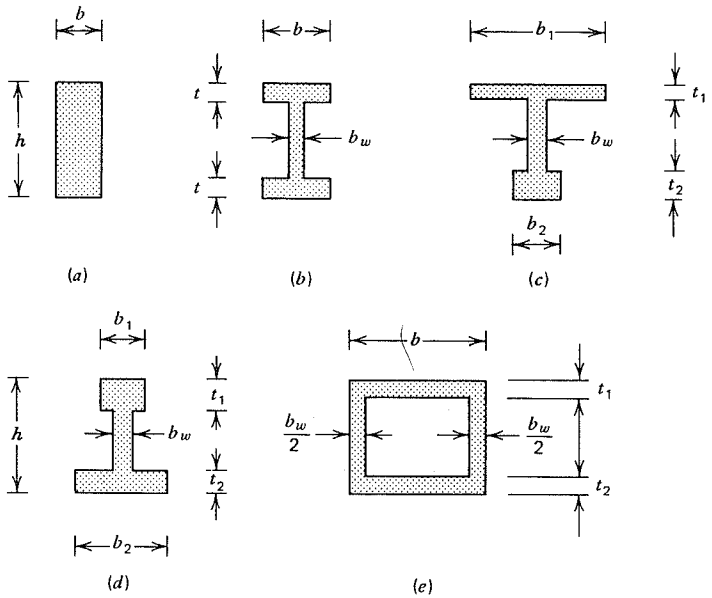

FIGURE 4.16 Types of beam cross sections. (*a*) Rectangular beam. (*b*) Symmetrical I-beam. (*c*) T-beam. (*d*) Inverted T-beam. (*e*) Hollow-box beam.

It is not always necessary or desirable to satisfy requirements for S_1 and S_2 exactly. In some cases a broad top flange is desired to provide a useful surface, as for bridge decks or building floors. Considering the flexural strength of a member, it is often desirable to provide a generous top flange so that, should the beam be overloaded, the concrete stresses will remain low, and a ductile failure insured though yielding of the tensile steel. In such cases, the compressive stress at the top face of the beam at full service load will be well below the allowed value. For long-span girders with a high ratio of self-weight to superimposed load, there is little danger of overstressing the bottom flange in compression at transfer, and the bottom flange may, in some cases, be eliminated altogether, resulting in a T-section.

In practice, the beam depth may be selected first, on the basis of a desirable span-depth ratio, or from requirements of headroom and clearance. The ratio of span to total depth for prestressed construction is considerably higher than is usual for reinforced concrete. Typical values for various types of prestressed members are given in Table 4.1. In all cases, continuity will permit use of larger span-depth ratios than for simple spans.

Once the depth of a beam is chosen, it is desirable to have a measure of the relative flexural efficiency of the cross sections being compared. In general terms, the ratio of section modulus to concrete area, S/A_c, will serve as such a measure.

Table 4.1 Typical Span-Depth Ratios for Prestressed Members

I-beams and single-T beams	24–36
Double-T beams	30–40
Bridge girders	25–30
One-way solid slabs	35–50
One-way hollowcore slabs	40–50
Two-way solid flat plates	40–50

A beam characterized by a high ratio of S/A_c would represent a more efficient use of the material than one with a low ratio.

For the general case of nonsymmetrical cross sections, one would like simultaneously to maximize the ratios S_1/A_c and S_2/A_c. Since $S_1 = I/c_1$ and $S_2 = I/c_2$, these ratios can be rewritten as follows:

$$\frac{S_1}{A_c} = \frac{I_c}{A_c c_1} = \frac{r^2}{c_1} \tag{a}$$

$$\frac{S_2}{A_c} = \frac{I_c}{A_c c_2} = \frac{r^2}{c_2} \tag{b}$$

Thus, for given values of c_1 and c_2, the most efficient cross section is the one with the largest value of radius of gyration, that is, the one in which the concrete area is concentrated as nearly as practical toward the extreme top and bottom surfaces.

The terms at the right of Eqs. (a) and (b) will be recognized as the lower kern and upper kern dimensions of the section, respectively (see Section 3.4D).

It is convenient to express the distances represented by Eqs. (a) and (b) in nondimensional form, in terms of the distances c_1 and c_2 to the top and bottom faces of the member. With $k_1 = r^2/c_2$ and $k_2 = r^2/c_1$, these ratios are

$$\frac{k_1}{c_1} = \frac{r^2}{c_1 c_2} \tag{c}$$

$$\frac{k_2}{c_2} = \frac{r^2}{c_1 c_2} \tag{d}$$

Consequently, the single expression

$$Q = \frac{r^2}{c_1 c_2} \tag{4.25}$$

can be used as a convenient basis for comparing the flexural efficiency of competing cross sections of a given depth.

The efficiency factor Q can also be expressed in geometric terms. Noting that $h = c_1 + c_2$

$$Q = \frac{r^2}{c_1 c_2} \frac{c_1 + c_2}{h} \tag{e}$$

$$Q = \frac{k_1 + k_2}{h} \tag{4.26}$$

indicating that the Q factor is nothing more or less than the ratio of the total kern depth to the total section depth.

Clearly, those I- and T-shaped cross sections with relatively thin webs and flanges will display higher Q factors than will cross sections with thicker parts. However, practical considerations place an upper limit on the degree of slenderness that can be achieved. The overall proportions of a beam must be chosen considering the possibility of lateral buckling of the loaded member, if it is not supported against lateral movement by connected construction. This is particularly a factor during the handling of precast members. Thin compression flanges always present the danger of local buckling when loaded. Thin overhanging flanges are vulnerable to breakage during the handling and erection of precast elements.

The minimum thickness of the web is often determined by minimum clearances needed for the prestressing tendons and the auxiliary reinforcement, and the requirements of concrete cover for the outermost steel. Although web thicknesses of less than 5 in. may be satisfactory to carry shear stresses with a reasonable amount of web reinforcement, such thin webs are often difficult to place without risk of voids or air pockets. Normally a 5-in. web width should be considered the practical minimum (Ref. 4.7). Web widths are usually smaller in European practice than in the United States.

In general, well-designed I-beams have an efficiency factor close to 0.50. Q factors less than about 0.45 indicate too heavy a section, and values larger than about 0.55 indicate an excessively slender section of questionable practicality (Ref. 4.3). Many standards sections, such as, single and double-T beams, have relatively low Q values, but are used because of their practical advantages.

4.4 STANDARD SECTIONS

Certain standard cross-sectional shapes have evolved over the years for floor and roof panels, wall panels, beams, and columns, as well as for short and medium span highway bridge girders. Members with these standard shapes can be mass-produced by precasting plants, often using long-line methods and permanent, reusable metal forms. Great cost savings are possible, compared with construction that requires special forming, either in a precasting plant or at the construction site. Consequently, standard sections are often used, even though properties may not be optimum for a particular set of design constraints and even though the section efficiency could be improved by shape modification.

The most common standard sections used for building construction are described in section 12.2, and those shapes most often employed for bridges up to medium span are discussed in Section 12.7. Reference 4.6 contains useful tables of section properties of standard precast sections, as well as load tables for particular prestressing configurations.

4.5 CONCRETE PROTECTION AND SPACING OF TENDONS

To provide tendons, ducts, and reinforcing bars with adequate protection against corrosion and fire, it is necessary to maintain a certain minimum thickness of concrete cover outside of the outermost steel. The thickness required varies depending on the type of construction, condition of exposure, class of member, and type of reinforcement.

The ACI Code imposes the minimum cover distances for prestressed concrete shown in Table 4.2. When tendons are enclosed in ducts, as is usual for post-tensioned members, cover distances apply to the duct and the metal end-

Table 4.2 ACI Code Requirements for Concrete Protection for Prestressed and Non-prestressed Reinforcement, Ducts, and End Fittings

Exposure condition and class of member	Minimum cover in.	Minimum cover mm
(a) Concrete cast against and permanently exposed to earth	3	70
(b) Concrete exposed to earth or weather:		
Wall panels, slabs, joists	1	30
Other members	$1\frac{1}{2}$	40
(c) Concrete not exposed to weather or in contact with ground:		
Slabs, walls, joists	3/4	20
Beams, columns		
Primary reinforcement	$1\frac{1}{2}$	40
Ties, stirrups, spirals	1	20
Shells, folded plates:		
No. 5 bar, W31 or D31 wire and smaller	3/8	10
Other reinforcement d_b, but not less than	3/4	20

fittings. Normally, tendons are enclosed in transverse stirrup bar reinforcement, in which case cover distances are measured to the outside of the stirrups, and are somewhat less than required for primary reinforcement, which may consist of both tendons and non-prestressed reinforcing bars.

If the prestressed member is designed for a service load tension in excess of $6\sqrt{f'_c}$ (see Table 3.1), cracking of the concrete is likely and according to ACI Code, the minimum cover requirements of Table 4.2 must be increased 50 percent. For precast members, improved dimensional control in construction of forms and placement of steel justifies some reduction in cover for the non-prestressed bar reinforcement, and special provisions of the ACI Code account for this.

Normally, it is necessary to maintain a certain minimum distance between parallel tendons or reinforcing bars to ensure proper placement of concrete around them. Air pockets below the steel should be avoided, and full contact between the bars or tendons and concrete is desirable to optimize bond strength. The ACI Code specifies that the minimum clear distance between adjacent bars in a layer should not be less than the nominal bar diameter d_b, nor 1 in. Where the reinforcement is placed in two or more layers, the clear distance between layers must not be less than 1 in. and the bars in the upper layer should be placed directly above those in the bottom layer. These provisions are interpreted to apply to prestressing strands, as well as reinforcing bars, although "bundling" is permitted (see next paragraph).

At the ends of pretensioned members, spacing requirements are increased to ensure proper transfer of prestress force by bond. According to ACI Code, the clear distance between pretensioning tendons in the end region must not be less than $4d_b$ for wires and $3d_b$ for strands. Elsewhere along the span, it is permissible to bundle the reinforcement, that is, to place groups of no more than four tendons or bars in contact so that they act as a unit. If this is done and if spacing limitations are based on the diameter d_b, a unit of bundled tendons or bars is treated as a single bar or tendon of diameter corresponding to the total equivalent area.

When post-tensioning ducts are arranged closely together vertically, adequate spacing must be provided to prevent the tendons, when tensioned, from breaking through the duct. Experience indicates that a clear spacing of ducts of one and one-third times the size of the coarse aggregate and not less than 1 in. will be satisfactory.

4.6 LOAD BALANCING AS A DESIGN TOOL

It was pointed out in Section 1.3 that the effect of a change in the alignment of a prestressing tendon in a beam is to produce a vertical force on the beam at that location. Prestressing a member with curved or deflected tendons thus has the effect of introducing a set of equivalent loads, and these may be treated just as any other loads in finding moments or deflections. Each particular tendon profile produces its own unique set of equivalent forces. Typical tendon profiles, with corresponding equivalent loads and moment diagrams, were illustrated in Fig. 1.8. Both Fig. 1.8 and Section 1.3 should be reviewed carefully.

The equivalent load concept offers an alternative approach to the determination of required prestress force and eccentricity. The prestress force and tendon profile can be established so that external loads that will act are exactly counteracted by the vertical forces resulting from prestressing. The net result, for that particular set of external loads, is that the beam is subjected only to axial compression, and no bending moment. The selection of the load to be balanced is left to the judgement of the designer. Often the balanced load chosen is the sum of the self-weight and superimposed dead load.

The design approach described in this section was introduced in the United States by T. Y. Lin in 1963 (Refs. 4.8 and 4.9), and is known as the *load-balancing method*. The fundamentals will be illustrated in the context of the simply supported, uniformly loaded beam of Fig. 4.17*a*. The beam is to be designed for a balanced load consisting of its own weight w_o, the superimposed dead load w_d, and some fractional part of the live load denoted by $k_b w_l$. Since the external load is uniformly distributed, it is reasonable to adopt a tendon having a parabolic shape. It is easily shown that a parabolic tendon will produce a uniformly distributed upward load equal to

$$w_p = \frac{8Py}{l^2} \tag{4.27}$$

where P is the magnitude of the prestress force, y is the maximum sag of the tendon measured with respect to the chord between its end points, and l is the span.

If the downward load exactly equals the upward load from the tendon, these two loads cancel and no bending stress is produced, as shown in Fig. 4.17*b*. The bending stresses due to prestress eccentricity are equal and opposite to the bending stresses resulting from the external load. The net resulting stress is uniform compression f_a equal to that produced by the axial force $P\cos\theta$. Excluding consideration of time-dependent effects, the beam would show no vertical deflection.

If the live load is removed or increased, then bending stresses and deflections will result because of the *unbalanced* portion of the load. Stresses resulting from this differential loading must be calculated and superimposed on the axial compression to obtain the net stresses for the unbalanced state. If we refer to Fig. 4.17*c*, the bending stresses f'_b resulting from removal of the partial live loading are superimposed on the uniform compressive stress f_a, resulting from the combination of eccentric prestress force and full balanced load to produce the final stress distribution shown.

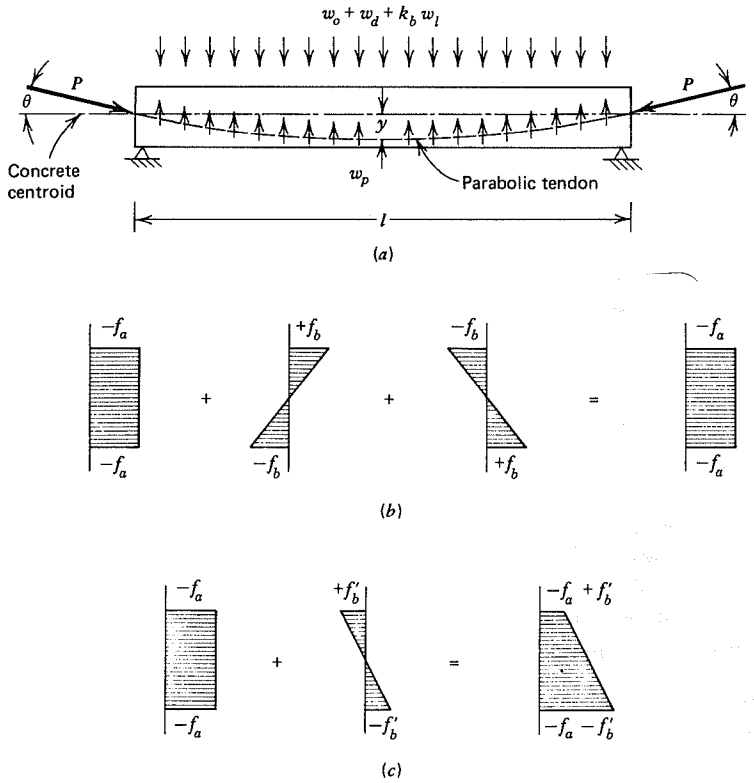

FIGURE 4.17 Load balancing for a uniformly loaded beam. (*a*) External and equivalent loads. (*b*) Concrete stresses resulting from axial and bending effects of prestress plus bending resulting from balanced external load. (*c*) Concrete stresses resulting when load $k_b w_l$ is removed.

Loads other than uniformly distributed would lead naturally to the selection of other tendon configurations. For example, if the external load consisted of a single concentration at midspan, a deflected tendon such as that of Fig. 1.8*a* would be chosen, with maximum eccentricity at midspan, varying linearly to zero eccentricity at the supports. A third-point loading would lead the designer to select a tendon deflected at the third points. A uniformly loaded cantilever beam would best be stressed using a tendon in which the eccentricity varied parabolically, from zero at the free end to y at the fixed support, in which case the upward reaction of the tendon would be

$$w_p = \frac{2Py}{l^2} \tag{4.28}$$

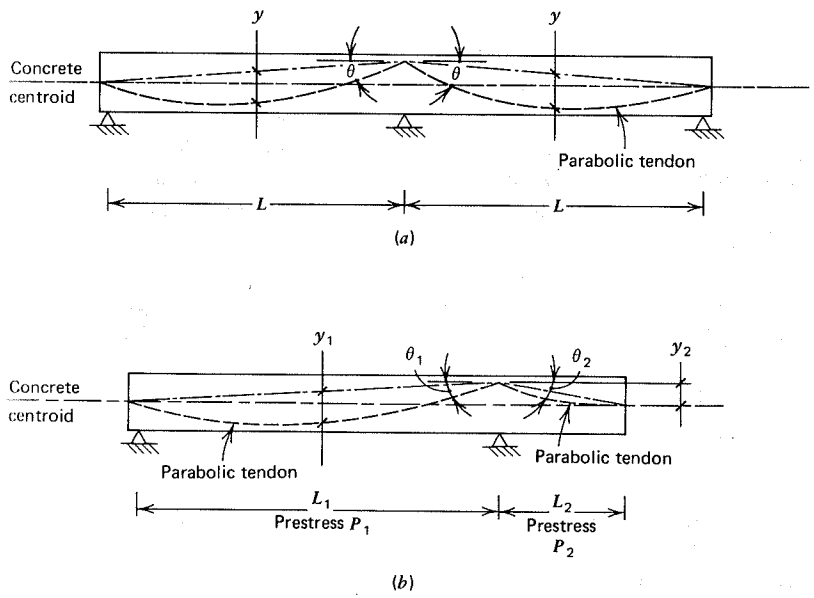

FIGURE 4.18 Load-balancing tendon profiles for uniformly loaded beams continuous over supports. (*a*) Two-span continuous beam. (*b*) Beam with cantilever.

It should be clear that for simple spans designed by the load-balancing concept, it is necessary for the tendon to have zero eccentricity at the supports, because the moment due to superimposed loads is zero there. Any tendon eccentricity would produce an unbalanced moment (in itself an equivalent load) equal to the horizontal component of the prestress force times its eccentricity.

For spans continuous over supports, this restriction does not apply. In Fig. 4.18*a*, if the prestress force is the same in the two spans adjacent to the interior support, and if the slope of the tendon is the same on either side, then the net bending moment applied to the beam at that location is zero. The only unbalanced load is the vertical force resulting from the change of tendon slope. This passes directly into the support. In such a case, the tendon may be raised to the maximum eccentricity permitted by requirements of concrete cover, maximizing the sag y in the adjacent spans and minimizing the prestress force required to carry the specified load. At the simply supported ends, the requirement of zero eccentricity must be retained.

At the free end of a cantilever beam (Fig. 4.18*b*), the steel eccentricity must be zero. The slope of the tendon there must match the slope of the concrete centroid, usually zero. In Fig. 4.18*b*, it is unlikely that the tendon slope θ_1 will equal the tendon slope θ_2; consequently, if the prestress force P_1 is the same as P_2, a net moment at the right support will result from prestressing. This could be

avoided by using separate tendons for each span, each with its own value of prestress such that the horizontal components balance.

In practice, the load-balancing method of design starts with selection of a trial beam cross section, based on experience and judgment. An appropriate span–depth ratio is often applied. The tendon profile is selected using the maximum available eccentricity, and the prestress force is calculated. The trial design may then be checked to ensure that concrete stresses are within the allowable limits should the live load be totally absent or fully in place, when bending stresses will be superimposed on the axial compressive stresses. There is no assurance that the section will be adequate for these load stages, nor that adequate strength will be provided should the member be overloaded. Revision may be necessary.

It should further be observed that obtaining a uniform compressive concrete stress at the balanced load stage does not ensure that the member will have zero deflection at this stage. The reason for this is that the uniform stress distribution is made up of two parts: that from the eccentric prestress force and that from the external loads. The prestress force varies with time because of shrinkage, creep, and relaxation, changing the vertical deflection associated with the prestress force. Concurrently, the beam will experience creep deflection under the combined effects of the diminishing prestress force and the external loads, a part of which may be sustained and a part of which may be short-term. However, if load balancing is carried out based on the effective prestress force P_e plus self-weight and external dead load only, the result may be near-zero deflection for that combination.

The load-balancing method provides the engineer with a useful tool. For simple spans, it leads the designer to choose a sensible tendon profile and focuses attention very early on the matter of deflection. But the most important advantages become evident in the design of indeterminate prestressed members, including both continuous beams and two-way slabs. For such cases, at least for one unique loading, the member carries only axial compression but no bending. This greatly simplifies the analysis.

EXAMPLE: Beam Design Initiating With Load Balancing

A post-tensioned beam is to be designed to carry a uniformly distributed load over a 30-ft span, as illustrated by Fig. 4.19*a*. In addition to its own weight, it must carry a dead load of 150 plf and a service live load of 600 plf. Concrete strength of 4,000 psi will be attained at 28 days; at time of transfer of prestress force, the strength will be 3,000 psi. Prestress loss may be assumed at 20 percent of P_i. On the basis that about one quarter of the live load will be sustained over a substantial time period, k_b of 0.25 will be used in determining the balanced load. (Span = 9.1 m, w_d = 2.2 kN / m, w_l = 8.8 kN / m, f'_c = 28 MPa, and f'_{ci} = 21 MPa.)

On the basis of an arbitrarily chosen span–depth ratio of 18, a trial section of 20 in. total depth is selected, having a 10-in. width. The calculated self-weight of the

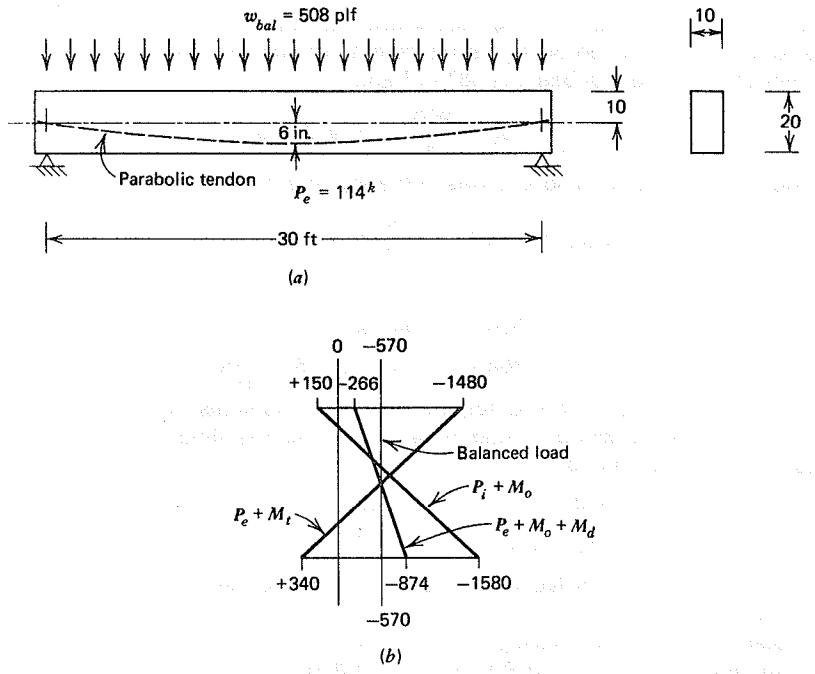

FIGURE 4.19 Example of design by load balancing. (*a*) Beam profile and cross section. (*b*) Flexural stresses at maximum moment section.

beam is 208 plf and the selected load to be balanced is

$$w_{bal} = w_o + w_d + k_b w_l = 208 + 150 + 150 = 508 \text{ plf}$$

Based on a minimum concrete cover from the steel centroid to the bottom face of the beam of 4 in., the maximum eccentricity that can be used for the 20-in. trial section is 6 in. A parabolic tendon will be used to produce a uniformly distributed upward tendon reaction. To equilibrate the sustained downward loading, the prestress force P_e after losses, from Eq. (4.27), should be

$$P_e = \frac{w_{bal} l^2}{8y} = \frac{508 \times 900}{8 \times 0.5} = 114{,}000 \text{ lb (507 kN)}$$

and the corresponding initial prestress force is

$$P_i = \frac{P_e}{R} = \frac{114{,}000}{0.8} = 143{,}000 \text{ lb (636 kN)}$$

For the balanced load stage, the concrete will be subjected to a uniform compressive stress of

$$f_{bal} = \frac{114{,}000}{200} = -570 \text{ psi}$$

as shown in Fig. 4.19*b*. Should the partial live load of 150 plf be removed, the stresses to be superimposed on f_{bal} result from a net *upward* load of 150 plf. The section modulus for the trial beam is 667 in.^{3} and

$$M_{unbal} = 150 \times \frac{900}{8} = 16{,}900 \text{ ft-lb}$$

Hence, the unbalanced bending stresses at the top and bottom faces are

$$f_{unbal} = 16{,}900 \times \frac{12}{667} = 304 \text{ psi}$$

Thus, the net stresses are

$$f_1 = -570 + 304 = -266 \text{ psi } (-1.8 \text{ MPa})$$

$$f_2 = -570 - 304 = -874 \text{ psi } (-6.0 \text{ MPa})$$

Similarly, if the *full* live load should act, the stresses to be superimposed are those resulting from a net *downward* load of 450 plf. The resulting stresses in the concrete at full service load are

$$f_1 = -570 - 910 = -1{,}480 \text{ psi } (-10.2 \text{ MPa})$$

$$f_2 = -570 + 910 = +340 \text{ psi } (+2.3 \text{ MPa})$$

Stresses in the concrete with live load absent and live load fully in place are shown in Fig. 4.19*b*.

It is also necessary to investigate the stresses in the initial unloaded stage, when the member is subjected to P_i plus moment due to its own weight.

$$M_o = 208 \times \frac{900}{8} = 23{,}400 \text{ ft-lb}$$

Hence, in the initial stage:

$$f_1 = -\frac{143{,}000}{200}\left(1 - \frac{6 \times 10}{33.35}\right) - \frac{23{,}400 \times 12}{667} = +150 \text{ psi } (+1.0 \text{ MPa})$$

$$f_2 = -\frac{143{,}000}{200}\left(1 + \frac{6 \times 10}{33.35}\right) + \frac{23{,}400 \times 12}{667} = -1{,}580 \text{ psi } (-10.9 \text{ MPa})$$

The stresses in the unloaded and full service load stages must be checked against these permitted by Code. With $f'_c = 4{,}000$ psi and $f'_{ci} = 3{,}000$ psi, the permitted stresses are:

$f_{ti} = +165$ psi (+ 1.1 MPa) $\quad f_{ts} = +380$ psi (+ 2.6 MPa)

$f_{ci} = -1{,}800$ psi (− 12.4 MPa) $\quad f_{cs} = -1{,}800$ psi (− 12.4 MPa)

The actual stresses, shown in Fig. 4.19*b*, are within these limits and acceptably close, and no revision will be made in the trial 10 × 20 in. (254 × 508 mm) cross section on the basis of stress limits.

The ultimate flexural strength of the members must now be checked, to insure that an adequate factor of safety against collapse has been provided. The required P_i of 143,000 lb will be provided using stranded Grade 250 cable, with $f_{pu} = 250{,}000$ psi and $f_{py} = 212{,}000$ psi. Referring to Table 3.2, the initial stress immediately after transfer must not exceed $0.74 \times 250{,}000 = 185{,}000$ psi, or $0.82 \times 212{,}000 = 174{,}000$ psi, which controls in this case. Accordingly, the required area of tendon steel is

$$A_p = 143{,}000 / 174{,}000 = 0.82 \text{ in.}^2 \ (529 \text{ mm}^2)$$

This will be provided using eight $\frac{7}{16}$ in. strands, giving an actual area of 0.864 in.^{2} (Table 2.2). The resulting stresses at the initial and final stages are

$$f_{pi} = \frac{143{,}000}{0.864} = 166{,}000 \text{ psi}$$

$$f_{pe} = \frac{114{,}000}{0.864} = 132{,}000 \text{ psi}$$

Using the ACI approximate equation for steel stress at failure [see Eq. (3.21)], with $\rho_p = 0.864 / 160 = 0.0054$, and $\gamma_p = 0.40$ for the ordinary Grade 250 tendons, the stress f_{ps} is given by

$$f_{ps} = f_{pu}\left(1 - \frac{\gamma_p}{\beta_1}\frac{\rho_p f_{pu}}{f'_c}\right)$$

$$= 250\left(1 - \frac{0.40}{0.85}\frac{0.0054 \times 250}{4}\right)$$

$$= 210 \text{ ksi}$$

Then,

$$a = \frac{A_{ps} f_{ps}}{0.85 f'_c b}$$

$$= \frac{0.864 \times 210}{0.85 \times 4 \times 10} = 5.34 \text{ in. } (136 \text{ mm})$$

The nominal flexural strength is

$$M_n = A_p f_{ps}\left(d - \frac{a}{2}\right) = 0.864 \times 210{,}000\left(16 - \frac{5.34}{2}\right)\frac{1}{12}$$

$$= 202{,}000 \text{ ft-lb } (275 \text{ kN-m})$$

This must be reduced by the factor $\phi = 0.90$ as usual to obtain design strength:

$$\phi M_n = 0.90 \times 202{,}000 = 182{,}000 \text{ ft-lb } (247 \text{ kN-m})$$

It will be recalled that the ACI load factors with respect to dead and live loads are, respectively, 1.4 and 1.7 (see Table 1.2). The safety factor obtained in the present case will be evaluated with respect to the service live load moment of 67,500 ft-lb, assuming that dead loads may be 1.4 times the calculated values, in keeping with the ACI requirements. Accordingly,

$$182 = 1.4(23.4 + 16.9) + F_l(67.5)$$

$$F_l = 1.86$$

This exceeds the ACI minimum of 1.7 and the design is judged satisfactory.

4.7 FLEXURAL DESIGN BASED ON PARTIAL PRESTRESSING

There is a distinct trend in current design practice toward the use of partially prestressed beams, in which flexural tensile cracking is permitted in the concrete in the service load stage or for occasional overloads (Refs. 4.10 to 4.16). Cracks are usually small and well distributed, and normally close completely when the load that produced them is removed.

It is argued convincingly that cracking has long been an accepted feature of reinforced concrete members and that there is no reason to penalize prestressed concrete designs by requiring that flexural cracks be eliminated completely, even though this is possible. Furthermore, the condition of no tension is never attained in a prestressed structure. If combined effects including shear or torsion are taken into account, the calculated principal stresses usually exceed the tensile strength of the concrete. In regions of concentrated loads, load transfer, or anchorage of tendons, tensile stresses cannot be avoided. Also, in most cases, a structure is prestressed in only one direction, so that in the transverse direction it acts as ordinary reinforced concrete. In view of these facts, it is hard to justify a requirement for no flexural cracking.

The advantages of partial prestressing are important. A smaller prestress force will be required, permitting reduction in the number of tendons and anchorages. The necessary flexural strength may be provided in such cases either by a combination of prestressed tendons and non-prestressed reinforcing bars, or by an adequate number of high-tensile tendons prestressed to a level lower than the permitted limit. In some cases, a combination of stressed and unstressed tendons is used. Since the prestressing force is smaller, the size of the bottom flange, which is required mainly to resist the compression when a beam is in the unloaded stage, can be reduced or eliminated altogether. This leads in turn to significant simplification and cost reduction in the construction of forms, as well as resulting in structures that are more pleasing esthetically. Furthermore, by relaxing the requirement for little or no service load tension in the concrete, a significant improvement can be made in the deflection characteristics of a beam. Troublesome upward camber in the unloaded stage can be avoided, and the prestress force selected primarily to produce the desired deflection for a particular loading condition. In addition, the behavior of partially prestressed beams, should they be overloaded to failure, is apt to be superior to that of fully prestressed beams, because the improved ductility provides ample warning of distress. Such points have been discussed more fully in Section 3.9.

The present ACI Code permits tensile stress in the concrete of $6\sqrt{f'_c}$ at full service load. This is slightly below the usual modulus of rupture. No cracking should occur if the tension is limited to this value, and the design methods presented earlier in this chapter are fully applicable.

The Code also permits flexural tension as high as $12\sqrt{f'_c}$ at full service load, provided that deflection calculations accounting for the cracked section confirm that deflections are within specified limits and that normal concrete cover requirements are increased by 50 percent. This tensile stress is above the modulus of rupture, so flexural cracks can be expected. A partially prestressed beam design results. It is clear that tensile stresses calculated on the basis of an uncracked concrete section for such designs are *nominal stresses* only. Nevertheless, they may serve as the basis for proportioning beam sections, and the equations of Section 4.2 are generally used without modification for designs satisfying this stress limit.

More rational methods for the design of partially prestressed beams are available. The first, described in Section 4.7A, is similar to the approach currently used to design reinforced concrete beams, in that the section is proportioned and steel area selected to provide the necessary strength at factored loads. The second, described in Section 4.7B, starts with the determination of prestress force and eccentricities to balance a selected load. In either case, all relevant limit states must be considered in the total design, and generally some iteration will be required.

A. STRENGTH APPROACH TO THE DESIGN OF PARTIALLY PRESTRESSED BEAMS

The first method for the design of a partially prestressed concrete beam starts with provision of *strength* sufficient to resist hypothetical overloads, which are calculated by applying overload factors to the expected service dead and live loads. After the required concrete and steel areas are determined, an amount of prestress force may be specified to produce a member with the desired deflection or cracking properties. The stresses at service load may be considered almost irrelevant, provided that all requirements of strength and serviceability are met (see Section 1.9).

It will be recognized that this is exactly analogous to the preferred design method for ordinary reinforced concrete, by which the cross-sectional dimensions and required reinforcement are found based on providing design strength just equal to strength required at factored loads. After this, service load deflections and cracking are investigated, and the design modified, if necessary. Service load stresses are not usually calculated.

This approach to design is appealing, because in all but unusual cases the most important single characteristic of a member, reinforced or prestressed, is its strength, which establishes the degree of safety incorporated. There are some complications when using the method for prestressed concrete, however. For reinforced concrete, consideration is usually limited to under-reinforced beams, for which the steel bars are at the yield stress at failure. With the tensile force known, the compressive area of the cross section is easily calculated from the summation of horizontal forces. With the centroid of the compression area known, the internal resisting lever arm is known and an explicit equation can be

written for the ultimate resisting moment. This equation can be rearranged to permit direct solution for the required concrete dimensions and tensile steel area (Ref. 4.17). For prestressed concrete, on the other hand, the stress in the steel at flexural failure is some value f_{ps}, usually less than the tensile strength f_{pu}. It may be more or less than the nominal yield stress f_{py}. The compression concrete area, which is a function of steel stress at failure, is not easily established at the outset, so the internal lever arm between compressive and tensile resultants is not known.

However, in practical cases, a trial concrete section may be found by assuming that the tendon stress at failure is 0.9 times the ultimate strength f_{pu}. Refinement will be found necessary only in cases when there is an unusually large percentage of steel. For flanged sections, the internal lever arm at failure is very nearly equal to the distance from the tensile steel centroid to the middepth of the flange.

On this basis, a strength design procedure for partially prestressed beams may be developed as follows:

1. Find the required ultimate flexural strength M_u by applying overload factors to the calculated dead loads and specified service live loads. According to the usual specifications, the nominal strength required of the member is $M_n = M_u/\phi$, where ϕ is a capacity reduction factor equal to 0.90 for bending.
2. A trial depth is assumed for the concrete section based on maximum span–depth ratio or experience. Top flange dimensions may be based on functional requirements or other criteria.
3. The internal lever arm z is assumed equal to the distance from the steel centroid to the middepth of the flange or, in the case of a rectangular section, equal to $0.80h$. If the steel stress at failure is taken to be $0.90f_{pu}$, then the required area of the tendon is

$$A_p = \frac{M_n}{0.9f_{pu}z} \tag{4.29}$$

4. Assuming for design purposes that the actual concrete stress distribution can be replaced by an equivalent rectangular stress block at uniform stress intensity $0.85f'_c$, the required area of compression concrete is

$$A'_c = \frac{M_n}{0.85f'_c z} \tag{4.30}$$

   This gives the required area of the top flange, after making allowance for the contribution, if any, of the web area in compression. The trial section is modified if necessary.
5. The web width can now be chosen based on shear strength requirements or the practical need for concrete cover for tendons and other steel.
6. The amount of prestress force is chosen to produce the desired deflection characteristics for the member. A criterion of zero deflection under the combined effects of prestress and partial service load (often full dead load) may be selected. The load-balancing concept described in Section 4.6 is used for determining the required prestress force.
7. Flexural tensile stress in the concrete at full service load is then checked, and if it exceeds the modulus of rupture significantly, crack widths should be checked using either of the two methods of Section 4.8. Analysis of the stresses in the cracked elastic section can be done using the method of Section 3.10. In some cases, non-prestressed reinforcing bars may be added specifically for crack control.

EXAMPLE: Design Based on Strength Requirements and Partial Prestressing

A beam having a T cross section is to be designed to carry a service live load of 1,200 plf and superimposed dead load of 400 plf in addition to its own weight, on an 80-ft simple span, as shown in Fig. 4.20*a*. The member will be post-tensioned using tendons composed of Grade 250 stranded cable. Concrete strength at 28 days is specified to be 5,000 psi. A partially prestressed design based on strength will be adopted, with the additional requirement that zero deflection is to be obtained under full service dead load. (w_l = 17.5 kN / m, w_d = 5.8 kN / m, span = 24.4 m, and f'_c = 34 MPa.)

In lieu of other restrictions, a trial member depth of one-twentieth of the span, or 4 ft (1,219 mm), will be selected. Functional requirements dictate a flange width

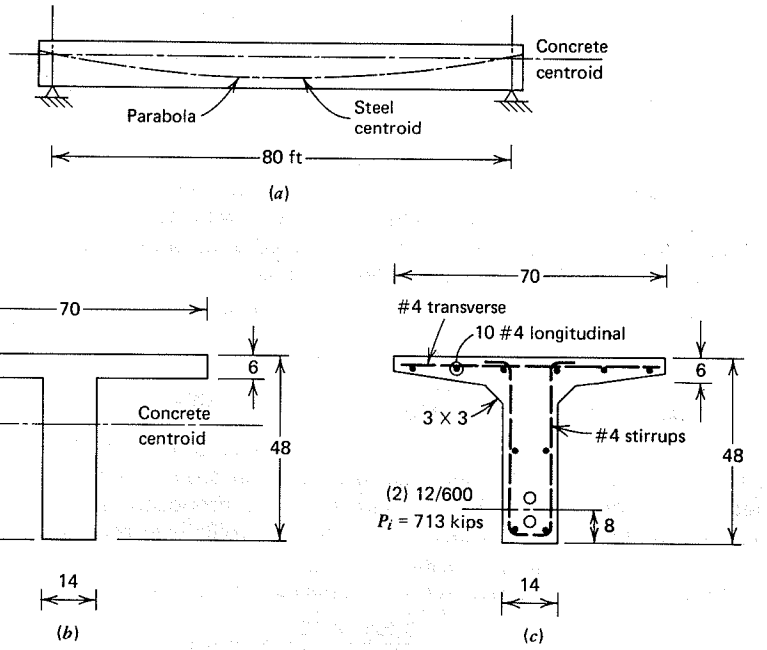

FIGURE 4.20 Partial prestress design example. (*a*) Beam profile. (*b*) Idealized section. (*c*) Final section.

of 70 in. (1.778 mm) having an average thickness of 6 in. (152 mm). Anticipated requirements for ducts and anchorages, as well as requirements for web reinforcement lead to a choice of 14 in. (356 mm) web width. The trial section, shown in Fig. 4.20*b*, has the following properties:

$$I_c = 229{,}000 \text{ in.}^4 \ (95.3 \times 10^9 \text{ mm}^4)$$

$$S_1 = 13{,}500 \text{ in.}^3 \ (221 \times 10^6 \text{ mm}^3)$$

$$S_2 = 7{,}380 \text{ in.}^3 \ (121 \times 10^6 \text{ mm}^3)$$

$$c_1 = 17.0 \text{ in. (432 mm)}$$

$$c_2 = 31.0 \text{ in. (787 mm)}$$

$$A_c = 1{,}010 \text{ in.}^2 \ (652 \times 10^3 \text{ mm}^2)$$

$$w_o = 1{,}050 \text{ plf (15.3 kN / m)}$$

The dead and live load moments are:

$$M_o = \tfrac{1}{8} \times 1.050 \times 6{,}400 = 840 \text{ ft-kips}$$

$$M_d = \tfrac{1}{8} \times 0.400 \times 6{,}400 = 320 \text{ ft-kips}$$

$$M_l = \tfrac{1}{8} \times 1.200 \times 6{,}400 = 960 \text{ ft-kips}$$

If we apply the usual ACI overload factors, the required flexural strength is

$$M_u = 1.4(840 + 320) + 1.7(960) = 3{,}260 \text{ ft-kips}$$

and with $\phi = 0.90$ for bending, the member must have a nominal strength of

$$M_n = \frac{3{,}260}{0.90} = 3{,}620 \text{ ft-kips (4909 kN-m)}$$

The internal lever arm at ultimate load may be assumed equal to the distance between the steel centroid and the middepth of the compression flange. Anticipating the use of two tendons arranged vertically, with appropriate clearance and concrete cover, the steel centroid will be placed 8 in. from the bottom face of the beam at midspan. Thus, the internal lever arm is

$$z = 48 - 8 - 3 = 37 \text{ in.}$$

From Eq. (4.29) the tentative steel area required is

$$A_p = \frac{3{,}620 \times 12}{0.9 \times 250 \times 37} = 5.22 \text{ in.}^2 \ (3368 \text{ mm}^2)$$

Two tendons will be used, each composed of twelve Grade 250 strands of 0.600-in. nominal diameter (see Appendix B), providing an area of 5.20 in.^{2} Check of the sheath diameter, which is 3 in., confirms that the proposed placement is satisfactory. The tendons will be draped to a parabolic profile with zero eccentricity at the supports and will be grouted after stressing.

From Eq. (4.30) the required compressive concrete area is

$$A'_c = \frac{3{,}620 \times 12}{0.85 \times 5 \times 37} = 276 \text{ in.}^2$$

The full 70-in. flange width may be considered effective; hence, the depth of the

stress block at ultimate load is

$$a = \frac{276}{70} = 3.94 \text{ in.}$$

Indicating that the revised internal lever arm is

$$z = 48 - 8 - \frac{3.94}{2} = 38 \text{ in.}$$

No practical difference in required steel area results.

The stress in the steel at ultimate load may now be estimated using the ACI approximate equation. With the actual steel ratio $\rho_p = 5.20 / 2{,}800 = 0.00186$, and $\gamma_p = 0.40$ for ordinary Grade 250 strands, from Eq. (3.21) the steel stress at failure is

$$f_{ps} = f_{pu}\left(1 - 0.5\rho_p \frac{f_{pu}}{f'_c}\right)$$

$$= 250\left(1 - 0.5 \times 0.00186 \times \frac{250}{5}\right)$$

$$= 238 \text{ ksi (1,640 MPa)}$$

This is within 6 percent of the value of $0.90 \times 250 = 225$ ksi assumed in sizing the steel and no revision is needed.

The amount of prestressing of the selected steel area will now be determined based on the specification that the full dead load of 1,450 plf will be balanced by the uplift of the parabolic curved tendons. With sag $y = 48.0 - 8.0 - 17.0 = 23.0$ in., Eq. (4.27) gives

$$P_e = \frac{(w_o + w_d)l^2}{8y} = \frac{1.450 \times 6{,}400 \times 12}{8 \times 23.0} = 606 \text{ kips (2,695 kN)}$$

If losses are assumed to be 15 percent, then

$$P_i = \frac{606}{0.85} = 713 \text{ kips (3,171 kN)}$$

and the initial stress in the tendons is

$$f_{pi} = \frac{713}{5.20} = 137 \text{ ksi}$$

According to the Code, the permitted upper limit for standard Grade 250 tendons with $f_{pu} = 250$ ksi and $f_{py} = 213$ ksi is 175 ksi; the actual initial prestress is 78 percent of this allowed value. Use of the lower value permits the desired zero deflection to be attained at full dead load.

To control cracking in the member prior to post-tensioning, non-prestressed longitudinal bars will be added in an amount equal to 0.0018 times the gross section of the concrete. The total area of

$$A_t = 0.0018(14 \times 48 + 6 \times 56) = 1.81 \text{ in.}^2 \ (1{,}168 \text{ mm}^2)$$

is very nearly provided by 10 No. 4 bars. The arrangement of steel is given by Fig. 4.20*c*, which also shows the location of the two 12-strand tendons. The non-stressed bars will also aid the grouted tendons in controlling and distributing flexural cracking.

As a matter of interest, the nominal stresses will be calculated in the member for the unloaded and full service load stages. The stresses due to the component effects are as follows:

$$P_i\text{: } f_1 = -\frac{713{,}000}{1{,}010}\left(1 - \frac{23.0 \times 17.0}{227}\right) = +510 \text{ psi}$$

$$f_2 = -\frac{713{,}000}{1{,}010}\left(1 + \frac{23.0 \times 31.0}{227}\right) = -2{,}920 \text{ psi}$$

$$P_e\text{: } f_1 = 510 \times 0.85 = +430 \text{ psi}$$

$$f_2 = -2{,}920 \times 0.85 = -2480 \text{ psi}$$

$$M_o\text{: } f_1 = \frac{840 \times 12{,}000 \times 17.0}{229{,}000} = -750 \text{ psi}$$

$$f_2 = \frac{840 \times 12{,}000 \times 31.0}{229{,}000} = +1{,}360 \text{ psi}$$

$$M_d + M_l\text{: } f_1 = \frac{1{,}280 \times 12{,}000 \times 17.0}{229{,}000} = -1{,}140 \text{ psi}$$

$$f_2 = \frac{1{,}280 \times 12{,}000 \times 31.0}{229{,}0000} = +2{,}080 \text{ psi}$$

In the unloaded stage, the top and bottom surface stresses are, respectively,

$$P_i + M_o\text{: } f_1 = +510 - 750 = -240 \text{ psi}$$

$$f_2 = -2{,}920 + 1{,}360 = -1{,}560 \text{ psi}$$

and in the full service load stage

$$P_e + M_t\text{: } f_1 = +430 - 750 - 1{,}140 = -1{,}460 \text{ psi}$$

$$f_2 = -2{,}480 + 1{,}360 + 2{,}080 = +960 \text{ psi}$$

Comparison of the bottom face tension with the ACI upper limit of $12\sqrt{5{,}000} = 849$ psi indicates that the design does *not* satisfy the usual Code restriction on nominal flexural tension in prestressed members. However, an "escape clause" is included in the Code to the effect that the limiting tensile stress "... may be exceeded when it is shown experimentally or analytically that performance will not be impaired." In the present instance, the full required strength is provided, and service load performance is improved over allowable stress design through the deflection control permitted by partial prestressing.

B. LOAD-BALANCING APPROACH TO THE DESIGN OF PARTIALLY PRESTRESSED BEAMS

A second method for the design of partially prestressed beams starts with the selection of prestress force and eccentricity to balance a selected load, usually the total dead load (see Section 4.6). The tendons are used at their full allowable stress, and steel area A_p is determined accordingly. The tensile force required to provide the necessary flexural strength at factored loads will generally be greater than can be developed in the prestressed tendon alone, and so supplementary non-prestressed bar reinforcement is added specifically for this purpose. It was shown in Section 3.10 that the non-prestressed bars will almost always be stressed to their yield strength at ultimate load.

This alternative approach to the design of partially prestressed beams, based on load balancing, can be described in detail as follows:

1. A trial member depth is assumed, based on maximum span–depth ratio or experience with similar designs. Top flange dimensions may be based on functional requirements or other criteria.
2. The web width is chosen based on shear strength requirements or on the requirements for concrete cover for tendons and stirrups.
3. The amount of prestress force is calculated to produce the desired deflection for a selected load. Often a zero deflection under the combined effects of prestress and total dead load is specified. The required tendon area A_p is found, using the full allowable steel stress.
4. The required flexural strength M_u is calculated using factored loads as usual. The nominal flexural strength $M_n = M_u/\phi$ is then found.
5. The total required tensile force at ultimate moment is calculated, and the tendon area A_p is augmented by bar reinforcement having area A_s to provide that total force. The prestressed steel can be assumed to act at $0.90f_{pu}$ and the bar reinforcement at f_y in this preliminary calculation.
6. The flexural strength of the beam is then checked, and adjustments are made to the trial design, if necessary.
7. Flexural tensile stress in the concrete at full service load is then checked, and if it exceeds the modulus of rupture significantly, crack widths are checked using the methods of Section 4.8.

This method contrasts with that described earlier in this section in that it will usually result in a design combining prestressed and non-prestressed flexural tensile reinforcement. By making use of the full allowable stress in the tendons in the initial stage, the amount of prestressing steel is reduced, generally resulting in a more economical design that still satisfies all requirements of strength and serviceability.

EXAMPLE: Design Based on Load Balancing and Partial Prestressing

The beam of the preceding example is to be redesigned based on load balancing, with the total tensile steel force at ultimate load provided with a combination of prestressed and non-prestressed reinforcement.

The same trial concrete cross section will be used as in the preceding example, with total depth 48 in., flange width 70 in., average flange thickness 6 in., and web width 14 in. Section properties are as determined in the earlier example, and moments due to self-weight, external dead load, and service live load are the same as before.

With tendon eccentricity varying parabolically from 23.0 in. at midspan to zero at the supports, the sag $y = 23.0$ in., and from Eq. (4.27), the effective prestress

force needed to balance the self-weight and external dead load is:

$$P_e = \frac{w_b l^2}{8y} = \frac{1.450 \times 80^2 \times 12}{8 \times 23.0} = 606 \text{ kips (2,695 kN)}$$

With 15 percent losses assumed as before, this corresponds to an initial prestress force $P_i = 606 / 0.85 = 713$ kips (3,171 kN). The tendons will be used at their full allowable stress, not greater than $f_{pi} = 0.82 f_{py}$ and not greater than $0.74 f_{pu}$. For Grade 250 tendons with $f_{pu} = 250$ ksi and $f_{py} = 213$ ksi, this gives $f_{pi} = 175$ ksi, and the required area of prestressing steel is

$$A_p = \frac{713}{175} = 4.07 \text{ in.}^2 \text{ (2,626 mm}^2\text{)}$$

This can be provided very nearly using two tendons, each with nine strands of Grade 250 steel having nominal diameter of 0.600 in. each (see Appendix B). The actual total area $A_p = 3.90$ in.^{2}, when stressed to $f_{pi} = 175$ ksi, will produce a force of 683 kips, about 4 percent below the desired value of 713 kips, but close enough, considering the approximate nature of the prestress loss estimate and deflection calculations.

The nominal flexural strength required at factored loads is $M_n = 3{,}620$ ft-kips, as found in the preceding example. The internal lever arm will be estimated, equal to the distance from the tensile steel to the middepth of the compression flange, and it will further be assumed that both prestressed and non-prestressed reinforcement have the same effective depth, that is, $d_p = d = 40$ in. Thus, the internal lever arm is approximately 37 in., and the required tensile steel force at ultimate load is

$$T = \frac{3{,}620 \times 12}{37} = 1{,}174 \text{ kips (5,222 kN)}$$

If the stress in the tendons is taken as $0.90 f_{pu} = 0.90 \times 250 = 225$ ksi, and if the non-prestressed bars are at yield stress $f_y = 60$ ksi, the area of non-prestressed bars required is

$$A_s = \frac{1{,}174 - 3.90 \times 225}{60} = 4.94 \text{ in.}^2 \text{ (3,187 mm}^2\text{)}$$

This will tentatively be provided using four No. 10 Grade 60 bars, giving an area of 5.06 in.^{2}.

The flexural strength will now be checked using the ACI approximate equation for f_{ps}. With $\rho = 5.06 / 2{,}800 = 0.00181$, $\rho_p = 3.90 / 2{,}800 = 0.00139$, $\gamma_p = 0.40$ for standard Grade 250 strands, and $\beta_1 = 0.80$, the stress according to Eq. (3.22) is

$$f_{ps} = f_{pu}\left(1 - \frac{\gamma_p}{\beta_1}\left[\frac{\rho_p f_{pu}}{f'_c} + \frac{d}{d_p}(\omega - \omega')\right]\right)$$

$$= 250\left(1 - \frac{0.40}{0.80}\left[\frac{0.00139 \times 250}{5} + \frac{0.00181 \times 60}{5}\right]\right)$$

$$= 239 \text{ ksi (1,648 MPa)}$$

The depth of the stress block at failure, according to Eq. (3.29), is

$$a = \frac{A_p f_{ps} + A_s f_y}{0.85 f'_c b}$$

$$= \frac{3.90 \times 239 + 5.06 \times 60}{0.85 \times 5 \times 70}$$

$$= 4.15 \text{ in. (105 mm)}$$

after which the flexural strength is easily found from Eq. (3.28). With $d = d_p = 40$ in. (1,016 mm), the flexural strength is

$$M_n = (A_p f_{ps} + A_s f_y)(d - a/2)$$

$$= (3.90 \times 239 + 5.06 \times 60) \times 37.93 / 12$$

$$= 3{,}905 \text{ ft-kips (5295 kN-m)}$$

This is about 8 percent above the required $M_n = 3{,}620$ ft-kips, the difference resulting from the combined effects of the stress in the tendons being slightly higher than assumed in the preliminary design, the internal lever arm being slightly greater, and the upward rounding of the steel area A_s. Refinement of the design, using $f_{ps} = 239$ ksi and an internal lever arm of 37.93 in., from the calculations just completed, indicates that an area $A_s = 3.55$ in.^{2} will provide the needed strength M_n. Two No. 9 and two No. 8 bars, with $A_s = 3.57$ in.^{2}, will be used rather than four No. 10 bars tentatively selected.

The nominal stresses in the concrete for the initial stage immediately after transfer and for the service load stage are the same as those calculated for the preceding example, because the prestress eccentricity and force are the same as before, although the force is provided using a smaller area A_p at higher stress.

Additional Comments

1. The design just completed uses a total of eighteen 0.600-in. diameter strands in two tendons, whereas the preceding design required 24 strands of the same size. This saving was achieved by adding four non-prestressed bars to augment the tendon area providing the needed flexural strength. The second design, which meets the same requirements of deflection control and strength, would almost certainly be more economical.
2. The calculations for the second example, which used a combination of prestressed and non-prestressed reinforcement, neglected the influence of the reinforcing bars in modifying prestress losses and deflections. Such effects are discussed in several of the references cited.

4.8 FLEXURAL CRACK CONTROL

Tensile stress due to flexure in concrete members at service load can be limited to any desired value, or eliminated completely, by prestressing. However, both technical and economic factors have resulted in a trend toward partial prestressing, such that tensile cracks may exist under normal conditions in service. For

designs based on partial prestressing, it is advisable to give special attention to the matter of cracking, both from the viewpoint of appearance, and because of possible corrosion of the highly stressed steel tendons if exposed by excessively wide cracks.

Parameters of importance with respect to crack width have been established by tests and observation of structural performance. They include:

1. Surface characteristics of the tensile reinforcement, which may include both prestressed tendons and non-prestressed bar steel.
2. Distribution of steel over the concrete cross section.
3. Amount of concrete cover.
4. Ratio of total reinforcement area to concrete area.
5. Increase in steel stress as the member is loaded.
6. Concrete tensile strength.
7. Size and shape of the member.

Ideally, a method for controlling cracking should reflect the influence of each of these variables, although this does not appear practical at present.

Practical methods that have been proposed may be placed in one of two categories: (a) those based on limiting the nominal tensile stress in the concrete, and (b) those based on computation of probable maximum crack width, followed by comparison with limit values. The following paragraphs summarize these two approaches to the problem.

A. NOMINAL CONCRETE TENSILE STRESS

The simplest method of crack control is based on calculation of a *nominal tensile stress* in the concrete at the load stage of interest, as proposed by Abeles (Refs. 4.18 to 4.20). By this method, the nominal concrete tensile stress is computed, based on properties of the concrete cross section assumed to be uncracked and homogeneous, even though that nominal stress exceeds the modulus of rupture. The maximum crack width is related to nominal tensile stress f_w by empirically derived equations, corresponding to crack widths w of 0.004 in., 0.008 in., and 0.012 in., as follows:

For strands:

$$f_{0.004} = 800 + 500(p - 0.3) \tag{4.31a}$$

$$f_{0.008} = 900 + 1{,}200(p - 0.3) \tag{4.31b}$$

$$f_{0.012} = 1{,}100 + 1{,}300(p - 0.3) \tag{4.31c}$$

For round bars or smooth wires:

$$f_{0.004} = 700 + 450(p - 0.3) \tag{4.32a}$$

$$f_{0.008} = 850 + 600(p - 0.3) \tag{4.32b}$$

$$f_{0.012} = 1{,}000 + 800(p - 0.3) \tag{4.32c}$$

where the nominal stresses f_w are expressed in psi, and p is the total *percentage* of steel, including both tendons and reinforcing bars, expressed in terms of the total beam depth times the width. Thus, if strands are used having a total area of 1.00 in.^{2} in a beam of width 12 in. and total depth 24 in., and if a maximum crack width of 0.008 in. is specified, then

$$p = \frac{100 \times 1.00}{12 \times 24} = 0.35 \text{ percent}$$

and, from Eq. (4.31*b*)

$$f_{0.008} = 900 + 1.200(0.35 - 0.3) = 960 \text{ psi}$$

If the nominal tensile stress at service load exceeds the value of f_w computed in this way, then cracks having maximum width in excess of 0.008 in. could be expected, and the designer has the choice of either (a) increasing the amount of prestress force, so that the nominal tensile stress at service load is reduced to the value computed, or (b) increasing the steel ratio by adding reinforcing bars, so that the computed stress for the selected crack width limit is increased to the nominal value at service load.

It should be noted that Eqs. (4.31) and (4.32) are based on a limited number of tests, and must be regarded as tentative. In addition, the tests included only beams of rectangular cross section. The resulting equations may underestimate crack widths in T-beams.

B. CALCULATION OF MAXIMUM CRACK WIDTH

Several methods have been proposed for direct calculation of crack widths.

The first approach uses the Gergely–Lutz equation, which provides the basis for ACI Code provisions relating to cracking in *reinforced concrete* beams (Refs. 4.18 and 4.21). Although Code provisions are stated in slightly different form, the basic equation for predicting the maximum crack width at the tension face of a reinforced concrete beam is

$$w = 0.076 R f_s \sqrt[3]{d_c A} \tag{4.33}$$

in which w is the maximum width of a crack in thousandth of an inch and f_s is the steel stress at the load for which crack width is to be determined, measured in ksi. The geometric parameters are shown in Fig 4.21. Terms are defined as follows:

d_c = thickness of concrete cover measured from the tension face to the center of bar closest to that face, in.

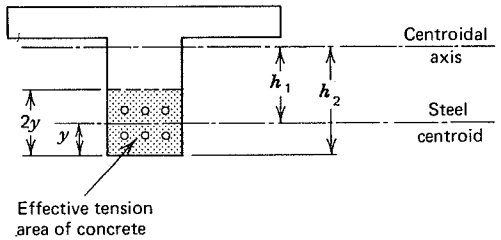

FIGURE 4.21 Geometric parameters used in the Gergely–Lutz crack-width equation.

R = ratio of distances from the tension face and from the steel centroid to the neutral axis, equal to h_2/h_1

A_t = total effective tension area of concrete surrounding the reinforcement and having the same centroid, in.^{2}

A = concrete tension area tributary to one bar, equal to A_t divided by the number of bars, in.^{2}

For *prestressed* beams, it is proposed that the same equation be used, except that an *incremental steel stress* in the tendon, Δf_s, be used rather than f_s. The increment is equal to the increase in tension as the member is loaded from the decompression load to the load for which crack width is to be found. The decompression load is defined here as the load that produces zero flexural stress at the level of the steel. Computation of steel stress after cracking can be based on the method of Section 3.10.

Equation (4.33) is based on experiments using normal deformed bar reinforcement. Available test evidence indicates that it can be used with reasonable accuracy for beams prestressed with strand and containing supplementary deformed bar reinforcement. If bar reinforcement is not used, a modifying factor of 1.8 has been suggested to account for the difference in bond properties between strand and deformed bars. If plain round bars or individual wires are used rather than strand, a further modifying factor of 1.5 to 2.0 is appropriate (Ref. 4.18).

Alternative equations for the prediction of crack width, also based on the incremental stress in the tendons past decompression of the concrete, have been proposed by Nawy and Huang (Ref. 4.22) and Nawy and Chiang (Ref. 4.23). These equations, derived from tests of pretensioned and post-tensioned beams having T- and I-shaped cross sections, are as follows:

For pretensioned beams:

$$w' = 5.85 \times 10^{-5} \Delta f_s \frac{A_t}{\Sigma_o} \qquad (4.34a)$$

For post-tensioned beams:

$$w' = 6.51 \times 10^{-5} \Delta f_s \frac{A_t}{\Sigma_o} \qquad (4.34b)$$

in which w' is the maximum crack width at the level of the reinforcement nearest the tension face of the beam, in., A_t is the total effective tension area of concrete, in.^{2}, Δf_s is the increment of stress in the tendon beyond the decompression load, ksi, and Σ_o is the total perimeter of tensile reinforcement, prestressed and non-prestressed, in. Application of these equations requires determination of Δf_s using a cracked section analysis, as does the Gergely–Lutz method (see Section 3.10). Based on limited comparisons, it appears that the Gergely–Lutz adaptation proposed here and the Nawy approach give comparable results (Ref. 4.16).

C. TOLERABLE CRACK WIDTH

From the viewpoint of appearance, crack widths up to about 0.015 in. will seldom be objectionable. With respect to protection of tendons and bar reinforcement against corrosion, the permissible crack width depends on conditions of exposure. For reinforced concrete members, present provisions of the ACI Code imply acceptable maximum crack widths of 0.016 in. for members with only interior exposure, and 0.013 in. for exterior exposure. ACI Committee 224 (Ref. 4.18) has recommended the values given in Table 4.3 for reinforced concrete members subject to various exposure conditions. These values are reasonably in agreement with those found in Ref. 4.19 for prestressed members, and may serve as a guide until recommendations are codified.

It should be recognized that cracking in concrete beams is a random phenomenon, and that crack widths in a structure can exceed the computed maximum. Isolated cracks in excess of twice the computed maximum can sometimes occur, although generally the coefficient of variation of crack width is about 40 percent.

Table 4.3 Tolerable Crack Widths

Exposure Condition	Maximum Allowable Crack Width	
	in.	mm
Dry air or protective membrane	0.016	0.41
Humidity, moist air, soil	0.012	0.30
De-icing chemicals	0.007	0.18
Seawater and seawater spray; wetting and drying	0.006	0.15
Water-retaining structures	0.004	0.10

Limited test data indicate that the increase of maximum crack width resulting from sustained loading of about two years duration is about 100 percent. High-cycle repeated loading increases crack widths by a factor that ranges from 1.5 to 4, depending on the load level.

No provisions are contained in the ACI Code pertaining specifically to crack widths in prestressed members. Special requirements are included, however, for the special case of beams with unbonded prestressing tendons, based on obervations that such members develop larger cracks and fail at lower loads than do otherwise identical members with bonded tendons. For such cases, a minimum area of bonded reinforcement, A_s, is required as given by the equation:

$$A_s = 0.004A \tag{4.35}$$

where A is defined here as the area of that part of the gross concrete cross section between the flexural tension face and the center of gravity. This reinforcement is to be uniformly distributed over the precompressed tensile zone, as close as possible to the extreme tension face. It must have a length one-third of the clear span in the positive moment region, and in the negative moment region must extend one-sixth of the clear span on each side of the support.

4.9 BOND STRESS, TRANSFER LENGTH, AND DEVELOPMENT LENGTH

In prestressed concrete beams, there are certain forces acting that tend to cause the steel tendons to slip through the surrounding concrete. These produce bond stresses or shearing stresses acting on the interface between steel and concrete. The tendency to slip is resisted by a combination of adhesion, friction, and mechanical bond between the two materials. There are two types of bond stresses to consider: flexural bond stress and transfer bond stress.

Flexural bond stresses arise because of the change in tension along the tendon resulting from differences in bending moment at adjacent sections. They are proportional to the rate of change of bending moment, hence, to the shear force at a given location along the span. Provided that the concrete member is uncracked, the magnitude of flexural bond stress is very low. After cracking, flexural bond stresses are higher by an order of magnitude than before. They can be calculated using the same equations that have been developed for ordinary reinforced concrete members (Ref. 4.17). The resulting stress is only a nominal, average value, however, and immediately adjacent to the cracks, the actual bond stresses bear little relation to the calculated values. On one side of a flexural crack, stresses are well below the nominal level and may even act in the opposite direction. On the other side of the same crack, they are much higher and commonly cause local, nonprogressive destruction of bond.

Flexural bond stress need not be considered in designing prestressed concrete beams, either before or after cracking. Even though local bond failure may

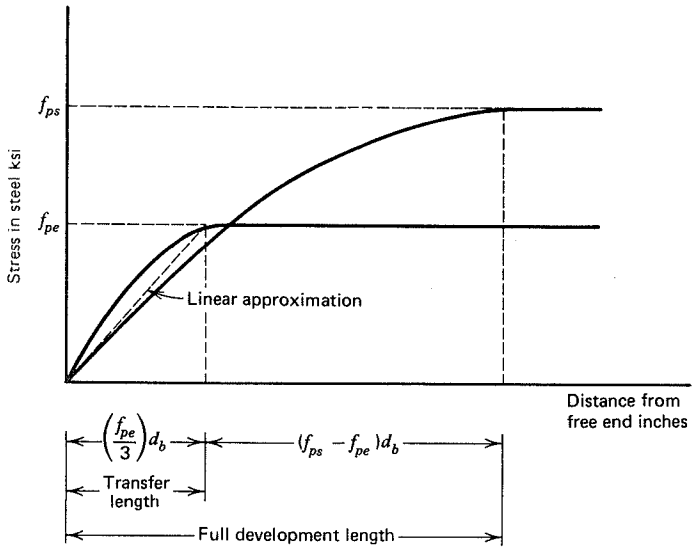

FIGURE 4.22 Transfer and development lengths for pretensioned strand.

occur, general failure cannot take place as long as adequate end anchorage is provided for the tendon, either in the form of mechanical anchorages or strand embedment.

For pretensioned beams, when the external jacking force is released, the prestressing force is transferred from the steel to the concrete near the ends of the member by bond over a distance that is known as the *transfer length*. Within this length, the stress buildup is gradual from zero to the effective prestress level, as indicated by Fig. 4.22. Some slip often occurs between steel and concrete. A wire cut off flush with the end of a beam will normally sink into the concrete slightly, but this slip is confined to the extreme end of the tendon, and stability is restored under a combination of friction and mechanical bond.

The transfer length depends on a number of factors, including the steel tensile stress, the concrete strength, the configuration of the steel cross section (e.g., wires vs. strands), the condition of the surface of the steel, and the suddenness with which the jacking force is released. Steel wires that are slightly rusted will require shorter transfer length than will clean bright wires. Tests indicate that if the release of jacking tension is sudden, as will be the case if the tendon is flame cut or parted with a grinding disc when under tension, the required transfer length will be substantially greater than if the force is gradually applied (Refs. 4.24 to 4.26).

It should be observed that, at the end of a pretensioned beam, the conditions resisting slip are quite different from those existing for a steel bar in an ordinary reinforced concrete beam. When the bar is stressed in tension, there is a slight

reduction in diameter because of the Poisson effect, with the result that there is a radial tension acting across the interface between steel and concrete. This tends to reduce the frictional resistance to slip. For a prestressed tendon, the diameter reduction has already taken place when the concrete is poured. When the jacking force is removed, the tension near the ends of the member is much less than before. This reduction in longitudinal stress is accompanied by a slight increase in the diameter of the steel, causing radial compression across the interface, which enhances the frictional resistance to pullout. This "swelling" has been shown to be important for wires, although in the more usual case of strands the mechanical resistance to slip provided by the irregular surface is at least equally important.

The effective prestress f_{pe} is essentially constant as the beam is loaded gradually up to the service load level. Should the beam be overloaded, there will be a large increase in steel stress until, at flexural failure a stress f_{ps} is attained that may be close to the tensile strength f_{pu} of the steel. Overstressing beyond service load produces somewhat reduced stresses within the original transfer length, as suggested by Fig. 4.22. A *development length* much greater than the original transfer length is required to reach the failure stress f_{ps} in the steel, as shown.

On the basis of tests of prestressing strand (Ref. 4.26), the effective prestress f_{pe} may be assumed to act at a transfer length from the end of the member equal to

$$l_t = \left(\frac{f_{pe}}{3}\right) d_b \tag{a}$$

where l_t is given in inches, the nominal strand diameter d_b is in inches, and the effective prestress f_{pe} is ksi. The value 3 in the denominator is a usually conservative estimate of the concrete strength f'_{ci} at the time of transfer. In investigating stresses near the ends of prestressed members such as short cantilevers, railroad ties, or truss members, it may be important to recognize that the full value of prestress force is not acting in the end region. Within the transfer length it is adequate and safe to assume a linear variation of prestress as shown in Fig. 4.22.

The same tests indicate that the additional distance past the original transfer length necessary to develop the failure strength of the steel is closely represented by the expression

$$l'_t = (f_{ps} - f_{pe}) d_b \tag{b}$$

where the quantity in parentheses is the stress increment above the effective prestress level, in ksi units, to reach the calculated steel stress at flexural failure.

Thus, the total development length is

$$l_d = l_t + l'_t$$

$$= \left(\frac{f_{pe}}{3}\right) d_b + (f_{ps} - f_{pe}) d_b \tag{c}$$

as shown in Fig. 4.22, or

$$l_d = \left(f_{ps} - \tfrac{2}{3} f_{pe}\right) d_b \tag{4.36}$$

A review of test data from a number of bond and anchorage investigations has indicated that the expressions just given may be somewhat unconservative estimates of transfer length and development length, particularly for larger strand diameters and relatively low-strength concrete (Ref. 4.27). As a result of this review, it was recommended that the transfer length be computed from

$$l_t = 1.5 \frac{f_{pi}}{f'_{ci}} d_b - 4.6 \tag{c}$$

rather than from Eq. (a), and that the additional distance past the original transfer length needed to develop the failure strength of the tendon be computed from

$$l'_t = 1.25 (f_{pu} - f_{pe}) d_b \tag{d}$$

Note that f_{pi} is used in the equation for l_t, rather than f_{pe}, and that f_{pu} is used in computing l'_t rather than f_{ps}. Both are expressed in ksi units.

The ACI Code does not require that flexural bond stresses be checked, either for pretensioned or post-tensioned beams, but for pretensioned strand it is required that the full *development length* given by Eq. (4.36) be provided beyond the critical bending section. Investigation may be limited to those cross sections nearest each end of the member that are required to develop their full flexural strength under the specified factored loads.

In the event that sheathed tendons are used near the ends of a span (see Section 4.2E), no prestress force will be transferred from the blanketed strands until the end of the sheathing is reached. From that point inward toward the center of the span, transfer of prestress by bond is less than normally effective, because of the lack of vertical compression from the beam reaction and because flexural tensile stresses may exist in the concrete. Based on tests (Ref. 4.28), the ACI Code requires that the development length given by Eq. (4.36) be doubled for sheathed tendons.

4.10 ANCHORAGE ZONE DESIGN

In prestressed concrete beams, the prestressing force is introduced as a load concentration, often acting over a relatively small fraction of the total member depth. For post-tensioned beams with mechanical anchorages, the load is applied at the end face, as shown by Fig. 4.23*a*, and heavy longitudinal compressive stress exists immediately under the anchorage plate, as suggested by Fig. 4.23*b*. With increasing distance from the end face, the concrete stresses are distributed more generally through the depth (Fig. 4.23*c*), but not until a distance from the end face roughly equal to the depth of the beam does the stress distribution become linear (Fig. 4.23*d*), as predicted by elastic analysis for the effect of the eccentric prestress force. For pretensioned beams, the same comments apply, except that conditions are less severe because the load is introduced more gradually over the transfer length (see Section 4.9).

The change in direction of the principal compressive stresses shown in Fig. 4.23*a* is accompanied by significant principal tensile stress acting in the perpendicular direction. This tensile stress is likely to produce longitudinal cracking in the end zone, often along the axis of the prestressing force as shown.

The pattern and magnitude of the concrete stresses depend on the location and distribution of the concentrated forces applied by the tendons. Numerous studies have been made using the theory of elasticity, photoelasticity, and finite-element analysis, all generally based on a two-dimension representation of

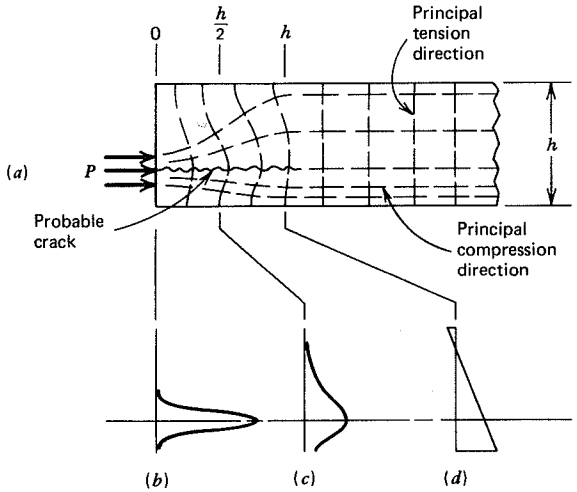

FIGURE 4.23 Stresses in end zone of post-tensioned beam. (*a*) Anchorage force P and principal stress directions. (*b*) Concrete compressive stresses under anchorage bearing plate. (*c*) Compressive stresses at $h/2$ from end face. (*d*) Compressive stresses at h from end face.

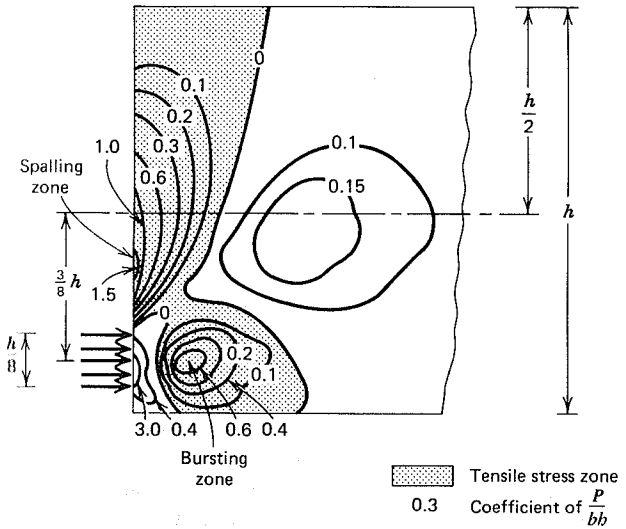

FIGURE 4.24 Contours of equal vertical stress. Adapted from Ref. 4.29.

the stress state. Typical results are shown in Fig. 4.24. Here a post-tensioned beam is loaded uniformly over a height equal to $h/8$, at eccentricity $3h/8$. Contour lines are drawn through points of equal vertical tension, with coefficients expressing the ratio of vertical stress to average longitudinal compression, P/bh. Typically, there are high *bursting stresses* along the axis of the load a short distance inside the end zone and high *spalling stresses* near the loaded face.

Elastic studies such as those just mentioned are relevant mainly in predicting the probable location of cracks and their direction, but they give little useful information about the state of stress after cracking; hence, they provide no rational basis for the design of the end zone reinforcement. There is inelastic action at a relatively low load because of the high concentration of stress in the concrete. Also, the concrete must crack before the end zone reinforcement becomes effective, yet the presence of cracks invalidates the analysis, as does the presence of the reinforcement. Present design methods are based mainly on the satisfaction of equilibrium requirements within the end zone, assumed to be cracked, and on information developed from tests.

A. POST-TENSIONED BEAMS

In many post-tensioned prestressed beams, solid end blocks are provided, as shown in Fig. 4.25, having width equal to the narrower of the top or bottom flange width. These end blocks are of little use in reducing vertical tension or avoiding cracking along the tendon path. In fact, both analysis and tests have

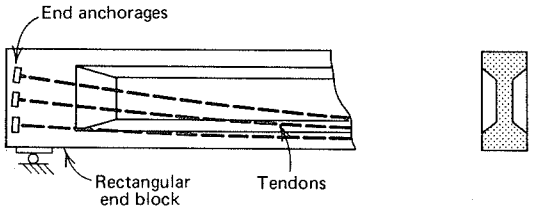

FIGURE 4.25 Post-tensioned I-beam with rectangular end block.

shown that beams with rectangular end blocks actually develop higher vertical tension for a given prestress force than do otherwise identical beams without them (Ref 4.29). Stresses in the reinforcement are higher and the cracks are wider. However, end blocks are often provided for other reasons. They may be necessary to provide room for the anchorage hardware. In addition, they provide greater bearing area to carry the high compression load at the anchorage, and they are helpful in avoiding splitting failure immediately under the anchorage plate, where heavy compressive stress tends to cause diagonal cracks emanating from the corners of the plate. These may lead to failure by spalling off of the side face of the web (Refs. 4.30 and 4.31).

Rational design of reinforcement for bursting and spalling tension must recognize that horizontal cracking is likely. If adequate reinforcement is provided so that the cracks are restricted to the local region and are no more than about 0.010 to 0.015 in. in width, then these cracks will not be detrimental to the performance of the beam. They normally will not lengthen or widen appreciably should the member be overloaded, because the tension in the tendons in the end zone, if the tendons are bonded along their length by grouting, does not increase much even if overloads are applied. Consequently, the design of reinforcement to resist bursting tension can be based on the initial prestressing force $A_p f_{pi}$, using a permissible stress for the reinforcement that is low enough that cracks will be acceptably small. Alternatively, if the anchorage zone is designed to develop the full tensile strength of the tendons $A_p f_{pu}$, the reinforcement can be designed to act at its yield strength f_y.

Reinforcement to resist bursting and spalling tension should be in the form of vertical bars of relatively small diameter and closely spaced, as shown in Fig. 4.26. They should be well anchored at the top and bottom. Closed hoop stirrups are generally used, looping around supplementary longitudinal bars provided at the corners to improve anchorage. For the design of such reinforcement in the ends of post-tensioned beams, Gergely and Sozen have developed a method based on equilibriium requirements in the end block after cracking (Ref. 4.29).

Figure 4.27*a* shows the end region of a post-tensioned beam for which the prestressing force P_i is applied as a concentrated load at the end face, with eccentricity e from the concrete centroid. At some distance l from the end face, the compressive stress distribution is linear as shown. Figure 4.27*b* shows the

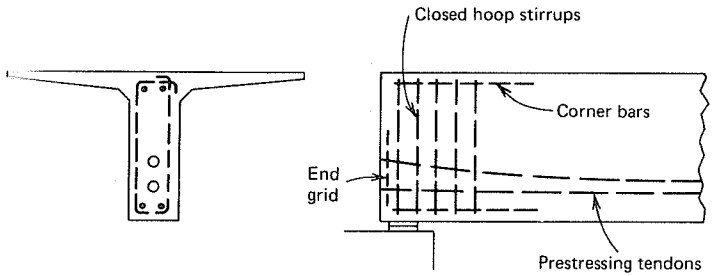

FIGURE 4.26 End-zone reinforcement for post-tensioned beam.

forces and stresses acting on the free body 0123 bounded by the edges of the member, by an assumed horizontal crack along the face 12, and by the inside end face 23 of the anchorage zone.

In general, both a moment and shear force will be produced on the face 12 by the horizontal forces. The shear is resisted by aggregate interlock and the necessary resisting moment is provided by the tensile force T from the end zone reinforcement and the compressive resultant force C from the concrete. The height c of the free body, determined by the level of the crack, is established from the condition that the moment due to the horizontal forces will be a maximum at the level at which the crack forms. In practical cases, moments may be calculated at increments of height, starting at the bottom of the beam, and plotted as a function of distance from the bottom. Typical results are shown in Fig. 4.27*c*. At the level of the load, a net clockwise bending moment causing vertical tension deep within the end zone is indicated, gradually changing to net counterclockwise moment causing vertical tension near the end face in the upper part of the end region.[6]

Knowing the maximum bending moment to be resisted, the forces T and C can be calculated if the distance between those forces can be estimated. For post-tensioned beams, stirrups should be provided within a distance $h/2$ from the end face to resist T, and the center of effort of those stirrup forces is easily found. The location of C must be estimated. It is usually assumed to be at a distance h from the end face. Accordingly, the tensile force to be resisted by the end stirrups is

$$T = \frac{M_{max}}{h - x} \tag{4.37}$$

where M_{max} is the maximum bending moment to be resisted and x is the distance from the end face to the centroid of the vertical steel within the distance

[6]Repetitive calculations can be avoided by recalling that the maximum moment values occur at the level or levels of zero shear.

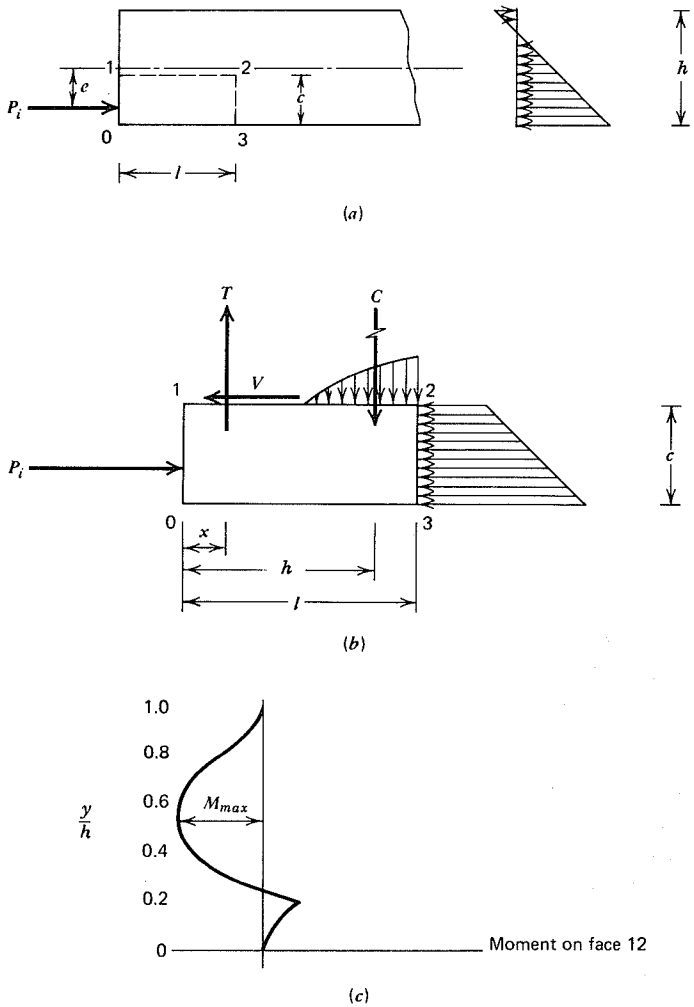

FIGURE 4.27 End-zone analysis of post-tensioned beam. (*a*) End of beam showing free-body location. (*b*) Forces on free body. (*c*) Variation of moment with depth.

$h/2$. The total required area of steel reinforcement is

$$A_t = \frac{T}{f_s} \tag{4.38}$$

where f_s is an allowable stress chosen on the basis of crack control. A value of $f_s = 20{,}000$ psi has been found to be satisfactory.

If more than one post-tensioned tendon is to be used, as is frequently the case, consideration should be given to the reinforcement needed as each tendon is tensioned in sequence. Depending on the order of tensioning, the controlling stage may not be when all tendons are stressed.

The method described is simple conceptually and gives reasonable results. It is easily adapted to cases where the load is applied at several levels, and can also be used for I-beams or beam of other shape. It is based on the initial prestress force P_i and permissible stirrup stress rather than strength. Since the stirrup stress recommended is less than one-half of the yield stress for the bar reinforcement currently used and since the tendon force at the anchorage does not increase significantly as the beam is loaded to failure, an adequate margin of strength is assured.

In addition to vertical tensile stress in the bursting and spalling zones, end zone distress may be caused by the high concentration of longitudinal compression under the bearing plates of the anchorages. The bearing stress on the concrete caused by post-tensioning anchorages, according to ACI Code Commentary, should not exceed the following:

Immediately after the tendon anchorage[7]:

$$f_b = 0.8 f'_{ci} \sqrt{\frac{A_2}{A_1} - 0.2} \qquad \text{and} \qquad \leq 1.25 f'_{ci} \tag{4.39a}$$

After allowance for prestress losses:

$$f_b = 0.6 f'_c \sqrt{\frac{A_2}{A_1}} \qquad \text{and} \qquad \leq f'_c \tag{4.39b}$$

where A_1 = bearing area of anchor plate
A_2 = maximum area of the portion of the anchorage surface that is geometrically similar to, and concentric with, the area of the anchor plate

The definition of A_2 may be clarified by Fig. 4.28, which shows the loaded area A_1 under the anchor plate and the largest concentric area A_2 that can be superimposed within the bounds of the beam end face.

[7]Although the ACI Code Commentary implies that bearing stress should be checked immediately after anchorage, with force $A_p f_{pi}$, the ACI Code requires that bearing stress be checked for the jacking force $A_p f_{pj}$. The Code seems more correct.

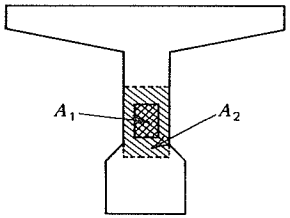

FIGURE 4.28 End bearing areas for post-tensioned beam.

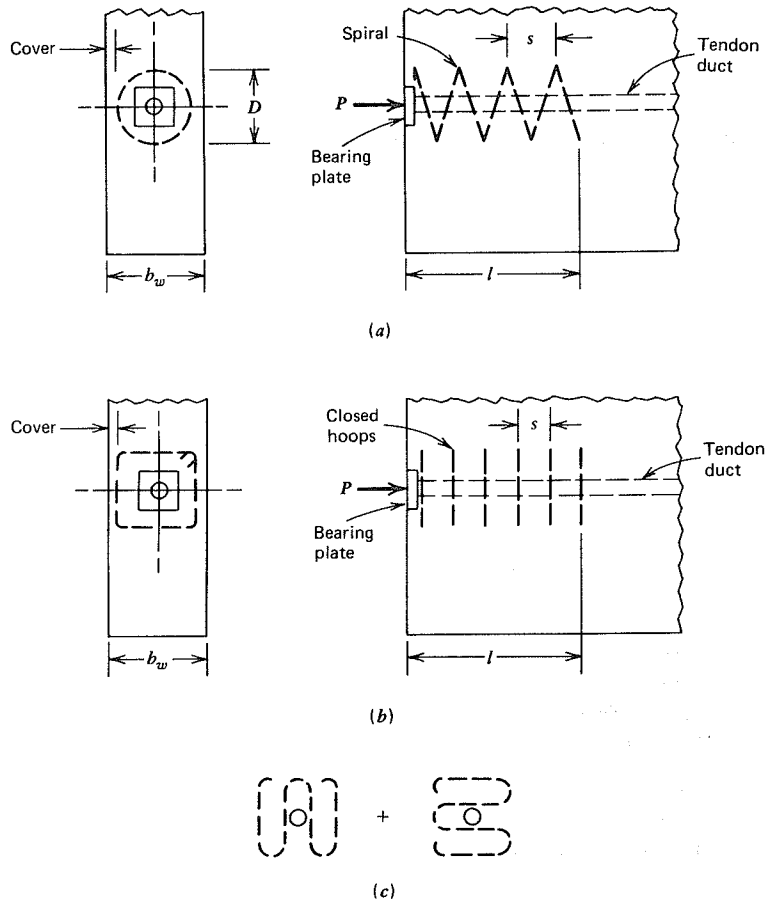

FIGURE 4.29 Special reinforcement under post-tensioning anchorage plate. (*a*) Spiral reinforcement. (*b*) Closed hoop reinforcement. (*c*) Orthogonal reinforcement. Adapted from Ref. 4.31.

Supplementary reinforcement directly under the anchor plate is required because of the tendency for diagonal splitting cracks to form, radiating outward from the corners of the bearing plate and possibly leading to spalling off of the outer face of the web at the anchorage. The most efficient reinforcement of this type is a continuous spiral, as shown in Fig. 4.29*a*. Such spirals enhance the strength of the concrete locally, acting in the same way as spiral confinement steel in columns, and are effective in resisting the splitting failure just described. Such spirals should have a diameter about equal to the diagonal dimension of the anchor plate, if used in solid end blocks or relatively wide webs, and in narrower webs should be as large as possible consistent with concrete cover requirements at the sides. They should begin very close to the anchor plate, and should have a minimum length about twice the side dimension of the plate (Ref. 4.31).

Where spiral confining steel cannot be used, closed hoops may be substituted, as show in Fig. 4.29*b*. These are not as effective as spirals, generally, and a substantial improvement is made using pairs of orthogonal grid bars, as shown in Fig. 4.29*c*, in place of each closed hoop.

The specification of such spirals, hoops, or grids is usually based on test information developed by the manufacturer of the anchorage hardware, although design equations are suggested in Ref. 4.31 based on the same approach used in the design of spiral steel in columns.

EXAMPLE: Design of End Zone Reinforcement for Post-Tensioned Beam

End zone reinforcement is to be designed for the rectangular post-tensioned beam shown in Fig. 4.30*a*. An initial prestress force P_i of 250 kips is applied by two tendons having eccentricity of 10.5 in., producing longitudinal stresses in the concrete that vary linearly from 2,153 psi compression at the bottom to 764 psi tension at the top. Closed vertical stirrups will be used as shown in Fig. 4.30*b*, at an allowable stress of 20,000 psi ($b = 305$ mm, $h = 762$ mm, $P_i = 1{,}112$ kN, $e = 267$ mm, $f_2 = -14.8$ MPa, $f_1 = +5.3$ MPa, and $f_s = 138$ MPa.)

For computational purposes, the beam will be divided into 3 in. increments of height, and the concrete stress at the center of each increment will be assumed to act uniformly through the depth of that increment. Values are given in Fig. 4.30*c*. The moments from these stresses and from the concentrated tendon forces are computed at 3 in. intervals, clockwise moments being taken positive. Results are given in Table 4.4 and are plotted in Fig. 4.30*d*. It is seen that a maximum moment of 388 in.-kips is obtained, acting at a distance 15 in. above the bottom of the beam to cause tension near the end face (spalling zone).

The centroid of the stirrup forces within a distance $h/2$ from the end face will be assumed to be at $x = 8$ in. Then, from Eq. (4.37) the maximum tension to be resisted is

$$T = \frac{388{,}000}{30 - 8} = 17{,}600 \text{ lb } (78 \text{ kN})$$

The total amount of reinforcement in the spalling zone, based on the allowable

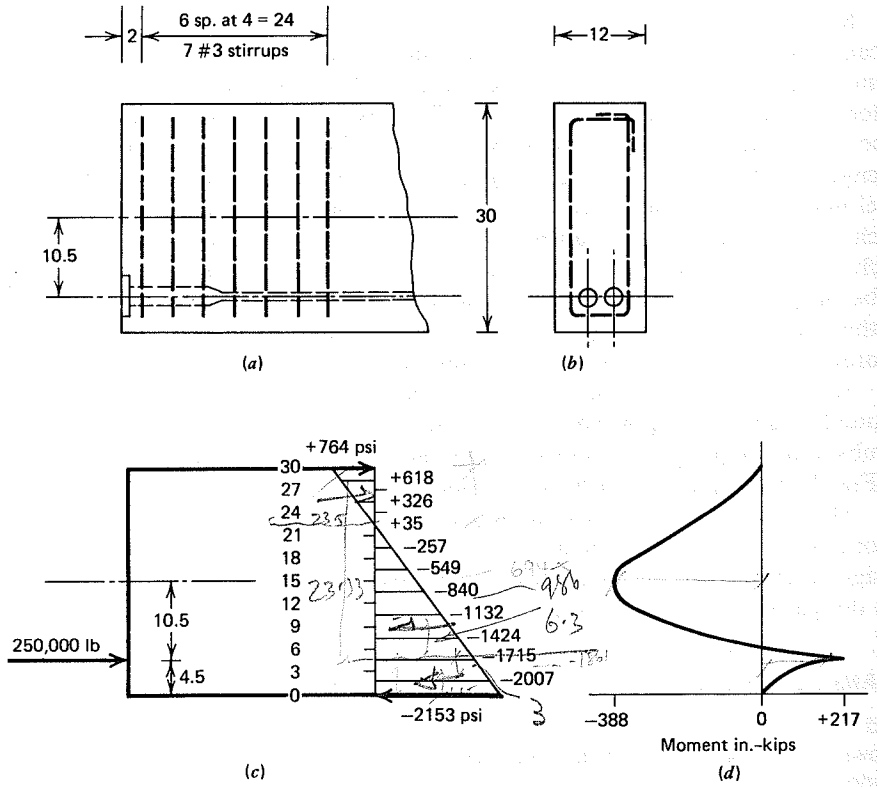

FIGURE 4.30 Design of anchorage zone reinforcement. (*a*) End zone. (*b*) Cross section. (*c*) Forces and stresses. (*d*) Moments.

stress of 20,000 psi, is found from Eq. (4.38):

$$A_t = \frac{17{,}600}{20{,}000} = 0.88 \text{ in.}^2 \text{ (568 mm}^2\text{)}$$

Four No. 3 closed loop stirrups provide an area of $4 \times 0.11 \times 2 = 0.88$ in.^{2}, exactly as required. The first stirrup will be placed 2 in. from the end face, followed by three stirrups at 4 in. spacing within the distance $h/2 = 15$ in., as shown in Fig. 4.30*a*. This places the steel centroid 8 in. from the end face as assumed.

A second moment maximum, of opposite sign and of value 217 in.-kips, is indicated by Fig. 4.30*d*, with associated tension at the level of the prestress force some distance inward from the end face (bursting zone). The tensile force of

$$T = \frac{217{,}000}{22} = 9{,}860 \text{ lb (44 kN)}$$

can be accommodated by three additional stirrups, providing a total of seven no. 3 stirrups at 4 in. spacing. End zone reinforcement, shown in Fig. 4.30*a*, is thus included through a distance approximately equal to h from the end face.

Table 4.4 Moments at Horizontal Section of End Zone Design Example

Distance from bottom (in.)	Moment of concrete stresses (in.-kips)	Moment of prestress force (in.-kips)	Net moment (in.-kips)
0	0	0	0
3	+108	0	+108
4.5	+217	→ 0	+217
6	+418	−375	+43
9	+897	−1,125	−228
12	+1,514	−1,875	−361
15	+2,237	−2,625	−338
18	+3,035	−3,375	−340
21	−3,877	−4,125	−248
24	+4,731	−4,875	−144
27	−5,566	−5,625	−59
30	+6,349	−6,375	−26[a]

[a]Nonzero value results from stepwise incremental stresses used.

In addition to the stirrup reinforcement just calculated, supplementary reinforcement will be provided directly under the anchor plates, in the form of orthogonal grids, similar to Fig. 4.29*c*. Based on anchorage manufacturer's recommendations, these plates will be fabricated of 1/4-in. diameter bar, with outside dimensions 9 × 9 in., with six sets of bars providing a total length l of 10 in.

B. PRETENSIONED BEAMS

The state of stress in the end region of pretensioned beams is much less severe than for post-tensioned beams, because of the gradual input of prestress force along the transfer length. Solid end blocks are generally not provided, but reinforcement for bursting and spalling stresses should always be used, unless tests prove it unnecessary for a particular type of member.

The equilibrium analysis used to design end zone stirrups for post-tensioned beams can also be used for pretensioned end zones. However, based on tests at the laboratories of the Portland Cement Association, Marshall and Mattock have proposed a very simple equation for the design of end zone reinforcement (Ref. 4.32). The total stirrup tension S is expressed in terms of the total longitudinal prestress force P by the relation

$$\frac{S}{P} = 0.0106\frac{h}{l_t}$$

where h is the total beam depth and l_t is the transfer length. Tests indicate that the stirrup stress varies approximately linearly from maximum close to the end

face to zero near the end of the crack. Thus, if f_s is a *permissible* stirrup stress when the initial prestress force P_i is applied, the average stress in the stirrups can be taken as $f_s/2$ and the total cross-sectional area of stirrups necessary, A_t, is given by

$$\frac{A_t f_s}{2P_i} = 0.0106\frac{h}{l_t}$$

or

$$A_t = 0.021\frac{P_i h}{f_s l_t} \tag{4.40}$$

An allowable stress $f_s = 20{,}000$ psi has been found in tests to produce acceptably small crack widths. The transfer length l_t may either be calculated by Eq. (a) of Section 4.9 or may be assumed to equal 50 times the nominal diameter of the strand. The required reinforcement having total area A_t should be distributed uniformly over a length equal to $h/5$ measured from the end face of the beam, according to recommendations made in Ref. 4.32, and for most efficient crack control, the first stirrup should be placed as close to the end face as possible.

Equation (4.40) was developed from tests of I-section girders in which the prestress was applied by two groups of tendons, one near the top of the beam and one near the bottom. It generally gives good results for such cases, for which the longitudinal crack starts at the end face, usually near the middepth of the beam or close to the junction of lower flange and web. For other end-loading conditions, such as for the tendon group centered near middepth, Eq. (4.40) will give completely misleading results, as the crack will usually initiate in the bursting zone along the tendon centroidal axis some distance from the end face.

REFERENCES

4.1 Nilson, A. H., "Flexural Design Equations for Prestressed Concrete Members," *J. PCI*, Vol. 14, No. 1, February 1969, pp. 62–71.

4.2 Orbison, J. G., "Generalized Flexural Design Equations for Prestressed Concrete," *J. PCI*, Vol. 30, No. 2, March/April 1985, pp. 172–182.

4.3 Guyon, Y., *Limit State Design of Prestressed Concrete*, Vol. 1, Wiley, New York, 1972, 485 pp.

4.4 Guyon, Y., *Limit State Design of Prestressed Concrete*, Vol. 2, Wiley, New York, 1974, 769 pp.

4.5 Magnel, G., *Prestressed Concrete*, McGraw-Hill, New York, 1954, 345 pp.

4.6 *PCI Design Handbook*, 3rd ed., Prestressed Concrete Institute, Chicago, 1985.

4.7 Libby, J. R., *Modern Prestressed Concrete*, 3rd ed., Van Nostrand Reinhold, New York, 1984.

4.8 Lin, T. Y., "Load Balancing Method for Design and Analysis of Prestressed Concrete Structures," *J. ACI*, Vol. 60, No. 6, June 1963, pp. 719–742.

4.9 Lin, T. Y. and Burns, N. H., *Design of Prestressed Concrete Structures*, 3rd ed., New York, 1981, 646 pp.

4.10 Abeles, P. W., "Design of Partially Prestressed Concrete Beams," *J. ACI*, Vol. 64, No. 10, October 1967, pp. 669–677.

4.11 Moustafa, S. E., "Design of Partially Prestressed Concrete Flexural Members," *J. PCI*, Vol. 22, No. 3, May–June 1977, pp. 12–29.

4.12 Naaman, A. E. and Siriaksorn, A., "Serviceability Based Design of Partially Prestressed Beams," *J. PCI*, Vol. 24, No. 2, March–April 1979, pp. 64–89.

4.13 Tadros, M. K., "Expedient Service Load Analysis of Cracked Prestressed Concrete Sections," *J. PCI*, Vol. 27, No. 6, November–December 1982, pp. 86–111.

4.14 Inomata, S., "A Design Procedure for Partially Prestressed Concrete Beams Based on Strength and Serviceability," *J. PCI*, Vol. 27, No. 5, September–October 1982, pp. 100–116.

4.15 Naaman, A. E., "A Proposal to Extend Some Code Provisions on Reinforcement to Partial Prestressing," *J. PCI*, Vol. 26, No. 2, March–April 1981, pp. 74–91.

4.16 Peterson, D. N. and Tadros, M. K., "Simplified Flexural Design of Partially Prestressed Concrete Members," *J. PCI*, Vol. 30, No. 3, May–June 1985, pp. 50–69.

4.17 Nilson, A. H. and Winter, G., *Design of Concrete Structures*, 10th ed., McGraw-Hill, New York, 1986, 735 pp.

4.18 "Control of Cracking in Concrete Structures," Reported by ACI Committee 224, Concrete International, Vol. 2, No. 10, October 1980, pp. 35–76.

4.19 Abeles, P. W., "Design of Partially Prestressed Concrete Beams," *J. ACI*, Vol. 64, No. 10, October 1967, pp. 669–677.

4.20 Nilson, A. H., discussion of Ref. 4.19, *J. ACI*, Vol. 65, No. 4, April 1968, pp. 345–347.

4.21 Gergely, P. and Lutz, L. A., "Maximum Crack Width in Reinforced Concrete Flexural Members," *Causes, Mechanism, and Control of Cracking in Concrete*, ACI Special Publication SP-20, American Concrete Institute, Detroit, 1968, pp. 87–117.

4.22 Nawy, E. G. and Huang, P. T., "Crack and Deflection Control of Pretensioned Prestressed Beams," *J. PCI*, Vol. 22, No. 3, May–June 1977, pp. 30–47.

4.23 Nawy, E. G. and Chiang, J. Y., "Serviceability Behavior of Post-Tensioned Beams," *J. PCI*, Vol. 25, No. 1, January–February 1980, pp. 74–95.

4.24 Janney, J. R., "Nature of Bond in Pretensioned Prestressed Concrete," *J. ACI*, Vol, 25, No. 9, May 1954, pp. 717–736.

4.25 Hanson, N. W., "Influence of Surface Roughness of Prestressing Strand on Bond Performance," *J. PCI*, Vol. 14, No. 1, February 1969, pp. 32–45.

4.26 Hanson, N. W. and Kaar, P. H., "Flexural Bond Tests of Pretensioned Prestressed Beams," *J. ACI*, Vol. 30, No. 7, January 1959, pp. 783–802.

4.27 Zia, P. and Mostafa, T., "Development Length of Prestressing Strands," *J. PCI*, Vol. 22, No. 5, September–October 1977, pp. 54–65.

4.28 Kaar, P. H. and Magura, D. D., "Effect of Strand Blanketing on Performance of Pretensioned Girders," *J. PCI*, Vol. 10, No. 6, December 1965, pp. 20–34.

4.29 Gergely, P. and Sozen, M. A., "Design of Anchorage Zone Reinforcement in Prestressed Concrete Beams," *J. PCI*, Vol. 12, No. 2, April 1967, pp. 63–75.

4.30 Stone, W. C. and Breen, J. E., "Behavior of Post-Tensioned Girder Anchorage Zones," *J. PCI*, Vol. 29, No. 1, January–February 1984, pp. 64–109.

4.31 Stone, W. C. and Breen, J. E., "Design of Post-Tensioned Girder Anchorage Zones," *J. PCI*, Vol. 29, No. 2, March–April 1984, pp. 28–61.

4.32 Marshall, W. T. and Mattock, A. H., "Control of Horizontal Cracking in the Ends of Pretensioned Prestressed Concrete Girders," *J. PCI*, Vol. 7, No. 5, October 1962, pp. 56–74.

PROBLEMS

4.1 A pretensioned prestressed beam has a rectangular cross section of 6-in. width and 20-in. total depth. It is built using normal density concrete of design strength $f'_c = 4{,}000$ psi, and strength at transfer of $f'_{ci} = 3{,}000$ psi. Stress limits are as follows: $f_{ti} = 165$ psi, $f_{ci} = -1{,}800$ psi, $f_{ts} = 380$ psi, and $f_{cs} = -1{,}800$ psi. The effectiveness ratio R may be assumed equal to 0.80. For these conditions, find the initial prestress force P_i and eccentricity e, to maximize the superimposed load moment $M_d + M_l$ that can be carried without exceeded stress limits. What uniformly distributed load can be carried on a 30-ft simple span? What tendon profile would you recommend?

4.2 A rectangular pretensioned concrete beam is to be designed to carry superimposed dead and live loads of 300 plf and 1,000 plf, respectively, on a 40-ft simple span. Straight tendons will be used. Time-dependent losses will be approximately 16 percent of the initial stress in the steel. Determine the concrete dimensions (use $h = 2.5b$) and required prestress force and eccentricity, based on ACI limit stresses. Concrete strength $f'_c = 5{,}000$ psi and $f'_{ci} = 4{,}000$ psi.

4.3 A pretensioned beam is to carry a superimposed dead load of 600 plf and service live load of 1,200 plf on a 55-ft simple span. A symmetrical I-section with $b = 0.5h$ will be used. Flange thickness $h_f = 0.2h$ and web width $b_w = 0.4b$. The member will be prestressed using Grade 270 strands. Time-dependent losses are estimated at 20 percent of P_i. Normal density concrete will be used, with $f'_c = 5{,}000$ psi and $f'_{ci} = 3{,}000$ psi. (a) Using straight strands, find the required concrete dimensions, prestress force, and eccentricity. Select an appropriate number and size of tendons, and show by sketch their placement in the section. (b) Revise the design of part (a) using tendons deflected at the third points of the span, with eccentricity reduced to zero at the supports. (c) Comment on your results. In both cases, ACI stress limits are to be applied. You may assume that deflections are not critical, and that a tensile stress of $12\sqrt{f'_c}$ is permissible at full service load.

4.4 The T-beam of Fig. P4.4 is to be used on an 80-ft roof span and must carry superimposed load (dead and live) of 70 psf of roof surface at full service condition. No topping slab is used. Using stress limitations in the unloaded and full service load stage as imposed by the ACI Code, and assuming 22 percent losses, determine the best combination of prestress force and eccentricity at midspan. Maintain at least 3 in. from the steel centroid to the bottom face of the concrete. Strands will be harped at midspan. Choose appropriate prestressing steel using Grade 270 stranded cable. For the section shown, $A_c = 782$ in.^{2}, $I_c = 169{,}000$ in.^{4}, $c_1 = 12.8$ in., $w_o = 815$ plf. Specify $f'_c = 5{,}000$ psi and $f'_{ci} = 3{,}500$ psi.

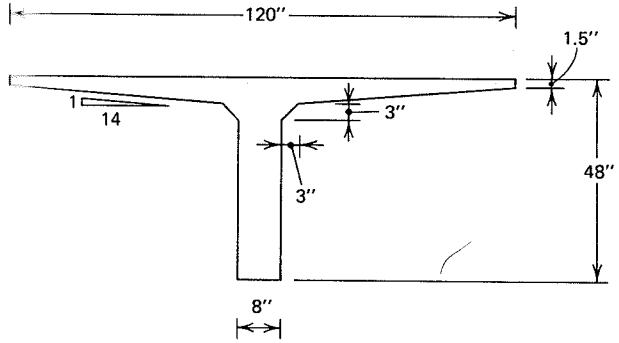

FIGURE P4.4

4.5 The double-T roof beam of Fig. P4.5 is to be constructed using lightweight concrete having density 120 pcf with compressive strength $f'_c = 5{,}000$ psi. At the time of

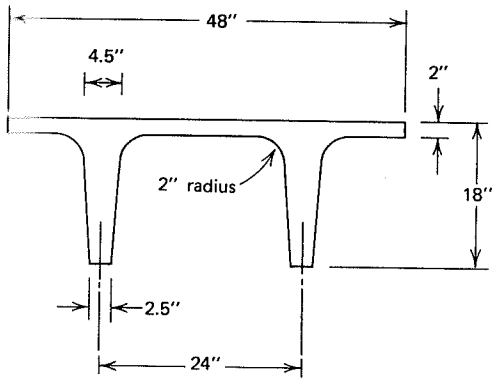

FIGURE P4.5

release of pretensioning force, f'_{ci} will be 4,000 psi. The member is intended for use on a 50-ft simple span, and must carry superimposed loads $w_d = 10$ psf and $w_l = 40$ psf uniformly distributed over the slab surface. Using ACI limit stresses, and assuming 15 percent losses, find the best combination of prestress force and eccentricity. Choose an appropriate size and number of Grade 250 strands. A minimum distance of 5 in. must be maintained from the steel centroid to the bottom face of the stems. What is the flexural efficiency of the beam section? Find the factor of safety against cracking and failure, both expressed in terms of live load increase. The section properties are $A_c = 208$ in.^{2}, $I_c = 5{,}944$ in.^{4}, and $c_1 = 5.44$ in.

4.6 A post-tensioned beam having the cross section shown in Fig. P4.6 will be used as a single-lane access ramp of 120-ft span. The flat, upper flange surface will serve as roadway and walk. The service live load providing the basis for design is 200 psf assumed uniformly distributed over the full width of flange and full span of girder. The weight of curbs (non-structural) and railings is 100 plf of span. Required clearances and visual factors limit the total depth to 66 in., and a web width of 14 in. is selected anticipating the need for placement of stirrups for shear and torsion (not a part of the present design problem), as well as prestressed and non-prestressed flexural steel. The average depth of flange, governed by transverse bending and shear requirements, will be 7 in. Design the girder for flexure, using partial prestressing, and incorporating the design requirement for a balanced load state when full dead load acts. Non-prestressed reinforcing bars may be used if required to provide the needed strength. Stresses in the member in the initial stage and full service load stage should be checked, but need not meet the restrictions of the ACI Code. Check the width of cracks, if any, at full service load, using either of the methods of Section 4.8. Concrete strengths are $f'_c = 6{,}000$ psi and $f'_{ci} = 4{,}500$ psi. Standard Grade 270 strands will be used for post-tensioning (e.g., Freyssinet system as shown in Appendix B). Grade 60 rebars may be used also. Time-dependent losses are estimated at 20 percent of the initial prestress force.

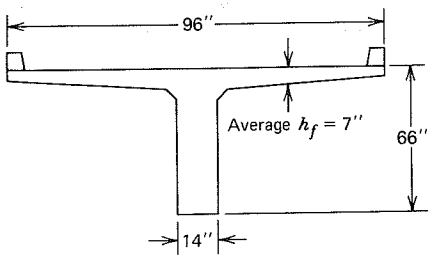

FIGURE P4.6

4.7 The I-beam shown in Fig. P4.7 is to be post-tensioned using three tendons, each containing seven 0.5-in. diameter Grade 270 strands. They will be tensioned to an initial value P_i of 202 kips each. To provide for anchorage hardware and to distribute concentrated forces, a solid end block will be provided having length equal to the member depth. Design the reinforcement for bursting and spalling tension for this beam, using closed hoop stirrups at an allowable stress $f_s = 20$ ksi. Note that the tendons will be tensioned in a sequence that can be specified by the designer. What is

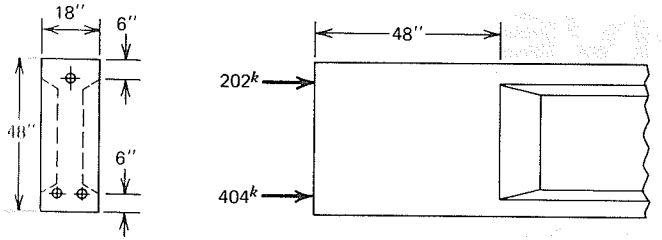

FIGURE P4.7

the minimum size bearing plate that can be used at the anchorages, given that the conduit carrying the tendons has outside diameter $3\frac{1}{4}$ in., and that no bearing is provided under this part of the plates. Concrete strengths are $f'_c = 5$ ksi and $f'_{ci} = 3.5$ ksi. Describe any other reinforcement that would be provided in the end zone.

4.8 The single T-beam shown in Fig. P4.8 is pretensioned using 14 Grade 270 0.50-in. diameter strands at an initial tension $f_{pi} = 0.70\, f_{pu}$. The strand pattern at the ends of the girder applies the force over a small area, and P_i can be considered to be a concentrated load for purposes of calculation, at eccentricity $e = 11.15$ in. The transfer length may be taken as 50-strand diameters. (a) Design the end zone reinforcement using the equilibrium method of Section 4.10A. (b) Redesign the end zone reinforcement using the PCA method of Section 4.10B, and comment on your results. For the section shown, $A_c = 570$ in.^{2}, $I_c = 68{,}900$ in.^{4}, $S_1 = 6{,}900$ in.^{3}, and $S_2 = 2{,}650$ in.^{3}.

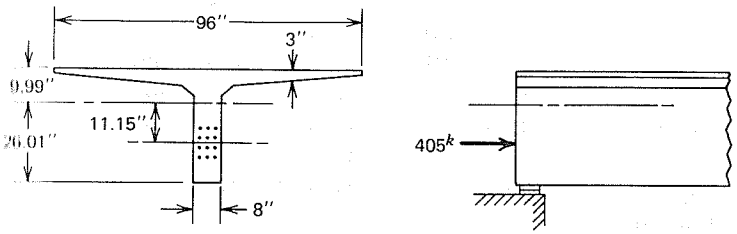

FIGURE P4.8

4.9 With reference to the pretensioned T-beam of Problem 4.8, an alternative design introduces the pretensioning force by two groups of seven Grade 270 0.50-in. diameter tendons, with the same initial tension as before, but with the first group centered at the concrete centroid and the second at an eccentricity of 22.30 in. (a) Design the end zone reinforcement using the equilibrium method of Section 4.10A. (b) Redesign the end zone reinforcement using the PCA method of Section 4.10B. Compare the results of Problem 4.9 with those of Problem 4.8 and comment.

FIVE

SHEAR AND TORSION

5.1 INTRODUCTION

Chapters 3 and 4 pertain mainly to the flexural stresses and flexural strength of beams. Beams must also be safe against premature failures of other types. These other failures may be more dangerous than flexural failure in the sense that, should catastrophic overloading and collapse occur, it might take place suddenly and without warning. Flexural shear failure is an example. Prestressed concrete beams normally contain special *shear reinforcement* to insure that flexural failure, which can be predicted accurately and which is usually preceded by obvious cracking and large deflections, will occur before shear failure, which is abrupt and more difficult to predict accurately.

Closely related to the shear stresses resulting from flexure in beams are those that are a consequence of torsion, or twisting of the beam, about its long axis. Torsional shear stresses, too, produce diagonal tension in the concrete. *Torsional reinforcement*, similar to shear reinforcement and, in many cases, combined with it, is required in members that must resist significant twisting moments. The basic aspects of torsional design will be presented later in this chapter, following consideration of flexural shear stresses and shear reinforcement.

Neither flexural shear analysis, nor torsional shear analysis is really concerned with shear stress as such. The shear stresses produced by actions of either type are usually much below the direct shear strength of the concrete. The real concern is with the *diagonal tension stress* in the concrete produced by shear stress, acting either alone or in combination with longitudinal normal stresses.

There are certain circumstances in which consideration of the direct shear strength of uncracked or cracked concrete is required. One example is the design of column brackets such as are used in precast construction to provide support for beams and girders. The *shear friction theory*, a useful design tool for such cases, will be described in Chapter 12.

5.2 SHEAR AND DIAGONAL TENSION IN UNCRACKED BEAMS

When the loads acting on a prestressed concrete beam are relatively low, the beam will be free of cracks and the concrete response will be nearly elastic. Under these circumstances, shear stresses, flexural stresses, and the principal stresses resulting from their combined action may be found based on familiar equations of mechanics. The concrete shear stress at any location is given by

$$v = \frac{V_{net}Q}{I_c b} \tag{5.1}$$

where V_{net} = net shear force at the cross section due to applied loads and prestressing
Q = static moment about the neutral axis of that portion of the cross section outside of the shear plane considered
I_c = moment of inertia of the cross section
b = width of the cross section at the shear plane considered

The longitudinal stress in the concrete may be found by the equation

$$f = -\frac{P}{A_c} \pm \frac{Pey}{I_c} \mp \frac{My}{I_c} \tag{5.2}$$

where P = prestress force
e = eccentricity of prestress force, measured positive downward
y = distance from the centroidal axis of the section to the point considered
A_c = area of concrete cross section
M = moments due to applied loads

and the upper and lower signs of each pair apply to calculation of stresses above and below the centroidal axis, respectively.

The beneficial influence of prestressing in reducing diagonal tension in concrete beams becomes evident when considering two concrete beams, one with non-prestressed bar reinforcement, as in Fig. 5.1*a*, and one prestressed, as in Fig. 5.1*c*.

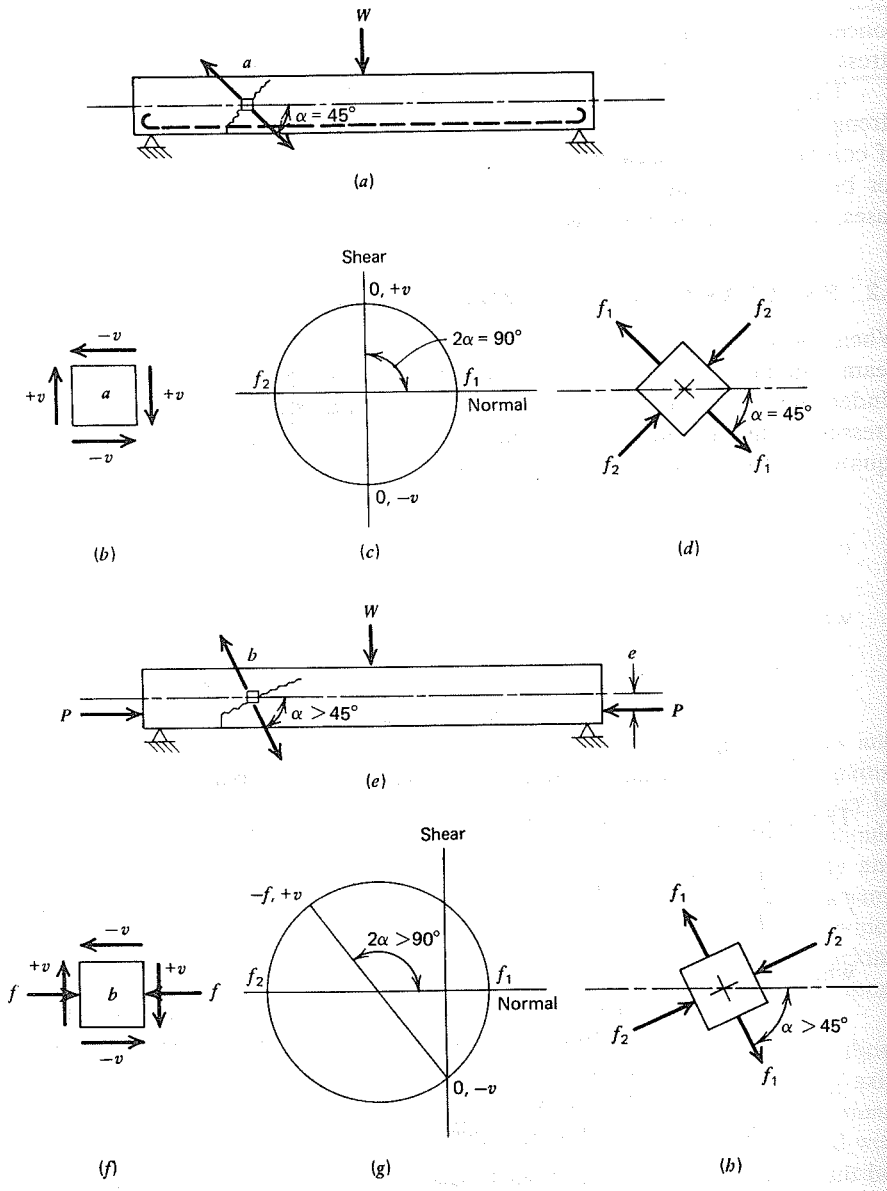

FIGURE 5.1 Effect of longitudinal prestress on diagonal tension and cracking.

A small element "a" located at the neutral axis of the reinforced concrete beam will be subjected to positive shear stresses v acting on its vertical faces, and negative shears of the same magnitude on the horizontal faces, as shown in Fig. 5.1*b*. Making use of Mohr's circle to find the principal stresses (Fig. 5.1*c*), it is found that the principal tension f_1 is equal (in absolute value) to the shear stress intensity and acts in a direction at 45 degrees to the axis of the beam, as shown in Fig. 5.1*d*. Equal principal compression acts in the perpendicular direction. Diagonal cracking, should it occur, will be at about 45 degrees to the horizontal axis of the member, as shown in idealized form in Fig. 5.1*a*.

The corresponding element "b" in the prestressed beam of Fig. 5.1*e* is subjected to identical shearing stresses v (Fig. 5.1*f*), and is subjected to horizontal compressive stress f. The Mohr's circle construction of Fig. 5.1*g* indicates that the principal tension f_1 is reduced to a much lower value than that of Fig. 5.1*c*, and acts in a direction making a substantially larger angle with the horizontal beam axis, as seen in Fig. 5.1*h*. Consequently, the diagonal tension crack of Fig. 5.1*e* is much flatter than before. If shear reinforcement is in the form of vertical stirrups, a larger number of those stirrips will cross the diagonal crack in the prestressed beam than would be true for the beam without prestressing, improving the effectiveness of the stirrups in transmitting shear across the crack.

It may also be seen from the principal stress constructions of Figs. 5.1*c* and 5.1*g* that diagonal tensile stress cannot be eliminated completely, no matter what the value of longitudinal compression, unless vertical precompression is introduced as well.

In addition to the effects just described, prestressing usually introduces a negative shear force, acting in an opposite sense to the load-induced shear, as a result of the inclination of the tendon, as shown in Fig. 5.2. Consequently, shear stresses in the uncracked beam are those corresponding to

$$V_{net} = V_{loads} - V_p \tag{5.3}$$

where V_p = the countershear of the tendons.

For beams having rectangular cross sections, the variation of shear stress through the depth of the member, given by Eq. (5.1), is parabolic, the value of v being zero at the top and bottom faces, and reaching a maximum at middepth. For beams of I cross section, such as Fig. 5.3*a*, commonly used for prestressed members, the shear stress increases abruptly at the transition from flange to web, because of the reduction of the section width b. The stress distribution of Fig. 5.3*b* is typical of I-beams, and is characterized by a nearly constant value of v throughout the depth of the web. The principal tensile stress in an I-beam can be found from the shear stresses of Fig. 5.3*b* and the longitudinal flexural stresses of Fig. 5.3*c*, which are usually about as shown at the service load level.

Typically, for I-beams, the maximum principal tension will not be found at the neutral axis, where the shear stress is greatest, but near the junction of the

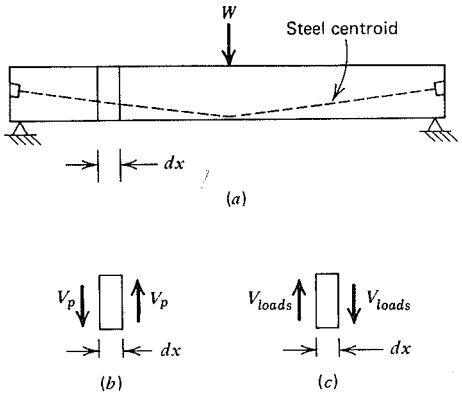

FIGURE 5.2 Effect of inclined tendons in reducing net shear force.

web and the lower flange, where the shear stress is also high, but where the longitudinal compression is reduced by the effect of the applied loads.

It should be noted further that the critical location for diagonal tension is usually not adjacent to the supports, even though the net external shear is highest there, because the longitudinal compression from prestressing is hardly reduced from its full value by the small external moments acting. A flexural stress distribution such as shown by the dotted line of Fig. 5.3*c* is typical, the exact variation depending on prestress eccentricity. Substantial longitudinal compression reduces the principal tensile stress near the supports. In addition, vertical compressive stress from the beam reactions prevents diagonal cracking close to the supports.

Consequently, diagonal tension cracking for uniformly loaded, simply supported prestressed I-beams is likely to occur at about the quarter points of the

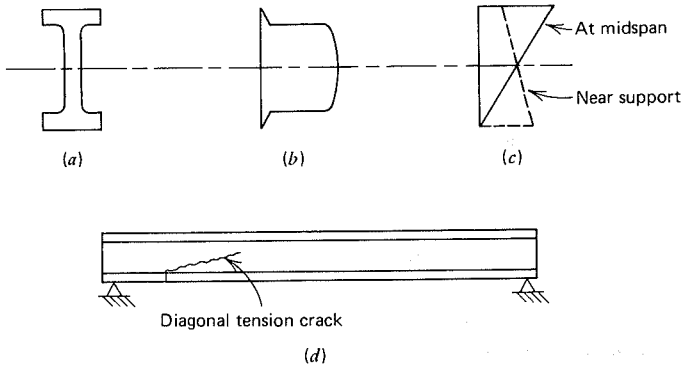

FIGURE 5.3 Diagonal tension cracking in prestressed concrete I-beam. (*a*) Cross section. (*b*) Shear stress variation. (*c*) Flexural stress variation. (*d*) Probable location of diagonal crack.

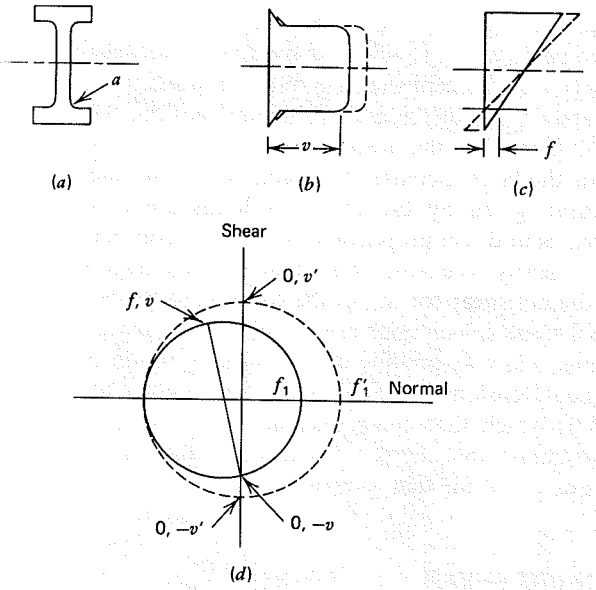

FIGURE 5.4 Principal stress increase upon overloading. (*a*) Cross section. (*b*) Shear stresses. (*c*) Flexural stresses. (*d*) Principal stress circle.

span, where the net shear forces are relatively large, and near the junction of the web and lower flange, where longitudinal compressive stresses are low and shear stresses are high. Should a diagonal crack form, it could be expected to appear about as shown in idealized form in Fig. 5.3*d*. This is confirmed by numerous tests.

The investigation of diagonal tension in uncracked beam webs is relevant mainly in predicting the load at which a diagonal crack will form, and in predicting the location and orientation of that crack. To base shear design upon an allowable tensile stress in the concrete at service load is unsafe, because relatively small increases in load above the service load level will produce disproportionate increases in diagonal tensile stress. This happens for two reasons.

First, consider the principal tensile stress at point *a* at the bottom of the web of the I-beam shown in Fig. 5.4*a*. At service loads, the shear stress distribution and flexural stress distribution are shown by the solid lines of Figs. 5.4*b* and 5.4*c*, respectively, with values v and f at the point of interest. The principal tensile stress f_1 of Fig. 5.4*d* may be obtained graphically or analytically.

Suppose now that the loads are increased by 20 percent, producing the increased shear stresses and flexural stresses shown by the dotted lines of Figs. 5.4*b* and 5.4*c*, respectively. From the modified principal stress construction

shown by the dotted lines of Fig. 5.4*d*, it is clear that reducing the flexural compression at point *a* to zero (which is achieved by a very modest increase in applied loads) together with a 20 percent increase in shear stress, is sufficient to produce a disproportionately large increase in principal tension. The increase shown is approximately 60 percent in the present case.

The second reason for the large increase in tension is that the shear stress is calculated for the net shear, given by Eq. (5.3). As loads are increased, the external shear V_{loads} increases in direct proportion, but V_p, the countershear from the inclined tendons, stays nearly constant. Thus, a small percentage increase in loads may easily double the net shear for which the beam is to be designed.

In summary, principal stress calculations are useful in visualizing the flow of stresses in uncracked beams, and may provide useful information on the location and orientation of diagonal tension cracking. Such calculations also provide information on the load at which that crack may be expected. However, they must never be used to evaluate the degree of safety inherent in a design. A strength-based analysis is essential for that purpose.

5.3 DIAGONAL CRACKING SHEAR

Extensive testing has shown that two types of diagonal cracking can occur in prestressed beams: *flexure-shear cracking* and *web-shear cracking* (Refs. 5.1 and 5.2). These are illustrated by Figs. 5.5*a* and 5.5*b*, respectively.

Flexure-shear cracks occur after flexural cracking has taken place. The flexural crack extends more or less vertically into the beam from the tension face. When a critical combination of flexural and shear stresses develops at the head of the flexural crack, that crack propagates in an inclined direction, often quite flat, as indicated by Fig. 5.5*a*. If web reinforcement is not provided, such a crack may produce what is known as a *shear-compression failure*, in which the compression area of the concrete near the top of the beam, reduced by the diagonal crack, is inadequate to resist forces resulting from flexure.

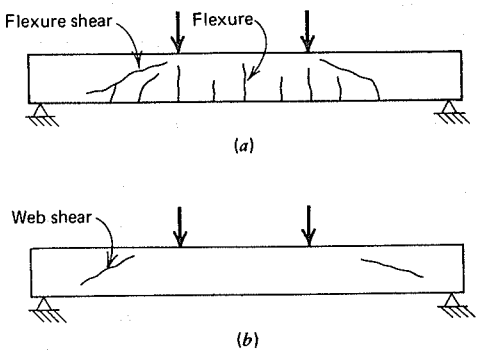

FIGURE 5.5 Types of inclined cracks. (*a*) Flexure-shear cracks. (*b*) Web-shear cracks.

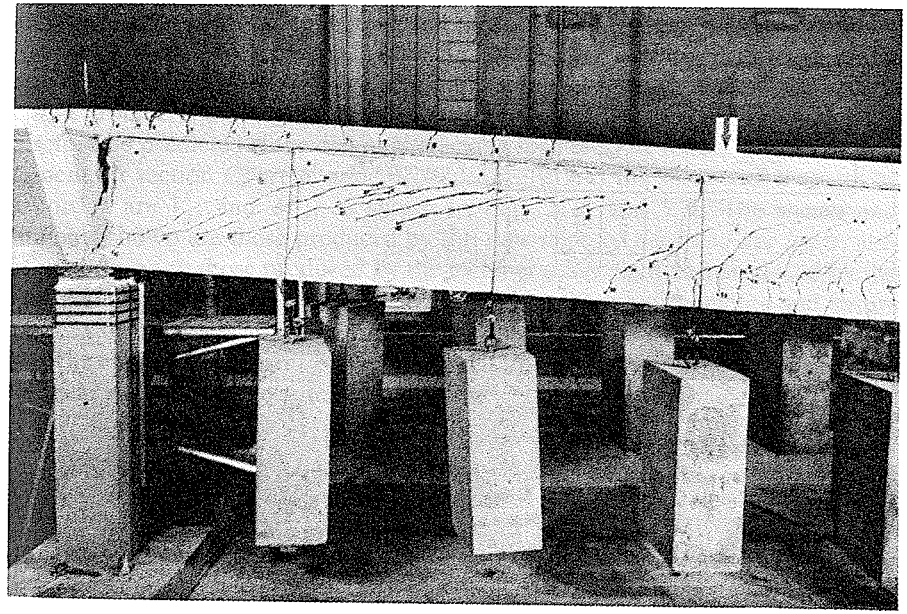

FIGURE 5.6 Web-shear cracking (left) and flexure-shear cracking (right) in continuous prestressed beam. Courtesy of Portland Cement Association.

Although flexure-shear cracking is the more common type, web-shear cracking may occur as shown in Fig. 5.5*b*, especially near the supports of heavily prestressed beams with relatively thin webs. This type of cracking initiates in the web, without previous flexural cracking, when the principal tension in the concrete becomes equal to the tensile strength of the material. This type of web distress leads to the sudden formation of a large inclined crack and, if web reinforcement is not present, will lead to failure of the beam in one of the following modes:

1. Separation of the tension flange from the web, as inclined cracks extend horizontally toward the supports.
2. Crushing of the web resulting from high compression acting parallel to the diagonal cracks, as the beam is transformed into the equivalent of a tied arch.
3. Secondary inclined tension cracking near the supports, which separates the compression flange from the web.

Typically, web-shear failures are more sudden than flexure-shear failures.

Figure 5.6 shows both web-shear cracking and flexure-shear cracking in a pretensioned beam with stirrup-reinforced web, tested at the laboratories of the Portland Cement Association. The cracks have been marked in ink on the beam surface for emphasis.

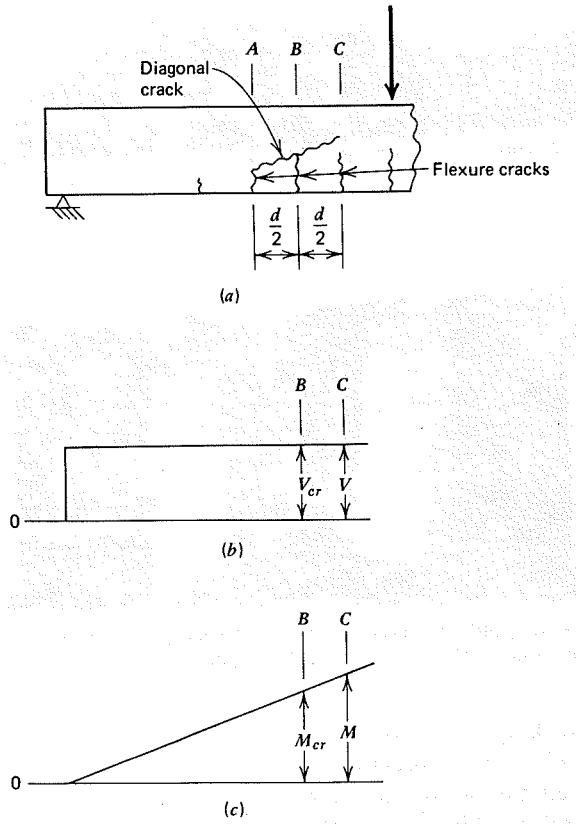

FIGURE 5.7 Flexure-shear cracking. (*a*) Idealized crack pattern. (*b*) Shear diagram. (*c*) Moment diagram.

In the case of flexure-shear cracking, tests have shown that the critical inclined crack has a horizontal projection at least equal to the effective beam depth d (Refs. 5.3, 5.4, and 5.5).[1] Therefore, it is the flexural cracking within a distance d, measured in the direction of decreasing moment from the section under consideration, that is associated with flexure-shear failure.

Figure 5.7*a* shows an idealized representation of flexure-shear cracking in the combined stress region of a beam (Refs. 5.6 and 5.7). The potential diagonal tension crack would initiate at the head of a previously formed flexural crack a distance d from the section C. Tests indicate that it is the formation of an *additional* flexural crack, midway between previously formed flexural cracks (i.e., at $d/2$ from C), that is the event that triggers actual collapse, and that must therefore be predicted if the diagonal cracking load is to be found. The shear and moment, at section C, are V and M, respectively, and the shear and moment at section B are V_{cr} and M_{cr}, as shown in Figs. 5.7*b* and 5.7*c*. The shears and moments shown are those produced by the *superimposed dead and live loads*, and act in addition to those produced by the member self-weight and produced by the prestressing tendon. The reason for distinguishing between moments and shears due to external loads and those due to self-weight will be clarified later.

The change in moment between sections B and C is equal to the area under the shear diagram between the two sections:

$$M - M_{cr} = \frac{1}{2}(V + V_{cr})\frac{d}{2}$$

or, since the difference between V and V_{cr} in the distance $d/2$ is small in most cases,

$$M - M_{cr} = \frac{Vd}{2}$$

Thus,

$$\frac{M}{V} - \frac{M_{cr}}{V} = \frac{d}{2}$$

and

$$V = \frac{M_{cr}}{M/V - d/2} \qquad \text{(a)}$$

This equation gives the shear V at section C due to superimposed dead and live loads when the moment at section B due to those loads is M_{cr}. Note that although the shear V appears on the right side of Eq. (a) as well as the left, it is not necessary that the value of V be known to make use of the equation. Only the ratio M/V, which is a characteristic of any given load pattern and stays constant as the superimposed loads increase proportionately, needs to be known.

The total shear at section C when the flexural crack develops at section B is the sum of that given by Eq. (a) plus the shear V_o due to self-weight and the shear V_p carried by the vertical component of the force in the curved or draped tendon. Furthermore, tests indicate that an increment of shear equal to $0.6b_w d\sqrt{f_c'}$ is

[1] In developing the design methods for shear and torsion in this chapter, the notation follows that of the ACI Code, in that the distance from the compression face of the beam to the centroid of the prestressing steel is defined as d for simplicity. Earlier in this text and in certain sections of the ACI Code, particularly with reference to partially prestressed beams, it was necessary to differentiate between effective depths d_p to the prestressing steel and d to the non-prestressed rebars.

required, after the flexural crack forms, for the inclined crack to develop, where b_w is the width of the section and d is the depth to the centroid of the prestressing steel (Refs. 5.3, 5.4, and 5.5). Thus, the total shear force V_{ci} that would produce flexure-shear failure is given by

$$V_{ci} = 0.6b_w d\sqrt{f_c'} + \frac{M_{cr}}{M/V - d/2} + V_o + V_p \tag{b}$$

In most cases, in the part of a span in which flexure-shear cracking is likely, the tendon slope is very small. Consequently, V_p has a small value that may conservatively be neglected, resulting in

$$V_{ci} = 0.6b_w d\sqrt{f_c'} + \frac{M_{cr}}{M/V - d/2} + V_o \tag{5.4}$$

The cracking moment M_{cr} in Eq. (5.4) is, by definition, that moment from superimposed dead and live loads, and acts in addition to the moment due to self-weight. M_{cr} may be calculated based on the tensile concrete stress at the bottom face equal to the modulus of rupture of the concrete, taken conservatively equal to $6\sqrt{f_c'}$. Thus,

$$f_o + \frac{M_{cr}c_2}{I_c} - f_{2p} = 6\sqrt{f_c'}$$

or

$$M_{cr} = \frac{I_c}{c_2}\left(6\sqrt{f_c'} + f_{2p} - f_o\right) \tag{5.5}$$

where f_o = flexural stress in the concrete at the bottom face of the beam due to self-weight
c_2 = distance from concrete centroid to the bottom face
I_c = moment of inertia of the concrete cross section
f_{2p} = concrete compressive stress at the bottom face resulting from axial and bending effects of the eccentric prestress force P_e

The sign convention used here, consistent with that of the ACI Code, treats all stresses as absolute values, without positive or negative sense.

The reason for separate consideration of self-weight and external loads is that self-weight is usually uniformly distributed, whereas superimposed loads may have any distribution. By separating the loads in this way, the ratio of M/V in Eq. (5.4) remains constant as external loads increase, facilitating the calculations. It should also be noted that whereas the analysis and design of web reinforcement to follow is based on ultimate strength at factored loads, the terms

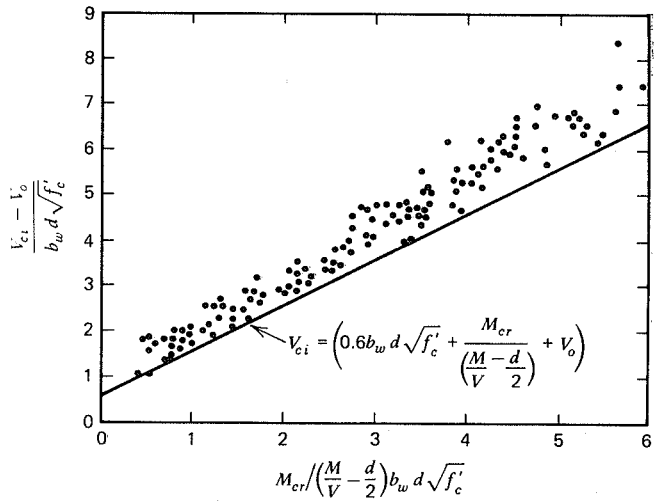

FIGURE 5.8 Comparison of Eq. (5.4) for V_{ci} with experimental data. From Ref. 5.7.

V_o and f_o used to predict diagonal cracking are based on the actual calculated self-weight without load factors. Figure 5.8 shows the close agreement between Eq. (5.4) and available experimental data (Ref. 5.7).

The second type of cracking, web-shear cracking, occurs when the maximum principal tensile stress resulting from the combination of shear and flexural stress, equals the tensile strength of the concrete. The concrete behavior is reasonably elastic up to failure in tension, so calculations may be based upon the ordinary equations of elasticity.

Principal stress calculations and tests of typical beams indicate that a web-shear crack may be expected to occur at, or below, the centroid of the concrete section (see Section 5.2 and Refs. 5.3 through 5.5). Beams for which the maximum principal tension is in the lower part of the cross section are likely to form flexural cracks, which lead to flexure-shear cracking rather than web-shear cracking. Consequently, the shear that will produce web-shear cracking may be estimated based on the principal tension at the concrete centroid.

The shear capacity of the member is reached if the principal tension becomes equal to the direct tensile strength of concrete, f_t'. Thus,

$$\sqrt{v_{cw}^2 + \left(\frac{f_{cc}}{2}\right)^2} - \frac{f_{cc}}{2} = f_t'$$

where v_{cw} = nominal shear stress in the concrete, $V_{cw}/b_w d$, resulting from *all* applied loads, dead and live
f_{cc} = compressive stress at the centroid of the concrete due to effective prestress force

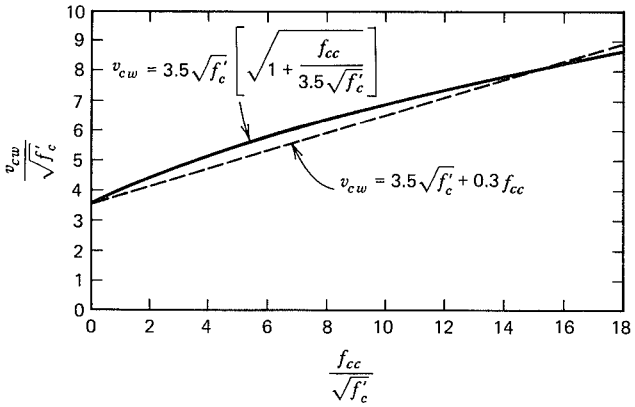

FIGURE 5.9 Nominal shear stress v_{cw} at web-shear cracking.

Solving for the nominal shear stress corresponding to diagonal cracking, we obtain

$$v_{cw} = f_t' \sqrt{1 + \frac{f_{cc}}{f_t'}}$$

The direct tensile strength may conservatively be taken equal to $3.5\sqrt{f_c'}$, indicating that

$$v_{cw} = 3.5\sqrt{f_c'} \sqrt{1 + \frac{f_{cc}}{3.5\sqrt{f_c'}}} \tag{5.6}$$

Figure 5.9 shows the functional relationship of Eq. (5.6). It also indicates that the results of the principal stress calculation can be closely approximated by the much simpler expression

$$v_{cw} = 3.5\sqrt{f_c'} + 0.3f_{cc} \tag{5.7}$$

The use of Eq. (5.7) is therefore recommended as the basis for design.

The external shear V_{cw} at which web-shear cracking is likely, based on Eq. (5.7), is increased by the vertical component of the prestress force V_p that normally acts in the opposite sense to the load-induced shear. Thus,

$$V_{cw} = b_w d\left(3.5\sqrt{f_c'} + 0.3f_{cc}\right) + V_p \tag{5.8}$$

In any given case, either flexure-shear or web-shear cracks may form. The shear force V_c at which diagonal cracking occurs should therefore be taken as the smaller of the two values V_{ci} and V_{cw}, given by Eqs. (5.4) and (5.8), respectively.

5.4 WEB REINFORCEMENT FOR SHEAR

It would be neither economical nor safe to design prestressed concrete beams of such proportions that all shear resistance is provided by the concrete alone. Non-prestressed web reinforcement is employed, of the same general form as used for reinforced concrete beams. Such web steel not only increases the shear strength of beams, but insures, should severe overloading produce a shear-related failure, that failure would be more ductile than otherwise. Yielding of the web reinforcement, accompanied by extensive concrete cracking, would give some warning of distress.

At least a minimum amount of web reinforcement is required in all prestressed beams. Exceptions may be made for members such as double-T beams of short to medium span that perform satisfactorily without such steel, or for slabs, where shear stress is characteristically low.

Infrequently, vertical or diagonal prestressing is used in the webs of beams. Although this offers the advantage that principal tensile stress and diagonal cracking in the concrete may be eliminated completely at service loads, such methods are not economical except in unusual cases. In addition, there is great practical difficulty controlling the amount of steel tension, because of large slip losses at the anchorages of the short tendons.

Typical forms of non-prestressed web reinforcement are shown in Fig. 5.10. For beams of ordinary dimensions, deformed reinforcing bars of sizes from No. 3 to No. 5 are common, and steel of Grades 40 or 60 is used. Steels of higher strength, used at corresponding higher stresses at service loads, are apt to permit excessively wide cracks. These not only would be visually objectionable, but would reduce the effectiveness of certain mechanisms of shear transfer, described later. In addition, the relatively sharp bends required for stirrups might lead to damage if the higher strength, more brittle steels were used.

Because stirrup bars are necessarily rather short, in most cases it is not possible to develop the full yield strength of the bars by bond alone within the available length of embedment. For this reason, special anchorage is provided in the form of hooks or bends as shown in Fig. 5.10. At the bottom of a typical stirrup, the reinforcing bar is bent into the form of a U, offering positive

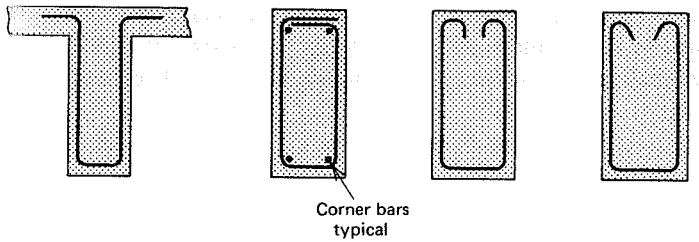

FIGURE 5.10 Types of web reinforcement.

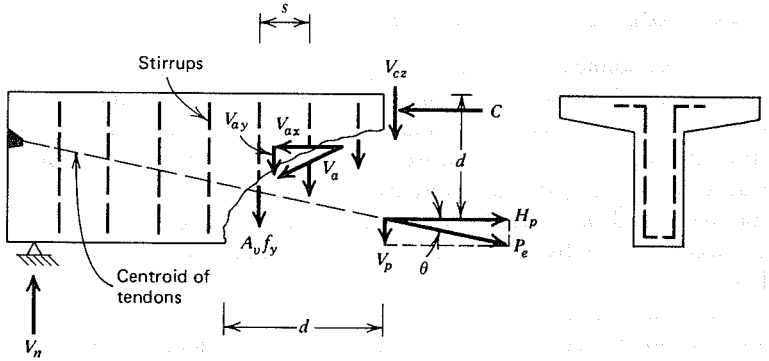

FIGURE 5.11 Shear transfer in partially cracked beam.

resistance to pullout. At the top, inward or outward facing bends or hooks are used.

In most cases, small diameter longitudinal bars are added to prestressed beams at the corners of the web reinforcement. These straight bars interlock with the stirrups to improve resistance to pullout, and serve the practical purpose of forming a rigid "cage" such that the web reinforcement can be fabricated outside of the beam forms, then dropped into position as a complete assembly.

The transfer of shear forces across the diagonally cracked section of a beam with web reinforcement may be understood after referring to Fig. 5.11. The figure shows the forces acting on a part of the beam between the diagonal cracked section and the adjacent support. Vertical U stirrups are shown at spacing s. For reasons already established, the analysis is based on conditions at the factored load stage, when the overloaded member is assumed to be at the point of incipient collapse.

Because of the presence of longitudinal compressive prestress in the concrete, the slope of the diagonal crack is generally considerably flatter than 45 degrees. It is assumed here, quite conservatively, that the horizontal projection of the crack has length d equal to the effective depth of the beam measured to the tendon centroid at the section of interest. Then, if the spacing of the web reinforcement in the direction of the member axis is s, the number of U stirrups crossing the diagonal crack is d/s. When the member is at incipient failure, the stirrups are stressed to their full yield strength f_y. It follows that the total contribution of the stirrups to transfer of shear across the cracked section is

$$V_s = \frac{A_v f_y d}{s} \tag{c}$$

where A_v is the total steel area of one stirrup, that is, two times the bar cross-sectional area for the typical case with U stirrups.

If the tendon centroid crosses the section of interest at slope θ, then the tendon transmits a shear force equal to the vertical component of the prestressing force. Although the tendon force increases as the member is overloaded, it will be assumed conservatively that it has a value equal to the effective prestress P_e. Thus, the vertical component is

$$V_p = P_e \sin\theta \tag{d}$$

A third contribution to shear transfer comes from frictional resistance along the naturally rough interface formed by the crack. Even though cracking will take place perpendicular to the direction of principal tension such that no shear displacements might be expected, it has been confirmed by tests that a significant redistribution of internal forces takes place upon cracking such that some tendency to slip exists along the interface. This is resisted by the roughness of the surface and the interlocking of the aggregate. The resisting force V_a associated with *aggregate interlock* acts on the free body in the direction represented in Fig. 5.11. Its vertical component is V_{ay}.

Finally, the concrete in the uncracked compression zone above the diagonal crack provides a resisting force V_{cz}.

Setting the summation of vertical forces equal to zero (Fig. 5.11) leads to the expression for nominal shear strength:

$$V_n = A_v f_y \frac{d}{s} + V_{cz} + V_p + V_{ay} \tag{5.9}$$

In spite of intensive research over a period of years, the magnitude of the individual contributions of V_{cz} and V_{ay} in Eq. (5.9) are not known. From tests, it appears that a conservative basis for design is to assume that their combined contribution is no less than V_c, the shear force that caused the diagonal crack to occur. The magnitude of V_c, in turn, may be determined either by web-shear cracking or flexure-shear cracking, and should be taken as the smaller of V_{ci} and V_{cw}, given by Eqs. (5.4) and (5.8), respectively.

If, in addition, the vertical component of the prestress force is neglected (this can be justified because of the small angle of tendon slope in the region of greatest interest), then Eq. (5.9) may be simplified to the following expression for ultimate shear strength:

$$V_n = A_v f_y \frac{d}{s} + V_c \tag{5.10}$$

If the "excess shear" above that which is resisted by the concrete is identified as $(V_n - V_c)$, and if the web reinforcement ratio is defined such that

$$\rho_v = \frac{A_v}{b_w s}$$

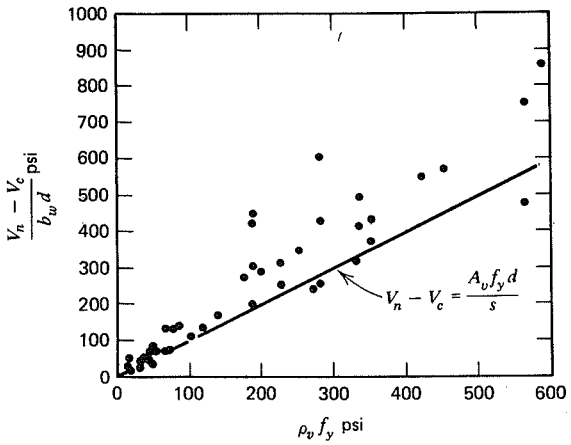

FIGURE 5.12 Increase in shear strength of a prestressed member resulting from web reinforcement. From Ref. 5.5.

then Eq. (5.10) may be restated as

$$\frac{V_n - V_c}{b_w d} = \rho_v f_y \tag{5.11}$$

A comparison of the shear strength predicted by Eq. (5.11) with experimental data is given in Fig. 5.12. It is seen that the equation gives a conservative lower limit to the experimental data in all but a few cases; these too are close to the value given by Eq. (5.11).

5.5 SHEAR DESIGN CRITERIA OF THE ACI CODE

A. DESIGN BASIS

The shear provisions of the ACI Code correlate directly with the development of the preceding articles. Design is to be based on conditions in the member at a hypothetical overload stage, with calculated dead loads and service live loads multiplied by the usual overload factors, except where otherwise noted.

The design of cross sections subject to shear is to be based on the relation:

$$V_u \le \phi V_n \tag{5.12}$$

where V_u = shear force applied at factored loads
V_n = nominal shear strength of the section
ϕ = strength reduction factor, taken equal to 0.85 for shear

The nominal shear strength V_n is calculated from the equation

$$V_n = V_c + V_s \tag{5.13}$$

where V_c = nominal shear strength provided by the concrete
V_s = nominal shear strength provided by the shear reinforcement

The value of V_c is to be calculated according to Section B.

The first critical section for shear is assumed to be at a distance $h/2$ from the face of a support, and sections located a distance less than $h/2$ are designed for the shear computed at $h/2$. This provision recognizes the beneficial effect of vertical compression in the concrete caused by the reaction. In special circumstances, those benefits are not obtained, and the shear at the support face may become critical.

B. NOMINAL SHEAR STRENGTH PROVIDED BY THE CONCRETE

In Eq. (5.13), the value of V_c is to be taken equal to the smaller of V_{ci} and V_{cw}, determined by flexure-shear cracking and web-shear cracking, respectively. These values are based on Eqs. (5.4) and (5.8).

First, in Eq. (5.4) for flexure-shear cracking, the term $d/2$ may be deleted, for the sake of simplicity. This has the effect of relating flexure-shear cracking to the load that causes flexural cracking at the section considered, rather than at a distance $d/2$ from the section considered, and makes the equation somewhat more conservative. Then, with slight notational changes,

$$V_{ci} = 0.6\sqrt{f_c'}\, b_w d + V_o + \frac{V_i}{M_{max}} M_{cr} \tag{5.14}$$

where b_w is the width of a rectangular section or the web width of a flanged section, and d is the depth from the compression face of the member to the centroid of the prestressing steel. On the basis of tests, the latter value need not be taken less than $0.80h$ for this and all other Code provisions relating to shear, except as specifically noted otherwise.

In Eq. (5.14), V_i and M_{max} are, respectively, the factored[2] shear and bending moment at the section considered, resulting from the *superimposed* dead load and live load, and M_{cr} is the moment causing flexural cracking, computed by Eq. (5.5):

$$M_{cr} = \frac{I_c}{c_2}\left(6\sqrt{f_c'} + f_{2p} - f_o\right) \tag{5.5}$$

[2]Note that load factors, which are applicable identically to numerator and denominator here, will cancel; unfactored V_i and M_{max} can be used.

In Eq. (5.14), V_o is the shear due to the self-weight of the member and is computed without load factor. In Eq. (5.5), f_o is the flexural stress at the bottom face of the beam, resulting from the self-weight of the member and is computed without load factor. The reason for separate consideration of self-weight was explained earlier.

In applying Eq. (5.14), V_{ci} need not be taken less than $1.7\sqrt{f_c'}\,b_w d$, according to the Code.

The nominal shear strength corresponding to web-shear cracking is computed from Eq. (5.8) without modification:

$$V_{cw} = \left(3.5\sqrt{f_c'} + 0.3f_{cc}\right)b_w d + V_p \tag{5.15}$$

where V_p is the vertical component of the effective prestress force at the section:

$$V_p = P_e \sin\theta \tag{5.16}$$

in which θ is the slope of the tendon centroid line at the section.

Instead of using Eq. (5.15), V_{cw} may be computed as the shear force corresponding to the dead load plus live load that results in a principal tensile stress of $4\sqrt{f_c'}$ at the centroid of the member, or at the intersection of the flange and web when the centroidal axis is in the flange.

For members with an effective prestress force not less than 40 percent of the tensile strength of the flexural reinforcement, an alternative to the use of Eqs. (5.14) and (5.15) is permitted. The shear force V_c may be taken equal to

$$V_c = \left(0.6\sqrt{f_c'} + 700\frac{V_u d}{M_u}\right)b_w d \tag{5.17}$$

In this equation, V_u and M_u are the factored shear and moment resulting from *all* loads, at the section considered, and the quantity $V_u d/M_u$ is not to be taken greater than 1.0. If Eq. (5.17) is used, V_c need not be taken less than $2\sqrt{f_c'}\,b_w d$ and must not be taken larger than $5\sqrt{f_c'}\,b_w d$. In this equation, the actual effective depth d to the centroid of the prestressing tendons is to be used in computing the term $V_u d/M_u$, according to ACI Code. The usual lower bound for d of $0.80h$ may be used in the final term $b_w d$, which merely translates the nominal average shear stress v_c to shear force V_c.

Equation (5.17) is appealing in that it is simple to use compared with the more accurate Eqs. (5.14) and (5.15), but it may give very conservative and uneconomical results for certain classes of members.

C. REQUIRED AREA OF WEB REINFORCEMENT

When shear reinforcement perpendicular to the axis of the member is used, its contribution to shear strength is

$$V_s = \frac{A_v f_y d}{s} \tag{5.18}$$

as derived in Section 5.4, but the value of V_s is not to be taken larger than $8\sqrt{f_c'}\,b_w d$.

The total nominal shear strength V_n is found by summing the contributions of the steel and the concrete:

$$V_n = \frac{A_v f_y d}{s} + V_c \tag{5.19}$$

From Eq. (5.12), in the limiting case, and Eq. (5.13):

$$V_u = \phi V_n$$
$$= \phi(V_s + V_c)$$

from which

$$V_u = \phi\left(\frac{A_v f_y d}{s} + V_c\right) \tag{5.20}$$

The required cross-sectional area of one stirrup A_v may be calculated by suitable transposition of Eq. (5.20):

$$A_v = \frac{(V_u - \phi V_c)s}{\phi f_y d} \tag{5.21}$$

Normally, in practical design, the engineer will select a trial stirrup size, for which the required spacing is found. Thus, a more convenient form of Eq. (5.21) is:

$$s = \frac{\phi A_v f_y d}{V_u - \phi V_c} \tag{5.22}$$

If the spacing determined for the trial stirrup size is too close for placement economy or practicality, or if it is so large that maximum spacing requirements control over too great a part of the beam span, then a revised bar size is selected and the calculation repeated.

D. MINIMUM WEB REINFORCEMENT

At least a certain minimum area of shear reinforcement is to be provided in all prestressed concrete members, where the total factored shear force V_u is greater than one-half of the shear strength ϕV_c provided by the concrete. Based on successful performance, the following types of members are excepted from this requirement:

1. Slabs and footings.
2. Concrete joist construction (including ribbed members such as double-T beams).
3. Beams with a total depth not greater than the largest of 10 in., two and one-half times the thickness of the flange, and one-half of the web width.

The minimum area of shear reinforcement to be provided in all other cases is to be taken equal to the *smaller* of the following values:

$$A_v = 50\frac{b_w s}{f_y} \tag{5.23}$$

and

$$A_v = \frac{A_p}{80}\frac{f_{pu}}{f_y}\frac{s}{d}\sqrt{\frac{d}{b_w}} \tag{5.24}$$

in which A_p is the cross-sectional area of the prestressing steel, f_y is the yield stress of the stirrup steel, and f_{pu} is the ultimate tensile strength of the prestressing steel. All other terms are as previously defined.

Note that a decrease in b_w will result in a decrease in A_v, according to Eq. (5.23), but an increase in A_v, according to Eq. (5.24). The first equation was originally based on studies of reinforced concrete beams with web reinforcement, having a ratio of depth-to-web width of about two. The second equation was derived specifically for prestressed concrete beams, and was intended to ensure that in sections with narrow webs, the ratio of web reinforcement would be greater than in thick-webbed sections. Equation (5.24) will generally require less shear reinforcement that Eq. (5.23); however, according to ACI Code, it may be used only if the effective prestress is not less than 40 percent of the tensile strength of the prestressed reinforcement.

The ACI Code contains, in addition, certain restrictions on the maximum spacing of web reinforcement to insure that any potential diagonal crack will be crossed by at least a minimum amount of web steel. For prestressed members, this maximum spacing is not to exceed the smaller of $0.75h$ or 24 in. If the value of V_s exceeds $4\sqrt{f_c'}\,b_w d$, these limits are reduced by one-half.

E. LIGHTWEIGHT CONCRETE

Lightweight aggregate concretes are often used for prestressed members. Although the provisions of the ACI Code for shear design that have just been summarized pertain to members using normal weight concrete, they may be applied to those built of lightweight concrete with the following modification:

1. When the split-cylinder strength f_{ct} is specified for the lightweight concrete, the provisions for V_c shall be modified by substituting $f_{ct}/6.7$ for $\sqrt{f_c'}$, but the value of $f_{ct}/6.7$ shall not exceed $\sqrt{f_c'}$.
2. When f_{ct} is not specified, all values of $\sqrt{f_c'}$ affecting V_c and M_{cr} shall be multiplied by 0.75 for "all-lightweight" concrete and 0.85 for "sand-lightweight" concrete.

F. ANCHORAGE OF WEB STEEL

Web reinforcement should be carried as close to the compression and tension surfaces of the member as cover requirements and the proximity of other reinforcement will permit. According to the Code, stirrups must extend a distance d from the extreme compression face, and must be anchored at both ends by one of the following means:

1. A standard hook plus an effective embedment of $0.5l_d$. The $0.5l_d$ of embedment of a stirrup leg shall be taken as the distance between the middepth of the member $d/2$ and the start of the hook (point of tangency).
2. Embedment above or below the middepth $d/2$ of the beam on the compression side for a full development length l_d but not less than 24 bar diameters, or for deformed bars or deformed wire 12 in.
3. For No. 5 bars and D31 wire and smaller, bending around the longitudinal reinforcement through at least 135 degrees, plus, for stirrups with design stress exceeding 40,000 psi, an effective embedment of $0.33l_d$. The $0.33l_d$ embedment of a stirrup leg shall be taken as the distance between the middepth of the member $d/2$ and start of the hook (point of tangency).

The basic development length l_d is to be taken as

$$l_d = \frac{0.04A_b f_y}{\sqrt{f_c'}} \tag{5.25a}$$

but not less than

$$l_d = 0.0004 d_b f_y \tag{5.25b}$$

where A_b = bar cross-sectional area, in.^{2}
d_b = bar diameter, in.

For "all-lightweight" concrete this length is increased by 33 percent, and for "sand-lightweight" it is increased by 18 percent.

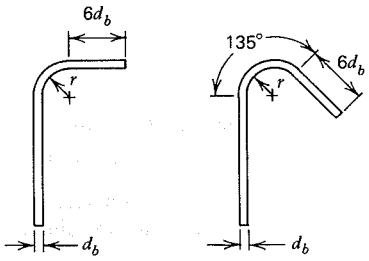

FIGURE 5.13 Standard hooks for stirrups and ties of size No. 5 or smaller.

The dimensions of hooks have been standardized, and for the common sizes, No. 5 and smaller, are as shown in Fig. 5.13. The minimum inside diameter of bend should be four bar diameters. Large beams may require the use of heavier stirrups, for which special, more restrictive Code provisions apply. The use of hooked stirrups and ties is limited to No. 8 bars or smaller.

G. DESIGN PRACTICE

It is clear that the design of web reinforcement becomes quite complex, even for ordinary cases. This is particularly true if V_C is based on the more refined approach using Eqs. (5.14) and (5.15) for V_{ci} and V_{cw}, respectively, because many of the parameters in those equations vary depending on the location along the span. Use of a computer program will greatly facilitate the calculation of required stirrup spacings.

Alternatively, it may be advantageous to determine web steel requirements by plotting the variation of applied and resisting shears along the span, as shown in Fig. 5.14 for a uniformly loaded member. The excess shear may be quickly established at any location from such a diagram, and a practical arrangement of

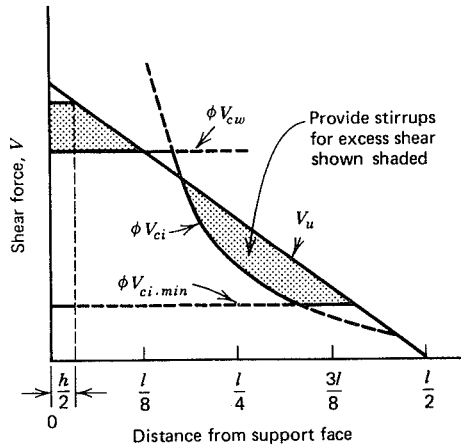

FIGURE 5.14 Basis for design of stirrups in uniformly loaded beam.

stirrups selected. In placing stirrups, usually three or four constant spacings are selected, to approximate the continuously varying requirement such as indicated by Fig. 5.14.

5.6 EXAMPLE: DESIGN OF WEB REINFORCEMENT FOR SHEAR

The I-beam of Fig. 5.15 is to carry a superimposed dead load of 345 plf and service live load of 1,220 plf in addition to its own weight of 255 plf. It is to be built of concrete with $f'_c = 5{,}000$ psi and is prestressed using tendons with $f_{pu} = 270{,}000$ psi to an effective force $P_e = 288$ kips. Find the required spacing of vertical U stirrups at a point 10 ft from the left support, if f_y for the stirrup steel is 40,000 psi. ($w_o = 3.72$ kN/m, $w_d = 5.03$ kN/m, $w_l = 17.80$ kN/m, $f'_c = 35$ MPa, $f_{pu} = 1{,}860$ MPa, $f_y = 276$ MPa, $P_e = 1{,}281$ kN, and the section at $x = 3.05$ m.)

It is easily established that the properties of the uncracked concrete cross section are: $I_c = 24{,}200$ in.^{4}, $A_c = 245$ in.^{2}, and $r^2 = 99$ in.^{2} (10.1×10^9 mm^4, 158×10^3 mm^2, and 64×10^3 mm^2.)

The tendon depth d through the central part of the span is 24.5 in. and the eccentricity $e = 11.4$ in. From a 15-ft distance, the eccentricity is reduced linearly to zero at the support. Thus, at the section of interest, the eccentricity is

$$e = 11.4 \times \frac{10}{15} = 7.6 \text{ in. (193 mm)}$$

The corresponding depth d is 13.1 + 7.6 = 20.7 in. In accordance with the Code, the effective depth in shear calculations will be assumed at $0.80 \times 29 = 23.2$ in. (589 mm).

The nominal shear strength for flexural-shear cracking is found with the aid of Eqs. (5.14) and (5.5). At the given section, the stress in the concrete at the bottom

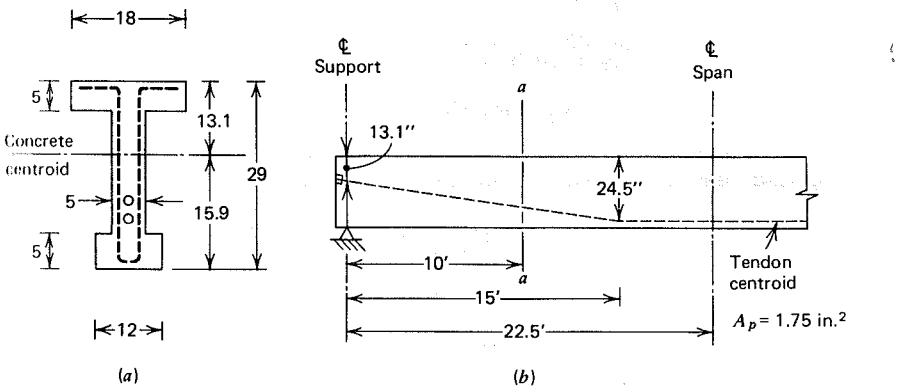

FIGURE 5.15 Shear design example. (*a*) Cross section. (*b*) Profile.

face due to prestress alone is

$$f_{2p} = -\frac{P_e}{A_c}\left(1 + \frac{ec_2}{r^2}\right)$$

$$= -\frac{288{,}000}{245}\left(1 + \frac{7.6 \times 15.9}{99}\right)$$

$$= -2{,}600 \text{ psi}$$

The self-weight moment and shear at $x = 10$ ft are, respectively,

$$M_o = \frac{w_o x}{2}(l - x)$$

$$= \frac{0.255 \times 10}{2}(45 - 10)$$

$$= 45 \text{ ft-kips (61 kN-m)}$$

$$V_o = w_o\left(\frac{l}{2} - x\right)$$

$$= 0.255\left(\frac{45}{2} - 10\right)$$

$$= 3.19 \text{ kips (14.19 kN)}$$

The moment M_o produces a tensile stress at the bottom of the beam equal to

$$f_o = \frac{M_o c_2}{I_c}$$

$$= \frac{45{,}000 \times 12 \times 15.9}{24{,}200}$$

$$= 355 \text{ psi}$$

Then, from Eq. (5.5)

$$M_{cr} = \frac{I_c}{c_2}\left(6\sqrt{f'_c} + f_{2p} - f_o\right)$$

$$= \frac{24{,}200}{15.9}(6\sqrt{5{,}000} + 2{,}600 - 355)\frac{1}{12{,}000}$$

$$= 339 \text{ ft-kips (460 kN-m)}$$

The shear and moment at the section 10 ft from the support, resulting from the superimposed dead load of 345 plf and live load of 1,220 plf, are, respectively

$$V_i = 1.565\left(\frac{45}{2} - 10\right)$$

$$= 19.56 \text{ kips}$$

$$M_{max} = \frac{1.565 \times 10}{2}(45 - 10)$$

$$= 274 \text{ ft-kips}$$

Thus, from Eq. (5.14) the value of V_{ci} is

$$V_{ci} = 0.6\sqrt{f'_c}\, b_w d + V_o + \frac{V_i}{M_{max}} M_{cr}$$

$$= 0.6\sqrt{5{,}000} \times 5 \times 23.2 + 3{,}190 + \frac{19{,}560}{274{,}000} \times 339{,}000$$

$$= 32{,}310 \text{ lb (144 kN)}$$

Note that the lower limit of $1.7\sqrt{5{,}000} \times 5 \times 23.2 = 13{,}940$ lb does not control here.

The nominal shear strength for web-shear cracking is found from Eq. (5.15). With $P_e = 288$ kips, the centroidal stress in the concrete is

$$f_{cc} = \frac{288{,}000}{245} = 1{,}170 \text{ psi}$$

The vertical component of the effective prestress force is

$$V_p = 288 \times \frac{11.4}{15 \times 12}$$

$$= 18.24 \text{ kips}$$

Then, from Eq. (5.15)

$$V_{cw} = \left(3.5\sqrt{f'_c} + 0.3 f_{cc}\right) b_w d + V_p$$

$$= (3.5\sqrt{5{,}000} + 0.3 \times 1{,}170) \times 5 \times 23.2 + 18{,}240$$

$$= 87{,}660 \text{ lb (390 kN)}$$

In the present case, flexure-shear cracking controls, and $V_c = V_{ci} = 32{,}310$ lb = 32.31 kips (144 kN).

The total shear force at $x = 10$ ft at factored loads is

$$V_u = [1.4(0.255 + 0.345) + 1.7 \times 1.220]12.5$$

$$= 36.43 \text{ kips (162 kN)}$$

Thus, the excess shear stress, $(V_u - \phi V_c) = \phi V_s = 36.43 - 0.85 \times 32.31 = 8.97$ kips, is well below the upper limit of $8 \times 0.85\sqrt{5{,}000} \times 5 \times 23.2 = 55.8$ kips and is below $4 \times 0.85\sqrt{5{,}000} \times 5 \times 23.2 = 27.9$ kips so that normal spacing limitations apply.

For trial purposes, No. 3 U stirrups will be selected, providing an area per stirrup of $A_v = 2 \times 0.11 = 0.22$ in.^{2} From Eq. (5.22)

$$s = \frac{\phi A_v f_y d}{V_u - \phi V_c}$$

$$= \frac{0.85 \times 0.22 \times 40{,}000 \times 23.2}{8{,}970}$$

$$= 19.3 \text{ in. (490 mm)}$$

Checking minimum web steel area by Eqs. (5.23) and (5.24):

$$A_v = 50\frac{b_w s}{f_y}$$

$$= \left(\frac{50 \times 5}{40{,}000}\right)s$$

$$= 0.00625s$$

and

$$A_v = \frac{A_p}{80}\frac{f_{pu}}{f_y}\frac{s}{d}\sqrt{\frac{d}{b_w}}$$

$$= \frac{1.75}{80} \times \frac{275}{40}\frac{s}{23.2}\sqrt{\frac{23.2}{5}}$$

$$= 0.01396s$$

The smaller of the two requirements controls, and for No. 3 stirrups with $A_v = 0.22$ in.^{2} the maximum spacing $s = 35$ in. In addition, the maximum spacing is not to exceed the smaller of 24 in. or $0.75 \times 29 = 22$ in. The calculated requirement of $s = 19.3$ in. controls in any case. This will be rounded off to $s = 18$ in. for practical reasons.

5.7 TORSION IN CONCRETE STRUCTURES

Reinforced or prestressed concrete members may be subjected to torsional moments, which cause a member to twist about its long axis. Although such torsional moments may act alone, more often they act in conjunction with bending moments and shear forces.

For many years, designers of concrete structures have tended to regard torsion as a secondary effect, relying on the capacity of a typical indeterminate structure to redistribute internal forces until an alternative equilibrium state is found. A common example occurs in the design of spandrel beams supporting the edge of a monolithic floor, as shown in Fig. 5.16. A distributed load applied to the floor causes twisting moments m_t to be applied, more or less uniformly along the length of the edge beam. These are equilibrated by resisting torques M_t provided by the building columns at A and B. Spandrel beam cross sections near

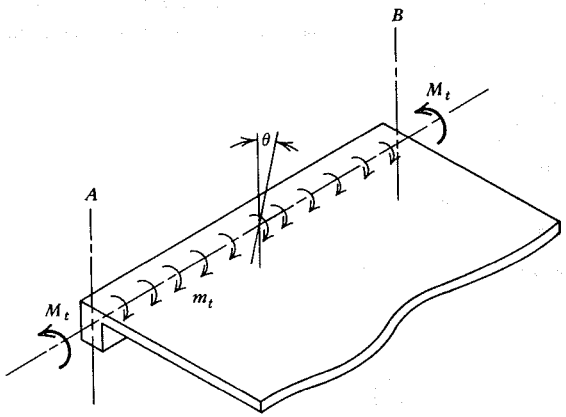

FIGURE 5.16 Spandrel beam subject to torsion.

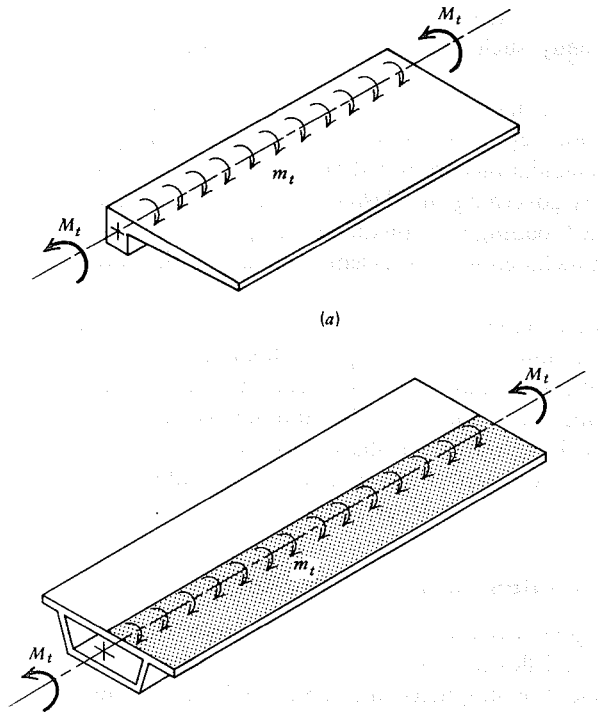

FIGURE 5.17 Torsion members. (*a*) Cantilevered slab. (*b*) Box girder bridge.

midspan tend to rotate with respect to the corresponding sections near the columns, as shown.

If no special attention is given to torsion in designing the spandrel and its reinforcement, some torsional cracking is likely to occur, reducing its stiffness and its capacity to provide edge restraint for the slab. If the slab is reinforced accordingly, in most cases no difficulty will be experienced.

Although indeterminate structures seek to accommodate to the assumptions of the designer in this way, it is dangerous to attempt to exploit this to too great an extent. Redistribution in some cases may be accompanied by excessive cracking and large deflections. In other cases, the required ductility may not be available.

Furthermore, in many types of structures, torsion is a primary design condition. The beam of Fig. 5.17*a*, for example, carries a cantilevered slab, and *must* possess adequate torsional resistance to carry the load. The box-girder bridge of Fig. 5.17*b*, when loaded in one traffic lane as indicated by the shaded area, develops torsional stresses that are a dominant part of the design. Other

examples are easily found, such as helical stairways and curved beams. Engineers may expect to encounter many such design problems in which torsion is the primary loading.

The behavior of concrete structures carrying torsion or combined loading is not yet fully understood. Research in recent years has shed much light on this behavior, yet present recommendations are based largely on test observation, not theory. Specific requirements governing the design of *reinforced* concrete members for torsion and combined loading were included for the first time in the 1971 ACI Code. These have been included with no essential change in the current 1983 Code.

Code provisions do not include coverage of prestressed concrete members subject to torsion. It appears, however, that an approach similar to that used for reinforced concrete is applicable, and tentative recommendations have been proposed (Ref. 5.10). The approach, which will be summarized in the following sections, combines theory with experimental observation to arrive at a practical design method. The material presented must be regarded as tentative, however, subject to revision as new information is developed.

5.8 TORSION DESIGN OF PRESTRESSED CONCRETE

In studying the behavior of prestressed concrete members subject to loading that combines torsion, bending, and flexural shear, it is first necessary to discuss the effects of torsion acting alone. For simplicity, the subject will be introduced with reference to rectangular members, but the conclusions apply to more complicated shapes with slight modifications, as will be discussed further.

A. TORSION IN BEAMS WITHOUT WEB REINFORCEMENT

Figure 5.18*a* shows a portion of a prismatic member *without prestress force*, with equal and opposite torques T acting at each end. If the material is elastic, St. Venant's torsion theory indicates that torsional shear stresses are distributed over the cross section, as shown by the solid lines in Fig. 5.18*b*. The largest shear stress occurs at the middle of the wide faces and is equal to

$$t_{max} = \frac{T}{\eta x^2 y} \tag{5.26}$$

where η is a coefficient that depends on the shape of the cross section, and x and y are, respectively, the shorter and longer sides. If the material is inelastic, the stress distribution is similar, as shown by the dashed lines, and the maximum shear stress is still given by Eq. (5.26) except that η assumes a different value.

Shear stresses act in pairs on an element at or near the wide surface, as shown in Fig. 5.18*a*. It is easily shown that this state of stress corresponds exactly

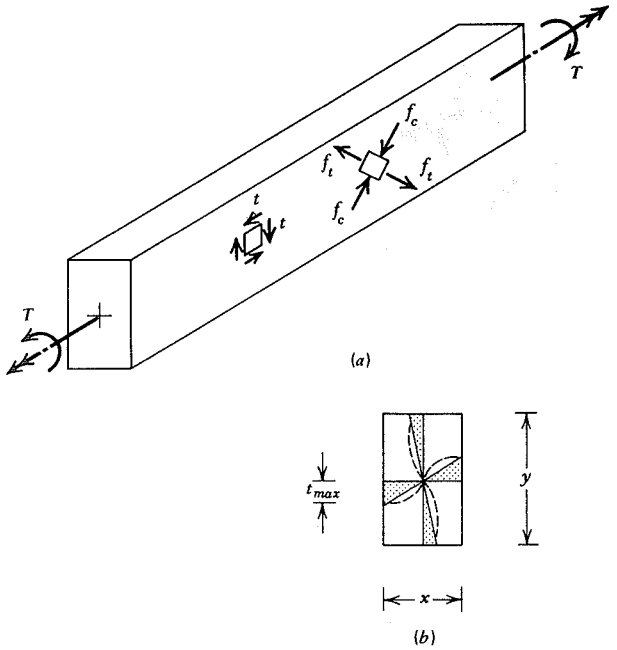

FIGURE 5.18 Stresses caused by torsion.

to a state described by equal tension and compression stresses on the faces of an element at 45 degrees to the direction of shear.

When the diagonal tension stresses exceed the tensile strength of the concrete, a crack forms at some accidentally weaker location and spreads immediately across the beam, as shown in Fig. 5.19*a*. Tests confirm that the crack forms at 45 degrees on the near face, and that the extensions of the crack on the two narrower faces are also at about 45 degrees with the member axis. The fracture line on the far face connects the cracks at the short faces, establishing a warped failure surface.

For purposes of analysis, this surface can be replaced by a plane section inclined at 45 degrees to the axis, as in Fig. 5.19*b*. The applied torque T can be resolved into a component T_b causing bending about the axis a–a of the failure plane, and a component T_t that causes twisting. Tests indicate that failure is associated with the bending component, not the twisting.

The section modulus of the failure plane about a–a is

$$Z = \frac{1}{6}\frac{x^2 y}{\sin 45°}$$

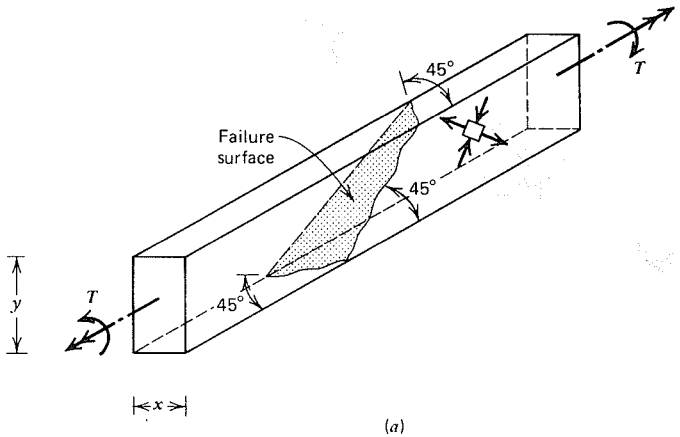

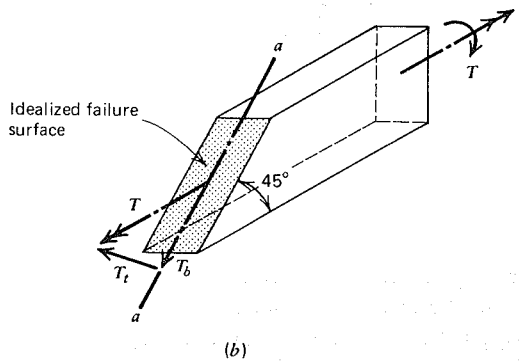

FIGURE 5.19 Torsional cracking of beam without web reinforcement. (*a*) Skewed bending failure. (*b*) Idealized failure model.

and the maximum tensile stress resulting from the moment component T_b is

$$f_t = \frac{T_b}{Z} = \frac{6T \sin 45° \cos 45°}{x^2 y}$$

Simplified, this becomes

$$f_t = \frac{T}{\frac{1}{3}x^2 y} \tag{5.27}$$

It is seen that the tension stress calculated by this *skew bending theory* is identical with the St. Venant's shear stress of Eq. (5.26) with $\eta = 1/3$.

If f_t were the only stress acting, cracking should occur when f_t becomes equal to f_r, the modulus of rupture of concrete, usually taken as $7.5\sqrt{f_c'}$. However, at right angles to the tension, there is equal compression. This results in a reduction in the tensile strength of about 15 percent (see Section 2.10). Consequently, a crack forms and the unreinforced member fails when $f_t = 6\sqrt{f_c'}$. Thus, the failure torque T_{cr} of a non-prestressed beam without web steel (or the cracking torque of one with web steel) can be predicted from the equation

$$T_{cr} = 6\sqrt{f_c'}\left(\tfrac{1}{3}x^2 y\right) \tag{5.28}$$

For *prestressed* concrete members without web steel, an analogous development is valid. Failure is attained when the maximum principal tensile stress, resulting from the combined action of torsion and compression, reaches the direct tensile strength of the concrete, which for present purposes is taken equal to $0.10f_c'$. On this basis it is shown in Ref. 5.9 that the cracking torque of a prestressed beam is given by the equation

$$T_{cr}' = 6\sqrt{f_c'}\sqrt{1 + 10f_{cc}/f_c'}\left(\eta x^2 y\right) \tag{5.29}$$

or $T_{cr}' = T_{cr}\sqrt{1 + 10f_{cc}/f_c'}$, where f_{cc} is the average longitudinal prestress P_e/A_c.

Equation (5.29) permits experimental evaluation of the shape factor η based on measured cracking torque. From tests of 218 prestressed rectangular beams, with varying eccentricity of prestress (Ref. 5.10), it appears that a reasonably conservative lower bound for the shape factor η is given by

$$\eta = \frac{0.35}{0.75 + (x/y)} \tag{5.30}$$

For *flanged sections*, the torsional strength may be taken conservatively as the sum of the torsional strengths of the web and projecting flanges. Accordingly, the term $\eta x^2 y$ in Eq. (5.29) is replaced by $\Sigma \eta x^2 y$, where x and y are, respectively, the smaller and larger side dimensions of each of the component rectangles. T and L sections may be subdivided to maximize $\Sigma \eta x^2 y$. The effective width of the projecting flanges should not be taken greater than three times the flange thickness.

Based on limited testing, it appears that the ACI Code approach for non-prestressed *box sections* applies to prestressed box sections also (Ref. 5.8). For such members with a wall thickness h not less than $x/4$, where x is the overall width of the box section, the torsional strength may be taken as that of a comparable solid rectangular section with the same overall dimensions. If the wall thickness h is less than $x/4$, but greater than $x/10$, the torsional strength of the box section is reduced by the factor $4h/x$ on the right-hand side of Eq. (5.29).

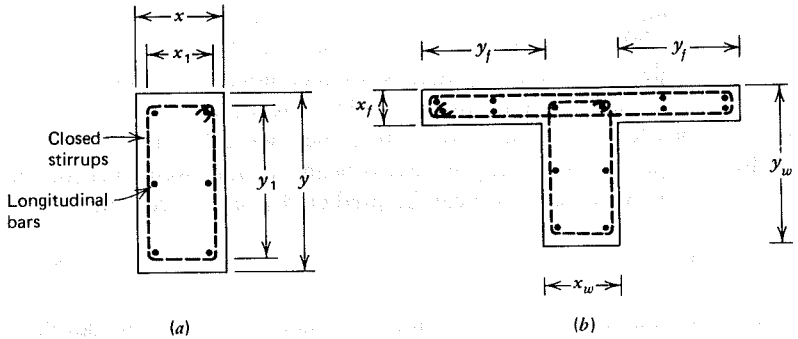

FIGURE 5.20 Torsion reinforcement. (*a*) Rectangular section. (*b*) Flanged section.

B. TORSION IN BEAMS WITH WEB REINFORCEMENT

To obtain increased resistance to torsion, in both non-prestressed and prestressed beams, reinforcement is provided consisting of closely spaced closed stirrups and longitudinal bars. Even though a member may be adequately reinforced in this way, as in Fig. 5.20, the concrete cracks at a torque equal to, or only somewhat larger than, that in an unreinforced member. Only after cracking does the reinforcement become effective. The cracks form a spiral pattern, as shown for one single crack in Fig. 5.19*a*. Actually, a great number of such cracks develop at close spacing.

Upon cracking, the torsional resistance of the concrete in a *non-prestressed member* drops to about half of that of the uncracked member, the remainder being resisted by the reinforcement. Failure occurs by skew bending. The stirrup steel may or may not be stressed to its yield strength, depending on the location of the crack and orientation of the stirrup leg.

The torsional strength of a *non-prestressed member* can be analyzed considering the equilibrium of the internal forces that are transmitted across the potential failure surface shown in Fig. 5.21. The figure shows the partially cracked failure surface, including the compression zone of concrete (shaded) and the horizontal and vertical stirrup forces S_h and S_v of all the stirrups intersecting the failure surface, except for those located in the compression zone.

It is shown in Ref. 5.11 that the total resisting torque contributed by the steel reinforcement is given by the expression

$$T_s = \alpha_t \frac{x_1 y_1}{s} A_t f_y$$

where s = spacing of stirrups along the axis of the member, in.
A_t = cross-sectional area of one stirrup leg, in.^{2}
f_y = yield strength of stirrup steel, psi

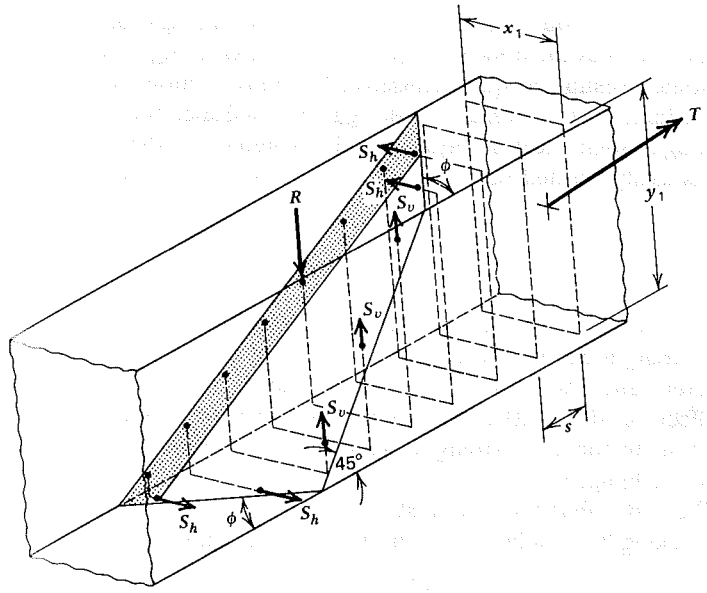

FIGURE 5.21 Torsion resistance of cracked beam with web steel.

and the coefficient α_t accounts for crack geometry, stirrup stress at failure, and other parameters. This coefficient has been established empirically as

$$\alpha_t = 0.66 + 0.33 \frac{y_1}{x_1} \tag{5.31}$$

not to exceed 1.5.

For non-prestressed members, after cracking, the torque T_c resisted by the concrete is diminished to about one-half the cracking torque. Taking the ratio of the two conservatively to be 40 percent, then from Eq. (5.28)

$$T_c = 0.4\left(\tfrac{1}{3}x^2 y\right)6\sqrt{f_c'} \tag{5.32}$$

The total nominal torsion strength for a non-prestressed member is then

$$T_n = T_c + T_s$$

or

$$T_n = 2.4\sqrt{f_c'}\,\frac{x^2 y}{3} + \alpha_t \frac{x_1 y_1}{s} A_t f_y \tag{5.33}$$

This torque will be developed only if the stirrups are sufficiently closely spaced so that any failure surface will intersect an adequate number of stirrups.

The role of the longitudinal bar reinforcement is not fully understood, but it has been shown by tests that T_n can be developed only if such reinforcement is

provided. Its chief functions are probably (1) to anchor the stirrups, particularly at the corners, which enables them to develop their full yield strength, and (2) to provide at least some resisting torque themselves by dowel action, where they cross the failure surface. It is customary to design torsional members such that the volume of longitudinal steel is equal to the volume of the transverse reinforcement. It is easily verified that this is so if the total area of longitudinal steel is

$$A_l = 2A_t \frac{x_1 + y_1}{s} \tag{5.34}$$

For *prestressed members* subject to torsion, limited tests show that the ultimate torsional strength can be expressed as the sum of the strengths contributed by the concrete and the web reinforcement, just as for non-prestressed members. The effect of the prestress is to increase the contribution of the concrete to the ultimate torsional strength, while the contribution of the reinforcement remains unchanged.

Figure 5.22 illustrates that for non-prestressed members, the concrete resisting torque after cracking T_c is only a fraction of the torque causing cracking T_{cr}.

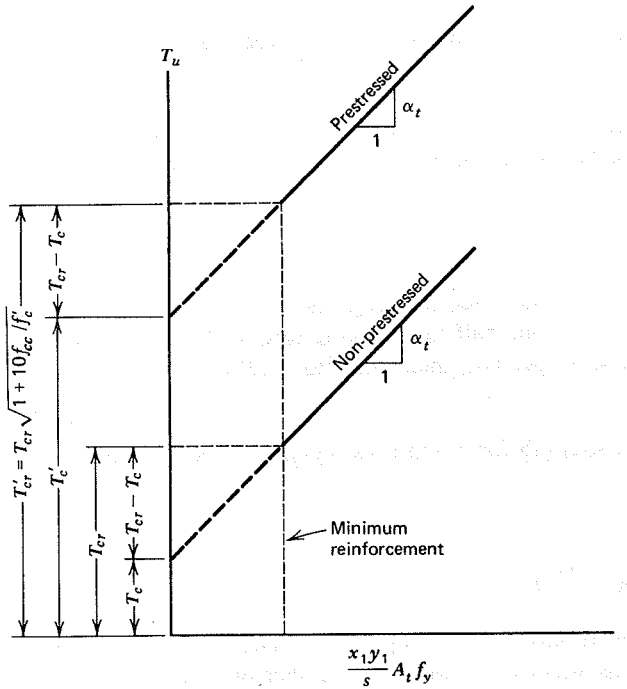

FIGURE 5.22 Ultimate torque for reinforced and prestressed members. From Ref. 5.10.

The reduced resistance is taken equal to 40 percent of the cracking torque, as pointed out earlier, in present design practice.

Likewise for prestressed members, the resistance of the concrete after cracking is only a fraction, but a greater fraction, of the torque causing cracking. Accordingly, the ultimate torque for a prestressed member can be expressed as

$$T_n = T_c' + T_s$$

or

$$T_n = T_c' + \alpha_t \frac{x_1 y_1}{s} A_t f_y$$

where the terms of T_s are exactly as defined earlier for non-prestressed members, and T_c' is the torsional resistance of the concrete after cracking.

It is proposed in Ref. 5.8 that the reduction in concrete torque, upon cracking, for a prestressed concrete beam be taken equal to that reduction upon cracking for the equivalent non-prestressed member. This is illustrated by Fig. 5.22. From Eq. (5.32) the torsional resistance, after cracking, of a non-prestressed beam is

$$T_c = 0.133(x^2 y)6\sqrt{f_c'}$$

Thus, with reference to Fig. 5.22

$$T_c' = T_{cr}\sqrt{1 + 10f_{cc}/f_c'} - (T_{cr} - T_c)$$

or

$$T_c' = (\eta x^2 y)6\sqrt{f_c'}\left(\sqrt{1 + 10f_{cc}/f_c'} - k\right) \tag{5.35}$$

where $k = (1 - T_c/T_{cr}) = (1 - 0.133/\eta)$.

Then the total nominal resisting torque T_n for a rectangular prestressed member with web reinforcement is

$$T_n = T_c' + T_s$$

or

$$T_n = (\eta x^2 y)6\sqrt{f_c'}\left(\sqrt{1 + 10f_{cc}/f_c'} - k\right) + \alpha_t \frac{x_1 y_1}{s} A_t f_y \tag{5.36}$$

The equivalent expression for a flanged section is obtained by substitution of $\Sigma \eta x^2 y$ for $\eta x^2 y$ in Eq. (5.36). In such a case, the coefficient k may be

determined on the basis of the largest component rectangle. For a box section, the reduction factor $4h/x$ may be applied within the limits indicated earlier.

5.9 TORSION PLUS SHEAR

It was pointed out in Section 5.7 that concrete members designed to carry torsion alone are quite unusual. It is much more common that a beam subject to the usual moments and shears must also resist torsion. In an uncracked member, shear forces as well as torques produce shear stresses. It must be expected, therefore, that simultaneous application of shear forces and torques will produce an interaction that will reduce the strength of a member compared with what it would be if shear or torsion were acting alone.

A. COMBINED LOADING IN BEAMS WITHOUT WEB REINFORCEMENT

No satisfactory theories of this complex interaction have yet been developed so that reliance must be placed on the available experimental evidence (Refs. 5.10, 5.12 through 5.14). Recommendations must be regarded as tentative.

Tests have shown that the interaction between torsion and shear for prestressed beams without web reinforcement can be adequately represented by a circular curve. Let V_{cr} and T_{cr} be the cracking shear and cracking torque of the prestressed member when subjected, respectively, to flexural shear or to torsion alone, computed according to the methods of Sections 5.3 and 5.8.[3] It will be recalled that, for all practical purposes, failure occurs at these same values almost immediately following cracking, so that, for members without web reinforcement, V_{cr} and T_{cr} adequately represent their ultimate strengths in the two modes. Furthermore, let V_n and T_n, respectively, represent the shear capacity and the torsion capacity under combined loading, that is, when the member is subject to simultaneous flexural shear and torsion. Available test results are reasonably well represented by the circular interaction equation

$$\left(\frac{V_n}{V_{cr}}\right)^2 + \left(\frac{T_n}{T_{cr}}\right)^2 = 1 \tag{5.37}$$

where V_n = shear force at failure under combined loading
T_n = torsional moment at failure under combined loading
V_{cr} = the lesser of V_{ci} and V_{cw} computed according to Section 5.3
$T_{cr} = 6\sqrt{f_c'}\sqrt{1 + 10f_{cc}/f_c'}\,\Sigma\eta x^2 y$

A graphical representation of this equation is shown in Fig. 5.23. It is seen that this interaction curve is quite favorable, that is, the two modes do not very

[3] T_{cr} was defined for the prestressed beam as T_{cr}' by Eq. (5.29). The prime will be deleted from this point on for the sake of simplification.

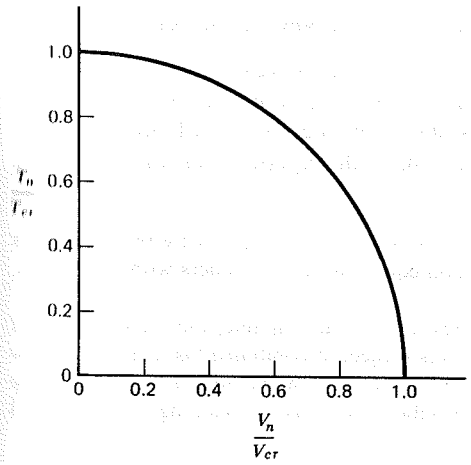

FIGURE 5.23 Interaction curve for combined torsion plus flexural shear.

strongly interfere with each other. For instance, if a member carries a torque $T_{cr}/2$, that is, one-half of its pure torsion capacity, the curve shows that it can carry simultaneously about $0.85V_{cr}$, that is, only about 15 percent less than it could carry if no torsion were present at all.

After suitable algebraic transformation, Eq. 5.37 results in the following:

$$V_n = \frac{V_{cr}}{\sqrt{1 + \left(\frac{V_{cr}}{T_{cr}}\right)^2\left(\frac{T_n}{V_n}\right)^2}} \tag{5.38}$$

$$T_n = \frac{T_{cr}}{\sqrt{1 + \left(\frac{T_{cr}}{V_{cr}}\right)^2\left(\frac{V_n}{T_n}\right)^2}} \tag{5.39}$$

The terms in the numerators of Eqs. (5.38) and (5.39) are the cracking stresses for shear and torsion, respectively, if shear or torsion is acting alone. The factors in the denominators of these equations account for the interaction between torsion and shear.

Note further that, although the unknowns V_n and T_n appear on the right sides of these two equations, it is not necessary to know their values at the outset of the calculations, but only the ratio of torsion to flexural shear at the section of interest, T_n/V_n, or in the design case, T_u/V_u, which is constant and known for given loads.

B. COMBINED LOADING IN BEAMS WITH WEB REINFORCEMENT

Although experimental verification is sparse, it appears reasonable to proceed, in designing members with web reinforcement subject to combined loading, following the same general approach established for members without web reinforcement. Pending more extensive research, both experimental and analytical, the following assumptions are made:

1. In members with stirrups, the portion of the total torsion carried by the concrete is determined by the same type of interaction equation as in members without stirrups; that is, a circular interaction law holds.
2. To carry the excess torque, above that resisted by the concrete, the same amount of reinforcement must be provided in members subject to combined loading as would be required for members carrying torsion alone. This torsional reinforcement is to be added to that required in the same member for carrying bending moments and flexural shears.

On the basis of the first assumption and with reference to Eqs. (5.38) and (5.39), the interaction equations for the nominal shear and torsion carried by the concrete, in beams with web reinforcement, are

$$V_c^* = \frac{V_c}{\sqrt{1 + (\beta T_n / V_n)^2}} \tag{5.40}$$

$$T_c^* = \frac{T_c'}{\sqrt{1 + (V_n / \beta T_n)^2}} \tag{5.41}$$

where V_c^* = shear force carried by concrete under combined loading
T_c^* = torsion force carried by the concrete under combined loading
V_c = the lesser of V_{ci} and V_{cw} computed according to Section 5.3
$T_c' = 6\sqrt{f_c'}(\sqrt{1 + 10 f_{cc}/f_c'} - k)\Sigma \eta x^2 y$
$\beta = \frac{1}{2}\left(\frac{V_c}{T_c'}\right)$
$k = 1 - 0.133/\eta$
$\eta = \frac{0.35}{0.75 + x/y}$

The basis of Eqs. (5.40) and (5.41) is found in Ref. 5.10.

From the second assumption, if the torque T_u actually applied to the member is larger than that carried by the concrete, then reinforcement must be provided to carry the excess. Recasting Eq. (5.36) to apply to the combined stress case, we obtain

$$T_n = T_c^* + \alpha_t \frac{x_1 y_1}{s} A_t f_y \tag{5.42}$$

where T_c^* is given by Eq. (5.41).

For the design case, setting $T_n = T_u$ at factored loads, and transposing terms, one obtains

$$(T_u - T_c^*) = \alpha_t \frac{x_1 y_1}{s} A_t f_y$$

from which

$$A_t = \frac{(T_u - T_c^*)s}{\alpha_t f_y x_1 y_1} \tag{5.43}$$

Note that the web reinforcement for torsion, determined by Eq. (5.43), must be in the form of closed stirrups, and is in addition to that required for flexural shear. The latter is to be found by Eq. (5.18), with the substitution of V_c^* from Eq. (5.40) for V_c in that equation.

For design purposes, it is consistent with earlier procedures to introduce the capacity reduction factor $\phi = 0.85$ for torsion in computing the nominal strengths. Thus, for design,

$$A_t = \frac{(T_u - \phi T_c^*)s}{\alpha_t \phi f_y x_1 y_1} \tag{5.44}$$

where T_u is the design torque at factored loads.

C. MAXIMUM AND MINIMUM WEB REINFORCEMENT

To avoid brittle failure upon cracking, a minimum amount of web reinforcement must be provided in members subject to combined stress. Tests reported in Ref. 5.10 indicate that the minimum web reinforcement required by ACI Code for flexural shear is insufficient to insure ductility in beams with a high ratio of torsion to shear. Accordingly, it is recommended that a beam should be reinforced for no less than the cracking torque.

Consideration must also be given to the possibility of over-reinforcing the member such that a sudden compressive failure of the concrete might occur before the stirrup steel yields. To avoid this type of failure, an upper limit must be placed on web reinforcement by specifying a maximum nominal torque

$T_{n,max}$. Based on available tests, it is recommended in Ref. 5.8 as follows:

1. For members subject to torsion alone:

$$T_{n,max} = C\sqrt{f'_c}\sqrt{1 + 10f_{cc}/f'_c}\,(\Sigma\eta x^2 y) \tag{5.45}$$

where

$$C = 14 - 13.33\left(\frac{f_{cc}}{f'_c}\right)$$

2. For members subject to combined loading:

$$T^*_{n,max} = \frac{C'\sqrt{f'_c}}{\sqrt{1 + \left(\frac{C'}{10}\right)^2\left(\frac{V_n}{T_n}\right)^2\left(\frac{\Sigma\eta x^2 y}{b_w d}\right)^2}}(\Sigma\eta x^2 y) \tag{5.46}$$

$$V^*_{n,max} = \frac{10\sqrt{f'_c}}{\sqrt{1 + \left(\frac{10}{C'}\right)^2\left(\frac{T_n}{V_n}\right)^2\left(\frac{b_w d}{\Sigma\eta x^2 y}\right)^2}}(b_w d) \tag{5.47}$$

where

$$C' = C\sqrt{1 + 10f_{cc}/f'_c}$$

D. LIMITATIONS

To insure the development of ultimate torsional strength and to control cracking and stiffness at service load, the maximum yield strength of the stirrup reinforcement should be limited to 60 ksi. To properly control spiral cracking, the maximum spacing of torsional stirrups should not exceed $(x_1 + y_1)/4$ or 12 in. whichever is smaller. Longitudinal bars must be provided, well distributed around the perimeter of the closed stirrups, at a spacing that should not exceed 12 in.

For reinforced concrete members, the ACI Code permits the torsional effect to be neglected if the torsional shear stress is less than 25 percent of the cracking stress. This same requirement would seem justified for prestressed beams. Specifically, the influence of torsion may be neglected if T_u is less than

$$T_{u,min} = 1.5\sqrt{f'_c}\sqrt{1 + 10f_{cc}/f'_c}\,(\Sigma\eta x^2 y) \tag{5.48}$$

5.10 EXAMPLE: DESIGN OF PRESTRESSED BEAM FOR COMBINED LOADING

The rectangular beam of 30 ft clear span shown in Fig. 5.24 is to carry a superimposed dead load of 1.85 kips/ft and service live load of 1.20 kips/ft, both at eccentricity of 9 in., in addition to its own weight of 0.38 kips/ft. The beam is prestressed with a force after losses of P_e = 300 kips, with steel centroid at effective depth 24 in. The specified 28-day concrete strength f'_c = 5,000 psi. Design the reinforcement required for shear and torsion, at a section $h/2$ from the support face, using steel of f_y = 40,000 psi. (Span = 9.14 m, w_o = 5.5 kN/m, w_d = 27.0 kN/m, w_l = 17.5 kN/m, e = 229 mm, P_e = 1,334 kN, d = 618 mm, f'_c = 34 MPa, and f_y = 276 MPa.)

The usual ACI load factors are applied to obtain the factored loads:

$$w_1 = 1.4 \times 0.38 = 0.53 \text{ kips/ft}$$

$$w_2 = 1.4 \times 1.85 + 1.7 \times 1.20 = 4.63 \text{ kips/ft}$$

The total shear force and torque at the face of supports are, respectively,

$$V_u = 5.16(30/2) = 77.4 \text{ kips}$$

$$T_u = 4.63(9/12)(30/2) = 52.1 \text{ ft-kips}$$

In accordance with the ACI Code provisions for shear, the first critical section will

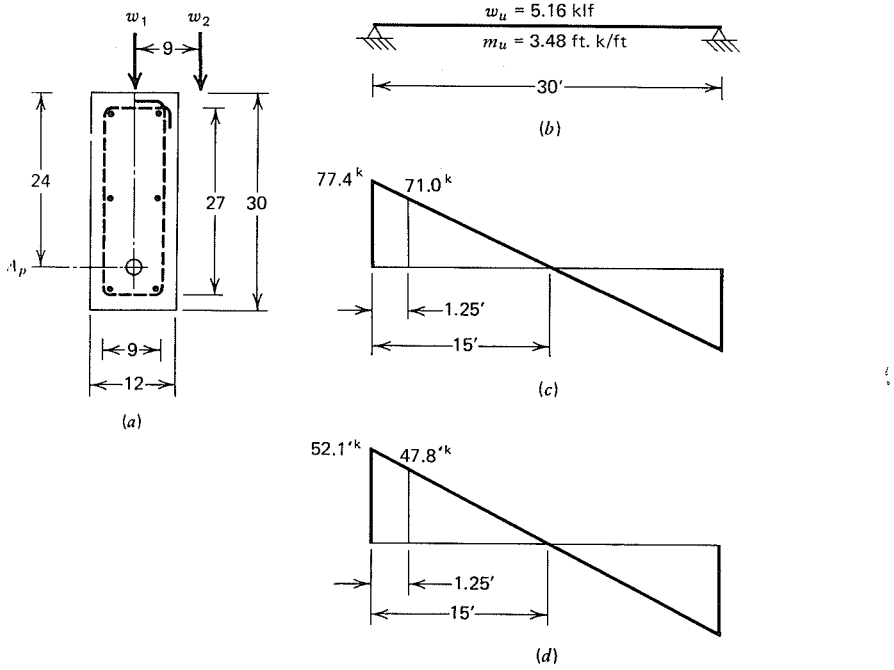

FIGURE 5.24 Torsion design example. (*a*) Cross section. (*b*) Loads. (*c*) Shear. (*d*) Torque.

be assumed at a distance $h/2 = 1.25$ ft from the support face. The values of shear and torque at that section are, respectively, 71.0 kips and 47.8 ft-kips, as shown in Fig. 5.24. First, for reference, from Eq. (5.30) with $x/y = 12/30 = 0.40$,

$$\eta = \frac{0.35}{0.75 + 0.40} = 0.304$$

and

$$\eta x^2 y = 0.304 \times 144 \times 30$$
$$= 1{,}310 \text{ in.}^3$$

Also,

$$b_w d = 12 \times 24$$
$$= 288 \text{ in.}^2$$

With the concrete stress at the section centroid

$$f_{cc} = \frac{P_e}{A_c} = \frac{300{,}000}{12 \times 30} = 833 \text{ psi}$$

from Eq. (5.48):

$$T_{u,min} = 1.5\sqrt{f_c'}\sqrt{1 + 10 f_{cc}/f_c'}\,(\eta x^2 y)$$
$$= 1.5\sqrt{5{,}000}\sqrt{1 + 8{,}330/5{,}000}\,(1{,}310)$$
$$= 227{,}000 \text{ in.-lb} = 18.9 \text{ ft-kips}$$

The actual nominal torsion of 47.8 ft-kips is well above this value, confirming that torsion must be considered in designing the member.

The upper limits of torsion and shear are determined from Eqs. (5.46) and (5.47), respectively with

$$C = 14 - 13.33(833 / 5{,}000) = 11.78$$
$$C' = 11.78\sqrt{1 + 8{,}330 / 5{,}000} = 19.23$$

$$T_{n,max}^* = \frac{C'\sqrt{f_c'}}{\sqrt{1 + \left(\frac{C'}{10}\right)^2\left(\frac{V_u}{T_u}\right)^2\left(\frac{\eta x^2 y}{b_w d}\right)^2}}(\eta x^2 y)$$

$$= \frac{19.23\sqrt{5{,}000}}{\sqrt{1 + \left(\frac{19.23}{10}\right)^2\left(\frac{71.0}{47.8 \times 12}\right)^2\left(\frac{1{,}310}{288}\right)^2}}\left(\frac{1{,}310}{12{,}000}\right)$$

$$= 101 \text{ ft-kips} > 47.8 \text{ ft-kips}$$

$$V_{n,max}^* = \frac{10\sqrt{f_c'}}{\sqrt{1 + \left(\frac{10}{C'}\right)^2\left(\frac{T_u}{V_u}\right)^2\left(\frac{b_w d}{\eta x^2 y}\right)^2}}(b_w d)$$

$$= \frac{10\sqrt{5{,}000}}{\sqrt{1 + \left(\frac{10}{19.23}\right)^2\left(\frac{47.8 \times 12}{71.0}\right)^2\left(\frac{288}{1{,}310}\right)^2}}\left(\frac{288}{1{,}000}\right)$$

$$= 150 \text{ kips} > 71 \text{ kips}$$

It is confirmed that the maximum values of forces acting are below the allowed upper limits in each case.

The interaction equations will next be employed to determine the contribution of the concrete section to resisting torsion and shear forces. With

$$k = 1 - \frac{0.133}{\eta}$$
$$= 1 - \frac{0.133}{0.304}$$
$$= 0.563$$

then from Eq. (5.35):

$$T_c' = 6\sqrt{f_c'}\left(\sqrt{1 + 10 f_{cc}/f_c'} - k\right)(\eta x^2 y)$$
$$= 6\sqrt{5{,}000}\left(\sqrt{1 + 8{,}330/5{,}000} - 0.563\right)\left(\frac{1{,}310}{1{,}000}\right)$$
$$= 595 \text{ in.-kips}$$

For V_c, the approximate Eq. (5.17) will be used:

$$V_c = \left(0.6\sqrt{f_c'} + 700\frac{V_u d}{M_u}\right) b_w d$$

but not less than $2\sqrt{f_c'}\,b_w d$ and not to exceed $5\sqrt{f_c'}\,b_w d$. The upper limitation controls in this case and

$$V_c = 5\sqrt{5{,}000} \times 288 / 1{,}000 = 102 \text{ kips}$$

Then with $\beta = \frac{1}{2}(102/595) = 0.086$, application of Eq. (5.41) results in

$$T_c^* = \frac{T_c'}{\sqrt{1 + \left(\frac{V_u}{\beta T_u}\right)^2}}$$

$$= \frac{595}{\sqrt{1 + \left(\frac{71.0}{0.086 \times 47.8 \times 12}\right)^2}}$$

$$= 339 \text{ in.-kips}$$

while Eq. (5.40) indicates

$$V_c^* = \frac{V_c}{\sqrt{1 + \left(\frac{\beta T_u}{V_u}\right)^2}}$$

$$= \frac{102}{\sqrt{1 + \left(\frac{0.086 \times 47.8 \times 12}{71.0}\right)^2}}$$

$$= 83.8 \text{ kips}$$

The web steel required for torsion will be in the form of closed stirrups placed with

$1\frac{1}{2}$ in. cover measured to the center of the steel, as shown in Fig. 5.24, giving $x_1 = 9$ in. and $y_1 = 27$ in. From Eq. (5.31):

$$\alpha_t = 0.66 + 0.33\left(\frac{27}{9}\right)$$
$$= 1.65$$

but not to exceed 1.50, which controls in this case. The required cross-sectional area of *one leg* of a torsion stirrup is found from Eq. (5.44)

$$A_t = \frac{(T_u - \phi T_c^*)\, s}{\alpha_t \phi f_y x_1 y_1}$$
$$= \frac{(47.8 \times 12 - 0.85 \times 339)\, s}{1.50 \times 0.85 \times 40 \times 9 \times 27}$$
$$= 0.0230s \text{ in.}^2$$

The maximum spacing of such stirrups is not to exceed the smaller of 12 in. or:

$$s_{max} = \frac{x_1 + y_1}{4}$$
$$= \frac{9 + 27}{4}$$
$$= 9 \text{ in.}$$

which controls here.

Next the required reinforcement for flexural shear will be found. Since $V_u = 71.0$ kips is less than $V_c^* = 83.8$ kips, only the minimum steel is needed for flexural shear. From Eq. (5.23)

$$A_v = \frac{50 b_w s}{f_y}$$
$$= \frac{50 \times 12}{40{,}000} s$$
$$= 0.015s$$

The minimum required cross-sectional area per vertical leg is therefore $A_v / 2 = 0.0075s$. This minimum requirement is easily met by the stirrups provided for torsion.

No. 4 bars will be selected for the closed hoop stirrup reinforcement, the area of one vertical leg being 0.20 in.^{2} Setting this provided area equal to the requirement of $0.0230s$ indicates the required spacing is

$$\frac{0.20}{0.0230} = 8.70 \text{ in.}$$

A practical spacing of 8 in. will be selected. The required longitudinal non-prestressed reinforcement is found from Eq. (5.34):

$$A_l = 2A_t \frac{x_1 + y_1}{s}$$
$$= 2 \times 0.0245(9 + 27)$$
$$= 1.62 \text{ in.}^2$$

This will be met by six No. 5 bars, arranged as shown in Fig. 5.24, that provide a total area of 1.84 in.^{2} The maximum spacing of 12 in. is very nearly met by the arrangement of six bars, allowing for placement clearances.

5.11 COMPRESSION FIELD THEORY FOR SHEAR AND TORSION DESIGN

The ACI Code method of design for shear in prestressed beams, presented in the first part of this chapter, is in essence empirical. Although generally leading to safe designs, the ACI Code approach lacks a proper physical model for the behavior of beams subject to flexural shear. A somewhat vague rationalization is followed in adopting the diagonal cracking load, V_{ci} or V_{cw}, of a member without web steel as the "concrete contribution" V_c to the shear strength of an otherwise identical member with web steel (see Section 5.4).

The ACI Code contains no recommendations for the design of prestressed concrete beams subject to torsion, or combined shear and torsion, although recommendations pertaining to non-prestressed reinforced concrete beams are included. The method for torsion design of prestressed beams included in the second part of this chapter represents an adaptation of the approach found in the ACI Code for non-prestressed beams. Here, too, the lack of a proper physical model is conspicuous, and a number of more or less arbitrary assumptions are made in the development, but the results correlate quite well with the available test data.

An alternative approach to the design of prestressed beams for flexural shear and for flexural shear combined with torsion, recently incorporated into the Canadian National Standard for concrete structures and closely related to methods followed in European design codes, is derived from the *compression field theory* (Refs. 5.15 and 5.16). The approach is based on a simple, easily visualized model for the behavior of members with web reinforcement, and can be applied in a unified way to both reinforced concrete and prestressed concrete members, as well as partially prestressed beams falling between those limit cases. In its complete implementation, it can be used to predict not only the ultimate strength but also the full load-deformation response as loads are gradually increased from zero to failure.

Although it appears that some simplifications must be made if the compression field theory is to be used in practical design, there is a strong likelihood that significant changes in the ACI Code relating to shear and torsion will come about based on this approach. Space limitations do not permit a presentation of the alternative method here. The interested reader should consult Ref. 5.15 for a complete development. Codified design procedures will be found in Ref. 5.16.

REFERENCES

5.1 ASCE–ACI Joint Committee 426, "The Shear Strength of Reinforced Concrete Members," Chs. 1–4, *J. Struct. Div., ASCE*, Vol. 99, No. ST6, June 1973, pp. 1091–1187.

5.2 MacGregor, J. G. and Hanson, J. M., "Proposed Changes in Shear Provisions for Reinforced and Prestressed Concrete Beams," *J. ACI*, Vol. 66, No. 4, April 1969, pp. 276–288.

5.3 MacGregor, J. G., Sozen, M. A., and Siess, C. P., "Strength and Behavior of Prestressed Concrete Beams with Web Reinforcement," Structural Research Series No. 201, University of Illinois, August 1960.

5.4 Sozen, M. A., Zwoyer, E. M., and Siess, C. P., *Strength in Shear of Beams without Web Reinforcement*, Bulletin No. 452, University of Illinois, Engineering Experimental Station, Urbana, 1959.

5.5 MacGregor, J. G., Sozen, M. A., and Siess, C. P., "Strength of Concrete Beams with Web Reinforcement," *J. ACI*, Vol. 62, No. 12, December 1965, pp. 1503–1519.

5.6 ACI Standard *Building Code Requirements for Reinforcement Concrete*, ACI 318–63, American Concrete Institute, Detroit, 1963, 143 pp.

5.7 ACI Committee Report *Commentary on Building Code Requirements for Reinforced Concrete*, ACI 318–63, American Concrete Institute Special Publication SP-10, 1965, 91 pp.

5.8 Zia, P. and McGee, W. D., "Torsion Design of Prestressed Concrete," *J. PCI*, Vol. 19, No. 2, March–April 1974, pp. 46–65.

5.9 Hsu, T. T. C., "Torsion of Structural Concrete—Uniformly Prestressed Members Without Web Reinforcement," *J. PCI*, Vol. 13, No. 2, April 1968, pp. 34–44.

5.10 McGee, W. D. and Zia, P., *Prestressed Concrete Members Under Torsion, Shear, and Bending*, Research Report, Department of Civil Engineering, North Carolina State University, Raleigh, N.C., July 1973, 212 pp.

5.11 Nilson, A. H. and Winter, G., *Design of Concrete Structures*, 10th ed., McGraw-Hill, New York, 1986.

5.12 GangaRao, H. V. S. and Zia, P., Rectangular Prestressed Beams in Torsion and Bending, *J. Struct. Div., ASCE*, Vol. 99, No. ST1, January 1973, pp. 183–198.

5.13 Henry, R. L. and Zia, P., "Prestressed Beams in Torsion, Bending, and Shear," *J. Struct. Div., ASCE*, Vol. 100, No. ST5, May 1974, pp. 933–952.

5.14 Hsu, T. C. C., *Torsion of Reinforced Concrete*, Van Nostrand Reinhold, New York, 1984, 516 pp.

5.15 Collins, M. P. and Mitchell, D., "Shear and Torsion Design of Prestressed and Non-Prestressed Concrete Beams," *J. PCI*, Vol. 25, No. 5, September–October 1980, pp. 32–100.

5.16 "Design of Concrete Structures for Buildings," CAN3-A23.3-M84, Canadian Standards Association, Toronto, 1984.

PROBLEMS

5.1 Establish the required spacing of No. 3 U stirrups at a beam cross section subject to factored load shear V_u of 35.55 kips and moment M_u of 474 ft-kips. Web width $b_w = 5$ in., effective depth $d = 24$ in., and total depth $h = 30$ in. The concrete shear contribution may be based on the approximate relationship of Eq. (5.17). Use $f_y = 40{,}000$ psi for stirrup steel and take $f'_c = 5{,}000$ psi.

5.2 The pretensioned beam shown in Fig. P5.2 is designed to carry a superimposed dead load of 500 plf and live load of 900 plf in addition to its own weight of 300 plf on a 50-ft simple span. Ten 1/2-in. diameter strands having $f_{pu} = 270{,}000$ psi are used to provide an effective prestress force P_e of 218 kips. The strands are positioned with eccentricity 12.5 in. at midspan and deflected at the third points to zero eccentricity at the supports. Normal density concrete is used, with $f'_c = 5{,}000$ psi. (a) Prepare a diagram showing the values of V_u, V_{ci}, and V_{cw} as a function of distance along the span. (b) Superimpose on the same diagram the values obtained by the simplified equation (5.17). (c) Based on the excess shears obtained in part (a) find the required spacing of No. 3 vertical U stirrups along the span. Stirrups will have yield stress $f_y = 40{,}000$ psi. For the section shown, $A_c = 288$ in.^{2}, $I_c = 28{,}700$ in.^{4}, $c_1 = 13.5$ in., $A_p = 1.53$ in.^{2}

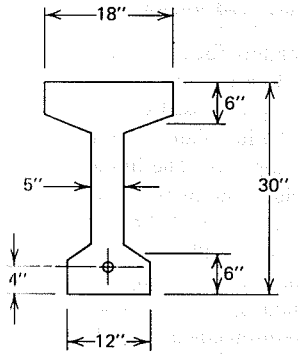

FIGURE P5.2

5.3 The girder shown in Fig. P5.3 is post-tensioned using a single tendon containing 19 0.600-in. diameter strands of Grade 270 steel. Eccentricity at the center of the 80-ft simple span is 32 in., varying parabolically to zero at the supports. The effective

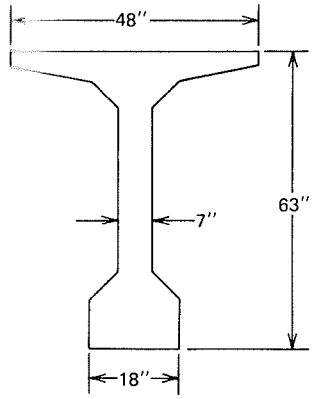

FIGURE P5.3

prestress force after all losses is $P_e = 660$ kips. The girder must carry its own weight of 920 plf, a superimposed dead load of 600 plf, and a service live load of 2,200 plf uniformly distributed over the span. Concrete compressive strength is $f_c' = 6{,}000$ psi. Design the web reinforcement, using stirrups with $f_y = 60{,}000$ psi. The section properties are: $A_c = 880$ in.^{2}, $I_c = 440{,}000$ in.^{4}, $c_2 = 38$ in., and $A_p = 4.12$ in.^{2}.

5.4 Design the web reinforcement for shear for the girder bridge of Problem 4.6. The live load may be considered to be applied fully over the entire width of the top flange, so that torsion need not be considered. For the stirrups, use $f_y = 50{,}000$ psi. Show in a sketch your proposed design, giving spacing of all stirrups and typical bar bending details.

5.5 Referring again to the girder of Problems 4.6 and 5.4, consider the possibility that the live load may be applied over only the right half of the bridge, causing torsional moments to act simultaneously with flexure and vertical shear. The ends of the girder are restrained torsionally, as well as supported vertically. Redesign the web reinforcement for the girder, accounting for both vertical shear and torsion.

5.6 Fig. P5.6 shows a typical precast prestressed concrete spandrel beam such as is used in parking deck structures. The beam extends above the deck to form a parapet wall, and a bracket is provided at the bottom to carry precast prestressed double-T floor beams. The spandrel beam is pretensioned with six 0.5-in. diameter Grade 270 strands, with centroid of prestress force 69 in. from the top face. The initial tension $P_i = 174$ kips; after all losses $P_e = 135$ kips. Loads include the member self-weight of 725 plf plus a service live load of 1,500 plf and dead load of 2,685 plf, both applied to the bracket with eccentricity 8 in. from the wall–beam centerline. Supporting columns are 12 in. square and spaced 28 ft. on centers. Design the torsion and shear reinforcement for this beam, using $f_c' = 5{,}000$ psi and $f_y = 40{,}000$ psi. (Note: In the projecting ledge, in addition to torsional reinforcement, supplementary steel would be needed to carry the eccentric loads. This would be designed using the shear friction method described in Chapter 12.)

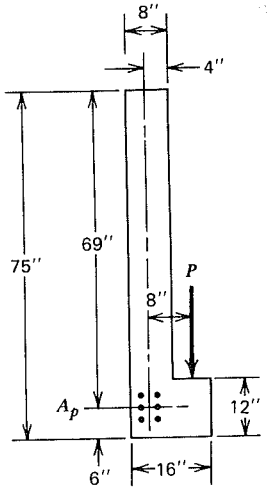

FIGURE P5.6

SIX

PARTIAL LOSS OF PRESTRESS FORCE

6.1 INTRODUCTION

The lack of success experienced in early attempts to prestress concrete was due, in most cases, to failure to appreciate the significance of the inevitable partial loss of prestress force. Doubts relative to the permanence of prestressing persisted into the 1940s. It was only with the success of the dramatic bridges of Freyssinet, such as that shown in Fig. 1.1, that the engineering profession began to accept that prestress losses could be calculated and allowed for in the design, and that their effect could be minimized through careful selection of the proper materials.

As discussed in Section 1.7, losses of prestressing force can be grouped into two categories; those that occur immediately during construction of the member, and those that occur over an extended period of time. The *prestress jacking force* P_j may be immediately reduced by losses due to friction, anchorage slip, and elastic shortening of the compressed concrete. In this book, the prestress force, after those losses, has been called the *initial prestress force* P_i. As time passes, the force gradually reduces further, rapidly at first but then more slowly, because of length changes resulting from shrinkage and creep of the concrete, and because of relaxation of the highly stressed steel. After a period of many months, or even

years, further stress changes become insignificant, and a nearly constant prestress force is attained. This has been defined as the *effective prestress force* P_e.

The jacking pressure P_j is the largest force that will act on the steel tendon during the normal life of a member, and the jacking operation may be thought of as a performance test of the tendon.

For pretensioned members, P_j never acts on the concrete, but only on the permanent anchorages of the casting bed. The tension is reduced along the length of the strand by friction at cable deflection points and beam end forms. In addition, the steel force is reduced by slip at the anchorages and, immediately upon transfer, by elastic shortening of the concrete.

For post-tensioned members, the jacking force is, in fact, actually applied to the concrete during stressing, but it exists at its full value only at the jacking end of the member. Elsewhere it is diminished by frictional losses. Immediately upon transfer, the post-tensioning force is reduced by anchorage slip. Elastic shortening may account for further losses.

The jacking force P_j is of somewhat secondary interest to the designer. Of primary interest are the initial prestress P_i immediately after transfer, and the final or effective prestress P_e after all losses have occurred. These were related in Section 3.3 in terms of the effectiveness ratio R by the equation

$$P_e = RP_i \tag{3.1}$$

All time-dependent losses, specifically those due to creep, shrinkage, and relaxation, all of which affect both pretensioned and post-tensioned members, are included in the coefficient R.

The estimation of losses may be done on several different levels. In most cases in practical design, detailed calculation of losses is not necessary. It is possible to adopt reasonably accurate lump sum approximations of prestress loss. Such expressions are included in the AASHTO Interim Specification for Bridges and other documents (Refs. 6.1 and 6.2), and are summarized in Section 6.2.

For cases in which greater accuracy is required, it is necessary to estimate the separate losses, taking account of the special conditions of member geometry, material properties, and construction methods that apply. Methods for making more detailed estimates of this type are outlined in Sections 6.3 through 6.10 of this chapter. The information on material properties found in Chapter 2 will be helpful. Additional guidance can be found in the recommendations of the Task Committee on Losses of the ACI-ASCE Joint Committee 423 on Prestressed Concrete (Ref. 6.3).

Accuracy of loss estimation may be still further improved by accounting for the interdependence of time-dependent losses, using discrete time intervals for the calculations. A practical method for doing so is described in Section 6.11.

For prestressed structures of major importance or for which unusual methods or materials are to be used, it may be advisable to base loss calculations on specific information obtained for the materials to be used, methods of curing, ambient exposure conditions, and other such construction information. For structures such as precast or cast-in-place segmental cantilever bridges, for example, it may be appropriate and necessary to obtain this information in order to maintain control of the geometry of the bridge during construction.

Actual losses, which may be greater or smaller than the estimated losses, have little effect on the ultimate flexural strength of a prestressed beam. Losses do affect service load behavior such as deflection or camber, cracking load, and crack widths, as well as deformations during construction. The overestimation of prestress losses, which may seem to be on the conservative side, can actually be as detrimental as underestimation. Overestimation may lead the designer to specify too much prestress, resulting in excessive camber and troublesome horizontal movements in structures. It is necessary that the best possible appraisal of losses be made in each case, commensurate with the importance of the construction.

6.2 LUMP SUM ESTIMATES OF LOSSES

As early as 1958, ACI-ASCE Joint Committee 423 recognized the need for approximate expressions to be used to estimate prestress losses in routine design. The following values were recommended in Ref. 6.4 for lump sum losses, including those due to elastic shortening, shrinkage, creep, and relaxation, but excluding losses due to friction and anchorage slip:

For pretensioning: 35,000 psi (241 MPa)
For post-tensioning: 25,000 psi (172 MPa)

Losses due to friction, assumed to apply only to post-tensioned members, were to be calculated separately, by the equations of Section 6.4.

This basis for the calculation of losses was incorporated in the 1963 ACI Code Commentary, although it is not in the current 1983 Commentary. Many thousands of prestressed concrete structures were built from designs based on these losses, and where member sizes, materials, construction procedures, amount of prestress, and environmental conditions were not out of the ordinary, this approach proved quite satisfactory.

The same lump sum values were included in the AASHO (AASHTO) Specifications then in effect for highway bridges. Most prestressed concrete bridges now in service were designed using these values and, in general, the performance and serviceability of these bridges have been excellent. These loss values were based on use of normal-weight concrete, normal prestress levels, and average conditions of exposure.

Modifications are included in the 1983 AASHTO Specification (Ref. 6.1) which provides that the lump sum losses of Table 6.1 be used for prestressed members or structures of usual design. The modifications reflect research that has

Table 6.1 AASHTO Lump Sum Losses

Type of prestressing steel	Total loss	
	f'_c = 4,000 psi (28 MPa)	f'_c = 5,000 psi (34 MPa)
Pretensioning:		
Strand		45,000 psi (310 MPa)
Post-tensioning:[a]		
Wire or strand	32,000 psi (221 MPa)	33,000 psi (228 MPa)
Bars	22,000 psi (152 MPa)	23,000 psi (159 MPa)

Source: From Ref. 6.1.
[a]Losses due to friction are excluded. Friction losses should be computed according to Section 6.4.

shown that certain of the assumptions made in the original development of lump sum loss values could be improved. This is particularly true with respect to steel relaxation loss, but applies to some extent to shrinkage and concrete creep losses as well.

Table 6.1 includes concrete strengths of 4,000 and 5,000 psi. The lump sum loss values may be used for bridges with concrete strengths 500 psi above or below the values of 4,000 and 5,000 psi listed in the table headings. Thus, the range of concrete strength covered may be considered to extend from 3,500 to 5,500 psi. The values were developed on the assumption that the full allowable compressive stress of concrete is required by stress conditions during the life of the member. For structures or elements where the concrete strength is determined on the basis of the nominal minimums in the specifications, and where full utilization of the allowable compressive stresses does not occur during the life of the structure, the lump sum loss values given will be higher than the actual losses.

The lump sum loss values presented in the AASHTO Specification include elastic shortening losses, as well as the time-dependent losses due to shrinkage, creep, and relaxation. Elastic shortening losses, easily calculated by the method given in Section 6.6, must be deducted from the lump sum losses if the recommended values are used as the basis for determining the effectiveness ratio R of Eq. (3.1).

Recommendations for lump sum losses for post-tensioned members published by the Post-Tensioning Institute (Ref. 6.2) are reproduced in Table 6.2. The tabulated values have the same basis as the AASHTO recommendations, that is, they include elastic shortening, creep, shrinkage, and relaxation effects, but do not include friction or anchorage slip losses. They are comparable to the AASHTO recommendations, but differentiate between the losses expected in

Table 6.2 PTI Lump Sum Losses for Post-Tensioned Members

Type of Post-Tensioning Steel	Total Loss[a]	
	Slabs	Beams and Joists
Stress-relieved grade 270 strand and stress-relieved grade 240 wire	30,000 psi (207 MPa)	35,000 psi (241 MPa)
Bars	20,000 psi (138 MPa)	25,000 psi (172 MPa)
Low-relaxation grade 270 strand	15,000 psi (103 MPa)	20,000 psi (138 MPa)

Source: From Ref. 6.2.
[a]Losses due to friction are excluded. Friction losses should be computed according to the equations in Section 6.4.

slabs and those for beams and joists. In addition, recommendations are included for low-relaxation strand, now widely used.

It is to be emphasized that the treatment of losses as lump sum quantities is recommended only for "standard" conditions. For members of unusual proportions, exceptionally long span, or lightweight concrete, for example, a separate estimate of the individual losses should be made using the methods described in the following sections.

6.3 DETAILED ESTIMATION OF LOSSES

For cases where lump sum estimates of loss are inadequate, it is necessary to estimate each of the losses separately, using either assumed data or, for major works, using data developed for the particular job at hand. The separate contributions are then summed to obtain the total loss.

The detailed calculation of prestress losses resulting from the various contributing factors is complicated because the rate of loss resulting from one effect is continually being altered by changes resulting from other causes. For example, the relaxation of stress in the tendons, usually studied in the laboratory at constant strain, is affected in a beam by length changes due to shrinkage and creep of the concrete. Creep, which is generally defined for a known and constant load, occurs in a prestressed concrete beam as the prestress force causing creep gradually diminishes because of relaxation, shrinkage, and creep itself. It is extremely difficult to establish the separate prestress losses accurately because of this interdependence. The calculations are further complicated by uncertainties in predicting load history and environmental conditions during the life of the member.

The following six sections provide the theoretical background needed to calculate the individual loss effects. The immediate losses due to friction, anchorage slip, and elastic shortening of the concrete are discussed in Sections 6.4, 6.5, and 6.6, respectively, and the time-dependent losses associated with concrete creep, concrete shrinkage, and steel relaxation are treated in Sections 6.7, 6.8, and 6.9. Although time-dependent losses are treated here as if they occur independently, certain arbitrary adjustments, based on more accurate calculations, are recommended to account for their interdependence. If greater refinement is necessary, a time-step approach, such as described in Section 6.11, should be used.

6.4 LOSSES DUE TO FRICTION

For post-tensioned members, the tendons are usually anchored at one end and stretched with the jacks at the other end. As the steel slides through the duct, frictional resistance is developed, with the result that the tension at the anchored end is less than the tension at the jack. The total friction loss is the sum of the *wobble friction* due to unintentional misalignment, and the *curvature friction* due to the intentional curvature of the tendon. These effects will be considered separately, then combined.

Wobble friction loss would be present even if a straight tendon were specified because, in actual cases, the duct cannot be perfectly straight. The amount of loss depends on the type of tendon and duct used, as well as on the care taken during construction. The incremental stress loss dP due to wobble friction in a short length dx of tendon can be expressed as

$$dP = KP\,dx \tag{a}$$

where the prestress force P is a function of distance x along the span, and K is a wobble friction coefficient, expressed in units of pounds loss per pound of prestress force per foot of duct. Typical ranges of values have been established by tests. The values given in Table 6.3 are those found in the ACI Code Commentary, based on earlier recommendations by the PCI Committee on Prestress Losses (Ref. 6.5).

The equation for those losses associated with the *intended* curvature of the tendon will be developed with reference to Fig. 6.1. Figure 6.1*a* shows a curved tendon subjected to a force P_s at the jacking end. The reduced force at a distance l is P_x. In most practical cases, the actual tendon curve can be replaced by a circular arc for calculating friction loss, as suggested in the sketch.

The loss of force in the short length defined by the angle change $d\alpha$ is dP, as shown in Fig. 6.1*b*. Here P is the value of the prestress force at the location considered. The equilibrium polygon of forces acting on the short segment, shown in Fig. 6.1*c*, indicates that the component of force normal to the tendon is

Table 6.3 Friction Coefficients for Post-Tensioning Tendons

Type of Tendon	Wobble Coefficient K per foot	Curvature coefficient μ
Grouted tendons in metal sheathing		
Wire tendons	0.0010–0.0015	0.15–0.25
High-strength bars	0.0001–0.0006	0.08–0.30
Seven-wire strand	0.0005–0.0020	0.15–0.25
Unbonded tendons		
Mastic coated		
Wire tendons	0.0010–0.0020	0.05–0.15
Seven-wire strand	0.0010–0.0020	0.05–0.15
Pregreased		
Wire tendons	0.0003–0.0020	0.05–0.15
Seven-wire strand	0.0003–0.0020	0.05–0.15

Source: Adapted with permission of the American Concrete Institute from ACI Building Code Commentary 318R-83.

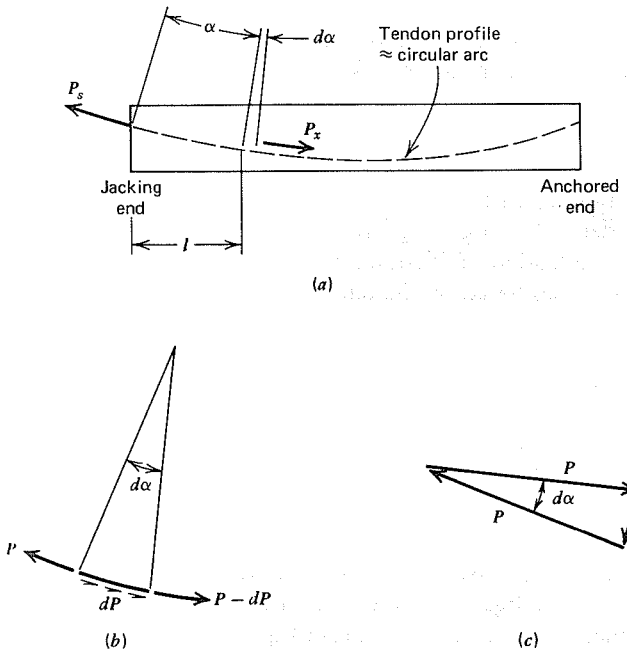

FIGURE 6.1 Loss of prestress due to curvature friction. (*a*) Tendon geometry. (*b*) Frictional effect in incremental length. (*c*) Force polygon.

equal to $P\,d\alpha$. If the coefficient of friction between tendon and duct is μ, the incremental stress loss dP due to curvature friction is

$$dP = \mu P\,d\alpha \tag{b}$$

Values of μ have been established by experiment and are given in Table 6.2.

Combining Eqs. (a) and (b), the sum of wobble and curvature losses in the incremental length is

$$dP = KP\,dx + \mu P\,d\alpha$$

The friction loss is conveniently expressed as the ratio dP/P at the location considered. If we do this, then integrate between appropriate limits,

$$\int_{P_x}^{P_s} \frac{dP}{P} = \int_0^l K\,dx + \int_0^\alpha \mu\,d\alpha$$

$$\ln \frac{P_s}{P_x} = Kl + \mu\alpha$$

This leads to the desired relation between the prestress force P_s at the jack and the reduced value P_x at a distance l from the jack:

$$P_s = P_x e^{Kl+\mu\alpha} \tag{6.1}$$

where e is the base of natural logarithms.

Equation (6.1) was derived recognizing that the prestress force P is a function of distance along the tendon. If frictional losses are sufficiently low, it is satisfactory to calculate the losses based on the tension P_x at the distance l from the jack:

$$P_s - P_x = KP_x l + \mu P_x \alpha$$

from which

$$P_s = P_x(1 + Kl + \mu\alpha) \tag{6.2}$$

According to the ACI Code, this approximation is acceptable if $(Kl + \mu\alpha) \leq 0.30$.

The relations established by Eqs. (6.1) and (6.2) may also be expressed in terms of *loss in stress*, rather than loss in force. From Eq. (6.1)

$$P_x = P_s e^{-(Kl+\mu\alpha)}$$

and the loss of force due to curvature and wobble friction is

$$\Delta P_{fr} = P_s - P_x = P_s(1 - e^{-(Kl+\mu\alpha)})$$

Dividing by the tendon area A_p gives the loss in stress resulting from friction:

$$\Delta f_{fr} = f_p(1 - e^{-(Kl+\mu\alpha)}) \tag{6.3}$$

where f_p is the tendon stress at the jack. Alternately, from the approximate relation given by Eq. (6.2)

$$\Delta P_{fr} = P_s - P_x = P_x(Kl + \mu\alpha)$$

$$\approx P_s(Kl + \mu\alpha)$$

or, in terms of stresses:

$$\Delta f_{fr} = f_p(Kl + \mu\alpha) \tag{6.4}$$

For tendon profiles composed of a combination of straight and curved segments, the losses may be calculated progressively, starting at the jacking end. For each segment, the force at the end nearest the jack is equivalent to P_s, and is equal to the reduced force P_x calculated at the end of the preceding segment.

A geometric problem often encountered, in determining prestress losses due to friction, is to fit a circular arc through three known points, for example, the tendon coordinates at the two ends and midpoint of a span, and to find the central angle α. If the curve is relatively flat, as is usually true, an approximate calculation will suffice. In Fig. 6.2, if the central angle is α, the slope at either end is $\alpha/2$. Then

$$\tan\frac{\alpha}{2} = \frac{m}{x/2} = \frac{2m}{x}$$

The distance m is approximately equal to twice the sag y. Also, for small angles, the tangent of an angle is about equal to the angle itself, measured in radians.

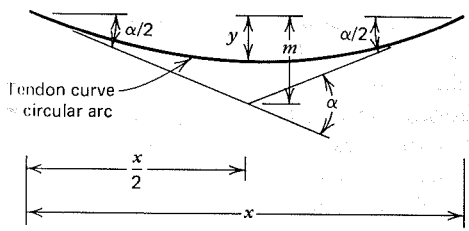

FIGURE 6.2 Approximate determination of central angle for a tendon.

Consequently,

$$\frac{\alpha}{2} = \frac{4y}{x}$$

and

$$\alpha = \frac{8y}{x} \text{ radians} \tag{6.5}$$

It should be noted that although Eq. (6.5) is approximate for a circular arc, it is exact for a parabola passing through the specified points; a parabolic tendon is often used in practice.

6.5 ANCHORAGE SLIP

In post-tensioned members, when the jacking force is released, the steel tension is transferred to the concrete by special anchorages of one type or another (see Appendix B). Inevitably, there is a small amount of slip at the anchorages upon transfer, as the wedges seat themselves into the tendons, or as the anchorage hardware deforms. Typically, anchorage "set" is in the range from $\frac{1}{8}$ in. to $\frac{1}{4}$ in. A similar situation is obtained in pretensioning, when the prestressing force is transferred from the jacks to the permanent anchorages of the casting bed through strandholding chucks. In either case, anchorage slip loss may be compensated for by overstressing, provided its magnitude is known.

Given the amount of slip characteristic of the specified hardware, the anchorage slip loss can easily be calculated from the expression

$$\Delta f_{anc} = \frac{\Delta l}{l} E_p \tag{6.6}$$

where Δl = amount of slip
l = tendon length
E_p = elastic modulus of the prestressing steel

Equation (6.6) is based on the assumption that the slip is uniformly distributed over the length of the tendon. This is approximately so for pretensioning, and may apply for post-tensioning, if the tendon is well greased or encased in low-friction plastic sheathing, and if wobble and curvature are small. For many post-tensioned beams, however, the anchorage slip loss is mostly confined to a region close to the jacking anchorage. Distribution along the tendon is prevented by reverse friction as the tendon slips inward, and the steel stress throughout much of the tendon length may be unaffected by anchorage slip. A more detailed discussion will be found in Refs. 6.2 and 6.6.

The importance of anchorage slip also depends on the length of the member or casting bed. For very short tendons, anchorage set will produce high slip losses. For long tendons or casting beds, slip becomes insignificant.

6.6 ELASTIC SHORTENING OF THE CONCRETE

When prestress force is transferred to a member, there will be elastic shortening of the concrete as it is compressed. For pretensioned members, in which the tendon is bonded to the concrete at the time of transfer, the change in steel strain is the same as the concrete compressive strain at the level of the steel centroid, and losses may be calculated accordingly. For post-tensioned members having a single tendon, the elastic deformation of the concrete takes place when the jacking force is applied, and there is automatic compensation for elastic shortening loss, which therefore need not be calculated. This will not be the case, however, if several tendons are tensioned sequentially.

First considering pretensioned beams, the concrete compressive stress at the level of the steel centroid when eccentric prestress plus self-weight are acting, immediately after transfer, is

$$f_{cs} = -\frac{P_i}{A_c}\left(1 + \frac{e^2}{r^2}\right) + \frac{M_o e}{I_c} \tag{6.7}$$

where P_i = initial prestress force (see below)
A_c = area of concrete section
e = eccentricity of steel centroid with respect to concrete centroid
r = radius of gyration of concrete section
M_o = moment due to self-weight of the member
I_c = moment of inertia of concrete section

Introducing the modular ratio $n_p = E_p/E_c$, the loss of stress in the tendon due to elastic shortening of the concrete is

$$\Delta f_{el} = n_p f_{cs} \tag{6.8}$$

The value of E_c to be used in computing n_p must be that of the concrete at the time of tensioning.

Some comment is necessary regarding the value of prestress force P_i to be used in Eq. (6.7). P_i is the prestress force after the losses being calculated have occurred. It is usually adequate to estimate P_i as about 10 percent less than P_j. It may be corrected later, with P_i set equal to the jacking force P_j less the sum of losses due to anchorage slip, friction, elastic shortening (based on the assumed P_i value) and any relaxation that may have occurred prior to the time of transfer. An iterative procedure will converge rapidly to give an improved value of P_i. However, such refinement is seldom necessary.

For post-tensioned beams, if all the steel is tensioned at once there will be no loss due to elastic shortening. However, for the common case where multiple tendons are used, with the tendons tensioned in sequence, there will be losses. The first tendon anchored will lose stress when the second is tensioned, the first and second will lose stress when the third is tensioned, and so on. The elastic shortening loss can be calculated for each tendon in turn, starting with the last tendon, for which there will be no loss. The procedure is time-consuming if there are more than a few tendons, however, and is further complicated by the uncertainty as to when the self-weight is introduced. When post-tensioning tendons are tensioned in sequential order to the same tension, it is satisfactory to calculate the loss of stress for the entire group of tendons equal to 0.5 times the value obtained using Eqs. (6.7) and (6.8). With other post-tensioning procedures, the multiplier may vary from 0 to 0.5 (Ref. 6.3).

For pretensioned beams, the stress loss due to elastic shortening will normally differ along the span, according to the variation of eccentricity and self-weight moment. It is generally necessary to calculate the loss only at the maximum moment section. For post-tensioned beams, the tendon is not bonded to the concrete when elastic shortening takes place, so the stress change in the tendon tends to be the same everywhere along the span, even though eccentricity and moment vary. To account for this, f_{cs} should be calculated at intervals along the span using Eq. (6.7) and the average value used in Eq. (6.8) to find the stress loss in the tendon or tendons.

For the increasingly common type of construction in which pretensioning and post-tensioning are combined in a single member, the loss of stress in the pretensioned strands as post-tensioning is introduced must not be neglected.

6.7 CREEP OF CONCRETE

Creep of concrete was discussed in Section 2.11, in which it was pointed out that concrete subjected to a sustained compression load will first deform elastically, then will continue to strain over an extended period of time. The *ultimate creep coefficient* was defined by Eq. (2.9):

$$C_u = \frac{\varepsilon_{cu}}{\varepsilon_{ci}} \tag{2.9}$$

where ε_{ci} is the initial elastic strain and ε_{cu} is the additional strain due to creep after a long period of time. Typical values of C_u range from about 1.6 to 3.2, the lower coefficients corresponding to the higher concrete compressive strengths (see Table 2.5). In prestressed concrete members, the concrete stresses due to prestressing force are sustained in nature, and the resulting concrete creep is an important cause of loss of prestress force.

The interdependence of time-dependent losses was mentioned in Section 6.3. In prestressed concrete beams, the compression causing creep is not constant, but diminishes with the passage of time, because of relaxation of stress in the steel and shrinkage of the concrete, as well as because of length changes associated with creep itself. This interdependence may be accounted for by adopting a step-by-step approach in calculating time-dependent losses, in which the stresses acting at the beginning of a specific time interval, causing the next increment of deformation, or relaxation, reflect all losses that have occurred up to that time. The PCI Method of calculating losses, described in Section 6.11, uses such an approach. For present purposes, losses are treated individually, for better appreciation of the role played by each. Practical calculations are often carried out on this basis as well, with arbitrary adjustments to account for interdependence.

The concrete stress that provides the basis for creep loss calculations is that at the level of the steel centroid, when the eccentric prestress force plus all sustained loads are acting. Equation (6.7) may be used, except that the moment M_o should be replaced by the moment due to *all* dead loads. To account, in an approximate way, for the gradual reduction of prestress force as creep, shrinkage, and relaxation occur, it is recommended that a value of $0.9P_i$ be substituted for P_i for creep calculations. For precast members that later receive a cast-in-place slab or topping, the moment of inertia of the composite section should be used in calculating the stress caused by loads applied after the cast-in-place concrete has hardened.

After f_{cs} is found, the loss of steel stress associated with concrete creep can be determined from the expression

$$\Delta f_{cp} = C_u n_p f_{cs} \tag{6.9}$$

when $n_p = E_p/E_c$ as usual. It is recommended in Ref. 6.7 that an average value of $C_u = 2.35$ can be used where specific data are not available, and that for average relative humidity H greater than 40 percent this value be reduced by applying a multiplication factor of $(1.27 - 0.0067H)$. The ACI-ASCE Task Committee report (Ref. 6.3) contains the recommendation that C_u be taken equal to 2.0 for pretensioned members and 1.6 for post-tensioned members, and that those values should be reduced by 20 percent for members made using sand-lightweight concrete.

For pretensioned and grouted post-tensioned members, the loss of prestress due to creep will depend on the concrete stress at the particular section of interest. The loss due to creep will usually be calculated at the section or sections of maximum moment. For unbonded post-tensioned beams, however, the reduction in steel stress will be more or less uniform along the entire length of the tendon. In creep loss calculations for this case, an average value of f_{cs} between the anchorages may be used.

If, for improved accuracy of loss estimation, a step-by-step analysis of time-dependent losses is to be made, the creep-time relation given by Eq. (2.12) may be employed. For other than "standard" conditions of loading, Eq. (2.13) can be introduced.

6.8 CONCRETE SHRINKAGE

Drying shrinkage of concrete permits a reduction of strain in the prestressing steel equal to the shrinkage strain of the concrete. The resulting steel stress loss is an important component of the total prestress loss for all types of prestressed concrete beams.

Ultimate concrete strains resulting from drying shrinkage may fall in the range from about 500×10^{-6} to $1{,}000 \times 10^{-6}$. According to Ref. 6.7 (see also Section 2.11B), ultimate shrinkage strain for moist-cured concrete can be taken equal to 800×10^{-6} in the absence of specific data, and for steam-cured concrete a value of 730×10^{-6} can be used. The time rates of shrinkage for these two cases were given by Eqs. (2.13*a*) and (2.13*b*), and the correction factors for other than "standard" conditions of humidity were given by Eqs. (2.14*a*) and (2.14*b*). The report of the ACI-ASCE Task Committee (Ref. 6.3) incorporates a recommendation that ultimate shrinkage strain be taken equal to 820×10^{-6}, and that that value be multiplied by two correction factors: the first depending on relative humidity, equal to $(100 - H)/100$, and the second depending on the volume-to-surface ratio V/S for the member, equal to $(1 - 0.06V/S)$, where V/S is expressed in inches.

Only the part of the shrinkage that occurs after transfer of prestressing force to the member need be considered. For pretensioned construction, transfer commonly takes place only 24 hours after pouring, and nearly all of the shrinkage takes place subsequent to that time. However, post-tensioned members are seldom stressed at an earlier age than seven days, and often much later than that. The curves of Fig. 2.12 indicate that about 10 to 15 percent of the ultimate shrinkage may already have occurred at seven days. If stressing is delayed until age 28 days, about 35 to 45 percent of the shrinkage would have occurred.

For total shrinkage loss calculation, or for calculations based on the step-by-step approach, the amount of shrinkage occurring in the specific time interval is the difference between the shrinkage at the beginning of the interval and that at the end. For such determinations, Fig. 2.12 and the equations of Section 2.11 may be used.

Once the amount of concrete shrinkage strain has been determined, the loss of tensile stress in the steel resulting from that shrinkage can easily be found, by multiplying the strain by the modulus of elasticity of the prestressing steel:

$$\Delta f_{sh} = E_p \varepsilon_{sh} \tag{6.10}$$

where ε_{sh} is the amount of shrinkage strain occurring during the period under consideration.

6.9 RELAXATION OF STEEL

Prestressing tendons are held stressed at essentially constant length during the lifetime of a member, although there is some reduction in length due to concrete creep and shrinkage. As was discussed in Section 2.6, there will be a gradual reduction of stress in the steel under these conditions resulting from *relaxation*, even though the length is held nearly constant. The amount of relaxation depends on the intensity of steel stress as well as time and, for stress-relieved steel, the ratio of reduced stress f_p to initial stress f_{pi} can be estimated using Eq. (2.1):

$$\frac{f_p}{f_{pi}} = 1 - \frac{\log t}{10}\left(\frac{f_{pi}}{f_{py}} - 0.55\right) \tag{2.1}$$

where f_{py} is the effective yield stress, t is the time in hours after stressing, $\log t$ is to the base 10, and f_{pi}/f_{py} is not less than 0.55. For present purposes, this relation may be restated in terms of the loss of steel stress resulting from relaxation:

$$\Delta f_{rel} = f_{pi}\frac{\log t}{10}\left(\frac{f_{pi}}{f_{py}} - 0.55\right) \tag{6.11a}$$

For step-by-step loss analysis, the loss increment in any time interval resulting from steel relation may be based on Eq. (2.2), which may be restated as

$$\Delta f_{rel} = f_{pi}\left(\frac{\log t_n - \log t_r}{10}\right)\left(\frac{f_{pi}}{f_{py}} - 0.55\right) \tag{6.12a}$$

in which t_n is the time at the end of the interval and t_r is the time at the beginning of the interval. The same equation is useful in estimating relaxation loss for pretensioned members, for which the relaxation loss that takes place before the concrete is cast should be subtracted from the total relaxation loss to obtain the change in steel stress as the beam ages from the initial to the final condition.

Low-relaxation steels are used commonly in current practice. For such steels, the loss of prestress due to relaxation is much lower, and Eqs. (6.11*a*) and

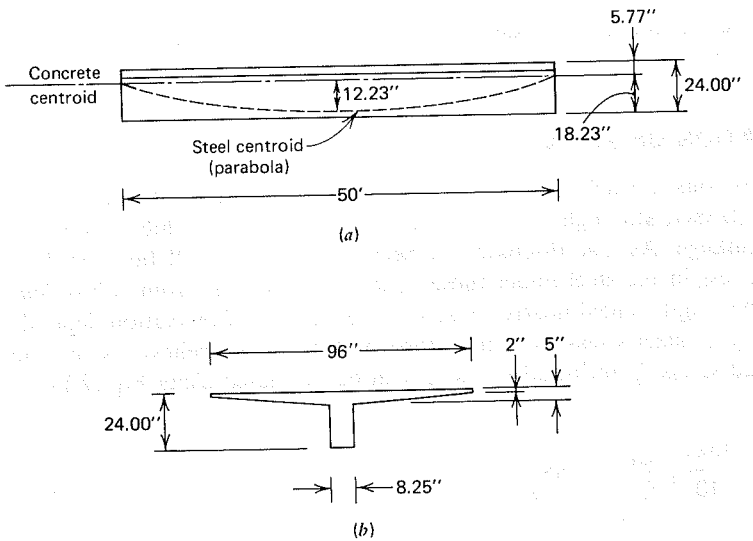

FIGURE 6.3 Beam for loss calculation example of Section 6.10. (*a*) Profile. (*b*) Cross section.

(6.12*a*) should be replaced with the following:

$$\Delta f_{rel} = f_{pi}\frac{\log t}{45}\left(\frac{f_{pi}}{f_{py}} - 0.55\right) \qquad (6.11b)$$

$$\Delta f_{rel} = f_{pi}\left(\frac{\log t_n - \log t_r}{45}\right)\left(\frac{f_{pi}}{f_{py}} - 0.55\right) \qquad (6.12b)$$

Relaxation loss will be diminished because of the effects of concrete shrinkage and creep, which reduce the stress intensity in the steel. This interaction may be accounted for in an approximate way by substituting $0.90f_{pi}$ for f_{pi} in the above equations. More elaborate recommendations are found in Ref. 6.3.

6.10 EXAMPLE: CALCULATION OF SEPARATE LOSSES

The beam shown in Fig. 6.3 is to be post-tensioned using twelve 0.5-in. diameter (12.7 mm) stress-relieved Grade 270 strands in a single duct. The total jacking tension of 300 kips (1,334 kN) will be applied to all strands at once, when the concrete is at age 28 days. Jacking will be at one end only. It has been determined by test that slip of 0.10 in. (2.54 mm) can be expected at the anchorage. The tendon will be grouted after stressing and anchoring. Other design data are as follows:

$A_p = 12 \times 0.153 = 1.836$ in.^{2} (1,185 mm^2)

$A_c = 524$ in.^{2} (338×10^3 mm^2)

$I_c = 22{,}040$ in.^{4} (9.17×10^9 mm^4)

$r^2 = 42.06$ in.^{2} (27.6×10^3 mm)

$w_o = 546$ plf (7.97 kN / m)

$E_c = 4{,}000{,}000$ psi (27.6×10^3 kN / mm^2)

$E_p = 27{,}000{,}000$ psi (186×10^3 kN / mm^2)

$f'_c = 5{,}000$ psi (34 kN / mm^2)

$C_u = 2.35$

Find the separate contributions to loss of prestress force at the end of a five-year period, during which time the only permanent sustained load will be the self-weight of the beam.

The estimate of loss of prestress will be based on consideration of the separate contributions to total loss, as outlined in Sections 6.4 to 6.9. The interdependence of creep, shrinkage, and relaxation losses will be accounted for in an approximate way by a downward adjustment of the force for which the respective losses are calculated.

(A) FRICTION LOSS

The actual parabolic tendon will be approximated as a circular arc for calculating friction losses. From Eq. (6.5), the central angle is

$$\alpha = \frac{8 \times 12.23}{50 \times 12} = 0.163 \text{ radian}$$

Consulting Table 6.3 for values of the wobble friction coefficient and the curvature friction coefficient for seven-wire strand in metal sheathing, representative values $K = 0.0010$ and $\mu = 0.20$ are selected. The parameter

$$(Kl + \mu\alpha) = 0.0010 \times 50 + 0.20 \times 0.163$$
$$0.0826.$$

is substantially less than 0.30, indicating that the approximate friction loss Eq. (6.4) may be used. The steel stress at the jack is $f_{pj} = 300{,}000/1.836 = 163{,}000$ psi, and the loss of stress due to friction, over the full length of the beam, from Eq. (6.4), is

$$\Delta f_{fr} = 163{,}000 \times 0.0826$$
$$= 13{,}500 \text{ psi (93 MPa)}$$

Thus, the stress at the far end of the tendon at this stage is

$$f_p = 163{,}000 - 13{,}500 = 149{,}500 \text{ psi (1,031 MPa)}$$

At midspan, based on a linear variation, the stress in the tendon is 156,000 psi (1,076 MPa).

(B) ANCHORAGE SLIP LOSS

As pointed out in Section 6.5, except for strands in plastic sheathing and for which the curvature is small, the slip effect is confined to the region close to the jacking anchorage. In the present example, it will be assumed that the slip effect does not propagate beyond about 10 ft from the end of the beam. Consequently, for the midspan section of interest:

$$\Delta f_{anc} = 0$$

(C) ELASTIC SHORTENING LOSS

With all 12 strands tensioned at once with a single jack, the elastic shortening of the concrete will take place during the jacking operation, and will be fully compensated for by additional extension of the jack. As a result, elastic shortening loss is

$$\Delta f_{el} = 0$$

Summarizing, the initial prestress in the steel at midspan, after appropriate consideration of losses due to friction, anchorage slip, and elastic shortening, is 156,000 psi, and the initial prestress force at that location is

$$P_i = 156{,}000 \times 1.836 = 286{,}000 \text{ lb } (1{,}272 \text{ kN})$$

(D) CREEP LOSS

The loss in tension due to concrete creep will be calculated at the maximum moment section at midspan, for the condition of prestress plus self-weight. To account, in an approximate way, for the gradual reduction of prestress force due to creep, shrinkage, and relaxation as creep goes on, the prestress force used in computation will be reduced to $0.9P_i$ or 257 kips. The maximum moment produced by the beam weight is

$$M_o = \tfrac{1}{8} \times 546 \times 50^2 = 171{,}000 \text{ ft-lb}$$

and, from Eq. (6.7), the concrete stress at the level of the steel centroid is

$$f_{cs} = -\frac{257{,}000}{524}\left(1 + \frac{12.23^2}{42.06}\right) + \frac{171{,}000 \times 12 \times 12.23}{22{,}040}$$

$$= -1{,}096 \text{ psi}$$

Then from Eq. (6.9), with $n_p = E_p / E_c = 6.75$, the loss of stress in the steel resulting from concrete creep is

$$\Delta f_{cp} = 2.35 \times 6.75 \times 1{,}096$$

$$= 17{,}400 \text{ psi } (120 \text{ MPa})$$

(E) SHRINKAGE LOSS

Shrinkage loss calculation will be based on an assumed ultimate shrinkage strain for the concrete of 800×10^{-6}. The amount of shrinkage affecting the stress in the tendon is that that occurs after stressing and anchoring the steel at concrete age 28 days. From Fig. 2.11 it is seen that for moist-cured concrete, 44 percent of the ultimate shrinkage could be expected to occur before that time. Consequently, the remaining shrinkage is $800 \times 10^{-6} \times 0.56 = 448 \times 10^{-6}$, and from Eq. (6.10) the loss in steel stress associated with that strain reduction is

$$\Delta f_{sh} = 27 \times 10^6 \times 448 \times 10^{-6}$$

$$= 12{,}100 \text{ psi } (83 \text{ MPa})$$

(F) RELAXATION LOSS

The gradual reduction of steel stress resulting from the combined effects of creep, shrinkage, and relaxation will be accounted for in determining relaxation loss by using a reduced value of prestress force of $0.9P_i$ in the calculation. The corresponding steel stress is $0.9 \times 156{,}000 = 140{,}000$ psi. Referring to Fig. 2.4, we see that the effective yield stress for Grade 270 strand is $f_{py} = 230{,}000$ psi. Then from Eq. (6.11), at time five years or 44,000 hours, the loss of stress in the steel due to the relaxation is estimated to be

$$\Delta f_{rel} = 140{,}000 \times \frac{4.64}{10}\left(\frac{140}{230} - 0.55\right)$$

$$= 3{,}800 \text{ psi } (26 \text{ MPa})$$

(G) SUMMARY AND COMPARISON WITH LUMP SUM ESTIMATES

The losses of prestress resulting from all causes are summarized in Table 6.4. The initial jacking stress $f_{pj} = 163{,}000$ psi is reduced due to friction losses to $f_{pi} = 156{,}000$ psi at midspan. Anchorage slip loss effect is confined to the local region near the jacking end, and no elastic shortening losses occur because all 12 strands were

Table 6.4 Summary of Losses for the Example of Section 6.10

Source	Loss		
	psi	MPa	Percent of f_{pi}
Friction	6,800	47	4
Anchorage slip	0	0	0
Elastic shortening	0	0	0
Creep	17,400	120	11
Shrinkage	12,100	83	8
Relaxation	3,800	26	2

tensioned at once. After a five-year period after transfer, the initial tension at midspan is reduced because of creep, shrinkage, and relaxation to an effective prestress f_{pe} = 122,700 psi.

The losses are also expressed as a percentage of initial stress f_{pi} in Table 6.4. It is seen that the immediate loss is only four percent of f_{pi} for this beam, because there are no elastic shortening losses, whereas time-dependent losses total 21 percent of f_{pi}. The effectiveness ratio for the beam is $R = 122{,}700 / 156{,}000 = 0.79$, close to the value of 0.80 used in most of the design examples of earlier chapters.

It is interesting to compare the results with lump sum estimates based on the recommendations of the AASHTO Specification and the recommendations of the Post-Tensioning Institute. The sum of losses due to elastic shortening (none in this case), creep, shrinkage and relaxation is 33,300 psi. For f'_c = 5,000 psi, the AASHTO value from Table 6.1 is 33,000 psi, and the PTI recommendation from Table 6.2 is 35,000 psi. Either of these lump sum estimates would be completely satisfactory in the present case.

6.11 ESTIMATION OF LOSSES BY THE TIME-STEP METHOD

The loss calculations of the preceding articles, and the example just presented, recognized the interdependence of creep, shrinkage, and relaxation losses in an approximate way, by an arbitrary reduction of 10 percent of the initial prestress force P_i to obtain the force for which creep and relaxation losses were calculated. For cases requiring greater accuracy, losses may be calculated for discrete time steps over the period of interest. The prestress force causing losses during any time step is taken equal to the value at the end of the preceding time step, accounting for losses due to all causes up to that time. Accuracy may be improved to any desired degree by reducing the length and increasing the number of time steps. Computer programs are available for such analysis (Refs. 6.8 and 6.9).

A step-by-step method has been developed by the PCI Committee on Prestress Losses that uses only a small number of time steps and, consequently, is well suited for use in calculations by slide rule or electronic calculator, as well as by computer (Ref. 6.5). The time interval for each step is increased with the age of the concrete. Four time steps are used as follows:

1. For pretensioned members: from the time of anchorage of the prestressing steel until the age of prestressing the concrete.
   For post-tensioned members: from the time when curing ends until the age of prestressing the concrete.
2. From the end of step (1) until age 30 days, or the time when a member is subjected to load in addition to its own weight.
3. From the end of step (2) until age one year.
4. From the end of step (3) until the end of service life.

The PCI method for determining losses resulting from the interrelated time-dependent effects will produce a more accurate estimate than the method suggested in Sections 6,7, 6.8, and 6.9, and the accuracy may be still further improved, within the general format of the PCI method, by increasing the number of time steps. When significant changes in loading are expected, time intervals other than those recommended may be used. The cost of such refinement, of course, is additional computational effort. This may or may not be justified in a given case.

Loss calculations using the time-step method are usually combined with deflection calculations, because deflections are influenced strongly by the amount of prestress loss (Ref. 6.10). A detailed study of prestress losses and deflection calculations using the time-step method and an example using this approach will be found in Chapter 9.

An additional factor to be considered in more exact calculation of prestress loss in some members is the effect of non-prestressed bar reinforcement. It has been shown (Refs. 6.11 and 6.12) that such rebars, often included in partially prestressed beams to augment flexural strength and control cracking, may significantly affect both loss of prestress force and deflection.

REFERENCES

6.1 Standard Specifications for Highway Bridges, 13th ed., American Association of State Highway and Transportation Officials (AASHTO), Washington, D.C., 1983.

6.2 *Post-Tensioning Manual*, 4th ed. Post-Tensioning Institute, Phoenix, 1985.

6.3 Zia, P., Preston, H. K., Scott, N. L., and Workman, E. B., "Estimating Prestress Losses," *Concrete International*, Vol. 1, No. 6, June 1979, pp. 32–38.

6.4 "Tentative Recommendations for Prestressed Concrete," reported by ACI-ASCE Joint Committee 423, *J. ACI*, Vol. 54, No. 7, January 1958, pp. 548–578.

6.5 "Recommendations for Estimating Prestress Losses," reported by PCI Committee on Prestress Losses, *J. PCI*, Vol. 20, No. 4, July–August 1975, pp. 43–75.

6.6 Huang, T., "Anchorage Takeup Loss in Posttensioned Members," *J. PCI*, Vol. 14, No. 4, August 1969, pp. 30–35.

6.7 Branson, D. E., *Deformation on Concrete Structures*, McGraw-Hill, New York, 1977, 546 pp.

6.8 Sinno, R. and Furr, H. L., "Computer Program for Predicting Prestress Loss and Camber," *J. PCI*, Vol. 17, No. 5, September–October 1972, pp. 27–38.

6.9 Tadros, M. K., Ghali, A., and Dilger, W. H., "Time-Dependent Prestress Loss and Deflection in Prestressed Concrete Members," *J. PCI*, Vol. 20, No. 3, May–June 1975, pp. 86–98.

6.10 "Deflections of Prestressed Concrete Members," reported by ACI Committee 435, *J. ACI*, Vol. 60, No. 12, December 1963, pp. 1697–1728.

6.11 Tadros, M. K., Ghali, A., and Dilger, W. H., "Effect of Non-Prestressed Steel on Prestress Loss and Deflection," *J. PCI*, Vol. 22, No. 2, March–April 1977, pp. 50–63.

6.12 Tadros, M. K., Ghali, A., and Meyer, A. W., "Prestress Loss and Deflection of Precast Concrete Members," *J. PCI*, Vol. 30, No. 1, January–February 1985, pp. 114–141.

PROBLEMS

6.1 A pretensioned, prestressed concrete girder is to be built, with the same span and cross section as the girder in the example of Section 6.10. Pretensioning will be applied using twelve 0.5-in. diameter stress-relieved Grade 270 strands, six of which are deflected upward at the one-quarter points of the span, to have zero eccentricity at the supports, the remainder being straight strands. The jacking force is 300,000 lb. Slip losses are fully compensated by overjacking, and friction at the tendon deflection points is negligible. Compute all losses, and express each as a percentage of the initial prestress f_{pi} at midspan. Calculate the effectiveness ratio R. Compare the sum of losses due to elastic shortening, creep, shrinkage, and relaxation with the AASHTO recommended loss of Table 6.1. High early-strength concrete will be used, with f'_c = 5,000 psi. Steam-curing will be utilized, and prestress force will be transferred to the girder at age three days, when f'_{ci} = 3,500 psi.

6.2 The beam shown in Fig. P6.2, of 70-ft span, is post-tensioned using eighteen 0.5-in. diameter stress-relieved Grade 270 strands in a single tendon having parabolic profile, with e = 18 in. at midspan and zero at the supports. The jacking force is P_j = 618 kips and is applied at one end only. Calculate the separate losses at midspan and express each loss as a percentage of f_{pi} at midspan. Creep effects may be assumed to occur under the combined effects of prestress, self-weight, and superimposed dead load of 600 plf. The beam is moist-cured and is prestressed when the concrete has reached age seven days. Anchorage slip = 0.20 in., coefficient of curvature friction = 0.20, coefficient of wobble friction = 0.0010, creep coefficient = 2.35. Member properties are as follows: A_c = 737 in.^{2}, I_c = 192,000 in.^{4}, $c_1 = c_2$ = 24 in., f'_c = 5,000 psi, E_c = 4,030,000 psi, E_p = 27,000,000 psi, and w_c = 150 pcf.

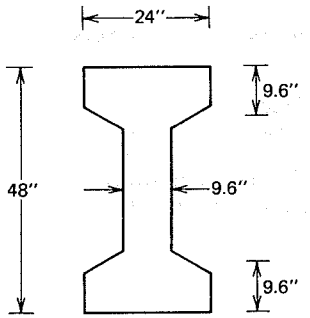

FIGURE P6.2

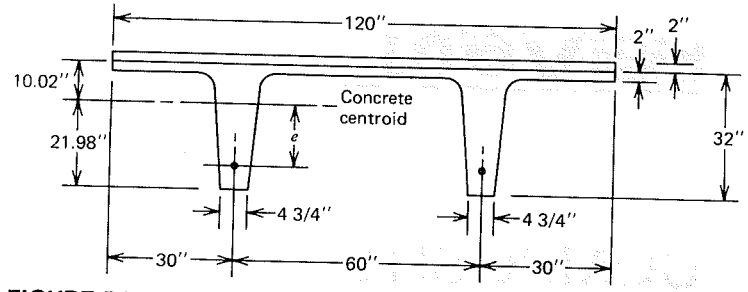

FIGURE P6.3

6.3 The standard pretensioned double-T beam of Fig. P6.3 is to be used on a 70-ft span with no superimposed dead load except for the 2-in. nonstructural topping. The initial prestress force P_i of 347 kips will be applied using a total of twelve 0.5-in. diameter Grade 270 stress-relieved strands. Slip losses will be fully compensated during jacking, and friction losses are negligible. The member will be steam-cured and the prestress force released at age three days. Shrinkage and creep subsequent to transfer may be assumed to take place at a relative humidity of 70 percent. Section properties are: A_c = 615 in.^{2}, I_c = 59,720 in.^{4}, w_o = 641 plf, w_{top} = 250 plf, A_p = 1.836 in.^{2}. Concrete has specified strength f'_c = 5,000 psi, and at transfer f'_{ci} = 3,500 psi. Tendons are depressed at midspan only; the tendon eccentricity at midspan is 18.73 in., and at the supports is 12.81 in. Calculate the jacking force P_j to be specified and find the individual and total losses, using the methods of Sections 6.4 to 6.9. Compare with AASHTO lump sum amount, and compute the effectiveness ratio R.

6.4 Recalculate the losses for the beam of Problem 6.3 based on the use of low-relaxation strands. The jacking force P_j will be the same as before.

SEVEN

COMPOSITE BEAMS

7.1 TYPES OF COMPOSITE CONSTRUCTION

The term composite construction, applied to prestressed concrete, usually refers to construction in which a precast concrete member acts in combination with cast-in-place concrete, poured at a later time and bonded to it. Often the precast element is a pretensioned slab or single-T or double-T beam. In such cases, a relatively thin topping slab is used, often unreinforced but sometimes containing wire mesh. Another frequently employed form of composite construction combines a pretensioned precast I-beam with a cast-in-place reinforced concrete slab to form a composite member having a bulb-T section. In either case, the cast-in-place slab meets functional requirements by providing a smooth, useful surface and, in addition, substantially stiffens and strengthens the precast unit. A pretensioned composite member may be further prestressed by post-tensioning after the slab has hardened.

Composite construction offers the advantages of precasting, including factory prefabrication of standardized sections, reuse of forms, long-line tensioning of strands, and excellent quality control. On the construction site, formwork and scaffolding are largely eliminated, permitting rapid field erection of the structure with little interference to work or traffic below.

Composite construction may take many forms. The types of members most common to United States practice are shown in Fig. 7.1. In each case, the precast

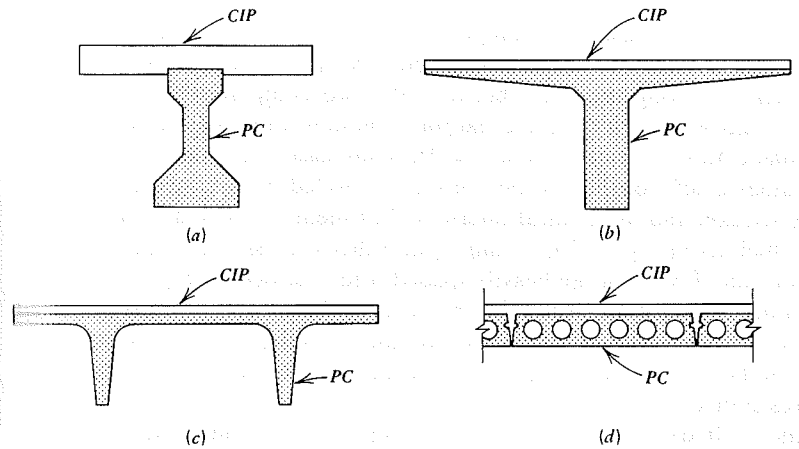

FIGURE 7.1 Typical composite sections. (*a*) AASHTO bridge girder. (*b*) Single-T girder. (*c*) Double-T beam. (*d*) Hollowcore slab.

(*PC*) part of the section is shown shaded, and the cast-in-place (*CIP*) portion is left unshaded to differentiate the two.

The bridge girder section shown in Fig. 7.1*a* has been used extensively for short-to-medium-span highway bridges. The dimensions of the precast I-sections have been standardized by AASHTO in six sizes, ranging in depth from 28 to 72 in. (Ref. 7.1 and Appendix A). The unsymmetrical I-section is used in conjunction with a cast-in-place roadway slab, creating a bulb-T beam with a composite concrete centroid close to the underside of the slab.

The single-T section beam shown in Fig. 7.1*b* is often used for medium-to-long-span roof deck and floor systems, as in parking garages, for example. With the increasing use of partial prestressing, which avoids the need for large bottom flanges to resist heavy initial prestressing forces, such cross sections are found suitable for members of all types including bridges as well as buildings. They are normally placed side by side with flange tips in contact. The thickness of the topping slab is typically 2 to 3 in. for buildings, but may be substantially deeper for bridges. The construction may include intermediate diaphragms, often prestressed laterally to ensure that the entire assembly acts as a unit.

The double-T beam of Fig. 7.1*c* is typical of the production of numerous precasting plants. Such beams are widely used for short and medium spans, mostly for floors and roofs in buildings, and are often designed for composite action with a 2 in. topping slab. The same comments apply to the hollowcore precast deck planks shown in cross section in Fig. 7.1*d*.

Section properties for the most common single-T and double-T beams and for hollowcore slabs, all for both with and without topping slab, are tabulated in Ref. 7.2, which also includes safe load tables.

An essential prerequisite for composition action is good bond between the precast concrete and the cast-in-place concrete. Flexural shear causes a tendency for horizontal slip along the plane between the two components. Considerable resistance to slip is provided by the natural adhesion and friction between the poured-in-place and the precast concrete. In many cases, the top surface of the precast element is left rough, screeded but not troweled, to improve the transfer of shear by friction and mechanical interlock. For members with a broad surface of contact, such as in Figs. 7.1*b*, *c*, and *d*, no other provision is made for shear transfer, as a rule. For the more heavily loaded bridge girders of Fig. 7.1*a*, with a smaller contact interface, the web reinforcement of the precast beam is projected upward into the cast-in-place slab. This provides dowel action in resisting slip, and locks the two components together to insure the development of maximum frictional resistance.

In almost all cases, the quality of concrete specified and attained in the precast member is superior to that in the cast-in-place part of a composite section. Concrete cast under plant conditions, where quality control is easily maintained, is generally of strength from 5,000 to 6,000 psi. Concrete cast on the construction site is of more variable quality and lower strength, usually in the range from 3,000 to 4,000 psi. Such differences must be accounted for in design.

7.2 LOAD STAGES

A composite member must perform in a satisfactory way under any load or combination of loads that may act upon it during its useful life. The analysis and design of composite beams will usually require consideration of at least the following load stages:

1. Initial prestress P_i plus self-weight of the precast beam.
2. Effective prestress P_e plus noncomposite and composite dead loads.
3. Effective prestress P_e plus all dead load plus service live load.
4. Factored overload.

Loads introduced before the cast-in-place concrete hardens cause stresses associated with bending of the precast section about its own centroidal axis. Loads applied after the cast-in-place concrete hardens cause bending about the centroid of the composite member. Stresses already present in the precast part of the member are modified and, in addition, stresses are introduced in the newly placed concrete.

In some cases, it is economical to carry all superimposed loads by composite action. This can be done through the use of temporary shoring of the precast unit during the period when the slab is poured and is curing. When shores are removed, the weight of the slab, as well as all subsequently applied loads, cause bending about the composite centroid.

As a general rule, stresses resulting from load stages 1 through 3 may be found based on the assumption of elastic behavior, with section properties calculated for the noncomposite or composite beam, whichever is appropriate.

Tests have proved that when composite members are subject to overloads, the full strength of the combined section is developed, provided that effective shear transfer is maintained across the interface between components (Refs. 7.3 and 7.4). Both steel and concrete are normally stressed well into their inelastic ranges, and the consequences of strain discontinuities are minimal. The strength of composite members may be calculated as if the construction were homogeneous.

Normally, the load stages that control the design of composite prestressed beams are stage 1, when limitations on tensile and compressive stresses at the top and bottom, respectively, of the precast unit must be satisfied, stage 3, when service load stress limits on compression at the top and tension at the bottom of the composite section must not be exceeded, and stage 4, when the member must develop adequate strength to resist overloads, developing a suitable margin of safety. In addition, stage 2 must be considered in predicting time-dependent loss of prestress force and long-term deflection.

7.3 SECTION PROPERTIES AND ELASTIC FLEXURAL STRESSES

In calculating stresses in composite beams, it is necessary to differentiate between loads acting on the precast beam and those introduced after the cast-in-place part of the section is added, when full composite action can be developed. Stresses produced by bending of the composite member may be superimposed directly upon those already present in the precast portion. Clearly, bending is about a different centroid in each case, and two different sets of section properties must be used.

Notation is established by reference to Fig. 7.2, which shows a precast I-section to which is added a cast-in-place slab. In referring to section properties, the subscripts p and c relate, respectively, to properties of the precast and composite sections. Similarly, dead loads affecting only the precast portion will be subscripted p, and those causing stresses associated with composite action will be subscripted c.

Elastic stresses acting on the member at any stage may be found by the methods of Chapter 3, using the appropriate section properties. It will be assumed that the member is uncracked at all stages of present interest.

The stresses at various load stages, for a typical composite beam, are shown in Fig. 7.3. Immediately after transfer, the initial prestress force P_i acts on the member. Normally, the self-weight of the precast portion is immediately superimposed. The stresses at the top and bottom of the precast beam are given by

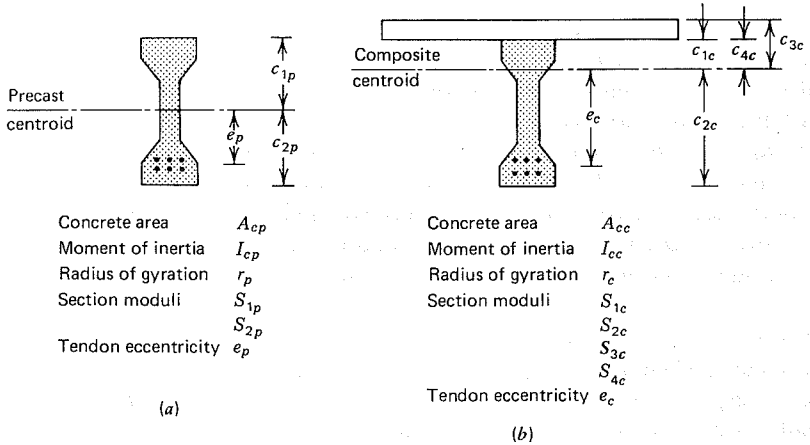

FIGURE 7.2 Properties of precast and composite cross sections. (*a*) Precast section. (*b*) Composite section.

distribution (2) of Fig. 7.3*b* and are, respectively:

$$f_1 = -\frac{P_i}{A_{cp}}\left(1 - \frac{e_p c_{1p}}{r_p^2}\right) - \frac{M_o}{S_{1p}} \tag{7.1a}$$

$$f_2 = -\frac{P_i}{A_{cp}}\left(1 + \frac{e_p c_{2p}}{r_p^2}\right) + \frac{M_o}{S_{2p}} \tag{7.1b}$$

where M_o is the moment due to the self-weight of the precast member, and other terms are as previously defined.

It will be assumed that all time-dependent losses occur at this point, so that concrete stresses are gradually modified to those shown as distribution (3), when P_e acts, together with self-weight.

Usually the only important noncomposite dead load other than that of the precast beam itself is the weight of the wet concrete slab. This causes bending about the centroid of the precast unit, with stresses as shown in Fig. 7.3*c*. These stresses, when superimposed on those already present, produce distribution (4) of Fig. 7.3*d*. At this stage, the stresses at the top and bottom of the precast concrete beam are, respectively:

$$f_1 = -\frac{P_e}{A_{cp}}\left(1 - \frac{e_p c_{1p}}{r_p^2}\right) - \frac{M_o + M_{dp}}{S_{1p}} \tag{7.2a}$$

$$f_2 = -\frac{P_e}{A_{cp}}\left(1 + \frac{e_p c_{2p}}{r_p^2}\right) + \frac{M_o + M_{dp}}{S_{2p}} \tag{7.2b}$$

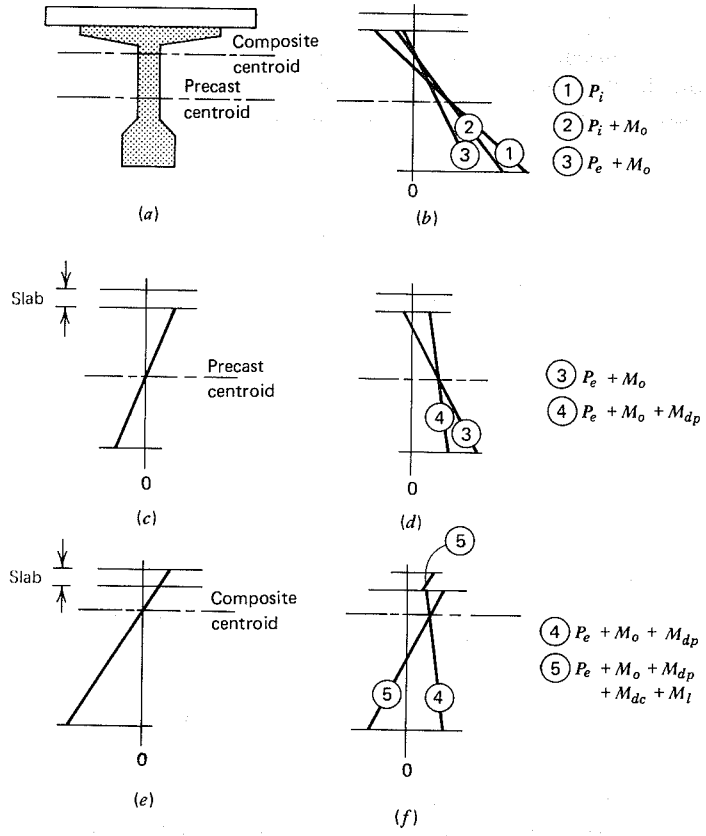

FIGURE 7.3 Elastic stresses in an uncracked composite beam. (*a*) Cross section. (*b*) Prestress plus self-weight. (*c*) Increment due to noncomposite loads. (*d*) Prestress plus noncomposite loads. (*e*) Increment due to composite loads. (*f*) Prestress plus noncomposite and composite loads.

where M_{dp} is moment due to dead loads, exclusive of the member self-weight, that cause bending of the noncomposite section.

After the freshly poured concrete slab has hardened and acquired its strength, the effective centroid shifts upward of that of the composite section, and all loads applied subsequently cause bending about the composite centroid. These include dead loads applied after the slab has hardened, such as pavement surface, piping, and sidewalks for bridges, or finish floors, ceilings, and suspended utilities in the case of buildings. Live load almost always acts on the composite section only.

The incremental stresses due to composite loads, shown in Fig. 7.3*e*, are superimposed on prior stresses in the precast section to produce the stress

distribution (5) shown in Fig. 7.3*f*. Note that, since there are no prior stresses in the slab (disregarding shrinkage and creep effects), distribution (5) shows a stress discontinuity at the level of the interface between precast and cast-in-place components. The stresses in the precast concrete at stage (5) are given by the equations:

$$f_1 = -\frac{P_e}{A_{cp}}\left(1 - \frac{e_p c_{1p}}{r_p^2}\right) - \frac{M_o + M_{dp}}{S_{1p}} - \frac{M_{dc} + M_l}{S_{1c}} \tag{7.3a}$$

$$f_2 = -\frac{P_e}{A_{cp}}\left(1 + \frac{e_p c_{2p}}{r_p^2}\right) + \frac{M_o + M_{dp}}{S_{2p}} + \frac{M_{dc} + M_l}{S_{2c}} \tag{7.3b}$$

and those at the top and bottom of the slab are, respectively,

$$f_3 = -\frac{M_{dc} + M_l}{S_{3c}} \tag{7.3c}$$

$$f_4 = -\frac{M_{dc} + M_l}{S_{4c}} \tag{7.3d}$$

In these equations, M_{dc} is the moment caused by dead loads introduced after composite action is obtained, and M_l is the moment due to the superimposed live loads.

It has already been noted that the precast concrete is ordinarily of higher strength than the cast-in-place concrete, which must be placed and cured under field conditions. The elastic stresses in the composite beam will be affected by the difference in the E_c values of the concretes. This difference may be accounted for in the calculations by making use of the transformed section concept, by which the cast-in-place concrete of lower grade may be transformed into a smaller equivalent amount of precast concrete of higher quality.

Figure 7.4*a* shows the actual composite cross section composed of two grades of concrete, and Fig. 7.4*b* shows the equivalent transformed homogeneous section, for which the slab concrete has the same strength and elastic properties as the concrete in the precast web. In Fig. 7.4*a*, the flange width b is the *effective flange width* defined, for composite members, by the same rules used for homogeneous sections (see Section 3.7D). At any level of the cross section a distance y above the centroidal axis, the flexural strains must be the same in the actual and transformed sections. If f_c and f_{cp} are, respectively, the concrete stresses at the level y in the actual and transformed sections, and if E_c and E_{cp} are, respectively, the elastic moduli of the concrete in the actual slab and the equivalent precast slab, then, since the strains are equal:

$$\frac{f_c}{E_c} = \frac{f_{cp}}{E_{cp}}$$

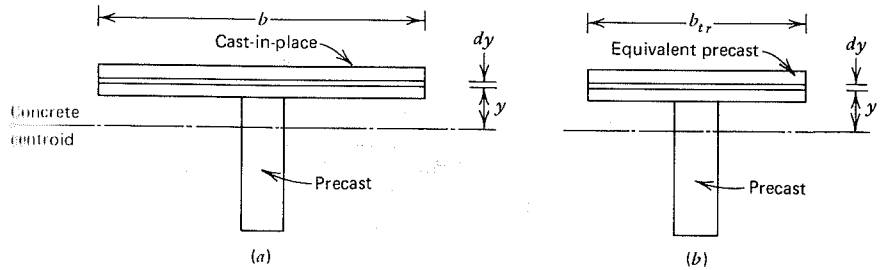

FIGURE 7.4 Transformed composite cross section. (*a*) Actual section. (*b*) Transformed section.

or

$$f_c = \frac{E_c}{E_{cp}} f_{cp} = n f_{cp}$$

where n = the modular ratio of the two concretes, a number normally less than unity.

The equivalent section will provide the proper resistance if the differential compressive force is the same in either case, that is:

$$dC = f_c b\, dy = f_{cp} b_{tr}\, dy$$

substituting nf_{cp} for f_c and cancelling like terms:

$$b_{tr} = nb \tag{7.4}$$

That is, a *reduced width* b_{tr}, based on the modular ratio n, is to be substituted for the actual width b in the calculation of section properties. After this substitution, the section properties may be found as if the beam were composed uniformly of the higher strength concrete used for the precast web.

The equations presented in this section for flexural stresses in the precast and cast-in-place concrete disregard the influence of differential shrinkage and creep effects between the two component parts of a composite beam. Generally, for any period following slab casting and bonding of the slab to the precast beam, shrinkage plus creep strain at the bottom surface of the slab would exceed shrinkage plus creep strain at the top of the precast beam, if the two were not bonded together. As a result of this, additional longitudinal shearing stresses are developed at the bonded interface. An eccentric longitudinal force acts inward toward the center of the beam and tends to produce additional downward deflection as well as modifying the longitudinal stresses computed by the preceding equations. The importance of this effect depends, among other things, on the amount of shrinkage and creep for the materials at their particular stress levels, on the time-sequence of construction, on whether or not shoring is used, and on

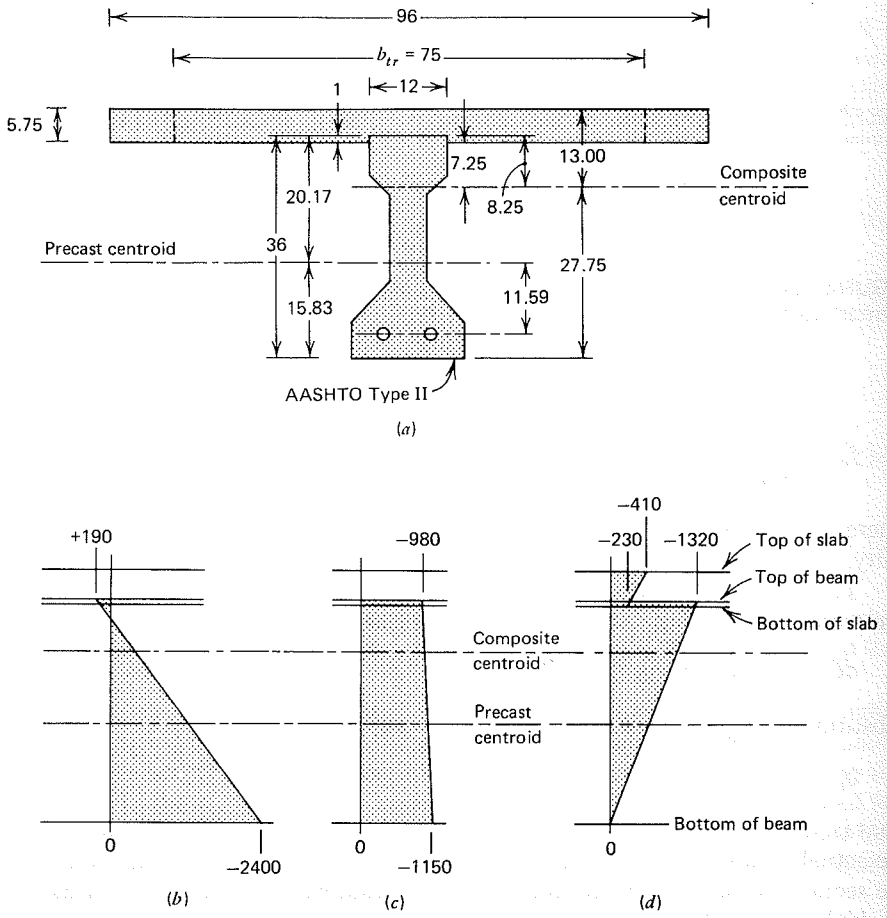

FIGURE 7.5 AASHTO bridge girder cross section and stress distributions. (*a*) Cross section. (*b*) $P_i + M_o$. (*c*) $P_e + M_o + M_{dp}$. (*d*) $P_e + M_o + M_{dp} + M_{dc} + M_l$.

whether or not the slab is subject to tensile cracking due to the restraint forces. A comprehensive treatment of this subject will be found in Ref. 7.5.

EXAMPLE: Calculation of Elastic Flexural Stresses in Bridge Girder

A 3-ft depth AASHTO Type II girder, precast and pretensioned, will be used with a 5.75 in. × 96 in. cast-in-place slab to form a composite beam that will span 55 ft between simple supports. The cross section geometry is shown in Fig. 7.5*a*. The precast beam will be made using concrete with f'_c = 5,000 psi and $E_c = 4.07 \times 10^6$ psi, and the slab concrete has f'_c = 3,000 psi and $E_c = 3.15 \times 10^6$ psi. An initial prestress force of 468 kips, applied 11.59 in. below the centroid of the precast beam, is reduced by time-dependent losses to 398 kips. (h = 914 mm, slab = 146 × 2438 mm, span 16.76 m, beam f'_c = 34 MPa, slab f'_c = 21 MPa, beam E_c = 28,000 MPa, slab E_c = 22,000 MPa, P_i = 2,081 kN, P_e = 1,770 kN, and e = 294 mm.) The loads and corresponding moments to be carried are as follows:

Precast girder:	w_o = 385 plf (5.6 kN/m)	M_o = 146 ft-kips (198 kN-m)
Concrete slab:	w_{dp} = 575 plf (8.4 kN/m)	M_{dp} = 218 ft-kips (296 kN-m)
Superimposed dead load:	w_{dc} = 185 plf (2.7 kN/m)	M_{dc} = 70 ft-kips (95 kN-m)
Live load:	w_l = 1,158 plf (16.9 kN/m)	M_l = 438 ft-kips (594 kN-m)

Find the flexural stresses in the beam corresponding to the following load combinations: (1) initial prestress plus self-weight of the precast beam, (2) effective prestress plus all noncomposite dead loads, and (3) effective prestress plus full service loads. Unshored construction will be assumed.

The properties of the AASHTO Type II precast beam are available from Appendix A and are summarized in Table 7.1. The girder self-weight is immediately

Table 7.1 Summary of Section Properties for AASHTO Bridge Girder Example

Precast Beam	Composite Beam
A_{cp} = 369 in.^{2} (238×10^3 mm^2)	A_{cc} = 799 in.^{2} (515×10^3 mm^2)
c_{1p} = 20.17 in. (512 mm)	c_{1c} = 8.25 in. (210 mm)
c_{2p} = 15.83 in. (402 mm)	c_{2c} = 27.75 in. (705 mm)
I_{cp} = 50,980 in.^{4} (21.2×10^9 mm^4)	c_{3c} = 13.00 in. (330 mm)
r_p^2 = 138 in.^{2} (89.0×10^3 mm^2)	c_{4c} = 7.25 in. (184 mm)
s_{1p} = 2,528 in.^{3} (41.4×10^6 mm^3)	I_{cc} = 149,000 in.^{4} (62.0×10^9 mm^4)
s_{2p} = 3,220 in.^{3} (52.8×10^6 mm^3)	r_c^2 = 162 in.^{2} (105×10^3 mm^2)
	S_{1c} = 18,000 in.^{3} (295×10^6 mm^3)
	S_{2c} = 5,300 in.^{3} (87×10^6 mm^3)
	S_{3c} = 11,400 in.^{3} (187×10^6 mm^3)
	S_{4c} = 20,550 in.^{3} (337×10^6 mm^3)

superimposed when the initial prestress force is applied to the precast girder, and stresses in the concrete at the top and bottom of the section may be found using Eqs. (7.1*a*) and (7.1*b*):

$$f_1 = -\frac{P_i}{A_{cp}}\left(1 - \frac{e_p c_{1p}}{r_p^2}\right) - \frac{M_o}{S_{1p}}$$

$$= -\frac{468{,}000}{369}\left(1 - \frac{11.59 \times 20.17}{138}\right) - \frac{146{,}000 \times 12}{2{,}528}$$

$$= +190 \text{ psi } (+1.3 \text{ MPa})$$

$$f_2 = -\frac{P_i}{A_{cp}}\left(1 + \frac{e_p c_{2p}}{r_p^2}\right) + \frac{M_o}{S_{2p}}$$

$$= -\frac{468{,}000}{369}\left(1 + \frac{11.59 \times 15.83}{138}\right) + \frac{146{,}000 \times 12}{3{,}220}$$

$$= -2{,}400 \text{ psi } (-16.5 \text{ MPa})$$

as shown in Fig. 7.5*b*.

The freshly poured concrete slab causes stresses in the precast section resulting from the additional noncomposite moment of 218 ft-kips. From Eqs. (7.2*a*) and (7.2*b*):

$$f_1 = -\frac{P_e}{A_{cp}}\left(1 - \frac{e_p c_{1p}}{r_p^2}\right) - \frac{M_o + M_{dp}}{S_{1p}}$$

$$= -\frac{398{,}000}{369}\left(1 - \frac{11.59 \times 20.17}{138}\right) - \frac{(146 + 218) \times 12{,}000}{2{,}528}$$

$$= -980 \text{ psi } (-6.8 \text{ MPa})$$

$$f_2 = -\frac{P_e}{A_{cp}}\left(1 + \frac{e_p c_{2p}}{r_p^2}\right) + \frac{M_o + M_{dp}}{S_{2p}}$$

$$= -\frac{398{,}000}{369}\left(1 + \frac{11.59 \times 15.83}{138}\right) + \frac{(146 + 218) \times 12{,}000}{3{,}220}$$

$$= -1{,}150 \text{ psi } (-7.9 \text{ MPa})$$

The properties of the composite cross section must now be found. With modular ratio $n = 3.15 / 4.07 = 0.775$, the transformed width of the compression flange is $b_{tr} = 0.775 \times 96 = 75$ in., as shown in Fig. 7.5*a*, providing a compression flange area of 430 in.^{2} If one takes moments of areas about the top face of the slab to locate the composite centroid:

$$c_{3c} = \frac{369 \times 24.92 + 430 \times 2.87}{369 + 430} = 13.00 \text{ in.}$$

Accordingly, the distances c_{1c} and c_{2c} from the composite centroid to the top and bottom faces of the precast section are, respectively, 8.25 and 27.75 in., and the distance c_{4c} to the bottom of the slab is 7.25 in., as shown in Fig. 7.5*a*.

The moment of inertia of the transformed slab concrete about its own centroidal axis is

$$I_{slab} = \frac{1}{12} \times 75 \times 5.75^3 = 1{,}190 \text{ in.}^4$$

and, making use of the transfer axis theorem, the moment of inertia of the composite section about its own axis is

$$I_{cc} = 50{,}980 + 369(27.75 - 15.83)^2 + 1{,}190 + 430(13.00 - 2.87)^2$$

$$= 149{,}000 \text{ in.}^4$$

The section moduli to the top and bottom of the precast section and to the top and bottom of the slab are, respectively:

$$S_{1c} = \frac{149{,}000}{8.25} = 18{,}000 \text{ in.}^3$$

$$S_{2c} = \frac{149{,}000}{27.75} = 5{,}300 \text{ in.}^3$$

$$S_{3c} = \frac{149{,}000}{13.00} = 11{,}400 \text{ in.}^3$$

$$S_{4c} = \frac{149{,}000}{7.25} = 20{,}550 \text{ in.}^3$$

All section properties for the composite section are summarized in Table 7.1.

The incremental stresses applied at the top and bottom of the precast member as composite dead and live loads are introduced are

$$f_1 = -\frac{(70 + 438)12{,}000}{18{,}000} = -340 \text{ psi } (-2.3 \text{ MPa})$$

$$f_2 = +\frac{(70 + 438)12{,}000}{5{,}300} = +1{,}150 \text{ psi } (+7.9 \text{ MPa})$$

These stresses associated with composite action are superimposed on the stresses already present because of the bending of the noncomposite section, Fig. 7.5*c*, to obtain the total service load stresses

$$f_1 = -980 - 340 = -1{,}320 \text{ psi } (-9.1 \text{ MPa})$$

$$f_2 = -1{,}150 + 1{,}150 = 0$$

at the top and bottom faces, respectively, as shown in Fig. 7.5*d*. The stresses at the top and bottom faces of the concrete slab may be found similarly, except that the stresses found for the transformed slab area must be transformed back, in turn, to stresses acting on the actual concrete, multiplying by the modular ratio n. Based on Eqs. (7.3*c*) and (7.3*d*), these stresses are:

$$f_3 = -\frac{(70 + 438)12{,}000}{11{,}400} \times 0.775 = -410 \text{ psi } (-2.8 \text{ MPa})$$

$$f_4 = -\frac{(70 + 438)12{,}000}{20{,}550} \times 0.775 = -230 \text{ psi } (-1.6 \text{ MPa})$$

The final stress distribution for the composite section at full service load is as shown by Fig. 7.5*d*.

7.4 FLEXURAL STRENGTH

If proper provision is made for the transfer of horizontal shear forces across the interface between the components of a composite member, then the entire cross section can be considered effective in the calculation of ultimate flexural strength.

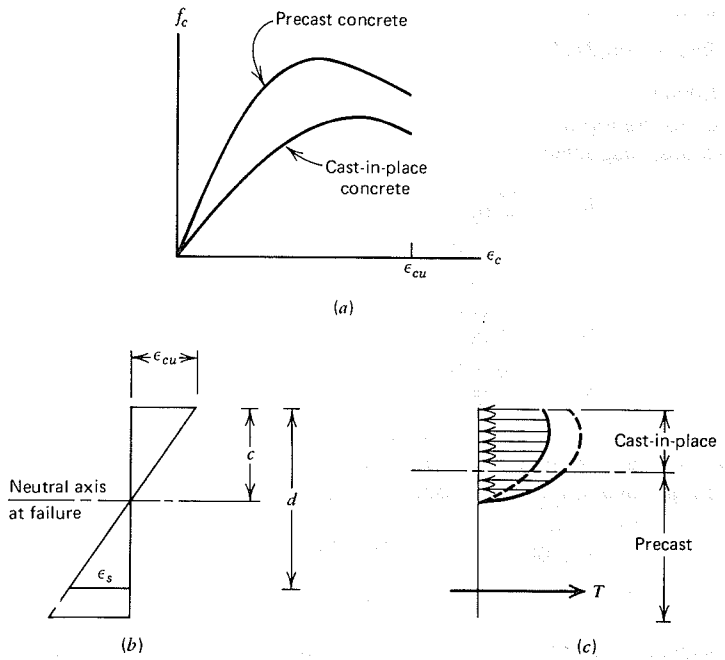

FIGURE 7.6 Strain and stress distributions for a composite section at failure load. (*a*) Comparative stress–strain curves. (*b*) Strains at failure. (*c*) Stresses at failure.

At large compressive strains, the difference in elastic moduli of the cast-in-place and precast concrete, which led to use of a transformed compressive flange width in elastic calculations, has no meaning and, consequently, the calculations should be based on the full effective flange width, determined by the usual criteria. Furthermore, the relatively small strain discontinuity at the interface between precast and cast-in-place concrete, resulting from prior bending of the noncomposite precast section, can be ignored without serious error at the overload stage. However, the differences in concrete compressive stress at a given strain in the two materials will produce a discontinuity in concrete stress at the interface, as illustrated in Fig. 7.6.

Figure 7.6*a* shows compressive stress–strain curves typical of the precast and cast-in-place concrete. The distribution of strain in the concrete at incipient failure is represented in Fig. 7.6*b*. The stress distributions shown in Fig. 7.6*c* are obtained from the respective stress–strain curves, the curve of higher stress applying below the interface and the curve of lower stress applying above the interface.

To account for such a stress distribution in design would result in complicated expressions for failure moment. It is unnecessary to do so in most cases, because for the T-section, the ultimate neutral axis is usually quite high in the section and often, in fact, is above the interface level. In addition, the resisting moment is governed by the steel and not the concrete strength. Thus, in most practical cases, the strength calculations may be based on a homogeneous section composed of the weaker, cast-in-place, concrete.

EXAMPLE: Ultimate Flexural Strength of Composite Bridge Girder

Find the ultimate flexural strength of the 36 in. AASHTO Type II bridge girder, with cast-in-place composite slab, studied in the preceding example and shown in cross section in Fig. 7.5*a*. The prestressing steel consists of nineteen 1/2-in. diameter stress-relieved strands having a total cross section of 2.75 in.^{2} The ultimate strength of the steel is $f_{pu} = 250{,}000$ psi. ($A_p = 1{,}774$ mm^2, $f_{pu} = 1{,}723$ MPa, and $h = 914$ mm.)

The ultimate flexural strength will be determined based on the ACI approximate expression for stress in the steel at failure.

First the effective compressive flange width will be determined, using the ACI criteria:

$$b \le \tfrac{1}{4} \times 55 \times 12 = 165 \text{ in.}$$
$$b \le (16 \times 5.75 + 12) = 104 \text{ in.}$$
$$b \le 96 \text{ in. (controls)}$$

The steel ratio is

$$\rho_p = \frac{A_p}{bd} = \frac{2.75}{96 \times 36.51} = 0.00078$$

The steel stress at failure will be calculated using the ACI approximate equation of Section 3.8A. From Eq. (3.21)

$$f_{ps} = f_{pu}\left(1 - \frac{\gamma_p}{\beta_1}\frac{\rho_p f_{pu}}{f'_c}\right)$$

where, for ordinary stress-relieved wire, $\gamma_p = 0.40$, and, for 3,000 psi concrete, $\beta_1 = 0.85$. With $f_{pu} = 250$ ksi and $f'_c = 3{,}000$ psi, as used in the slab, the steel stress at flexural failure is

$$f_{ps} = 250\left(1 - \frac{0.40}{0.85}\frac{0.00078 \times 250}{3}\right)$$
$$= 240 \text{ ksi (1,655 MPa)}$$

The stress-block depth a will be calculated assuming that it is less than the flange thickness $h = 5.75$ in. From Eq. (3.26)

$$a = \frac{A_p f_{ps}}{0.85 f'_c b}$$
$$= \frac{2.75 \times 240}{0.85 \times 3 \times 96}$$
$$= 2.70 \text{ in. (69 mm)}$$

confirming the assumption on which the calculation was based. Then, from Eq.

(3.27), the design strength of the composite girder is:

$$\phi M_n = \phi A_p f_{ps}(d_p - \frac{a}{2})$$
$$= 0.90 \times 2.75 \times 240\,(36.51 - 1.35)/12$$
$$= 1{,}740 \text{ ft-kips } (2{,}360 \text{ kN-m})$$

This value will be compared with the required strength found by applying the usual ACI load factors to dead and live load moments:

$$M_u = 1.4(146 + 218 + 70) + 1.7(438)$$
$$= 1{,}353 \text{ ft-kips } (1835 \text{ kN-m})$$

confirming that adequate strength is available should the member be overloaded.

7.5 HORIZONTAL SHEAR TRANSFER

As flexural loading is applied to a composite prestressed beam such as that shown in Fig. 7.7*a*, there is a tendency for the cast-in-place slab to slip horizontally, the bottom face of the slab tending to move outward with respect to the top face of the precast web, which tends to displace inward. If this slip is not prevented, the flange and the web will act as two separate beams, each resisting its portion of the load independently by bending about its own centroidal axis, as in Fig. 7.7*b*. The development of full composite action depends on the prevention of slip.

To prevent slip, there must be a means for transferring shear forces across the interface between the two components of the composite member. The shear forces produced by the usual bending loads act inward on the slab, toward the section of maximum moment, and outward on the web, as shown in Fig. 7.7*c*.

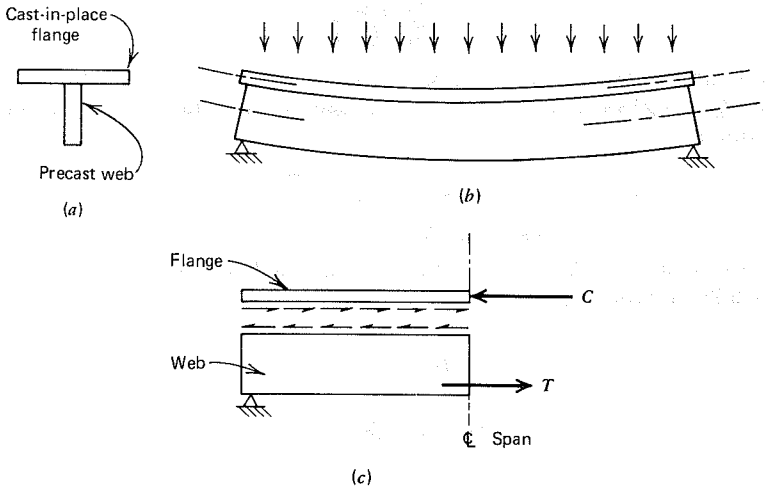

FIGURE 7.7 Composite action in T-beam. (*a*) Section. (*b*) Noncomposite behavior. (*c*) Shear stresses on interface.

Shear resistance along the interface may be provided by the natural adhesion and friction between the cast-in-place and the precast concrete. It will be enhanced if the top of the precast unit is deliberately roughened, rather than troweled smooth. This is usually done, and for composite beams having a broad contact surface, such as those of Figs. 7.1*b*, *c*, and *d*, no other provision need be made for transfer of shear force. Tests have confirmed that full composite behavior is assured up the flexural failure load in members of this type.

For more heavily loaded beams with a smaller contact interface, such as that of Fig. 7.1*a*, vertical stirrups placed in the beam web to resist diagonal tensile stresses are usually extended upward and anchored in the cast-in-place slab. This not only provides slip resistance through dowel action, but improves frictional resistance by holding the two components in intimate contact. In addition, a roughened surface is usually specified. In special cases, shear keys may be formed in the top of the web, projecting upward into the flange, although these are actually ineffective until some slip occurs.

For an elastic uncracked beam, the intensity of the horizontal shearing stress due to bending can be calculated from the familiar expression

$$v_h = \frac{VQ}{Ib_v} \qquad (7.5a)$$

where v_h = shear stress intensity, psi
V = vertical shear force at the section, lb
Q = static moment, about the centroidal axis of the entire section, of the area of the cross section between the horizontal plane considered and the extreme compression face, in.[3]
I = moment of inertia of the entire section about its own centroidal axis, in.[4]
b_v = width of the shear plane under investigation, in.

Although Eq. (7.5*a*) was used to calculate the interface shearing stress at failure in early research (Refs. 7.4 and 7.6), it was recognized that it does not give a true representation of stresses because the influence of cracking is ignored and because of the assumption of elastic concrete response. A simpler, and no less valid, basis for comparison is provided by calculating the nominal shear stress intensity at failure, defined by the equation

$$v_h = \frac{V}{b_v d_p} \qquad (7.5b)$$

where d_p is the distance from the extreme compression face of the member to the centroid of the prestressing steel for the entire composite section.[1] Present design

[1]Although the ACI Code is not clear as to the definition of d_p when applied to composite prestressed concrete beams, it is usually taken to be the larger of the actual d_p or $0.80h$, as is usual for other shear calculations.

procedures are based on nominal shear stress limits, calculated by Eq. (7.5*b*), determined by test.

Accordingly, following ACI Code provisions, one computes the nominal horizontal shear strength of a composite beam from the equation:

$$V_{nh} = v_{nh} b_v d_p \tag{7.6}$$

where values of v_{nh} are established from tests of members with varying conditions of surface roughness and varying amounts of vertical tie steel crossing the interface. Specifically:

1. When concrete surfaces are clean, free of laitance, and intentionally roughened, $v_{nh} = 80$ psi.
2. When minimum ties are provided and contact surfaces are clean and free of laitance, but not intentionally roughened, $v_{nh} = 80$ psi.
3. When minimum ties are provided and contact surfaces are clean, free of laitance, and intentionally roughened, $v_{nh} = 350$ psi.

In applying these provisions, to be considered suitably roughened, the top surface of the precast unit must be left with a full amplitude of approximately 1/4 in. Minimum ties are defined to be the same as the minimum required for shear reinforcement in the web, that is,

$$A_{v,\min} = \frac{50 b_w s}{f_y} \tag{7.7}$$

where b_w = web width of the precast unit, s = longitudinal spacing of the web steel along the beam, and f_y = yield strength of the stirrups. In addition, the tie spacing must not exceed four times the least dimension of the supported element (i.e., the concrete slab), or 24 in., according to ACI Code. Ties for horizontal shear may consist of single bars, multiple leg stirrups, or the vertical legs of welded wire fabric. Normally, the stirrups provided for diagonal tension reinforcement in the web are simply extended upward into the cast-in-place slab. Suitable anchorage must be provided. This generally requires the use of 90 degree bends or hooks.

After computing the horizontal shear strength in this way, the basic design requirement is:

$$V_u \le \phi V_{nh} \tag{7.8}$$

where V_u = total factored vertical shear force at the section, and $\phi = 0.85$.

The horizontal shear force to be transferred may be determined by an alternate method, according to ACI Code, by computing the actual change in compressive or tensile force in an element in any segment of the beam, and providing for transfer of that force as horizontal shear to the supporting element. If this procedure is followed, the factored horizontal shear force must not exceed the horizontal shear strength ϕV_{nh} calculated by Eq. (7.6), with the area of the contact surface A_c being substituted for $b_v d_p$ in that equation.

If the shear force V_u at a section exceeds $350 \phi b_v d_p$, then design for horizontal shear may be done employing the shear friction analysis of Section 12.4 (Ref. 7.7). The basis, in this case, is to provide for transfer of the maximum compression or tension force that may act on either component of the composite section when loads are increased to incipient failure. With reference to Fig. 7.7*c*, the flexural compression C or tension T to be transferred between the sections of maximum moment and zero moment can be taken, for design purposes, to be the smaller of

$$C = 0.85 f_c' h_f b \tag{7.9}$$

or

$$T = A_p f_{ps} \tag{7.10}$$

where all terms are as previously defined. In Eq. (7.9), f_c' is the specified compressive strength of the slab concrete. Using this approach, the maximum shear force V_{nh} that can be transferred between the sections of maximum and zero moment depends on the number, size, and yield strength of the stirrups crossing the interface, as well as on the roughness of the surface. The method is very simple to apply, and details will be clear after study of Section 12.4. In designing for interface shear by the shear friction method, acceptance is implied of slight movements along the interface at loads near failure, such that the elastic distribution of shear forces along the span becomes irrelevant. Redistribution at loads near failure produces near-uniform shear.

EXAMPLE: Investigation of Horizontal Shear Transfer

The AASHTO Type II girder with cast-in-place slab studied in the preceding examples contains web reinforcement consisting of No. 4 U stirrups that are extended upward into the slab and anchored by a standard 90 degree bend. The proposed spacing of Grade 60 stirrups varies from 5 in. (127 mm) on centers at the supports to a maximum of 21 in. (533 mm) on centers through the central part of the span. A total of 29 stirrups is provided in each half of the span. The top surface of the precast beam is screeded such that it meets Code requirements for "intentional roughening," with approximately 0.25 in. (6.35 mm) full amplitude. Determine if the shear transfer mechanism provided is adequate.

The factored load is computed from actual dead load and service live loads by the usual ACI procedures:

$$w_u = (385 + 575 + 185)1.4 + 1{,}158 \times 1.7$$
$$= 3{,}572 \text{ plf } (53 \text{ kN/m})$$

corresponding to a shear of

$$V_u = 3{,}572 \times 55/2 = 98{,}230 \text{ lb (443 kN)}$$

For the composite beam, the effective depth to the steel centroid (assumed to be constant here) is 36.51 in. and the width of the shear interface at the top of the precast member is 12 in.

According to the Code, for roughened surface and ties, the design shear strength may be taken equal to $\phi V_{nh} = 0.85 \times 350 \times 12 \times 36.51 = 130$ kips, well above the value of $V_u = 98.2$ kips. The maximum spacing of the ties must not exceed four times the slab thickness, nor 24 in., according to ACI Code. The proposed maximum spacing of 21 in. will satisfy both criteria.

For comparison, the design will be checked using the shear friction method. The force to be transferred between midspan and support, to develop the flexural strength of the beam, is the lower of:

$$C = 0.85 f'_c h_f b$$
$$= 0.85 \times 3.00 \times 5.75 \times 96$$
$$= 1{,}408 \text{ kips (6,263 kN)}$$

and, referring to the results of the strength analysis of Section 7.4,

$$T = A_p f_{ps}$$
$$= 2.75 \times 240$$
$$= 660 \text{ kips (2,936 kN)}$$

and T controls, as will almost always be the case. With a friction factor between cast-in-place and precast concrete of 1.0, according to the ACI Code (see Section 12.4), the required steel area crossing the interface in the half-span is found, from Eq. (12.4), to be

$$A_{vf} = \frac{V_u}{\phi \mu f_y}$$
$$= \frac{660{,}000}{0.85 \times 1.0 \times 60{,}000}$$
$$= 12.94 \text{ in.}^2 \text{ (8,349 mm}^2\text{)}$$

The proposed total of 29 stirrups, each with area $2 \times 0.20 = 0.40$ in.^{2}, provides

$$A_{vf} = 29 \times 0.40 = 11.60 \text{ in.}^2 \text{ (7,484 mm}^2\text{)}$$

slightly less than required. Spacing will be reduced near midspan to 20 in. to provide four additional stirrups in each half-span, meeting requirements according to the shear friction method.

According to ACI Code, a composite beam that meets shear transfer requirements based on unit shear stresses v_{nh} at the interface need not be checked using the shear friction method. The shear friction analysis would be employed only if V_u exceeds $350 \phi b_v d_p$. However, it will usually be found that the spacing of ties required according to the shear friction analysis will be much closer than the minimum as dictated by the several criteria to be applied when using the unit shear stress approach. It is recognized that the minimum spacing will generally apply only close to midspan, whereas nearer the supports requirements for diagonal tension reinforcement in the web will require a closer spacing of ties. However, it is prudent in designing composite members for which ties are required for horizontal shear transfer to check that the total number provided between midspan and support is at least equal to that required by the shear friction approach.

7.6 SHEAR AND DIAGONAL TENSION

There are no special problems associated with the design of composite prestressed beams to resist diagonal tension in the web. In general, the concepts and design specifications of Chapter 5 apply to composite members without change (Ref. 7.8). Because shear design is based on conditions in the member at factored loads, that is, at incipient failure, it is not relevant whether the loads are applied to the precast section alone or to the composite member.

The entire composite member may be assumed to resist vertical shear, assuming it behaves as a monolithically cast member of the same cross-sectional shape. The calculation of V_c may usually be based upon the strength of the concrete in the precast part of composite members (normally of the higher compressive strength) because most of the shear resistance is provided by the precast web rather than by the cast-in-place flange.

As usual, the nominal shear stress is computed on the basis of the web width. For I-sections such as that of Fig. 7.1*a*, it is appropriate and conservative to use the narrowest width of the web, disregarding the top flange of the precast section. For sections having a tapered web, such as Fig. 7.1*c*, it is acceptable to base the calculations on the average width of the stems.

Web reinforcement is normally not necessary or provided for slab units such as Fig. 7.1*d*, or for double-Ts (actually ribbed slab units) such as Fig. 7.1*c*. For other cases, such as single Ts, Fig. 7.1*b*, and I-sections (Fig. 7.1*a*) stirrups are provided. The stirrups are carried up into the slab and suitably anchored with a 90 degree bend or a hook. For composite bridge girders, such as shown in Fig. 7.1*a*, the stirrups are normally carried above the top of the precast section and are anchored in the cast-in-place concrete, as noted in Section 7.5.

REFERENCES

7.1 *AASHTO Standard Specifications for Highway Bridges*, 13th ed., American Association of State Highway and Transportation Officials, Washington, D.C., 1983, 394 pp.

7.2 *PCI Design Handbook*, 3rd ed., Prestressed Concrete Institute, Chicago, 1985.

7.3 Hanson, N. W., "Precast Prestressed Concrete Bridges: (2) Horizontal Shear Connections," *J. Res. and Dev. Lab.*, Portland Cement Association, Vol. 2, No. 2, May 1960, pp. 38–58.

7.4 Saemann, J. C. and Washa, G. W., "Horizontal Shear Connections Between Precast Beams and Cast-in-Place Slabs," *J. ACI*, Vol. 61, No. 11, November 1964, pp. 1383–1409.

7.5 Branson, D. E., *Deformation of Concrete Structures*, McGraw-Hill, New York, 1977.

7.6 ACI-ASCE Committee 333, "Tentative Recommendations for the Design of Composite Beams and Girders for Buildings," *J. ACI*, Vol. 57, No. 6, December 1960, pp. 609–628.

7.7 Mast, R. F., "Auxiliary Reinforcement in Concrete Connections," *J. Struct. Div. ASCE*, Vol. 94, No. ST6, June 1968, pp. 1485–1504.

7.8 Mattock, A. H. and Kaar, P. H., "Precast Prestressed Concrete Bridges: (4) Shear Tests of Continuous Girders," *J. Res. and Dev. Lab.*, Portland Cement Association, Vol. 3, No. 1, January 1961, pp. 19–46.

PROBLEMS

7.1 The uniformly loaded 50-ft span composite T-beam of Fig. P7.1 incorporates a cast-in-place slab with $f'_c = 3{,}000$ psi. The prestressed steel area is $A_p = 1.73$ in.^{2}, and separate calculations indicated that the steel stress at failure is $f_{ps} = 230{,}000$ psi. It is designed to carry a total factored load, including self-weight, of 2.65 kips per ft. Web reinforcement consisting of No. 3 U stirrups has $f_y = 60{,}000$ psi, and spacing varies from 5 in. at the supports to 20 in. at midspan. It is carried up into the slab and is properly anchored. The top face of the precast unit will be roughened according to ACI Code requirements. (a) Calculate the nominal horizontal shear strength at the interface according to the basic ACI Code method and confirm that it is greater than the strength required. (b) According to the alternative shear friction method of analysis, calculate the number and spacing of stirrups needed between midspan and support.

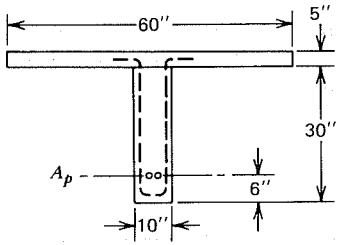

FIGURE P7.1

7.2 The precast double-T floor unit shown in Fig. P7.2 has concrete strength $f'_c = 5{,}000$ psi and is prestressed using a total of ten 0.5-in. diameter Grade 270 strands having eccentricity at midspan of 14.15 in. Initial prestress $f_{pi} = 189$ ksi. A 2-in. topping slab will be placed, with $f'_c = 3{,}000$ psi. The units will carry a service live load of 79 psf and external dead load of 15 psf, in addition to self-weight, on a 50-ft simple

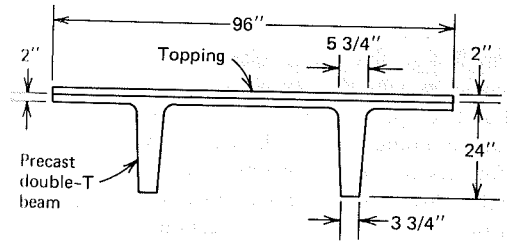

FIGURE P7.2

span. Properties of the precast unit are as follows:

$A_c = 401$ in.^{2}
$I_c = 20{,}985$ in.^{4}
$c_1 = 6.85$ in.
$c_2 = 17.15$ in.
$S_1 = 3{,}063$ in.^{3}
$S_2 = 1{,}224$ in.^{3}
$w_o = 418$ plf
$A_p = 1.53$ in.^{2}

(a) Confirm that horizontal shear strength at the interface is adequate. (b) Calculate the flexural stresses in the member, immediately after release of prestress force and at full service load. Loss of prestress due to time-dependent effects may be taken at 18 percent. Compare with ACI Code allowable stresses. (c) Compute the flexural strength of the composite unit and compare with the required value.

7.3 A parking deck structure is planned, composed of 70-ft span precast single-T beams as shown in Fig. P7.3. After erection of the Ts, a 5-in. slab will be cast in place, to act in a composite sense with the precast Ts. For the precast units, $f'_c = 5{,}000$ psi and $f'_{ci} = 3{,}500$ psi, and the cast-in-place concrete has strength $f'_c = 3{,}000$ psi. The precast beams will be pretensioned using 0.5-in. diameter Grade 250 strands,

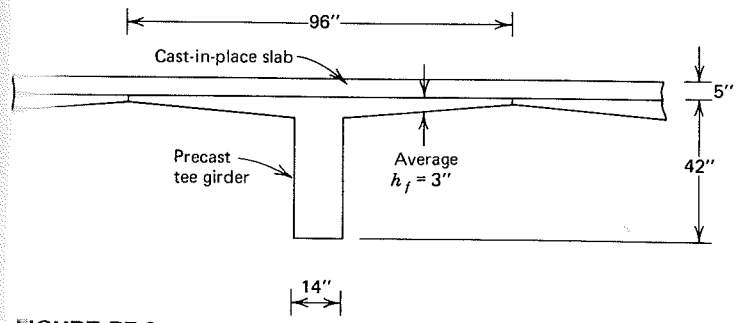

FIGURE P7.3

deflected at midspan, with eccentricity reduced to the lower kern point at the supports. Pretensioning should be applied so that ACI Code stress limits are not exceeded in the initial stage or when self-weight plus fresh concrete slab weight is acting. After the slab has hardened and composite action can be assured, the units will be further prestressed by post-tensioning, using additional 0.5-in diameter strands in metal ducts, to carry the full service live load of 150 psf without exceeding ACI Code stress limits. Time-dependent losses in the pretensioned strands may be assumed at 18 percent, occurring in the casting yard prior to erection of the girders and subsequent post-tensioning. Elastic loss of pretensioning when post-tensioning is applied should be taken into account. Subsequent losses in the post-tensioned strands may be taken at 20 percent. (a) Find the required pretensioning force and number of strands. (b) Find the additional prestress to be applied by post-tensioning. (c) Check flexural stresses in the concrete at all significant load stages. (d) Calculate the flexural strength of the composite beam and compare with the required strength at factored loads. (d) Check the adequacy of the beams for transferring horizontal shear at the interface. The top of the precast units will be intentionally roughened according to ACI Code specifications. Should the stirrups provided for diagonal tension in the web be carried into the 5-in. slab? Section properties for the single-T precast unit are: $A_c = 834$ in.^{2}, $I_c = 127{,}000$ in.^{4}, $c_1 = 15.3$ in., $c_2 = 26.7$ in., $S_1 = 8{,}300$ in.^{3}, $S_2 = 4{,}757$ in.^{3}, $w_o = 869$ plf.

EIGHT

CONTINUOUS BEAMS AND FRAMES

8.1 SIMPLE SPANS VERSUS CONTINUITY

Most prestressed concrete construction in the United States at the present time consists of statically determinate beams and girders, floor and roof deck panels, and wall units. There are several reasons for this. In contrast to reinforced concrete construction, which is mostly cast-in-place and for which continuity is the natural condition, a large proportion of prestressed concrete is also precast. This offers great advantages by avoiding forming, shoring, and tensioning in the field, and permits high-quality construction at low cost. But the structure arrives on the site in pieces, much as does a steel structure, and extra expense and effort is needed to obtain continuity.

In addition, for continuous spans, the diagram of maximum design moments has local peaks, usually at the supports. For concrete structures using ordinary non-prestressed bar steel, the resisting moment is easily varied to match the controlling moments at various sections by cutting off or bending bars where they are not needed. For prestressed members, the main reinforcement is usually a continuous tendon of constant cross section, the area of which is determined by requirements at the section of greatest moment. For continuous spans in which

moment requirements vary greatly along the total length, this may result in an uneconomical design.

Frictional losses may also become large for continuous prestressed spans, for which the tendon profile is likely to have several changes of curvature.

Finally, as will be discussed in more detail later, statically indeterminate prestressed beams characteristically develop *secondary moments* as a result of prestressing, introducing a complication to the design process.

However, there are important advantages associated with indeterminate structures of prestressed concrete, as with structures of other types. Design moments are smaller for given spans and loads than for determinate structures, and deflection is reduced. By continuing post-tensioning tendons over several spans, fewer anchorages are required and the labor cost of stressing is greatly reduced. Joint rigidity in continuous frames provides an important mechanism to resist horizontal loads such as are induced by wind, blast, or seismic forces.

Because of the advantages, continuous prestressed concrete construction is increasingly common in the United States, and this trend is expected to continue. Two-way, continuous, flat plate slabs are used extensively, and have proven both functional and highly economical. For medium and long span bridges, the economic and esthetic advantages of continuity are dominant considerations. Many ingenious arrangements have been developed to avoid the problems listed earlier.

In many instances, precast pretensioned components are post-tensioned together in the field to obtain the advantages of continuity, as well as the economy associated with plant production. This system has been widely exploited for medium span bridges, for which entire spans are often precast and pretensioned to carry their own weight and construction loads, then post-tensioned at the construction site to provide continuity for superimposed dead and live loads. Segmentally precast bridges of long span are normally designed for full continuity.

Continuous prestressed construction is well established in Europe, and may be expected to become common in the United States because of further technical development and changing economic conditions (Refs. 8.1 to 8.6).

8.2 TENDON PROFILES AND STRESSING ARRANGEMENTS

The tendon profiles used for continuous spans are closely related to the variation of bending moment due to the dead and live loads, just as was true for statically determinate simple span beams. In general, moments resulting from prestressing should vary in the same way as those moments due to the applied loads and act in the opposite sense. It follows that a reasonable tendon profile may be established by dividing all ordinates of the applied load moment diagram by a constant to obtain tendon eccentricities along the span.

For example, for the two-span continuous beam of Fig. 8.1*a*, a uniformly distributed load will produce the moment diagram of Fig. 8.1*b*. Moments vary

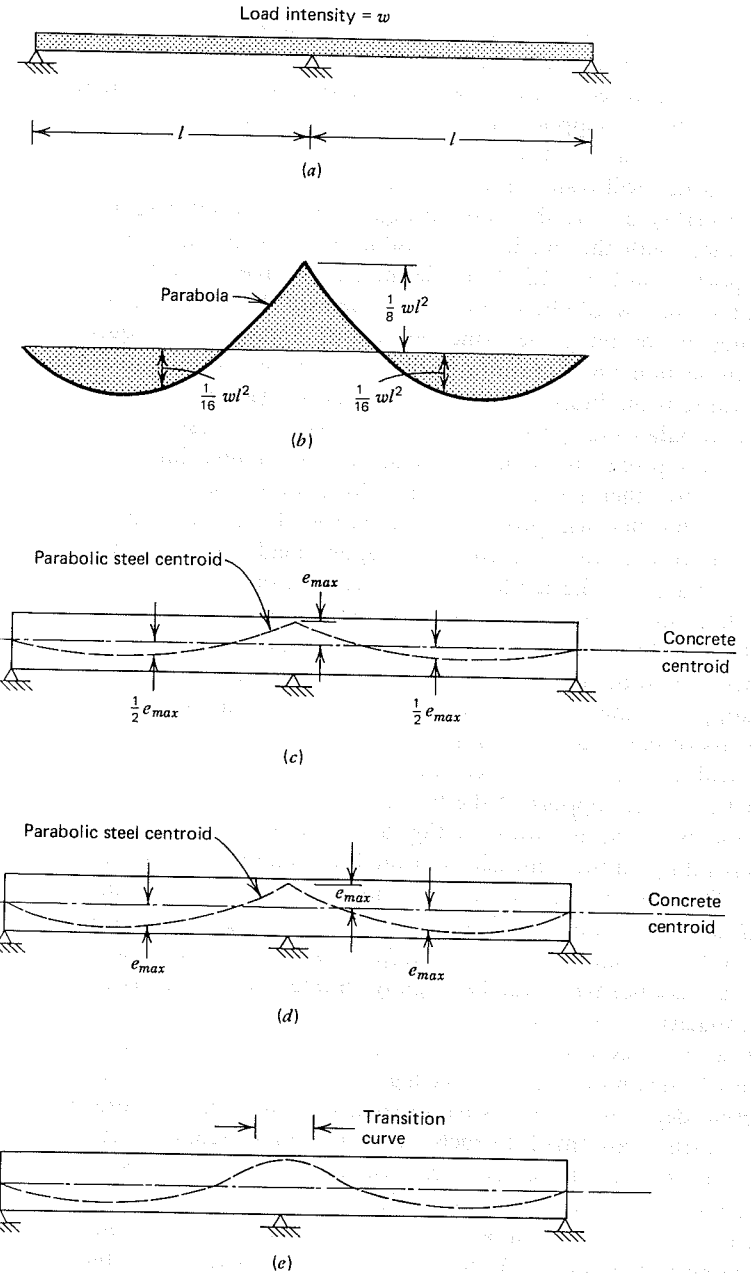

FIGURE 8.1 Basis for selecting tendon profile. (*a*) Loads. (*b*) Moment due to loads. (*c*) Tendon profile based on moment diagram. (*d*) Tendon profile based on maximum sag. (*e*) Practical tendon profile.

parabolically, reaching a maximum value of $wl^2/8$ at the central support. The moment at the center of each span is $wl^2/16$. Accordingly, a tendon might be selected for which the eccentricity varied parabolically, with maximum eccentricity over the central support, and eccentricity just one-half that amount at midspan, as shown in Fig. 8.1*c*.

Although this will result in a *concordant tendon*, as described in Section 8.7, it would probably not be the best arrangement. Economy would be improved using a tendon with the maximum possible eccentricity, at both midspan and center support, as in Fig. 8.1*d*. A smaller prestress force would be required, using such a profile, than would be necessary for the case shown in Fig. 8.1*c*. This may be confirmed by recalling the principle of load balancing, or equivalent loads, described in Section 4.6, that confirms that the prestress force required to balance a given loading is minimized by maximizing the sag (Refs. 8.7 and 8.8).

The load-balancing approach generally provides the best insight in determining the tendon profile for continuous beams, often revealing possibilities not clearly shown by other methods. Designing for load balancing, the engineer is led to select a profile that will produce equivalent loads on the beam that are equal and opposite to those resulting from the applied loads. A distributed load would be carried by a parabolic tendon, a set of concentrated loads by a segmentally linear tendon, and so on, as was true for the simple spans discussed in Section 4.6. At the simply supported ends of exterior spans of continuous beams, the eccentricity should be zero, because the load-induced moments are zero there. At interior supports, the eccentricity may be the maximum value permitted by requirements of concrete protection for the steel.

Practical considerations preclude the sharp change in the tendon slope shown at the center support of the beam of Fig. 8.1*d*. In real cases, a transition curve would be used, as shown in Fig. 8.1*e*. The length of the transition curve varies, depending on the dimensions of the beam and the flexibility of the tendon and duct. The difference in equivalent load produced by the idealized tendon of Fig. 8.1*d* and the more practical arrangement of Fig. 8.1*e*, with a transition curve, may be accounted for in the analysis, but is usually neglected. Although the service load behavior will be slightly different than assumed, the ultimate flexural capacity is not affected.

The several reversals of curvature typical of post-tensioning tendons for continuous beams may result in very high frictional losses. For slabs (Fig. 8.2*a*), the concrete depth is small relative to span lengths and, therefore, the required tendon curvatures are small. In such cases, continuous tendons may be used over three or four spans without excessive frictional losses. For other cases, special arrangements may be used to avoid difficulty.

For example, a two-span beam, such as that of Fig. 8.1*e*, might be tensioned from both ends simultaneously by using two jacks. Alternately, the beam might be jacked from only one end, but overtensioned temporarily to bring the tension in the farther span up to the desired value. After this, the jacking force is reduced to the specified initial level.

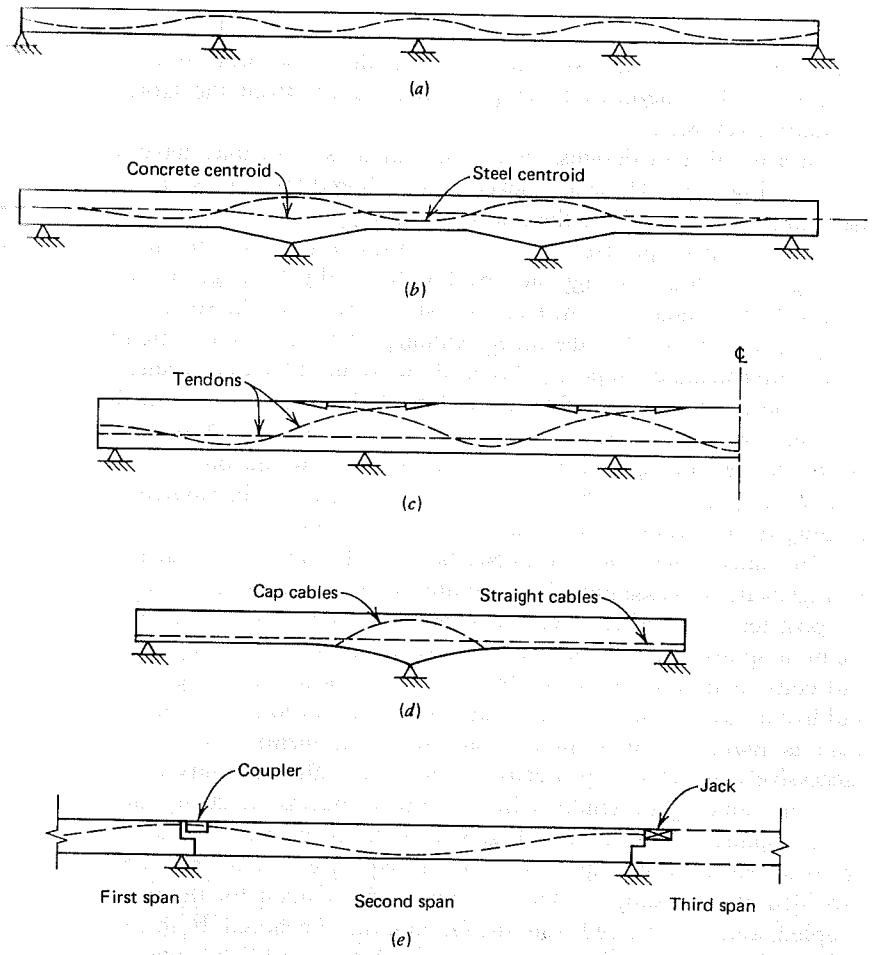

FIGURE 8.2 Tendon profiles for cast-in-place continuous beams. (*a*) Continuous tendons in slabs. (*b*) Beam with varying depth. (*c*) Use of intermediate anchorages. (*d*) Cap cables. (*e*) Span-by-span construction.

Other tendon arrangements for post-tensioned cast-in-place construction are shown in Fig. 8.2. The needed eccentricity of tendon may be achieved without excessive cable curvatures by curving the bottom flange of the girder, as in Fig. 8.2*b*. The effective eccentricity is the distance from the steel centroid to the concrete centroid, the depth of which varies as shown.

The overlapping intermediate anchorages of Fig. 8.2*c* reduce the length of the prestressing units and, thus, reduce frictional losses. The tendons are brought out of the upper surface of the beam. Long stressing cavities must be provided to accommodate the jacks and anchorages. These cavities are later filled with

unstressed concrete. It is usually necessary, when such a scheme is used, to place several straight tendons over the entire length of the beam initially to prevent cracking at the intermediate supports that results from the large effective eccentricity (Ref. 8.1).

In a number of designs, short discontinuous cap cables have been used, as shown in Fig. 8.2*d*. These are jacked and anchored in pockets cast in the soffit of the beam on either side of the intermediate supports.

Span-by-span prestressing of continuous beams may be accomplished by splicing of tendons, as suggested by Fig. 8.2*e*. High-strength bars are normally used, with threaded ends engaged by coupling sleeves. The spans are constructed and prestressed one after the other. Although the couplers are often located close to the intermediate supports, this leads to some difficulty because the tendons should be as close as possible to the top of the beam there, and the clearances required for splicing prevent this optimum arrangement. A better scheme is to locate the tendon splices at construction joints at the one-fifth points of the successive spans, where the individual tendons may be distributed vertically, still keeping the centroid of the group at the desired level.

In many cases, for continuous beams, the most economical and practical arrangement is to assemble the structure using precast pretensioned elements that are post-tensioned after assembly to provide for partial continuity. For short to medium spans, the elements span between supports, carrying their own weight and construction loads as simple spans. After post-tensioning, added dead load and live loads are carried by continuous action. For long span bridges, often each span is made up of a number of precast segments that are post-tensioned successively as erection proceeds. In this case, full continuity may be obtained.

The splicing of tendons in continuous beams made up of pretensioned precast spans is illustrated by Fig. 8.3*a*. After placing the precast elements, they are post-tensioned one span at a time in sequence, a temporary anchorage being provided at each support. The post-tensioning tendon for the next span is then coupled, and it is stressed from the far end, then anchored. In this way continuity may be provided for resisting superimposed dead and live loads.

Cap cables may also be used to join precast beams, as shown in Fig. 8.3*b*. These cables provide negative bending resistance over the intermediate supports, and the pretensioning provides for the positive moments in the spans.

The construction of a long span bridge by the cantilever method is illustrated by Fig. 8.3*c*. In this case short segments of the central span are precast or cast-in-place sequentially. The tendons that are necessary over the supports are successively curved downward into the webs of the girder and are anchored to the segments as they are progressively set in place, cantilevering outward toward midspan. Continuity cables start at the top of the girder, about at the points of contraflexure. These tendons curve downward to be at the bottom of the girder at midspan. They are tensioned and anchored in recesses formed into the top of the girder.

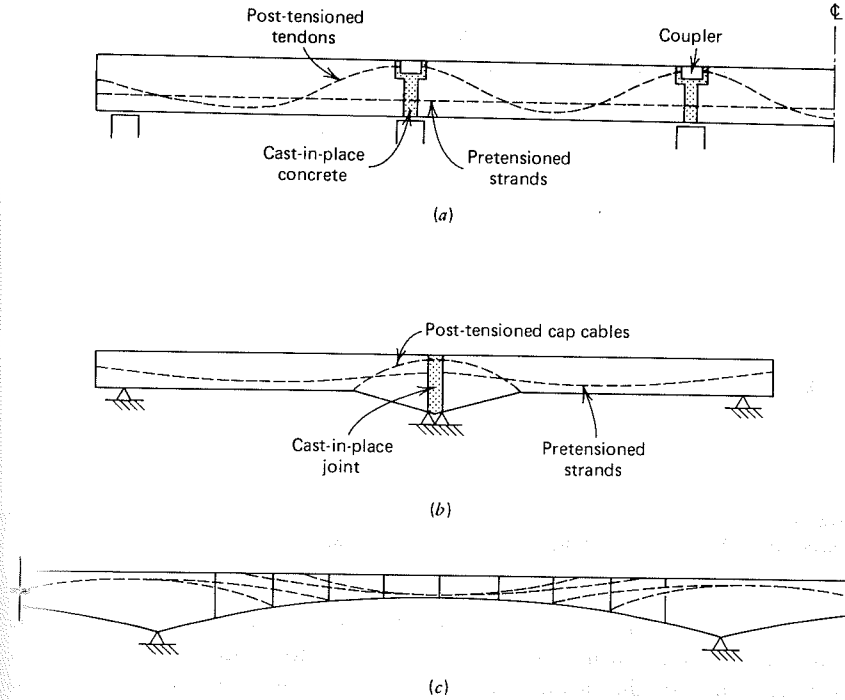

FIGURE 8.3 Tendon profiles for continuous beams using precast elements. (*a*) Coupled continuous tendons. (*b*) Cap cables at intermediate support. (*c*) Precast segments post-tensioned in sequence.

The variations are many, for both cast-in-place and precast construction, and considerable engineering ingenuity has been demonstrated in the development of special techniques. *For continuous members of all types, it is absolutely essential that provision be made for the axial shortening associated with post-tensioning.* Otherwise, the calculated prestress will not be attained.

8.3 ELASTIC ANALYSIS FOR THE EFFECTS OF PRESTRESSING

When an eccentric prestressing force is applied to a statically *determinate* beam, shown in Fig. 8.4, bending moments are induced, equal to the product of the force times the distance between the steel centroid and the concrete centroid. The beam will deflect when prestressed, usually cambering upward, but no external reactions are produced. If the effect of member self-weight is excluded from consideration, the compressive stress resultant C coincides with the centroid of the prestressing steel, as shown.

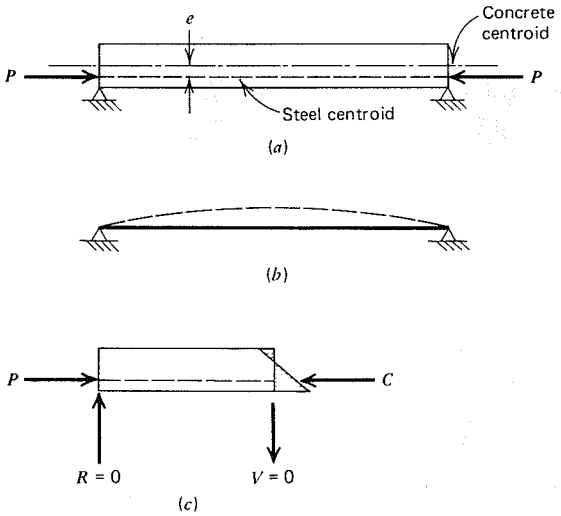

FIGURE 8.4 Statically determinate beam. (*a*) Beam profile. (*b*) Deflection due to prestressing. (*c*) Free-body diagram of portion of beam.

For a statically *indeterminate* beam, the action is more complex. The moment just described, which will now be referred to as the *primary moment*, causes a tendency for the beam to deflect as before, but it is restrained by the redundant system of supports. Reactions are produced at those supports, giving rise to *secondary moments* in the beam. In this case, the total moment produced at any section by prestressing is the sum of the primary and secondary moments.

The effect of prestressing a statically indeterminate beam may be understood with reference to Figs. 8.5 and 8.6. The beam of Fig. 8.5*a* is subjected to a prestressing force P with a constant eccentricity e. The primary bending moment Pe would cause the central part of the continuous beam to rise off its support, as in Fig. 8.5*b*, if it were free to do so. It is restrained against this displacement by the redundant support system, however. To provide this restraint, a downward force R is developed at the center support, as shown in Fig. 8.5*c*. This force is equilibrated by the reactions $R/2$ at each end of the continuous span. The actual deflected shape of the continuous beam, subjected to the prestressing force P, and constrained to zero deflection at all supports, is represented in Fig. 8.5*d*.

The support forces due to prestressing can be found using the classical method of superposition (Ref. 8.9). Appropriate redundant reactions are selected such that their removal will result in a statically stable and determinate primary structure. The redundants are replaced by unknown forces, and the values of these forces adjusted so that zero deflection is obtained at the corresponding support locations.

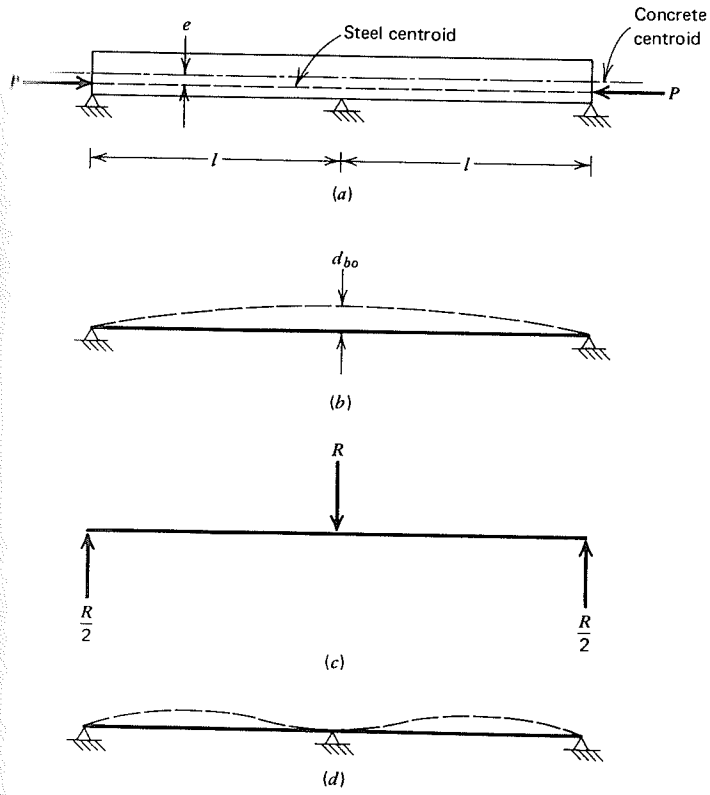

FIGURE 8.5 Forces and deflections for statically indeterminate beam. (*a*) Beam profile. (*b*) Deflection if center support were removed. (*c*) Reactions at supports due to prestressing. (*d*) Actual deflection due to prestressing.

For the present example, it would be convenient to treat the center support force as the redundant. With that redundant restraint removed, the deflection d_{bo} of Fig. 8.5*b*, resulting from the applied prestress force, can be found by any convenient method, such as moment-area, conjugate beam, virtual work, and so on. The force R of Fig. 8.5*c* is then found from the condition that it must produce an equal and opposite deflection, so that the sum of the two deflection components at that location is zero.

The bending moments for the beam of Fig. 8.5 are shown in Fig. 8.6. Since the eccentricity is constant, for this example the primary moment $M_1 = Pe$ is constant (Fig. 8.6*a*). The reactions resulting from prestressing produce the secondary moments $M_2 = Rl/2$ at the center support. Since the secondary moments of any continuous prestressed beam are caused by forces acting at the

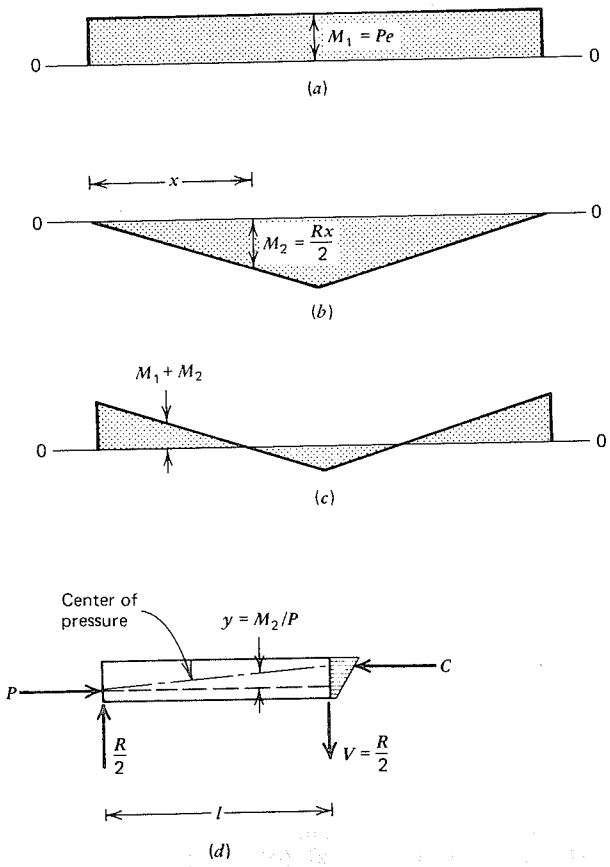

FIGURE 8.6 Moments and thrust line for a statically indeterminate beam. (*a*) Primary moments due to prestressing. (*b*) Secondary moments due to support reactions. (*c*) Total moments due to prestressing. (*d*) Free-body diagram of one-half of the beam.

supports only, these secondary moments must always vary linearly between the supports, as shown here.

The total moment due to prestressing the indeterminate beam is equal to the sum of the primary and secondary moments, and is shown in Fig. 8.6*c*. The points of zero bending moment may be identified with the points of inflection for the deflection curve of Fig. 8.5*d*.

The magnitude of the secondary moments in any given case depends on the particular tendon profile selected. For special cases, the secondary moments may be zero (see Section 8.7), but this is not usually so. They are often comparable to the primary moments, and in many cases may be larger, even though they are called secondary.

The centroid of the concrete stress distribution for a continuous beam will not, in general, be at the same level as the steel centroid, as was true for simple span beams, because of the existence of secondary moments. This is shown for the present example by the free-body diagram of Fig. 8.6*d*. The clockwise secondary moment, equal to the reaction $R/2$ the distance l to the center support, is equilibrated by the internal counterclockwise couple, consisting of the compressive resultant C times the lever arm to the steel centroid. Elsewhere along the span, the distance to the *center of pressure*, or *thrust line*, from the steel centroid varies linearly with distance from the support, as does the secondary moment M_2. Specifically, referring to Fig. 8.6*d*,

$$y = \frac{M_2}{P} \tag{8.1}$$

where y = distance from steel centroid to thrust line
M_2 = secondary moment due to prestressing
P = prestress force

Note that the primary moments are directly proportional to the prestress force. Consequently, the reactions due to prestressing, and the secondary moments are proportional to the prestress force, as are the total moments generated by prestressing. It follows that the displacement y of the thrust line from the steel centroid does not change as losses gradually reduce the prestress force from P_i to P_e. The location of the thrust line for a given steel profile is fixed.

The concrete stresses resulting from prestressing a continuous beam may be found from the equations of Section 3.4, except that e^*, the eccentricity of the thrust line with respect to the concrete centroid, must be substituted for e, the eccentricity of the steel centroid, because the center of compression no longer coincides with the center of tension. Thus, for a continuous beam, the longitudinal stresses in the concrete at the top and bottom face, resulting from initial prestress are

$$f_1 = -\frac{P_i}{A_c}\left(1 - \frac{e^* c_1}{r^2}\right) \tag{8.2a}$$

$$f_2 = -\frac{P_i}{A_c}\left(1 + \frac{e^* c_2}{r^2}\right) \tag{8.2b}$$

and, after all losses have occurred, the effective prestress force produces the concrete stresses

$$f_1 = -\frac{P_e}{A_c}\left(1 - \frac{e^* c_1}{r^2}\right) \tag{8.3a}$$

$$f_2 = -\frac{P_e}{A_c}\left(1 + \frac{e^* c_2}{r^2}\right) \tag{8.3b}$$

where e^* is the distance from the concrete centroid to the thrust line, and all other terms are previously defined. Note that e^* is negative when the thrust line is above the neutral axis.

The support reactions that result from prestressing a statically indeterminate beam produce shear forces, as well as bending moments, and these should be considered in the analysis.

An example of the calculation of secondary moments, thrust line, and stresses resulting from prestressing a continuous beam will be found in Section 8.5, following the development of an alternative approach to the analysis of such members.

8.4 EQUIVALENT LOAD ANALYSIS

The total moments resulting from prestressing a continuous member may be found directly, without considering the separate contributions of primary and secondary moments, by the method of equivalent loads. The equivalent loads produced by various prestressing tendon profiles were described in Section 1.3 (see also Fig. 1.8), and the use of the equivalent load approach in the design of statically determinate simple span beams was presented in Section 4.6.

The equivalent load approach is based on consideration of the vertical forces that are applied to a member wherever there is a change in the alignment of the prestressing tendons. These forces produce moments, just as any other system of external loads. The stresses resulting from these moments must be combined with the uniform axial compression P/A_c due to prestressing to obtain the total stresses at any section.

The concept of equivalent loads is particularly advantageous for continuous beams. The vertical forces that correspond to the particular tendon profile are found, making use of the relations developed in Sections 1.3 and 4.6. The structure can then be analyzed for the effects of these equivalent loads by using any of the available methods for indeterminate analysis, such as moment distribution or matrix analysis (Ref. 8.9).

For an indeterminate structure, the moments found from such an analysis are the *total moments* due to prestressing, and include the secondary moments due to support reactions as well as the primary moments due to tendon eccentricity. Secondary moments may be found, if needed, by subtracting the primary moments, easily determined, from the total moments obtained from the equivalent load analysis.

If the equivalent loads due to prestressing should be exactly equal and opposite to the applied loads, then all transverse forces cancel. For this unique balanced load condition, there are no bending moments applied to the beam. No flexural stresses exist, but only the axial stresses produced by the longitudinal component of the prestressing force. For such a condition, there are no displacements of the beam other than axial shortening, and the question of determinancy or indeterminancy becomes irrelevant (Refs. 8.7 and 8.8). Should the balancing load be removed or should an increment of load be added, moments must be found for the unbalanced portion of the load. To obtain the net concrete stresses, the stresses resulting from these moments may be added to the uniform compressive stress resulting from prestressing.

The equivalent load method simplifies the analysis and design of indeterminate beams by eliminating, in service load analysis, the need to calculate the reactions and secondary moments due to prestressing. When such secondary moments must be found, in connection with ultimate load analysis, the equivalent load method provides the most convenient way to obtain those secondary moments by subtracting the primary from the total moments. Furthermore, it is an aid to the designer in selecting the most advantageous tendon profile and in understanding the effects of linear transformation and concordancy of tendons, discussed in Sections 8.6 and 8.7.

Although the method of superposition of deflections first described is quite convenient where there are only one or two redundant reactions, for more highly indeterminate members, the method of equivalent loads permits a more systematic solution, and is better suited for use with existing computer programs.

8.5 EXAMPLE: INDETERMINATE PRESTRESSED BEAM

The two-span rectangular beam of Fig. 8.7*a* has width $b = 12$ in. and total depth $h = 22$ in. It is prestressed using a continuous tendon with a parabolic profile in each span, with eccentricities as indicated. The beam will carry an effective prestress force P_e, after all losses, of 200 kips. Differences in tension along the span due to friction may be neglected. Find the primary, secondary, and total moments resulting from prestressing, as well as the support reactions and location of the thrust lines: (1) using the method of superposition of deflections, and (2) using the method of equivalent loads. Find the concrete stress at support B due to prestressing. ($b = 305$ mm, $h = 559$ mm, $e = +152, -152, +152$ mm, span $= 2 \times 0.14$ m, and $P_e = 890$ kN.)

(1) METHOD OF SUPERPOSITION

The primary moments resulting from the prestress force are easily found by multiplying the eccentricities of Fig. 8.7*a* by the prestress force of 200 kips, assumed constant over the full 60-ft length. The resulting primary moments are given by Fig. 8.7*b*.

The given structure is indeterminate to the first degree. Following the usual procedure for the method of superposition, a redundant is selected such that its removal will leave a stable and determinate primary structure. In this case, the reaction at B will be treated as redundant; the primary structure becomes a single-span beam, simply supported at A and C.

This primary structure will first be subjected to the moments M_1 due to prestressing, and the deflection found at point B. This deflection is numerically

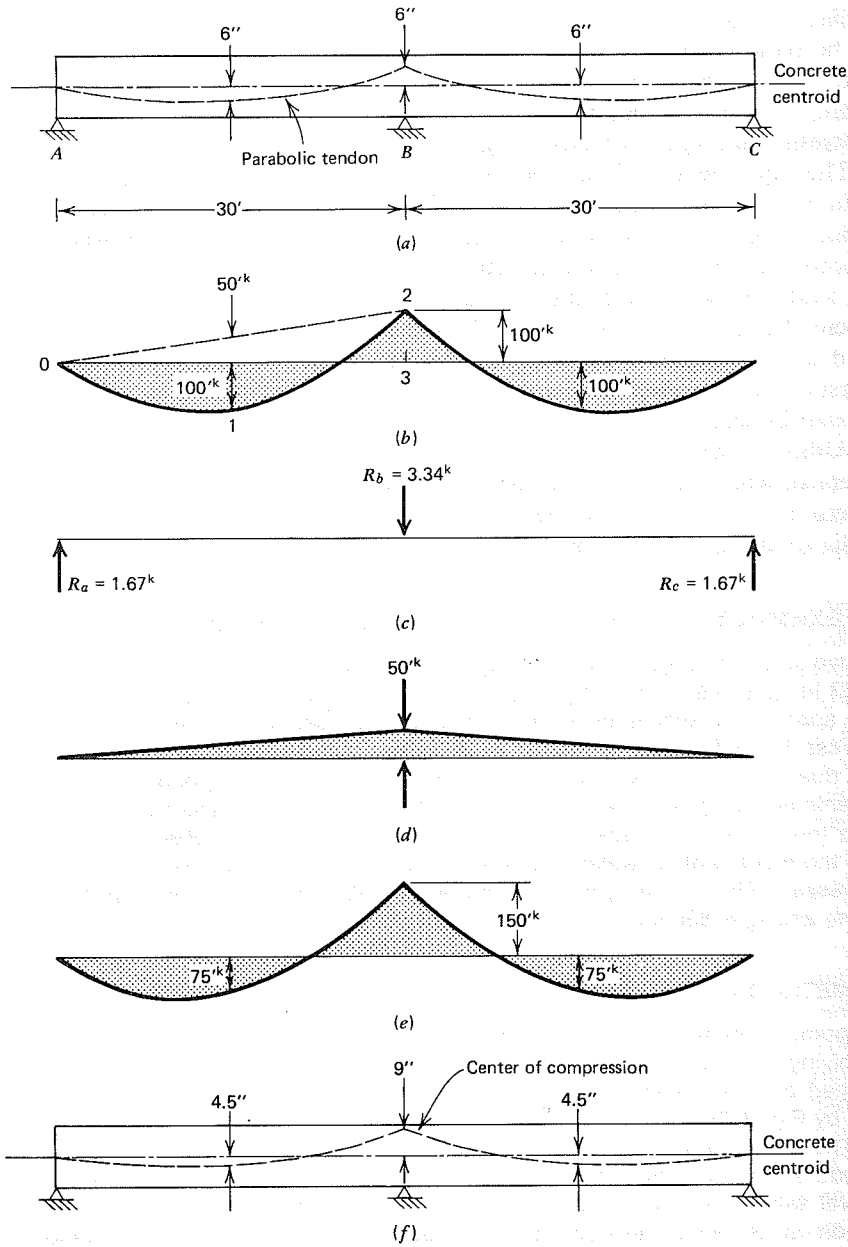

FIGURE 8.7 Indeterminate beam analysis by method of superposition. (*a*) Beam profile. (*b*) Primary moments M_1. (*c*) Reactions due to prestress. (*d*) Secondary moments M_2. (*e*) Total moments $M_1 + M_2$. (*f*) Thrust line due to prestress.

equal to the distance of point A, on the elastic curve, from the horizontal tangent to the elastic curve through point B. This can easily be found using the second moment-area principle (Ref. 8.9). First, it is convenient, in taking moments of the M/EI area, to divide the diagram for span AB into the positive area included within the parabola 012 and the negative triangular area 023 (Fig. 8.7*b*). Then, when we take moments about A, the deflection sought is equal to

$$d_{bo} = \frac{1}{EI}[(150 \times 30 \times \tfrac{2}{3} \times 15) - (100 \times 30 \times \tfrac{1}{2} \times 20)]$$

$$= \frac{15{,}000}{EI} \text{ ft}$$

upward; that is, the beam would rise off the support B if not restrained by a still-unknown downward force R_b at that point.

Next, the primary structure of span AC will be subjected to the unknown reaction R_b with corresponding reactions at A and C of $R_b/2$, as shown by Fig. 8.7*c*. The resulting moment diagram is linear, of the shape shown by Fig. 8.7*d*, with a maximum value $15R_b$. The downward deflection of point B due to the force R_b is

$$d_{bb} = \frac{1}{EI}(15R_b \times 30 \times \tfrac{1}{2} \times 20) = \frac{4{,}500}{EI} R_b$$

For satisfaction of the condition of compatibility, the upward deflection due to the primary prestressing moments d_{bo} must equal d_{bb}, the downward deflection due to R_b, that is, the net deflection must be zero at the support. Thus

$$4{,}500R_b = 15{,}000$$

$$R_b = 3.34 \text{ kips}$$

$$R_a = R_c = 1.67 \text{ kips (7.43 kN)}$$

The secondary moment M_2 varies linearly from 0 at the exterior supports to the value of $1.67 \times 30 = 50$ ft-kips at support B, as indicated by Fig. 8.7*d*. These secondary moments are superimposed on the primary moments M_1, to obtain the total moments due to prestressing shown in Fig. 8.7*e*.

The thrust line resulting from the application of prestress is presented in Fig. 8.7*f*. Its location is found by computing distances from the steel centroid line using Eq. (8.1). Thus, at B, the center of compression is

$$y_b = \frac{50 \times 12}{200} = 3 \text{ in. (76 mm)}$$

above the steel centroid, or 9 in. above the concrete centroid. Similar calculations indicate that at midspan the thrust line is 1.5 in. above the steel centroid or 4.5 in. below the concrete centroid. The deviation of the thrust line from the steel centroid varies linearly from 0 at the exterior supports to 3 in. at the center support.

The location of the thrust line may also be found directly, from the total moments of Fig. 8.7*e*, by using the condition that these moments are produced by the compressive resultant, acting at its own eccentricity e^* from the concrete

centroid. Thus, at B,

$$e^* = \frac{150 \times 12}{200} = 9 \text{ in. (229 mm)}$$

and, at midspan,

$$e^* = \frac{75 \times 12}{200} = 4.5 \text{ in. (114 mm)}$$

The concrete stresses at the top and bottom face at B are found using Eqs. (8.3*a*) and (8.3*b*). With $A_c = 264$ in.^{2}, $I_c = 10{,}600$ in.^{4}, and $r^2 = 40.2$ in.^{2} these stresses are, respectively,

$$f_1 = -\frac{200{,}000}{264}\left(1 + \frac{9 \times 11}{40.2}\right) = -2{,}620 \text{ psi } (-18.1 \text{ MPa})$$

$$f_2 = -\frac{200{,}000}{264}\left(1 - \frac{9 \times 11}{40.2}\right) = +1{,}110 \text{ psi } (+7.7 \text{ MPa})$$

(2) METHOD OF EQUIVALENT LOADS

The same results may be found by using the method of equivalent loads. From Eq. (4.27) of Section 4.6, is known that a parabolic tendon having total sag y will produce a uniformly distributed upward load on a member equal to

$$w_p = \frac{8Py}{l^2} \qquad (4.27)$$

For the present case, the sag, measured with respect to a line between tendon locations at the supports of either span, is 9 in. Thus,

$$w_p = \frac{8 \times 200 \times 9}{30^2 \times 12} = 1.33 \text{ kips / ft } (19.4 \text{ kN / m})$$

acting upward, as in Fig. 8.8*a*. The two-span indeterminate beam will be analyzed for this load, using the method of moment distribution (Ref. 8.9). Fixed end moments at the left and right ends of each span are $1.33 \times 30^2/12 = 100$ ft-kips. These are recorded, with appropriate signs, in Fig. 8.8*b*. Two cycles of moment distribution are executed to obtain the final moments of 0 at the exterior supports and 150 ft-kips at the center support. The final moment diagram is given in Fig. 8.8*c*. These are the total moments due to prestressing, and include the contributions of both primary and secondary moments. Primary moments are easily found, multiplying the tendon eccentricity by the value of P_e, and are shown in Fig. 8.8*d*. Secondary moments are determined by subtracting primary from total moments, and are given by the diagram of Fig. 8.8*e*. All results are identical to those obtained by the method of superposition. The thrust line and concrete stresses are found just as before.

With the total effect of prestressing established, there is little difficulty in superimposing the effects of other loads to establish net moments and stresses at any location.

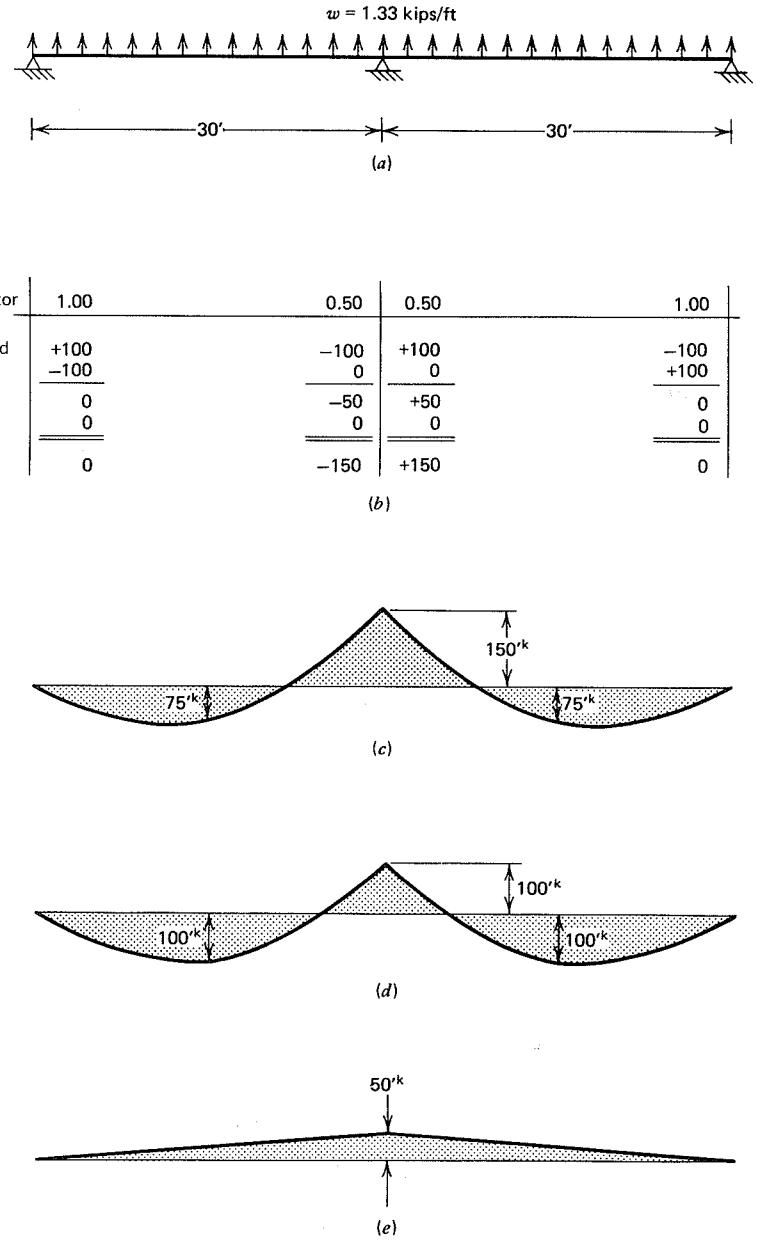

FIGURE 8.8 Indeterminate beam analysis by the method of equivalent loads. (*a*) Equivalent load from prestressing. (*b*) Analysis by moment distribution. (*c*) Total moments M. (*d*) Primary moments M_1. (*e*) Secondary moments $M_2 = M - M_1$.

8.6 LINEAR TRANSFORMATION

It will be noted, from the review of Sections 8.3 and 8.4, that the thrust line, locating the center of pressure in any span of an indeterminate beam, has the same basic shape as the steel centroid line in that span. Its profile may be obtained by rotating the profile of the steel centroid line an appropriate amount about its end. This is so because the deviation of the thrust line from the steel centroid is directly proportional to the secondary moment, which in turn varies linearly with distance from the support.

This procedure, by which a line of given characteristic shape is rotated about one end or the other, without changing that shape within the span, is known as *linear transformation*. The thrust line is said to be a linearly transformed version of the steel centroid line.

It is an interesting fact, of considerable practical importance, that *any steel profile may be linearly transformed to a new position in a span, yet produce exactly the same thrust line as before*. The reactions induced by prestressing will differ for different steel profiles, and the secondary and primary moments will be different, but the total moment, that is, the sum of the primary and secondary moments, will be unchanged. Consequently, the thrust line must be in the same position.

This will be illustrated by the beams of Figs. 8.9 and 8.10. In each case, all conditions are the same as for the beam shown in Fig. 8.7, except that linearly transformed versions of the original steel profile are used.

The beam of Fig. 8.9*a* uses a parabolic tendon in each span with the same 9 in. sag as before. However, the steel centroid passes through the concrete centroid at the center support B, as well as at the exterior supports A and C. The analysis was performed using the method of superposition. The primary moments M_1 of Fig. 8.9*b*, when applied to the beam, require the reactions shown in Fig. 8.9*c* to maintain zero support deflections. The secondary moments of Fig. 8.9*d*, when superimposed upon the primary moments, produce the total moments due to prestressing, shown in Fig. 8.9*f*. These are seen to be identically the same as the final moments obtained for the same beam, with the tendon profile shown in Fig. 8.7*a*. The thrust line, shown in Fig. 8.9*f*, is also identically the same as before.

Another alternative design is shown in Fig. 8.10*a*. Again, a parabolic tendon with the same 9 in. sag is used, but in this case with 9 in. eccentricity at the center support. Primary moments are obtained and shown in Fig. 8.10*b*. For this particular moment diagram, analysis by the method by superposition indicates that there is no tendency for the beam to move up or down from its support at B, that is, the deflection at B of the primary structure AC, when loaded with moments M_1, is zero. As a result, there are no induced reactions and no secondary moments. The total moments of Fig. 8.10*e* are identical to the primary moments of Fig. 8.10*b*. Once again, the same thrust line is obtained, because the final moments due to prestressing are the same as in the previous two cases.

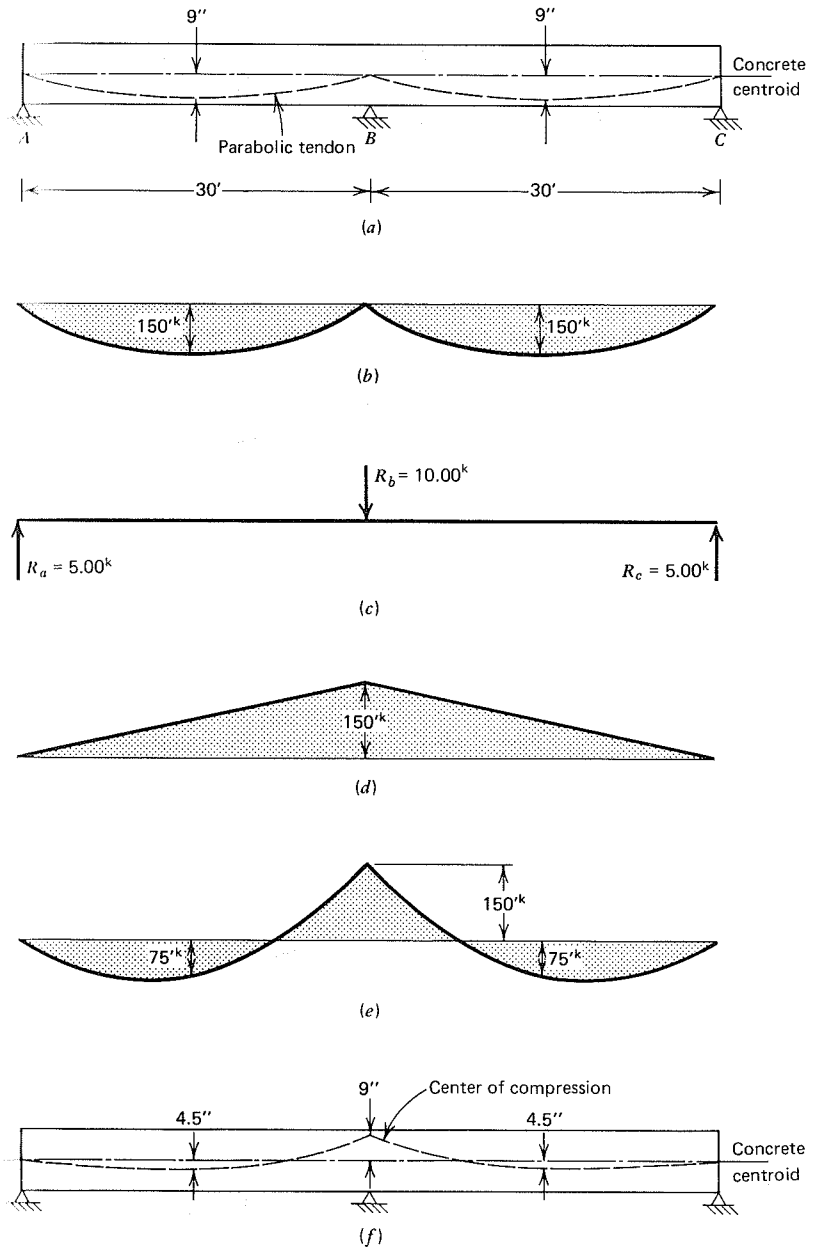

FIGURE 8.9 Indeterminate beam with modified tendon profile. (*a*) Beam profile. (*b*) Primary moments M_1. (*c*) Reactions due to prestress. (*d*) Secondary moments M_2. (*e*) Total moments $M_1 + M_2$. (*f*) Thrust line due to prestress.

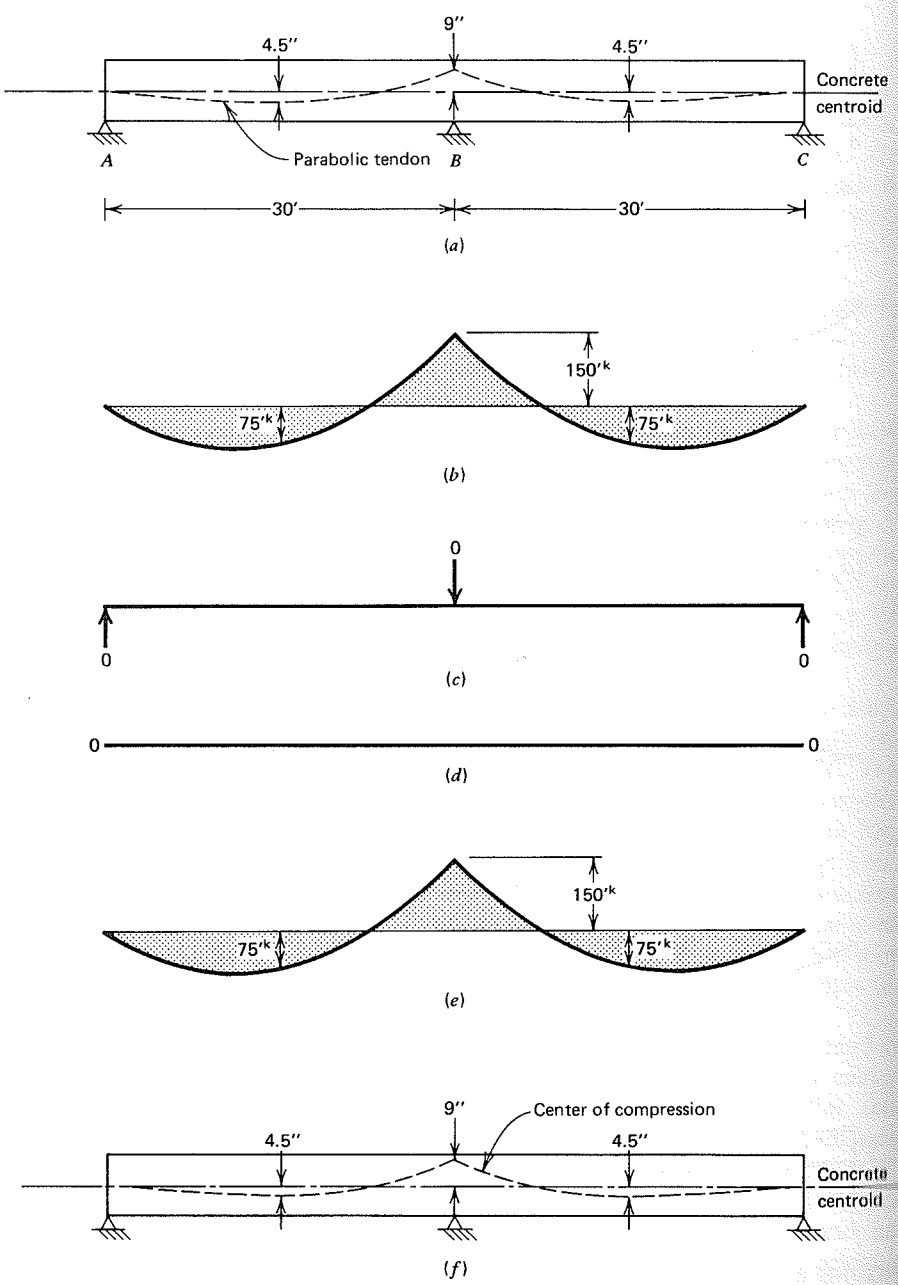

FIGURE 8.10 Indeterminate beam with concordant tendon. (*a*) Beam profile. (*b*) Primary moments M_1. (*c*) Reactions due to prestress. (*d*) Secondary moments M_2. (*e*) Total moments $M_1 + M_2$. (*f*) Thrust line due to prestress.

Figures 8.7, 8.9, and 8.10 should be studied carefully and compared. Primary moments, prestress reactions, and secondary moments are completely different in each case, yet the same thrust line is obtained and, consequently, the same concrete stresses will be produced by prestressing.

The examples confirm that a tendon profile may be linearly transformed without modifying the thrust line produced. This is always true. Although the reason may not be immediately evident, it will become so after consideration of equivalent loads. The same tendon shape was used for all three cases. The equivalent upward load, 1.33 kips per foot, was unchanged by the small rotations of the steel centroid line. Consequently, the total moments, obtained from that equivalent load, must be the same in all three cases, even though the primary and secondary moments must differ.

It is a necessary restriction that the transformed steel centroid line must still intersect the concrete centroid at the freely supported ends of continuous spans. Changes in the eccentricity at the free end would produce changes in the moment applied at the beam end. This represents a modification of the equivalent load, which would produce a different diagram of total moment and different thrust line.

The concept of linear transformation is of great use to the designer of prestressed concrete structures, because it permits the relocation of the steel centroid, as may be desirable to maintain adequate concrete cover for the tendon, for example, without changing the thrust line or the concrete stresses in the structure.

8.7 CONCORDANT TENDONS

The tendon profile selected for use in the beam of Fig. 8.10 was unique because, for that particular tendon, no reactions were generated by prestressing and, consequently, no secondary moments were developed. The thrust line produced by prestressing coincided with the steel centroid line, as would be the case for a simple span, statically determinate beam. Such a tendon is called a concordant tendon.

There are any number of concordant tendons possible for a given continuous prestressed concrete beam. The most obvious one is a steel profile that coincides everywhere with the concrete centroid. For this case, no primary bending moments are generated by prestressing and so no support reactions are possible, and no secondary moments. This observation is of limited practical use, because centroidally prestressed beams are generally highly uneconomical.

The beam examples of Figs. 8.7, 8.9, and 8.10 suggest another basis for concordancy: a tendon that coincides with the thrust line obtained using a nonconcordant tendon is itself a concordant tendon. The steel profile used for the example of Fig. 8.10 was selected this way, and for that profile, no prestress reactions and no secondary moments were found. The proof of concordancy for such a tendon is simple. It has been shown that the thrust line in any given case is

a linearly transformed steel centroid line. Any other linearly transformed version of the steel centroid line would produce identically the same thrust line, *including the one that matches the thrust line itself*. Consequently, a tendon that follows that thrust line is concordant.

Actually, *any valid moment diagram for a continuous member provides the basis for a concordant tendon profile*, with the steel eccentricity taken equal to a constant times the moment ordinate at any point. This too may be simply proved. For any arbitrary system of loads, the moment diagram for the span in question is obtained on the basis that there is no deflection at the supports. If the beam deflections were to be calculated at the supports, using moment-area theorems or other means, those deflections would be zero. A steel centroid line that has eccentricities directly proportional to the ordinates of any such moment diagram would produce primary moments varying this same way. Support deflections of the primary structure, acted upon by those moments, would also be zero. No reactions or secondary moments would be produced by prestressing, and the requirements for concordancy would be satisfied.

Although use of a concordant tendon in a given instance offers the possibility of simplified analysis, there is little practical advantage in terms of structural behavior. The most economical design in a given case is usually obtained with the steel centroid as high as possible over the supports, and as low as possible near midspan, an arrangement that will not generally result in a concordant tendon.

8.8 CONCRETE STRESSES IN THE ELASTIC RANGE

There is no special difficulty associated with the calculation of concrete stresses for the initial and service load stages for indeterminate prestressed beams. The moments M_o, M_d, and M_l due respectively to member self-weight, superimposed dead load, and service live load must be found for each of the sections of interest by an analysis that accounts for the effects of continuity. As for any indeterminate structure, a continuous prestressed concrete beam or frame must be analyzed for alternate live loadings to determine the maximum moments at all critical sections. The investigation of minimum moments in the spans should not be neglected, as they may be of sign opposite to the maximum moments.

For initial conditions, immediately after transfer, the effect of prestressing is found using Eqs. (8.2*a*) and (8.2*b*). At midspan, where gravity moments are generally positive, the stress in the concrete at the top and bottom faces of the beam are, respectively,

$$f_1 = -\frac{P_i}{A_c}\left(1 - \frac{e^*c_1}{r^2}\right) - \frac{M_o}{S_1} \tag{8.4a}$$

$$f_2 = -\frac{P_i}{A_c}\left(1 + \frac{e^*c_2}{r^2}\right) + \frac{M_o}{S_2} \tag{8.4b}$$

The same equations apply for the negative bending regions near the supports, except that the sign of the stress associated with M_o is reversed in each case. The eccentricity of the thrust line e^* is negative if measured upward from the concrete centroid; otherwise, it is positive.

At the full service load stage, when all prestress losses are assumed to have already occurred, concrete stresses due to prestressing are found based on Eqs. (8.3*a*) and (8.3*b*), and stresses due to the total service load are superimposed. With $M_t = M_o + M_d + M_l$, the resulting stress in the positive bending region at the top and bottom faces of the concrete are, respectively

$$f_1 = -\frac{P_e}{A_c}\left(1 - \frac{e^*c_1}{r^2}\right) - \frac{M_t}{S_1} \tag{8.5a}$$

$$f_2 = -\frac{P_e}{A_c}\left(1 + \frac{e^*c_2}{r^2}\right) + \frac{M_t}{S_2} \tag{8.5b}$$

As before, the sign of the stress associated with the gravity moments must be reversed in determining net stress in the negative bending regions.

According to ACI Code, service load stresses may be based on the properties of the uncracked concrete section, even though the nominal concrete tensile stress may be as high as $12\sqrt{f_c'}$, well above the modulus of rupture.

The method of load balancing offers considerable simplification in determining the concrete stresses within the elastic range. The equivalent load that results from prestressing may be easily found, referring to Sections 1.3 and 4.6. If the external loads acting are just equal and opposite to the equivalent loads, then there is no bending, no flexural stress, and no deflection (except axial) of the continuous member. Consequently, an indeterminate analysis becomes unnecessary. The net stress in the concrete is simply uniform compression, P_e/A_c, for the balanced load stage. Often this load state is that produced by effective prestress plus total dead load.

When the service live load is applied, bending of the continuous member results, and the concrete stresses resulting from that increment of load must be found by an analysis that accounts for continuity. These flexural stresses must be superimposed at any section on the axial compression produced by the balanced loading.

Although the method of load balancing avoids the immediate need to calculate reactions and secondary moments due to prestressing, they must eventually be found to evaluate the factor of safety against collapse. Secondary moments and shears from prestressing may add to, or subtract from, the moments and shears due to gravity loads.

8.9 FLEXURAL STRENGTH

The ultimate flexural strength should always be checked, for continuous prestressed concrete beams, just as for simple spans, because the desired degree of safety against collapse is not automatically insured by satisfaction of stress limits at service load. Load factors, such as those of the ACI Code, are applied to the calculated dead loads and service live loads to obtain the minimum hypothetical overload that the member should be capable of resisting. Moments corresponding to these overloads are determined at all critical sections, and compared with the flexural strength of the beam at those sections. The moment analysis may be performed by using any of the standard methods for continuous beams and frames. The strength of sections in flexure, in turn, can be found by the methods of Sections 3.7 and 3.8, incorporating the usual strength reduction factors.

For several reasons the load-balancing approach to the analysis of continuous members is not useful at overload stages or incipient failure. When overloaded, the member is well beyond the range of elastic response, and the superposition of stresses, which is implicit in load balancing, is not valid. Also, the equivalent loads computed for load-balancing analysis are usually determined for the effective prestress force P_e, which is assumed to have constant value along the span and to remain unchanged as loads are applied. These conditions are at least approximately met up to service load, but not much beyond that stage. When the beam is severely overloaded, the stress in the tendon increases, the amount of the increase depending on the location along the span, whether or not the tendons are grouted or otherwise bonded to the concrete, and the extent of concrete cracking. Any calculation of equivalent load would have to recognize this change in tendon stress, a procedure that would involve great practical difficulty.

For any indeterminate structure, moments may be found based on an elastic analysis, or based on the assumption of some degree of plastic behavior. Plastic analysis assumes the formation of one or more *plastic hinges* at critical moment sections, followed by some amount of *redistribution of the elastic moments*, until finally a collapse mechanism is formed. This type of analysis, for prestressed concrete structures, will be discussed in Section 8.10.

It is conservative to perform the strength analysis based on elastic moments. The moments at all sections are considered to increase linearly with load until, at some location, the capacity of the beam or frame is reached, establishing the failure load. This procedure is conservative, in that it neglects the capacity of almost all beams and frames to redistribute moments, to some extent, before actual collapse. For concrete structures it is also inconsistent, because the flexural strength of individual sections is computed on the basis of nonlinear, inelastic material behavior, even though the beam or frame is assumed to respond elastically. However, because of the difficulty in predicting rotation capacities, present United States practice for both reinforced and prestressed concrete members follows essentially this procedure. It is always on the safe side to neglect moment redistribution. The actual failure load would not be less, and may be substantially more, than that computed.

Thus, the ultimate moments that must be resisted may be found, for the factored loads, by using any of the well-known methods for analysis of elastic beams and frames. Ordinarily, for solutions performed using a hand calculator, the method of moment distribution is used, whereas for computer solutions the matrix methods, incorporated in a wide selection of software, are almost universally adopted (Ref. 8.9).

In either case, members are represented by their centerlines. Moments of inertia, upon which member stiffnesses are based, may be computed for the uncracked concrete sections, neglecting the influence of the steel and cracking. Provided that a consistent set of assumptions is adopted for all members of the indeterminate structure, no significant error will result from this, because it is the relative stiffnesses of the members that are of consequence, not the absolute stiffnesses, in determining moments.

Loads to be included in the elastic flexural analysis are the member self-weight, the superimposed dead loads, and the live loads, each with the appropriate load factor specified by the Code. It has been pointed out already that load balancing is not appropriate at the ultimate load stage and, therefore, equivalent loads due to prestressing are not to be included.

The proper treatment of secondary moments in factored-load analysis of indeterminate prestressed structures has been the subject of much debate (Refs. 8.10 to 8.15). In the 1971 ACI Code, it was stated that the effect of moments due to prestressing, including secondary moments, shall be neglected when calculating the factored-load moments to be resisted. The accompanying ACI Code Commentary stated that the secondary moments produced by the prestress force in a nonconcordant tendon disappear at the capacity at which, because of plastic hinge formation, the structure becomes statically determinate. Therefore, according to that edition of the Code and Commentary, factored moments at the critical sections of a continuous prestressed beam are only those resulting from dead and live loads. However, elsewhere in the Code, it was stated that behavior shall be determined by elastic analysis with only a modest amount of redistribution of moments due to plastic hinging permitted.

That such a procedure is inconsistent and, in some cases, unsafe, was pointed out in Refs. 8.10 to 8.13 and elsewhere. The secondary moments generally continue to act, possibly at their full value, as the load is increased, and may influence the moments at all sections of a structure through the full range of loads up to failure.

The only circumstances under which it can be certain that secondary moments disappear are when full moment redistribution can be assured through formation of plastic hinges that have adequate rotation capacity. The procedure established by the 1971 ACI Code, where only limited rotation was permitted at

critical sections, on the one hand, but secondary moments were ignored, on the other hand, was clearly erroneous.

But the final value of secondary moments is uncertain. It has been pointed out that the secondary moments, which depend on the external reactions caused by prestressing a statically indeterminate beam, undoubtedly change as the beam stiffness changes because of flexural and other cracking. They are further modified by time-dependent effects, and even limited inelastic rotation at the more highly stressed sections will have some influence on reactions and the resulting moments.

The 1971 error was corrected in the 1977 ACI Code. The 1983 Code requires consideration of secondary moments, using a load factor of 1.0, up to and including the ultimate load. But it should be noted that, in many practical cases, secondary moments *reduce* moments due to gravity loads at some sections. In this case, a more conservative procedure would be to account for secondary moments when their sign increases design moments, but to disregard them when they are of opposite sign.

Presently, most designers probably calculate secondary moments based on the effective prestress force P_e, and include these moments with load factor of 1.0, according to ACI Code, when checking strength provided against the required strength at critical sections. However, Code procedures may not represent the last word on this controversial topic.

8.10 MOMENT REDISTRIBUTION AND LIMIT ANALYSIS

If the loads acting on an indeterminate structure should gradually be increased, the limiting flexural capacity will eventually be reached at one (or possibly more than one) section of the structure. If the member at that location possesses the capacity to rotate plastically, at a resisting moment that is essentially constant, then *redistribution of moments* is possible. If the loads produce a sufficient number of *plastic hinges* in a given case, then a collapse mechanism will form, and the collapse load can be calculated on the basis that each hinging section provides a resistance equal to its flexural strength. After the formation of one or more plastic hinges, the ratios between moments at the critical sections will no longer be the same as the elastic moment ratios.

The principles of limit analysis, based on plastic behavior, are well known and will not be developed in detail here (see Ref. 8.16). The essential aspects can be demonstrated by the simple example shown in Fig. 8.11. Figure 8.11*a* shows a single span beam with fixed support at the left end and roller support at the right, the structure thus being indeterminate to the first degree. It carries a single concentrated load at midspan. That load is increased gradually until the elastic bending moment at the fixed support, $3/16Pl$, is just equal to the plastic moment

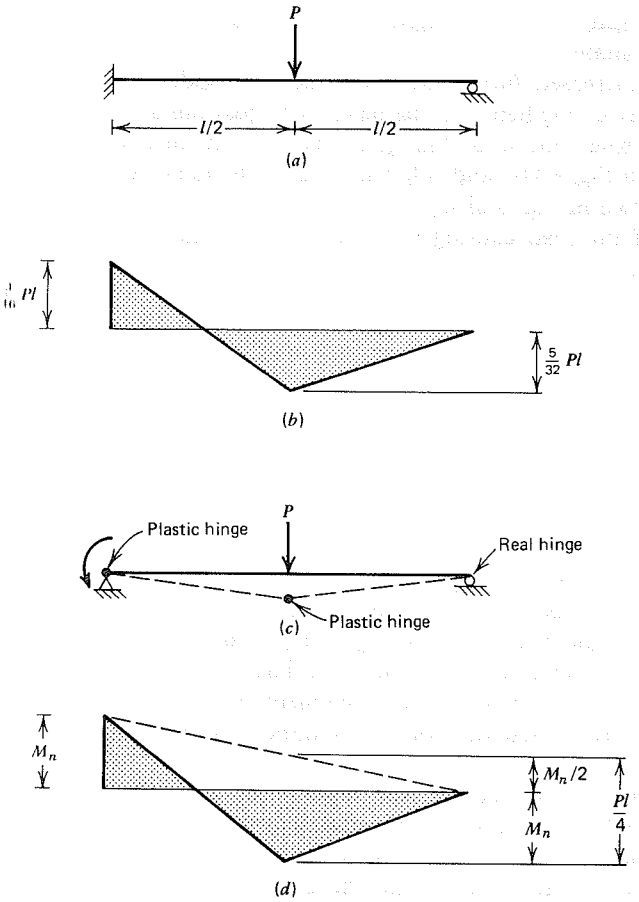

FIGURE 8.11 Moment redistribution in statically indeterminate beam. (*a*) Indeterminate beam. (*b*) Elastic moment diagram. (*c*) Collapse mechanism. (*d*) Plastic moment diagram.

capacity of the beam section M_n. This load is

$$P = \frac{16M_n}{3l} = 5.33\frac{M_n}{l} \qquad \text{(a)}$$

At this stage the positive moment under the load is $5/32Pl$, as shown in Fig. 8.11*b*. The beam still responds elastically everywhere but at the left support, where plastic rotation occurs. At that point, the actual fixed support can be replaced for analysis with a plastic hinge offering a known resisting moment M_n.

Because a redundant reaction has been replaced by a known moment, the beam is now statically determinate.

The load can be increased further until the moment under the load also becomes equal to M_n (assuming here that the beam has equal capacity in positive and negative bending), where the second hinge forms. The structure then forms a mechanism, as shown in Fig. 8.11*c*, and collapse occurs. The moment diagram at the collapse load is shown in Fig. 8.11*d*.

The magnitude of the load causing collapse is easily calculated from the geometry of Fig. 8.11*d*:

$$M_n + \frac{M_n}{2} = \frac{Pl}{4}$$

from which

$$P = \frac{6M_n}{l} \qquad \text{(b)}$$

By comparing Eqs. (a) and (b), it is evident that an increase in P of 12.5 percent is possible for this example, beyond that load that caused the formation of the first plastic hinge, before the beam will actually collapse. Because of the formation of plastic hinges, a redistribution of moments has occurred such that, at failure, the ratio between positive and negative moments is equal to the ratio of resisting moments *provided* in designing the beam, rather than the ratio of elastic moments.

There is a direct relation between the amount of redistribution to be achieved and the amount of plastic rotation required at the critical sections of a beam to produce the desired redistribution. In general, the greater the modification of the elastic moment ratio, the greater the rotation capacity required to accomplish this change. If the beam of Fig. 8.11 had been designed with resisting moments consistent with the elastic moment diagram of Fig. 8.11*b*, no rotation would have been required at the two critical sections, and the beam would (theoretically) have yielded at the same instant at the left support and at midspan. On the other hand, if the resisting moment at the left support had been deliberately reduced (and the resistance at midspan correspondingly increased), then substantial plastic rotation at the support would have been required before the strength at midspan could be realized.

The simple example chosen illustrates clearly the difference between elastic moment analysis and plastic moment analysis, and the necessity for plastic rotation capacity at the location of hinges if the failure load predicted by plastic analysis is to be achieved. Plastic analysis is widely used for steel structures, where rotation capacity is usually adequate because of the great ductility of the steel. It has not been generally accepted for reinforced or prestressed concrete

structures, because of the more limited amount of rotation that can be achieved at the hinging sections, and the practical difficulty of predicting the rotation capacity that is available in specific cases.

It has been shown experimentally and analytically that prestressed concrete sections with relatively small amounts of steel are capable of substantial plastic rotation, whereas those with relatively large amounts of steel behave in a more brittle fashion. Accordingly and in lieu of more exact calculations of rotation requirements and capacities, the ACI Code permits a limited amount of redistribution of elastic moments depending on the reinforcement index. Defining

$$\omega = \frac{\rho f_y}{f_c'} \qquad \text{where } \rho = \frac{A_s}{bd}$$

$$\omega' = \frac{\rho' f_y}{f_c'} \qquad \text{where } \rho' = \frac{A_s'}{bd}$$

$$\omega_p = \frac{\rho_p f_{ps}}{f_c'} \qquad \text{where } \rho_p = \frac{A_p}{bd_p}$$

according to the ACI Code, negative moments calculated by elastic theory for any assumed loading arrangement may be increased or decreased by not more than the following percentages:

For rectangular sections with prestressing steel only:

$$\text{Percent} = 20\left[1 - \frac{\omega_p}{0.36\beta_1}\right] \qquad (8.6a)$$

For rectangular sections with prestressing steel and non-prestressed reinforcement:

$$\text{Percent} = 20\left[1 - \frac{\omega_p + \dfrac{d}{d_p}(\omega - \omega')}{0.36\beta_1}\right] \qquad (8.6b)$$

For flanged sections:

$$\text{Percent} = 20\left[1 - \frac{\omega_{pw} + \dfrac{d}{d_p}(\omega_w - \omega_w')}{0.36\beta_1}\right] \qquad (8.6c)$$

provided that these modified negative moments are used for calculating moments at sections within the spans for the same loading arrangement. Flanged sections with stress-block depth equal to or less than the flange thickness should be treated as rectangular sections. Redistribution of negative moments according to Eqs. (8.6*a*), (8.6*b*), or (8.6*c*) is permitted only when the section at which moment is reduced is so designed that the reinforcement index:

$$\omega_p$$

or

$$\omega_p + \frac{d}{d_p}(\omega - \omega')$$

or

$$\omega_{pw} + \frac{d}{d_p}(\omega_w - \omega'_w)$$

whichever is applicable, is not greater than $0.24\beta_1$. In addition, for such readjustment, bonded reinforcement must be provided at the supports, having an area not less than $A_s = 0.004A$, where A is the area of that part of the cross section between the flexural tension face and the centroid of the cross section.

These provisions for prestressed beams are exactly analogous to the ACI Code provisions for redistribution of negative moments in reinforced concrete beams. Through use of this limited amount of moment redistribution, many of the economic and practical benefits of plastic analysis can be realized without the complexity of a true plastic analysis of the indeterminate prestressed concrete structure.

It is worth repeating that for prestressed structures in which full redistribution of moments through plastic hinge formation cannot be assured, it is necessary to consider the secondary moments due to prestressing when calculating moments at critical sections. Although the magnitude of these moments is uncertain, it appears conservative to calculate them based on effective prestress force, and to include these moments, with load factor of 1.0, when calculating the required resistance M_u (according to ACI Code), at least at those sections where design moments are increased by secondary moments. At locations where they are decreased, a convincing argument can be made for disregarding their effect, although the ACI Code does not presently call for this.

8.11 INDETERMINATE FRAMES

All of the fundamentals of the behavior of indeterminate structures that have been presented in studying beams apply with equal validity to frames. For

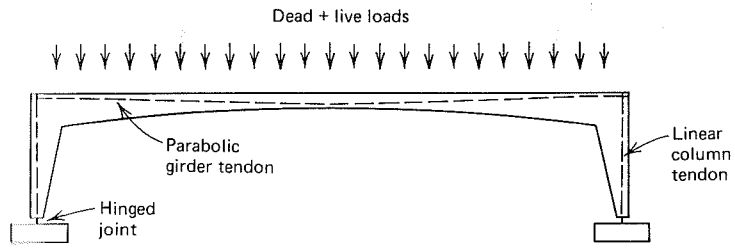

FIGURE 8.12 Prestressed portal frame.

frames, prestressing generally develops secondary as well as primary moments. As for beams, the equivalent load approach is useful in establishing optimum tendon profiles, and may avoid the necessity for considering secondary moments, at least up to the service load stage. In frames, special attention must be paid to the axial shortening of members that accompanies prestressing, because if the structure is restrained against this tendency to shorten, the intended prestress may not be achieved and large secondary moments may be caused.

The rigid jointed portal frame of Fig. 8.12, indeterminate to the first degree, will serve to illustrate certain fundamental principles. The uniformly distributed dead and live loads acting on the girder lead to selection of a parabolic tendon profile, with the steel centroid close to the top surface of the girder at the columns and near the bottom face at midspan, maximizing the sag. The moments produced at the girder-to-column joints by the eccentric girder tendon will be balanced by countermoments produced by the column tendon eccentricity there. At the column bases, where hinged supports are provided, the tendon eccentricity is zero.

Figure 8.13*a* shows the equivalent vertical loads acting on the girder as a result of the curvature of the tendon. This load produces an upward deflection, accompanied by rotation of the knee joints,which causes inward displacement at the bottom of the columns. The supports prevent this displacement, and reaction forces act outward on the columns.

The axial component of prestress force causes a tendency for the girder to shorten, as in Fig. 8.13*b*. This too causes outward reactions on the frame at the bottom of the columns, producing flexural deformations of both columns and girder. The outward forces due to support restraint tend to produce tensile stress in the girder. This causes a reduction in the effective prestress that must be accounted for in the design.

The deformations and reactive forces caused by dead and live loads are similar in nature. Figure 8.13*c* shows the vertical reactions and inward-directed thrust at the bases of the columns, typical of any portal frame.

When prestressing force and dead load effects are superimposed, as in Fig. 8.13*d*, in most designs the net transverse load on the girder will be upward, and

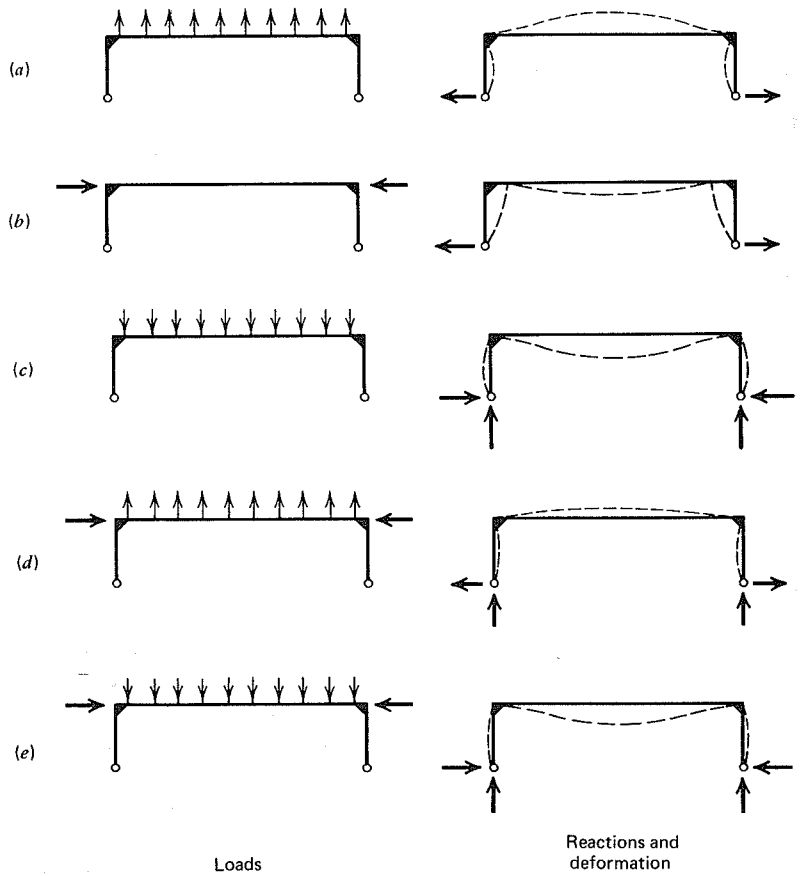

FIGURE 8.13 Effects of prestressing and loading of portal frame. (*a*) Equivalent load of prestress. (*b*) Axial component of prestress. (*c*) Superimposed dead and live loads. (*d*) Prestress and dead load. (*e*) Prestress and dead and live loads.

the girder will deflect upward accordingly. Support reactions are obtained by superposition of those of the type shown in Figs. 8.13*a*, *b*, and *c*. For this load stage, it is likely that the net horizontal reaction at the columns will be outward, rather than inward as would usually be the case for non-prestressed portal frames.

Finally, when the full servive load acts, together with prestress and superimposed dead and live loads, the girder deflects downward, as in Fig. 8.13*e*. The thrust at the base of the columns is now inward, but it will be much less than otherwise would be obtained, because of the combined effects of girder shortening and flexure resulting from prestress. This reduction of foundation force permits lighter foundations to be used. In addition, column moments, being directly proportional to the horizontal thrust, will be much reduced. This may

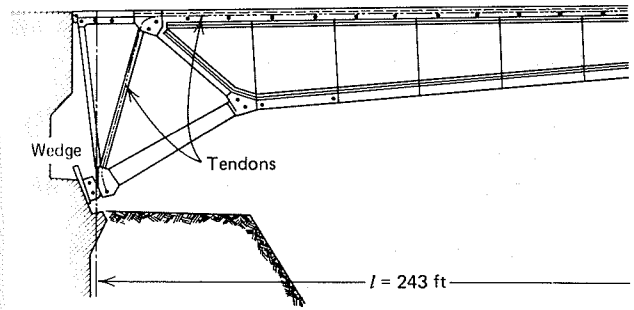

FIGURE 8.14 Freyssinet's portal frame with adjustable inclined struts at the supports. After Ref. 8.2.

permit prestressing in the columns to be eliminated with tensile stresses in the columns resisted by ordinary bar reinforcement.

The relative magnitudes of the various effects just discussed and, consequently, the direction of the reactive forces and displacements, depends not only on the magnitudes of prestress force and applied loads, but on the relative stiffness of the columns and the girder. Stiff columns produce a high degree of restraint, large reduction of prestress in the girder (see Fig. 8.13*b*), and large moments at the knee joints to produce downward deflection of the girder at midspan. Slender columns will deform more readily, permitting axial shortening of the girder with little restraint or loss of prestress. The horizontal thrust at the supports will be less, as well as the column moments.

Time-dependent deformation of the concrete due to shrinkage and creep assumes great importance when constructing prestressed frames, particularly of long span. The columns must be designed to permit the inevitable axial shortening of the girder without suffering damage themselves. Several ingenious schemes have been devised to accomplish this. The slender bridges over the Marne by Freyssinet (see Fig. 1.1) were very shallow portal frames that used a triangulated support at each end that provided the equivalent of very stiff columns. The

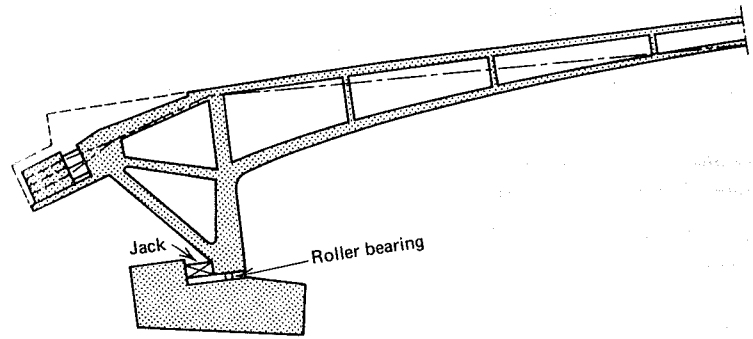

FIGURE 8.15 Support detail of the Rosenstein Bridge at Struttgart. After Ref. 8.2.

sloping compression members of the end support frames could be adjusted by hydraulic jacks and wedges (Fig. 8.14) when shortening of the beam was sufficient to cause noticeable girder deflection at midspan.

In other designs, the shortening has been accommodated by use of a sliding joint detail. Figure 8.15 shows a portal frame support of this type, used for the Rosenstein Bridge in Stuttgart. Jacks provides the needed inward movement, as shrinkage and creep deformations occurred, maintaining the desired reactions and controlling bending moments applied at the ends of the span.

REFERENCES

8.1 Leonhardt, F., "Continuous Prestressed Concrete Beams," *J. ACI*, Vol. 24, No. 7, March 1953, pp. 617–634.

8.2 Leonhardt, F., *Prestressed Concrete Design and Construction*, Wilhelm Ernst and Sons, Berlin, 1964.

8.3 Abeles, P. W. and Bardhan-Roy, B. K., *Prestressed Concrete Designer's Handbook*, 3rd ed., Cement and Concrete Association, Wexham Springs, Slough, England, 1981.

8.4 Guyon, Y., *Limit State Design of Prestressed Concrete*, Vol. 2, Wiley, New York, 1974.

8.5 Bachmann, H., "Design of Partially Prestressed Concrete Structures Based on Swiss Experiences," *J. PCI*, Vol. 29, No. 4, July–August 1984, pp. 84–105.

8.6 Freyermuth, C. L., "Practice in Partial Prestressing for Continuous Post-Tensioned Structures in North America," *J. PCI*, Vol. 30, No. 1, January–February 1985, pp. 154–182.

8.7 Lin, T. Y., "Load Balancing Method for Design and Analysis of Prestressed Concrete Structures," *J. ACI*, Vol. 60, No. 6, June 1963, pp. 719–742.

8.8 Discussion of Ref. 8.7, *J. ACI*, Vol. 60, No. 12, December 1963, pp. 1843–1881.

8.9 Norris, C. H., Wilbur, J. B., and Utku, S., *Elementary Structural Analysis*, 3rd ed., McGraw-Hill, New York, 1976.

8.10 Lin, T. Y. and Thornton, K., "Secondary Moment and Moment Redistribution in Continuous Prestressed Concrete Beams," *J. PCI*, Vol. 17, No. 1, January–February 1972, pp. 1–20.

8.11 *AASHTO Standard Specification for Highway Bridges*, 13th ed., American Association of State Highway and Transportation Officials, Washington, D.C. 1983.

8.12 Mattock, A. H., "Discussion of Proposed Revision of ACI 318–63: Building Code Requirements for Reinforced Concrete," *J. ACI*, Vol. 67, No. 9, September 1970, p. 710.

8.13 Mattock, A. H., Discussion of Ref. 8.10, *J. PCI*, Vol. 17, No. 4, July –August 1972, pp. 86–88.

8.14 Mattock, A. H., Yamazaki, J., and Kattula, B. T., "Comparative Study of Prestressed Concrete Beams With and Without Bond," *J. ACI*, Vol. 68, No. 2, February 1971, pp. 116–125.

8.15 *Proceedings International Symposium on Nonlinearity and Continuity in Prestressed Concrete*, Vols. 1, 2, 3, and prepared discussions, University of Waterloo, July 1983.

8.16 Nilson, A. H. and Winter, G., *Design of Concrete Structures*, 10th ed. McGraw-Hill, New York, 1986.

PROBLEMS

8.1 The prestressed concrete beam shown in Fig. P8.1 is fixed at the left end and roller-supported at the right. It is post-tensioned with a single tendon with a parabolic profile, with indicated eccentricities. (a) Locate the pressure line due to application of a prestress force of 240 kips. (b) Find the primary, secondary, and total moments due to prestressing at the face of the fixed support. (c) What is the magnitude and direction of the reaction produced at the roller by prestressing? (d) What minor adjustment could be made in the tendon profile to produce a concordant tendon?

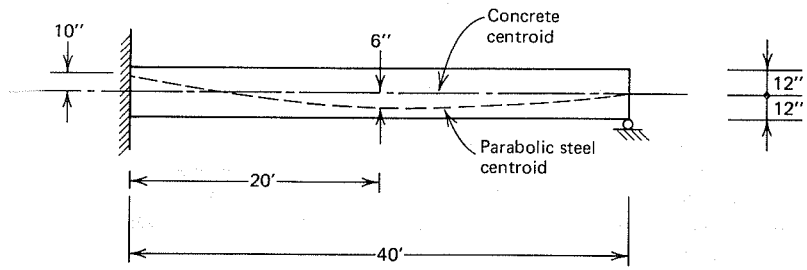

FIGURE P8.1

8.2 A concrete beam having width 12 in. and total depth 24 in. is continuous over two 48-ft spans with hinge or roller supports at three points. It is post-tensioned with tendons providing effective prestress P_e after losses of 230,000 lb. The tendon profile in each span is parabolic, with 0 eccentricity at the exterior supports, −8 in. eccentricity at the interior support, and +8 in. eccentricity at the center of each span. Using the method of equivalent loads: (a) Find the primary moments resulting from prestressing. (b) Find the support reactions and secondary moments resulting from prestressing. (c) Draw the combined moment diagram resulting from prestressing and locate the pressure line along the span. (d) Find the distributions of concrete flexural stress at midspan and at the interior support resulting from: (1) effective prestress plus total dead load of 500 plf, and (2) effective prestress plus total dead load plus a superimposed live load of 300 plf.

8.3 Solve Problem 8.2 using the method of superposition (consistent deformation). Comment on the relative merits of the alternative methods of analysis.

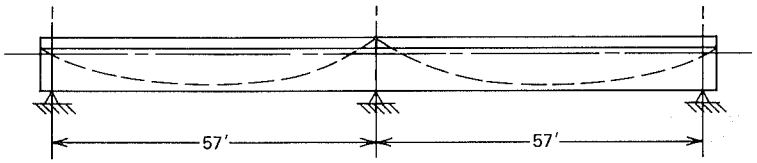

(a)

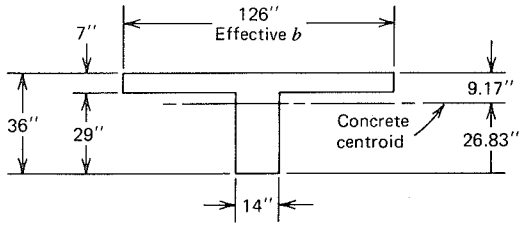

(b)

FIGURE P8.4

8.4 A parking garage structure is to be designed using two-span cast-in-place post-tensioned T-beams spaced at 26.9 ft laterally, as shown in Fig. P8.4. The monolithic slab is 7 in. in total thickness, and based on trial calculations, a web width of 14 in. and total depth of 36 in. has been chosen. Post-tensioning will be carried out from the two exterior supports to minimize friction losses using a single tendon with 1/2-in. diameter Grade 270 strands in a metal duct, grouted after anchoring. The tendon will be overstressed to compensate for slip losses. Tendon eccentricity will be −5.17 in. at the center support, 0 in. at the exterior supports, and +23.83 in. at midspan. Service dead load is 2.78 kips/ft including self-weight, and service live load is 0.800 kips/ft. It is specified that effective prestress equivalent load should balance 70 percent of the total dead load. Concrete strengths are f'_c = 5,000 psi, f'_{ci} = 4,000 psi. ACI Code allowable stresses will be imposed, with a limitation on a flexural tensile stress at service loads of $6\sqrt{f'_c}$. Losses due to shrinkage, creep, and relaxation may be assumed at 17 percent of P_i. (a) Based on the requirement for balancing 70 percent of dead load, find the required effective prestress force P_e and compute P_i based on assumed losses. (b) Find the primary, secondary, and total moments resulting from initial prestress. (c) Calculate stresses at all critical sections of the T-beam resulting from P_i and total dead load, and from P_e plus full service load. Compare with ACI Code limits and revise the design if necessary. (d) Calculate the required flexural strength at all critical sections at factored loads, including secondary moments with load factor of 1.0, and compare with strength provided. Non-prestressed Grade 60 rebars may be added if necessary to increase M_n. (e) Calculate the required spacing of No. 4 Grade 60 U stirrups along the span. (f) Calculate the deflection at midspan resulting from application of full live load, and compare with ACI Code limits. (Note: Although a complete design would require consideration of a loading case with live load on one span only, for present purposes consideration may be limited to dead and live load on both spans.)

NINE

DEFLECTIONS

9.1 INTRODUCTION

Prestressed concrete beams typically are more slender than reinforced concrete beams. Because of the high span-to-depth ratios that are characteristic of prestressed concrete, the prediction of deflections demands special attention. Failure to give proper consideration to deformations may cause several types of problems.

For many members, particularly those designed for full rather than partial prestressing, the problem may be upward deflection, or camber, which may increase with time as a result of concrete creep. Camber of bridge girders, for example, may result in an uneven road profile, producing uncomfortable or even dangerous ride characteristics. Excessive camber of roof decks may interfere with proper drainage. For floors, excessive upward or downward displacement may cause cracking of partitions or other nonstructural elements, ill-fitting windows or doors, or misalignment of sensitive equipment. In some cases, differential vertical displacement between adjacent precast floor units, caused by unintentional variation of material properties, prestress force, or tendon placement, may cause difficulty.

For a typical beam, application of prestress force will produce upward camber. The effect of concrete shrinkage, creep, and steel relaxation is gradually to reduce the camber produced by the initial force as that force is diminished. However, the creep effect is twofold. Although it produces loss of prestress force, tending to reduce the camber, creep strains in the concrete usually increase the negative curvature associated with prestress and, hence, increase the camber. Either of these time-dependent effects may predominate, depending on the details of the design and the material properties.

Dead and live loads usually produce downward deflections that superimpose on the upward deflection due to prestress. In the case of sustained loads, these too are time-dependent because of concrete creep.

By prestressing, it is possible to control deflections to a remarkable degree. In fact, it is only through deflection control that the high span-to-depth ratios typical of prestressed concrete can be achieved. A prestressed beam of a given cross section is considerably stiffer than a reinforced concrete beam of the same section, because cracking is reduced or eliminated by prestressing. Thus, all or nearly all of the cross section contributes to the moment of inertia and the flexural rigidity. Even more important, the net deflection in service can be minimized or even eliminated altogether using the load-balancing approach (see Section 1.3 and 4.6). In considering the effect of creep on deflections, it should be noted that if load balancing is achieved under the combined action of effective prestress and long-term gravity loads, then uniform compression stress results through the depth of the beam and the effects of creep are minimized. Zero deflection can be obtained for the balanced load stage.

Although prediction of deflection of prestressed concrete members is complicated by such factors as the gradual reduction of prestress force due to time-dependent losses, the direct effect of concrete creep, and (for partially prestressed beams) the influence of concrete cracking, relatively simple procedures can be followed that permit calculation of deflections within acceptable limits of accuracy. The calculation can be done at any of several levels, depending on the nature and importance of the work. In many cases, it would be sufficient to place limitations on span-to-depth ratio, based on experience, or using values such as found in Table 4.1 of Section 4.3. For calculation of deflections, the approximate methods described in Section 9.3 will be sufficiently accurate for most ordinary designs. In special cases where it is important to obtain the best possible estimate of deflections at all load stages, as for long span bridges, for example, the most satisfactory approach is to use a time-step summation procedure, as described in Section 9.4. By this method, the time-dependent changes of prestress force, material properties, and loading can be accounted for with the needed accuracy. The time-step method also provides the best means for estimating losses in prestress force, as suggested in Section 6.11.

In some cases, limitations are placed on the total deflection resulting from the combined effects of prestress, dead load, and service live load. More often, limitations are set on the immediate deflection due to full service live load and on the deflection component that will occur *after* nonstructural elements such as walls (which could be damaged by large deflections) are in place. In the latter case, the deflection of interest is the sum of the long-term deflection resulting from all sustained loads (including prestress) and the immediate deflection resulting from any additional live load. The ACI Code includes restrictions on these deflection components.

It should be emphasized that *all* deflection calculations for prestressed concrete members are merely estimates and are affected by uncertainties relating

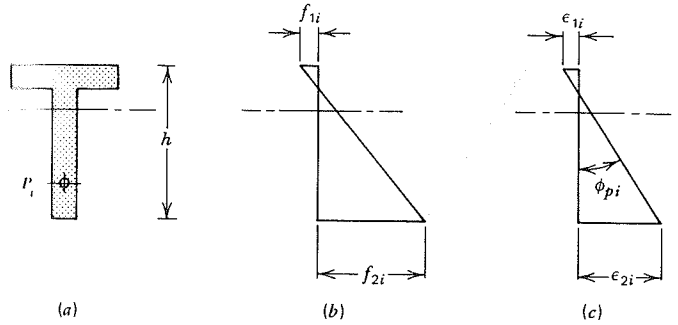

FIGURE 9.1 Stresses and strains resulting from initial prestress force P_i. (*a*) Cross section. (*b*) Stresses. (*c*) Strains.

to material properties, which are time-dependent and affected by influences such as temperature and humidity, and by uncertainties relating to the time of application and duration of the loads that may act.

9.2 BASIS FOR THE CALCULATIONS

If the prestress force is accurately known, if the materials are stressed only within their elastic ranges, and if the concrete remains uncracked, then the calculation of deflection of a prestressed flexural member presents no special difficulty. Camber resulting from prestressing can be calculated either on the basis of curvatures, or directly from the prestress moment diagram, using familiar tools such as the moment-area method. Alternately, the effect of prestressing may be considered in terms of equivalent loads. Deflections resulting from dead and live loads are then calculated as for any other flexural member and are superimposed on prestress deflections to obtain net values at the load stages of interest.

The concrete strains and stresses in a typical beam, resulting from the application of initial prestress force P_i, may appear as shown in Fig. 9.1. Concrete stresses are found from the equations of Chapter 3, after which the strains are easily obtained by the relation $\varepsilon_c = f_c/E_c$. If the total depth of the section is h, then the curvature at a particular section due to P_i is

$$\phi_{pi} = \frac{\varepsilon_{2i} - \varepsilon_{1i}}{h} \tag{9.1}$$

with due regard for sign. If tensile strain is taken positive, as usual, then a negative sign will indicate concave-downward curvature and upward camber for a simple span.

Concrete stresses and strains in the member after losses are shown in Fig. 9.2. Stresses decrease, compared with those of Fig. 9.1, because of the loss of prestress force. However, because of the combined effects of shrinkage and creep,

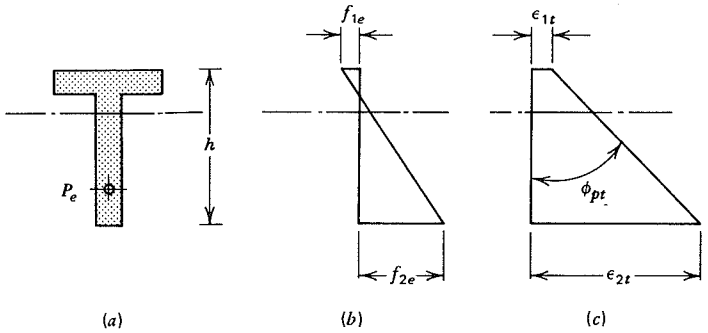

FIGURE 9.2 Stresses and strains resulting from effective prestress force P_e after losses. (*a*) Cross section. (*b*) Stresses. (*c*) Strains.

there is an increase of strains in the compressive sense. After losses, the curvature is

$$\phi_{pt} = \frac{\varepsilon_{2t} - \varepsilon_{1t}}{h} \tag{9.2}$$

For computational purposes, it is convenient to consider the curvature after losses, ϕ_{pt}, as the sum of three parts: (1) the instantaneous curvature ϕ_{pi} occurring immediately upon application of P_i, (2) the change in curvature $d\phi_1$ corresponding to loss of prestress from relaxation, shrinkage, and creep, and (3) the change in curvature $d\phi_2$ resulting from the direct effect of concrete creep under sustained compression (Ref. 9.1). Thus,

$$\phi_{pt} = \phi_{pi} + d\phi_1 + d\phi_2 \tag{9.3}$$

The curvatures ϕ_{pi} and ϕ_{pt} vary along a span. Values at intervals may be calculated to establish the shape of the curvature diagram, which may then be treated as an elastic load in deflection calculations.

In many cases, in computing deflections due to prestress force, it is simpler to work with moments rather than curvatures. For statically determinate beams, the prestress moment diagram is directly proportional to the eccentricity diagram, since $M = Pe$. Moment ordinates are converted to M/EI ordinates, and the M/EI diagram considered an elastic load in finding deflections by the moment-area or conjugate beam method. The equivalence of the two methods is obvious, since from elementary mechanics

$$\phi = \frac{M}{E_c I_c} = \frac{Pe}{E_c I_c} \tag{9.4}$$

Thus, for the beam of Fig. 9.3*a*, having a parabolic tendon of eccentricity e at midspan, diminishing to zero at the supports, a parabolic moment diagram with maximum ordinate Pe is obtained. This is readily converted to the M/EI

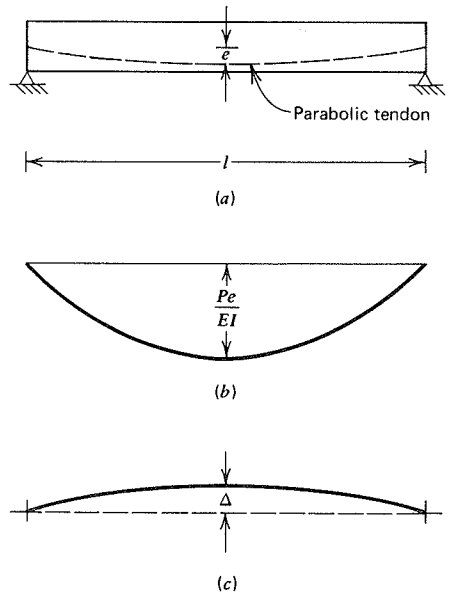

FIGURE 9.3 Deflection due to prestressing. (*a*) Profile. (*b*) Elastic loads. (*c*) Deflection curve.

diagram of Fig. 9.3*b*. If we apply the moment-area method, the flexural displacement Δ due to prestress P is found by taking moments of the M/EI area, between midspan and support, about the support point:

$$\Delta = \frac{Pe}{EI} \times \frac{l}{2} \times \frac{2}{3} \times \frac{5}{8} \times \frac{l}{2}$$

$$= \frac{5}{48} \frac{Pel^2}{EI}$$

This, and other cases that occur frequently, are summarized in Fig. 9.4 for reference. Figures 9.4*b*, *c*, and *d* give the midspan deflections for tendons harped at midspan, at the third points, and at the quarter points of the span, respectively, and passing through the concrete centroid at the supports in all cases. Figure 9.4*e* gives the midspan deflection produced by a straight tendon having constant eccentricity e.

Other cases may be obtained by superposition. For example, if the parabolic tendon of Fig. 9.4*f* has eccentricity e_1 at the supports, plus an incremental eccentricity e_2 at midspan, the total deflection at midspan due to prestressing is found by superimposing cases (a) and (e), as shown in Fig. 9.4*f*.

A third alternative in finding the deflection due to prestressing is to translate the prestress effect into equivalent loads, which permits use of handbook equations for deflections such as are available for the usual loadings.

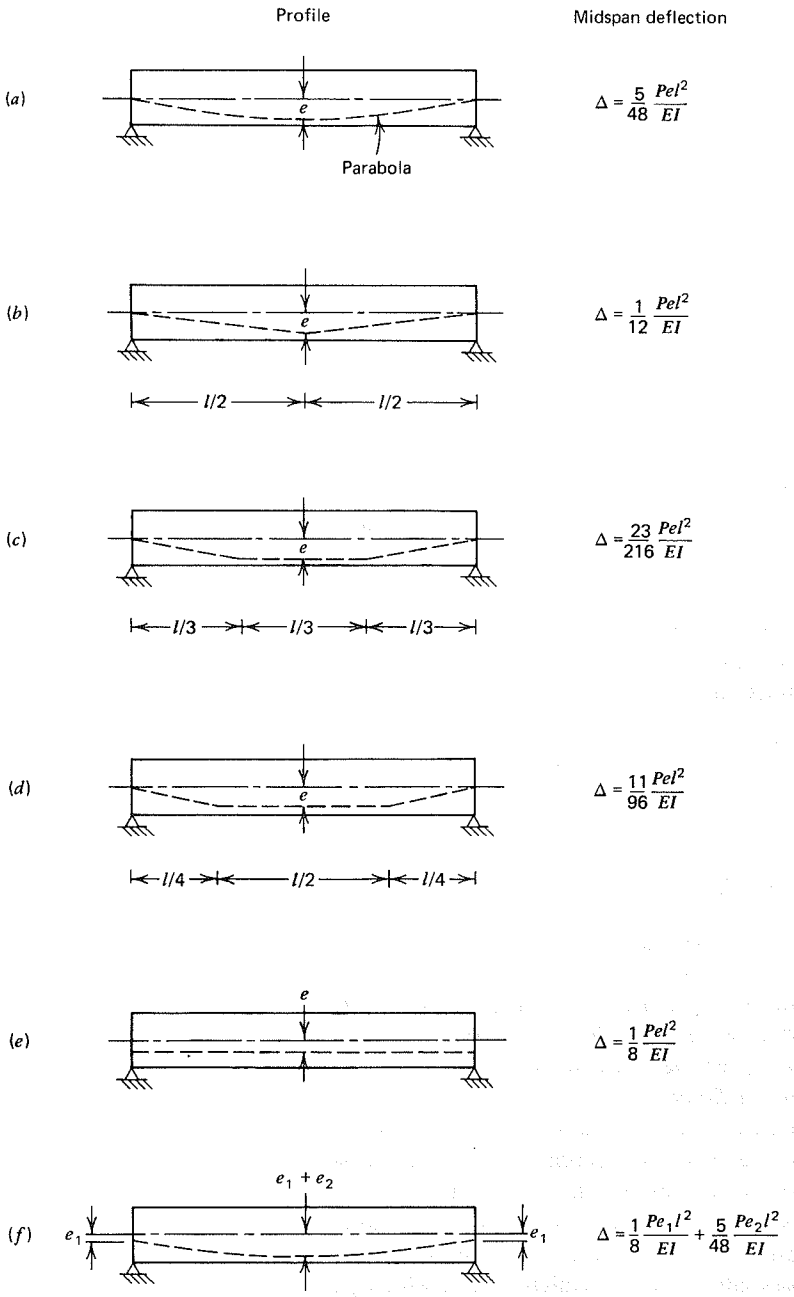

FIGURE 9.4 Prestress deflections for various tendon profiles.

To illustrate that identical results may be obtained by the method of equivalent loads, it will be recalled that the equivalent upward load produced on a concrete member by a parabolic tendon is

$$w = \frac{8Pe}{l^2} \tag{4.27}$$

It may be confirmed in any standard reference that the deflection due to a uniform load on a simple span is

$$\Delta = \frac{5}{384}\frac{wl^4}{EI}$$

Substituting the equivalent prestress load:

$$\Delta = \frac{5 \times 8}{384}\frac{Pel^4}{l^2EI}$$

$$= \frac{5}{48}\frac{Pel^2}{EI}$$

as already found by the method of moment areas. Similar confirmation may be obtained for the other load cases shown.

If the beam or slab is uncracked, the moment of inertia used in the calculations may be taken as that of the gross concrete cross section without serious error. If there is an unusually large amount of steel present, accuracy will be improved by the use of the properties of the transformed section.

If cracking is present, the stiffness of a member may be substantially reduced. However, even partially prestressed concrete members crack only at discrete locations. Between cracks, the flexural stiffness is approximately that of the uncracked concrete section. In such cases, use of an *effective moment of inertia* is recommended, as described in Section 9.6.

9.3 APPROXIMATE METHOD FOR DEFLECTION CALCULATION

Although deflection at intermediate states may be important in certain cases, normally to be considered are the initial stage, when a beam is acted upon by the initial prestress force P_i and its own weight, and one or more combinations of load in service, when the prestress force is reduced by losses to P_e and when deflections are modified by concrete creep under sustained loads. Initial deflections are easily found. Time-dependent effects are estimated using either of two methods, as follows.

A. USE OF CREEP COEFFICIENT AND AVERAGE PRESTRESS FORCE

The *short-term deflection* Δ_{pi} due to the initial prestress force P_i may be found based on the variation of curvature along the span, making use of moment-area principles. The initial curvatures ϕ_{pi} may be calculated from strains (Eq. 9.1), but it is usually more direct to work from the prestress moment diagram, and the corresponding variation of $P_i e/E_c I_c$ along the span. For common cases, the midspan deflection Δ_{pi} may be calculated directly by the equations in Fig. 9.4.

Usually Δ_{pi} is upward, and for normal conditions, the member self-weight is superimposed immediately upon prestressing. The immediate downward deflection Δ_o due to self-weight, which is usually uniformly distributed, is easily found by conventional methods. The net deflection upon prestressing is

$$\Delta = -\Delta_{pi} + \Delta_o \tag{9.5}$$

where negative values indicate upward displacement.

In consideration of *long-term effects*, reference is made to Eq. (9.3), which indicates that the curvatures (or deflections) resulting from prestressing force P_e after losses may be computed as the sum of the initial curvatures (or deflections) plus changes due to reduction of prestress and due to concrete creep. Equation (9.3) may be restated as follows:

$$\phi_{pt} = -\frac{P_i e_x}{E_c I_c} + (P_i - P_e)\frac{e_x}{E_c I_c} - \left(\frac{P_i + P_e}{2}\right)\frac{e_x}{E_c I_c} C_u \tag{9.6}$$

where C_u is the creep coefficient (see Chapter 2). The subscript x used with e indicates that the eccentricity varies along the span. The first term in Eq. (9.6) is the initial negative curvature, the second term is the reduction in that initial curvature because of the loss of prestress, and the third term is the increase in negative curvature because of concrete creep. Here the important approximation is made that creep occurs under a constant prestress force, equal to the average of the initial and final values.

Corresponding to that approximation, the final deflection of the member under the action of P_e is

$$\Delta = -\Delta_{pi} + (\Delta_{pi} - \Delta_{pe}) - \frac{\Delta_{pi} + \Delta_{pe}}{2} C_u$$

or simply

$$\Delta = -\Delta_{pe} - \frac{\Delta_{pi} + \Delta_{pe}}{2} C_u \tag{9.7}$$

where the first term is easily obtained by direct proportion:

$$\Delta_{pe} = \Delta_{pi}\frac{P_e}{P_i} \tag{9.8}$$

The long-term deflection due to self-weight is also modified by creep, and may be obtained applying the creep coefficient to the instantaneous value. Thus, the total member deflection, after losses and creep deflections when effective prestress and self-weight act, is given by

$$\Delta = -\Delta_{pe} - \frac{\Delta_{pi} + \Delta_{pe}}{2} C_u + \Delta_o(1 + C_u) \tag{9.9}$$

The deflection due to superimposed loads may now be added, with creep coefficient introduced to account for the long-term effect of the sustained dead loads, to obtain the net deflection at full service loading:

$$\Delta = -\Delta_{pe} - \frac{\Delta_{pi} + \Delta_{pe}}{2} C_u + (\Delta_o + \Delta_d)(1 + C_u) + \Delta_l \tag{9.10}$$

where Δ_d and Δ_l are the immediate deflections due to superimposed dead and live loads, respectively.

Although the value of E_c increases with time, as the concrete gains strength, in approximate calculations such as just described it is usually adequate to consider E_c constant, using the ACI Code value given by Eq. (2.3) or, for higher strength concretes, using the value predicted by Eq. (2.5), in either case with f_c' taken as the full specified compressive strength of the concrete.[1] The ultimate creep coefficient C_u is also usually considered to have a constant value in approximate calculations, even though it is known to depend on the age of the concrete at the time of loading.

B. LONG-TERM DEFLECTION MULTIPLIERS

An alternative approach to the approximate calculation of long-term deflection of prestressed members under prestress and sustained loads is to apply a simple multiplier to the immediate elastic deflections. This approach is similar to that

[1] It has been suggested that E_c in Eq. (9.6) be taken equal to E_{ci}, the value of the elastic modulus at time of release. This is clearly a more reasonable basis for the first term in that equation, although the second and third terms represent effects taking place while E_c gradually increases from E_{ci} to its full value. Recognizing that typically f_{ci}' is about equal to 70 percent of f_c', for which E_{ci} = 84 percent of E_c, it can be concluded that, in an approximate calculation based on Eq. (9.6), use of E_c based on the design strength f_c' is justified.

Table 9.1 Multipliers for Estimating Long-Term Cambers and Deflections for Typical Precast Members[a]

	Without composite topping	With composite topping
At erection:		
1. Downward deflection—apply to elastic deflection due to member weight at release of prestress.	1.85	1.85
2. Upward camber—apply to elastic camber due to prestress at time of release of prestress.	1.80	1.80
Final:		
3. Downward deflection—apply to elastic deflection due to member weight at release of prestress.	2.70	2.40
4. Upward camber—apply to elastic camber due to prestress at time of release of prestress.	2.45	2.20
5. Downward deflection—apply to elastic deflection due to superimposed dead load only.	3.00	3.00
6. Downward deflection—apply to elastic deflection caused by composite topping.	—	2.30

[a]Adapted from Ref. 9.2. Multipliers result in the total initial plus time-dependent deflection, whereas the multipliers found in the ACI Code for long-term effects in non-prestressed beams give the *additional* deflection to be added to the initial deflection.

used, according to ACI Code procedures, for ordinary reinforced concrete beams. Multipliers have been derived in Ref. 9.2 for precast prestressed members,[2] with or without composite topping slabs, to estimate the total long-term effects of prestressing, member self-weight, and the composite slab if present, and are shown in Table 9.1. To use these multipliers, which result in the *total* (immediate plus time-dependent) deflection components, the upward and downward components of the initial elastic camber should be separated to take into account the effects of loss of prestress, which affects only the upward component. In Table 9.1, the term "erection" refers to the time the precast member is placed in the structure, assumed to be from 30 to 60 days following casting; thus, both immediate and partial time-dependent effects are included at this stage. The term "final" refers to the stage at which all loss and creep effects have occurred.

9.4 REFINED CALCULATIONS USING INCREMENTAL TIME STEPS

In calculating the deflection resulting from prestress force, the method presented in Section 9.3A treated time-dependent changes in a very approximate way. Two

[2]Although derived originally for precast pretensioned members, they are often applied to post-tensioned beams in approximate calculations.

load stages were considered: the initial stage, when prestress P_i acts, and the final stage, after all time-dependent losses, when the prestress force is P_e. With reference to Eq. (9.6), the initial curvature $P_i e_x/E_c I_c$ was reduced to account for the prestress loss $(P_i - P_e)$, then increased to account for the effect of creep strain in increasing the curvatures along the span. In computing the last component, we made the approximation that concrete creep occurred under a constant prestress force, equal to the average value $(P_i + P_e)/2$. Such an approach should prove sufficiently accurate for all but unusual cases.

For greater refinement, it is necessary to account for time-dependent changes in prestress force in a way that recognizes the interaction of the effects of creep, shrinkage, and relaxation. Creep does not proceed under a constant force, but under a force that is continuously reducing because of the combined effects of shrinkage, relaxation, and creep itself. This may be accounted for using a summation procedure, based on the incremental changes occurring in a series of discrete time steps (Ref. 9.1). This also provides the most accurate means to predict the time-dependent *loss of prestress force* due to creep, shrinkage, and relaxation. Such a step-by-step method, although still approximate, permits improvement in accuracy to any desired degree by reducing the length and increasing the number of the time steps considered.

The determination of curvatures and deflections by such means requires information not only on the ultimate creep, shrinkage, and relaxation coefficients, but on the variation of those quantities with time. The information contained in Chapter 2 will prove useful in this respect (see also Refs. 9.4 to 9.6).

For the step-by-step method, Eq. (9.6) is replaced, in effect, by the following summation, to obtain the curvature ϕ_{pt} at any section at time t:

$$\phi_{pt} = -\frac{P_i e_x}{E_c I_c} + \sum_0^t (P_{n-1} - P_n)\frac{e_x}{E_c I_c} - \sum_0^t (C_n - C_{n-1})P_{n-1}\frac{e_x}{E_c I_c} \qquad (9.11)$$

where the subscripts $(n-1)$ and (n) define the beginning and end of a particular time step. It will be recalled that the first term is the instantaneous curvature occurring upon application of the prestress force P_i, the second term is the decrease in curvature corresponding to the loss of prestress from creep, shrinkage, and relaxation, and the third term is the increase in curvature resulting from creep.

The prestress force at the end of any time step is equal to the initial prestress P_i less the losses caused by shrinkage, creep, and relaxation. Losses caused by shrinkage, and relaxation could easily be obtained by application of the shrinkage and relaxation coefficients and time functions of Chapter 2. However, the effect of creep must be accounted for by summing the curvature changes in all time steps up to the time (t), because the force causing creep is continuously reducing.

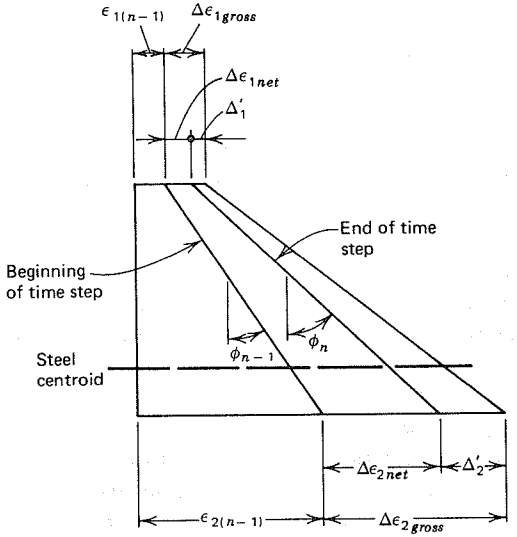

FIGURE 9.5 Strain changes and rotations at time step n.

In practice, it is convenient to treat all losses in the same summation. Curvature changes represented by the second and third terms of Eq. (9.11) are obtained concurrently at each step by a sequence of calculations that accounts both for prestress loss from all causes and creep curvature, and provides for the summation indicated symbolically by Eq. (9.11).

First, the initial curvature, term 1 of Eq. (9.11), is determined, either from Eq. (9.1) or Eq. (9.4). Then, for the next and each subsequent time step, the following sequence of calculations is performed (refer to Fig. 9.5):

1. Obtain the gross increase in creep strain at each extreme fiber, $\Delta\varepsilon_{1\,gross}$ and $\Delta\varepsilon_{2\,gross}$ by multiplying the stress at the beginning of the time step by the *increment* of unit creep strain for that interval.
2. Determine the corresponding creep strain at the level of the steel centroid.
3. Sum the creep strain determined in Step 2 and the shrinkage strain *increment* for the time interval to obtain the total change in strain at the level of the steel centroid.
4. Multiply the total strain found in Step 3 by E_p, and add the increment of relaxation loss to obtain the total steel stress loss for the interval.
5. Find the change in concrete stress at the extreme fibers corresponding to the loss in steel stress, and divide by E_c to obtain the corresponding strain changes Δ_1' and Δ_2'.
6. Determine the net changes in creep strain at the extreme fibers, $\Delta\varepsilon_{1\,net}$ and $\Delta\varepsilon_{2\,net}$, by subtracting the strain changes of Step 5 from the gross changes of Step 1.
7. Obtain the increase in curvature

$$(\phi_n - \phi_{n-1}) = \frac{\Delta\varepsilon_{2\,net} - \Delta\varepsilon_{1\,net}}{h}$$

from the net strains determined in Step 6, and sum with the curvatures present at the beginning of the time step to obtain total curvatures.

8. Find the stresses in the extreme fibers at the end of the time interval by finding the algebraic sum of the initial stress and the change in stress determined in Step 5. These are the stresses with which the computational sequence begins at the next time step.

The effect of the computational sequence just described is to calculate creep curvature, term 3 of Eq. (9.11), based on the prestress force at the beginning of the time step, then to calculate the curvature change due to losses, term 2 of Eq. (9.11), based on the shrinkage and relaxation occurring during the time step, and the creep corresponding to the prestress force acting at the beginning of the time step.

The calculations described must be performed at a sufficient number of locations along the span to establish the shape of the curvature diagram with reasonable accuracy, at least at midspan, the quarter points, and the supports. The calculation of beam deflections from the curvature diagram is a routine matter, and may proceed using the moment-area method or other means.

The instantaneous and long-term deflections due to transverse loads may now be superimposed to obtain net deflections at the load stages of interest. In this case, creep does not require the summation approach, because the sustained load causing creep is constant. Instantaneous deflections due to the sustained load may be multiplied directly by the creep coefficient to obtain long-term deflections.

9.5 EXAMPLE: DEFLECTION CALCULATIONS

Calculate the midspan deflection of the 40-ft span I-beam of Fig. 9.6 at age 0, 30, 180, and 360 days, using the step-by-step method of Section 9.4. Compare the resulting deflection at 360 days with that obtained using the approximate method of Section 9.3A. The member, originally studied in connection with elastic stress analysis in Section 3.4, is to carry its own weight of 183 plf and will be subjected to a service live load of 550 plf. (Span = 12.19 m, w_o = 2.7 kN / m, and w_l = 8.0 kN / m.) The following data are given:

P_i = 169,000 lb (752 kN)	I_c = 12,000 in.^{4} (4.99 × 10^9 mm^4)
A_p = 0.966 in.^{2} (623 mm^2)	r^2 = 68.2 in.^{2} (44.0 × 10^3 mm^2)
f_y = 210,000 psi (1,448 MPa)	E_c = 4,030,000 psi (27,800 MPa)[3]
f_{pi} = 175,000 psi (1,207 MPa)	C_u = 2.35
A_c = 176 in.^{2} (114 × 10^3 mm^2)	$\varepsilon_{sh,\,u}$ = 800 × 10^{-6}

The member will be constructed of normal density concrete, moist-cured, and will be prestressed at age seven days.

[3]For simplicity in this illustration, E_c will be taken as constant, although the variation of E_c with time could easily be incorporated in the solution.

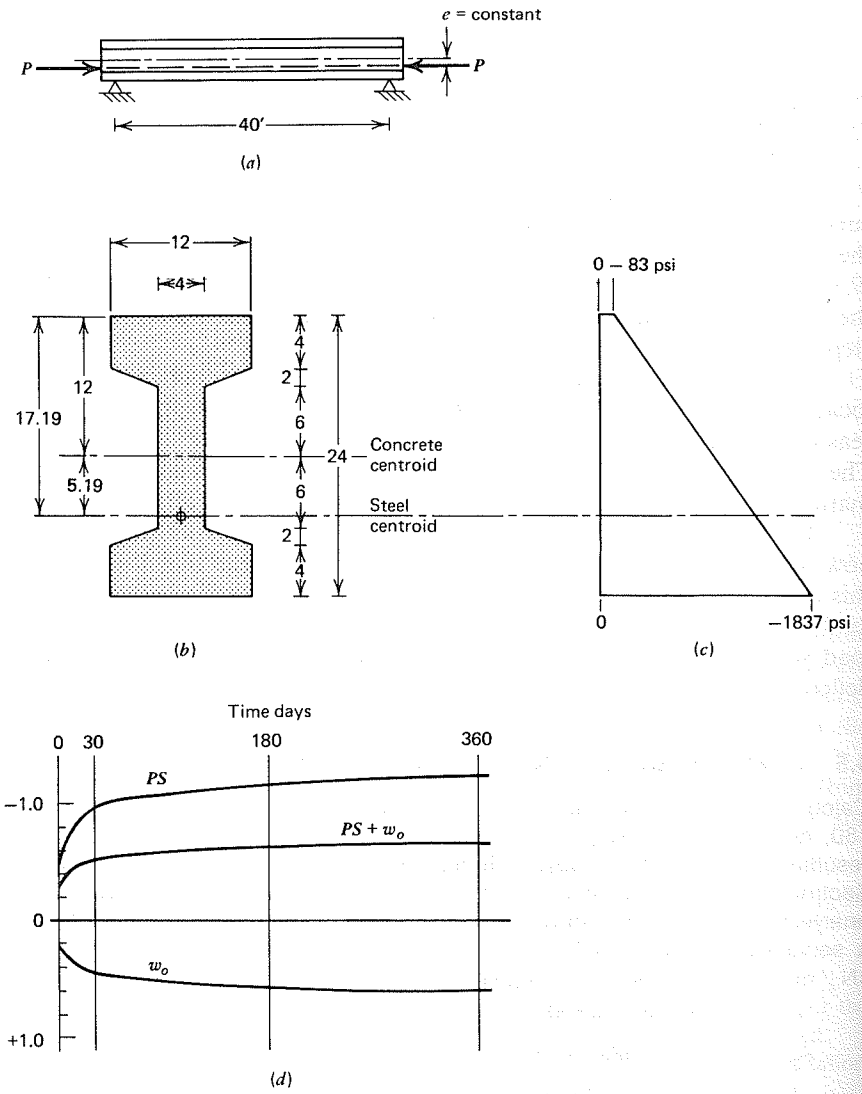

FIGURE 9.6 Deflection example. (*a*) Elevation. (*b*) Cross section. (*c*) Concrete stresses resulting from $P_i = 169$ kips. (*d*) Midspan deflection.

A. TIME-STEP METHOD

It is convenient to determine deflections due to prestress, self-weight, and superimposed loads separately, then to superimpose the results.

In the calculations of Section 3.4, it is shown that the concrete stresses due to P_i at the top and bottom of the section are, respectively, -83 and -1837 psi. The corresponding concrete strains are

$$\varepsilon_1 = \frac{f_1}{E_c} = \frac{83}{4{,}030{,}000} = 21 \times 10^{-6}$$

$$\varepsilon_2 = \frac{f_2}{E_c} = \frac{1{,}837}{4{,}030{,}000} = 456 \times 10^{-6}$$

Then, from Eq. (9.1), the initial curvature is

$$\phi_{pi} = \frac{\varepsilon_{2i} - \varepsilon_{1i}}{h}$$

$$= \frac{-456 + 21}{24} \times 10^{-6} = -18.14 \times 10^{-6} \text{ rad / in.}$$

The identical result may be obtained from Eq. (9.4):

$$\phi_{pi} = -\frac{P_i e_x}{E_c I_c}$$

$$= \frac{169{,}000 \times 5.19}{4{,}030{,}000 \times 12{,}000} = -18.14 \times 10^{-6} \text{ rad / in.}$$

The corresponding upward camber may be found by the moment-area method or by reference to Fig. 9.4*e*:

$$\Delta_{pi} = \phi_{pi} \frac{l^2}{8}$$

$$= -18.14 \times 10^{-6}(40 \times 12)^2 / 8$$

$$= -0.52 \text{ in. (13 mm)}$$

The time-dependent changes in deflection due to relaxation, shrinkage, and concrete creep will be determined based on the material information given in Chapter 2.

The ultimate creep coefficient C_u of 2.35 corresponds to a unit creep strain of

$$\delta_u = \frac{C_u}{E_c} = \frac{2.35}{4{,}030{,}000} = 0.583 \times 10^{-6}$$

The time variation of δ may be obtained from Eq. (2.12*b*). For example, at 30 days:

$$\delta_t = \frac{30^{0.60}}{10 + 30^{0.60}} \times 0.583 \times 10^{-6}$$

$$= 0.254 \times 10^{-6}$$

Similar calculations result in the data summarized in column 2 of Table 9.2. The increment of creep strain for each time step is given in column 3.

Shrinkage calculations must account for the fact that the beam is poured and commences volumetric change seven days before stressing, hence, at time -7 days. With $\varepsilon_{sh,u} = 800 \times 10^{-6}$ and time function as given by Eq. (2.15*a*), a typical calculation is as follows:

$$\varepsilon_{sh,30} = \frac{37}{35 + 37}(800 \times 10^{-6})$$

$$= 411 \times 10^{-6}$$

Table 9.2 Time-Dependent Parameters for Loss Calculations

(1) Time	(2) Creep	(3) Creep	(4) Shrinkage	(5) Shrinkage	(6) Relaxation	(7) Relaxation	(8) Increment
Days	$\delta_t \times 10^{-6}$	$\Delta\delta_t \times 10^{-6}$	$\varepsilon_{sh,t} \times 10^{-6}$	$\Delta\varepsilon_{sh,t} \times 10^{-6}$	f_p/f_{pi}	$1 - f_p/f_{pi}$	$\Delta(1 - f_p/f_{pi})$
−7			0				
0	0		133	133	1.000		
30	0.254	0.254	411	278	0.919	0.081	0.081
180	0.404	0.150	674	263	0.897	0.103	0.022
360	0.451	0.047	730	56	0.888	0.112	0.009

Calculations at other time steps yield the data of column 4 of Table 9.2, with the increments in each step in column 5.

Loss of stress in the steel due to relaxation is given by Eq. (2.1). With yield stress of 210 ksi and initial stress of 175 ksi, the stress ratio at 30 days, or 720 hours, is

$$\frac{f_p}{f_{pi}} = 1 - \frac{\log 720}{10}\left(\frac{175}{210} - 0.55\right)$$

$$= 0.919$$

corresponding to a loss ratio of 1.000 − 0.919 = 0.081. Similar calculations at all time steps provide the information of column 6, Table 9.2, with the incremental changes given in column 7.

The calculation of time-dependent changes in curvature and deflection can now proceed, following steps 1 through 8 of Section 9.4. For purposes of demonstrating the method, only three time steps will be used.

The first time step will be taken from the time of prestressing, time 0, to time 30 days. At the beginning of that time step, concrete fiber stresses are

$$f_1 = -83 \text{ psi}$$

$$f_2 = -1{,}837 \text{ psi}$$

Applying the unit creep increment of 0.254×10^{-6} for the first step results in gross creep strains of

$$\Delta\varepsilon_{1\,gross} = 83 \times 0.254 \times 10^{-6} = 21 \times 10^{-6}$$

$$\Delta\varepsilon_{2\,gross} = 1{,}837 \times 0.254 \times 10^{-6} = 467 \times 10^{-6}$$

The gross creep at the level of the prestressing steel is

$$\Delta\varepsilon_{pgross} = \left[21 + \frac{17.19}{24}(467 - 21)\right] \times 10^{-6}$$

$$= 340 \times 10^{-6}$$

The shrinkage strain increment for the first time step, from Table 9.2, is 278×10^{-6}. The relaxation of steel stress, based on the incremental loss ratio is

$$\Delta f_{p,\,rel} = 0.081 \times 175{,}000$$

$$= 14{,}200 \text{ psi}$$

Consequently, the total loss of steel stress during time step 1 is

$$\Delta f_p = (\varepsilon_{cr} + \varepsilon_{sh})E_p + \Delta f_{p,\,rel}$$

$$= (340 + 278) \times 10^{-6} \times 27 \times 10^6 + 14{,}200$$

$$= 30{,}900 \text{ psi}$$

The corresponding changes in concrete stress at the top and bottom face are:

$$\Delta f_1 = +\frac{\Delta P}{A_c}\left(1 - \frac{ec_1}{r^2}\right)$$

$$= \frac{0.966 \times 30{,}900}{176}\left(1 - \frac{5.19 \times 12}{68.2}\right)$$

$$= +14 \text{ psi}$$

$$\Delta f_2 = +\frac{\Delta P}{A_c}\left(1 + \frac{ec_2}{r^2}\right)$$

$$= \frac{0.966 \times 30{,}900}{176}\left(1 + \frac{5.19 \times 12}{68.2}\right)$$

$$= +324 \text{ psi}$$

These stresses are divided by the elastic modulus of the concrete to obtain the corresponding changes in concrete strain:

$$\Delta_1 = 14/4{,}030{,}000 = 3 \times 10^{-6}$$

$$\Delta_2 = 324/4{,}030{,}000 = 80 \times 10^{-6}$$

The gross strains, first obtained, are now adjusted by these values to obtain the net strains at the top and bottom faces of the concrete section:

$$\Delta\varepsilon_{1\,net} = (21 - 3) \times 10^{-6} = 18 \times 10^{-6}$$

$$\Delta\varepsilon_{2\,net} = (467 - 80) \times 10^{-6} = 387 \times 10^{-6}$$

The curvature increment during the first time step is easily found based on these strains:

$$\phi_{30} - \phi_0 = \frac{(-387 + 18)10^{-6}}{24} = -15.38 \times 10^{-6}$$

Thus, the total curvature, as of the end of time step 1, is

$$\phi_{pi} + \Delta\phi = (-18.14 - 15.38)10^{-6}$$

$$= -33.52 \times 10^{-6}$$

This curvature, which is constant along the span as a result of the constant eccentricity, is easily translated into upward deflection at midspan:

$$\Delta_{30} = \phi_{30}\frac{l^2}{8}$$

$$= -33.52 \times 10^{-6}\,\frac{(40 \times 12)^2}{8}$$

$$= -0.97 \text{ in. } (-25 \text{ mm})$$

Concrete stresses at the top and bottom faces at the beginning of the next time step are obtained by taking the algebraic sum of the stresses at the start of the first time step and the change in stress that resulted from losses:

$$f_1 = -83 + 14 = -69 \text{ psi}$$

$$f_2 = -1837 + 324 = -1513 \text{ psi}$$

The results of all calculations described to this point are summarized in Table 9.3 at time 30 days. Corresponding calculations at the second and third time steps are summarized as well.

Based on total curvature at the end of each time step, found by the summation process just described, the upward cambers due to prestress force at times 0, 30, 180, and 360 days are, respectively, 0.52, 0.97, 1.18, and 1.24 in., as given in the final column of Table 9.3. These cambers are plotted as a function of time in days in Fig. 9.6*d*.

Next, the deflections due to the self-weight of 183 plf are found. The instantaneous deflection, downward, is

$$\Delta_o = \frac{5wl^4}{384E_c I_c}$$

$$= \frac{5 \times 183(40 \times 12)^4}{384 \times 4{,}030{,}000 \times 12{,}000 \times 12}$$

$$= 0.218 \text{ in. (6 mm)}$$

The time-dependent increase in this value is found by introducing the creep coefficient $C_u = 2.35$, with time multipliers obtained by Eq. (2.12*a*):

$$\Delta_t = \Delta_o(1 + C_t)$$

$$\Delta_{30} = 0.218(1 + 0.435 \times 2.35) = 0.44 \text{ in. (11 mm)}$$

$$\Delta_{180} = 0.218(1 + 0.693 \times 2.35) = 0.57 \text{ in. (14 mm)}$$

$$\Delta_{360} = 0.218(1 + 0.774 \times 2.35) = 0.61 \text{ in. (15 mm)}$$

These values, too, are plotted as a function of time in Fig. 9.6*d*, and the net deflection resulting from the combined effect of prestress and dead load is shown.

The instantaneous deflection resulting from application of the live load of 550 plf is

$$\Delta_l = 0.218 \times \frac{550}{183} = 0.66 \text{ (17 mm)}$$

Thus, the net deflection at time 360 days, due to prestress, and dead and live loads will be

$$\Delta_{net} = -1.24 + 0.61 + 0.66$$

$$= +0.03 \text{ in. (1 mm)}$$

The beam would be almost level at this load stage, but with the short-term live load removed, a net upward camber of 0.63 in. could be expected.

Table 9.3 Summary of Calculations for Deflection due to Prestress

Time	Concrete stress at start of time step		Gross creep strain increment		Gross steel strain increment	Shrinkage strain increment	Steel relaxation increment	Total stress loss increment	Concrete stress change resulting from losses	
Days	f_1 psi	f_2 psi	$\Delta\varepsilon_{1g}$ $\times 10^{-6}$	$\Delta\varepsilon_{2g}$ $\times 10^{-6}$	$\Delta\varepsilon_p$ $\times 10^{-6}$	$\Delta\varepsilon_{sh}$ $\times 10^{-6}$	$\Delta f_{p,rel}$ psi	Δf_p psi	Δf_1 psi	Δf_2 psi
0										
30	−83	−1,837	21	467	340	278	14,200	30,900	+14	+324
180	−69	−1,513	10	227	165	263	3,850	15,400	+ 7	+162
360	−62	−1,351	3	64	47	56	1,575	4,400	+ 2	+ 46

Time	Concrete strain change resulting from losses		Net creep strain increment		Curvature increment	Total curvature	Midspan deflection
Days	$\Delta\varepsilon_1$ $\times 10^{-6}$	$\Delta\varepsilon_2$ $\times 10^{-6}$	$\Delta\varepsilon_{1\,net}$ $\times 10^{-6}$	$\Delta\varepsilon_{2\,net}$ $\times 10^{-6}$	$\Delta\phi$ $\times 10^{-6}$ rad	$\Sigma\phi$ $\times 10^{-6}$ rad	Δ_p in.
0						18.14	0.52
30	+3	+80	18	387	15.38	33.52	0.97
180	+2	+40	8	187	7.46	40.98	1.18
360	+1	+11	2	53	2.13	43.11	1.24

Table 9.4 Summary of Deflections

(1) Time	(2) Δ_p		(3) Δ_o		(4) Δ_l		(5) $\Delta_p + \Delta_o$		(6) $\Delta_p + \Delta_o + \Delta_l$	
Days	in.	mm	in.	mm	in.	mm	in.	mm	in.	mm
0	−0.52	−13	+0.22	+6	+0.66	+17	−0.30	−8	+0.36	+9
30	−0.97	−25	+0.44	+11	+0.66	+17	−0.53	−13	+0.13	+3
180	−1.18	−30	+0.57	+14	+0.66	+17	−0.61	−15	+0.05	+1
360	−1.24	−31	+0.61	+15	+0.66	+17	−0.63	−16	+0.03	+1

Component deflections and net deflections at the end of each time step are summarized in Table 9.4. Column 5 represents the beam camber for the unloaded member, and column 6 is the deflection with the full live load acting.

In the present case, the step-by-step method was demonstrated using only three time steps, with increments of loss and deflection calculated at ages 30, 180, and 360 days. If deflections are sufficiently critical that use of the step-by-step method is indicated, at least nine or ten steps should be used. A suggested sequence might use calculations at ages from one day to three years, for example, with short steps at the beginning of the sequence and longer steps at the end. Although the work would become tedious if performed manually, the deflection analysis can be programmed for computer. A number of such programs are available, as described in Refs. 9.7 to 9.9, for example, permitting the accurate calculation of both deflections and prestress losses.

B. APPROXIMATE METHOD

For comparison, prestress camber at 360 days will be found using the approximate method of Section 9.3A. The loss of prestress will be taken the same as for the previous calculations, and at the end of 360 days will total

$$\Delta f_p = 30{,}900 + 15{,}400 + 4{,}400$$
$$= 50{,}700 \text{ psi (350 MPa)}$$

as shown in Table 9.3. This corresponds to loss in force of $0.966 \times 50{,}700 = 49{,}000$ lb. Thus,

$$P_e = P_i - \Delta P$$
$$= 169 - 49$$
$$= 120 \text{ kips (534 kN)}$$

The immediate deflection upward due to prestress is

$$\Delta_{pi} = -0.52 \text{ in. (13 mm)}$$

as before, whereas

$$\Delta_{pe} = -0.52 \times \frac{120}{169}$$
$$= -0.37 \text{ in. (9 mm)}$$

The creep coefficient at time 360 days is $C_t = 0.774 \times 2.35 = 1.82$. Thus, from Eq. (9.7), the total deflection due to prestress force at 360 days is estimated at

$$\Delta_{360} = -\Delta_{pe} - \frac{\Delta_{pi} + \Delta_{pe}}{2} C_t$$
$$= -0.37 - \frac{0.52 + 0.37}{2} \times 1.82$$
$$= -1.18 \text{ in. (30 mm)}$$

This compares very favorably with the value of 1.24 in. obtained by the step-by-step approach. Agreement would not normally be so good.

9.6 DEFLECTION OF PARTIALLY PRESTRESSED BEAMS

Partially prestressed beams have been defined earlier in this text (see Sections 1.5, 3.9, and 4.7) as prestressed beams in which some flexural tension cracking is permitted at full service load. The advantages of partial compared with full prestressing are becoming more generally recognized, and partially prestressed beams are likely to be used with increasing frequency in practice.

One of the main advantages is improved deflection control. Troublesome upward camber due to prestress when the beam is lightly loaded can be avoided by using a smaller prestress force. However, this means that the net downward deflection when full service load is in place will be greater than for a fully prestressed member. Consequently, it is particularly important to make a close estimate of the deflection of partially prestressed beams at the controlling load stages.

Calculations are complicated by the influence of flexural cracks that reduce the moment of inertia in some regions of the beam. It has been shown (Refs. 9.10 to 9.13) that the deflection of partially cracked prestressed beams can be calculated using an *effective moment of inertia* I_e that depends on the extent of cracking. The method is analogous to that used in computing deflections of non-prestressed beams, according to the ACI Code, for which

$$I_e = \left(\frac{M_{cr}}{M_a}\right)^3 I_g + \left[1 - \left(\frac{M_{cr}}{M_a}\right)^3\right] I_{cr} \quad \text{and} \quad \leq I_g \tag{9.12}$$

where I_g = moment of inertia of the gross concrete section
I_{cr} = moment of inertia of the fully cracked transformed concrete section
M_{cr} = cracking moment = $f_r I_g / c_2$
M_a = maximum moment acting in the span
f_r = modulus of rupture for concrete = $7.5\sqrt{f'_c}$
c_2 = distance from section centroid to tension face of beam

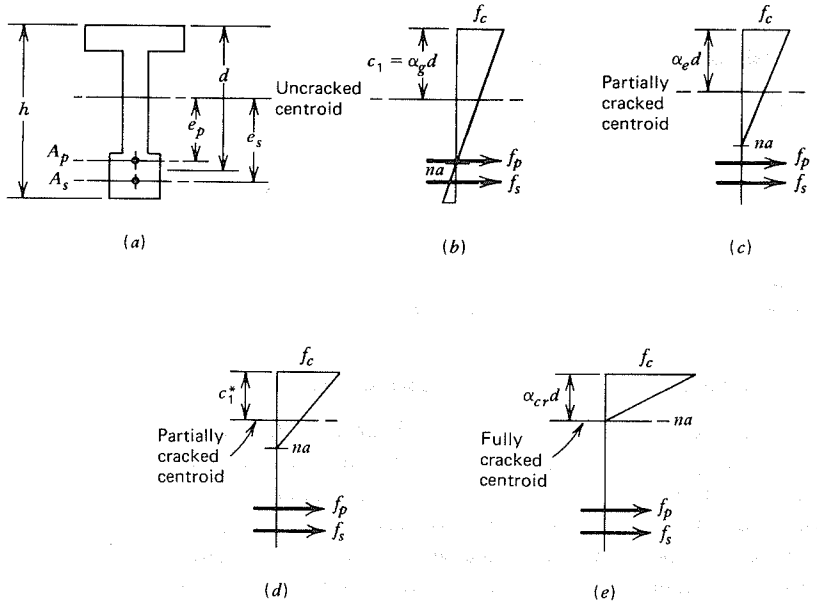

FIGURE 9.7 Concrete flexural stress distributions for partially prestressed beam. (*a*) Beam cross section. (*b*) Stresses in uncracked section. (*c*) Stresses for ficticious effective section. (*d*) Stresses after cracking at section with maximum tensile stress. (*e*) Stresses at cracked section neglecting influence of prestress force P_e. From Ref. 9.13.

For partially prestressed beams, a complication arises because the neutral axis (level of zero flexural stress and strain) is not at the centroidal axis of the section, as it is for reinforced concrete beams, but depends on the magnitude of the prestressing force and the external load. A practical method to account for this, as well as for the influences of non-prestressed tensile reinforcement and time-dependent effects, is presented in Refs. 9.11 to 9.13, and will be summarized here.

A. IMMEDIATE ELASTIC DEFLECTION

The stress distributions for a partially prestressed beam at several load stages are shown in Fig. 9.7. For the uncracked section, Fig. 9.7*b*, the centroidal axis is a distance $\alpha_g d$ from the compression face (equal to c_1 by the notation used earlier). Because of the axial compression from P_e, the neutral axis *na* does not coincide with the concrete centroid.

When loads are increased to produce cracking at the section of maximum flexural tension, the stress distribution of Fig. 9.7*d* results. With tension concrete disregarded as usual, the new neutral axis *na* and the new centroidal axis, a distance c_1^* from the compression face, could be found by methods presented in Ref. 9.14 or 9.15.

For deflection calculation, a *fictitious effective cross section* is used, with stresses as shown in Fig. 9.7*c*. The moment of inertia I_e of the effective cross section depends on the ratio of maximum moment to cracking moment for the member. Note that for the fictitious effective cross section, the neutral axis *na* will be between the limits defined by Figs. 9.7*b* and 9.7*d*. Correspondingly, the centroidal distance $\alpha_e d$ in Fig. 9.7*c* is between the centroidal distances of Fig. 9.7*b* and Fig. 9.7*d*. Finally, Fig. 9.7*e* shows the stress distribution that would result if the ratio of moment to effective prestress force P_e was very large. This stress distribution is referred to as the "fully cracked" distribution, and corresponds to the case of ordinary non-prestressed reinforced concrete. For this case, it is seen that the neutral axis coincides with the centroidal axis, a distance $\alpha_{cr} d$ from the compression face.

In the procedure that follows, the fully cracked distribution of Fig. 9.7*e* will be used as the lower bound case for the cracked section, rather than that of Fig. 9.7*d*. That is, I_{cr} and α_{cr} are the lower limits of I_e and α_e when interpolation is used to find the latter two values. The advantage of this simplifying assumption is that the values of Fig. 9.7*e* are constant, whereas those of Fig. 9.7*d* vary with the load level. The value of I_{cr} is calculated based on the transformed section, as usual for reinforced concrete.[4]

Figure 9.8 shows the strains and curvatures at the load stages of interest. Figure 9.9 shows the idealized moment-deflection diagram. As shown earlier in connection with Fig. 9.4, deflection can always be stated in the terms:

$$\Delta = \frac{KML^2}{EI} \tag{9.13}$$

where the multiplier K depends on the distribution of the load. Thus, for a central concentrated load $K = 1/12$ for a uniformly distributed load, $K = 5/48$, and so on. Figure 9.9 is drawn in terms of KM vs. Δ rather than M vs. Δ, so that a single line with slope $= E_c I_g / L^2$ can be applied to the deflection under different load distributions (different K's), such as those due to prestress, dead load, and live load in a typical problem.

With reference to strain distribution (1) of Fig. 9.8 and to Fig. 9.9, the deflection corresponding to the prestress curvature ϕ'_p is

$$\Delta'_p = \frac{K_p P_e e_p L^2}{E_c I_g} \tag{9.14a}$$

[4] It has been pointed out in Ref. 9.18 that this simplification may result in overestimation of live load deflection for partially cracked prestressed beams. Use of design charts for I and α of the partially cracked section of Fig. 9.7*d* (see Ref. 9.15) would avoid this.

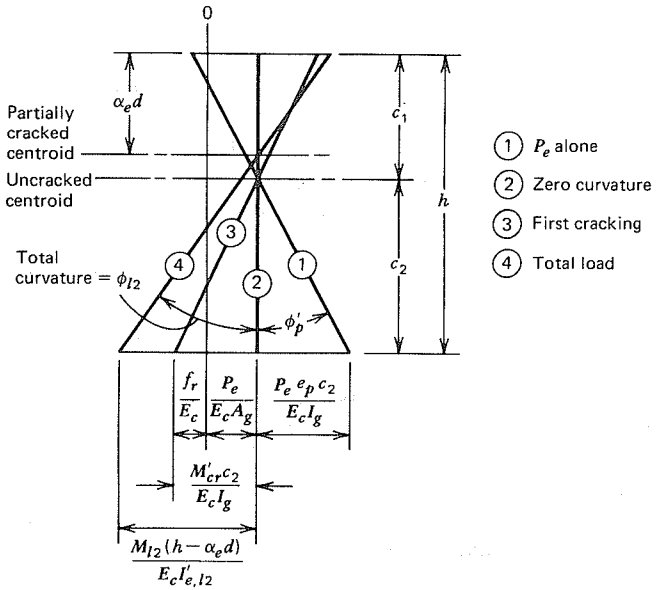

FIGURE 9.8 Strains and curvatures for section loaded into the cracking range. From Ref. 9.11.

and at the time the initial prestress force P_i is applied

$$\Delta_p = \Delta'_p \frac{E_c P_i}{E_{ci} P_e} \tag{9.14b}$$

The dead load deflection[5] shown in Fig. 9.9 is

$$\Delta'_d = \frac{K_d M_d L^2}{E_c I_g} \tag{9.15a}$$

and, when the initial prestress force P_i acts, is

$$\Delta_d = \Delta'_d \frac{E_c}{E_{ci}} \tag{9.15b}$$

For the zero-deflection state corresponding to strain distribution (2) of Fig. 9.8

[5]Here dead load is defined to include both member self-weight and superimposed dead load. In calculating long-term deflections, it is usually necessary to separate these two components, as illustrated in the example of Section 9.6C.

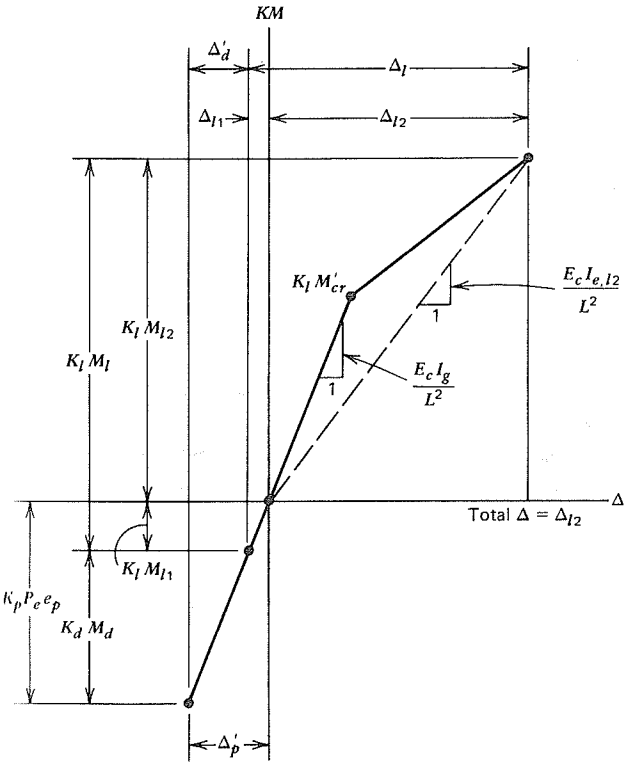

FIGURE 9.9 Moment vs. deflection for prestressed beam loaded into the cracking range. From Ref. 9.11.

and with reference to Fig. 9.9, a moment increment $K_l M_{l1}$ must be imposed:

$$K_l M_{l1} = K_p P_e e_p - K_d M_d$$

or

$$M_{l1} = \frac{K_p}{K_l} P_e e_p - \frac{K_d}{K_l} M_d \tag{9.16}$$

Up to this load, the beam is uncracked so

$$\Delta_{l1} = \frac{K_{l1} M_{l1} L^2}{E_c I_g} \tag{9.17}$$

Distribution (3) of Fig. 9.8 corresponds to first cracking, with the bottom-face tension stress equal to the modulus of rupture f_r. From Fig. 9.8

$$\frac{M'_{cr}c_2}{E_cI_g} = \frac{f_r}{E_c} + \frac{P_e}{E_cA_g}$$

Solving for the cracking moment gives

$$M'_{cr} = \frac{f_rI_g}{c_2} + \frac{P_eI_g}{A_gc_2} \tag{9.18}$$

This moment value is identified in Fig. 9.9, and is the net positive moment above zero required to crack the section.

Strain distribution (4) of Fig. 9.8 corresponds to the total service load. With reference to Fig. 9.9, $K_lM_l = K_lM_{l1} + K_lM_{l2}$, so

$$M_{l2} = M_l - M_{l1} \tag{9.19}$$

Then the deflection component Δ_{l2}, which is identical to the net downward deflection Δ, as is evident from Fig. 9.9, is

$$\Delta = \Delta_{l2} = \frac{K_lM_{l2}L^2}{E_cI_{e,l2}} \tag{9.20}$$

Then the total live load deflection is easily calculated as the sum of Δ_{l1} and Δ_{l2}. In Eq. (9.20), the effective moment of inertia is calculated, with reference to Fig. 9.9, as

$$I_{e,l2} = \left(\frac{M'_{cr}}{M_{l2}}\right)^3 I_g + \left[1 - \left(\frac{M'_{cr}}{M_{l2}}\right)^3\right] I_{cr} \quad \text{and} \quad \leq I_g \tag{9.21}$$

It should be noted that, by this "unified" procedure, the deflection for a non-prestressed beam is obtained simply by setting $P_e = 0$ and $M_{l2} = M_d + M_l$. Then Eq. (9.21) becomes identical to Eq. (9.12).

Several alternate procedures have been proposed for including the effect of cracking on the deflection of partially prestressed beams based on the I_e concept. These are summarized in Ref. 9.13, and may be identified with reference to Figs. 9.8 and 9.9 as follows:

1. Applying I_e in calculating the deflection increment measured from the effective prestress plus dead load deflection point (see Fig. 9.9). This is the basis of the PCI Handbook method described in Ref. 9.3 (see Ref. 9.6 also).
2. Applying I_e for the deflection increment measured from the zero-deflection point, as presented in detail in this section. This relates directly to the calculations for reinforced concrete (non-prestressed) beams when $P_e = 0$.
3. Applying I_e for the deflection increment measured from the decompression load (see Fig. 9.8) when the concrete stress at the bottom face of the beam is zero. This corresponds to a downward deflection, but can also be related to the calculations for reinforced concrete beams, for which I_e is applied starting at zero load when $f_2 = 0$.

B. LONG-TERM DEFLECTION

In Section 9.3B, an approximate method for predicting total deflections of prestressed beams was described that employed simple multipliers applied to the initial elastic deflections to obtain total (immediate plus time-dependent) deflections under sustained loads. The multipliers derived in Ref. 9.2 and reproduced in Table 9.1 are widely used and appear to give good results. It is suggested in Ref. 9.13 that these multipliers can also provide the basis for approximate calculation of the deflections of partially prestressed beams.

An important factor in partially prestressed beams is that the total tensile force required at factored loads is often provided by a combination of prestressed steel having area A_p and non-prestressed steel having area A_s. The two steels normally are placed at about the same effective depth. It has been shown that such non-prestressed steel, which is not subject to creep under sustained load, significantly affects both prestress losses and deflections (Refs. 9.16 and 9.17). In a simple span, non-prestressed steel reduces camber due to prestress; hence, under service load, the member will have a larger downward deflection.

To account for such non-prestressed steel, it is suggested in Ref. 9.13 that the basic multipliers of Table 9.1, defined here as C_1, be modified, depending on the areas A_p and A_s, to obtain new multipliers C_2. These are used instead of C_1 to compute the total (immediate plus time-dependent) deflection due to prestress and sustained loads. The multiplier C_2 is found from:

$$C_2 = \frac{C_1 + A_s/A_p}{1 + A_s/A_p} \tag{9.22}$$

where C_1 = basic multiplier of Table 9.1
A_p = area of prestressed reinforcement
A_s = area of non-prestressed reinforcement

provided that $A_s/A_p \leq 1$.

The method of deflection calculation just described, based on proposals in Refs. 9.11 to 9.13, is a rational extension of methods long used for non-prestressed reinforced concrete beams. Although complicated, it has the merit that it is applicable over the full range from zero prestressing (ordinary reinforced concrete) to full prestressing (no cracking at service load). Simplified

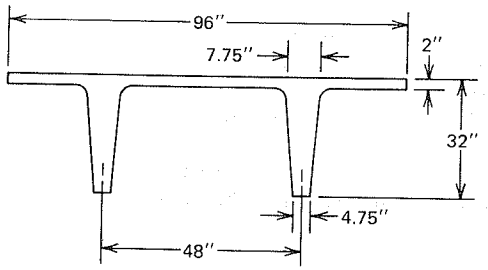

FIGURE 9.10 Precast pretensioned double-T beam (standard PCI 8DT32 section).

methods have been proposed (Ref. 9.18) that appear to account for the influence of all important parameters, and some design aids in the form of charts are available. Considering the uncertainties associated with the magnitude, time of application, and duration of loads, and the actual material properties, simplified methods are probably justified and further development along these lines is anticipated.

C. EXAMPLE: Deflection Calculations for A Partially Prestressed Beam[6]

Figure 9.10 shows the cross section of a precast pretensioned double-T beam that will be used on a 70-ft simple span. An initial prestress force just after transfer, $P_i = 416$ kips, will be provided using sixteen 1/2-in. diameter Grade 270 strands. Tendon eccentricity at midspan is $e_c = 17.46$ in., varying linearly to $e_e = 8.21$ in. at the supports. After losses, $P_e = 361$ kips. Four additional 1/2-in. diameter non-prestressed strands will be provided, following the same profile as the prestressed strands. A superimposed dead load $w_{ds} = 80$ lb/ft will be applied at age two months from the time of transfer, and a live load $w_l = 680$ lb/ft must be carried, in addition to the member self-weight of $w_{do} = 591$ lb/ft. The following additional member data are given:

$A_c = 567$ in.^{2}	$f'_c = 5{,}000$ psi
$I_g = 55{,}460$ in.^{4}	$f_r = 530$ psi
$c_1 = 10.79$ in.	$E_c = 4{,}070{,}000$ psi
$c_2 = 21.21$ in.	$E_{ci} = 3{,}410{,}000$ psi
$f'_{ci} = 3{,}500$ psi	

It is required to calculate the immediate and long-term deflections, following the methods of Section 9.6A and 9.6B.

[6]Adapted from Ref. 9.13.

For the given member, moments are found to be:

Self-weight:	$M_{do} = 362$ ft-kips
Superimposed dead load:	$M_{ds} = 49$ ft-kips
Service live load:	$M_l = 417$ ft-kips

It is easily confirmed that under effective prestress plus full service dead and live loads, the flexural tensile stress at the bottom face of the beam at midspan is 753 psi, above f_r, indicating that the beam is partially cracked at service load.

(1) IMMEDIATE DEFLECTIONS

The fictitious camber due to prestress is found using Eq. (9.14*a*) in conjunction with the deflection multipliers from Fig. 9.4*b* and Fig. 9.4*e*, superimposing the effects of a constant eccentricity $e = 8.21$ in. and an eccentricity varying linearly from zero at supports to $e = 17.46 - 8.21 = 9.25$ in. at midspan. Thus

$$\Delta'_p = \frac{1}{12}\frac{361 \times 9.25 \times 70^2 \times 12^2}{4{,}070 \times 55{,}460} + \frac{1}{8}\frac{361 \times 8.21 \times 70^2 \times 12^2}{4{,}070 \times 55{,}460}$$

$$\Delta'_p = 2.03 \text{ in}$$

Then, from Eq. 9.14*b*, when the prestress force is first applied:

$$\Delta_p = 2.03\frac{4.07 \times 416}{3.41 \times 361} = 2.79 \text{ in.}$$

For future reference, the overall deflection coefficient for prestress effect will be found, with reference to Eq. (9.14*a*):

$$K_p \times 17.46 = \frac{1}{12}(9.25) + \frac{1}{8}(8.21)$$

$$K_p = 0.1029$$

For dead and live loads, $K_d = K_l = 5/48 = 0.1042$. The fictitious deflection due to total dead load is found from Eq. (9.15*a*):

$$\Delta'_d = \frac{5}{48}\frac{(362 + 49) \times 70^2 \times 12^2 \times 12}{4{,}070 \times 55{,}460} = 1.61 \text{ in.}$$

That part of the live load that must be added to produce zero deflection is found from Eq. (9.16):

$$M_{l1} = \frac{0.1029}{0.1042} \times 361 \times \frac{17.46}{12} - (362 + 49) = 108 \text{ ft-kips}$$

and the corresponding deflection component, from Eq. (9.17), is

$$\Delta_{l1} = \frac{5}{48}\frac{108 \times 12 \times 70^2 \times 12^2}{4{,}070 \times 55{,}460} = 0.42 \text{ in.}$$

The net moment (above zero) to produce flexural cracking is given by Eq. (9.18):

$$M'_{cr} = \frac{0.530 \times 55{,}460}{21.21 \times 12} + \frac{361 \times 55{,}460}{567 \times 21.21 \times 12} = 254 \text{ ft-kips}$$

From Eq. (9.19), the incremental live load moment is

$$M_{l2} = 417 - 108 = 309 \text{ ft-kips}$$

For determining the effective moment of inertia using Eq. (9.21), the moment ratio will be needed as follows:

$$\left(\frac{M'_{cr}}{M_{l2}}\right)^3 = \left(\frac{254}{309}\right)^3 = 0.555$$

The moment of inertia of the fully cracked, transformed cross section is computed according to standard methods for reinforced concrete, and is $I_{cr} = 13{,}630$ in.^{4}. Then, from Eq. (9.21):

$$I_{e,l2} = 0.555 \times 55{,}460 + (1 - 0.555) \times 13{,}630 = 36{,}850 \text{ in.}^4$$

Using this value, the net downward deflection, from Eq. (9.20), is

$$\Delta = \Delta_{l2} = \frac{5}{48} \frac{309 \times 12 \times 70^2 \times 12^2}{4{,}070 \times 36{,}850} = 1.82 \text{ in.}$$

The total live load deflection is simply the sum of the parts:

$$\Delta_l = \Delta_{l1} + \Delta_{l2} = 0.42 + 1.82 = 2.24 \text{ in.}$$

(2) LONG-TERM DEFLECTIONS

The long-term deflections will be found using the multipliers C_1 from Table 9.1, modified to reflect the influence of the non-prestressed tendons according to Eq. (9.22). For the given beam, with 16 tensioned and four untensioned strands, $A_s / A_p = 0.25$. From Eq. (9.22):

For upward camber due to prestress: $C_2 = \dfrac{2.45 + 0.25}{1 + 0.25} = 2.16$

For deflection due to self-weight: $C_2 = \dfrac{2.70 + 0.25}{1 + 0.25} = 2.36$

For deflection due to superimposed dead load: $C_2 = \dfrac{3.00 + 0.25}{1 + 0.25} = 2.60$

The immediate camber due to prestress, $\Delta_p = 2.79$ in., increases to a final value of $2.79 \times 2.16 = 6.03$ in. upward deflection.

The fictitious dead load deflection, $\Delta'_d = 1.61$ in. computed earlier must be separated into its component parts due to self-weight (imposed immediately upon transfer) and superimposed dead load (applied at age two months), respectively

$$\Delta'_{do} = 1.61 \times 362/411 = 1.42 \text{ in.}$$

$$\Delta'_{ds} = 1.61 \times 49/411 = 0.19 \text{ in.}$$

Then, for the self-weight, making use of Eq. (9.15*b*),

$$\Delta_{do} = 1.42 \times 4.07/3.41 = 1.69 \text{ in.}$$

and the total long-term deflection component is $1.69 \times 2.36 = 3.99$ in. downward.

For the superimposed dead load, the long-term downward deflection is $0.19 \times 2.60 = 0.49$ in.

The live load deflection, calculated earlier, is 2.24 in. downward. Thus, the total long-term deflection of the beam is:

$$\Delta = -6.03 + 3.99 + 0.49 + 2.24 = 0.69 \text{ in.}$$

downward. Results will be compared with allowable deflections under the ACI Code in the Section 9.8.

9.7 COMPOSITE MEMBERS

Determination of the deflection of composite prestressed concrete beams introduces few new concepts, although there are practical complications because of the need to relate the time-dependent material parameters to the time-sequence of construction operations, such as casting the slab, achievement of full composite action, and possible step-by-step tensioning of the steel. Appropriate section properties must be used at the various stages in the computations.

Even if the approximate approach of Section 9.3 is followed, it is normally necessary to use two time-steps: the first from time of transfer of prestress until the time of casting the slab, and the second from the time the slab is cast until the service load stage, when all losses may be assumed to have occurred.

Initial camber due to prestress, and deflection due to self-weight of the precast unit and weight of the freshly poured slab may be found by procedures already described, with no change, using properties of the precast section. The effect of creep due to prestress and other sustained loads, together with the effect of losses of prestress force, must be determined in two stages: prior to and after casting of the slab. Appropriate values of shrinkage, creep, and relaxation coefficients may be established by applying the time functions of Chapter 2 to the ultimate values of the parameters. Live load deflection may be calculated in the usual way, using properties of the composite beam.

A new consideration in the case of composite beams is the effect of differential shrinkage and creep between the precast and cast-in-place parts of the section. As already pointed out in Section 7.3, for any given period following slab casting and bonding of the slab to the precast beam, shrinkage and creep strain at the bottom of the slab would generally exceed the corresponding strains at the top of the precast beam, if the two were not in fact bonded together. Longitudinal shear stresses at the interface prevent slip, so the strains are forced to be the same. But the inward (toward the center of a simple span) force applied by these shears to the top of the precast unit tends to produce an additional downward deflection. This may or may not be significant, depending on the particular material properties, the time-sequence of construction, whether or not shoring is used, and to what extent the cast-in-place slab is subject to cracking, which would tend to relieve the interface shear forces. See Ref. 9.6 for a comprehensive treatment.

9.8 ALLOWABLE DEFLECTIONS

The deflections that are considered acceptable vary widely depending on the particular type of construction and circumstances. Functional requirements of the member or structure may impose limits. Nonstructural elements carried by the prestressed construction may be damaged if deflections due to short- or long-term loads are too great. Drainage of long roof spans may be affected.

Table 9.5 Maximum Allowable Computed Deflections of the ACI Code[a]

Type of member	Deflection to be considered	Deflection limitation
Flat roofs not supporting or attached to nonstructural elements likely to be damaged by large deflections	Immediate deflection due to the live load, L	l*/180
Floors not supporting or attached to nonstructural elements likely to be damaged by large deflections	Immediate deflection due to the live load, L	l/360
Roof or floor construction supporting or attached to nonstructural elements likely to be damaged by large deflections	That part of the total deflection which occurs after attachment of the nonstructural elements, the sum of the long-time deflection due to all sustained loads and the immediate deflection due to any additional live load.†	l‡/480
Roof or floor construction supporting or attached to nonstructural elements not likely to be damaged by large deflections		l§/240

[a]Adapted with permission of the American Concrete Institute from ACI Building Code 318–83

*This limit is not intended to safeguard against ponding. Ponding should be checked by suitable calculations of deflection, including the added deflections due to ponded water, and considering long-time effects of all sustained loads, camber, construction tolerances, and the reliability of provisions for drainage.

†The long-time deflection may be reduced by the amount of deflection which occurs before attachment of the nonstructural elements. This amount shall be determined on the basis of accepted engineering data relating to the time-deflection characteristics of members similar to those being considered.

‡This limit may be exceeded if adequate measures are taken to prevent damage to supported or attached elements.

§But not greater than the tolerance provided for the nonstructural elements. This limit may be exceeded if camber is provided so that the total deflection minus the camber does not exceed the limitation.

Riding properties of bridges may be unsatisfactory if the supporting structure is too flexible.

Certain limits are included in the ACI Code, applicable to building construction. These are given in Table 9.5. The deflection limitation in each case, expressed as a fractional part of the span, depends on the type of member and supported construction. In some cases, the limit applies to live load deflection only, although in other cases it applies to incremental deflections expected after attachment of nonstructural elements.

For bridges, the AASHTO Specification requires that for simple or continuous spans, the deflection due to live load plus impact should not exceed 1/800 of the span, except on bridges in urban areas used in part by pedestrians, on which the ratio preferably shall be 1/1000. The deflection of cantilever arms due to live load plus impact is limited to 1/300 of the cantilever arm except for the case including pedestrian use, where the ratio preferably shall be 1/375 according to the Specification.

To illustrate these limits for the double-T beam studied in Section 9.6C, having 70-ft. span, the live load deflection limit would be $70 \times 12/180 = 4.67$ in. if it were used as a roof girder, and $70 \times 12/360 = 2.33$ in. if used as a floor girder, if no vulnerable nonstructural elements were attached. The computed deflection of 2.24 in. is acceptable in either case.

The sum of the time-dependent deflection and the short-time effects of superimposed dead and live load deflection can be found by deducting the immediate camber of 2.79 in., due to prestress, and the immediate deflection of 1.69 in., due to self-weight, from the total long-term deflection of 0.69. Thus

$$\Delta = 0.69 + 2.79 - 1.69 = 1.79 \text{ in.}$$

downward. According to the ACI Code limits of Table 9.5, the limit value if the member is attached to elements *likely* to be damaged by large deflections is $70 \times 12/480 = 1.75$ in. If the supported elements are *not likely* to be damaged, then the limit is $70 \times 12/240 = 3.50$ in. The member is marginal in the first case, but would be fully satisfactory in the second.

REFERENCES

9.1 "Deflections of Prestressed Concrete Members," ACI Committee 435, *J. ACI*, Vol. 60, No. 12, December 1963, pp. 1697–1727.

9.2 Martin, L. D., "A Rational Method for Estimating Camber and Deflection of Precast Prestressed Members," *J. PCI*, Vol. 22, No. 1, January–February 1977, pp. 100–108.

9.3 *PCI Design Handbook*, 3rd ed., Prestressed Concrete Institute, Chicago, 1985.

9.4 Branson, D. E., "The Deformation of Non-Composite and Composite Prestressed Concrete Members," ACI Special Publication SP-43, *Deflections of Concrete Structures*, American Concrete Institute, Detroit, 1974, pp. 83–127.

9.5 Branson, D. E. and Kripanarayanan, K. M., "Loss of Prestress, Camber, and Deflection of Non-Composite and Composite Prestressed Concrete Structures," *J. PCI*, Vol. 16, No. 5, September–October 1971, pp. 22–52.

9.6 Branson, D. E., *Deformation of Concrete Structures*, McGraw-Hill, New York, 1977.

9.7 Sinno, R. and Furr, H. L., "Computer Program for Predicting Prestress Loss and Camber," *J. PCI*, Vol. 17, No. 5, September–October 1972, pp. 27–38.

9.8 Suttikan, C., *A Generalized Solution for Time-Dependent Response and Strength of Noncomposite and Composite Prestressed Concrete Beams*, Ph.D. dissertation, Department of Civil Engineering, University of Texas, Austin, Texas, August 1978.

9.9 Turner, D. B., *A Computer Program for Predicting the Deflection of Nonprestressed and Partially Prestressed Members by Unified Procedures*, M.S. thesis, Department of Civil Engineering, University of Iowa, Iowa City, Iowa, May 1983.

9.10 Branson, D. E., "Instantaneous and Time-Dependent Deflections of Simple and Continuous Reinforced Concrete Beams," *HPR Report*, No. 7, Part 1, Alabama Highway Department, Bureau of Public Roads, August 1963, pp. 1–78.

9.11 Branson, D. E. and Trost, H., "Unified Procedures for Predicting the Deflection and Centroidal Axis Location of Partially Cracked Nonprestressed and Prestressed Concrete Members," *J. ACI*, Vol. 79, No. 2, March–April 1982, pp. 119–130.

9.12 Branson, D. E. and Trost, H., "Application of the I-Effective Method in Calculating Deflections of Partially Prestressed Members," *J. PCI*, Vol. 27, No. 5, September–October 1982, pp. 62–77.

9.13 Branson, D. E. and Shaikh, A. F., "Deflection of Partially Prestressed Members," Special Publication SP-86: *Deflection of Concrete Structures*, American Concrete Institute, Detroit, 1985, pp. 323–363.

9.14 Nilson, A. H., "Flexural Stresses After Cracking in Partially Prestressed Beams," *J. PCI*, Vol. 21, No. 4, July–August 1976, pp. 72–81.

9.15 Tadros, M. K., "Expedient Service Load Analysis of Cracked Prestressed Concrete Sections," *J. PCI*, Vol. 27, No. 6, November–December 1982, pp. 86–111.

9.16 Shaikh, A. F. and Branson, D. E., "Non-Tensioned Steel in Prestressed Concrete Beams," *J. PCI*, Vol. 15, No. 1, February 1970, pp. 14–36.

9.17 Tadros, M. K., Ghali, A., and Dilger, W. H., "Effect of Non-Prestressed Steel on Prestress Loss and Deflection," *J. PCI*, Vol. 22, No. 2, March–April 1977, pp. 50–63.

9.18 Tadros, M. K., Ghali, A., and Meyer, A. W., "Prestress Loss and Deflection of Precast Concrete Members," *J. PCI*, Vol. 30, No. 1, January–February 1985, pp. 114–141.

PROBLEMS

9.1 The concrete T-beam shown in Fig. P9.1 is post-tensioned at an initial force $P_i = 229$ kips that reduces after one year to an effective value $P_e = 183$ kips. In addition to its own weight, the beam will carry a superimposed short-term live load of 21.5 kips at midspan. Using the approximate method of Section 9.3A, find (a) the initial deflection of the unloaded girder, and (b) the deflection at age one year of the loaded girder. The following data are given: $A_c = 450$ in.^{2}, $c_1 = 8$ in., $I_c = 24{,}600$ in.^{4}, $E_c = 3{,}500{,}000$ psi, $C_u = 2.5$.

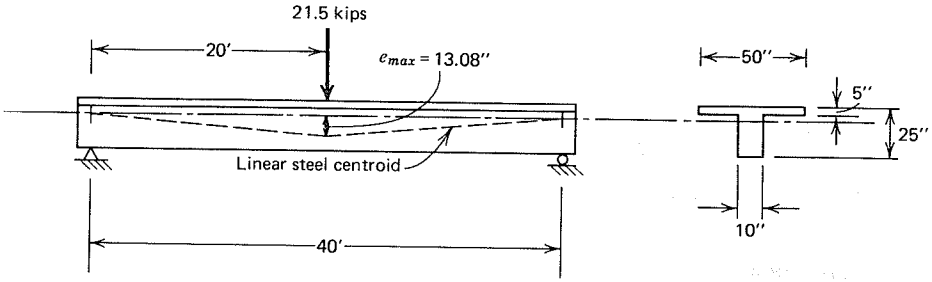

FIGURE P9.1

9.2 Find the deflections of the beam of Problem 9.1 by using the method of incremental time steps described in Section 9.5. Consider the beam at time zero, one month, three months, six months, and one year. The following additional data are given: $A_p = 1.31$ in.^{2}, $f_y = 210{,}000$ psi, $f_{pi} = 175{,}000$ psi, $\varepsilon_{sh,u} = 650 \times 10^{-6}$. Use material properties as given in Chapter 2. The beam is poured three days before transfer, and is steam cured. Compare with the results of Problem 9.1 and comment.

9.3 The standard double-T section beam of Fig. P9.3 is to be used on a simple span of 46 ft. Tendons are harped at midspan, with eccentricity varying as shown in the sketch. The initial prestress in the six 0.5-in. diameter low-relaxation strands is 200 ksi; after time-dependent losses, this is reduced to 160 ksi. Compute the camber immediately after transfer, when initial prestress plus self-weight act, after all time-dependent losses, when effective prestress plus self-weight act, and at full service load when live load of 600 plf is added to effective prestress plus self-weight. (a) Compute the required deflections based on Eqs. (9.5) through (9.10), neglecting cracking. (b) Compute the deflections using the multipliers of Table 9.1. (c) Compute the deflections using the I_e method of Section 9.6. Compare results of parts (a), (b), and (c) and comment. The following data are given: $A_c = 344$ in.^{2}, $I_g = 9{,}300$ in.^{4}, $c_1 = 4.73$ in., $c_2 = 13.27$ in., $A_p = 0.918$ in.^{2}, $w_o = 358$ plf, $f'_c = 5{,}000$ psi, $f'_{ci} = 3{,}500$ psi, $f_{pu} = 270{,}000$ psi, $C_u = 2.0$, $E_c = 4{,}030{,}000$ psi, $E_{ci} = 3{,}370{,}000$ psi, $E_p = 27{,}000{,}000$ psi.

9.4 For the post-tensioned T-beam of Problem 5.3, use the time-step method to find the deflections at midspan at the following load stages: (a) Immediately upon application of prestress force. The force just after transfer is $P_i = 770$ kips. (b) At age 30 days, due to prestress force, self-weight, and superimposed dead load. (c) At age 30 days,

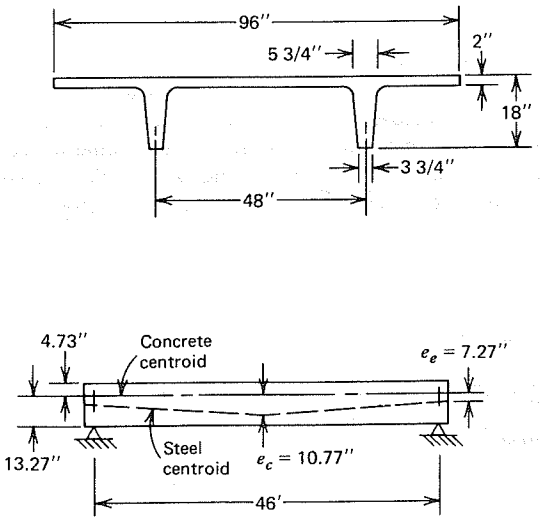

FIGURE P9.3

due to loads of (b) plus full service live load. (d) At age five years, due to all sustained loads. The ultimate creep coefficient $C_u = 2.00$, and the ultimate shrinkage strain is 500×10^{-6}. Refer to Chapter 2 for the time-variation of these properties, as well as steel relaxation as a function of time. The concrete will be moist-cured for seven days, and the girder will be post-tensioned immediately after that period. Superimposed dead load is applied at age 30 days. It is suggested that four time-steps be used, defined by times zero, seven days, 30 days, one year, and five years.

9.5 The post-tensioned T-beam shown in Fig. P9.5 has been designed for partial prestressing, and will carry a service live load of 1,200 lb/ft and superimposed dead load of 400 lb/ft, in addition to its own weight of 1,050 lb/ft, on an 80-ft simple

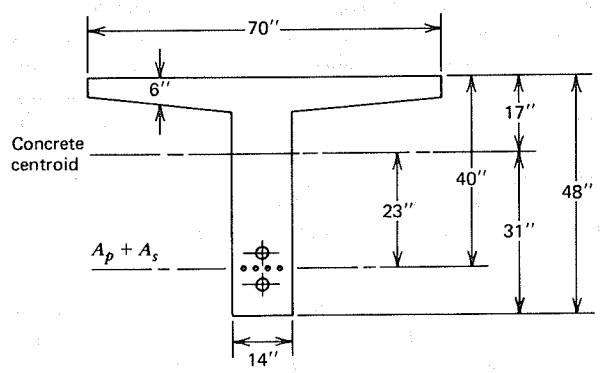

FIGURE P9.5

span. A prestress force $P_i = 713$ kips is provided using two tendons, each with nine strands of Grade 250 steel with nominal diameter 0.600 in. each, providing total $A_p = 3.90$ in.^{2}. Eccentricity varies parabolically from zero at the supports to 23.0 in. at midspan. After time-dependent losses, $P_e = 606$ kips. Non-prestressed reinforcement $A_s = 3.57$ in.^{2} is provided by four reinforcing bars with the same effective depth as the prestressed steel. The following additional information is given:

$I_g = 229{,}000$ in.^{4}; $c_1 = 17.0$ in.; $c_2 = 31.0$ in.; $A_c = 1{,}010$ in.^{2};

$f'_c = 5{,}000$ psi; $f'_{ci} = 3{,}500$ psi; $E_c = 4{,}030{,}000$ psi;

$E_{ci} = 3{,}370{,}000$ psi; $f_r = 530$ psi.

Find the immediate and long-term deflections for this member, using the methods of Section 9.6, and compare your answer with ACI Code limits for deflections. The member is proposed for use as a part of a floor system. Attached nonstructural elements can accommodate to moderate deflections without damage. (Note: This partially prestressed beam was designed, in the second example of Section 4.7, for load balancing under external dead load plus self-weight. Was the goal of zero deflection for this load stage achieved?)

TEN

SLABS

10.1 INTRODUCTION

Prestressed concrete slabs are used in civil engineering to provide flat, useful surfaces such as floors, roofs, decks, or walls. In its most basic form, a slab is a plate, the thickness of which is small relative to its length and width. Usually, the thickness is constant. The slab may be supported by walls, but more often it is carried by concrete beams that are generally poured monolithically with the slab, by structural steel beams, or directly by columns with no beams or girders.

Beam-supported slabs may be supported along two opposite edges only, as in Fig. 10.1*a*, in which case the structural action is essentially *one-way*. Loads applied to the surface are carried by the slab spanning in the direction perpendicular to the supported edges. On the other hand, there may be supports on all four sides of a slab panel, as in Fig. 10.1*b*, so that *two-way* action is obtained. Intermediate beams may be introduced to subdivide the slab, as shown in Fig. 10.1*c*. If the ratio of the short to the long side of a rectangular slab panel is less than about 0.5, most of the load is carried in the short direction because of the greater stiffness associated with the shorter span length. Thus, one-way action may be obtained, in effect, even though supports exist on four edges.

Prestressed concrete slabs are often carried directly by columns, as in Fig. 10.1*d*, without the use of beams or girders. Such slabs are described as *flat plates*. Although flat plates are generally cast-in-place, just as for the other types of slabs described, they may also be cast at ground level and lifted into their final position in the structure by jacks at the columns. These are termed *lift slabs*. Generally steel columns are used.

Closely related to the flat plate is the grid slab shown in Fig. 10.1*e*. To reduce dead load, voids are formed in the lower surface of the slab in a rectilinear pattern by reusable metal, fiberboard, or plastic form inserts. A two-way ribbed

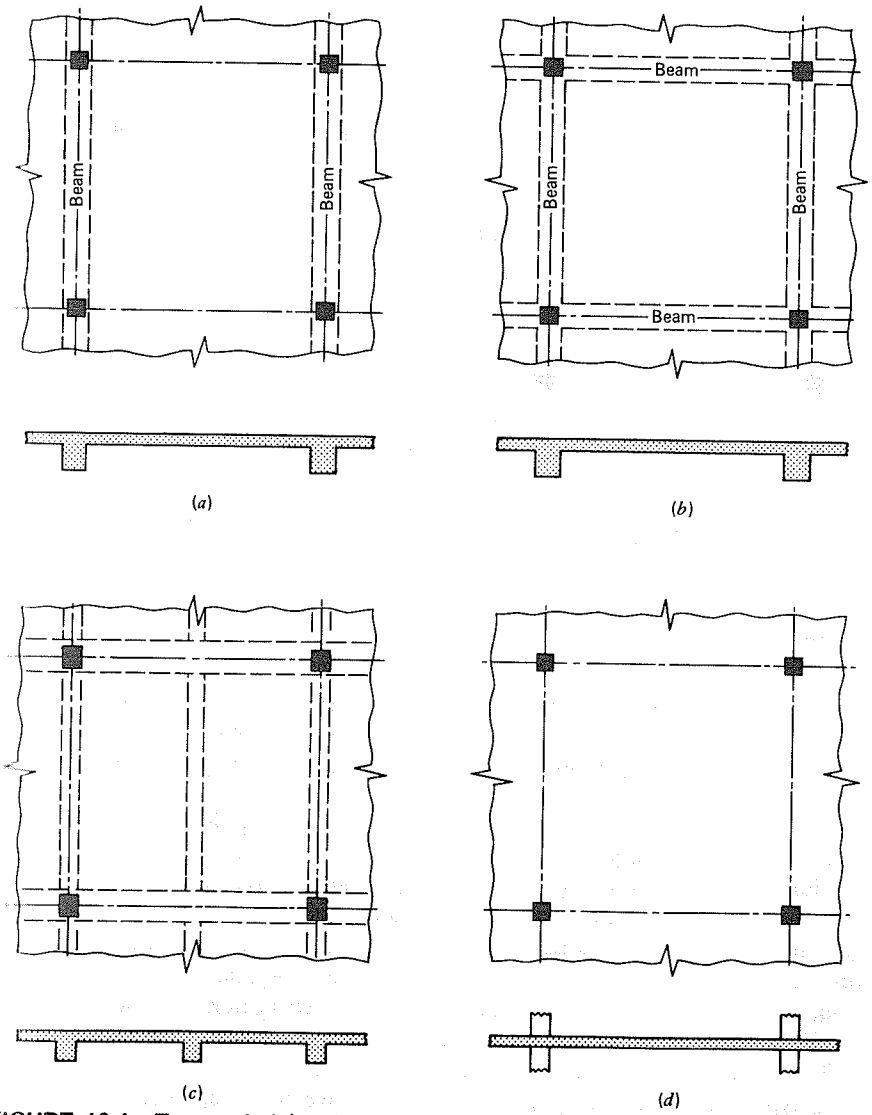

FIGURE 10.1 Types of slabs. (*a*) One-way slab. (*b*) Two-way slab. (*c*) One way slab. (*d*) Flat plate slab. (*e*) Grid slab. (*f*) Flat slab.

construction results. Generally, inserts are omitted near the columns, resulting in a solid slab better able to resist the local concentration of moments and shears.

The term *flat slab* is reserved for the type of beamless construction shown in Fig. 10.1*f* (although in a literal sense all the slab forms described are flat slabs). Flat slab construction is characterized by a locally thickened portion of the slab, termed a dropped panel, centered on the column, or by flared column tops, or

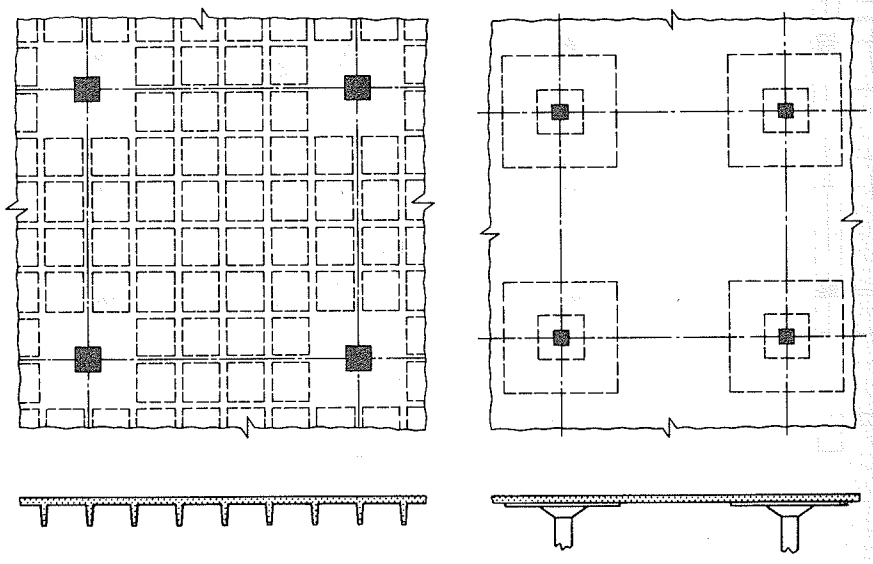

(e) (f)

FIGURE 10.1 (*Continued*)

both. These devices increase shear strength and negative bending resistance at the columns. The design trend is away from the use of either dropped panels or flared columns, in favor of flat plates incorporating special reinforcement to serve the same purpose.

Prestressed concrete slabs are usually designed for dead and live loads assumed to be uniformly distributed over the entire surface of an area bounded by column centerlines or beam centerlines. Pattern live loadings, for which certain panels are unloaded, may be considered to obtain maximum and minimum moments. Concentrated loads require special study. They are always supported by a width of slab greater than the contact width, because of two-way action, or in the case of one-way slabs, by lateral distribution steel that is always used. Very heavy fixed concentrated loads may require supporting beams.

The principal reinforcement in prestressed slabs generally consists of stranded cables, typically spaced between about two and five ft center-to-center, depending on the loads, spans, and slab thickness. Variable eccentricity is always specified, with a basic parabolic profile derived from the uniform loads to be carried, but incorporating local concave-downward transition curves over the column centerlines or supporting beams. The concrete protection for the tendons should not be less than one in. if the surface is exposed to earth or weather and not less than 3/4 in. if it is not exposed to weather or in contact with the ground, according to ACI Code.

Economic and construction considerations have generally resulted in the selection of greased and plastic-sheathed unbonded tendons for slabs. These considerations include higher friction during stressing of tendons of the type intended for later grouting, the necessity to protect unsheathed tendons against corrosion during construction, and the problems associated with grouting a large number of tendons in small diameter ducts. Non-prestressed bar reinforcement is commonly added in slabs for lateral distribution steel, and in the moment direction to control cracking and enhance flexural strength. It also increases shear strength at the columns of flat plate construction.

Prestressed concrete slabs must exhibit satisfactory behavior at all stages of loading. Allowable stresses must not be exceeded at the unloaded or full service load stages. Camber and deflection must be within acceptable limits. Adequate strength must be provided to resist the specified degree of overloading.

Any of these requirements may serve as the starting point in proportioning the slab. Recognizing that deflections may govern for relatively thin members such as slabs, many designers start with an assumed slab depth, based on maximum span-to-depth ratios or personal experience, to insure adequate stiffness. For some types of slabs, notably flat plates, shear is critical. The initial estimate of slab thickness may be such as to satisfy shear strength requirements at the columns.

The concept of load balancing is specially useful for slabs, and usually provides the basis for establishing the best tendon profile, as well as the prestress force required to produce zero deflection for the selected load. The load to be balanced is often the full dead load.

10.2 ONE-WAY SLABS

It has been noted that for one-way slabs the main structural action is in the direction perpendicular to the two supported edges. It follows that the principal prestressing tendons are placed perpendicular to the supports, as shown for a single-span slab in Fig. 10.2*a*. Normally unbonded strands are employed, and some bonded bar reinforcement is included to provide a strength reserve and crack control. Consistent with the principle of load balancing, a parabolic tendon profile would be selected for the usual case of uniformly distributed load, with eccentricity varying from maximum at midspan to zero at the supported edges for the simply supported slab shown.

It is convenient for design purposes to isolate a typical slab strip of unit width, as shown in Fig. 10.2*a*. The load applied per unit area of slab surface is then equivalent to a distributed load per unit length along the strip of span l. All the equations developed in earlier chapters for beams can be applied, with no change, to the slab strip under consideration.[1] The required prestressing force

[1] This simplified analysis, which neglects lateral pressures between adjacent slab strips resulting from the Poisson effect, is slightly conservative. The slab will actually be slightly stiffer and stronger than assumed, but the difference is small and is almost always disregarded.

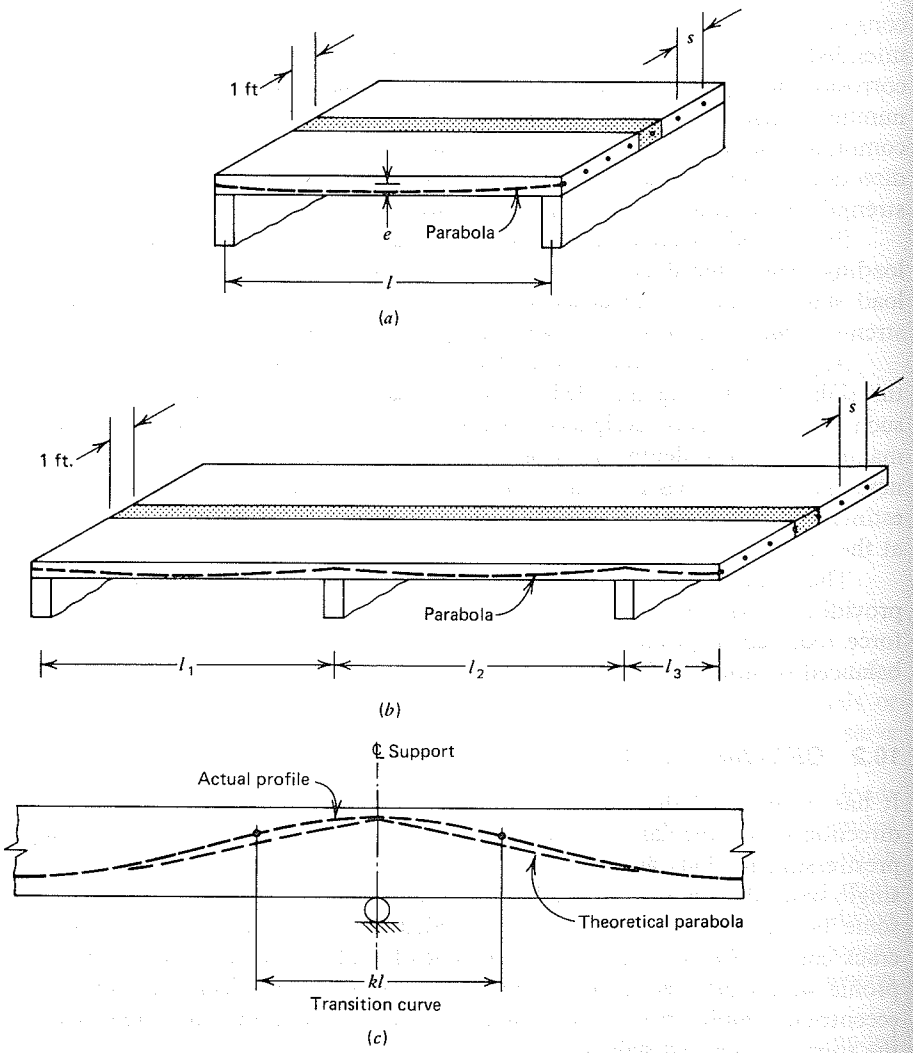

FIGURE 10.2 One-way slabs. (*a*) Simple span. (*b*) Continuous spans. (*c*) Detail at interior support.

determined will be that per unit width of slab. This can easily be translated into a required spacing s for tendons of known capacity. As a general guide, ACI Committee 423 has recommended that the spacing not exceed six to eight times the slab thickness h (Ref. 10.1). The maximum spacing permitted by the ACI Code is eight times the slab thickness, but not more than 5 ft. The Code further requires a minimum average prestress P_e/A_c of 125 psi on the slab section tributary to a tendon or tendon group.

One-way slabs are often continuous over several supports or cantilevered, as suggested by Fig. 10.2*b*. A design approach similar to that for simple spans is followed but, in this case, the continuous tendon may be raised over the interior supports to the maximum negative eccentricity permitted by requirements of concrete cover. Parabolic profiles are used in each span, with relatively short, concave-downward transition curves over the interior supports. These transitions have the effect of delivering the downward reaction from each tendon over a finite length kl, as in Fig. 10.2*c*, rather than at a point, as would be true for the theoretically correct but impractical profile shown. In ordinary cases, the value of k may be about 0.20. The difference between concentrated and distributed reactions may be accounted for in the design, but is usually disregarded, since the reversed curvature has only a minor influence on the elastic moments and usually does not affect ultimate moment capacity.[2]

The tendons may be continuous over two, three, or more spans. Because of the shallow depth of slabs compared with beams, the prestress loss due to friction is not as severe, and it does not preclude several reversals of curvature. The effect of frictional losses in slabs may be further minimized by jacking alternate tendons from opposite ends, or for tendons longer than about 150 ft, by jacking each tendon from both ends.

When unbonded tendons are used for continuous one-way slabs, special consideration must be given to the consequences of a catastrophic loading condition or a fire, which might cause failure of all the tendons in one span. This would lead to loss of prestress and load-carrying capacity in the other spans, with disastrous results. The minimum requirement for non-prestressed steel in members with unbonded tendons that is imposed by ACI Code:

$$A_s = 0.004A \tag{4.35}$$

is intended, at least in part, to guard against such total collapse, as well as to control cracking (see Section 4.8C). The amount of steel required by Eq. (4.35) is approximately equal to the minimum reinforcement for non-prestressed slabs. Because this steel is intended to function as part of an alternate load-carrying system, it should be detailed according to all requirements for development length, anchorage, and bar cutoff imposed by ACI Code for reinforced concrete (Ref. 10.1). The minimum length requirements quoted in Section 4.8C with reference to Eq. (4.35) are not adequate in this regard, and are intended merely to provide crack control.

Unless a concordant tendon system is used, post-tensioning a continuous slab will result in secondary moments, which affect both service load stresses and ultimate strength. They are most easily found using the method of equivalent loads (Section 8.4B) to obtain the total moments from prestressing, after which primary moments Pe are subtracted to obtain the secondary moments.

[2] Secondary moments may be slightly changed.

In calculating the resisting moments ϕM_n at critical sections, the steel stress at failure f_{ps} can be found using Eq. (3.23) or Eq. (3.24) of Section 3.8A. Because slab span-to-depth ratios are typically higher than 35, Eq. (3.24) will usually apply. In continuous slabs, an average of value of f_{ps} calculated at positive and negative moment sections along the slab should be used. The non-prestressed bar reinforcement just described can be included in computing flexural strength, and may be considered to act at the bar yield stress f_y.

In addition to the main prestressed steel perpendicular to the supports, one-way slabs should be provided with reinforcement in the direction parallel to the supports. This serves the purpose of controlling cracks due to shrinkage of the concrete or due to a decrease in temperature. It also serves to distribute any concentrated loads. Reinforcement for shrinkage and temperature effects and load distribution may be non-prestressed bar steel, as for ordinary reinforced concrete construction. The ACI Code specifies the following minimum ratios of reinforcement area to gross concrete area:

Slabs where Grade 40 or 50 deformed bars are used	0.0020
Slabs where Grade 60 deformed bars or welded wire fabric (smooth or deformed) are used	0.0018
Slabs where reinforcement with yield strength exceeding 60,000 psi measured at a yield strain of 0.35 percent is used	$\dfrac{0.0018 \times 60{,}000}{f_y}$

In no case are such reinforcing bars to be placed farther apart than five times the slab thickness or more than 18 in., and in no case is the steel ratio to be less than 0.0014. Use of non-prestressed bar steel does not eliminate shrinkage or temperature cracks, but does insure that these will be very narrow "hairline" cracks, well distributed throughout the slab and not detrimental in any way.

An alternative that may completely avoid cracking is to use centroidal post-tensioned tendons, parallel to the supported edges, to provide a uniform compressive stress in that direction. This scheme is not practical for narrow one-way slabs, because short prestressing is neither economical, nor accurate, but it has been successful for wide slabs. If such an arrangement is used, a minimum concrete compression of 100 psi should be maintained. Prestressing a slab in the transverse direction has the effect of reducing losses associated with elastic shortening and creep in the longitudinal direction, but it can be shown that the reduction is not significant.

The design of one-way slabs will seldom be controlled by shear, although shear strength should be checked by the usual equations for beams. The critical section is to be taken a distance $h/2$ from the support face. One-way slabs, essentially wide shallow beams, are more apt to be critical in flexure or governed by deflection. For slabs designed by the load-balancing method, it is the deflection due to the *unbalanced* load (usually the live load) that is important. In calculations, the moment of inertia of the gross concrete cross section may be used unless the flexural tensile stress exceeds $6\sqrt{f_c'}$, in which case the methods of Section 9.6 are available.

The ACI Code requires that deflection be calculated for slabs, as well as for all other prestressed members, and that the computed deflections should not exceed the limits given in Table 9.5.

Span-to-depth ratios provide a convenient starting point in proportioning one-way slabs. For single-span solid slabs, values between 35 and 40 are common. For fully continuous spans, ratios between 45 and 50 are often seen. The total required thickness is usually rounded to the next higher one-quarter in. for slabs up to 6 in. in thickness, and to the next higher one-half in. for thicker slabs.

A practical consideration that must not be overlooked in the design of slabs prestressed longitudinally, or both longitudinally and transversely, is that axial shortening of the slab must not be prevented by conditions at the supports. This shortening may be particularly significant for multiple span members of substantial total length or very wide slabs. To avoid problems resulting from slab shortening, a maximum average prestress of about 250 psi appears to be reasonable. The maximum length of a slab between construction joints should be limited to about 200 ft.

Some reinforcement should be included at end anchorages to avoid failure by splitting of the concrete. Two No. 4 bars are commonly used along the edge of the slab behind the anchorages, but they are ineffective in preventing horizontal splitting. Rebars perpendicular to the edge, bent down and hooked if necessary for anchorage, are often used.

10.3 TWO-WAY SLABS WITH ALL EDGES SUPPORTED: BEHAVIOR

Two-way slab systems may be supported by walls or relatively stiff beams on all four sides of each panel. Whereas the one-way slabs discussed in the preceding section deform under load into a cylindrical surface (Fig. 10.3*a*), a two-way edge-supported slab will bend into a dished shape (Fig. 10.3*b*). At any location, the slab is curved in both principal directions and, consequently, moments exist in both directions. Prestressing tendons are placed in two directions, parallel to the edges of the slab, each set providing for its share of the applied load.

Inspection of Fig. 10.3*b* will show that the curvature of the central part of the slab in the short direction is greater than that in the long direction. Since the bending moment is directly proportional to curvature, it may be concluded that the bending moment in the short direction is larger than that in the long direction. Furthermore, the short span curvature is less near the short edges of the panel than at the center of the slab. Consequently, a variation of short span moments exists across the width of the slab, moments reducing markedly as the

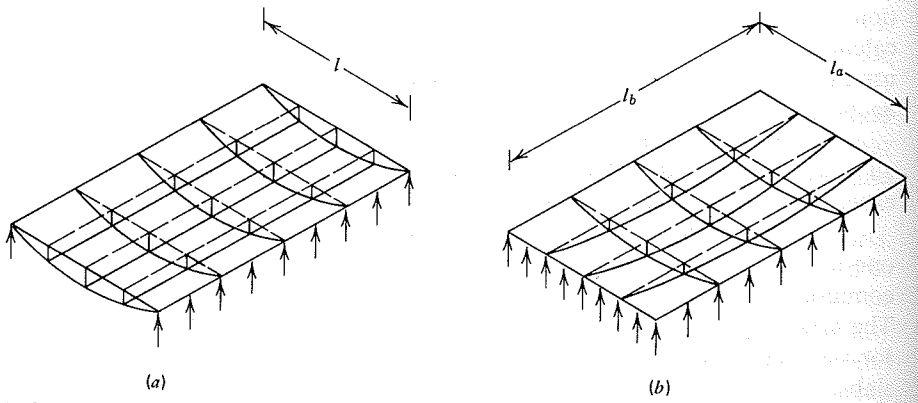

FIGURE 10.3 Deflected shape of uniformly loaded edge-supported slabs. (*a*) One-way slab with two edges supported. (*b*) Two-way slab with four edges supported.

supported edges are approached. Similar behavior is apparent in the long direction.

Loads applied to two-way slabs cause twisting moments, as well as bending moments. Careful study of Fig. 10.3*b* indicates that slab strips in either direction, at any location except the slab centerlines, must twist to conform to the flexural rotations in the perpendicular direction. The internal twisting moments developed by two-way slabs tend to reduce the bending moments that must be resisted.

It may be clear from this short discussion that the determination slab design moments, in even the relatively simple two-way slab shown, is a fairly difficult problem. Although solutions are available based on application of the theory of elasticity, practical cases are complicated by the continuity of the slab over one or more of the edges, torsional and vertical deflection of the edge beams, varying panel proportions, and so on. The more important variables are incorporated in an approximate way in practical methods of analysis.

10.4 TWO-DIRECTIONAL LOAD BALANCING FOR EDGE-SUPPORTED SLABS

The concept of load balancing, introduced in Chapter 1 and developed further in Chapter 4, is a useful tool for the analysis and design of two-way wall- or beam-supported slabs. The objective of load balancing for slabs, as for beams, is to provide an equivalent upward load from the curved tendons to exactly balance a specified downward load. For that unique loading, the slab is subjected only to a uniform compressive stress in its own plane, resulting from the prestress force. Neither bending moments nor twisting moments will exist and, consequently, the analysis is very much simplified. If the external load is sustained in nature, as is the prestress force, the slab will exhibit little camber or deflection.

Two-directional load balancing for slabs differs from linear load balancing for beams, in that the equivalent load on the slab produced by the tendons in one direction either adds to, or subtracts from, the equivalent load from the tendons in the perpendicular direction. The fractional part of the load to be carried by the tendons in either direction is more or less arbitrary, the only strict requirement being satisfaction of static equilibrium. Consideration of indeterminancy is avoided for the unique balanced load that produces no deflection.

The fundamentals of two-directional load balancing will be demonstrated in the context of the rectangular, wall-supported slab of Fig. 10.4. The load to be balanced is generally the dead load, and is uniformly distributed. This leads naturally to the choice of parabolic tendon profiles in each direction as shown. Simply supported edges, in turn, govern the choice of zero eccentricity over the walls.

From Eq. (4.27) of Chapter 4, the upward equivalent load, uniformly distributed, applied to the slab by parabolic tendons in the short span direction is

$$w_{pa} = \frac{8P_a y_a}{l_a^2} \tag{10.1a}$$

where w_{pa} is the upward load in terms of force per unit area of slab surface, P_a is the effective prestress force after losses in the l_a direction per unit of length along side l_b, and y_a is the maximum eccentricity of those tendons with respect to the middepth of the slab. Similarly, the tendons in the direction l_b produce an upward equivalent load of

$$w_{pb} = \frac{8P_b y_b}{l_b^2} \tag{10.1b}$$

For design, the sum of the two upward components is set equal to the load to be balanced:

$$w_b = \frac{8P_a y_a}{l_a^2} + \frac{8P_b y_b}{l_b^2} \tag{10.2}$$

and the required prestressing forces P_a and P_b determined accordingly.

Note that many combinations of P_a and P_b will satisfy the requirement of static equilibrium given by Eq. (10.2).

For rectangular panels, in general, the economical choice is to carry most of the load in the short direction. However, it is usually desirable to maintain a

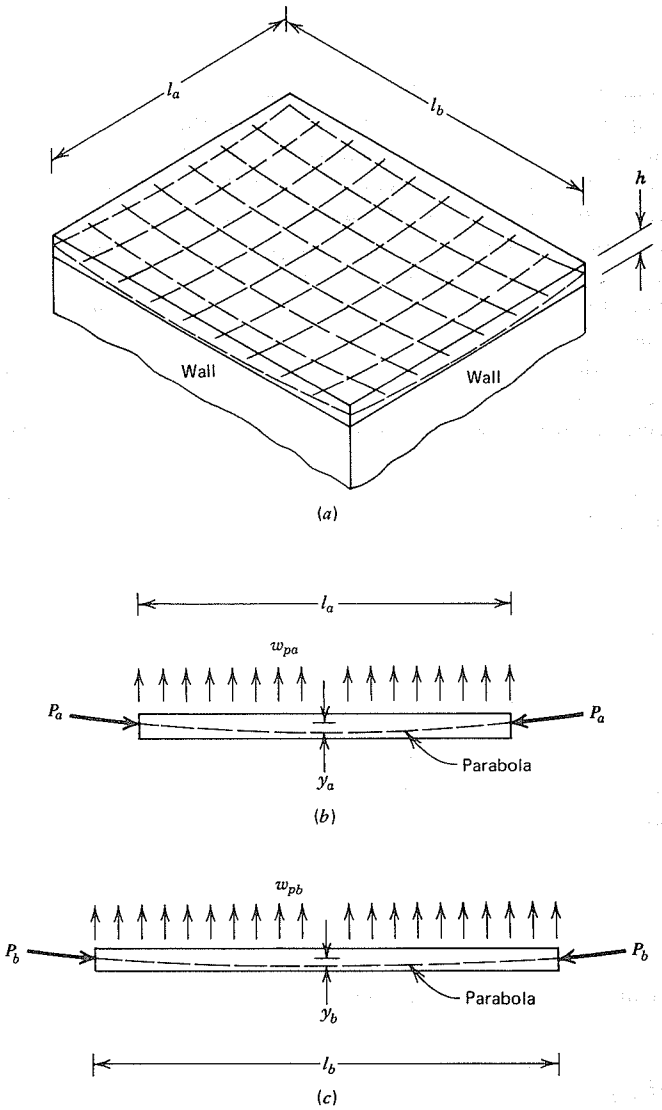

FIGURE 10.4 Wall-supported slab with two-directional tendon layout.

minimum precompression of about 100 psi in the long direction to control cracking and to provide for improved distribution of any locally applied load. This can be used to reduce the prestress required in the short direction by the amount w_{pb} from Eq. (10.1*b*).

Under the action of prestressing forces P_a and P_b plus the applied load w_b, the slab will be in a state of uniform compression P_a/bh in the direction of l_a and P_b/bh in the direction of l_b, where h is the slab thickness and b is the width of the unit strip, in appropriate units. Theoretically, the slab should be a completely level surface for this special loading, although this state will be only approximated in practice. This is because of uncertainties connected with losses and because of time-dependent effects on deflections.

If the slab is subjected to an incremental load above the balanced load, moments resulting from the unbalanced portion of the load may be determined using the methods of classical elasticity or the approximate methods described in Section 10.5. The resulting stresses in the slab (within the elastic range) are found by superimposing the uniform compression from the balanced loading and the flexural stresses associated with the moments due to the unbalanced loading. In the direction of l_a:

$$f_1 = -\frac{P_a}{bh} - \frac{M_a h}{2I_c}$$
$$f_2 = -\frac{P_a}{bh} + \frac{M_a h}{2I_c} \qquad (10.3a)$$

at the top and bottom face of the slab, respectively, and in the direction of l_b:

$$f_1 = -\frac{P_b}{bh} - \frac{M_b h}{2I_c}$$
$$f_2 = -\frac{P_b}{bh} + \frac{M_b h}{2I_c} \qquad (10.3b)$$

where M_a and M_b are the moments associated with the unbalanced portion of the load in the l_a and l_b directions, respectively, per unit strip of slab, and I_c is the moment of inertia of a unit strip of the slab section, which is assumed uncracked. Stresses in the unloaded stage and stresses at full service loading may be found in this way and compared against specified limits.

The arrangement of tendons suggested by Fig. 10.4 is not the only possibility, or even the best, from points of view other than load balancing. If an additional load is applied, the full service live load for example, the slab will deflect downward and the behavior described in Section 10.3 will result. A greater concentration of tendons in a central band in either direction would be more rational and more economical for that loading, although a slab designed with banded tendons would not be a level surface if the live load were removed. A banded arrangement of tendons would produce a slab with a greater strength reserve, should it be overloaded, than one with the same number of tendons at uniform spacing.

In two-way slabs, a practical problem may arise resulting from interference of the tendons passing in perpendicular directions in certain regions. In the simply supported panel shown in Fig. 10.4, for example, such tendon interference will occur in the central region and at the corners. For thicker slabs, it is sufficiently accurate to use the average eccentricity for calculations in each direction; the loads will redistribute accordingly, should severe overloading occur. For thinner slabs, for which the tendon diameter represents a more substantial fraction of the slab depth, it is advisable to use actual eccentricities, recognizing that stacking is unavoidable.

10.5 PRACTICAL ANALYSIS FOR UNBALANCED LOADING

If the loading applied to an edge-supported slab deviates from the balanced loading, the slab will deflect either upward or downward, and moments must be found recognizing the indeterminate nature of even a simply supported rectangular panel. Typically, stresses must be checked when full service live load causes downward deflection, and moments due to factored loads must be found in connection with strength analysis. Although the classical methods of elastic analysis provide solutions for very idealized situations, practical complications intrude and, as a result, approximate methods are favored that account for these complicating factors, if only in a simplified way.

Perhaps the most rational and comprehensive of the simplified approaches is known as Method 3, published in the Appendix to the 1963 edition of the ACI Code.[3] The method applies to slabs supported on four sides by walls or relatively stiff beams.[4] The ratio of short to long sides of a panel may vary between 1.0 and 0.5. Slabs for which the aspect ratio is less than 0.5 may be designed for one-way action. The edge restraint conditions considered are simply supported (torsional resistance negligible) and continuous across or fixed at the supports. Nine separate combinations of restraint are included.

For each set of variables within the stated ranges, coefficients are given that permit the direct calculation of moments. These coefficients are based on elastic analysis, but also account for inelastic redistribution of moments. The design moments in the two directions are computed from the expressions

$$M_a = C_a w l_a^2 \qquad (10.4a)$$

$$M_b = C_b w l_b^2 \qquad (10.4b)$$

[3]It is unfortunate that the method has been deleted from subsequent editions of the Code; however, its validity has not been questioned, and it continues to be a useful tool.

[4]For cases with more flexible beams, the stiffness of which is of the same order as the slab, or for two-way slabs supported directly on columns with no beams, the methods of Section 10.12 are appropriate.

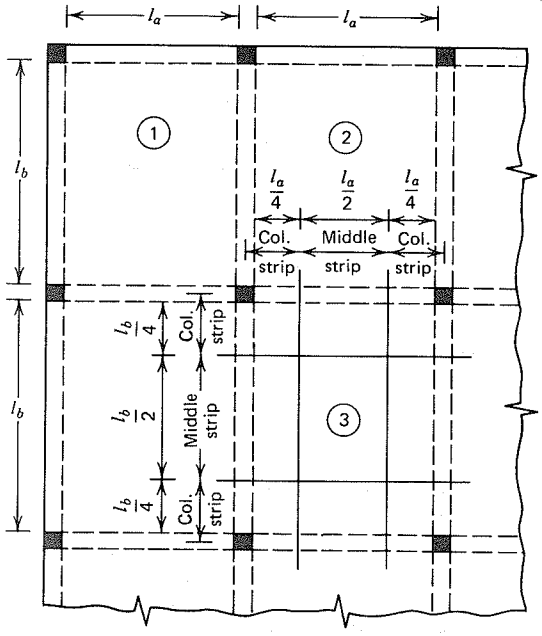

FIGURE 10.5 Beam-supported two-way slab.

where C_a and C_b = tabulated moment coefficients
w = uniformly distributed load per ft^2
l_a and l_b = length of clear span in short and long directions, respectively, ft

The method provides that each panel be divided, in both directions, into a middle strip whose width is one-half that of the panel, and two column strips of one-quarter of the panel width. As noted in Section 10.3, the moments in both directions are larger in the central region of the slab than in regions close to the edges. Correspondingly, Method 3 provides that the entire middle strip be designed for the full design moments calculated with the tabulated coefficient. In the column strips, this moment is assumed to decrease from its full value at the edge of the middle strip to one-third of this value at the edge of the panel.

Figure 10.5 shows a portion of the floor of a two-way beam-supported slab structure, with middle and column strips in both directions indicated for panel 3. The figure also illustrates certain of the possible edge conditions. Panel 1, for example, has two adjacent discontinuous exterior edges, while the other edges are continuous with neighboring panels. Panel 2 has one discontinuous and three continuous edges. The interior panel 3 has all edges continuous.

Tables 10.1 through 10.4, reproduced from the 1963 ACI Code, give coefficients for moments and shears in two-way slab panels.

Table 10.1 Coefficients for negative moments in slabs[a]

$M_{a,\text{neg}} = C_{a,\text{neg}} w l_a^2$
$M_{b,\text{neg}} = C_{b,\text{neg}} w l_b^2$
where w = total uniform dead plus live load

Ratio $m = \frac{l_a}{l_b}$		Case 1	Case 2	Case 3	Case 4	Case 5	Case 6	Case 7	Case 8	Case 9
1.00	$C_{a,\text{neg}}$		0.045		0.050	0.075	0.071		0.033	0.061
	$C_{b,\text{neg}}$		0.045	0.076	0.050			0.071	0.061	0.033
0.95	$C_{a,\text{neg}}$		0.050		0.055	0.079	0.075		0.038	0.065
	$C_{b,\text{neg}}$		0.041	0.072	0.045			0.067	0.056	0.029
0.90	$C_{a,\text{neg}}$		0.055		0.060	0.080	0.079		0.043	0.068
	$C_{b,\text{neg}}$		0.037	0.070	0.040			0.062	0.052	0.025
0.85	$C_{a,\text{neg}}$		0.060		0.066	0.082	0.083		0.049	0.072
	$C_{b,\text{neg}}$		0.031	0.065	0.034			0.057	0.046	0.021
0.80	$C_{a,\text{neg}}$		0.065		0.071	0.083	0.086		0.055	0.075
	$C_{b,\text{neg}}$		0.027	0.061	0.029			0.051	0.041	0.017
0.75	$C_{a,\text{neg}}$		0.069		0.076	0.085	0.088		0.061	0.078
	$C_{b,\text{neg}}$		0.022	0.056	0.024			0.044	0.036	0.014
0.70	$C_{a,\text{neg}}$		0.074		0.081	0.086	0.091		0.068	0.081
	$C_{b,\text{neg}}$		0.017	0.050	0.019			0.038	0.029	0.011
0.65	$C_{a,\text{neg}}$		0.077		0.085	0.087	0.093		0.074	0.083
	$C_{b,\text{neg}}$		0.014	0.043	0.015			0.031	0.024	0.008
0.60	$C_{a,\text{neg}}$		0.081		0.089	0.088	0.095		0.080	0.085
	$C_{b,\text{neg}}$		0.010	0.035	0.011			0.024	0.018	0.006
0.55	$C_{a,\text{neg}}$		0.084		0.092	0.089	0.096		0.085	0.086
	$C_{b,\text{neg}}$		0.007	0.028	0.008			0.019	0.014	0.005
0.50	$C_{a,\text{neg}}$		0.086		0.094	0.090	0.097		0.089	0.088
	$C_{b,\text{neg}}$		0.006	0.022	0.006			0.014	0.010	0.003

[a]A crosshatched edge indicates that the slab continues across or is fixed at the support; an unmarked edge indicates a support at which torsional resistance is negligible.

In the tables, the effects of dead loads are differentiated from the effects of live loads. Dead loads are always present in all panels of a floor system, although live loads may or may not act, and must be positioned for the maximum effect.

Table 10.1 gives moment coefficients for *negative moments at continuous edges*. Maximum negative edge moments are obtained when both panels adjacent to the particular edge carry full dead and live load. The moment is computed for this total load. Clearly, the same coefficients apply in calculating the maximum negative moments due to dead load alone, or live load only, which is assumed to

Table 10.2 Coefficients for Dead Load Positive Moments in Slabs[a]

$M_{a,\text{pos},dl} = C_{a,dl} w l_a^2$
$M_{b,\text{pos},dl} = C_{b,dl} w l_b^2$
where w = total uniform dead load

Ratio $m = \frac{l_a}{l_b}$		Case 1	Case 2	Case 3	Case 4	Case 5	Case 6	Case 7	Case 8	Case 9
1.00	$C_{a,dl}$	0.036	0.018	0.018	0.027	0.027	0.033	0.027	0.020	0.023
	$C_{b,dl}$	0.036	0.018	0.027	0.027	0.018	0.027	0.033	0.023	0.020
0.95	$C_{a,dl}$	0.040	0.020	0.021	0.030	0.028	0.036	0.031	0.022	0.024
	$C_{b,di}$	0.033	0.016	0.025	0.024	0.015	0.024	0.031	0.021	0.017
0.90	$C_{a,dl}$	0.045	0.022	0.025	0.033	0.029	0.039	0.035	0.025	0.026
	$C_{b,dl}$	0.029	0.014	0.024	0.022	0.013	0.021	0.028	0.019	0.015
0.85	$C_{a,dl}$	0.050	0.024	0.029	0.036	0.031	0.042	0.040	0.029	0.028
	$C_{b,dl}$	0.026	0.012	0.022	0.019	0.011	0.017	0.025	0.017	0.013
0.80	$C_{a,dl}$	0.056	0.026	0.034	0.039	0.032	0.045	0.045	0.032	0.029
	$C_{b,dl}$	0.023	0.011	0.020	0.016	0.009	0.015	0.022	0.015	0.010
0.75	$C_{a,dL}$	0.061	0.028	0.040	0.043	0.033	0.048	0.051	0.036	0.031
	$C_{b,dl}$	0.019	0.009	0.018	0.013	0.007	0.012	0.020	0.013	0.007
0.70	$C_{a,dl}$	0.068	0.030	0.046	0.046	0.035	0.051	0.058	0.040	0.033
	$C_{b,dl}$	0.016	0.007	0.016	0.011	0.005	0.009	0.017	0.011	0.006
0.65	$C_{a,dl}$	0.074	0.032	0.054	0.050	0.036	0.054	0.065	0.044	0.034
	$C_{b,dl}$	0.013	0.006	0.014	0.009	0.004	0.007	0.014	0.009	0.005
0.60	$C_{a,dl}$	0.081	0.034	0.062	0.053	0.037	0.056	0.073	0.048	0.036
	$C_{b,dl}$	0.010	0.004	0.011	0.007	0.003	0.006	0.012	0.007	0.004
0.55	$C_{a,dl}$	0.088	0.035	0.071	0.056	0.038	0.058	0.081	0.052	0.037
	$C_{b,dl}$	0.008	0.003	0.009	0.005	0.002	0.004	0.009	0.005	0.003
0.50	$C_{a,dl}$	0.095	0.037	0.080	0.059	0.039	0.061	0.089	0.056	0.038
	$C_{b,dl}$	0.006	0.002	0.007	0.004	0.001	0.003	0.007	0.004	0.002

[a]A crosshatched edge indicates that the slab continues across or is fixed at the support; an unmarked edge indicates a support at which torsional resistance is negligible.

be acting on both adjacent panels. Method 3 provides that *negative moments at discontinuous edges* will be assumed equal to one-third of the positive moments for the same direction. One must provide for such moments because some degree of restraint is provided by discontinuous edges, by the torsional rigidity of the edge beam, or by the supporting wall.

For *positive moments*, there will be little, if any, rotation at the continuous edges if *dead load* alone is acting, because the loads on both adjacent panels tend

Table 10.3 Coefficients for Live Load Positive Moments in Slabs[a]

$M_{a,\text{pos},ll} = C_{a,ll} w l_a^2$
$M_{b,\text{pos},ll} = C_{b,ll} w l_b^2$
where w = total uniform live load

Ratio $m = \frac{l_a}{l_b}$		Case 1	Case 2	Case 3	Case 4	Case 5	Case 6	Case 7	Case 8	Case 9
1.00	$C_{a,ll}$	0.036	0.027	0.027	0.032	0.032	0.035	0.032	0.028	0.030
	$C_{b,ll}$	0.036	0.027	0.032	0.032	0.027	0.032	0.035	0.030	0.028
0.95	$C_{a,ll}$	0.040	0.030	0.031	0.035	0.034	0.038	0.036	0.031	0.032
	$C_{b,ll}$	0.033	0.025	0.029	0.029	0.024	0.029	0.032	0.027	0.025
0.90	$C_{a,ll}$	0.045	0.034	0.035	0.039	0.037	0.042	0.040	0.035	0.036
	$C_{b,ll}$	0.029	0.022	0.027	0.026	0.021	0.025	0.029	0.024	0.022
0.85	$C_{a,ll}$	0.050	0.037	0.040	0.043	0.041	0.046	0.045	0.040	0.039
	$C_{b,ll}$	0.026	0.019	0.024	0.023	0.019	0.022	0.026	0.022	0.020
0.80	$C_{a,ll}$	0.056	0.041	0.045	0.048	0.044	0.051	0.051	0.044	0.042
	$C_{b,ll}$	0.023	0.017	0.022	0.020	0.016	0.019	0.023	0.019	0.017
0.75	$C_{a,ll}$	0.061	0.045	0.051	0.052	0.047	0.055	0.056	0.049	0.046
	$C_{b,ll}$	0.019	0.014	0.019	0.016	0.013	0.016	0.020	0.016	0.013
0.70	$C_{a,ll}$	0.068	0.049	0.057	0.057	0.051	0.060	0.063	0.054	0.050
	$C_{b,ll}$	0.016	0.012	0.016	0.014	0.011	0.013	0.017	0.014	0.011
0.65	$C_{a,ll}$	0.074	0.053	0.064	0.062	0.055	0.064	0.070	0.059	0.054
	$C_{b,ll}$	0.013	0.010	0.014	0.011	0.009	0.010	0.014	0.011	0.009
0.60	$C_{a,ll}$	0.081	0.058	0.071	0.067	0.059	0.068	0.077	0.065	0.059
	$C_{b,ll}$	0.010	0.007	0.011	0.009	0.007	0.008	0.011	0.009	0.007
0.55	$C_{a,ll}$	0.088	0.062	0.080	0.072	0.063	0.073	0.085	0.070	0.063
	$C_{b,ll}$	0.008	0.006	0.009	0.007	0.005	0.006	0.009	0.007	0.006
0.50	$C_{a,ll}$	0.095	0.066	0.088	0.077	0.067	0.078	0.092	0.076	0.067
	$C_{b,ll}$	0.006	0.004	0.007	0.005	0.004	0.005	0.007	0.005	0.004

[a]A crosshatched edge indicates that the slab continues across or is fixed at the support; an unmarked edge indicates a support at which torsional resistance is negligible.

to produce opposite rotations that cancel or nearly cancel. Hence, for this condition, the continuous edges can be regarded as fixed, and the appropriate coefficients for the dead load moments are given in Table 10.2. On the other hand, the maximum *live load moments* are obtained when the live load is placed only on the particular panel and not on any of the adjacent panels. In this case, some rotation will occur at all continuous edges. As an approximation, it is assumed that there is 50 percent restraint for calculating these live load moments, and the corresponding coefficients are given in Table 10.3.

Table 10.4 Ratio of Load W in l_a and l_b Directions for Shear in Slab and Load on Supports[a]

Ratio $m = \frac{l_a}{l_b}$		Case 1	Case 2	Case 3	Case 4	Case 5	Case 6	Case 7	Case 8	Case 9
1.00	W_a	0.50	0.50	0.17	0.50	0.83	0.71	0.29	0.33	0.67
	W_b	0.50	0.50	0.83	0.50	0.17	0.29	0.71	0.67	0.33
0.95	W_a	0.55	0.55	0.20	0.55	0.86	0.75	0.33	0.38	0.71
	W_b	0.45	0.45	0.80	0.45	0.14	0.25	0.67	0.62	0.29
0.90	W_a	0.60	0.60	0.23	0.60	0.88	0.79	0.38	0.43	0.75
	W_b	0.40	0.40	0.77	0.40	0.12	0.21	0.62	0.57	0.25
0.85	W_a	0.66	0.66	0.28	0.66	0.90	0.83	0.43	0.49	0.79
	W_b	0.34	0.34	0.72	0.34	0.10	0.17	0.57	0.51	0.21
0.80	W_a	0.71	0.71	0.33	0.71	0.92	0.86	0.49	0.55	0.83
	W_b	0.29	0.29	0.67	0.29	0.08	0.14	0.51	0.45	0.17
0.75	W_a	0.76	0.76	0.39	0.76	0.94	0.88	0.56	0.61	0.86
	W_b	0.24	0.24	0.61	0.24	0.06	0.12	0.44	0.39	0.14
0.70	W_a	0.81	0.81	0.45	0.81	0.95	0.91	0.62	0.68	0.89
	W_b	0.19	0.19	0.55	0.19	0.05	0.09	0.38	0.32	0.11
0.65	W_a	0.85	0.85	0.53	0.85	0.96	0.93	0.69	0.74	0.92
	W_b	0.15	0.15	0.47	0.15	0.04	0.07	0.31	0.26	0.08
0.60	W_a	0.89	0.89	0.61	0.89	0.97	0.95	0.76	0.80	0.94
	W_b	0.11	0.11	0.39	0.11	0.03	0.05	0.24	0.20	0.06
0.55	W_a	0.92	0.92	0.69	0.92	0.98	0.96	0.81	0.85	0.95
	W_b	0.08	0.08	0.31	0.08	0.02	0.04	0.19	0.15	0.05
0.50	W_a	0.94	0.94	0.76	0.94	0.99	0.97	0.86	0.89	0.97
	W_b	0.06	0.06	0.24	0.06	0.01	0.03	0.14	0.11	0.03

[a]A crosshatched edge indicates that the slab continues across or is fixed at the support; an unmarked edge indicates a support at which torsional resistance is negligible.

Finally, for computing shear in the slab and loads on the supporting beams, Table 10.4 gives the fractions of the total load W that are transmitted in the two directions.

10.6 DEFLECTION OF TWO-WAY SLABS

Edge-supported slabs are typically thin in relation to their span, and may exhibit excessively large deflections when loaded, even though they are satisfactory in all other respects. Early in the design, a trial slab depth should be selected such that need for later revision due to deflection restrictions will be unlikely. For pre-

stressed two-way slabs continuous over supported edges, the ratio of average span to total depth may be estimated to be from 45 to 50.

Slab deflections should always be calculated, and the results compared against limit values. Assuming that the slab has been designed for a balanced state under the combined action of prestress plus full dead load, then the deflection at any other load stage within the elastic range, such as at full service load, can be found considering only the incremental loading past the balanced load stage. Prestressed edge-supported slabs are mostly uncracked up to the service load stage, and the properties of the gross concrete cross section may be used in the calculations without serious error.

Classical methods of deflection analysis are of very limited use in practical cases, because the panel edges are generally neither fully fixed, nor perfectly hinged, but have some intermediate degree of fixity depending on the load and span conditions in the adjacent panels, and on the torsional restraint provided by the edge beams or supporting walls.

However, deflections may be calculated based on the approximate moment coefficients of Section 10.5, which include recognition of such effects in a self-consistent way. Such an approximate approach is fully justified here, because it is only the incremental deflection, not the total deflection that is to be found.

It will be recalled that the moment coefficient method of Section 10.5 is used to determine *maximum values* of positive and negative moments at the critical sections of slabs. The moment coefficients of Tables 10.1 through 10.3 have been established considering the possibility of loads acting on alternate panels and of other arrangements.

Consequently, in the deflection calculations, it would be incorrect to assume that those moments could act simultaneously at positive and negative critical sections.

Because the maximum deflection at the center of a slab panel will normally be obtained when live load acts on that panel, but not on the adjacent panels, deflection calculations should be based on the maximum positive moments found from the coefficients of Table 10.3, together with statically consistent negative moments at the supported edges.

This will be illustrated considering the middle strip of unit width in the long direction of a panel, as shown in Fig. 10.6*a*. The variation of moment for the uniformly distributed loading is parabolic, and by statics, the sum of the positive moment and the average of the two negative moments must be equal to $\overline{M} = \frac{1}{8}\overline{w}l_b^2$, where $\overline{w}$ is the fractional part of the load transmitted in the long direction of the panel. If full fixity were obtained at the supports, the negative moments would be $\frac{1}{12}\overline{w}l_b^2$, or $\frac{2}{3}\overline{M}$, and the positive moment would be $\frac{1}{24}\overline{w}l_b^2$, or $\frac{1}{3}\overline{M}$. But it has been noted earlier that the coefficients for maximum positive moments were derived assuming not 100 percent fixity, but 50 percent fixity. Accordingly, the moment baseline associated with the maximum positive moment M_{max} is as shown in Fig. 10.6*c*, and the statically consistent negative moments at the supports are $\frac{1}{2}M_{max}$.

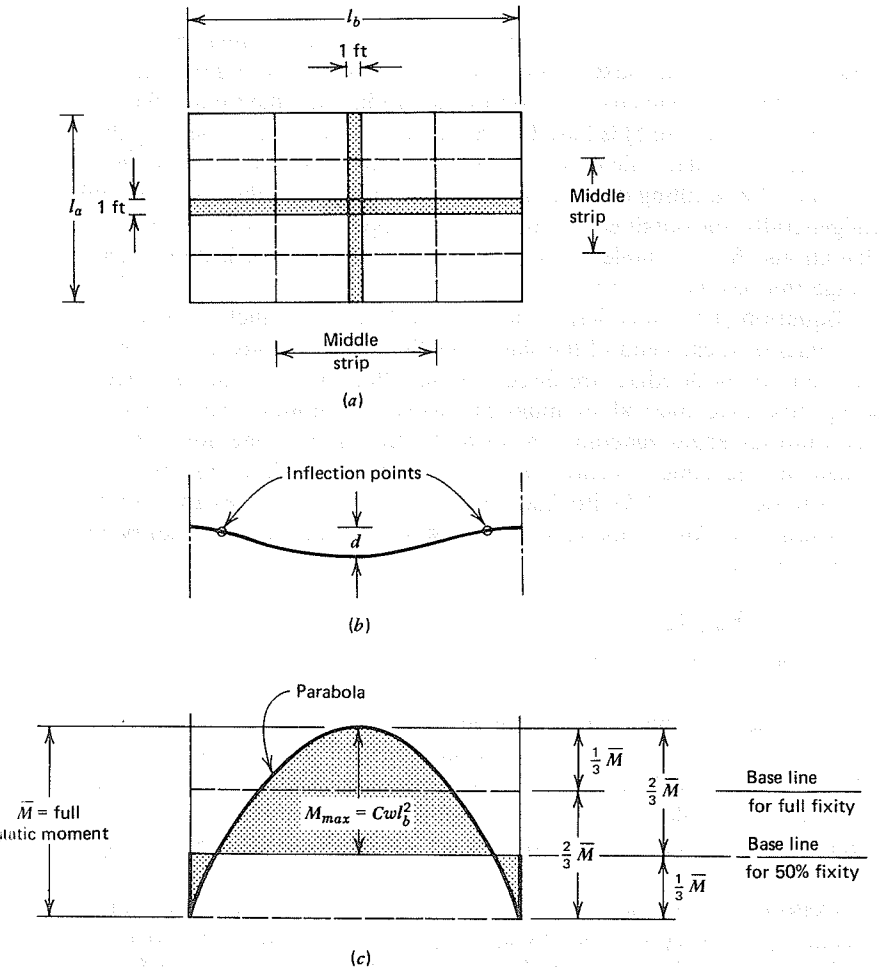

FIGURE 10.6 Basis for deflection analysis of two-way edge-supported slabs. (*a*) Plan view of slab. (*b*) Deflection curve of unit strip. (*c*) Diagram for maximum positive moment.

Deflection calculations are thus based on a parabolic moment curve, with maximum ordinate at midspan, and end moments equal to half that maximum.

The midspan deflection d of the slab strip shown in Fig. 10.6*b* can easily be found using the moment diagram of Fig. 10.6*c*, in conjunction with the moment-area principles. For the slab shown, with all edges continuous:

$$d = \frac{3}{32}\frac{M_{max}l_b^2}{E_cI_c} \tag{10.5}$$

where M_{max} is the positive live load moment obtained using the coefficients of Table 10.3, E_c is the elastic modulus of the concrete, and I_c is the moment of inertia of the concrete cross section of unit width, assumed uncracked.

Although Eq. (10.5) is based on a unit strip spanning in the long direction of the panel, a similar calculation could as easily have been made in the short direction. The resulting deflections should be the same, although small differences will generally be obtained because of the approximate nature of the moment calculations. A reasonable procedure is to calculate the deflection each way and average the results.

Equation (10.5) was derived for a typical interior panel, with equal restraining moments at each end of the slab strip. Similar equations can easily be derived where one or both edges are discontinuous. Bearing in mind that, according to the approximate method of moment analysis, minimum negative moments at discontinuous edges generally are to be taken equal to one-third of the positive moment in the same direction, it is clear that the resulting equations will differ very little from Eq. (10.5). For the special case where all edges are completely free of restraint, as for example, if a slab were supported on masonry walls, the midspan deflection is

$$d = \frac{5}{48}\frac{M_{max}l_b^2}{E_cI_c} \tag{10.6}$$

If the slab is supported on edge beams for which the deflection is significant, the midspan deflection of the beams on the short side of a slab panel may be added to the center deflection of a unit strip of the slab in the long direction, to obtain the total deflection at the center of the bay. Approximately the same result should be obtained adding the short-span slab deflection to the long span beam deflection.

Deflections calculated by the previous equations are the initial elastic deflections, resulting immediately upon application of short-term loads. Since the sustained effects of prestress and dead load have been accounted for separately through load balancing, usually only the short-term deflection associated with the live load is required. However, if all or part of the incremental loading is sustained in nature, the additional long-term deflection may be estimated by multiplying the immediate deflection caused by the sustained load by an appropriate factor. A value of 2.5 has often been used, although this may be unconservative in some cases.

10.7 FLEXURAL STRENGTH OF TWO-WAY SLABS

For slabs, as for other prestressed members, keeping stresses within acceptable limits in the unloaded and service load stages does not insure an adequate degree of safety against collapse. The ultimate strength of slabs for the overload stage should always be determined. Shear strength of edge-supported slabs is usually not critical, although the shear capacity of unit strips may be checked using ordinary beam equations, and compared against the shear strength required, based on the coefficients of Table 10.4. The ultimate flexural strength of slabs is likely to control.

It has been proposed that the yield line theory of ultimate load analysis be applied to prestressed concrete slabs. Basically a two-dimensional version of limit analysis, as is sometimes used for beams and frames, yield line theory assumes the formation of a sufficient number of plastic hinges in an arrangement that forms a mechanism, leading to collapse of the slab. The formation of such hinges, or yield lines, is accompanied by a redistribution of moments so that the elastic moment ratios are modified (Ref. 10.2).

Questions have been raised relative to the applicability of limit analysis, even to reinforced concrete, on the basis that the needed rotation capacity may not be available. Prestressing steel is less ductile than bar reinforcement, and prestressed concrete members show less rotation at critical sections at failure than reinforced concrete members. Although the application of yield line theory to prestressed slabs is an attractive possibility, it may be concluded that there is as yet insufficient experimental basis for doing so. It is recommended that moments be calculated by applying the usual load factors to the moments found from elastic analysis, or from the coefficients of Tables 10.1 through 10.3. The ACI Code permits some readjustment of elastic moments for prestressed flexural members [see Eq. (8.6) of Section 8.10]. These readjustments are often applied to slabs to improve overall economy of the design.

In investigating the ultimate load of slabs, it is no longer appropriate to superimpose load effects, cancelling the effect of prestress uplift against all or part of the surface loading, as is done at the load-balancing stage. Both concrete and steel are stressed into the nonlinear range, invalidating superposition. The prestressing force changes as the slab is overloaded, and the increase generally is not uniform along the length of the tendons. As the slab deflects for heavy overloads, the lateral distribution of moments across the critical sections changes, further invalidating the load-balancing approach. The moments to be carried must be found by applying load factors to the total dead load, including the weight of the slab, and the total live load. Secondary moments due to prestressing must be included, using a load factor of 1.0.

The secondary moments can be found easily using the method of equivalent loads (Section 8.4B) in conjunction with the moment coefficients of Tables 10.1 to 10.3 to find the total moments due to prestressing. The primary prestress moments $P_e e$ are subtracted from the total moments to obtain the secondary moments. The procedure will be illustrated in the following example.

After the moment analysis, the resisting moments at critical sections of the slab are found using beam equations as described in Section 10.2 for one-way slabs. The design is modified, if necessary, so that the strength at all sections ϕM_n

is at least equal to the required strength M_u. Non-prestressed bars should be added, according to Eq. (4.35), for crack control, and if needed to augment the flexural strength. For two-way systems, catastrophic loading beyond ultimate capacity in one bay is not generally as critical to other spans as in one-way systems, because considerable redistribution of forces is possible. Unless the reinforcing bars are used to increase the flexural strength, the minimum lengths quoted in Section 4.8C for crack-control steel are sufficient.

10.8 EXAMPLE: TWO-WAY WALL-SUPPORTED SLAB

A rectangular slab measuring 20 × 30 ft in plan is supported on masonry walls on four sides, offering negligible rotational restraint. The general arrangement is shown in Fig. 10.7. The slab is to be designed to carry a superimposed dead load of 9 psf in addition to its own weight, and will be subjected to a service live load of 50 psf. The condition of balanced load is specified when the full dead load acts. Concrete having 28-day compressive strength of 4,000 psi and $E_c = 3.6 \times 10^6$ psi

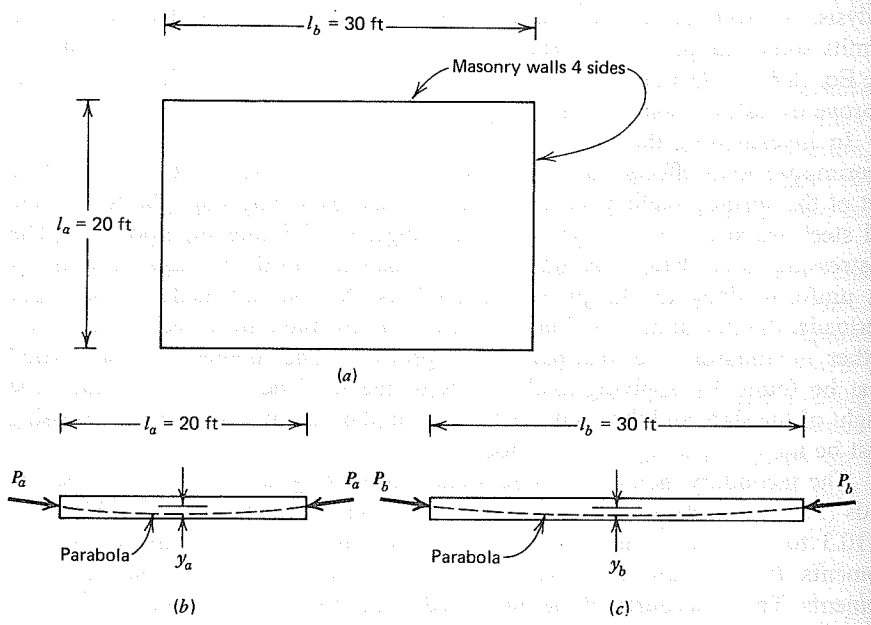

FIGURE 10.7 Design example: two-way slab. (*a*) Plan view. (*b*) Profile of short span. (*c*) Profile of long span.

is to be used. Unbonded, post-tensioned single-strand tendons will be used, and losses after anchorage may be taken at 15 percent of the initial prestress force (l_a = 6.09 m, l_b = 9.14 m, w_d = 0.43 kN/m^2, w_l = 2.40 kN/m^2, f_c' = 28 Mpa and E_c = 24,800 MPa).

A trial slab thickness will be selected based on a span–depth ratio of 45. For edge-supported slabs with side ratio l_b/l_a in the range from 1 to 2, the average span length may be used for this purpose.

$$h = \frac{(20 + 30)12}{2 \times 45} = 6.67 \text{ in.} \quad \text{try } h = 6.5 \text{ in. (165 mm)}$$

Since load balancing is desired for the full dead load stage, the design will be initiated at that stage, although all other significant stages must, of course, be checked. For the trial slab depth, the self-weight is 81 psf, and so the total dead load to be balanced is w_b = 81 + 9 = 90 psf (4.3 kN/m^2).

It is economical to carry most of the load in the short direction. A minimum uniform compression of 150 psi in the concrete in the long direction will be used to insure a crack-free structure. Since the balanced load is uniformly distributed, parabolic tendons will be used in both directions, as shown in Figs. 10.7*b* and 10.7*c*, with zero eccentricity at the supported edges. Given that a 3/4-in. cover must be maintained below the lowest tendons, according to the Code, and assuming that sheathed tendons will have an outer diameter of about 1/2 in., an average distance from the bottom of slab to the tendon centroid of 1 1/4 in. will be used for calculations. This gives a maximum sag for the tendons of 2 in. from the centroid of the 6.5-in. depth slab.

To maintain the selected average compression of 150 psi in the slab in the long direction, an effective prestress force is required of

$$P_b = 150 \times 6.5 \times 12 = 11{,}700 \text{ lb/ft strip (52 kN)}$$

corresponding to an initial value of 13,800 lb/ft strip. From Eq. (10.1*b*), with the tendon profile shown, this produces an uplift of

$$w_{pb} = \frac{8P_b y_b}{l_b^2} = \frac{8 \times 11{,}700 \times 2}{900 \times 12} = 17 \text{ psf}$$

Consequently, an uplift of w_{pa} = 90 − 17 = 73 psf must be provided by the tendons in the short direction. From Eq. (10.1*a*):

$$P_a = \frac{w_{pa} l_a^2}{8y_a} = \frac{73 \times 400 \times 12}{8 \times 2} = 21{,}900 \text{ lb/ft strip (97 kN)}$$

after losses, requiring an initial prestress force of 25,800 lb/ft strip. After losses,

this will produce an average compression in the concrete in the short direction of

$$\frac{P_a}{bh} = \frac{21{,}900}{12 \times 6.5} = 280 \text{ psi}$$

Grade 270 unbonded strand having a diameter of 0.600 in. is selected for each direction (see Appendix B) and tensioned to the full allowed value to produce an initial force of 41,000 lb per tendon after strand anchorage. The required spacing in the short direction is

$$s_a = \frac{41{,}000}{25{,}800} = 1.59 \text{ ft} = 19 \text{ in (483 mm)}$$

and in the long direction

$$s_b = \frac{41{,}000}{13{,}800} = 2.97 \text{ ft} = 36 \text{ in. (914 mm)}$$

These spacings correspond to about 3 and 5.5 times the slab thickness, respectively, confirming that design choices to this point are reasonable.

For crack control, bonded reinforcing bars having an area of $A_s = 0.004 \times 12 \times 3.25 = 0.16$ in.^{2} per ft will be provided using No. 4 bars at 16-in. centers. A length of 10 ft is specified for bars in the l_b direction, and 7 ft for those in the l_a direction, and they will be centered in the postive moment region in each case. In addition, non-prestressed reinforcement will be added at the end anchorages to avoid failure in that highly stressed region. Two horizontal No. 4 bars will be placed around the entire perimeter just inside the anchorages, and manufacturer's recommendations will be followed regarding special grids or spirals at the anchorages.

With the full dead load in place, and prestressing force and arrangement as indicated, a level slab should be obtained, very nearly.

The service live load of 50 psf will now be applied and concrete stresses and slab deflection checked. Making use of the moment coefficients of ACI Method 3, with $l_a/l_b = 20/30 = 0.67$, from Case 1 of Table 10.3 $C_a = 0.072$ and $C_b = 0.014$. Thus, the moments per 12-in. strip in the short and long directions, respectively, resulting from application of the live load of 50 psf are

$$M_a = 0.072 \times 50 \times 20^2 = 1{,}440 \text{ ft-lb}$$

$$M_b = 0.014 \times 50 \times 30^2 = 630 \text{ ft-lb}$$

The moment of inertia of a 12-in. strip of the slab is equal to $12 \times 6.5^3/12 = 275$ in.^{4} The bending stresses that superimpose on the uniform compression stress already existing in the balanced slab are

$$f_b = \frac{1{,}440 \times 12 \times 3.25}{275} = 204 \text{ psi}$$

in the short direction and

$$f_b = \frac{630 \times 12 \times 3.25}{275} = 89 \text{ psi}$$

in the long direction. The resulting stresses are

$$f_1 = -280 - 204 = -484 \text{ psi}$$

$$f_2 = -280 + 204 = -76 \text{ psi}$$

at the top and bottom surfaces in the short direction and

$$f_1 = -150 - 89 = -239 \text{ psi}$$

$$f_2 = -150 + 89 = -61 \text{ psi}$$

at the top and bottom surfaces in the long direction. This indicates a condition of no tension in the slab for full service load, and maximum compression well below the ACI limit stress of $0.45f'_c$.

Deflection at the center of the panel will be checked for the full live load condition using Eq. (10.6). In the short direction

$$d = \frac{5}{48} \frac{1{,}440 \times 12(20 \times 12)^2}{3.6 \times 10^6 \times 275} = 0.10 \text{ in. (3 mm)}$$

whereas an independent check using a central strip in the long direction confirms that

$$d = \frac{5}{48} \frac{630 \times 12(30 \times 12)^2}{3.6 \times 10^6 \times 275} = 0.10 \text{ in. (3 mm)}$$

This is well below the allowable live load deflection of $20 \times 12/360 = 0.67$ in. permitted by ACI Code.

Next, the flexural strength of the slab must be compared with the strength required at factored loads. Secondary moments will be estimated using the equivalent load method to find total prestress moments. With $w_b = 90$ psf, making use of the moment coefficients determined earlier, the total prestress moment per 12-in strip in the l_a direction is

$$M_a = 0.072 \times 90 \times 20^2 = 2{,}592 \text{ ft-lb}$$

corresponding to negative bending, that is, concave-downward curvature. The primary prestress moment in that direction is

$$M_1 = P_e e = 21{,}900 \times 2/12 = 3{,}650 \text{ ft-lb}$$

also negative. Thus, the secondary moment in that direction is

$$M_2 = M - M_1 = -2{,}592 + 3{,}650 = +1{,}058 \text{ ft-lb}$$

tending to reduce the negative curvature from the primary moment.

Similarly, in the l_b direction, the total prestress moment is

$$M_b = 0.014 \times 90 \times 30^2 = 1{,}134 \text{ ft-lb}$$

and the primary moment in that direction is

$$M_1 = 11{,}700 \times 2/12 = 1{,}950 \text{ ft-lb}$$

both tending toward concave-downward curvature. Thus, the secondary moment in the l_b direction is

$$M_2 = -1{,}134 + 1{,}950 = +816 \text{ ft-lb}^5$$

The total factored load moment to be resisted per 12-in. strip in the short direction is

$$M_u = 0.072(90 \times 1.4 + 50 \times 1.7)20^2 + 1{,}058 = 7{,}135 \text{ ft-lb}$$

The resisting moment will be found using the ACI approximate method. With $A_p = 0.217$ in.^{2} on 1.59-ft centers,

$$f_{pe} = \frac{41{,}000 \times 0.85}{0.217} = 161{,}000 \text{ psi}$$

$$\rho_p = \frac{0.217}{1.59 \times 12 \times 5.25} = 0.0022$$

[5]The analogy with the treatment of secondary moments for the continuous beam of Section 8.5 should be noted. Although the single-bay slab of the present example is simply supported, reactions are generated by prestressing. It can be shown using the theory of elasticity (see Ref. 10.3, for example) that a simply supported rectangular plate under gravity load will deflect upward at the corners unless the corners are held down by vertical support forces. These forces on the plate are equilibrated by upward reactions distributed along the ends. In the present case, with equivalent load from prestressing acting upward, upward reactions are induced at the corners, equilibrated by downward forces distributed along the edges. If the slab were freely suspended in space, without such forces, application of prestress would warp the slab. The existence of the nonuniform edge forces in the actual case produces the secondary moments that have been calculated, just as the reactions produced by prestressing the continuous beam of Section 8.5 produced secondary moments. The secondary moments reduce the negative primary moments in the spans in the present case, just as they reduced the primary moments in the spans in the continuous beam example.

and from Eq. (3.24):

$$f_{ps} = 161{,}000 + 10{,}000 + \frac{4{,}000}{300 \times 0.0022} = 177{,}000 \text{ psi}$$

From Eqs. (3.25) and (3.26):

$$a = \frac{0.217 \times 177{,}000}{1.59 \times 0.85 \times 4{,}000 \times 12} = 0.59 \text{ in.}$$

$$\phi M_n = \frac{0.90 \times 0.217 \times 177{,}000(5.25 - 0.59/2)}{1.59 \times 12} = 8{,}977 \text{ ft-lb}$$

This is well above the required value of 7,135 ft-lb. Similarly, in the long direction:

$$M_u = 0.014(90 \times 1.4 + 50 \times 1.7)30^2 + 816 = 3{,}475 \text{ ft-lb}$$

With $f_{pe} = 161{,}000$ and $\rho_p = 0.217/(2.97 \times 12 \times 5.25) = 0.0012$, the steel stress at failure is

$$f_{ps} = 161{,}000 + 10{,}000 + \frac{4{,}000}{300 \times 0.0012} = 182{,}000 \text{ psi}$$

and

$$a = \frac{0.217 \times 182{,}000}{2.97 \times 0.85 \times 4{,}000 \times 12} = 0.33 \text{ in.}$$

$$\phi M_n = \frac{0.90 \times 0.217 \times 182{,}000(5.25 - 0.33/2)}{2.97 \times 12} = 5{,}071 \text{ ft-lb}$$

which is well above the required $M_u = 3{,}475$ ft-lb.

Finally, the shear strength of the slab will be compared against the required capacity. Using the coefficients of Table 10.4, with the total load on the slab of

$$W = (90 \times 1.4 + 50 \times 1.7)20 \times 30 = 126{,}600 \text{ lb}$$

the shear force applied along the long edge is

$$V_u = \frac{126{,}600 \times 0.83}{2 \times 30} = 1{,}750 \text{ lb/ft}$$

and along the short edge is

$$V_u = \frac{126{,}600 \times 0.17}{2 \times 20} = 538 \text{ lb/ft}$$

Using the ACI approximate equation for shear strength, Eq. (5.17),

$$V_c = \left(0.6\sqrt{f'_c} + 700\frac{V_u d}{M_u}\right) b_w d \quad \text{but} \quad \geq 2\sqrt{f'_c}\, b_w d$$

$$\text{and} \quad \leq 5\sqrt{f'_c}\, b_w d$$

The last provision controls here and

$$\phi V_c = 0.85 \times 5\sqrt{4{,}000}\,(12 \times 5.25)$$
$$= 16{,}900 \text{ lb/ft}$$

Clearly, the slab is not shear-critical.

Additional Comments

1. The slab depth was chosen based on an assumed span-to-depth ratio of 45, and was post-tensioned to achieve a zero deflection for full dead load. The average concrete compression (centroidal stress) used in the short direction was 280 psi, and in the long direction, 150 psi. These are rather high.
2. With full service live load superimposed, concrete compressive stress is much below the allowable value, and no tensile stresses are present.
3. Live load deflection was well below the limit value.
4. Strength provided by the prestressed tendons was considerably above that required.
5. It can be concluded that a more economical design would result from use of a somewhat lower prestress force, resulting in lower concrete centroidal stresses, in both directions. Although the specified criterion of load balancing for full dead load would not be met, downward deflection under dead load is normal and perfectly acceptable for reinforced concrete slabs, and may be considered acceptable for prestressed slabs. A minimum centroidal prestress of 100 psi should be maintained in each direction for crack control, however.
6. It is common European practice to load balance for about 70 to 80 percent of full dead load, rather than 100 percent as was done in the present example (Ref. 8.5). In many cases, this amounts to decompression at the surface of the slab when full dead load is in place.

10.9 PRESTRESSED FLAT PLATE SLABS

Flat plate construction, the floor system in which there are no beams or other projections below the bottom surface of the slab, is well suited to prestressed concrete construction. It has been widely used for office buildings, institutional structures, apartment buildings, and hotels. For such cases, loads are not heavy,

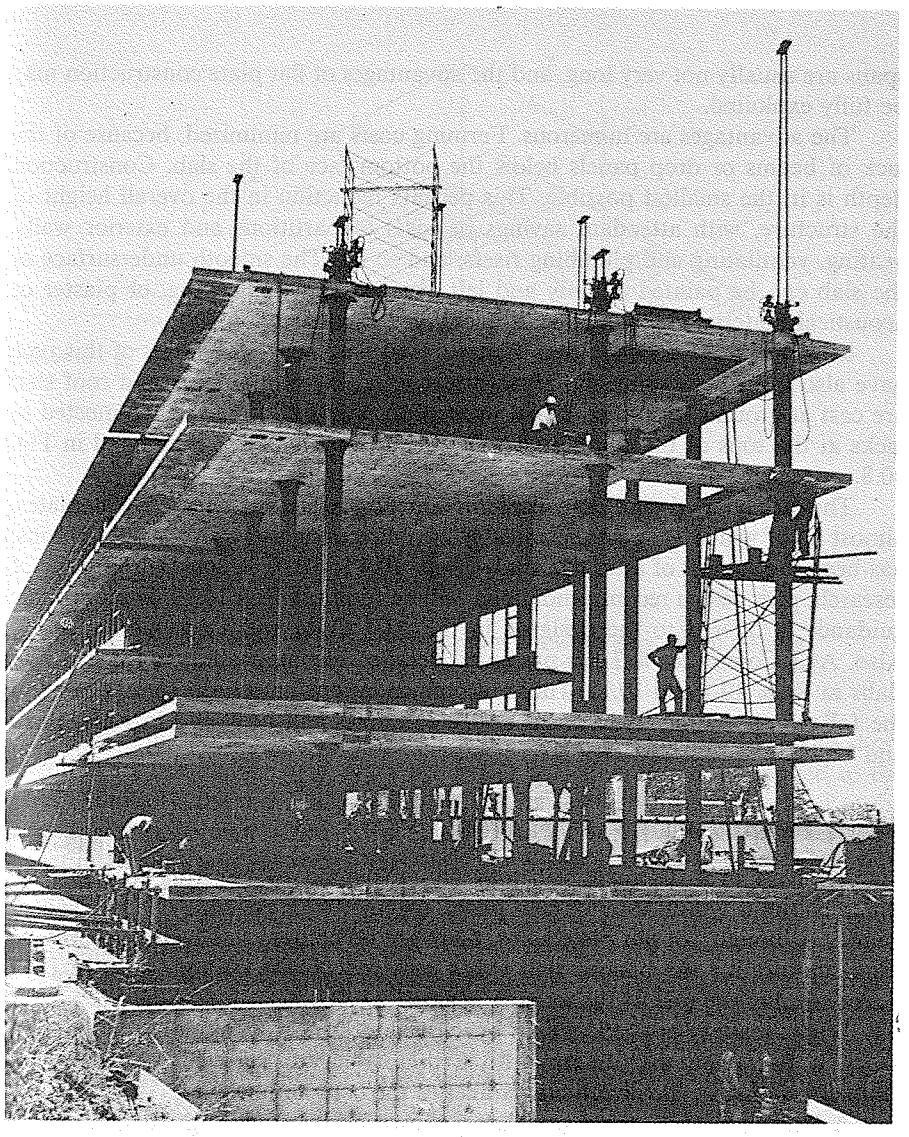

FIGURE 10.8 Lift-slab building under construction at Clemson College, South Carolina.

spans are usually not very long, and the advantages of flat plate construction may be fully exploited.

The advantages are numerous. Forming costs are minimized, because of the lack of beams or drop panels below the bottom face of the slab. Construction depth is in the smallest possible. This permits reduction in the overall height of the structure, with attendant savings in costs of partitions and exterior walls, heating, ventilating and plumbing risers, and so on. The smooth undersurface of the slab can be painted directly and left exposed as finish ceiling, or plaster or acoustical material can be applied directly to the concrete.

Most flat plate slabs are cast in place. However, many structures of this type have also been built using the lift-slab technique, by which floors and roof slab are cast at ground level, then raised to final position by lifting rods connected to jacks at the tops of the columns. This form of construction is illustrated in Fig. 10.8.

The behavior, design, and construction of prestressed concrete flat plates, almost all of which are post-tensioned in two directions using unbonded tendons, has been the subject of intensive study (Refs. 10.4 to 10.9). A concise summary of research, plus design recommendations, will be found in Ref. 10.10. Some specific guidance is offered to the designer in the ACI Code and Code Commentary. Also, ACI Committee 423 has presented detailed recommendations for two-way slabs in Refs. 10.1 and 10.12. Those recommendations have been incorporated in the following sections. Additional design examples will be found in Refs. 10.10 and 10.11.

10.10 BEHAVIOR OF FLAT PLATES

The behavior of a flat plate slab may be understood by referring to Fig. 10.9, which shows a typical interior slab panel, together with portions of the adjacent panels. Although, for flat plate slabs, there are no column line beams to provide edge support for the panels, slab strips centered on the column lines in each direction play the role of the missing beams.

When load is applied, either by curved prestressing tendons or external loads, a flat plate will deform into a doubly-curved surface, with principal moments acting in the directions parallel to the column lines.

A load applied to the central area, shown darkened in Fig. 10.9, is shared between strips of slab spanning in the short and long directions of the panel. The division of the load between short- and long-direction strips depends on the aspect ratio of the panel, and on the boundary conditions, as was true for edge-supported slabs. The strips of slab each carry their share of the load to the slab column strips, shown shaded, which act as edge-support beams for the panel although their thickness is no greater than that of the central portion of the slab.

Note that the portion of the load that is carried by the middle strip in the long direction is delivered to the column strips spanning in the short direction of

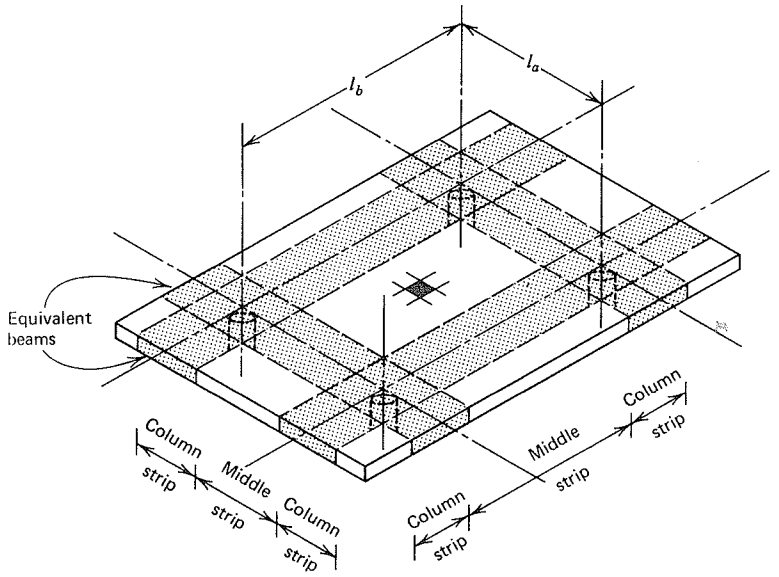

FIGURE 10.9 Two-way flat plate floor system showing equivalent beams.

the panel. This portion of the total load, plus that carried directly in the short direction by the middle strip, sums up to 100 percent of the load applied to the panel. Similarly, the short-direction middle strips deliver a part of the load to the long-direction column strips. This load, plus that carried directly in the long direction by the middle strips, includes 100 percent of the applied load. It is clearly a requirement of statics that for column-supported slabs, 100 percent of the applied load must be accounted for in *each* direction, jointly by the column strips and middle strips.[6]

Figure 10.10*a* shows a flat plate floor supported by columns at *a*, *b*, *c*, and *d*, and carrying load *w* per unit of surface area. Figure 10.10*b* indicates the moment diagram for the direction of span l_1. In this direction, the slab may be considered as a broad, flat beam of width l_2. Accordingly, the load per unit length of span is wl_2.

In any span of a continuous beam, the sum of the midspan positive moment and the average of the negative moments at adjacent supports is equal to the midspan positive moment of a corresponding simply supported beam. In terms of

[6] This conclusion is not a contradiction of Section 10.4, in which it was pointed out that the applied load could be assigned more or less arbitrarily to slab strips in either direction, for edge-supported slabs. In that discussion, loads on the edge beams were not considered.

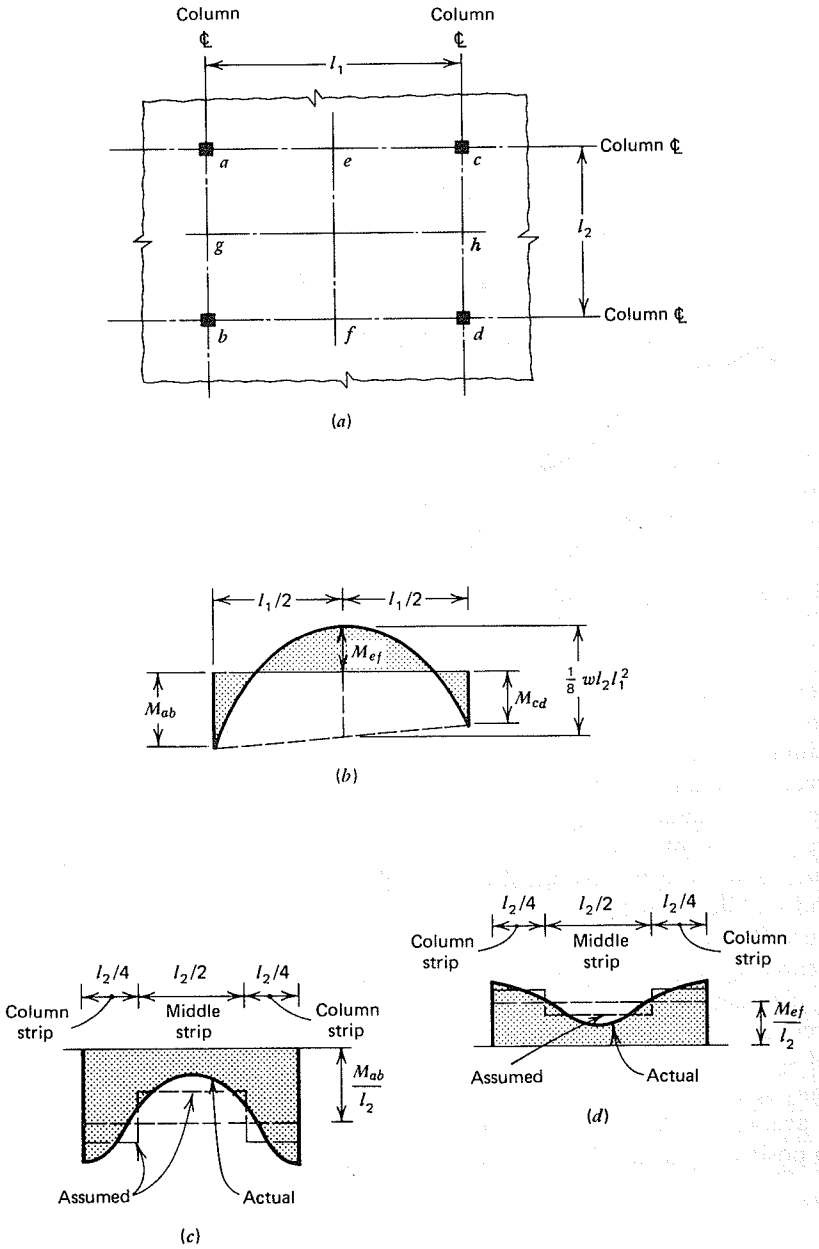

FIGURE 10.10 Moments in flat plate floors. (*a*) Plan. (*b*) Moments in l_1 direction. (*c*) Variation of moment across width *ab*. (*d*) Variation of moment across width *ef*.

the slab, this requirement of statics may be written

$$\tfrac{1}{2}(M_{ab} + M_{cd}) + M_{ef} = \tfrac{1}{8}wl_2l_1^2 \qquad (10.7a)$$

A similar requirement exists in the perpendicular direction, leading to

$$\tfrac{1}{2}(M_{ac} + M_{bd}) + M_{gh} = \tfrac{1}{8}wl_1l_2^2 \qquad (10.7b)$$

These statements disclose nothing about the relative magnitudes of the support moments and span moments. The proportion of the total static moment that is associated with each critical section must be found from an elastic analysis, which considers the relative stiffnesses and loadings of all panels in a continuous strip of floor, as well as the stiffnesses of connected columns. Alternatively, empirical methods that have been found to be reliable under restricted conditions may be adopted.

The moments across the width of critical sections, such as across the lines *ab* or *ef*, are not constant, but vary as shown qualitatively in Fig. 10.10*c* and 10.10*d*. Along the column centerlines, where curvatures are greater, moments are greater, whereas along a line at the centerline of the panel, curvatures are more gradual and the corresponding moments are smaller. For design purposes, it is convenient to divide the panel in each direction into column strips and middle strips, as shown. Within the limits of each strip, the moment is assumed constant.

It is clear, considering this lateral distribution of moments, that the best distribution of tendons is likely to be nonuniform across the width of a slab panel, in either direction. Cables will be rather widely spaced in the middle strips, and closer together in the column strips.

Prestressed concrete flat plates are statically indeterminate structures and, in general, the application of prestressing force produces not only primary moments, but secondary moments associated with the support reactions resulting from prestressing. The concept of equivalent load is useful in the design of flat plates, as it was for edge-supported slabs, in that the combined primary and secondary moments may be determined based on the equivalent loads from the tendons. Secondary moments may be calculated by deducting the easily determined primary moments from the total moments resulting from the equivalent load analysis.

The load-balancing approach to design, by which the upward equivalent load from prestressing is cancelled against a selected downward load applied to the slab, is also useful. For that special loading, assuming that the applied load, as well as the prestress force, is sustained in nature, the slab is in a state of uniform compression and will show near-zero deflection. If the load is then increased to full service load, only the effect of the incremental load above the

balanced load need be considered, and the stresses and deflections for that incremental load superimposed upon those of the balanced load stage.

At the ultimate load stage, such superposition is not valid, and the design strength of the slab must be compared against the required strength, found by applying the usual load factors to the calculated dead loads and service live loads. At this stage, secondary moments, if present, must be considered, just as for continuous beams, with a load factor of 1.0.

10.11 THE BALANCED LOAD STAGE

The load-balancing approach to design is specially useful in treating flat plates. The tendons can be arranged so that a specified loading, for example, the total dead load, can be cancelled by the upward equivalent load from prestressing.

An orthogonal grid of parabolic tendons, concave-upward, is specified for each slab panel. The short, concave-downward, transition curves characteristic of each tendon as it passes over the column lines, where tendons pass from one slab panel to the next, produce downward reactions that must be accommodated by special bands of tendons along these column lines in each direction.

Load-balancing design for a flat plate system may be developed from either of two different points of view. The first derives from the method of analysis of two-way edge-supported plates, and the second treats the slab as a system of broad shallow beams, first in one direction and then the other.

The first approach is illustrated by the rectangular slab of Fig. 10.11, which shows a typical interior panel of a flat plate floor. The uniformly distributed load to be balanced is carried by a two-way network of tendons of parabolic shape, uniformly spaced along either side l_1 or l_2. The panel is considered to be supported at its edges along the column lines in each direction. The proportion of the load to be carried in one direction or the other is more or less arbitrary, as for all edge-supported slabs. Assume for the present example that 60 percent of the load is assigned to the short direction l_2 and 40 percent to the long direction l_1. The required tendon network is shown in Fig. 10.11*a*. Parabolic tendons are used, concave-upward, near the top of the slab at the column lines and close to the bottom at midspan.

But the change in slope of the tendons of the primary network, as they cross the column lines, produces a downward reaction on the slab strips along the column lines. A true line loading would be obtained for the sharply bent tendons shown, but such a profile is not practical. In actual cases, a transition curve, concave-downward, would produce a strip loading of finite width along the column lines.

The downward load on the column strips must be resisted by a second set of tendons, placed along those column strips, as shown in Fig. 10.11*b*. If 40 percent of the load were carried in the long direction of the slab, then the column strips in the short direction would pick up that load and transmit it to the columns.

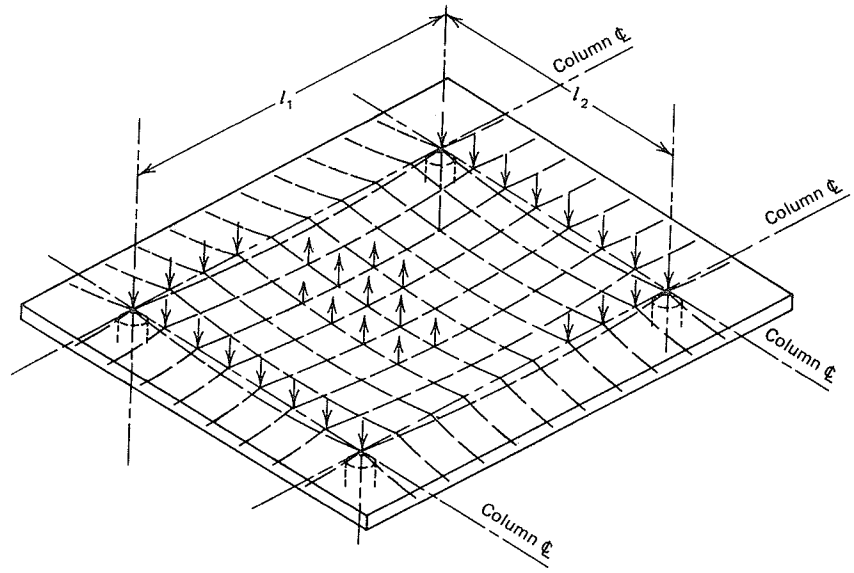

(*a*)

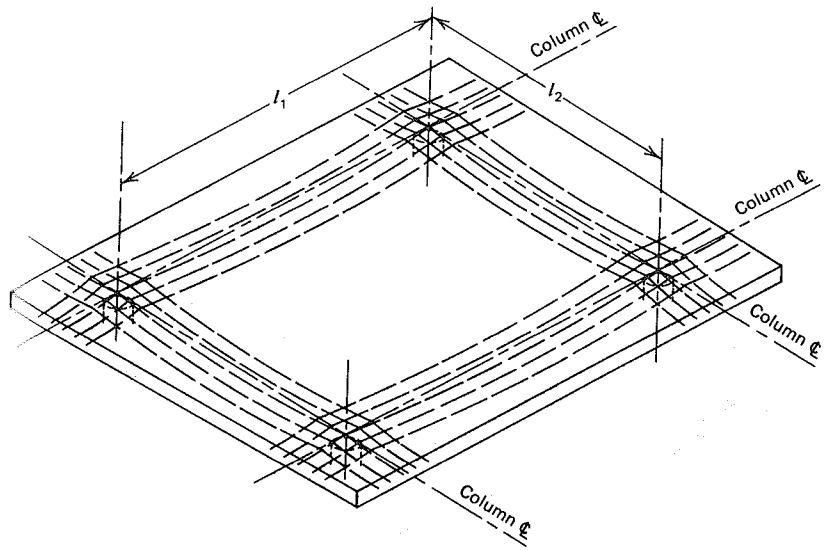

(*b*)

FIGURE 10.11 Load balancing for flat plate as two-way slab. (*a*) Distributed tendons. (*b*) Banded tendons.

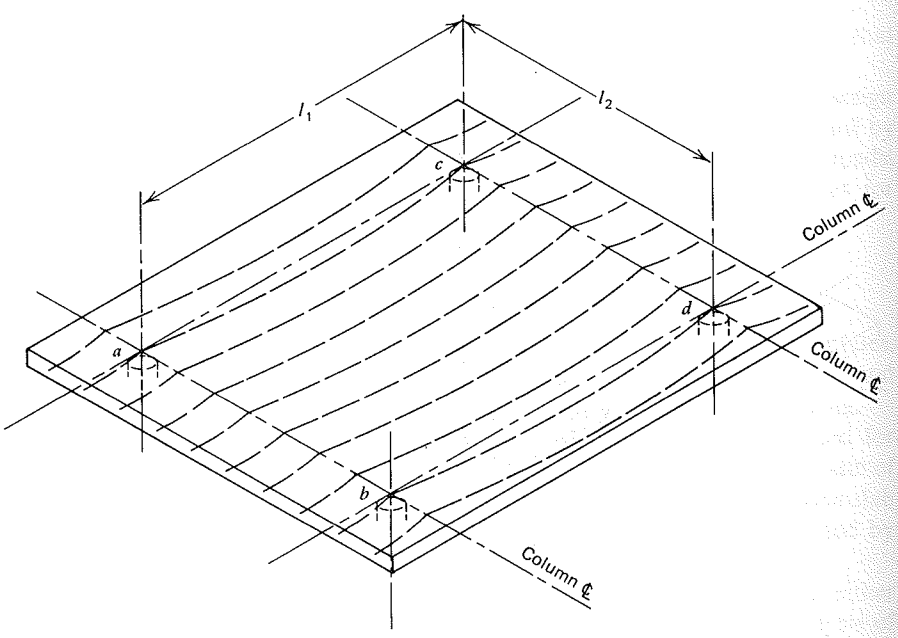

(*a*)

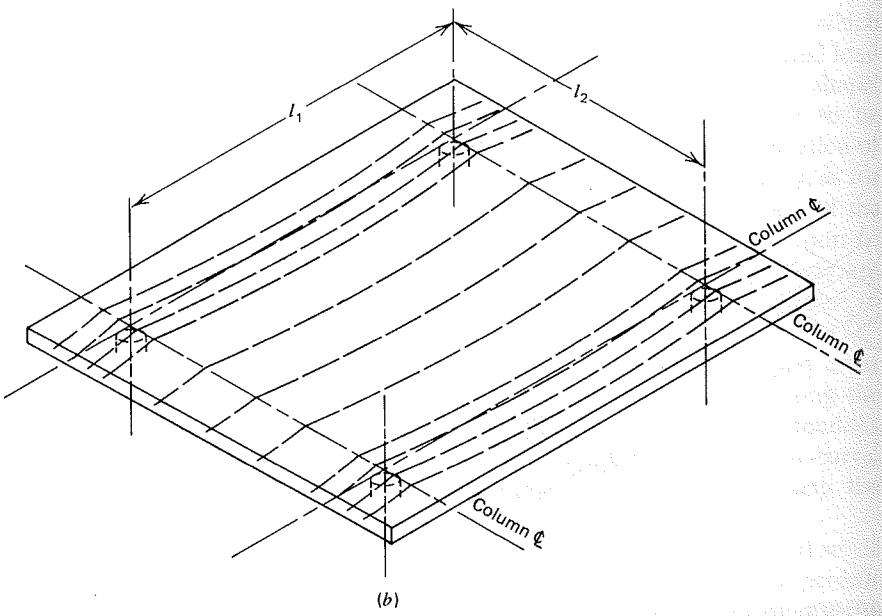

(*b*)

FIGURE 10.12 Load balancing for flat plate floor as wide-beam system. (*a*) Tendons uniformly distributed. (*b*) Tendons concentrated in column strips. (*c*) Two-way tendon pattern.

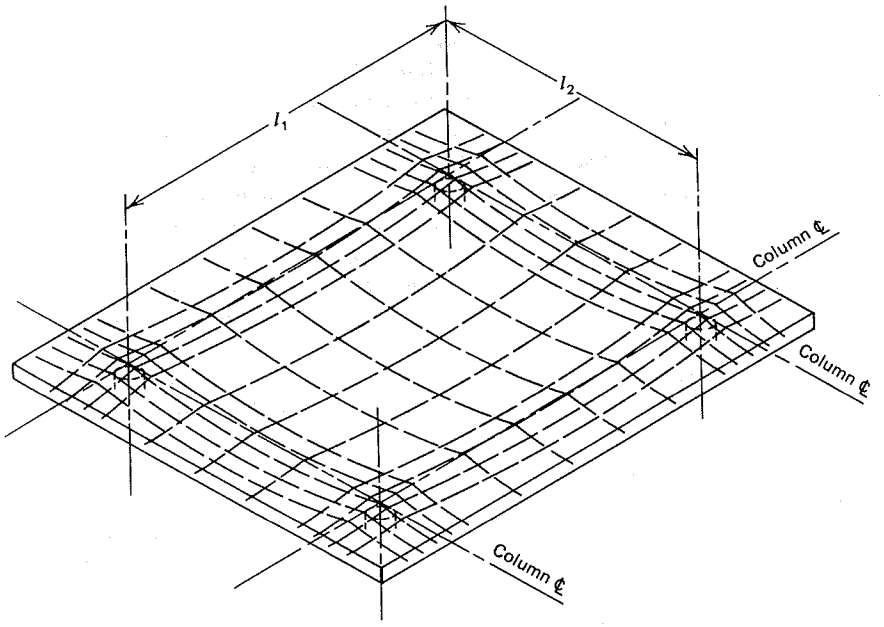

(*c*)

FIGURE 10.12 (*Continued*)

Note that the 60 percent carried directly the short way by the slab, plus the 40 percent carried by the short-direction column strips, accounts for 100 percent of the load, as required by statics. A corresponding analysis holds in the perpendicular direction.

The final arrangement of tendons is found by superimposing the arrangements of Figs. 10.11*a* and 10.11*b*, resulting in a rather wide spacing of cables in the central part of the panel and a concentrated band of tendons along the column lines in each direction.

The second approach to the analysis treats the slab as an orthogonal system of broad flat beams, each one of full panel width, and makes use directly of the fact that 100- percent of the load to be balanced must be carried in each of the two perpendicular directions. For purposes of analysis in the l_1 direction (Fig. 10.12*a*), the slab is considered to be supported continuously along the transverse column lines *ab* and *cd*. For the usual distributed loading, the designer would be led to select parabolic tendons, with maximum sag controlled by the requirements of cover at the top and bottom of the slab. However, it is known, based on elastic analysis and tests, that the lateral distribution of bending moments due to the applied load is not uniform across the width of the critical sections, but tends to concentrate near the column lines (see Section 10.9). According to information

presented in Refs. 10.4 and 10.12, for simple spans, between 55 and 60 percent of the moment will be concentrated in the column strips, and, for continuous spans, between 65 and 75 percent will be within the column strips, the remainder being assigned to the middle strips in each case. Anticipating such a distribution when the slab is subjected to full service live load or overloading, the designer is led to distribute the tendons in a like manner. The result is indicated in Fig. 10.12*b*. The total number of tendons per panel is the same as for Fig. 10.12*a*, but a large percentage is concentrated in bands along the column lines.

A corresponding situation exists in the direction l_2, the total number of tendons being sufficient to equilibrate 100 percent of the load to be balanced in that direction also.

The superposition of the tendons in each of the two perpendicular directions is shown in Fig. 10.12*c*. It is clear that the end results are the same as those of the analysis summarized in Fig. 10.11, although the reasoning is different. The second approach is simpler to apply in practice.

More recent research on flat plates prestressed with unbonded tendons (Refs. 10.6 through 10.9) indicates that it is unnecessary to concentrate the tendons near the column centerlines in *both* directions, as suggested by Figs. 10.11 and 10.12; the flexural strength of two-way prestressed slabs appears to be controlled by total tendon strength and the amount and location of non-prestressed reinforcement, rather than by tendon distribution. Although it is important that some tendons pass within the shear perimeter over columns, distribution elsewhere does not appear to be critical and any rational method that satisfies statics may be used (Ref. 10.1). Many, if not most, post-tensioned flat plates constructed recently have used the *one-way banded distribution* shown in Fig. 10.13, in which the tendons in one direction are spaced uniformly across the width of the slab. Those in the perpendicular direction are concentrated entirely in bands centered on the column lines. Use of this type of banded tendon distribution greatly simplifies the placement of tendons, and provides a significant reduction in field labor cost. It is interesting to observe that when banded tendons are used as shown in Fig. 10.13, the result is actually a one-way slab, spanning in the direction of the distributed tendons, with supports provided along the column lines in the perpendicular direction by heavily prestressed integral beams. The effectiveness of such an arrangement, confirmed by tests, indicates once again the more or less arbitrary way in which loads may be carried using the load-balancing approach, the main requirement being to satisfy statics. It should also be noted, however, that a perfectly level slab surface, even for the theoretical balanced load, is less likely using one-way banded tendons than with the two-way banded arrangements first described. The use of non-prestressed bonded bars to control cracking is particularly important.

The ACI Code provisions permit use of either two-way banded tendons (Fig. 10.12*c*) or one-way banded tendons (Fig. 10.13). The following requirements

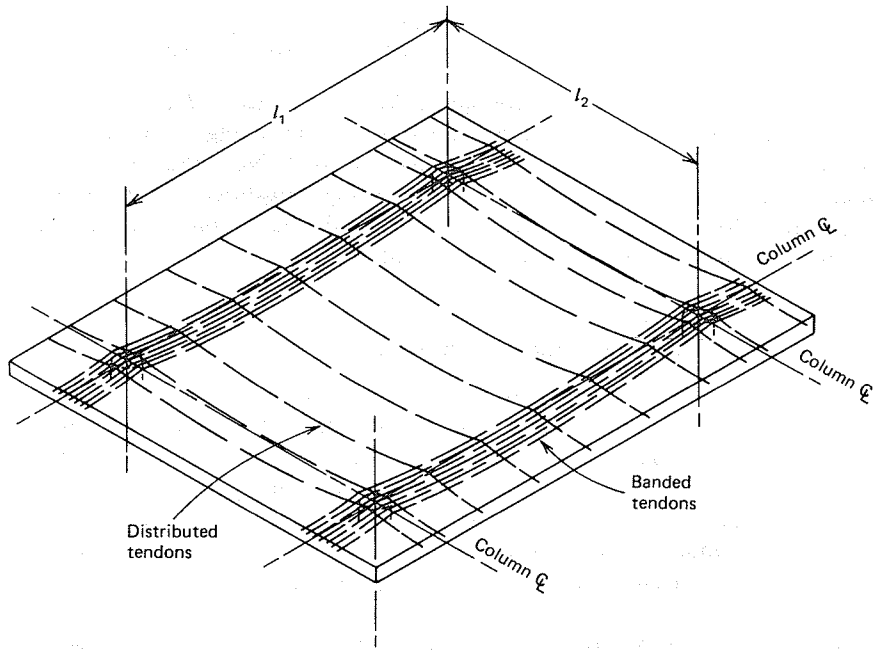

FIGURE 10.13 One-way banded tendon distribution.

pertain to placement of tendons and bar reinforcement:

1. The spacing of tendons or groups of tendons in one direction (i.e., the distributed tendons) shall not exceed eight times the slab thickness or 5 ft. The spacing shall provide a minimum average prestress (after allowance for all losses) of 125 psi on the slab section tributary to the tendon or tendon group. A minimum of two tendons shall be provided in each direction through the critical shear section over columns.
2. A minimum area of bonded reinforcement, $A_s = 0.00075hl$, shall be provided at the columns, where l is the length of the span in the direction parallel to that of the reinforcement being determined. At least four bars should be provided in each direction in the negative bending region. They should be placed within a slab width bounded by lines that are $1.5h$ outside the opposite faces of the column, where h is the total slab thickness. The maximum spacing of these bars is 12 in., and their minimum length is one-sixth the clear span on each side of the support.
3. Where service load positive moment gives concrete tensile stress in excess of $2\sqrt{f_c'}$, minimum bonded reinforcement, $A_s = N_c/0.5f_y$, shall be provided, where N_c is the tensile force in the concrete due to unfactored dead plus live load. When required, these bars should have length at least one-third of the clear span, with bars centered in the positive bending region.
4. When bonded reinforcement is used along with unbonded tendons to contribute to the needed flexural strength rather than solely for crack control, it should be detailed

according to all requirements for development length, anchorage, and cutoff imposed by ACI Code for reinforcement in conventional (non-prestressed) slabs.

In addition to these Code provisions, ACI Committee 423, in Ref. 10.1, suggests a maximum average prestress of 500 psi. If shortening of the slab is not likely to cause problems, a higher value may be used. Note that for one-way banded systems, according to Ref. 10.1, the average prestress is defined as the total prestress force after losses divided by the total area of concrete. This value is much lower than the prestress in the banded region.

10.12 THE EQUIVALENT FRAME METHOD

When flat plates are acted upon by loads other than the balanced load, deflections, curvatures, and moments result. Up to the full service load, stresses associated with the *unbalanced* part of the total load are found by flexural analysis of the slab. These stresses are easily superimposed on the uniform compression resulting from the balanced load to obtain net stresses. From a *factored-load analysis* of the slab, using *total* dead and live loads, the required flexural resistance of all critical sections can be found, and the margin of safety against failure determined.

A refined analysis, either for unbalanced service load or for factored ultimate load, is highly complex, involving not only variations of moments longitudinally and transversely, but requiring consideration of torsional stiffness, moment redistribution, and other effects. Fortunately, there are approximate methods available that give good results.

The most widely used approximate method for concrete slabs is the *equivalent frame method* of Chapter 13 of the ACI Code. The equivalent frame method, sometimes known as the beam method, is quite general, and can be applied to two-way slabs supported by beams on column lines, flat slabs with dropped panels or column capitals or both, grid slabs or waffle slabs, and flat plates, including lift slabs. Most prestressed two-way systems are flat plates, and only recommendations pertaining to them will be summarized here.

Certain of the provisions of Chapter 13 of the Code are *not* recommended for use in applying the approach to prestressed flat plates (Ref. 10.1). Coefficients for the lateral distribution of design moments across the width of critical sections were developed largely on the basis of tests of reinforced concrete slabs, and other sets of coefficients are appropriate for prestressed construction. Chapter 13 of the Code also includes an alternative method of analysis known as the *direct design method*, based on moment coefficients obtained mainly by testing reinforced concrete slabs. The direct design method should not be used for prestressed concrete.

By the equivalent frame method, the structure is divided for purposes of analysis into continuous frames, centered on the column lines and extending both

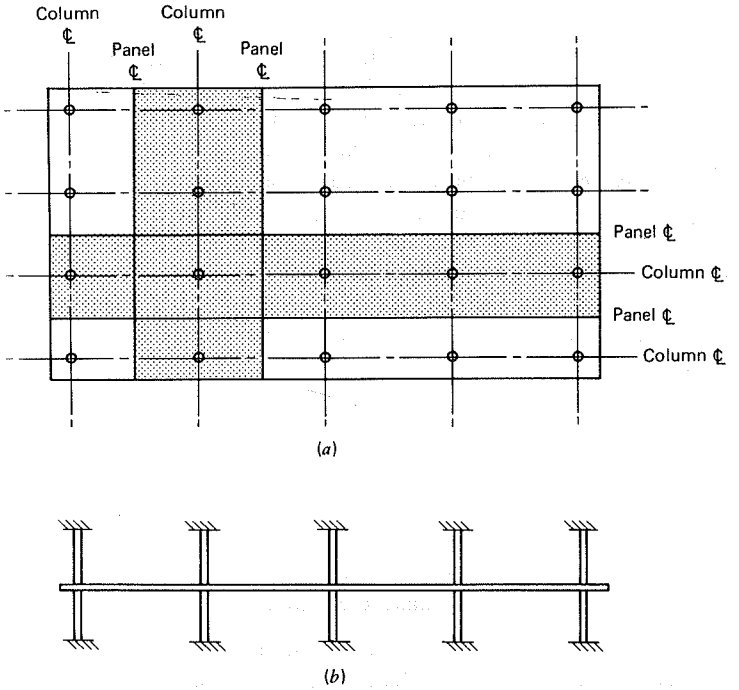

FIGURE 10.14 Building idealization for equivalent frame analysis. (*a*) Plan. (*b*) Elevation.

longitudinally and transversely, as shown by the shaded strips in Fig. 10.14. Each frame is composed of a row of columns and a broad continuous beam consisting of the portion of slab bounded by panel centerlines on either side of the columns. For vertical loading, each floor with its columns may be analyzed separately; the columns are assumed fixed at the floors above and below. In keeping with the requirements of statics, equivalent beams or frames in each direction must each carry 100 percent of the applied load. To maximize the effect of the live loads, alternate loading positions usually must be considered, although the ACI Code waives this requirement if the live load does not exceed three-quarters of the dead load.

When columns are relatively slender or not rigidly connected to the slab (as in the case of lift slabs), their stiffness may be neglected and continuous beam analysis applied. For other cases, it is necessary to account for the rotational resistance provided by the columns. Figure 10.15 shows the condition at an interior column with the slab spanning in the direction l_1.[7] According to the

[7]By Code notation, l_1 is the span length in the direction that moments are being determined and l_2 is the length of span transverse to l_1.

Code, the flat plate is to be considered as supported by a transverse slab strip or beam of width b equal to the dimension of the column in the direction of the moment analysis, and height h equal to the depth of the slab. The rotational restraint provided for the slab is influenced, not only by the flexural stiffness of the column, but by the torsional stiffness of the transverse beam as well, as indicated by the sections. With distributed torque m_t applied by the slab and resisting torque M_t provided by the column, the outer ends of the transverse slab strip will rotate to a greater degree than the central section, due to torsional deformation. To allow for this, the actual column and transverse slab strip are replaced by an equivalent column, defined so that the total flexibility (inverse of stiffness) of the equivalent column is the sum of the flexibilities of the actual column and the slab strip. Thus

$$\frac{1}{K_{ec}} = \frac{1}{\Sigma K_c} + \frac{1}{K_t} \tag{10.8}$$

where K_{ec} = flexural stiffness of equivalent column
K_c = flexural stiffness of actual column
K_t = torsional stiffness of transverse slab strip

all expressed in terms of moment per unit rotation. The flexural stiffness can be calculated by the usual equations of mechanics and for members having a uniform cross section is equal to $4E_cI/l$. The torsional stiffness of the transverse slab strip can be calculated by the expression

$$K_t = \Sigma \frac{9E_cC}{l_2\left(1 - \dfrac{c_2}{l_2}\right)^3} \tag{10.9}$$

where c_2 = transverse column dimension as shown in Fig. 10.15
C = cross-sectional constant for the transverse strip.

The summation applies to the typical case in which there are slab strips on both sides of the column. The constant C pertains to the torsional rigidity of the effective cross section, and for the slab strip shown in Fig. 10.15 is

$$C = \left(1 - 0.63\frac{x}{y}\right)\frac{x^3y}{3} \tag{10.10}$$

where x and y are, respectively, the smaller and larger dimensions of the rectangular cross section (h and b in Fig. 10.15).

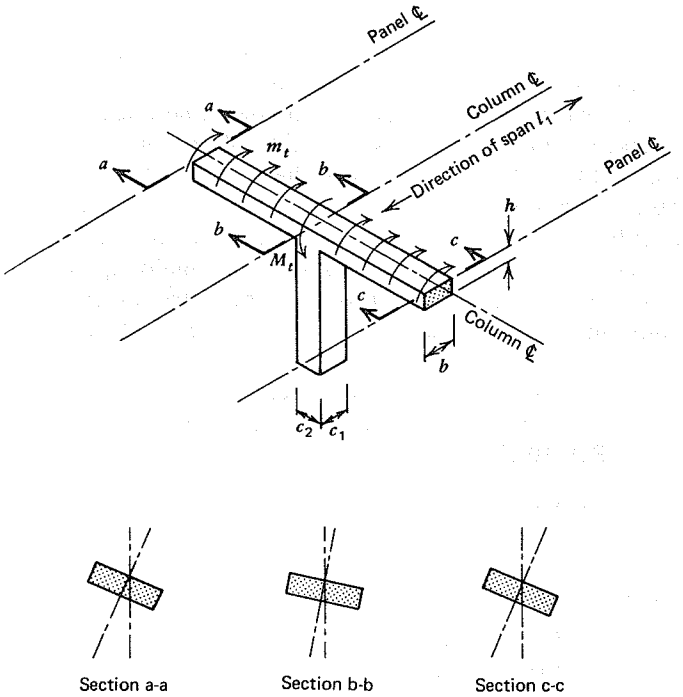

FIGURE 10.15 Basis of equivalent column.

With the effective stiffness of the slab strip and the columns found by this procedure, the analysis of the equivalent frame can proceed by any convenient means, such as by moment distribution or using standard computer programs.

Having found the total moments at positive and negative critical sections from the continuous beam or frame analysis, it still remains to distribute those moments across the width of the critical sections. For this purpose it is convenient to divide the total width of the slab into column strips and middle strips as suggested earlier. The column strip is defined as having a width on either side of the column equal to one-quarter of the smaller of the panel dimensions l_1 or l_2. A middle strip is bounded by two column strips. Moments at positive and negative bending sections are assumed to be constant within the bounds of a middle strip or column strip. For prestressed flat plates, the following distribution of moments at the critical sections is recommended (Ref. 10.12):

Simple spans:	55 to 60 percent to the column strip with the remainder to the middle strip
Continuous spans:	65 to 75 percent to the column strip with the remainder to the middle strip

Negative moments obtained from the analysis apply at the centerlines of supports. Since the support provided is not a knife-edge but is a broad band of slab spanning in the transverse direction, some reduction in the negative design moment is proper. The critical section for negative bending, in both column and middle strips, may be taken at the face of the supporting column, but in no case at a distance greater than $0.175l_1$ from the center of the column.

Service load flexural stresses caused by the moments from *unbalanced loads*, found by the equivalent frame method, may be calculated by the usual equations of mechanics. As tensile and compressive stresses are normally quite low, calculations are usually based on the uncracked section. These stresses are added algebraically to the uniform compressive stresses obtained for the balanced load state.

Limiting concrete stresses at service loads recommended for flat plates differ from the allowable stresses given in the ACI Code for other types of construction in the following respects (Ref. 10.12):

1. Compression in concrete
   - Negative moment areas around columns $0.30f_c'$
2. Tension in concrete:
   - Positive moment areas without the addition of non-prestressed reinforcement $2\sqrt{f_c'}$
   - Positive moment areas with the addition of non-prestressed reinforcement $6\sqrt{f_c'}$
   - Negative moment areas without the addition of non-prestressed reinforcement 0
   - Negative moment areas with the addition of non-prestressed reinforcement $6\sqrt{f_c'}$

All other stress limits of the ACI Code apply. The reader is referred to Ref. 10.12 for the background and rationale for these recommendations.

10.13 FLEXURAL STRENGTH OF FLAT PLATES

Although the concept of load balancing is of great use up to the service load stage, it has no validity at overload stages. Load balancing makes use of the principle of superposition, which is valid only within the elastic range of behavior. For the overload stage, both steel and concrete are stressed into the inelastic range. Steel stress increases disproportionately to load increase as cracking of the slab occurs. In addition, the increase in steel stress is not uniform along the length of the tendon.

The safety of the structure against collapse must be evaluated by comparing the resisting moment of all critical sections against the maximum moments that would act at those sections at the hypothetical factored load stage.

In calculating the flexural strength ϕM_n of slab sections, the ACI approximate equations for steel stress f_{ps} at failure, given in Section 3.8A, are usually adopted. Because span–depth ratios for two-way slabs are generally above 35, Eq. (3.24) applies. Flexural strength can be found using Eqs. (3.25) and (3.26). For flexure, $\phi = 0.90$ as usual. Non-prestressed bar reinforcement can be included in the strength calculations, considered to be stressed to f_y at the ultimate load, but only if it is detailed according to the usual requirements for bar reinforcement in flexural members.

The moments to be resisted at the critical sections are found using the equivalent frame method with factored loads. The loads are calculated by applying the usual load factors to the actual dead load (including the self-weight of the slab) and the service live load. Secondary moments, if any, due to prestressing must be included using a load factor of 1.0. Secondary moments are most conveniently found for two-way slabs by first calculating the total moments due to prestress using the equivalent load method in conjunction with the equivalent frame approach, then subtracting the primary prestress moments, equal to Pe, from the total to obtain the secondary moments.

It has been suggested that the collapse load for prestressed flat plates can be calculated using yield line theory (Refs. 10.4 and 10.5). Limited experimental evidence suggests that this may be valid. However, the yield line analysis implies a redistribution of elastic moments, which can occur only if adequate rotation capacity is available at the highly stressed sections. There are not sufficient data available at this time to support such an assumption. ACI Committee 423, in its tentative recommendations (Ref. 10.12), makes no mention of yield line theory, but endorses the ACI Code provision for statically indeterminate prestressed structures that the required ultimate resisting moments should be found from an elastic analysis, with the usual load factors included. A limited amount of redistribution is permitted for slabs, as it is for beams and frames, provided that the critical sections are sufficiently under-reinforced. Specifically, Eq. (8.6) may be applied.

10.14 SHEAR IN FLAT PLATES

Prestressed flat plates are apt to be critical in shear. When two-way slabs are supported directly by columns, there is a high concentration of shear stress near the columns. Tests of flat plate structures confirm that in many practical cases the capacity is governed by shear (Ref. 10.13).

A. FLAT PLATES WITHOUT SPECIAL SHEAR REINFORCEMENT

There are two kinds of shear that may be critical. The first is the familiar *beam-type shear* leading to diagonal tension failure, as in Fig. 10.16*a*. Likely to control mainly for long, narrow slabs, this mechanism is based on the slab acting

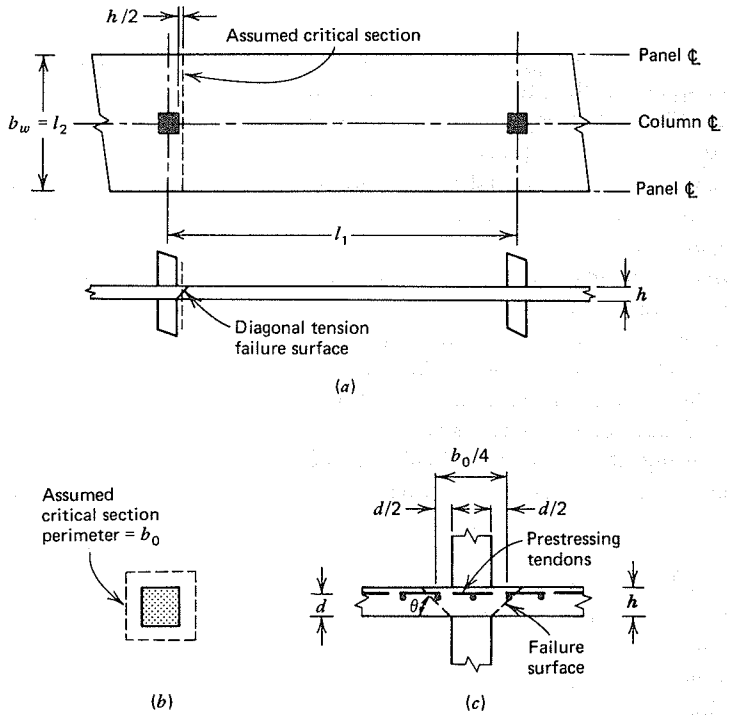

FIGURE 10.16 Shear failure in flat plates. (*a*) Beam-shear in rectangular panel. (*b*) Critical section for punching shear. (*c*) Failure surface for punching shear.

as a wide beam, spanning between supports provided by the perpendicular column strips. A potential diagonal crack extends in a plane across the entire width of the slab as shown. The critical section is taken a distance $h/2$ from the face of the column. As for beams, the design basis is $V_u \le \phi V_n$, where V_u is the shear force at factored loads and V_n is the nominal shear strength. The strength reduction factor ϕ is equal to 0.85 as usual for shear calculations. Normally, shear reinforcement is not provided for beam-shear in slabs, and so $V_n = V_c$, where V_c is computed as usual for beams. The effective depth need not be taken less than $0.80h$. The restriction that shear reinforcement must be provided whenever $V_u > \frac{1}{2}\phi V_c$ does not apply to slabs.

Alternatively, failure may occur by *punching shear*, with the potential diagonal crack following the surface of a truncated cone or pyramid around the column, as shown in Figs. 10.16*b* and 10.16*c*. The failure surface extends from the bottom of the slab at the column diagonally upward to the top surface. The angle of inclination with the horizontal θ depends on the amount of reinforcement in the slab and the degree of prestressing. It may range from about 20 to 45 degrees.

For design purposes, a critical section for shear is defined perpendicular to the plane of the slab and a distance $d/2$ from the face of the column, defining the shear perimeter b_o as shown in Figs. 10.16*b* and 10.16*c*. At that section, the basis for design is that $V_u \le \phi V_n$ as usual. In the absence of special shear reinforcement, $V_n = V_c$.

At such a critical section, in addition to the shearing stresses and horizontal compression resulting from prestress and bending, vertical or somewhat inclined compressive stress is present resulting from the reaction of the column. The simultaneous presence of vertical and biaxial horizontal compression increases the strength of the concrete in the area of the column. Tests have indicated that when punching shear failure occurs, the shear stress computed on the perimeter of the critical section is larger than in beams or one-way slabs, and according to the Code, the nominal shear strength may be taken equal to

$$V_c = \left(3.5\sqrt{f_c'} + 0.3f_{pc}\right)b_o d + V_p \tag{10.11}$$

where b_o is the shear perimeter, defined earlier, f_{pc} is the average value of the concrete compression after losses at the slab centroid for the two directions, and V_p is the vertical component of all effective prestress forces crossing the shear perimeter.[8] If Eq. (10.11) is used, the following conditions must be satisfied:

1. No portion of the column cross section will be closer to a discontinuous edge than four times the slab thickness h.
2. Concrete strength f_c' used in Eq. (10.11) must not be taken greater than 5,000 psi.
3. The concrete centroidal compression f_{pc} in each direction will not be less than 125 psi and will not be taken greater than 500 psi.

If these three conditions are not satisfied, the nominal shear strength at the column should be calculated using the same equation as for non-prestressed slabs:

$$V_c = (2 + 4/\beta_c)\sqrt{f_c'}\, b_o d \tag{10.12}$$

but not greater than $4\sqrt{f_c'}\, b_o d$. In Eq. (10.12), β_c is the ratio of the long side to short side of the column.

The nominal shear strength calculated from Eq. (10.11) or (10.12) must be reduced applying $\phi = 0.85$ for design purposes; the design basis is $V_u \le \phi V_c$ as usual.

[8]For thin slabs, V_p must be carefully evaluated, because the accuracy of placement of tendons in the field can have a great effect. The term V_p can conservatively be taken as zero in most cases.

B. TYPES OF SHEAR REINFORCEMENT

Special shear reinforcement is sometimes used at the columns for flat plates. It may take several forms. A few of these are shown in Fig. 10.17. The *shearheads* shown in Figs. 10.17*a* and *c* consist of standard structural steel shapes embedded in the slab and projecting beyond the column. They serve to increase the effective perimeter b_o of the critical section. In addition, they may contribute to the negative bending resistance of the slab.

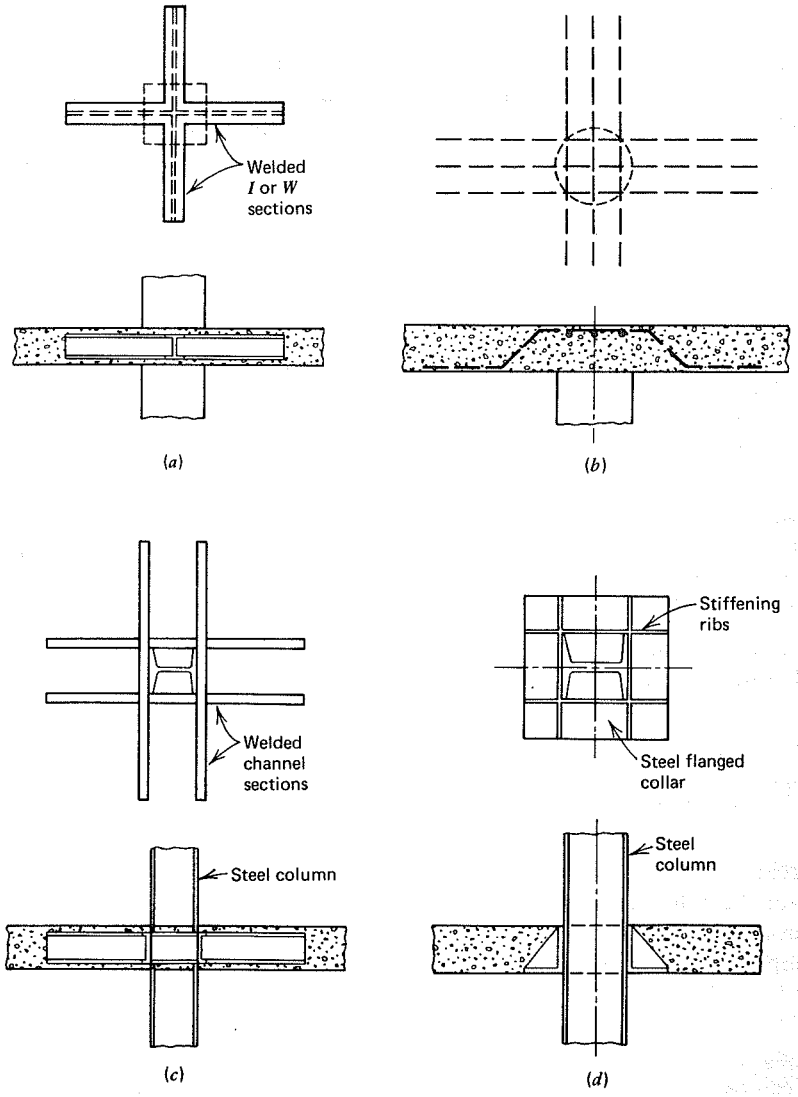

FIGURE 10.17 Shear reinforcement for flat plates.

The reinforcement shown in (*a*) is particularly suited for use with concrete columns. It consists of short lengths of *I*- or wide-flange beams, cut and welded at the crossing point, so that the arms are continuous through the column. The prestressing tendons pass over the top of the structural steel. Column bars pass vertically at the corners of the column without interference. The effectiveness of this type of shearhead has been well documented by tests (Ref. 10.13).

The channel frame of (*c*) is very similar in its action, but is adapted for use with steel columns, as are often used for lift slabs.

The bent bar arrangement of (*b*) is suited for use with concrete columns. The bars are usually bent at 45 degrees across the potential diagonal crack, and extend along the bottom of the slab a distance sufficient to develop their strength by bond.

The flanged collar of (*d*) is designed mainly for use with lift slabs. It consists of a flat bottom plate with vertical stiffening ribs. It may incorporate sockets for lifting rods, and usually is used in conjunction with shear pads welded directly to the column surfaces below the collar to transfer the vertical reaction. Moment transfer is generally considered negligible.

Since only limited test data are available for prestressed concrete flat plates with shear reinforcement, it is recommended that such shear reinforcement, if used, be designed according to methods that are well substantiated by test information for conventionally reinforced (nonprestressed) flat plates. These methods are described in detail and design examples are provided in Ref. 10.14.

10.15 TRANSFER OF MOMENTS AT COLUMNS

The analysis for punching shear in flat plates and flat slabs presented in Section 10.14 assumed that the shear force V_u was resisted by shearing stresses uniformly distributed around the perimeter b_0 of the critical section, a distance $d/2$ from the face of the supporting column. The nominal shear strength V_c was given by Eq. (10.11) or Eq. (10.12).

If significant moments are to be transferred from the slab to the columns, as would result from unbalanced gravity loads on either side of a column, or for exterior columns, or from horizontal loading due to wind or seismic effects, the shear stress on the critical section is no longer uniformly distributed.

The situation can be modeled as shown in Fig. 10.18*a*. Here V_u represents the total vertical reaction to be transferred to the column, and M_u represents the unbalanced moment to be transferred, both at factored loads. The vertical force V_u causes shear stress distributed more or less uniformly around the perimeter of the critical section as assumed earlier, represented by the inner pair of vertical arrows, acting downward. The unbalanced moment M_u causes horizontal flexural loading on the joint, represented by the forces T and C, and, in addition, causes

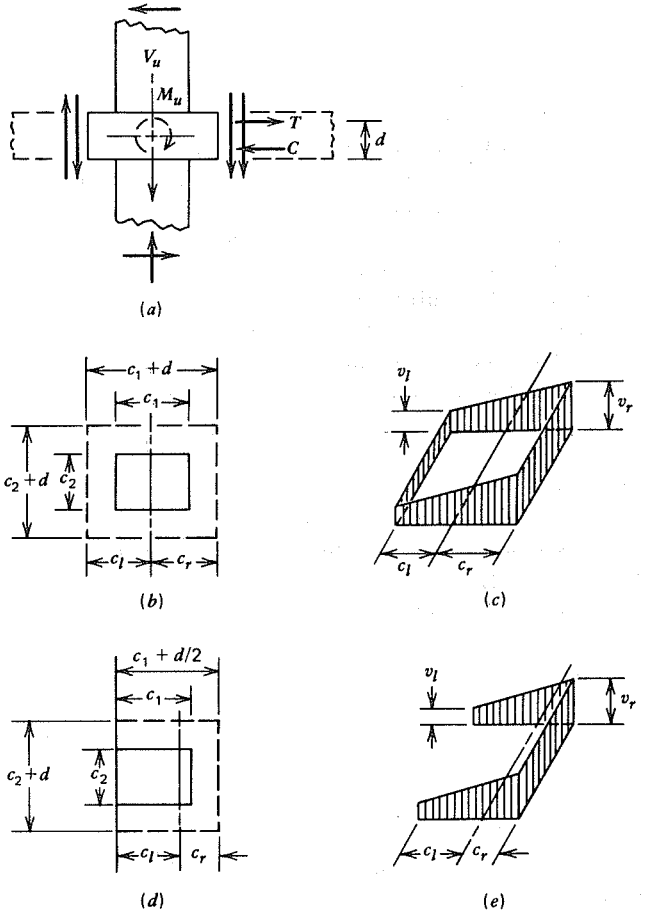

FIGURE 10.18 Transfer of moment from slab to column. (*a*) Forces resulting from vertical load and unbalanced moment. (*b*) Critical section for interior column. (*c*) Shear stress distribution for interior column. (*d*) Critical section for edge column. (*e*) Shear stress distribution for edge column.

shearing stresses, represented by the outer pair of vertical arrows, which add to the shear stresses otherwise present on the right side in the sketch and subtract on the left side.

Tests indicate that for square columns about 60 percent of the unbalanced moment is transferred by flexure (forces T and C in Fig. 10.18*a*) and about 40 percent by shear stresses on the faces of the critical section (Ref. 10.15). For rectangular columns, it is reasonable to suppose that the portion transferred by flexure increases as the width of the critical section that resists the moment increases, that is, as $c_2 + d$ becomes larger relative to $c_1 + d$ in Fig. 10.18*b*. According to the ACI Code, the moment considered to be transferred by flexure is

$$M_{ub} = \frac{1}{1 + \frac{2}{3}\sqrt{(c_1 + d)/(c_2 + d)}} M_u \tag{10.13a}$$

and that assumed to be transferred by shear is

$$M_{uv} = \left[1 - \frac{1}{1 + \frac{2}{3}\sqrt{(c_1 + d)/(c_2 + d)}}\right] M_u \tag{10.13b}$$

It is seen that for a square column these equations indicate that 60 percent of the unbalanced moment is transferred by flexure and 40 percent by shear, in accordance with the available data. If c_2 is very large relative to c_1, nearly all the moment is transferred by flexure.

The moment M_{ub} can be accommodated by concentrating slab column-strip tendons and bar reinforcement near the column. To be considered effective in transferring moment, all such reinforcement, bonded and unbonded, should be placed within a width between lines $1.5h$ on each side of the column, where h is the total slab thickness.

The moment M_{uv}, together with the vertical reaction delivered to the column, causes shear stresses assumed to vary linearly with distance from the centroid of the critical section, as indicated for an interior column by Fig. 10.18*c*. The stresses can be calculated from

$$v_l = \frac{V_u}{A_c} - \frac{M_{uv} c_l}{J_c} \tag{10.14a}$$

$$v_r = \frac{V_u}{A_c} + \frac{M_{uv} c_r}{J_c} \tag{10.14b}$$

where A_c = area of critical section $= 2d[(c_1 + d) + (c_2 + d)]$
c_l, c_r = distances from centroid of critical section to left and right face of section, respectively
J_c = property of critical section analogous to polar moment of inertia

The quantity J_c is to be calculated from

$$J_c = \frac{2d(c_1 + d)^3}{12} + \frac{2(c_1 + d)d^3}{12} + 2d(c_2 + d)\left(\frac{c_1 + d}{2}\right)^2 \tag{10.15}$$

Note the implication, in the use of the parameter J_c in the form of a polar

moment of inertia, that shear stresses indicated on the near and far faces of the critical section in Fig. 10.18*c* have horizontal as well as vertical components.

The maximum shear stress calculated according to Eq. (10.14*a*) or Eq. (10.14*b*) should not exceed ϕ times the shear strength based on Eq. (10.11) or Eq. (10.12), whichever applies. For present purposes, the shear strength must be expressed in terms of unit shear stress rather than shear force. Thus, corresponding to Eq. (10.11) and neglecting V_p:

$$v_c = 3.5\sqrt{f_c'} + 0.3f_{pc} \tag{10.16}$$

with f_{pc} taken equal to the average precompression in the direction of moment transfer. Corresponding to Eq. (10.12):

$$v_c = (2 + 4/\beta_c)\sqrt{f_c'} \tag{10.17}$$

but should not exceed $v_c = 4\sqrt{f_c'}$. Thus, with the nominal shear strength calculated according to Eq. (10.16) or Eq. (10.17) and the factored-load shear calculated from Eq. (10.14*a*) or Eq. (10.14*b*), the basic design requirement is $v_u \leq \phi v_c$, with $\phi = 0.85$ for shear.

Equations similar to those previously cited can be derived for the edge column shown in Fig. 10.18*d* and 10.18*e* or for a corner column. Note that although the centroidal distances c_l and c_r are equal for the interior column, this is not true for the edge column of Fig. 10.18*d* or for a corner column.

Many engineers, to avoid problems associated with transfer of moments at edge and corner columns, elect to cantilever the flat plate slab a distance beyond the exterior column lines a distance about equal to one-quarter of the typical interior span length. This results in a much improved condition, more nearly like that of an interior column. The unbalanced moment is apt to be less, and the critical shear perimeter is increased.

In its recommendations pertaining to moment transfer at exterior columns, ACI Committee 423 calls attention to the need for bonded reinforcement in the form of closed ties to act as torsional reinforcement along the edge of the slab adjacent to the column. This should be included if v_u exceeds $2\sqrt{f_c'}$, according to Ref. 10.1. It can be designed following the methods for torsion found in Chapter 5.

The application of moment to a column from a floor system introduces horizontal shear force to the column, as is clear from Fig. 10.18*a*. This shear should be considered in the design of lateral column ties.

10.16 DEFLECTION OF FLAT PLATES

Post-tensioned prestressed flat plates may be made quite thin. Although strength may be adequate at factored loads, and although service load cracking can be controlled by precompression in the slab, camber or deflection of such slabs can cause difficulty and should always be checked.

It is helpful in the initial design stage to select a trial slab thickness such that later revision of the design will be unnecessary. For prestressed post-tensioned flat plates continuous over two or more spans in each direction, a span-to-depth ratio of 40 to 45 may be used for floors, and a ratio of 45 to 48 for roofs. These limits may be increased to about 48 and 52, respectively, if later calculations verify that deflection is not excessive.

Generally, it is the incremental deflection due to live load that is of interest. This is certainly so for slabs designed for dead load balancing, which should produce a nearly level surface for the balanced load stage. Since only the incremental deflection due to unbalanced load is to be found, the use of an approximate method is fully justified.

The deflection of a uniformly loaded flat plate may be estimated by the equivalent frame method (Ref. 10.16). Originally developed for reinforced concrete two-way systems, the method is specially appropriate for prestressed flat plates, which are usually uncracked at service loads. The method is fully compatible with equivalent frame method for moment analysis presented in Section 10.12. The definition of column and middle strips, the longitudinal moment analysis, lateral moment distribution coefficients, and other details are the same as for the moment analysis, and so most of the needed quantities are already at hand.

A slab region bounded by column centerlines is shown in Fig. 10.19. The deflection calculation considers the deformation of such a typical region in one direction at a time after which the contributions in each direction are added to obtain the total deflection at any point of interest. Referring to Fig. 10.19*a*, the slab is considered to act as a broad, shallow beam of width equal to the panel dimension l_y and having the span l_x. At this stage, the slab is considered to rest on unyielding support lines at $x = 0$ and $x = l_x$. Note that all unit strips in the X direction will not deform identically, because of variation of moment across the width of the slab.

The slab is next analyzed for bending in the Y direction (Fig. 10.19*b*). Once again, the effect of variation of moment is shown.

The midpanel deflection can now be obtained as the sum of the midspan deflection of the column strip in one direction, and that of the middle strip in the other direction, as shown in Fig. 10.19*c*:

$$d_{max} = d_{cx} + d_{my} \tag{10.18a}$$

or

$$d_{max} = d_{cy} + d_{mx} \tag{10.18b}$$

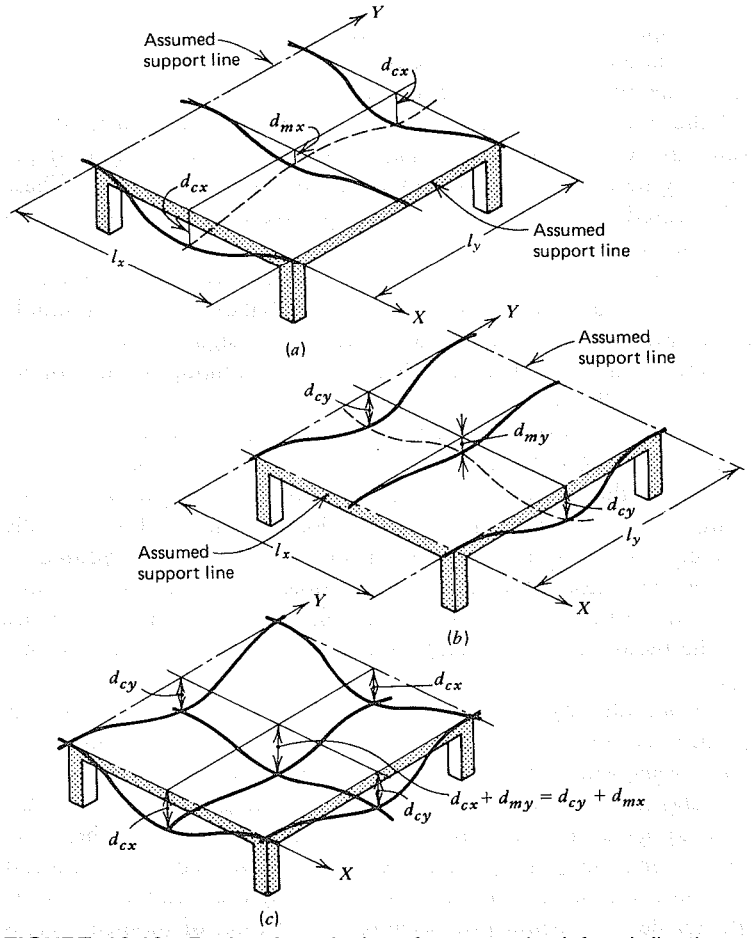

FIGURE 10.19 Basis of equivalent frame method for deflection analysis. (*a*) *X* direction bending. (*b*) *Y* direction bending. (*c*) Combined bending.

Although the floor area bounded by column centerlines (Fig. 10.19) was used to introduce the method, the actual calculations are more easily done for strips of floor in either direction bounded by panel centerlines, as for the moment analysis. Figure 10.20 shows such a strip of floor spanning in the X direction.

The strip is initially considered to have supports that are fully fixed at $x = 0$ and $x = l_x$, permitting neither deflection, nor rotation at those support lines. Deflections of the equivalent frame are calculated. The effect of the actual support rotations on midspan deflection is found later and the total deflection of the equivalent frame spanning in the X direction is taken as the sum of the three parts: that of the panel assumed to have fixed supports, plus that resulting from the rotation at each of the two support lines in turn.

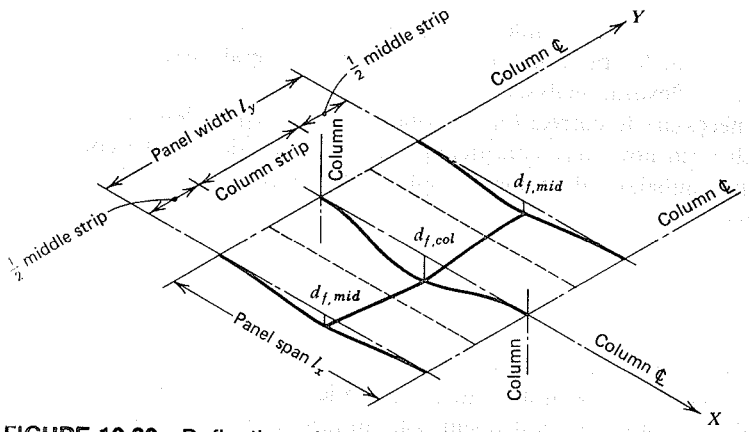

FIGURE 10.20 Deflection of column and middle strips in X direction.

Moment variation across the width of the panel is treated the same approximate way as for the flexural analysis of Section 10.12. Column strips and middle strips are defined as before, and the moment is assumed to be constant within the bounds of each. As suggested in Section 10.12, for simple spans, 55 to 60 percent of the total moment at critical sections may be assigned to the column strip, for continuous spans, 65 to 75 percent may be assigned to the column strip. In either case, the remaining percentage is assigned to the middle strip.

A "reference" deflection at midspan of the uniformly loaded full-panel-width equivalent frame with fixed ends can be established as:

$$d_{f,ref} = \frac{wl^4}{384E_cI_{frame}} \tag{10.19}$$

where w is the load per foot along the span of length l, and I_{frame} is the moment of inertia of the full-panel-width slab. This implies a uniform lateral distribution of moment across the panel width, with the slab deforming into a cylindrical surface. The effect of the actual moment variation, as well as possible difference in width of column strip and middle strip, is accounted for by multiplying the reference deflection by the ratio of M/EI for the strip to that of the frame:

$$d_{f,col} = d_{f,ref} \times \frac{M_{col}}{M_{frame}} \times \frac{E_cI_{frame}}{E_cI_{col}} \tag{10.20a}$$

$$d_{f,mid} = d_{f,ref} \times \frac{M_{mid}}{M_{frame}} \times \frac{E_cI_{frame}}{E_cI_{mid}} \tag{10.20b}$$

The subscripts relate the deflection d, the bending moment M, or moment of

inertia I to the column strip, middle strip, or full-width frame. Note that the ratio of strip moment to frame moment is simply the lateral distribution factor already used in the flexural analysis.

Next it is necessary to correct for the rotations of the equivalent frame at the supports, which until now were considered fixed. The rotation at the column is equal to the net unbalanced moment applied at the column, divided by the column stiffness:

$$\theta = \frac{M_{net}}{K_{ec}} \tag{10.21}$$

where θ = angle change in radians
M_{net} = difference in floor moments to left and right of column
K_{ec} = stiffness of equivalent column (see Section 10.12)

In some cases, the connection between floor slab and column transmits negligible moment, as for lift slabs. In such a case, the flexural analysis will indicate that the net moment applied at the column is zero. The end slopes for the slab may be found, in this case, using the second moment-area principle. The slope at the right end of an equivalent frame span, for example, is found by taking moments of the M/EI diagram for that span about the left end, then dividing by the span length.

Once the rotation at each end is known, the associated midspan deflection of the equivalent frame can be calculated. It is easily confirmed that the midspan deflection of a beam experiencing an end rotation of θ radians, the far end being fixed, is

$$d_\theta = \frac{\theta l}{8} \tag{10.22}$$

Thus, the total deflection at midspan of the column strip or middle strip is the sum of the three parts:

$$d_{col} = d_{f,col} + d_{\theta l} + d_{\theta r} \tag{10.23a}$$

$$d_{mid} = d_{f,mid} + d_{\theta l} + d_{\theta r} \tag{10.23b}$$

where the subscripts l and r refer to the left and right ends of the span, respectively.

The calculations described are repeated for the equivalent frame in the second direction of the structure, and the total deflection at midpanel obtained by summing the column strip deflection in one direction and the middle strip deflection in the other, as indicated by Eqs. (10.18).

The midpanel deflection should be the same whether calculated by Eq. (10.18a) or Eq. (10.18b). Actually, a difference will usually be obtained because of the approximate nature of the calculations. For very rectangular panels, the main contribution to midpanel deflection is that of the long-direction column strip. Consequently, the midpanel deflection is best estimated by summing that of the long-direction column strip and the short-direction middle strip. However, for exterior panels, the most important contribution is from the column strips perpendicular to the discontinuous edge, even though the long side of the panel may be parallel to the edge. Judgment is required.

The deflections found using the procedure described are short-term deflections such as would be caused by a live load intermittently applied. If the unbalanced load is sustained over an extended period, the increase of deflection due to concrete creep must be accounted for. For beams as well as slabs, it has long been the practice to estimate long-term deflection as a simple multiplier times the initial elastic deflection. A factor of two is often used.

An example of a flat plate deflection calculation is found in the following section.

10.17 EXAMPLE: FLAT PLATE DESIGN

A prestressed flat plate lift slab will be supported by steel columns spaced 25 ft on centers in each direction, as shown in Fig. 10.21a. Loads will be transferred from the slab to the 10 × 10 in. tubular columns by square lifting collars shown in Fig. 10.21b. The collar detail transmits no significant bending moment to the columns. The load to be carried includes the self-weight of the slab, an additional dead load of 12 psf, and a service live load of 50 psf. A balanced load condition is specified for full dead load. A typical interior panel is to be designed. Concrete compressive strength $f_c' = 5{,}000$ psi, and $E_c = 4{,}030{,}000$ psi. (Columns 254 × 254 mm at 7.62 m spacing, $w_d = 0.57$ kN / m^2, $w_l = 2.40$ kN / m^2, $f_c' = 34$ MPa^2, and $E_c = 27.8$ kN / mm^2.)

A trial depth of slab will be based on a span – depth ratio of 45:

$$h = \frac{25 \times 12}{45} = 6.7 \text{ in.} \qquad \text{try 7 in. (178 mm)}$$

For the 7-in. depth slab, using normal density concrete, the self-weight is 88 psf. Therefore, the total dead load, on which load balancing is to be based, is 88 + 12 = 100 psf. A two-directional network of parabolic tendons will be used. With a 3/4-in. concrete cover required at the top and bottom of the slab, and anticipating the outside diameter of the tendons to be about 1/2 in., the average distance from the slab surface to the top or bottom steel is 1 1/4 in. Thus, the maximum sag y for a typical interior span is 7 – 2.5 = 4.5 in., as shown in Fig. 10.21c. The short transition curve necessary over the column lines will be disregarded in the calculations.

The tendon layout and prestress force will be based on load balancing for a 100 psf dead load, the full load to be carried in each direction. The analysis is

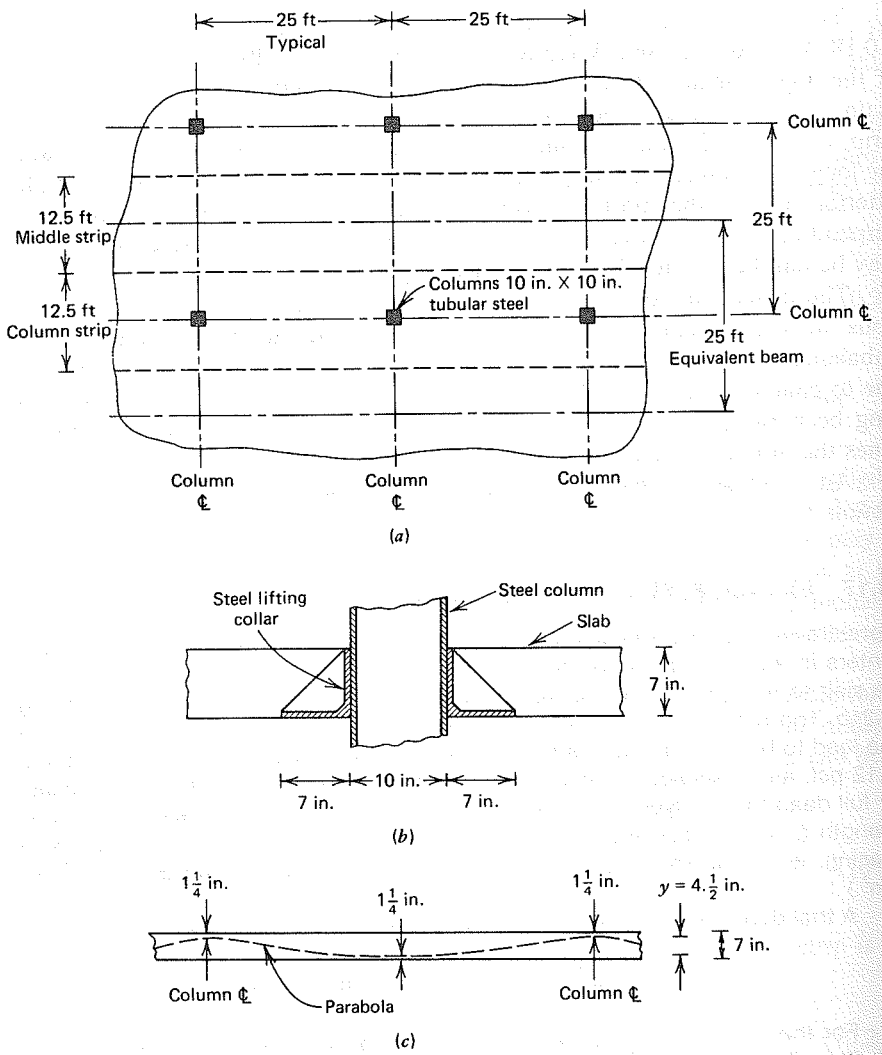

FIGURE 10.21 Flat plate design example. (*a*) Plan view of floor. (*b*) Detail of steel lifting collars. (*c*) Typical tendon profile.

based on an equivalent beam of full 25-ft panel width. In each direction, the effective prestress force required per 25-ft strip, from Eq. (4.27), is

$$P_e = \frac{wl_2l_1^2}{8y} = \frac{100 \times 25 \times 625 \times 12}{8 \times 4.5} = 521{,}000 \text{ lb } (2317 \text{ kN})$$

Assuming 20 percent loss of prestress force, the initial prestress force is 651,000 lb per 25 ft strip. Unbonded 0.600-in. diameter Grade 270 strands will be used, each providing an area of 0.217 in.^{2} For an initial prestress of $0.70f_{pu}$, each cable provides 41.0 kips force (Appendix A); thus, the number of tendons required per 25-ft strip is

$$N = \frac{651{,}000}{41{,}000} = 15.9 \qquad \text{use } 16$$

The number of these to be placed in the column strip is $0.75 \times 16 = 12$, the remaining four to be distributed over the width of the middle strip. This results in a spacing of tendons in the column strip of $12.5 \times 12/12 = 12.5$ in., and in the middle strip of $12.5 \times 12/4 = 37.5$ in. Thus, the maximum spacing is well below $8 \times 7 = 56$ in., as required by Code. The average prestress in the middle strip after losses is $(41{,}000 \times 0.8)/(37.5 \times 7) = 125$ psi, exactly the minimum permitted by Code. In the column strip, the average prestress is $(41{,}000 \times 0.8)/(12.5 \times 7) = 375$ psi, compared with a recommended maximum of 500 psi. This confirms that design decisions to this point are satisfactory.

Next the structure will be analyzed for the effect of applying the 50 psf service live load. Again, a 25-ft wide strip provides the basis; the analysis that follows applying in each direction of the structure. Alternate loadings will be considered to maximize moments at negative and positive bending sections.[9] For maximum negative moments at a typical support, the uniform live load of $50 \times 25 = 1{,}250$ plf will be applied to the two adjacent spans, as shown in Fig. 10.22*a*. The supports second removed from the one under study will be considered fixed, as permitted by ACI Code, and the analysis for moments done by moment distribution, with the results as shown.

For maximum positive moment in a typical span, only that span will be loaded, as in Fig. 10.22*b*. The resulting live load moment diagram is indicated.

Although not needed for present purposes, a third analysis is shown in Fig. 10.22*c* for later reference: the effect of dead load of $100 \times 25 = 2{,}500$ plf uniformly distributed over all spans.

Concrete stresses at full service load are found by superimposing the bending stresses due to live load moments on the uniform compression obtained for the balanced dead load.

The negative moments obtained from the live load analysis apply at the column centerlines, and may be reduced for design purposes to those at the support face. The shear at the column centerline resulting from the load that produced the maximum negative moment is (from Fig. 10.22*a*).

$$V = 1.25 \times \frac{25}{2} + \frac{82 - 32}{25} = 17.6 \text{ kips } (78 \text{ kN})$$

The effective support width is 24 in., based on the use of the lifting collar shown in Fig. 10.21*b*. Consequently, the negative moment at the face of supports is (see Ref.

[9] In the present case, the ratio of live to dead load is only 0.5, and the ACI Code permits use of a single loading case, with all panels fully loaded. Optionally, alternate loadings may be used with three-quarters of the factored live load acting. These more lenient provisions will not be used here.

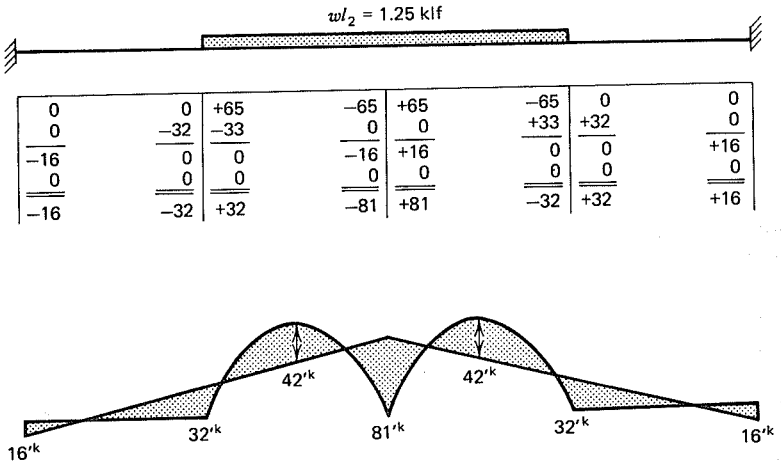

(*a*)

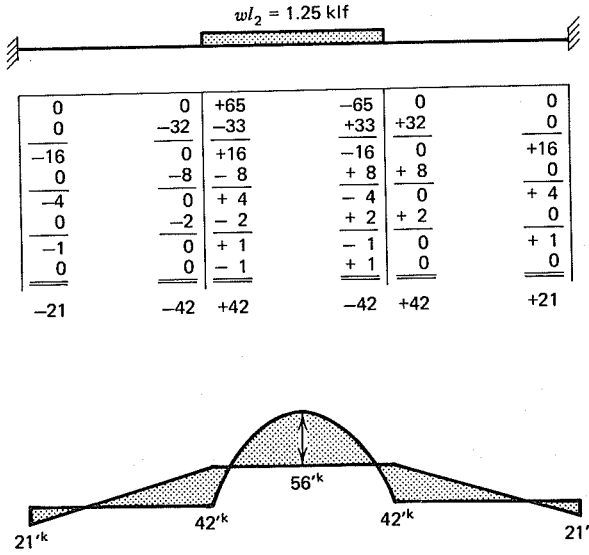

(*b*)

FIGURE 10.22 Moment analysis at service loads for flat plate example. (*a*) Maximum live load negative moment. (*b*) Maximum live load positive moment. (*c*) Dead load negative and positive moments.

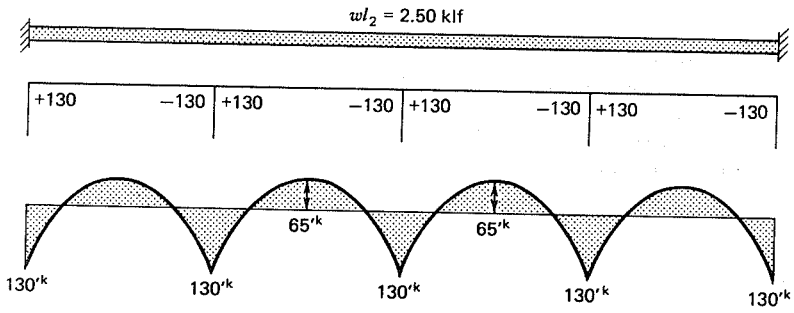

(*c*)

FIGURE 10.22 (*Continued*)

10.14, p. 526):

$$M_{neg} = M_{\ell} - \frac{Val}{3} = 81 - 17.6 \times \frac{2}{3} = 69 \text{ ft-kips (94 kN-m)}$$

The moment assigned to the column strip is 0.75 × 69 = 52 ft-kips. The moment of inertia of the column strip is

$$I_c = \frac{1}{12} \times 12.5 \times 12 \times 7^3 = 4{,}290 \text{ in.}^4$$

Consequently, the bending stress in the concrete in that strip is

$$f_b = \frac{52{,}000 \times 12 \times 3.5}{4{,}290} = 510 \text{ psi}$$

Thus, the concrete stresses at the top and bottom faces of the column strip, at the face of supports, are respectively

$$f_1 = -375 + 510 = +135 \text{ psi}$$
$$f_2 = -375 - 510 = -885 \text{ psi}$$

According to ACI Committee 423 recommendations, the allowable compression in the concrete is 0.30 × 5,000 = 1,500 psi, and the allowable tension (provided non-prestressed bonded steel is included) is $6\sqrt{5{,}000}$ = 424 psi. Both limits are well above the actual stresses.

The negative moment assigned to the middle strip is 0.25 × 69 = 17 ft-kips. The low-bending stresses in the middle strips, superimposed on the 125 psi compression, produce a stress that is not critical.

At the positive moment section, the total moment in each 25-ft strip is 56 ft-kips. Again, 75 percent, or 42 ft-kips, will be assigned to the column strip. Thus, the bending stresses in the column strip are

$$f_b = \frac{42{,}000 \times 12 \times 3.5}{4{,}290} = 411 \text{ psi}$$

and the net stresses at the top and bottom of the concrete slab are, respectively,

$$f_1 = -375 - 411 = -786 \text{ psi}$$
$$f_2 = -375 + 411 = +36 \text{ psi}$$

According to the recommendations, the allowable compression is 0.45 × 5,000 =

2,250 psi and the allowable tension, assuming no bonded rebars, is $2\sqrt{5,000} = 141$ psi. The actual stresses are satisfactory.

The middle strip positive moment of 14 ft-kips produces low flexural tension and compression stresses that are not critical.

Non-prestressed bar reinforcement must be provided at the top of the slab in the column region, in the amount

$$A_s = 0.00075 \times 7 \times 25 \times 12 = 1.58 \text{ in.}^2 \ (1{,}019 \text{ mm}^2)$$

Four No. 6 Grade 60 bars will be used in each direction, providing an area each way of 1.77 in.^{2} These will be placed close to the column, and will be $25/3 = 8$ ft long.

Beam shear will be checked at a section $h/2$ from the support face, or 15.5 in. from the column centerline (see Fig. 10.21*b*). The shear force at factored load is

$$V_u = \frac{22.4}{2}(1.4 \times 100 + 1.7 \times 50) \times 25 = 63{,}000 \text{ lb}$$

By ACI Code, the shear strength may be taken as $V_c = 2\sqrt{f_c'}\, b_w d = 2\sqrt{5,000} \times 25 \times 12 \times 5.75 = 244{,}000$ lb. Thus, $\phi V_c = 0.85 \times 244{,}000 = 207{,}000$ lb, substantially above V_u. Beam shear is not critical here.

Punching shear will be investigated at a critical perimeter $d/2$ from the toe of the lifting collar. The side dimension of the assumed critical section is $24 + 5.8 = 29.8$ in., and $b_0 = 119$ in. (refer to Fig. 10.21*b*). The shear force to be resisted may be based on the tributary area, neglecting the small reduction for load within the critical perimeter in this case:

$$V_u = 625(1.4 \times 100 + 1.7 \times 50) = 141{,}000 \text{ lb (627 kN)}$$

According to Eq. (10.11),

$$\phi V_c = 0.85(3.5\sqrt{5,000} + 0.3 \times 375)119 \times 5.75 = 209{,}000 \text{ lb}$$

It is clear that the slab is satisfactory without supplementary shear reinforcement by either beam shear or punching shear criterion.

The flexural strength will be checked for the full-width slab strip of 25 ft, in either direction, placing the loads to produce maximum moments at the critical sections. Referring to Fig. 10.22, and introducing the usual load factors, the negative moment applied at the column centerline, at factored loads, is[10]

$$M_{neg} = 1.4 \times 130 + 1.7 \times 81 = 320 \text{ ft-kips (434 kN-m)}$$

and the associated shear force is

$$V = \frac{25}{2}(1.4 \times 2.5 + 1.7 \times 1.25) + \frac{(81 - 32)1.7}{25} = 74 \text{ kips (329 kN)}$$

Consequently, the required flexural strength at the face of support is

$$M_{neg} = 320 - 74 \times \frac{2}{3} = 271 \text{ ft-kips (367 kN-m)}$$

[10]Note that for the present example, a typical interior panel, the application of prestress force produces no secondary moments.

The positive moment to be resisted is

$$M_{pos} = 1.4 \times 65 + 1.7 \times 56 = 186 \text{ ft-kips (252 kN-m)}$$

For the full 25-ft strip containing 16 tendons,

$$f_{pe} = \frac{521{,}000}{16 \times 0.217} = 150{,}000 \text{ psi}$$

$$A_p = 0.217 \times 16 = 3.472 \text{ in.}^2$$

$$\rho_p = \frac{3.472}{25 \times 12 \times 5.75} = 0.0020$$

and the stress in the unbonded tendons is estimated to be

$$f_{ps} = f_{pe} + 10{,}000 + \frac{f_c'}{300\rho_p}$$

$$= 150{,}000 + 10{,}000 + \frac{5{,}000}{300 \times 0.0020} = 168{,}000 \text{ psi}$$

The contribution of the four No. 6 bars added to meet requirements for bonded non-prestressed steel may be included in ultimate strength calculations. Then

$$a = \frac{A_p f_{ps} + A_s f_y}{0.85 f_c' b} = \frac{3.472 \times 168 + 1.77 \times 60}{0.85 \times 5 \times 300} = 0.54 \text{ in.}$$

$$\phi M_n = 0.90(3.472 \times 168 + 1.77 \times 60)(5.75 - 0.54/2)/12$$

$$= 283 \text{ ft-kips}$$

which is about four percent above that required for negative bending. Similar calculations confirm that the positive bending section has adequate flexural strength as well.

The live load deflection at the center of the typical panel will be checked, using the equivalent frame method. The moments of inertia for the full-width frame and the column or middle strips are respectively,

$$I_{frame} = \frac{1}{12} \times 25 \times 12 \times 7^3 = 8{,}580 \text{ in.}^4$$

$$I_{col} = I_{mid} = \frac{8{,}580}{2} = 4{,}290 \text{ in.}^4$$

The reference deflection is found from Eq. (10.19) to be

$$d_{f,ref} = \frac{50 \times 25 \times 25^4 \times 12^4}{384 \times 4{,}030{,}000 \times 12 \times 8{,}580} = 0.064 \text{ in.}$$

From Eqs. (10.20*a*) and (10.20*b*), the deflections of the column and middle strips, with ends assumed fixed, are

$$d_{f,col} = 0.064 \times 0.75 \times 2 = 0.096 \text{ in.}$$

$$d_{f,mid} = 0.064 \times 0.25 \times 2 = 0.032 \text{ in.}$$

For the present case, with no moment transmitted through the slab-to-column joint, the actual end rotations of the slab strip must be found from the moment diagram

for the slab, using moment area principles. Calculations are based on the diagram for maximum live load moment (Fig. 10.22*b*). The distance of a point on the elastic curve at the left support from a tangent to the elastic curve at the right support is found taking moments of the M/EI area about the left support:

$$\Delta = \frac{1}{EI}\left(98 \times 25 \times \frac{2}{3} \times \frac{25}{2} - 42 \times 25 \times \frac{25}{2}\right) = \frac{7{,}290}{EI}$$

The slope at the right support (the left support slope is the same, of opposite sign) is then easily calculated by dividing by the span length:

$$\theta_r = \frac{7{,}290}{25EI} = \frac{7{,}290 \times 1{,}000 \times 12^3}{25 \times 12 \times 4{,}030{,}000 \times 8{,}580} = 0.0012 \text{ radians}$$

From Eq. (10.22) the midspan deflection associated with the end rotation just found is

$$d_\theta = \frac{0.0012 \times 25 \times 12}{8} = 0.045 \text{ in.}$$

and from Eqs. (10.23*a*) and (10.23*b*), the midspan deflections of the column and middle strips are, respectively,

$$d_{col} = 0.096 + 0.045 \times 2 = 0.186 \text{ in. (5 mm)}$$

$$d_{mid} = 0.032 + 0.045 \times 2 = 0.122 \text{ in. (3 mm)}$$

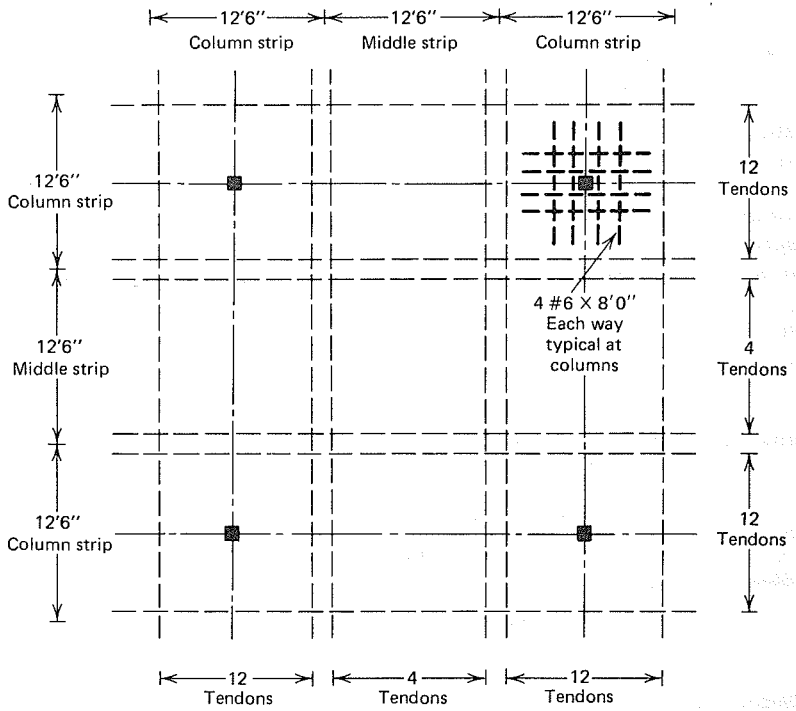

FIGURE 10.23 Reinforcing and prestress tendon layout for flat plate example.

Finally, from Eq. (10.18*a*), the live load deflection at the midpoint of the panel is found by summing the deflection of the column strip in one direction and the middle strip in the other:

$$d_{max} = 0.186 + 0.122 = 0.308 \text{ in. (8 mm)}$$

According to ACI Code, the limiting live load deflection is taken as 1/360 times the span, or 0.833 in. The design is satisfactory in this respect as well as all others.

The complete arrangement of prestressing tendons and non-prestressed bar reinforcement is shown in Fig. 10.23.

REFERENCES

10.1 "Recommendations for Concrete Members Prestressed With Unbonded Tendons," reported by ACI-ASCE Joint Committee 423, *Concrete International*, Vol. 5, No. 7, July 1983, pp. 61–76.

10.2 Jones, L. L. and Wood, R. H., *Yield Line Analysis of Slabs*, American Elsevier, New York, 1967, 405 pp.

10.3 Timoshenko, S. and Woinowsky–Krieger, S., *Theory of Plates and Shells*, 2nd ed., McGraw-Hill, New York, 1959, 580 pp.

10.4 Scordelis, A. C., Lin, T. Y., and Itaya, R., "Behavior of a Continuous Slab Prestressed in Two Directions," *J. ACI*, Vol. 56, No. 6, December 1959, pp. 441–460.

10.5 Rice, E. K. and Kulka, F., "Design of Prestressed Lift Slabs for Deflection Control," *J. ACI*, Vol. 56, No. 8, February 1960, pp. 681–693.

10.6 Hemakom, R., *Strength and Behavior of Post-Tensioned Flat Plates With Unbonded Tendons*, Ph.D. dissertation, Department of Civil Engineering, University of Texas, Austin, 1975.

10.7 Winter, V. C., *Tests of Four Panel Post-Tensioned Flat Plate With Unbonded Tendons*, Research Paper, Department of Civil Engineering, University of Texas, Austin, 1977.

10.8 Burns, N. H. and Hemakom, R., "Test of Scale Model Post-Tensioned Flat Plate," *J. Structural Division, ASCE*, Vol. 103, No. ST6, June 1977, pp. 1237–1255.

10.9 Gerber, L. L. and Burns, N. H., "Ultimate Strength Tests of Post-Tensioned Flat Plates," *J. PCI*, Vol. 16, No. 6, November–December 1971, pp. 40–58.

10.10 *Design of Post-Tensioned Slabs*, 2nd ed., Post-Tensioning Institute, Phoenix, 1984.

10.11 *Post-Tensioning Manual*, 4th ed., Post-Tensioning Institute, Phoenix, 1985, 406 pp.

10.12 "Tentative Recommendations for Prestressed Concrete Flat Plates," reported by ACI Committee 423, *J. ACI*, Vol. 71, No. 2, February 1974 (reaffirmed 1980), pp. 61–71.

10.13 Corley, W. G. and Hawkins, N. M., "Shearhead Reinforcement for Slabs," *J. ACI*, Vol. 65, No. 10, October 1968, pp. 811–824.

10.14 Nilson, A. H. and Winter, G., *Design of Concrete Structures*, 10th ed., McGraw-Hill, New York, 1986.

10.15 Hanson, N. W. and Hanson, J. M., "Shear and Moment Transfer Between Concrete Slabs and Columns," *J. Res. and Dev. Lab.* Portland Cement Association, Vol. 10, No. 1, January 1968, pp. 2–16.

10.16 Nilson, A. H. and Walters, D. B., "Deflection of Two-way Floor Systems by the Equivalent Frame Method," *J. ACI*, Vol. 72, No. 5, May 1975, pp. 210–218.

PROBLEMS

10.1 Figure P10.1 shows the cross section of a factory floor consisting of a three-span, one-way, continuous, solid concrete slab supported by monolithic concrete beams. The slab is to carry a superimposed service live load of 80 psf and superimposed dead load of 20 psf, in addition to its own weight. It will be post-tensioned using 0.600-in. diameter Grade 270 stranded tendons, unbonded, in plastic sheathing. Specified concrete strength is f'_c = 5,000 psi, and f'_{ci}, at the time of tensioning, will be 3,500 psi. Time-dependent losses may be assumed to be 20 percent of P_i. (a) Using the load-balancing approach, based on balancing the full dead load, calculate the necessary slab thickness, the initial and effective prestress force per foot of slab, and the spacing of tendons. (b) Calculate flexural stresses at all critical sections for the full service load condition. (c) Design the required non-prestressed bar reinforcement, longitudinal and transverse. (d) Check to ensure that the slab has the required flexural strength at factored loads. Include secondary moments, if any. Modify the design of bar reinforcement, if necessary. (e) Check the shear strength of the slab. (f) Calculate the deflections due to full service live load and compare with permissible values.

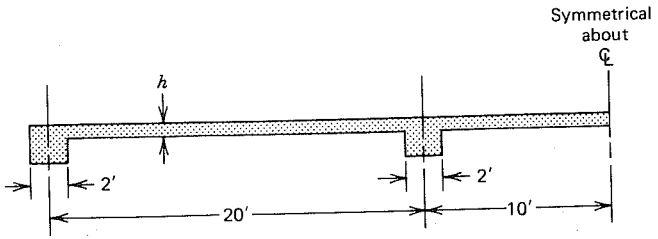

FIGURE P10.1

10.2 A two-way prestressed concrete slab, measuring 60 × 120 ft overall, is to be provided to carry a tennis court over an underground parking facility. Support will be provided by masonary walls on the perimeter, and steel framing along interior column lines, as shown in Fig. P10.2. An asphalt court surface 2-in. thick, weighing 25 psf, will be provided. (a) Design the slab for a balanced load consisting of the self-weight of the slab and the asphalt topping. Determine the required slab thickness, prestress force, and number and spacing of 1/2-in. diameter Grade 250 unbonded post-tensioning tendons. Concrete strengths f'_c = 5,000 psi and f'_{ci} =

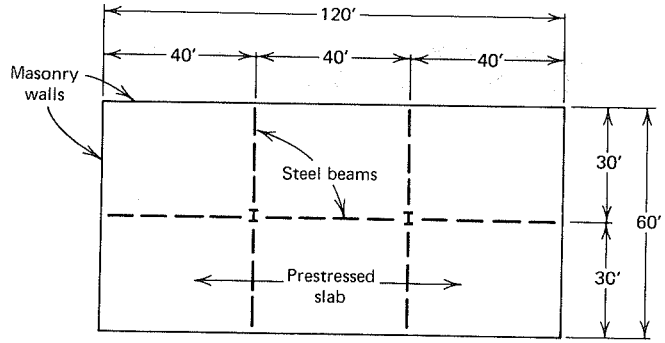

FIGURE P10.2

3,500 psi. (b) Check concrete flexural stresses in the fully loaded stage assuming live load of 100 psf. (c) Check the safety of the slab against flexural failure, applying the usual ACI load factors and strength reduction factors. Modify the design, if necessary. (d) What other aspects of the proposed structure should be investigated for a complete structural design?

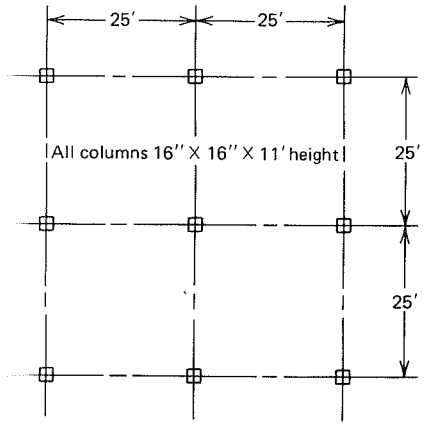

FIGURE P10.3

10.3 Fig. P10.3 shows a typical interior region of a prestressed concrete floor that is to be designed as a flat plate, using unbonded post-tensioned tendons. There will be no column capitals or dropped panels. Service live load is 80 psf; dead load consists of self-weight plus 20 psf superimposed. (a) Find the required slab thickness, tendon profile, required prestress force per ft, and spacing of tendons in the column and middle strips. A two-way banded tendon arrangement is specified. Prestress should be based on a balanced load consisting of self weight plus superimposed dead load. (b) Find the concrete stresses at all critical sections resulting from application of dead plus service live load. (c) Determine the size, spacing, and length of all required non-prestressed bonded flexural steel. (d) Check the flexural strength of the slab, and modify the design, if necessary. Note that, according to ACI Code, if the

live load does not exceed three-fourths of the dead load, maximum factored moments may be assumed to occur at all sections with full factored live load on the entire slab system. (e) Check for shear transfer at a typical interior column. If shear reinforcement is required, use 45 degree bent bars (see Ref. 10.14). (f) What is the deflection at the center of a typical panel when the full service live load is in place? Tendons will be 0.500-in. diameter Grade 250 unbonded strands. Concrete strength is f'_c = 5,000 psi and f'_{ci} = 3,500 psi. Assume 20 percent time-dependent losses.

10.4 Redesign the floor of Problem 10.3 using a one-way banded arrangement of tendons, similar to Fig. 10.13.

ELEVEN

AXIALLY LOADED MEMBERS

11.1 INTRODUCTION

The preceding chapters have focused on the analysis and design of flexural members: beams, for which the main loading is normal to the axis of the member, and slabs, with loads acting normal to the surface. Another class of members will now be considered: prismatic elements for which the main loading acts in the direction parallel to the long axis. Included are compression members, such as columns, truss components, wall panels, and pilings, and tension members such as are used in trusses, tie rods of arches and rigid frames, and hangers. Although the main loads in these cases are longitudinal, producing compression or tension, they may be combined with bending loads. Combined loading is normal in columns, where forces are often applied eccentrically by brackets, or where an equivalent eccentricity results from rigid-jointed continuous-frame action.

This chapter will present the basic features of the analysis and design of columns, including eccentric columns, and tension members. Special applications, such as trusses, pilings, foundation anchors, liquid storage tanks, and containment vessels will be described in Chapter 13.

11.2 BEHAVIOR OF PRESTRESSED COLUMNS

If a concrete column were subjected only to axial compression, there would be very little point in prestressing and thereby adding to the compression stress. However, the column that is loaded only with concentric compressive force is most unusual in structural practice. In most cases, columns carry bending moment as well, introduced by eccentric application of the load, as for precast columns with brackets, or by continuous rigid-jointed frame action, which transfers bending moments from the ends of the beam spans into the columns. Wind or earthquake forces may introduce direct tension combined with high bending stresses. Prestressing of columns will often be found advantageous, particularly when the ratio of bending moment to axial force is high.

Prestressed concrete columns may be categorized as *short* or *long*. In the first case, the strength depends only on the strength of the steel and concrete and the geometry of the cross section, whereas in the second, the strength may be significantly diminished by the effects of slenderness. The effect of slenderness on strength will be studied in Sections 11.5 and 11.6. The present discussion pertains to short columns, but provides a basis for later study of slender columns.

Deflection and cracking of prestressed columns at service loads are almost never serious problems. Furthermore, the investigation of stresses at service loads, based on elastic behavior of the materials, is of limited interest and has little to do with the safety of the column, which is the main concern. Consequently, present attention will be focused on the analysis to determine *strength* of eccentrically loaded, short, prestressed concrete columns (Refs. 11.1–11.3).

Figure 11.1*a* shows such a column, at incipient failure, with ultimate load P_n applied at eccentricity e with respect to the geometric center of the cross section.[1] Section dimensions b and h are, respectively, parallel and perpendicular to the axis of bending, as shown in Fig. 11.1*b*. The prestressing steel is arranged in two layers, each parallel to the axis of bending, and it will be assumed that the cross section is symmetrical, with equal steel areas A_{p1} and A_{p2}. The eccentric load is equilibrated at any section a–a along the length of the member by internal forces producing a net thrust equal and opposite to P_n, and moment M_n equal and opposite to $P_n e$.

Such a column may fail by either of two modes:

1. *For large eccentricities* the prestressing steel on the side of the column farther from the load will reach the yield condition in tension. Continued yielding will shift the neutral axis toward the loaded side of the member, reducing the concrete area available to resist compression, and eventually overloading the concrete. A *secondary* compression failure results when the compressive strain in the concrete becomes equal to the limiting value ε_{cu}.

[1]Note that a column carrying a concentric load P_n and bending moment M_n may be designed for an equivalent loading consisting of P_n acting at eccentricity $e = M_n / P_n$.

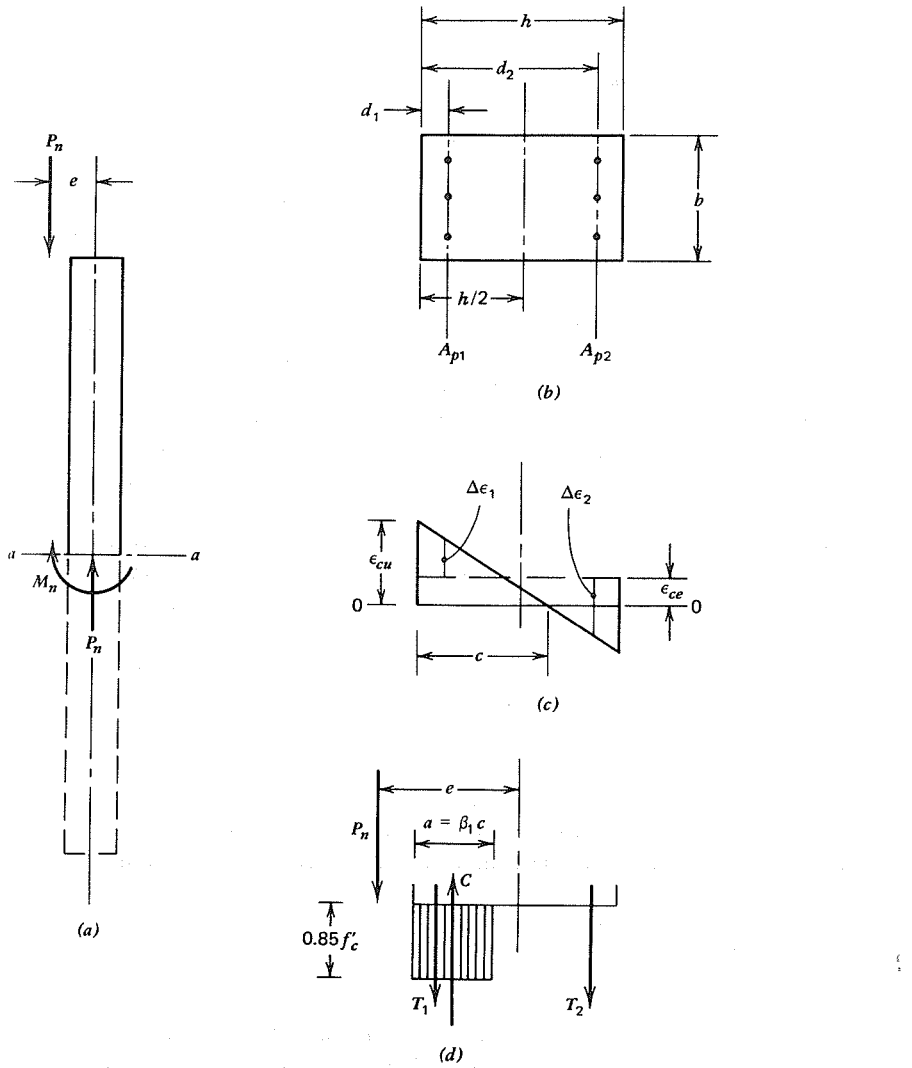

FIGURE 11.1 Short column with eccentric loading. (*a*) Free body of half-column. (*b*) Cross section. (*c*) Strain distribution. (*d*) Forces and equivalent stresses.

2. *For small eccentricities* a *primary* compression failure of the concrete will obtain when the maximum concrete strain on the loaded side of column reaches ε_{cu}. The steel on the far side of the column may be well below the yield stress when this occurs.

Clearly, it is also possible for some unique combination of P_n and M_n (or equivalent eccentricity) to obtain, simultaneously, tension yielding of the steel on

the side of the column farther from the load and crushing of the concrete in compression on the side nearer the load. Such a situation is referred to as *balanced failure*, occurring at load P_b and moment M_b. For columns, this condition does not have the significance that it did for beams, where a ductile yielding failure could be insured by setting an upper limit on steel ratio. For columns, the nature of the failure, that is, yielding or crushing, is determined by the ratio of the applied moment M_u and thrust P_u, established by analysis of the structure as a whole. The equivalent eccentricity that results may be larger or smaller than the eccentricity e_b for balanced failure, and so failure may be initiated either by concrete crushing or steel yielding in a particular case.

The strains in the concrete at section a–a are shown in Fig. 11.1*c*. A convenient reference strain state corresponds to the effective prestress force P_e, such that after creep, shrinkage, and relaxation have taken place, the concrete strain is uniformly at ε_{ce} compression. Also shown in Fig. 11.1*c* is the strain distribution in the concrete at incipient failure, when the neutral axis is a distance c from the loaded side of the column, and the concrete strain on that face is equal to the limiting value ε_{cu}.

Forces and stresses corresponding to the strains at incipient failure are given in Fig. 11.1*d*. The equivalent rectangular stress block, with uniform concrete stress intensity $0.85f_c'$ and depth $a = \beta_1 c$ is substituted for the actual concrete stress variation as usual.

With reference to Fig. 11.1*d*, requirements of equilibrium of the free body consisting of the upper half of the column indicate that

$$P_n = C - T_1 - T_2 \tag{11.1}$$

where the concrete compressive stress resultant $C = 0.85f_c'ab$, and T_1 and T_2 are, respectively, the tensile forces provided by steel areas A_{p1} and A_{p2}. Setting the summation of moments about the column centerline equal to zero indicates that

$$P_n e = C\left(\frac{h}{2} - \frac{a}{2}\right) - T_1\left(\frac{h}{2} - d_1\right) + T_2\left(d_2 - \frac{h}{2}\right) \tag{11.2}$$

Equations (11.1) and (11.2) do not at once permit calculation of the failure load P_n for a given eccentricity e, because the terms C, T_1, and T_2 on the right-hand sides, as well as a, are all dependent on the still-unknown location of the neutral axis at failure, a distance c from the face of the column (see Fig. 11.1*c*). The neutral axis dimension, in turn, depends on the magnitude of the forces C, T_1, and T_2.

One could, theoretically, express all unknowns on the right-hand sides of Eqs. (11.1) and (11.2) in terms of the neutral axis distance c, then, for a given eccentricity e, solve the two equations simultaneously for c and P_n. However, the computational difficulties would be substantial.

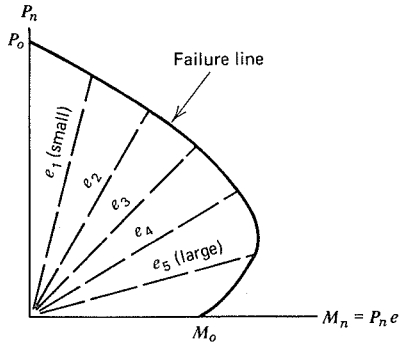

FIGURE 11.2 Interaction diagram for prestressed column.

It is more practical to approach the problem indirectly through the construction of an *interaction diagram* relating thrust P_n and moment M_n at failure. A typical diagram of this type is shown in Fig. 11.2. The solid line corresponds to a state of incipient failure for the particular column. Any combination of thrust and moment falling within the area bounded by that line can be carried with some margin of safety.

Radial lines may be drawn in Fig. 11.2 corresponding to discrete values of eccentricity, as shown. As the load is gradually increased from zero, for any eccentricity, the moment increases proportionately. When the load path represented by the radial eccentricity line reaches the solid interaction line, failure results. An eccentricity of zero (vertical eccentricity line) corresponds to a concentric compression failure at P_o, whereas an infinite eccentricity (horizontal eccentricity line) corresponds to failure at M_o in pure bending with no axial force. It will be seen that in the region of small eccentricity (compression failure), the addition of axial load will reduce the moment that can be carried. Conversely, in the region of high eccentricity (yielding failure), the addition of axial load increases the moment capacity.

A column failure interaction diagram such as Fig. 11.2 may be constructed for a given column geometry, material strengths, and prestress force by choosing successive, arbitrary locations for the ultimate neutral axis. Each choice corresponds to a particular eccentricity, failure load P_n, and failure moment M_n all of which can be found by a strain-compatibility analysis as follows.

A convenient starting point for the analysis is the effective prestress stage, prior to application of the external loads, when the prestress force is P_e and the concrete strain is ε_{ce}. Referring again to Fig. 11.1*c* shows that this compressive concrete strain is uniformly distributed over the depth of the section.

Application of the eccentric load will produce a linearly varying strain in the concrete. When the column is at incipient failure, the concrete strain on the side nearer to load will be ε_{cu} and the neutral axis will be at a distance c from that face, as shown in Fig. 11.1*c*.

The stresses and forces of Fig. 11.1*d* may be found on the basis of the strain distributions. For the arbitrarily selected value c, the concrete compressive resultant is

$$C = 0.85f_c'ab \tag{11.3}$$

Note that although the value of c may be greater than the column dimension h and, in fact, will be equal to infinity for the special case of concentric loading, in all calculations, the upper limit of a is the column dimension h.

The strain in the prestressing steel at effective prestress is

$$\varepsilon_{pe} = \frac{f_{pe}}{E_p} = \frac{P_e}{(A_{p1} + A_{p2})E_p} \tag{a}$$

The *change in strain* in the steel of area A_{p1} as the member passes from effective prestress stage to ultimate load is

$$\Delta\varepsilon_1 = \varepsilon_{cu}\frac{c - d_1}{c} - \varepsilon_{ce} \tag{b}$$

and the corresponding change in strain in the steel of area A_{p2} is

$$\Delta\varepsilon_2 = \varepsilon_{cu}\frac{d_2 - c}{c} + \varepsilon_{ce} \tag{c}$$

The steel forces T_1 and T_2 of Fig. 11.1*d* may be found based on the net strains in the respective steel areas. If these strains are below the proportional elastic limit, or yield strain, then

$$\begin{aligned} T_1 &= A_{p1}f_{p1} \\ &= A_{p1}E_p(\varepsilon_{pe} - \Delta\varepsilon_1) \\ T_1 &= A_{p1}E_p\left(\varepsilon_{pe} - \varepsilon_{cu}\frac{c - d_1}{c} + \varepsilon_{ce}\right) \end{aligned} \tag{11.4}$$

and

$$\begin{aligned} T_2 &= A_{p2}f_{p2} \\ &= A_{p2}E_{p2}(\varepsilon_{pe} + \Delta\varepsilon_2) \\ T_2 &= A_{p2}E_p\left(\varepsilon_{pe} + \varepsilon_{cu}\frac{d_2 - c}{c} + \varepsilon_{ce}\right) \end{aligned} \tag{11.5}$$

In applying these equations, careful attention must be given to signs, noting that c may be less than d_1 or larger than d_2, or intermediate between those values as shown.

If the strains represented by the quantities in parentheses in Eqs. (11.4) and (11.5) exceed the proportional limit, then the stresses corresponding to the particular strains must be found by reference to the actual stress–strain curve of the steel.

The failure load P_n may now be found by Eq. (11.1) and the failure moment M_n from Eq. (11.2) without difficulty, thus establishing *one point* on the failure interaction curve.

The analysis must be repeated, choosing other values of c, to establish the complete failure line. After the curve is defined this way, the failure load and moment for any value of eccentricity may be read directly from the graph, moving out the appropriate radial line to the point of intersection with the curve.

For design purposes, according to the ACI Code, the computed values of P_n and M_n must be modified by strength reduction factors ϕ to obtain the reduced values to be used as the design strengths:

$$P_{des} = \phi P_n \tag{11.6a}$$

$$M_{des} = \phi M_n \tag{11.6b}$$

The specified value of ϕ is 0.70 for columns with lateral ties (see Section 11.4) and 0.75 for columns with spiral reinforcement. In either case, the value of ϕ may be increased linearly, according to the Code, to 0.90, as the value of P_n decreases from the balanced load P_b to zero, thus matching at M_o the usual value of $\phi = 0.90$ for beams. In practical cases, ϕ may be increased linearly to 0.90 as ϕP_n decreases from $0.10f_c'A_g$ to zero.

In addition, according to the Code, the axial load design strength ϕP_n will not be taken greater than 0.85 (for members with spiral reinforcement) or 0.80 (for members with tie reinforcement) of the axial design strength ϕP_o in pure compression.

It is evident that the design of prestressed concrete columns is essentially a trial-and-error procedure. A trial column must be selected, the strength curve computed, and the capacity of that column compared against the capacity required. The same design approach is followed for ordinary reinforced concrete columns. Some useful design aids are available in the form of generalized interaction diagrams (Refs. 11.4 and 11.5), but in many cases, a strain-compatibility analysis such as that just described is necessary. A rather simple computer program may be prepared to perform the computations for as many trial designs as required.

11.3 EXAMPLE: CONSTRUCTION OF COLUMN INTERACTION DIAGRAM

The column of Fig. 11.3 measures 12 × 12 in. in cross section and is prestressed using eight 3/8-in. diameter Grade 250 strands in two layers. Total steel area is 0.640 in.^{2} The steel carries an effective prestress, after losses, of 150,000 psi, that, with E_p = 29,000,000 psi, corresponds to a strain ε_{pe} = 0.0052. The steel stress - strain curve is as shown in Fig. 2.4. Concrete strength is 6,000 psi, and the strain in the concrete when P_e = acts in ε_{ce} = 0.0005. The ultimate compressive strain may be taken as ε_{cu} = 0.003. (Column 305 × 305 mm, A_p = 413 mm^2, f_{pe} = 1034 MPa, E_p = 200 kN/mm^2, and f'_c = 41 MPa.) Establish the failure interaction diagram for this column, relating P_n and M_n. Superimpose on the same diagram the line corresponding to the ACI design strength, that is obtained by application of the appropriate ϕ factors.

The interaction curve will be established by selecting arbitrary values for the neutral axis dimension c, and for each value calculating the axial force and moment producing a state of incipient failure, using Eqs. (11.3), (11.4), (11.5), (11.1), and (11.2). Only representative points will be calculated here. The complete data are summarized in Table 11.1 and plotted in Fig. 11.4.

1. Assume the neutral axis distance c from the left face equals 8 in. (see Fig. 11.1c). Then $a = 0.75 \times 8 = 6$ in., and the compressive force resultant is found from Eq. (11.3):

$$C = 0.85 \times 6 \times 6 \times 12 = 367 \text{ kips}$$

The resultant force in the steel near the left face is given by Eq. (11.4):

$$T_1 = 0.32 \times 29{,}000(0.0052 - 0.0023 + 0.0005)$$

$$= 32 \text{ kips}$$

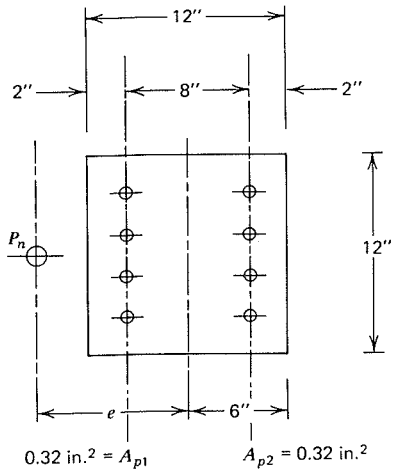

FIGURE 11.3 Cross section of column.

Table 11.1 Summary of Calculations for Column Design Example

Point	c (in.)	a (in.)	P_n (kips)	M_n (in.-kips)	ϕ	ϕP_n (kips)	ϕM_n (in.-kips)	e (in.)
1	8	6.0	275	1,213	0.70	193	849	4.4
2	10	7.5	376	1,125	0.70	263	788	3.0
3	12	9.0	473	899	0.70	331	629	1.9
4	15	11.3	616	319	0.70	431	223	0.5
5	∞	12.0	684	0	0.70	479	0	0
6	6	4.5	177	1,151	0.70	124	806	6.5
7	4	3.0	77	944	0.77	59	727	12.3
8	3	2.3	24	777	0.86	21	668	32.4
9	2	1.5	−33	559				−16.9

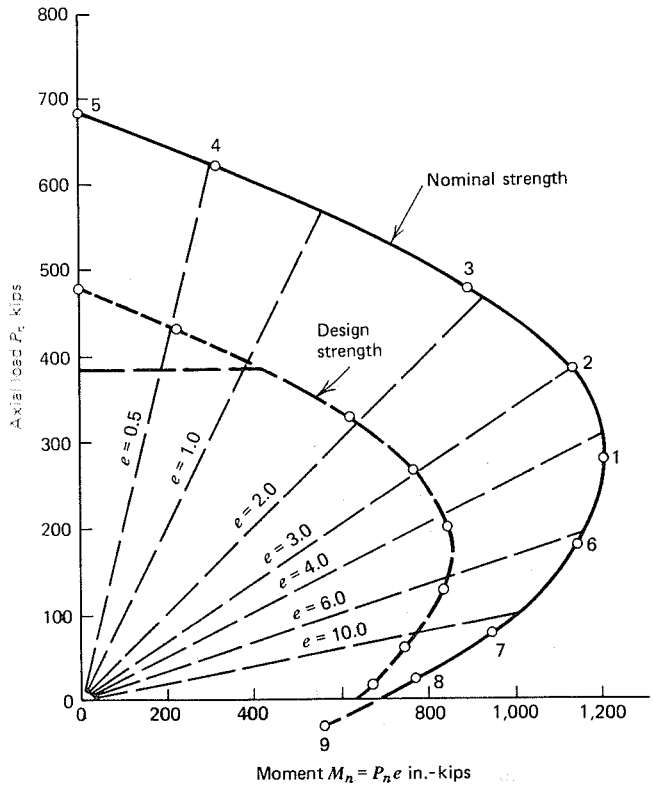

FIGURE 11.4 Interaction diagram for eccentric column example.

and T_2 on the right side is found from Eq. (11.5):

$$T_2 = 0.32 \times 29{,}000(0.0052 + 0.0008 + 0.0005)$$

$$T = 60 \text{ kips}$$

Summing vertical forces to determine P_n (Eq. 11.1):

$$P_n = 367 - 32 - 60 = 275 \text{ kips}$$

and the moment M_n is obtained using Eq. (11.2):

$$M_n = 367 \times 3 - 4 \times 32 + 4 \times 60 = 1{,}213 \text{ in-kips}$$

thus, determining point (1) on the interaction curve of Fig. 11.4. Other points are found in a similar fashion:

5. Assume $c = \infty$; $a = 12$ in. Then

$$C = 0.85 \times 6 \times 12 \times 12 = 734 \text{ kips}$$

$$T_1 = 0.32 \times 29{,}000(0.0052 - 0.0030 + 0.0005) = 25 \text{ kips}$$

$$T_2 = 25 \text{ kips}$$

$$P_n = 734 - 25 - 25 = 684 \text{ kips}$$

$$M_n = 0 - 4 \times 25 + 4 \times 25 = 0$$

6. Assume $c = 6$ in.; $a = 4.5$ in. Then

$$C = 0.85 \times 6 \times 4.5 \times 12 = 275 \text{ kips}$$

$$T_1 = 0.32 \times 29{,}000(0.0052 - 0.0020 + 0.0005) = 34 \text{ kips}$$

In this case, the total steel strain in the strand on the right side of the column is 0.0077, exceeding the yield strain shown by Fig. 2.4 for Grade 250 strand. A calculation based on the elastic modulus would be invalid, and steel stress of 200 ksi corresponding to that strain must be read directly from the graph. Then

$$T_2 = 0.32 \times 200 = 64 \text{ kips}$$

$$P_n = 275 - 34 - 64 = 177 \text{ kips}$$

$$M_n = 275 \times 3.75 - 4 \times 34 + 4 \times 64 = 1{,}151 \text{ in.-kips}$$

Similar conditions result for points (7) and (8).

9. Assume $c = 2$ in.; $a = 1.5$ in. Then

$$C = 0.85 \times 6 \times 1.5 \times 12 = 92 \text{ kips}$$

$$T_1 = 0.32 \times 29{,}000(0.0052 + 0 + 0.0005) = 53 \text{ kips}$$

$$T_2 = 0.32 \times 225 = 72 \text{ kips}$$

$$P_n = 92 - 53 - 72 = -33 \text{ kips}$$

$$M_n = 92 \times 5.25 - 4 \times 53 + 4 \times 72 = 559 \text{ in.-kips}$$

The negative sign of P_n in this case is an indication that the neutral axis location chosen is possible only if the column is subjected to a tensile load, rather than a compression load. The equivalent eccentricity, having increased to an infinite value at $P_n = 0$, has now changed sign, indicating that the tensile load must be applied on the opposite side of the column. Although mainly of academic interest, the last calculation does indicate the generality of the method, which can be applied to eccentric tensile members as well as eccentric compression members.

A total of nine points on the failure interaction line were calculated. All results are summarized in Table 11.1 and are plotted in Fig. 11.4.

Also shown in Fig. 11.4 is the design strength curve, obtained by application of the appropriate ϕ factors to P_n and M_n in accordance with Eqs. (11.6*a*) and (11.6*b*). The balanced failure load ϕP_b will be approximated by the value $0.10 \times 6 \times 144 = 86$ kips, according to ACI Code, thus, the approximate value of $P_b = 86/0.70 = 123$ kips. The value of ϕ will be increased linearly from 0.70 at $P_n = 123$ kips to 0.90 at $P_n = 0$, with the results indicated in Table 11.1 and Fig. 11.4. At higher loads, a value of $\phi = 0.70$ is applied to thrust and moment to obtain points on the design strength curve, except that a cutoff at $0.80\phi P_o = 383$ kips is applicable.

11.4 NON-PRESTRESSED REINFORCEMENT IN COLUMNS

Non-prestressed reinforcement is used in prestressed columns in the form of lateral ties or spirals and, in some cases, as supplementary longitudinal steel near the ends (Ref. 11.4).

According to the ACI Code; if compression members have an average prestress, P_e/A_g, less than 225 psi, then longitudinal bar reinforcement must be included. Requirements are the same as for ordinary reinforced concrete columns. Specifically, non-prestressed longitudinal steel must be used having a total area not less than 0.01 and not more than 0.08 times the gross area of the concrete cross section. At least four bars are required when a rectangular arrangement is selected, and at least six bars when the bar pattern is circular. If the average prestress is 225 psi or higher, these provisions do not apply.

Lateral reinforcement should always be provided, just as for reinforced concrete columns. When the main steel is arranged in a circular pattern, normally a continuous spiral winding is used, usually of plain round, underformed steel wire. If the main bars are set in a rectangular pattern, individual lateral ties are provided, spaced at a uniform interval along the column axis.

Such lateral reinforcement serves several important purposes: (1) By resisting the lateral expansion of the concrete that would normally occur because of longitudinal applied load, the transverse steel causes horizontal compression in the concrete. When superimposed on the longitudinal stress, this creates a state of triaxial compression. This not only increases the strength of the column, but improves its toughness by greatly increasing available ductility. (2) If non-prestressed compression steel is used supplementary to the longitudinal prestressing steel, these bars tend to buckle outward when loaded, as would any very slender compression element. Lateral ties or spirals are effective in preventing this type of premature failure. (3) When columns are subjected to horizontal shear forces, as from earthquake action, the lateral reinforcement serves to

increase the shear strength substantially. (4) Finally, lateral steel serves the practical function of holding the longitudinal steel in proper alignment and position as the concrete is poured.

Lateral steel is designed on the basis of empirical procedures that have been established by tests. According to ACI Code, if spiral reinforcement is used, the ratio of the volume of spiral steel reinforcement to volume of concrete core (with diameter measured out-to-out of the spiral) should not be less than

$$\rho_s = 0.45\left(\frac{A_g}{A_c} - 1\right)\frac{f_c'}{f_y} \tag{11.7}$$

where A_g is the gross concrete area, A_c is the area of the concrete core, and f_y is the specified yield strength of the spiral reinforcement (not to be taken greater than 60,000 psi). For case-in-place columns, the spiral wire should not be smaller than $\frac{3}{8}$ in. in diameter. In all cases, the pitch of the spiral (advancement in one complete turn) must be between one and three in. When lateral ties are used, they must be at least $\frac{3}{8}$ in. in diameter. Their spacing must not exceed 48 times the tie diameter, or the least dimension of the column, whichever is the smallest. Furthermore, they must be arranged such that every corner and alternate longitudinal bar, wire, or strand has lateral support provided by the corner of a tie having an included angle not greater than 135 degrees.

11.5 BEHAVIOR OF SLENDER COLUMNS

The columns considered in the preceding articles were *short columns*, of such proportions that their strength could be determined on the basis of the geometry of the cross section and the properties of the materials. In practice, many compression members are *long columns*, for which strength is reduced significantly by the effects of slenderness. Prestressed concrete columns, which use higher strength materials, are likely to have smaller cross sections than ordinary reinforced concrete columns, and the possibility of strength reduction due to slenderness should always be investigated (Refs. 11.6 to 11.8).

The idealized case of a perfectly straight, concentrically loaded, slender column was solved by Euler more than 200 years ago. If such a column is free of rotational restraint at its ends, it will fail by lateral buckling at the *critical load*

$$P_c = \frac{\pi^2 EI}{l_u^2} \tag{11.8}$$

where EI is the flexural stiffness of the member, and l_u is the unbraced length. This equation shows that the critical buckling load decreases rapidly as the length increases.

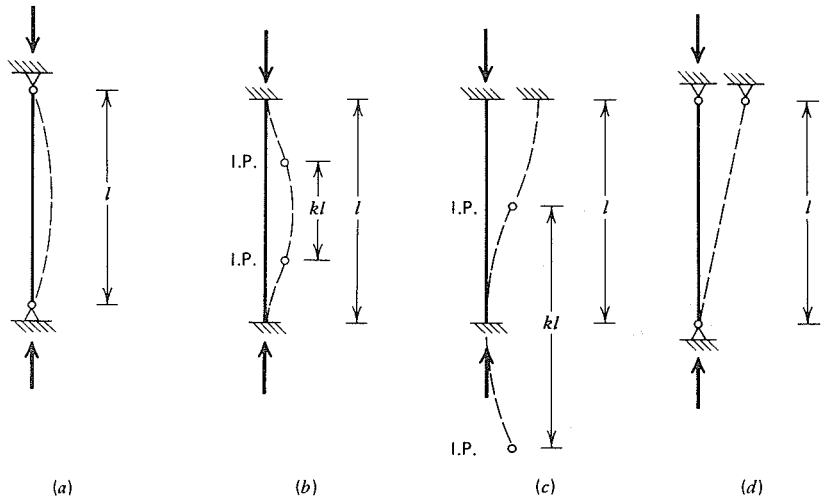

FIGURE 11.5 Buckled shapes and effective lengths of axially loaded columns. (*a*) Braced, hinged ends, $k = 1$. (*b*) Braced, fixed ends $k = 1/2$. (*c*) Unbraced, fixed ends, $k = 1$. (*d*) Unbraced, hinged ends, $k = \infty$.

The Euler equation may be generalized to apply to different conditions of end restraint through the introduction of an effective length factor k, applied to the actual length l_u such that

$$P_c = \frac{\pi^2 EI}{(kl_u)^2} \tag{11.9}$$

The value of k depends on the degree of rotational restraint that exists in a given case, and on whether or not lateral displacement of the ends of the column is prevented.

In many, if not most cases, concrete structures are braced against sidesway by walls, sufficiently strong and stiff in their own plane effectively to prevent such displacement. These walls may be provided expressly for that purpose, or they may be required otherwise, to enclose stairwells, elevator shafts, or utility ducts, for example.

For a column restrained against sway, having hinged ends as shown in Fig. 11.5*a*, the effective length kl_u is equal to the actual length l_u. When the critical load of Eq. (11.9) is reached, this column will buckle laterally, taking the shape of a half-sine wave as shown. In contrast, if the member is restrained against sway and is fixed against rotation at its ends (Fig. 11.5*b*), it will buckle into the shape of a full-sine wave, with points of inflection at the quarter points of its length. The portion of the column between these inflection points is in precisely the same

state as the hinged-end column considered first, and the buckling load of this fixed-ended column can be predicted from Eq. (11.9) with effective length factor $k = 0.5$.

The ends of columns in real structures are seldom either perfectly fixed or perfectly hinged, but are restrained by beams, which permit some limited rotation. Consequently, values of k intermediate between 1.0 and 0.5 can be expected for columns that are a part of frames braced against sway.

In some instances, concrete building frames *are* free to sway laterally, the sole resistance to horizontal displacement being provided, in such cases, by the rigid-jointed frame itself. The effective length of the columns is then much greater than before, and the critical buckling load is much less.

This is illustrated by the columns of Figs. 11.5*c* and 11.5*d*. If rotation of the column ends is prevented, but translation permitted, as in Fig. 11.5*c*, the effective length is equal to the actual length, and the effective length factor $k = 1.0$. If the ends are provided with no rotational restraint (Fig. 11.5*d*), the column would topple immediately, that is, the effective length factor is infinite. Thus, for columns in unbraced frames, the effective length factor k may be expected to vary from 1.0 to infinity.

The members considered up to this point were loaded concentrically. Actually, most columns are subjected simultaneously to compression and bending moments, the latter resulting from either eccentric application of the load or continuous frame action. The behavior of members subjected to combined loading, too, depends greatly on slenderness.

Figure 11.6*a* shows a member carrying axial load P at eccentricity e, producing a *primary moment* $M_o = Pe$, which is constant throughout the length. The member deflects laterally an amount y_o due to the moment M_o as shown by the dotted line.

But this lateral displacement causes an increase in bending moment, because of the increased eccentricity of load with respect to the deflected centerline of the column. The column deflects still further because of this increase in moment, which causes an additional moment increase in turn. The behavior is strictly nonlinear.

If the total lateral deflection of the member with respect to its original axis is y, then the final moment is

$$M = M_o + Py \tag{11.10}$$

The resulting deflected shape is shown by the dashed line of Figs. 11.6*a*, and 11.6*b*.

Slenderness may be accounted for in members subject to such combined loading by what is known as a *second-order analysis*, which includes the so-called P–Δ effect, which accounts for the moment increase resulting from lateral displacement. Deflections are calculated for the primary moments. Then the

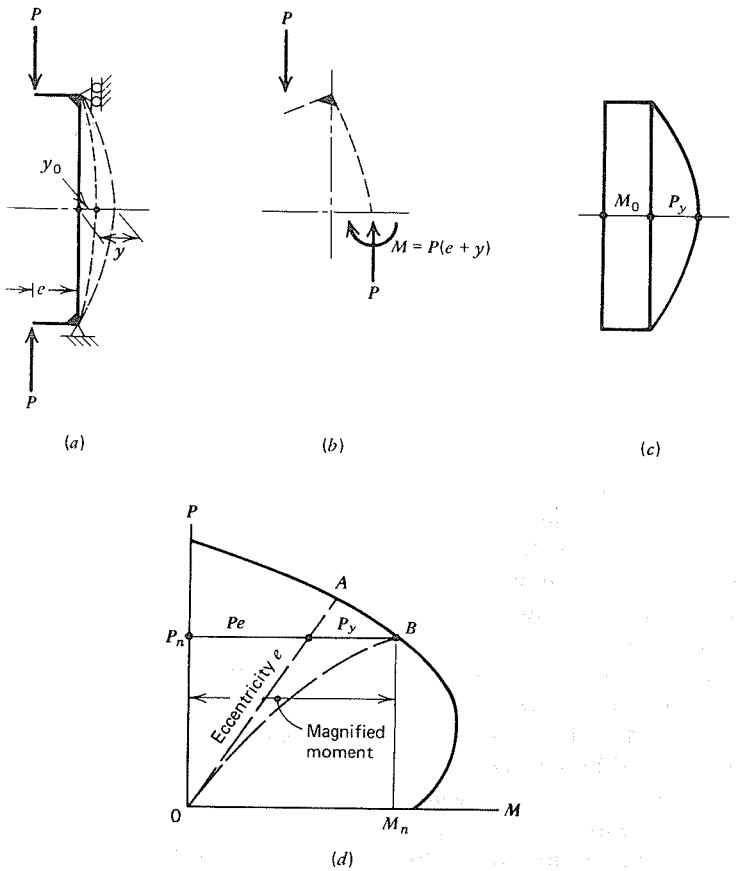

FIGURE 11.6 Behavior of slender columns. (*a*) Load and deflection curve. (*b*) Free body of half-column. (*c*) Moment diagram. (*d*) Interaction diagram for failure.

increase in moments that results from these lateral displacements is determined, and the deflections revised accordingly. The process is repeated in an iterative way until satisfactory convergence is obtained. But even with use of a computer, such an analysis is time-consuming and expensive. For ordinary design purposes, a satisfactory approximate solution is possible, based on *magnified moments*, as follows (Ref. 11.9).

The final deflection y of a slender column subjects to eccentric loading can be calculated from the deflection y_o by the following expression:

$$y = y_o \frac{1}{1 - P/P_c} \tag{11.11}$$

Then from Eqs. (11.10) and (11.11),

$$M_{max} = M_o + Py$$

$$M_{max} = M_o + Py_o \frac{1}{1 - P/P_c} \tag{11.2}$$

For design purposes, the last equation can be closely approximated by the simplified form:

$$M_{max} = M_o \frac{1}{1 - P/P_c} \tag{11.13}$$

where $1/(1 - P/P_c)$ is known as a *moment magnification factor*, accounting for the increase in primary moment M_o due to the lateral deflection of the column. Clearly, if the axial force P is much less than P_c, the maximum moment is about equal to the primary moment M_o. If P is close to P_c, the denominator approaches zero and the maximum moment approaches infinity.

The effect of moment magnification on the strength of a prestressed concrete column is illustrated by Fig. 11.6*d*, which shows a typical column strength interaction diagram. A short column loaded with eccentricity e will experience a linear increase of M with increasing P. The loading follows path OA until material failure is obtained at load and moment corresponding to point A. The strength is not diminished by slenderness.

However, if the same column is slender, significant moment magnification will occur. For given eccentricity e, as load is increased, the moment increases in a nonlinear way as indicated by Eq. (11.13) and as shown by Fig. 11.6*d*. The member fails at a load and moment corresponding to point B.

The direct addition of maximum moment caused by deflection to the full value of primary moment, implied in the preceding paragraphs, does not always result. Consider the alternative situations shown in Fig. 11.7. Figure 11.7*a* shows the load case just described, with eccentricities causing equal and and opposite end moments. This is the most unfavorable situation possible, for the maximum moment due to lateral deflection superimposes directly on the maximum (in this case constant) moment due to eccentricity. If the end moments act in the opposite sense but are unequal (Fig. 11.7*b*), then the maximum primary moment occurs at one end of the member, and the maximum moment due to deflection occurs near midlength. This less severe loading case may produce a magnified moment very little greater than the primary moment, as seen. In the third case (Fig. 11.7*c*), the end moments act in the *same* direction, producing a deflected shape having reverse curvature. In this instance, the magnified moments may or may not be greater than the primary moments, depending on the relative

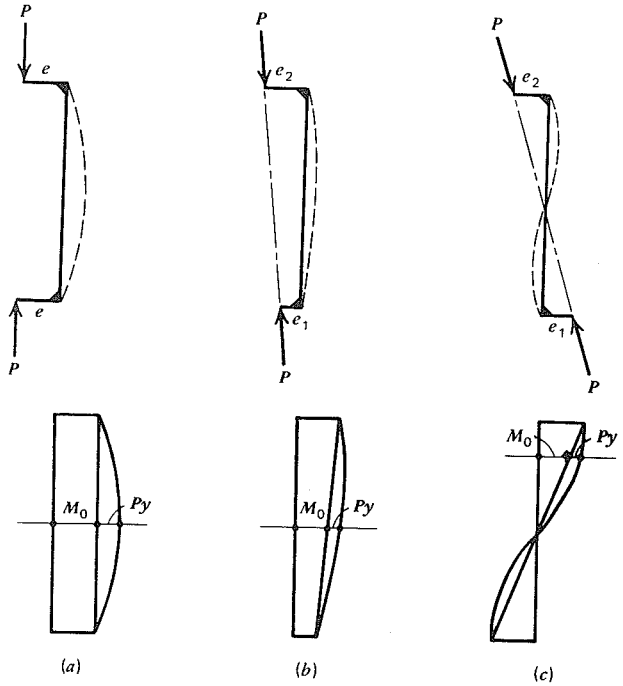

FIGURE 11.7 Superposition of primary and deflection moments for slender columns. (*a*) End moments equal and opposite direction. (*b*) End moments unequal and opposite direction. (*c*) End moments same direction.

magnitudes of the primary and deflection moments. The column may, or may not, be weakened by the effect of slenderness.

In practical design methods, such as described in Section 11.6, the influence of relative magnitude and direction of end moments is accounted for by using an *equivalent uniform moment*, based on the larger of the two end moments, modified to account for the possible alternate loading cases described.

Certain assumptions must be made relative to the effective stiffness of the column. The use of Eq. (11.13) to determine the magnified moment is predicated on calculation of the critical buckling load P_c from Eq. (11.9). The calculation of P_c depends, in turn, on the flexural stiffness EI of the column. Prestressed concrete columns are nonhomogeneous, consisting of steel, which is substantially elastic, and concrete, which is not. The concrete is subject to creep, and if the ratio of moment to axial load is high, it is subject to cracking as well. All these factors affect the effective stiffness. Although various "exact" methods have been proposed to calculate flexural rigidity taking account of these effects, the calculations are no more accurate than the assumptions on which they are based. It is

usually satisfactory to account for such influences in an approximate way, in the calculation of effective EI, by the methods described in Section 11.6.

11.6 PRACTICAL CONSIDERATION OF SLENDERNESS EFFECTS

The ACI Code does not include provisions relating to the design of slender prestressed concrete columns. However, it has been shown that Code methods intended for *reinforced* concrete columns can be applied to prestressed concrete columns with reasonable accuracy (Ref. 11.7). These provisions are based on the concepts and approaches presented in Section 11.5.

A. BRACED FRAMES

For a moment-resisting frame that is effectively braced against sidesway by shear walls or diagonally braced frames, the ACI Code equation for magnified moment, acting with the factored axial load P_u, can be written as

$$M_c = \delta M_2 \tag{11.14}$$

where the moment-magnification factor

$$\delta = \frac{C_m}{1 - P_u/(\phi P_c)} \geq 1 \tag{11.15}$$

The critical load P_c is given as

$$P_c = \frac{\pi^2 EI}{(kl_u)^2} \tag{11.16}$$

where l_u is defined as the unsupported length of the compression member.

In Eq. (11.15), the value of C_m is

$$C_m = 0.6 + 0.4\frac{M_1}{M_2} \geq 0.4 \tag{11.17}$$

for members braced against sidesway and without transverse loads between supports. Here M_2 is the larger of the two end moments, and M_1/M_2 is positive when the end moments produce single curvature and negative when they produce double curvature. The variation of C_m with M_1/M_2 is shown in Fig. 11.8. In Eq. (11.15), when the calculated value of δ is smaller than 1, this indicates that the larger of the two end moments M_2 is the largest moment in the column.

In this manner the ACI Code provides for the capacity-reducing effects of slenderness in braced frames by the moment-magnification factor δ. It is well

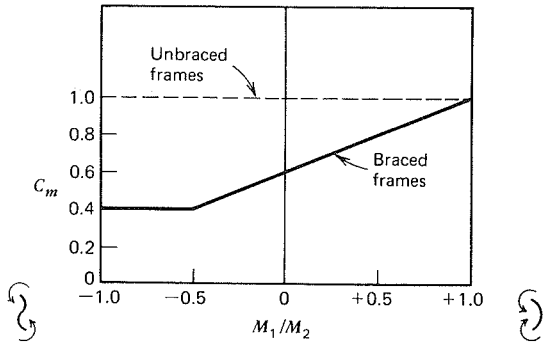

FIGURE 11.8 Values of C_m for slender columns in braced and unbraced frames.

known, of course, that for columns with no or very small applied moments (i.e., axially or nearly axially loaded columns), increasing slenderness also reduces the column strength. For this situation, the ACI Code provides the following:

> If computations show that there is no moment at both ends of a braced compression member, or that computed end eccentricities are less than $(0.6 + 0.03h)$ in., M_2 [in Eq. (11.14)] shall be based on a minimum eccentricity of $(0.6 + 0.03h)$ in., about each principal axis separately. [Here h is the thickness of the section in the direction perpendicular to the pertinent principal axis.] The ratio M_1/M_2 for calculating C_m [see Eq. (11.17)] shall be determined by either of the following:
>
> (a) When computed eccentricities are present, but less than $(0.6 + 0.03h)$ in., computed end moments may be used to evaluate M_1/M_2 in calculating C_m.
>
> (b) If computations show that there is essentially no moment at both ends of the member, the ratio M_1/M_2 shall be taken equal to one.

It is seen that for the case where design calculations show a column to be axially or nearly axially loaded, the ACI Code provides a minimum eccentricity that depends on the cross-sectional dimensions for calculating the moment M_2 and the moment-magnification factor δ in Eqs. (11.14) and (11.15). This provides for the effects of slenderness in axially or nearly axially loaded columns.

In homogeneous elastic members, such as steel columns, the rigidity EI is easily obtained from Young's modulus and the usual moment of inertia. Reinforced concrete columns, however, are nonhomogeneous, since they consist of both steel and concrete. Although steel is substantially elastic, concrete is not, and is, in addition, subject to creep and to cracking if tension occurs on the convex side of the column. All these factors affect the effective rigidity EI of a reinforced concrete member. If it possible by computer methods to calculate

fairly realistic effective rigidities that take these factors into account. Even these calculations are no more accurate than the assumptions on which they are based. On the basis of elaborate studies, both analytical and experimental, the ACI Code permits EI to be determined by either

$$EI = \frac{E_c I_g/5 + E_s I_s}{1 + \beta_d} \tag{11.18}$$

or by the simpler expression

$$EI = \frac{E_c I_g/2.5}{1 + \beta_d} \tag{11.19}$$

where E_c = modulus of elasticity of concrete, psi
I_g = moment of inertia of gross section of column, in.^{4}
E_s = modulus of elasticity of steel, psi
I_s = moment of inertia of reinforcement about centroidal axis of member cross section, in.^{4}
β_d = ratio of maximum factored dead load moment to maximum factored total load moment, always positive

The factor β_d accounts approximately for the effect of creep. That is, the larger the moments caused by sustained dead loads, the larger are the creep deformations and corresponding curvatures. Consequently, the larger the sustained loads relative to the temporary loads, the smaller the effective rigidity, as is correctly reflected in Eqs. (11.18) and (11.19).

An accurate determination of the effective length factor k is essential in connection with Eqs. (11.14) and (11.15). In Section 11.5, it was shown that for

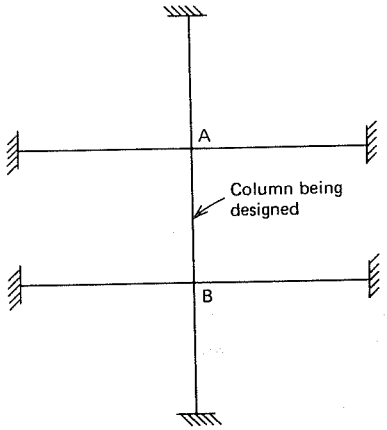

FIGURE 11.9 Section of rigid frame including column to be designed.

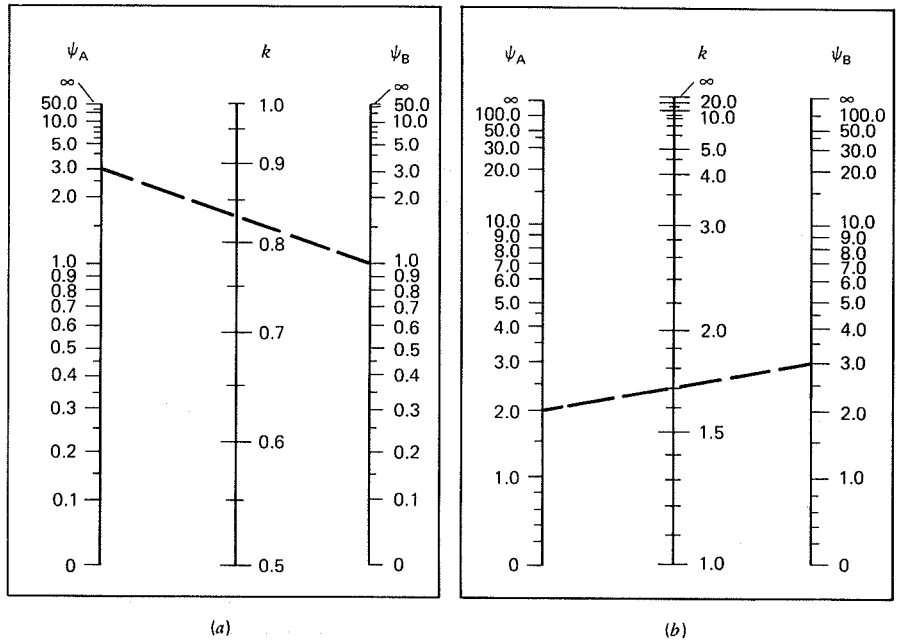

FIGURE 11.10 Alignment charts for effective length factor k. (*a*) Braced frames. (*b*) Unbraced frames.

frames braced against sidesway, k varies from $\frac{1}{2}$ to 1, whereas for laterally unbraced frames, it varies from 1 to ∞, depending on the degree of rotational restraint at both ends. This was illustrated in Fig. 11.5. For rigid frames, it is seen that this degree of rotational restraint depends on whether the rigidities of the beams framing into the column at top and bottom are large or small compared with the rigidity of the column itself. An approximate, but generally satisfactory way of determining k is by *alignment charts* based on isolating the given column plus all members framing into it at top and bottom, as shown in Fig. 11.9. The degree of end restraint at each end is $\psi = \Sigma(EI/l \text{ of columns})/\Sigma(EI/l \text{ of floor members})$. Only floor members that are in a plane at either end of the column are included. The value of k can then be read directly from the charts of Fig. 11.10, as illustrated by the dashed lines.

It is seen that k must be known before a column in a frame can be dimensioned. Yet k depends on the rigidity EI/l of the members to be dimensioned, as well as on that of the abutting members. Thus, the dimensioning process necessarily involves iteration; that is, one assumes member sizes, calculates rigidities and corresponding k values, and then calculates more accurate member sizes on the basis of these k values until assumed and final member sizes coincide or are satisfactorily close.

B. UNBRACED FRAMES

Where there is more than one column in a given frame or story of a building, sidesway can occur only by simultaneous lateral motion of all columns of the particular story. For bracing to be effective, it must be sufficiently rigid to brace all columns of that story when they are fully loaded. Bracing generally consists of shear walls, utility cores, or other wall-like components. Bracing that holds the upper ends of all columns fully immovable relative to the lower ends is, of course, impossible to achieve. Therefore, the function of adequate lateral bracing is to limit lateral deflections of one end relative to the other to insignificant and inconsequential amounts. The ACI Code Commentary suggests that "... a compression member braced against sidesway is a member in a story in which the bracing members [shear walls, etc.] have a total stiffness to resist lateral movement of that story, which is at least six times the sum of the lateral stiffness of all columns in that story." The ACI Code Commentary also presents a more accurate, although more complex criterion; it includes a number of other important matters on slender-column design, too elaborate to be included here.

Because sidesway can occur only for all columns of a story simultaneously rather than for any individual column, the ACI Code specifies that in frames not braced against sidesway, the value of δ that pertains to the loads causing sway should be computed for the entire story, assuming all columns to be fully loaded. Correspondingly, for lateral loads acting on unbraced frames, P_u and P_c are to be taken as ΣP_u and ΣP_c for all columns in the story in Eq. (11.15). Furthermore, for lateral loads, the equivalent moment correction factor C_m given by Eq. (11.17) does not apply, because the maximum sway moment will be located at the ends of the column, not near the midheight. Thus, for unbraced frames, Eq. (11.14) is replaced by:

$$M_c = \delta_b M_{2b} + \delta_s M_{2s} \tag{11.20}$$

where M_{2b} = value of larger factored end moment on compression member due to loads that result in no appreciable sidesway (i.e., gravity loads)

M_{2s} = value of larger factored end moment on compression member due to loads that result in appreciable sidesway (i.e., lateral loads)

both calculated by conventional elastic frame analysis. The moment magnification factors are

$$\delta_b = \frac{C_m}{1 - P_u/(\phi P_c)} \geq 1 \tag{11.21a}$$

$$\delta_s = \frac{1}{1 - \Sigma P_u/(\phi \Sigma P_c)} \geq 1 \tag{11.21b}$$

In Eq. (11.21*a*), the value of $C_m = 1.0$.

The moment-magnification method just discussed is both complicated and approximate, but until recently has been the only rational yet practical method of designing slender frame columns. The ACI Code now also permits a more accurate but more elaborate second-order analysis, often known as the P–Δ method. It is a method of frame analysis in which the effects of axial loads and of the sway deflections Δ on the bending moments are not estimated by approximate formulas but are explicitly calculated.

C. CRITERIA FOR NEGLECT OF SLENDERNESS

The procedure of designing slender columns is inevitably fairly lengthy, particularly since it generally involves a trial-and-error procedure. At the same time, studies of existing structures have shown that many actual building columns are sufficiently stocky so that slenderness effects reduce their capacities only by a few percent. To permit the designer to dispense with these procedures, the ACI Code provides limits of slenderness below which the effects of slenderness are insignificant and may be neglected.

These limits are adjusted to result in a maximum unaccounted reduction of column capacity of no more than five percent. The corresponding ACI Code provision may be stated as follows:

> For compression members braced against sidesway, the effects of slenderness may be neglected when kl_u/r is less than $34 - 12M_1/M_2$, and for compression members not braced against sidesway when kl_u/r is less than 22, l_u being the unsupported, free length of the column.

The radius of gyration r for rectangular columns may be taken as $0.30h$, where h is the overall cross-sectional dimension in the direction in which stability is being considered. For circular members, it may be taken as 0.25 times the diameter. For other shapes, r may be computed for the gross concrete section.

Although the equations just presented were developed from study of reinforced concrete columns, their use for prestressed concrete columns may be considered acceptable until further data and improved methods become available that pertain specifically to prestressed concrete. Rational methods have been proposed (Ref. 11.8), but it appears that further simplification is necessary before these could be considered for practical design. Certain design aids are available, such as those found in Ref. 11.11, which also contains recommendations pertaining to carrying out a "second-order analysis" in which the influence of column displacements on moments is considered directly, rather than through a moment-magnification approach.

11.7 BEHAVIOR OF TENSION MEMBERS

Concrete does not at first seem a natural choice for constructing a member subject dominantly to tensile loads. A *reinforced concrete* tensile member will

crack at relatively low loading, after which the reinforcing bars must carry all of the tension. The concrete, subsequent to cracking, serves mainly to provide some measure of corrosion protection for the steel. If cracking is extensive, even this function is not well served.

By prestressing the concrete, however, a tension member may be constructed that is superior in all respects to a reinforced concrete unit and, in several important ways, is superior to a comparable all-steel member.

It is evident that by applying an appropriate amount of compressive prestress, a tension member may be designed that will be free of concrete cracking under normal service conditions. This is of particular importance for tie members, which may be buried underground between arch foundations, for example.

Of greater significance, in many cases, is the fact that a prestressed concrete tension member will display much less elongation when loaded than will a comparable all-steel member designed for the same load. Prior to concrete cracking, the strain per unit load will be much less, because of the much larger effective cross section. After cracking, the steel tendon must carry all of the tension. However, the tendon has been "prestretched" during the prestressing of the concrete, and the additional elongation as the concrete is relieved of its compressive stress by the external loading is likely to be very small.

This point is illustrated by Fig. 11.11. The bare steel strand of Fig. 11.11*a*, if stressed by the specified service load Q, as shown in Fig. 11.11*b*, would exhibit an increase in length of the amount Δl directly proportional to the steel stress and inversely proportional to the modulus of elasticity. If the otherwise efficient, economical, high tensile strength wire or strand were to be used and if length l is substantial, an unacceptably large elongation could be expected.

However, if the wire were "prestretched" by a force P equal to Q, and if concrete were poured between suitable end-bearing plates, and furthermore, if the force P were then released after the concrete had hardened, then shortening of the strand would be largely prevented by the concrete, as seen in Fig. 11.11*c*. The length of the prestressed concrete member, with no external load applied, would be slightly less than the length $(l + \Delta l)$, because of elastic shortening of the concrete. (This would also reduce the prestress force to a value somewhat less than P).

If the external load Q is now applied, as in Fig. 11.11*d*, the member would elongate only by the amount $\Delta' l$, much less than the elongation Δl of Fig. 11.11*b*, because in this case elongation is governed by the transformed cross section of concrete rather than the area of the strand alone. In the service load stage, the concrete stress would be diminished to zero, and the force in the steel would be equal to Q.

The simplified example neglects factors such as creep and shrinkage of the concrete and relaxation of the steel, but serves to illustrate the deformation control possible for prestressed tension members.

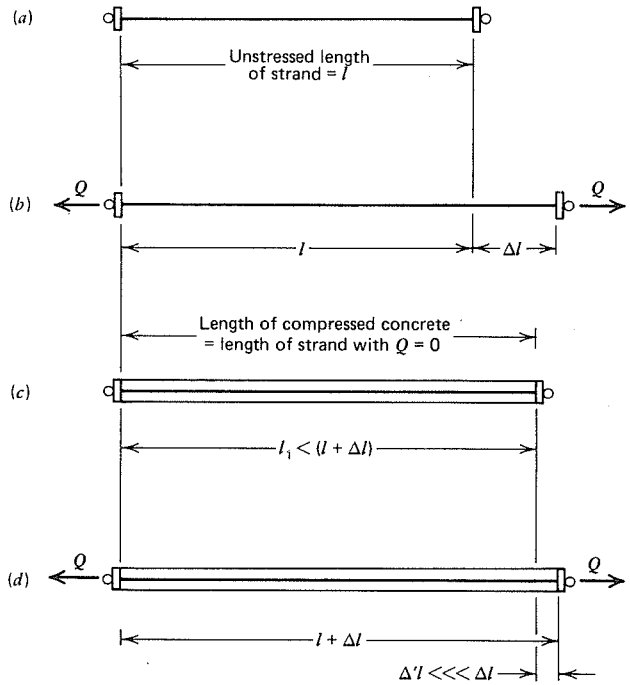

FIGURE 11.11 Use of prestressed concrete to limit tensile deformation.

A question that may be raised relative to prestressing tension members is whether or not the member, which typically will be rather long and slender, is vulnerable to buckling because of the prestress compression load. It can be shown analytically, and it has been confirmed experimentally that, in the case of post-tensioning, if the tendon is in close contact with the inside of the duct, then no tendency to buckle will result. Any slight lateral displacement of the concrete is accompanied by a corresponding displacement of the steel that provides the force producing the compression and, consequently, no bending moment is obtained. This is in contrast with the condition in the typical Euler column analysis, in which a slight lateral displacement of the member axis introduces bending moment as a result of the eccentricity of loading that accompanies that displacement.

The same argument obviously applies to pretensioned members as well; the prestressing forces cause no tendency to buckle. For post-tensioned elements in which the tendon is contained in an unusually large duct or a hollow box section, however, a buckling tendency does exist and calculations should always be made to insure that no problems will arise.

As long as both materials are stressed only in the elastic range, stresses and deformations may be found based on the net or transformed cross section,

whichever is applicable. The following notation will be used:

P_i = initial prestress force, after anchorage but before time-dependent losses
P_e = effective prestress force, after all losses
A_g = gross area of concrete cross section
A_p = area of steel tendon
A_c = net area of concrete cross section
A_t = transformed area of concrete cross section
n = modular ratio = E_p/E_c

The stress in the concrete immediately after transfer and anchorage is

$$f_{ci} = -\frac{P_i}{A_c} \tag{11.22}$$

After time-dependent losses have occurred, this stress is reduced to

$$f_{ce} = -\frac{P_e}{A_c} \tag{11.23}$$

and the stress in the steel is

$$f_{pe} = \frac{P_e}{A_p} \tag{11.24}$$

Because tensile loads applied to the member after this time cause equal elongation and tensile strain in both the concrete and steel, stress changes resulting from subsequent loading, prior to cracking, may be found using the transformed section approach.[2] If we replace the actual steel area A_p with its equivalent tensile concrete area, the transformed section is

$$A_t = A_g + (n-1)A_p \tag{11.25}$$

The stress changes in the concrete and steel, as an external tension Q is applied (up to the cracking load), are, respectively

$$\Delta f_c = \frac{Q}{A_t} \tag{11.26}$$

$$\Delta f_p = \frac{nQ}{A_t} \tag{11.27}$$

[2]This statement applies to both bonded and unbonded tension members. In practice, most tension members are bonded, being either pretensioned or grouted after post-tensioning

When superimposed on the stresses already present, these produce

$$f_c = -\frac{P_e}{A_c} + \frac{Q}{A_t} \tag{11.28}$$

$$f_p = f_{pe} + \frac{nQ}{A_t} \tag{11.29}$$

The cracking load Q_{cr} may be predicted using Eq. (11.28) by setting the concrete stress equal to the direct tensile strength of the material. This is generally in the range from $3\sqrt{f_c'}$ to $5\sqrt{f_c'}$ for normal density concrete and from $2\sqrt{f_c'}$ to $3.5\sqrt{f_c'}$ for lightweight concrete.

After cracking, the concrete is ineffective, and the entire tension must be resisted by the steel tendon. Denoting f_{pu} the tensile strength of the steel, the nominal strength of the tension member is

$$Q_n = A_p f_{pu} \tag{11.30a}$$

For design purposes this is reduced by the factor $\phi = 0.90$, which gives the design strength

$$\phi Q_n = \phi A_p f_{pu} \tag{11.30b}$$

Deformations will be found with respect to the original, unstressed length of the concrete. If we assume for present purposes that the member will be post-tensioned and grouted, the reduction in length as the concrete is initially stressed to P_i is

$$\Delta_i = -\frac{P_i l}{A_c E_c} \tag{11.31}$$

Creep deformation takes place while the prestress force reduces gradually from P_i to P_e. For most practical purposes, it will be sufficient to use an average value of force $(P_i + P_e)/2$ to compute total displacement after an extended time period:

$$\Delta_e = -\frac{l}{A_c E_c}\left[P_e + \left(\frac{P_i + P_e}{2}\right)C_u\right] \tag{11.32}$$

where C_u is the creep coefficient. Values of C_u and suitable modifying factors will be found in Chapter 2. If greater accuracy is required, an improved estimate of long-term deformation may be had using a time-step incremental approach, similar to that described in Chapter 9, in which the force causing creep during any time step is that computed, after losses, at the end of the preceding time step.

Assuming that the member has been designed to avoid cracking at service load, then the change in length at service load, with respect to the prestressed but unloaded length of the concrete member, is

$$\Delta_s = \frac{Ql}{A_t E_c} \tag{11.33}$$

11.8 EXAMPLE: BEHAVIOR OF PRESTRESSED CONCRETE TENSION ELEMENT

A concrete tension member 100-ft long has a 10 in. square cross section. It is post-tensioned with a force $P_i = 103$ kips using a single 12-wire tendon of Grade 250 steel, with total steel area $A_p = 0.589$ in.^{2} The wires are contained in a 1.5-in. diameter conduit, and are grouted after post-tensioning. Separate calculations indicate that after losses the prestress force will be $P_e = 88$ kips. Using values of $C_u = 2.0$, $E_p = 29 \times 10^3$ ksi, $E_c = 3.64 \times 10^3$ ksi, $n = 8$, and $f_t' = 0.475$ ksi find

1. The maximum tensile force Q that can be resisted without causing tension in the concrete.
2. The cracking load.
3. The failure load.
4. The safety factor against cracking and failure, if service load is defined to be the zero-tension load of part (1).
5. The elongation at P_i, P_e, and full service load

($l = 30.5$ m, $b = h = 254$ mm, $P_i = 458$ kN, $P_e = 391$ kN, $A_p = 380$ mm^2, conduit 38 mm diameter, $E_p = 200$ kN/mm^2, $E_c = 25.1$ kN/mm^2, $f_t' = 3.28$ MPa.)

Elastic stress calculations will require use of the transformed section. In the present case

$$A_g = 10 \times 10 = 100 \text{ in.}^2$$

$$A_c = 100 - \pi \times \frac{1.5^2}{4} = 98 \text{ in.}^2$$

$$A_t = A_g + (n-1)A_p$$

$$= 100 + 7 \times 0.589 = 104 \text{ in.}^2$$

The zero-tension load, defined here as the service load, can be found setting f_c in Eq. (11.28) equal to zero and solving for Q:

$$Q_o = \frac{A_t}{A_c} \times P_e$$

$$= \frac{104}{98} \times 88 = 93 \text{ kips (414 kN)}$$

Note that Q_o required to produce zero concrete tension is larger than the effective prestress force P_e. The reason for this is that the force P_e was applied to the net section of concrete, and the force Q_o required to return the concrete to the zero stress state is applied to the transformed section.

If we assume elastic behavior, the cracking load is also found using Eq. (11.28), in this case, setting the concrete stress equal to 475 psi. Thus

$$Q_{cr} = \left(f_c + \frac{P_e}{A_c}\right) A_t$$

$$= \left(0.475 + \frac{88}{98}\right) 104$$

$$= 142 \text{ kips (632 kN)}$$

But, assuming that the stress–strain curve of Fig. 2.4 for Grade 250 steel is applicable, the resulting steel stress of $142/0.589 = 240$ ksi is somewhat above the yield stress of 215 ksi. In all probability, cracking of the concrete would initiate soon after yielding of the steel and, therefore, the cracking tension will be taken equal to

$$Q_{cr} = 215 \times 0.589 = 127 \text{ kips (565 kN)}$$

The design strength is easily found using Eq. (11.30*b*).

$$\phi Q_n = 0.90 \times 0.589 \times 250$$

$$= 132 \text{ kips (587 kN)}$$

On the basis of these calculations, the safety factors against cracking and failure, with respect to the zero-tension load, are, respectively

$$F_{cr} = \frac{127}{93} = 1.37$$

$$F_u = \frac{132}{93} = 1.42$$

The relatively small spread between cracking and failure is typical of prestressed tension members, and illustrates well the dangers of basing designs on permissible tensile stress in the concrete. This point will be further discussed in the following section.

Deformations will next be calculated. Upon initial post-tensioning the concrete shortening is found from Eq. (11.31):

$$\Delta_i = -\frac{103 \times 1{,}200}{98 \times 3.64 \times 10^3} = -0.346 \text{ in. } (-9 \text{ mm})$$

After all losses have occurred, the total displacement with respect to the original length is found from Eq. (11.32):

$$\Delta_e = -\frac{1{,}200}{98 \times 3.64 \times 10^3}\left[88 + \left(\frac{103 + 88}{2}\right)2\right]$$

$$= -0.939 \text{ in. (24 mm)}$$

When the full service load acts, the deformation with respect to the prestressed but unloaded length is found from Eq. (11.33):

$$\Delta_s = \frac{93 \times 1{,}200}{104 \times 3.64 \times 10^3} = 0.294 \text{ in. (7 mm)}$$

It is of great relevance to compare this deformation with that that would be obtained if the bare steel tendon had been used to carry the same load, without prestressing. In such a case, the deformation at 93 kips would have been

$$\Delta_s = \frac{Ql}{A_p E_p} = \frac{93 \times 1{,}200}{0.589 \times 29 \times 10^3} = 6.53 \text{ in. (166 mm)}$$

This is 22 *times* the length increase associated with the prestressed concrete tie member.

11.9 DESIGN OF TENSION MEMBERS

The preceding example illustrated that a tension member designed on the basis of an allowable concrete stress may show a dangerously low factor of safety against failure. This suggests that the most direct route to the final design of such a structural component may well start with the consideration of strength, rather than stress limitations.

In most such cases, the design considerations, in order of importance, are as follows:

a. To provide a member having the strength adequate to resist a specified degree of overloading.
b. To control the elongation of the member at full service load, with reference to its unloaded length.
c. To provide crack control at service load, usually specifying zero concrete tension at this stage.

Accordingly, a suggested design procedure for tension members is as follows:

a. Select the steel area on the basis of the required strength, disregarding the presence of concrete, which will be cracked at ultimate load. Thus

$$Q_u = F_1 Q_d + F_2 Q_l$$

where Q_d and Q_l are the tensile forces corresponding to dead loads and service live loads, respectively, and F_1 and F_2 are the required load factors (e.g., 1.4 and 1.7, according to ACI Code). Then from Eq. (11.30*a*), $Q_n = A_p f_{pu} = Q_u/\phi$, and the required steel area is

$$A_p = \frac{Q_u}{\phi f_{pu}} \tag{11.34}$$

b. Next a maximum elongation Δ_s at full service load $Q_d + Q_l$ is established, based, for example, on maximum acceptable moments in a rigid frame if support displacement were to occur. Based on Eq. (11.33)

$$A_t = \frac{(Q_d + Q_l)l}{\Delta_s E_c} \tag{11.35}$$

giving the required transformed section area, from which

$$A_g = A_t - (n-1)A_p$$

and

$$A_c = A_g - A_{duct}$$

c. The amount of prestress is finally determined to provide the desired crack control. For the common case when zero tension is specified at service load, from Eq. (11.28).

$$P_e = \frac{A_c}{A_t}(Q_d + Q_l) \tag{11.36}$$

A design that is carried out in this order will be satisfactory for all specified conditions and will be completed without unnecessary repetition of effort.

11.10 EXAMPLE: DESIGN OF RIGID-FRAME TIE MEMBER

An athletic field house roof is supported by concrete rigid frames of 120-ft span, as shown in Fig. 11.12*a*. When subject to dead load plus full service live load, the frames will impose an outward thrust at each footing of $Q_d = 50$ kips and $Q_l = 85$ kips. A maximum outward displacement of 0.333 in. is acceptable under that loading. Using load and capacity reduction factors in accordance with ACI Code, design an appropriate prestressed tie member to connect the frame footings. The following data are given: $E_p = 27 \times 10^3$ ksi, $E_c = 3.64 \times 10^3$ ksi, $n = 8$, Grade 250 steel. ($l = 36.6$ m, $Q_d = 222$ kN, $Q_1 = 378$ kN, $d = 8$ mm, $E_p = 186$ kN/mm^2, and $E_c = 25.1$ kN/mm^2.)

The required area of steel is found using Eq. (11.34):

$$A_p = \frac{1.4 \times 50 + 1.7 \times 85}{0.90 \times 250} = 0.96 \text{ in.}^2 \text{ (619 mm}^2\text{)}$$

A single multistrand tendon consisting of twelve $\frac{3}{8}$-in. diameter strands is selected, providing a total steel area just equal to 0.96 in.^{2} The strands are enclosed in a 2.5-in. diameter duct.

From Eq. (11.35) the transformed area necessary to limit the elongation to the desired value is

$$A_t = \frac{(50 + 85) \times 120 \times 12}{0.333 \times 3.64 \times 10^3} = 160 \text{ in.}^2 \text{ (103} \times 10^3 \text{ mm}^2\text{)}$$

Thus,

$$A_g = 160 - 7 \times 0.96 = 153 \text{ in.}^2 \text{ (99} \times 10^3 \text{ mm}^2\text{)}$$

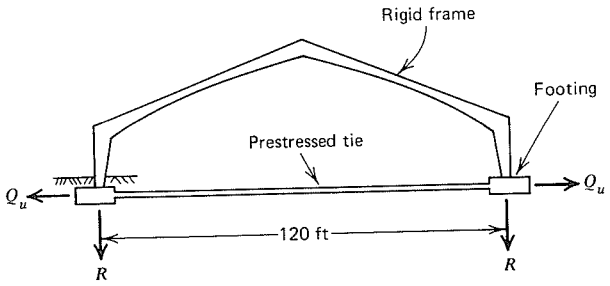

(a)

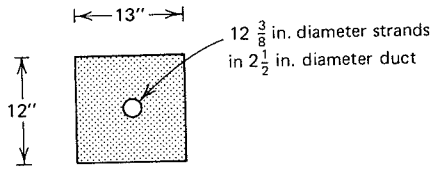

(b)

FIGURE 11.12 Prestressed tension tie for rigid frame, (*a*) Transverse section through building. (*b*) Cross section of footing tie.

A 12 × 13 in. gross cross section will be specified, as shown in Fig. 11.12*b*, providing $A_g = 156$ in.^{2} and $A_t = 163$ in.^{2} With a 2.5-in. diameter duct, the net concrete area is

$$A_c = 156 - \frac{\pi}{4}(2.5)^2 = 151 \text{ in.}^2 \ (97 \times 10^3 \text{ mm}^2)$$

From Eq. (11.36) the prestress force necessary to insure zero concrete tension at full service load is

$$P_e = \frac{151}{163}(50 + 85) = 125 \text{ kips (556 kN)}$$

Losses will be estimated based on $\varepsilon_{sh} = 800 \times 10^{-6}$, $C_u = 2.35$, and relaxation of 3.5 percent. The change in length due to creep of the concrete is based on a constant force assumed 15 percent larger than P_e:

$$\Delta_{cr} = \frac{1.15 P_e l C_u}{A_c E_c}$$

$$= \frac{1.15 \times 125 \times 120 \times 12 \times 2.35}{151 \times 3.64 \times 10^3}$$

$$= 0.88 \text{ in. (22 mm)}$$

and the length change due to shrinkage is

$$\Delta_{sh} = \varepsilon_{sh} l$$

$$= 800 \times 10^{-6} \times 120 \times 12$$

$$= 1.15 \text{ in. (29 mm)}$$

Accordingly, the loss in tension from these two causes is

$$\Delta P = \frac{(\Delta_{cr} + \Delta_{sh})}{l} E_p A_p$$

$$= \frac{2.03}{120 \times 12} \times 27 \times 10^3 \times 0.96$$

$$= 37 \text{ kips (165 kN)}$$

Allowing also for relaxation of 3.5 percent:

$$P_i = \frac{P_e - \Delta P}{1 - 0.035}$$

$$= \frac{125 + 37}{0.965} = 168 \text{ kips (747 kN)}$$

As a check on the force used for the creep calculations:

$$\frac{P_i + P_e}{2} = \frac{125 + 168}{2} = 147 \text{ kips (654 kN)}$$

very nearly the same as the value used of 1.15 × 125 = 144 kips. No revision is required. The final design is shown in Fig. 11.12.

REFERENCES

11.1 Zia, P. and Moreadith, F. L., "Ultimate Load Capacity of Prestressed Concrete Columns," *J. ACI*, Vol. 63, No. 7, July 1966, pp. 767–788.

11.2 Zia, P. and Guillermo, E. C., "Combined Bending and Axial Load in Prestressed Concrete Columns," *J. PCI*, Vol. 12, No. 3, June 1967, pp. 52–59.

11.3 Wilhelm, W. J. and Zia, P., "Effects of Creep and Shrinkage on Prestressed Concrete Columns," *J. Struct. Div. ASCE*, Vol. 96, No. ST10, October 1970, pp. 2103–2123.

11.4 *PCI Design Handbook*, 3rd ed., Prestressed Concrete Institute, Chicago, 1985.

11.5 Salmons, J. R. and McLaughlin, D. G., "Design Charts for Proportioning Rectangular Prestressed Concrete Columns," *J. PCI*, Vol. 27, No. 1, January–February 1982, pp. 120–143.

11.6 Nathan, N. D., "Slenderness of Prestressed Concrete Beam-Columns," *J. PCI*, Vol. 17, No. 6, November–December, 1972, pp. 45–57.

11.7 Nathan, N. D., "Applicability of ACI Slenderness Computations to Prestressed Concrete Sections," *J. PCI*, Vol. 20, No. 3, May–June 1975, pp. 68–85.

11.8 Nathan, N. D., "Rational Analysis and Design of Prestressed Concrete Beam Columns and Wall Panels," *J. PCI*, Vol. 30, No. 3, May–June 1985, pp. 82–133.

11.9 Nilson, A. H. and Winter, G., *Design of Concrete Structures*, 10th edition, McGraw-Hill, New York, 1986.

11.10 "Recommended Practice for the Design of Prestressed Columns and Walls," unpublished report of PCI Committee on Prestressed Columns.

PROBLEMS

11.1 The precast concrete column shown in Fig. P11.1 is pretensioned with eight 3/8-in. diameter Grade 250 strands tensioned to a stress that, after losses, reduces to f_{pe} = 150,000 psi. The steel has stress–strain characteristics as shown in Fig. 2.4. The concrete used has strength f'_c = 5,500 psi, and ultimate strain capacity ε_{cu} = 0.0035. At effective prestress, the concrete strain is 0.0007. Plot a failure interaction diagram for this member relating P_n and M_n with bending taking place about the strong axis as indicated in the figure. Calculate no fewer than ten well-spaced points along the curve. Show the "balanced failure" point on your diagram. Show also the curve of design strength, obtained by application of ACI strength reduction factors.

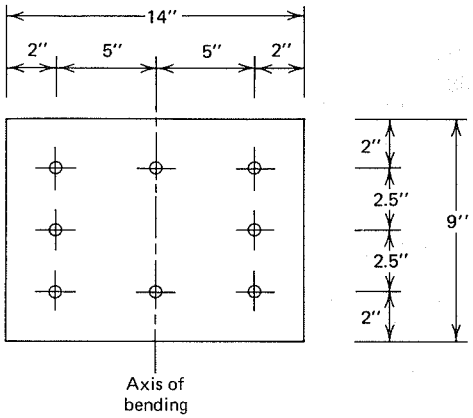

FIGURE P11.1

11.2 An alternative design is considered for the column of Problem 11.1, identical in all respects except that the prestress in the steel is reduced to f_{pe} = 75,000 psi. The corresponding strain in the concrete is 0.00035 Construct the interaction curve for this alternative design and compare with previous results.

TWELVE

PRECAST CONSTRUCTION

12.1 INTRODUCTION

Over the past 30 years, development of prestressed concrete in Europe and in the United States has taken place along quite different lines. In Europe, where the ratio of labor cost to material cost has been relatively low, innovative one-of-a-kind projects were economically feasible. Sophisticated design and construction techniques were used to achieve the ultimate in material savings. In the United States, where by contrast, the demand for skilled on-site building labor often exceeded the supply, economic conditions favored the greatest possible standardization of construction, replacing site labor by factory production of precast parts.

Conditions of practice here are changing. Construction labor is no longer scarce, and material costs are increasing. Advanced design and construction concepts are more often employed, both to save material and to extend the range of prestressed concrete beyond previous limits.

The advantages of precasting are clearly established, however. Because of mass production, less labor is required per unit, and unskilled local labor, which is much less expensive than skilled mobile construction labor, may be used. High-quality, high-strength concrete is more easily attained. Complex section shapes are made economically feasible by the repeated use of metal or fiberglass forms. The work can proceed with greater independence from weather and season. On-site construction time is reduced because of the prefabrication of parts, an important consideration in congested localities. Thus, the operation of

centrally located permanent precasting plants, supplying standard members within a shipping radius of several hundred miles, will comprise an important part of the total United States construction effort in the years ahead.

Many designs are likely to combine precasting with cast-in-place concrete to provide composite action or to develop continuity. The combination of pretensioning and post-tensioning has proved economically advantageous in many instances.

In addition, one can expect the greater use of temporary precasting yards set up at the site of heavy construction to produce members specially designed for particular projects. An example is the production of precast cellular segments for long span bridges. In other cases, site precasting will be used to reduce forming costs and speed construction, as for lift slabs or construction of shell roofs.

Many types of precast members have been developed, and much thought has been given to the design of connections for precast members, such that structural requirements are met and erection procedures simplified to the maximum degree. For economy, standard members and connections are used where possible. In other cases, when special components and details are justified, close collaboration is needed between the engineer and builder to develop the best arrangement.

The following sections describe some of the more common precast members and connections. Because of the many variations and important differences in design details, the discussion is generally descriptive. However, the shear friction theory, which has broad applicability in the design of connections and precast members, is described in detail in Section 12.4. Special Code provisions and reinforcement details for brackets, which are frequently used in precast structures, are found in Section 12.5.

12.2 PRECAST MEMBERS FOR BUILDINGS

Certain more-or-less standard forms of precast units have been developed for buildings. Though not completely standardized, they are widely available with minor local variations. At the same time, the precasting process is sufficiently adaptable so that special shapes can be produced economically, provided the number of repetitions of each unit is sufficiently large. This is particularly important for exterior wall panels, for example, for which a great variety of architectural treatment is needed.

A. FLOOR AND ROOF UNITS

Perhaps the most common of the standard shapes for buildings is the double-T floor or roof plank shown in Fig. 12.1*a*. These are available in 8- and 10-ft widths, with depths ranging from 12 to 32 in. The double-T is highly functional, because it not only meets structural requirements, but provides a flat useful surface. Often a 2-in. cast-in-place concrete topping slab is used over the top

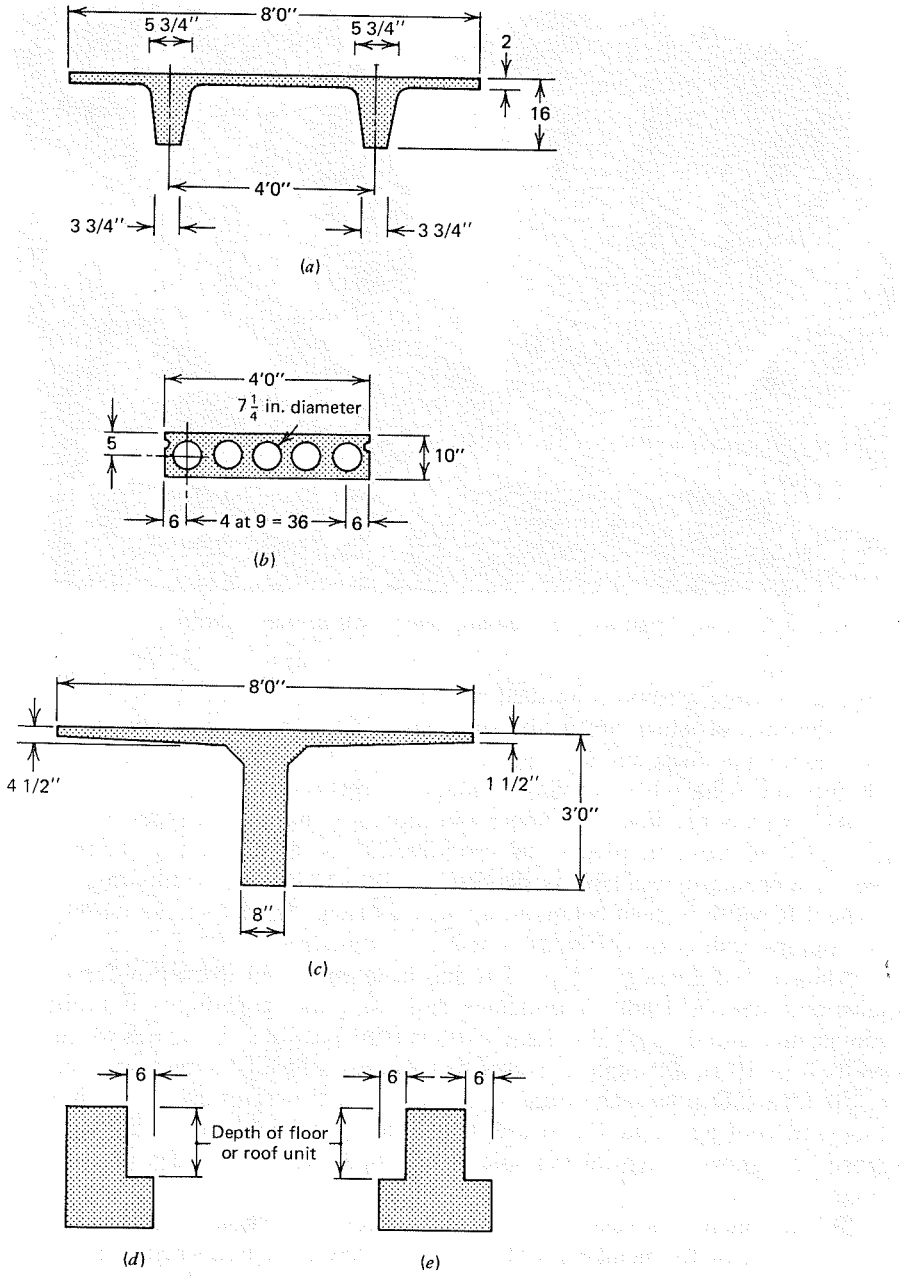

FIGURE 12.1 Typical standard sections. (*a*) Double-T section. (*b*) Hollowcore plank. (*c*) Single-T section. (*d*) L-section. (*e*) Inverted-T section.

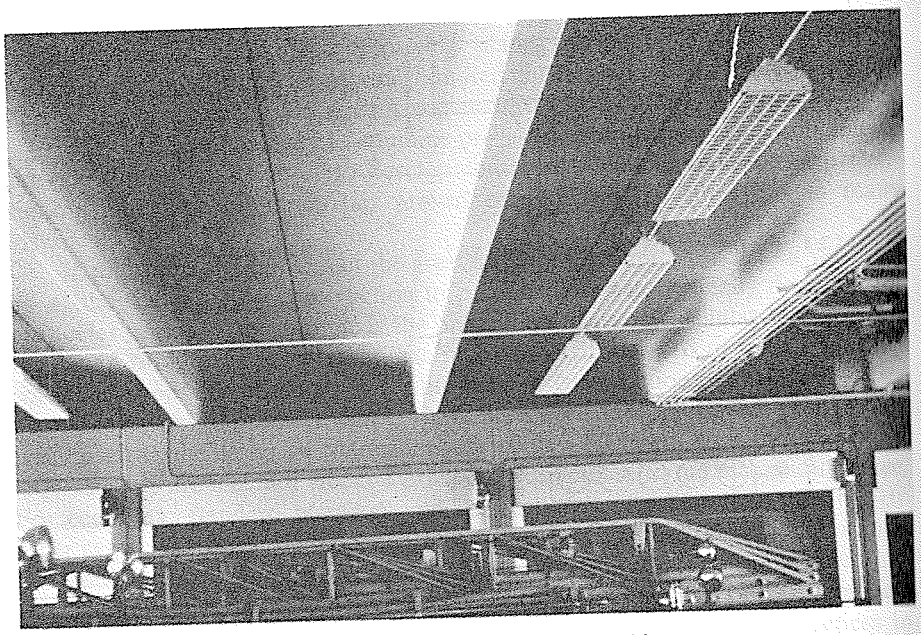

FIGURE 12.2 Long-span single-T beams used over parking garage.

flange to provide a smooth finished surface. The topping bonds to the precast units, the tops of which are deliberately left rough. Resulting composite action increases both stiffness and strength. Spans of about 30 ft are common, but spans well over 100 ft have been achieved using deep sections.

Also widely employed for floors and roofs are the various types of hollow-core slabs. A representative panel cross section is shown in Fig. 12.1*b*. Slab panels are ordinarily available in depths from 6 to 12 in., and widths from 2 to 8 ft. The 4-ft width is most common. Spans may range from 15 to about 40 ft. A 2-in. topping slab is also often used with these panels.

The single-T section of Fig. 12.1*c* has been employed frequently for longer spans and heavier loads in buildings such as parking garages, auditoriums, gymnasiums, and dining halls. Stem width is 8 in. as a rule, and flange widths are usually 8 or 10 ft, although narrower flanges are easily cast simply by blocking out the forms. Depths range from 36 to 48 in. Topping slabs are generally used. Floor and roof spans to 120 ft are not uncommon for members of this type. Figure 12.2 shows a typical example of long-span single-T beams used over a garage.

When concrete is cast against smooth steel or fiberglass formwork, as is generally the case for members of the types just described, and when care is taken in proportioning the mix and vibrating after placement, the resulting member has a surface that is very smooth and hard. Often this is left exposed in the completed structure with no additional finish other than paint. Flat plank provides a smooth ceiling overhead. Single- and double-Ts, too, may be left exposed and incorporated in the basic architectural scheme.

Section properties and safe load tables for double-T, single-T, and hollow-core deck sections will be found in Ref. 12.1. Properties for the more widely used sections are given in Appendix A.

B. BEAMS AND GIRDERS

Beam and girders of many shapes have been produced for the main framing members of precast prestressed concrete buildings. The shape and dimensions of

FIGURE 12.3 Commonwealth Title Building in Tacoma, showing floor and roof system composed of precast double-T beams supported by precast L-section girders. Courtesy of Concrete Technology Corporation, Tacoma, Washington.

these members are not as standard as was the case for deck units. Cross-sectional geometry is dictated not only by requirements of load and span, but often by the need to provide a shelf, or continuous corbel, for the end support of precast deck units framing in at right angles. Typical L- and inverted-T cross sections are seen in Figs. 12.1*d* and 12.1*e*.

Special attention should be given to detailing of reinforcement for sections of this type. Auxiliary web steel should project into the flange to provide for the vertical reactions from floor units. This steel may be designed using the shear friction approach (Section 12.4). Longitudinal prestressing steel, in the case of unsymmetrical L-beams, should have its centroid in the same vertical plane as the centroid of the concrete section, to avoid lateral warping due to prestress force.

Typical use of L-section beams to carry a double-T floor system is shown in Fig. 12.3.

C. COLUMNS

Columns, as well as floor beams and girders, are often precast. They may be prestressed (see Chapter 11), but more often are conventionally reinforced, even

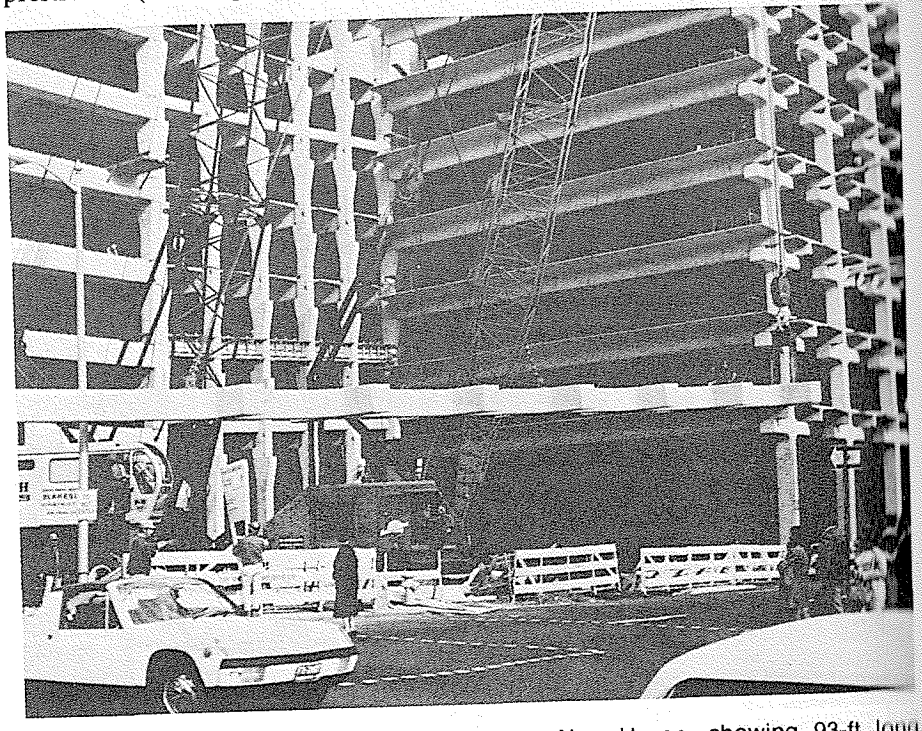

FIGURE 12.4 Crown Street Parking Garage, New Haven, showing 93-ft long precast tree columns carrying 36-in. depth single-T deck girders. Courtesy of Blakeslee Prestress, Inc.

though the rest of the work is prestressed. Rectangular cross sections are most common, but unusual shapes have been employed for special purposes. Columns are precast in the horizontal position, greatly simplifying formwork and facilitating the placement of concrete.

A variety of column details have been developed to support beams and girders. Brackets, such as described in Section 12.5, are used extensively in industrial construction, but may be visually or functionally objectionable in apartments or schools, for example. Alternative beam support details will be discussed in Section 12.3.

An unusual example of precast columns with corbels is shown in Fig. 12.4. Reinforced, but not prestressed, these 93-ft members were precast in one piece, each weighing 41 tons. Floor members are 9-ft width and 36-in. depth single-Ts resting on individual column haunches at each level.

D. EXTERIOR WALL PANELS

Many types of precast wall panels have been used to enclose multi- as well as single-story buildings. These may serve only as cladding, but often the walls are load bearing, and provide vertical support for floors and roofs. In addition, with proper attention to details, they can be effective in providing resistance to lateral forces on buildings.

The same double-T forms used to produce floor deck plank can be employed to manufacture wall panels. Widths are normally 8 ft, and typical surface thickness 2 or 3 in., with ribs 12 to 24 in. in depth. Such units provide vertical support for floors and roofs by using continuous corbels on the inside face, or by steel shelf angles anchored to inserts cast into the concrete.

Flat wall panels are often used as well, such as illustrated in Fig. 12.5. These may have various surface treatments, including exposed aggregate and patterned surfaces. Flat panels are sometimes cast with an internal layer of 2 to 4 in. of foam-insulating material, with structural concrete faces, inside and out, connected by shear clips.

The unusually large bearing wall panels shown in Fig. 12.6 are continuous over four stories of building height, carrying floor and roof loads directly to the foundation wall.

E. LARGE-PANEL CONSTRUCTION

Large-panel construction is the name given to the broad class of structural systems, some patented, in which precast floor panels span freely between precast interior and exterior wall panels. Generally no columns or beams are used. The walls enclose and subdivide the space, provide vertical support, and resist lateral loads. Wall panels are reinforced and may be pretensioned. They may serve as forms for cast-in-place reinforced concrete columns. In some cases, the com-

FIGURE 12.5 Tai Tung Village in Boston, with precast bearing walls and floor units joined by post-tensioning. Sepp Firnkas and Associates, Engineers; photograph courtesy of Prestressed Concrete Institute.

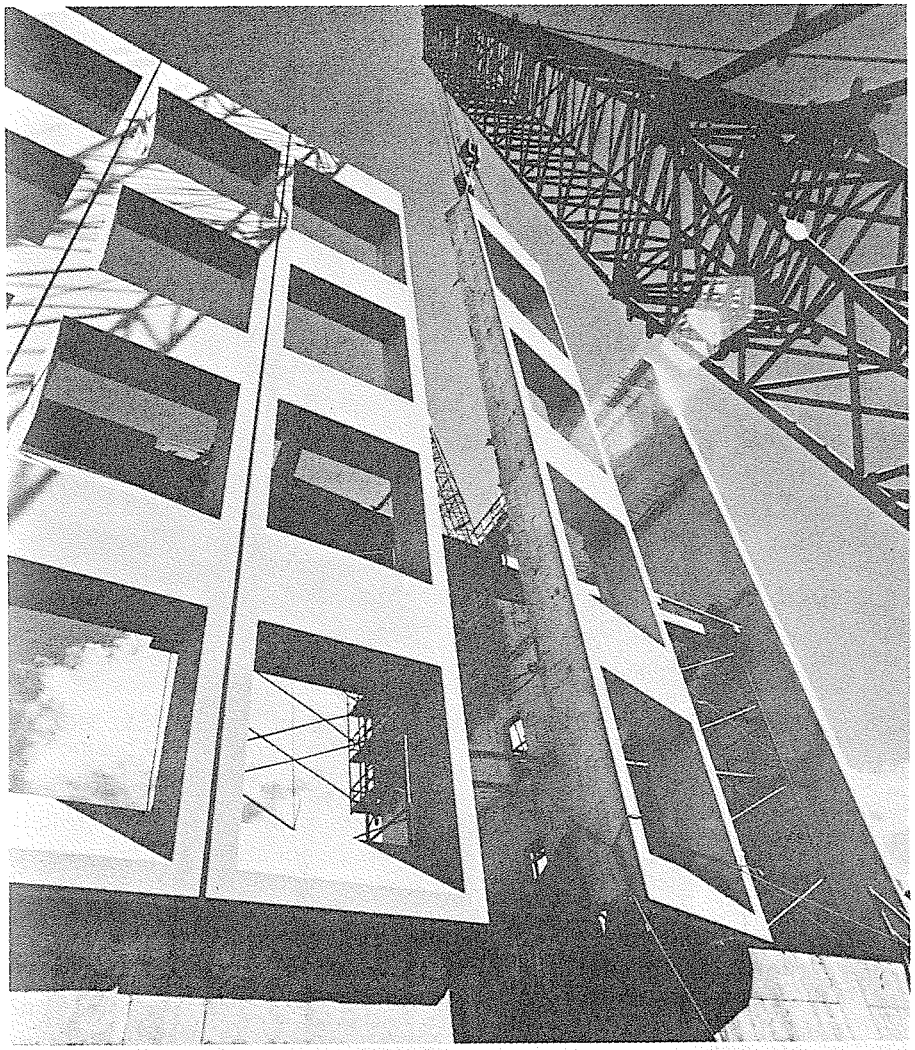

FIGURE 12.6 Precast, prestressed concrete load-bearing wall units having a total height of 62 ft and a weight of 35 tons each. Courtesy of Prestressed Concrete Institute.

pleted assemblage is post-tensioned, permitting the structure to act in an integrated sense in resisting horizontal loads due to wind or seismic action.

Figure 12.7 shows a variation of large-panel construction used for a 21-story hotel. Except for the service units; the structure consisted entirely of box-shaped, room-sized modules, completely prefabricated, and stacked on top of each other. In Europe, such precast modules, with plumbing, wiring, and heating prein-

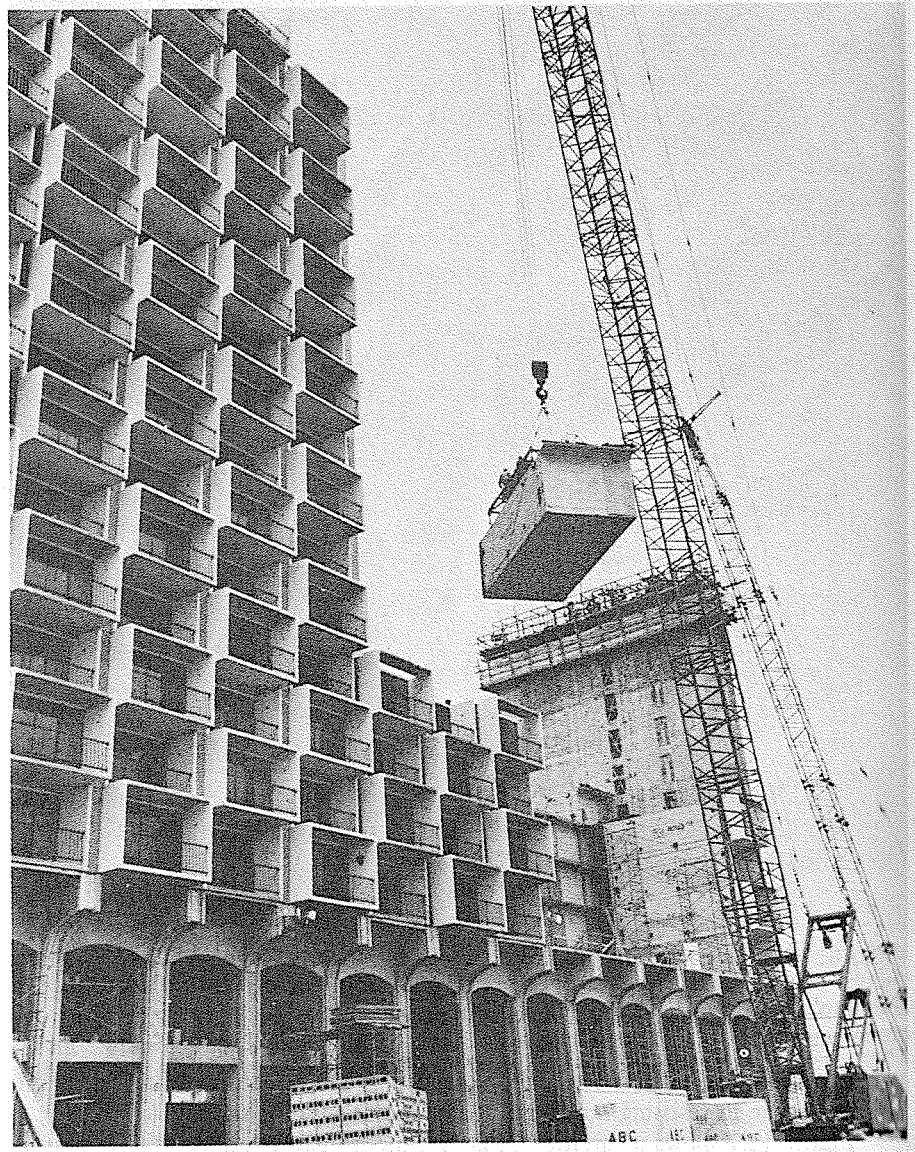

FIGURE 12.7 Precast room-size modules for 21-story hotel. Courtesy of Portland Cement Association.

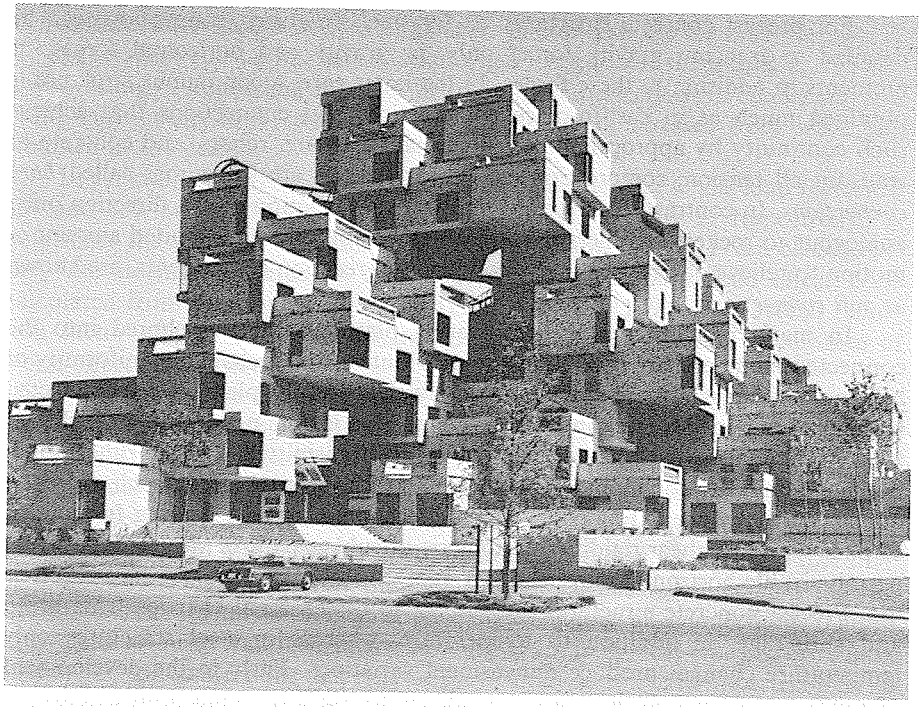

FIGURE 12.8 Habitat Village at Montreal, constructed as part of Expo 67. Courtesy of Portland Cement Association.

stalled, are widely used for multistory apartment buildings, as an alternative to making similar apartment structures in precast wall, roof, and floor panels, which are more easily shipped but less easily erected than box-shaped modules.

Perhaps the best-known example of precast modular design is Habitat 67 at Montreal, shown in Fig. 12.8. Post-tensioning tendons lock the residential units together, permitting dramatic cantilevers and open space in the seemingly random arrangement of boxes. The project may be regarded as a prototype in the development of industrialized housing that retains a large measure of uniqueness in the final result.

12.3 CONNECTION DETAILS

By their very nature, cast-in-place concrete structures tend to be monolithic and continuous. Connections, in the sense of joining two otherwise separate pieces, rarely occur in that type of construction. Precast structures, on the other hand, resemble steel construction in that the final structure consists of an assemblage of a large number of prefabricated elements that are connected together on the site.

For precast concrete structures, as for steel structures, connections can be detailed to transmit gravity forces only, or gravity and horizontal forces, or moments in addition to these forces. In the latter case, a continuous structure is obtained much as in cast-in-place construction, and connections that achieve such continuity by appropriate use of special hardware, rebars, and concrete to transmit all tension, compression, and shear stresses are sometimes called *hard connections*. In contrast, connections that transmit reaction in one direction only, analogous to rockers or rollers in steel structures, but permit a limited amount of motion to relieve other forces such as horizontal reaction components, are known as *soft connections*.

In many precast connections, bearing plates, suitably anchored into the connected members, are used to insure distribution and reasonable uniformity of bearing pressures. If these bearing plates are steel and the plates of the connected members are joined by welding, a hard connection is obtained in the sense that at least horizontal, as well as vertical, forces are transmitted. On the other hand, bearing details are common that permit relief of horizontal forces, such as by use of tetrafluorethylene (TFE) pads, which effectively eliminate bearing friction, or of pads with low shear rigidity (elastomeric or rubber pads of various types) that permit sizable horizontal movements.

Precast concrete structures are subject to dimensional changes from creep and shrinkage, in addition to temperature, whereas in steel structures only temperature changes produce dimensional variations. Early in the development of precast construction there was a tendency to use soft connections extensively to permit these dimensional changes to occur without causing restraint forces. More recent experience with soft connections indicates that the resulting structures tend to have insufficient resistance to lateral forces, such as those due to earthquake. For this reason, the present trend is toward the use of hard connections with a high degree of continuity. In connections of this sort, provision must be made for resistance to the restraint forces that are caused by volume changes.

Few specific recommendations are found in the ACI Code pertaining to the design of connections for precast members, for the reason that such construction is still regarded as somewhat special. A substantial amount of work has been done by industry-oriented groups toward formulating design recommendations and establishing more-or-less standard connection details. Of particular interest are the recommendations found in the PCI publication, *Connections for Precast Prestressed Concrete Buildings* (Ref. 12.2), formulated with the assistance of the PCI Committee on Connection Details and the PCI Seismic Committee. Additional design information, including load tables for standard connections, will be found in Ref. 12.1.

In the design of connections, it is prudent to select load factors that exceed those required for the members being connected. This is so because connections are generally subject to high stress concentrations, which preclude the attainment of much ductility should overloading occur. In contrast, the members connected are apt to show substantial deformation when loaded near the ultimate, and will give warning of impending collapse. In addition, imperfections in connections, as built, may cause large changes in the magnitude of stresses from what was assumed in the design.

In general, in designing members according to the ACI Code, load factors of 1.4 and 1.7 are applied to dead and live loads, D and L respectively, to determine the required strength. When volume change effects T are considered, they are normally treated as dead load, and the ultimate load effect U is calculated from the equation $U = 0.75(1.4D + 1.4T + 1.7L)$. The overall reduction factor of 0.75 is introduced, recognizing that simultaneous occurrence of worst effects is not likely.

However, for the design of brackets and corbels the ACI Code provides that the tensile force resulting from volume change effects should be included with the live load. Thus, a load factor of 1.7 is to be used. No overall reduction factor is used for corbels and brackets. PCI recommendations for load factors are still more conservative. In view of the importance of connections, and to further ensure that, should failure occur, it will be in the members connected rather than in the connections themselves, the PCI Committee has recommended that an additional load factor of 1.3 be applied in designing all connections. This is equivalent to an overall load factor of about 2 in. in typical cases. Others have noted that, for connections that may be particularly sensitive to imperfections, an overall factor of 2.5 is not excessive (Ref. 12.3).

Many types of connections have been developed for use with precast concrete members, with details varying depending on the forces to be transferred, plant facilities available, and the particular construction techniques and sequences to be followed. Certain of the more common types will be described below.

A. COLUMN BASE CONNECTIONS

Figure 12.9*a* shows a column base detail with projecting base plate. Four anchor bolts are used, with double nuts facilitating erection and leveling of the column. Typically, about 2 in. of nonshrink grout is used between the top of the pier, footing, or wall and the bottom of the steel base plate. Column reinforcement is welded to the top face of the base plate. Tests have confirmed that such column connections can transmit the full moment or which the column is designed, if properly detailed (Ref. 12.4).

An alternative base plate detail is shown in Fig. 12.9*b*, with the dimensions of the base plate the same as, or in some cases less than, the outside column dimensions. The advantage of this type of column is that it can be cast using long-line forms, without the need for special modification to accommodate the

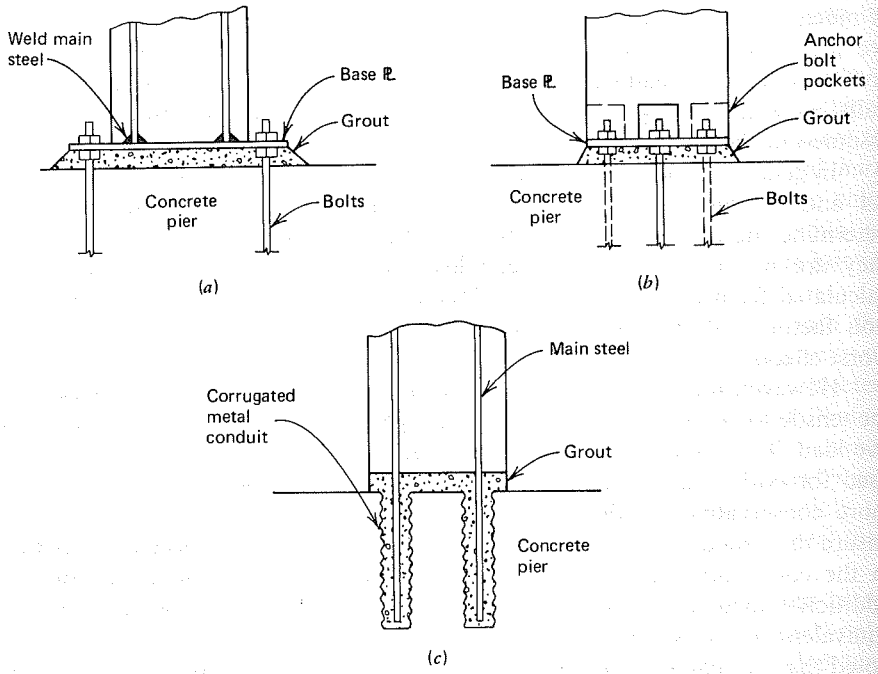

FIGURE 12.9 Column base connections.

projecting base plates of Fig. 12.9*a*. Anchor bolt pockets are provided, either centered on the four column faces as shown, or located at the corners. Ordinarily a double-nut system is used to facilitate leveling of the column, and nonshrink grout is placed after the column is set. Bolt pockets too are grouted, after the nuts are tightened. Column reinforcement, not shown here, would be welded to the top face of the plate as before.

In Fig. 12.9*c*, the main column reinforcement projects from the end of the precast member a sufficient distance to develop its strength by bond. The projecting rebars are inserted into grout-filled cold-formed steel conduits, which are embedded in the foundation when it is poured. Temporary bracing may be used to position the column until the grout has set and hardened, or temporary erection angles may be provided, bolted to two opposite column faces using inserts cast in the concrete.

In all cases described, confinement steel should be provided around the anchor bolts in the form of closed ties. A minimum of four No. 3 ties is recommended, placed at 3 in. centers near the top surface of the pier or wall in addition to the normal pattern of tie steel. Tie reinforcement in the columns, not shown in Fig. 12.9 for clarity, should be provided as usual.

B. BEAM-TO-COLUMN CONNECTIONS

Several alternative means for interconnecting beams and columns are illustrated in Fig. 12.10. In all cases, rectangular beams are shown, but similar details would apply to I-beams or single-Ts. The figure shows only the basic geometry of the joint in each case, and auxiliary reinforcement, anchors, and ties are omitted for the sake of clarity. Such steel is crucially important to the integrity of connections, and careful attention must be given to detailing. The design of such reinforcement may be based on the shear friction approach in most cases (Section

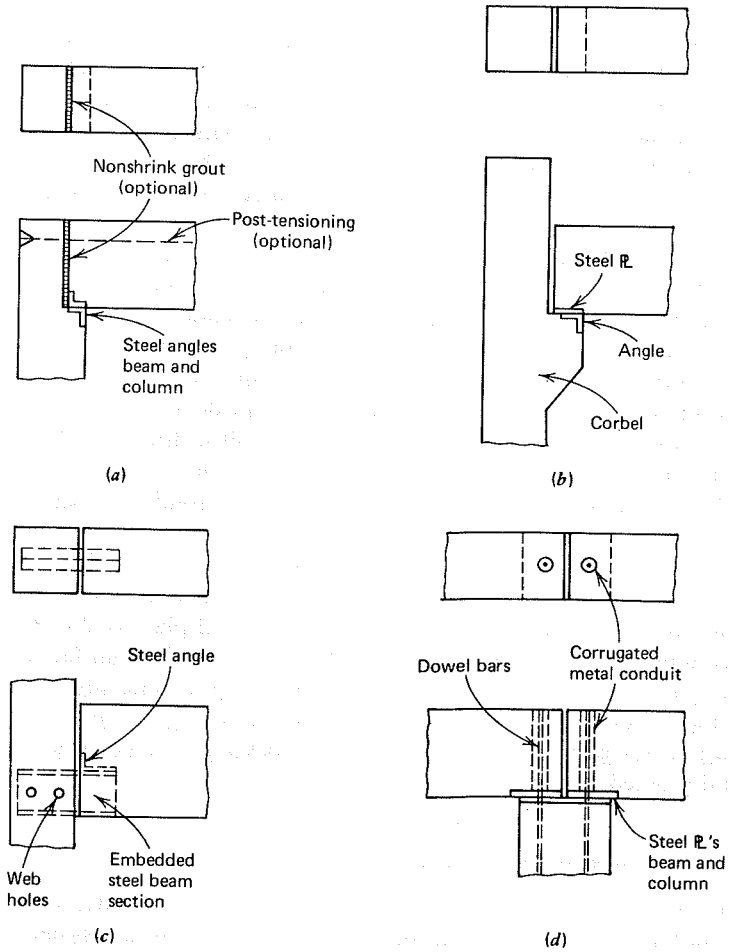

FIGURE 12.10 Beam-to-column connections.

12.4). Specific suggestions for steel details will be found in Ref. 12.2 and other sources listed at the end of this chapter.

Figure 12.10*a* shows a joint detail with a concealed haunch. Well-anchored bearing angles are provided at the column seat and the beam end. This type of connection may be used to provide vertical and horizontal reaction components only, or with the addition of nonshrink grout and post-tensioning at the top of the beam as shown, will serve as a moment connection as well. The tendon, in such case, passes through the column and is jacked and anchored from the outside. It may be continuous through the entire beam span, may be terminated in an internal anchor, or may be curved downward and anchored at the bottom face of the beam.

Figure 12.10*b* shows a typical bracket connection, common for industrial construction where the projecting bracket is not architecturally offensive. The seat angle at the upper corner of the bracket is welded to reinforcing bars anchored into the column, and special ties and moment bars provided in the bracket. A steel bearing plate is used at the bottom corner of the beam, anchored into the concrete. Design considerations for brackets will be discussed in detail in Section 12.5.

The embedded steel shape shown in Fig. 12.10*c* is used when it is necessary to avoid projections beyond the face of column or below the bottom of the beam. The steel, often a short piece of wide-flanged beam, is embedded in the column and projects outward a distance sufficient to provide the proper bearing for the beam. A socket is formed in casting the beam, with steel angle or plate at its top, to receive the beam stub. Alternately, a dapped-end beam detail may be used, similar to that shown but with the cutout extending the full width of the beam. Auxiliary reinforcement is specially critical in such cases. Holes provided in the web of the steel beam stub help to insure good concrete consolidation between flanges (Ref. 12.5).

Finally, Fig. 12.10*d* shows a doweled connection with bars projecting from the column into cold-formed steel tubing or conduit embedded in the beam ends. The tubes are grouted after the beams are in position. A steel plate is shown at the top of the column, with bearing plates also provided at the bottom faces of the beams. The connection may be made continuous by providing nonshrink grout between the beam ends, after which top post-tensioning is introduced. Alternately, non-prestressed rebars may be placed in blockout slots along the top of the beams and grouted in place (Ref. 12.6).

C. COLUMN-TO-COLUMN CONNECTIONS

Figure 12.11 shows several typical column-to-column splices. Generally, a non shrink grout is used between column members, and often a double-nut system is used to facilitate leveling of the upper column. Base plates may be slightly smaller than the external column dimensions if architectural requirements so

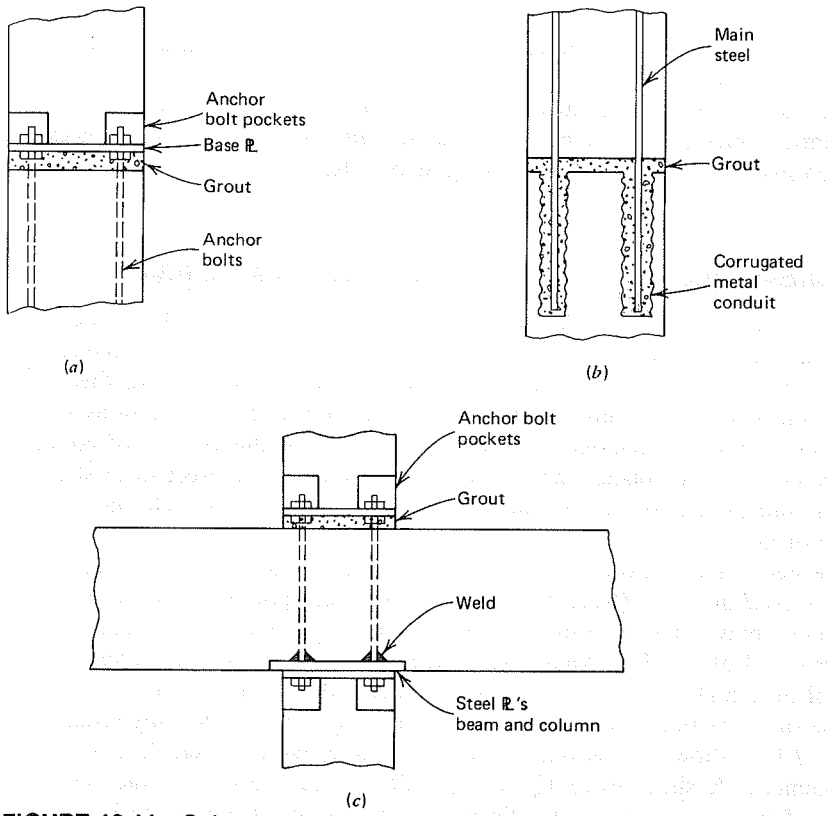

FIGURE 12.11 Column-to-column connections.

indicate. Tie steel and main steel have been omitted from the sketches for clarity, in most cases. Closely spaced ties should be placed in the columns immediately above and below the joint, as described earlier, in addition to the usual ties.

Figure 12.11*a* shows a detail using anchor bolt pockets and a double-nut system with anchor bolts. The bolt pockets would be packed with nonshrink grout after assembly of the parts. Bolts can also be located at the center of the column faces as in Fig. 12.9*b*.

The detail of Fig. 12.11*b* permits the main steel to be lap-spliced with that of the column below. Generally, clip angles would be provided, attached to inserts cast into the column faces to permit positioning of the upper column during erection.

One of many possibilities for splicing a column through a continuous beam is shown in Fig. 12.11*c*. Main reinforcement in both upper and lower columns should be welded to steel cap and base plates to transfer their load, and anchor

bolts should be detailed with the same consideration. Closely spaced ties must be provided in the columns, and in this case, in the beam as well, to transfer the load between columns.

The various types of connections shown and described are representative, but countless variations may be developed to suit the special circumstances in any given instance. Many details are suggested in Ref. 12.2.

12.4 SHEAR FRICTION METHOD FOR CONNECTION DESIGN

Chapter 5 dealt with shear in prestressed concrete beams in the context of flexural and torsional loading. In such cases, shear is used merely as a convenient measure of diagonal tension, which is the real concern. In contrast, there are circumstances such that direct shear may cause failure. Such situations occur commonly in precast concrete members, particularly in the vicinity of connections. Potential failure planes can be established along which direct shear stresses are high, and failure to provide adequate reinforcement across such planes may produce disastrous results.

The necessary reinforcement may be determined on the basis of the *shear friction method* of design (Refs. 12.7–12.10). The basic approach is to assume that the concrete may crack in an unfavorable manner, or that slip may occur along a predetermined plane of weakness. Reinforcement must be provided crossing the potential or actual crack or shear plane to prevent direct shear failure.

The shear friction theory is very simple, and the behavior is easily visualized. Figure 12.12*a* shows a cracked block of concrete, with the crack crossed by reinforcement. A shear force V_n acts parallel to the crack, and the resulting tendency for the upper block to slip relative to the lower is resisted largely by friction along the concrete interface at the crack. Since the crack surface is naturally rough and irregular, the effective coefficient of friction may be quite high. In addition, the irregular surface will cause the two blocks of concrete to separate slightly, as shown in Fig. 12.12*b*.

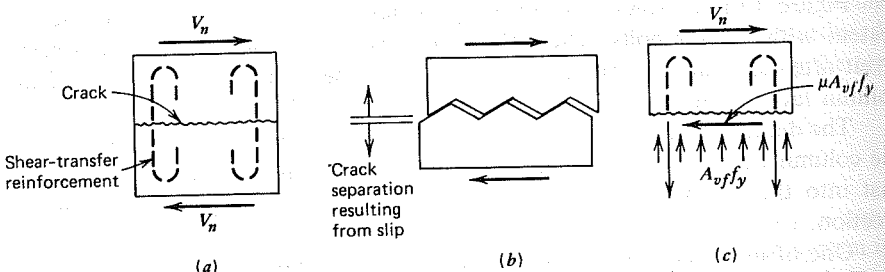

FIGURE 12.12 Basis of shear-friction theory. (*a*) Applied shear. (*b*) Enlarged representation of crack surface. (*c*) Free body of concrete above crack.

If reinforcement is present normal to the crack, then slip and subsequent separation of the concrete will stress the steel in tension. Tests have confirmed that well-anchored steel will be stressed to its yield strength when shear failure is obtained (Ref. 12.9). The resulting tensile force sets up an equal and opposite pressure between the concrete faces on either side of the crack. It is clear from the free body of Fig. 12.12*c* that the maximum value of this interface pressure is $A_{vf} f_y$, where A_{vf} is the total area of steel crossing the crack and f_y is its yield strength.

The concrete resistance to sliding may be expressed in terms of the normal force times a coefficient of friction μ. By setting the summation of horizontal forces equal to zero:

$$V_n = \mu A_{vf} f_y \tag{12.1}$$

Defining the steel ratio $\rho = A_{vf}/A_c$, where A_c in this case is the area of the cracked surface, Eq. (12.1) may be rewritten in terms of the nominal shear stress v_n:

$$v_n = \mu \rho f_y \tag{12.2}$$

The relative movement of the concrete on opposite sides of the crack also subjects the individual reinforcing bars to shearing action, and the dowel resistance of the bars to this shearing action contributes to shear resistance. It is customary to neglect the dowel effect for simplicity in design, and to compensate for this by using an artificially high value of the friction coefficient.

Based on early tests, μ may be taken equal to 1.4 for cracks in monolithic concrete, but V_n should not be assumed greater than $0.2 f_c' A_c$ or $800 A_c$ lb (Ref. 12.7).

In Fig. 12.13 the shear transfer strength predicted by Eq. (12.2) is compared with experimental values obtained in more recent tests conducted at the University of Washington (Ref. 12.9). It is evident that Eq. (12.2) gives a conservative estimate of shear strength. It is also clear that strength considerably in excess of the upper limit of 800 psi can be developed if appropriate reinforcement is provided. It has been proposed (Ref. 12.9) that a modified form of Eq. (12.2) be adopted when ρf_y exceeds 600 psi, as follows:

$$v_n = \mu \rho f_y \left(\frac{300}{\rho f_y} + 0.5 \right) \tag{12.3}$$

The strengths predicted by Eq. (12.3) (indicated by the dashed line in Fig. 12.13) appear to give a satisfactory correlation with experimental results for concrete strengths greater than 2,500 psi. Pending further data, it is recommended that an upper limit of v_n = 1,300 psi be imposed for Eq. (12.3).

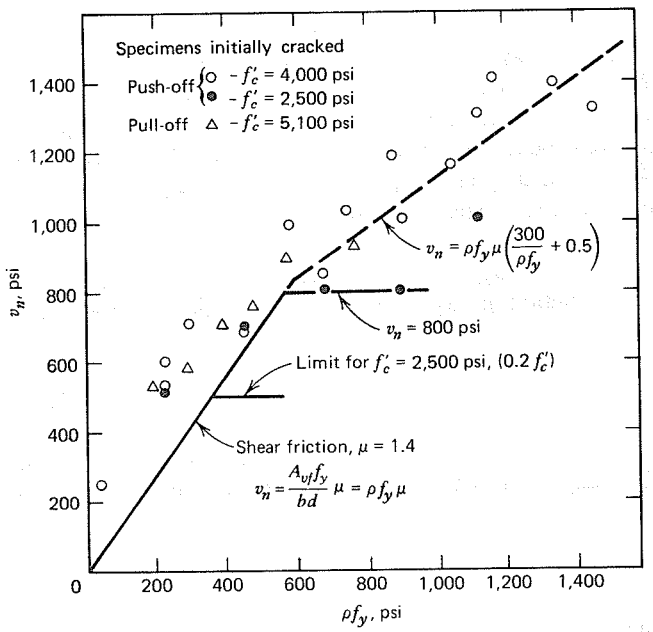

FIGURE 12.13 Calculated vs. experimental shear-transfer strength for initially cracked specimens.

The provisions of the ACI Code are based on Eq. (12.1). The design strength is to be taken equal to ϕV_n, where $\phi = 0.85$ for shear friction design and V_n is not to exceed the smaller of $0.2 f'_c A_c$ or $800 A_c$ lb. Recommendations for friction factor μ are as follows:

Concrete placed monolithically	1.4λ
Concrete placed against hardened concrete with surface intentionally roughened	1.0λ
Concrete placed against hardened concrete not intentionally roughened	0.6λ
Concrete anchored to as-rolled structural steel by headed studs or rebars	0.7λ

where $\lambda = 1.0$ for normal weight concrete, 0.85 for "sand-lightweight" concrete, and 0.75 for "all-lightweight" concrete. The yield strength of the reinforcement is not to exceed 60,000 psi. Direct tension across the shear plane, if present, is to be provided for by additional reinforcement, and permanent net compression across the shear plane may be taken as additive to the force in the shear friction reinforcement $A_{vf} f_y$ when calculating the required A_{vf}.

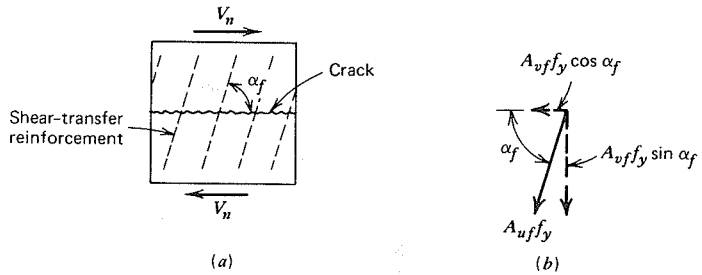

FIGURE 12.14 Shear-friction reinforcement inclined with respect to crack face.

When shear is transferred between concrete newly placed against hardened concrete, the surface roughness is an important variable; an intentionally roughened surface is defined to have a full amplitude of approximately $\frac{1}{4}$ in. In any case, the old surface must be clean and free of laitance. When shear is to be transferred between as-rolled steel and concrete, the steel must be clean and without paint, according to the ACI Code.

If V_u is the shear force to be resisted at factored loads, then with $V_u = \phi V_n$, the required steel area is found by transposition of Eq. (12.1):

$$A_{vf} = \frac{V_u}{\phi \mu f_y} \tag{12.4}$$

In some cases, the shear friction reinforcement may not cross the shear plane at 90 degrees as described in the preceding paragraphs. If the shear friction reinforcement is inclined to the shear plane so that the shear force is applied in the direction to increase tension in the steel, as in Fig. 12.14*a*, then the component of that tension parallel to the shear plane, shown in Fig. 12.14*b*, contributes to the resistance to slip. Then the shear strength may be computed from

$$V_n = A_{vf} f_y (\mu \sin \alpha_f + \cos \alpha_f) \tag{12.5}$$

in lieu of Eq. (12.1). Here α_f is the angle between the shear friction reinforcement and the shear plane. If α_f is larger than 90 degrees, that is, if the inclination of the steel is such that the tension in the bars tends to be reduced by the shear force, then the assumption that the steel stress equals f_y is not valid, and a better arrangement of bars should be found.

Certain precautions should be observed in applying the shear friction method of design. Reinforcement, of whatever type, should be well anchored to develop the yield strength of the steel, by the full development length or by hooks or bends, in the case of rebars, or by proper heads and welding, in the case of

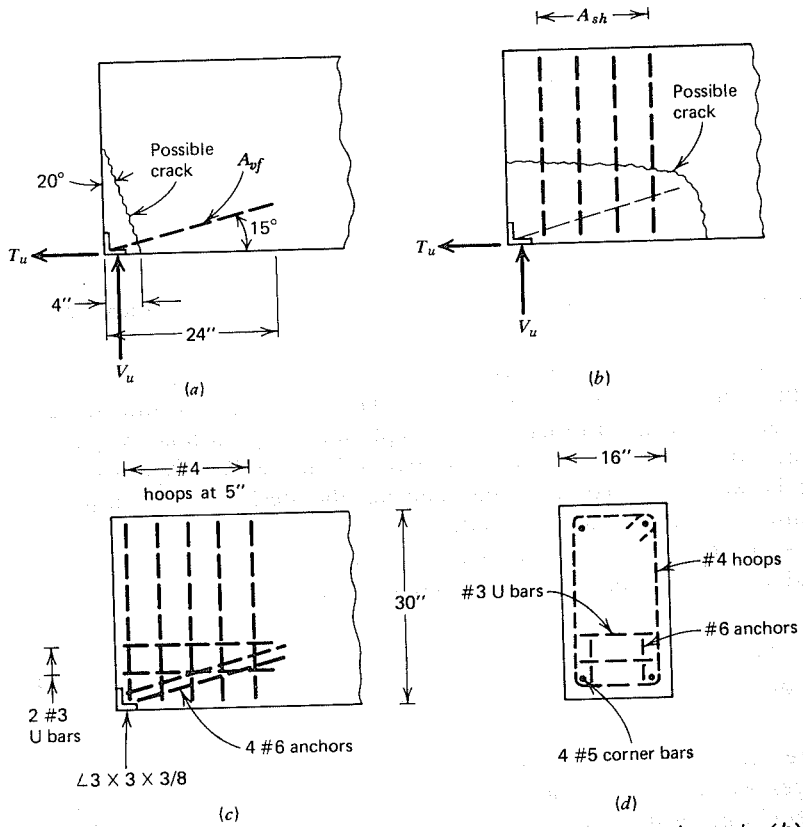

FIGURE 12.15 Design of beam-bearing shoe. (*a*) Diagonal crack. (*b*) Horizontal crack. (*c*) Reinforcement. (*d*) Cross section.

studs joining concrete to structural steel. The concrete should be well confined, and the liberal use of hoops has been recommended (Ref. 12.7). Care must be taken to consider all possible failure planes, and to provide sufficient well anchored steel across these planes.

EXAMPLE: Design of Beam Bearing Detail

A precast beam must be designed to resist a support reaction, at factored loads, of $V_u = 125$ kips applied to a 3 × 3 steel angle, as shown in Fig. 12.15. In lieu of a calculated value, a horizontal force T_u, resulting from restrained volume change, will be assumed at 20 percent of the vertical reaction, or 25 kips. Determine the required auxiliary reinforcement, using steel of yield strength $f_y = 60{,}000$ psi. Concrete design strength $f_c' = 5{,}000$ psi ($V_u = 556$ kN, $T_u = 111$ kN, $f_y = 522$ MPa, and $f_c' = 34$ MPa).

A potential crack will be assumed at 20 degrees, initiating at a point 4 in. (102 mm) from the end of the beam, as shown in Fig. 12.15*a*. The total required steel A_{vf} is the sum of that required to resist the effects of V_u and T_u. Equation (12.4) is modified accordingly:

$$A_{vf} = \frac{V_u \cos 20° + T_u \sin 20°}{\phi \mu f_y}$$

$$= \frac{117 + 9}{0.85 \times 1.4 \times 60}$$

$$= 1.76 \text{ in.}^2 \ (1136 \text{ mm}^2)$$

Four No. 6 bars will be used, providing an area of 1.77 in.^{2} They will be welded to the 3 × 3 angle and will extend into the beam a sufficient distance to develop the yield strength of the bars. According to the ACI Code, the development length for a No. 6 bar is 12 in. However, considering the uncertainty of the exact crack location, the bars will be extended twice the development length, or 24 in, into the beam as shown in Fig. 12.15*a*. The bars will be placed at an angle of 15 degrees with the bottom face of the member, approximately normal to the assumed crack.

The area of the cracked interface is

$$A_c = 16\left(\frac{4}{\sin 20°}\right) = 187 \text{ in.}^2$$

Thus, according to the ACI Code, the maximum nominal shear strength of the surface is not to exceed $V_n = 0.2 f_c' A_c = 187$ kips or $V_n = 800 A_c = 150$ kips. The maximum design strength to be used is $\phi V_n = 0.85 \times 150 = 128$ kips. The applied shear on the interface at factored loads is

$$V_u = 125 \cos 20° + 25 \sin 20° = 126 \text{ kips}$$

and so the design is judged satisfactory to this point.

A second possible crack must be considered, as shown in Fig. 12.15*b*, resulting from the tendency of the entire anchorage weldment to pull horizontally out of the beam. The required steel area A_{sh} and the concrete shear stress will be calculated based on the development of the full yield tension in the bars A_{vf}. (Note that the factor ϕ need not be used here because it has already been introduced in computing A_{vf}.)

$$A_{sh} = \frac{A_{vf} f_y \cos 15°}{\mu f_y}$$

$$= \frac{1.76 \times 0.966}{1.4}$$

$$= 1.21 \text{ in.}^2 \ (781 \text{ mm}^2)$$

Four No. 4 hoops will be used, providing an area of 1.57 in.^{2}

The maximum shear force that can be transferred, according to the ACI Code limits, will be based conservatively on a horizontal plane 24-in long. No strength reduction factor need be included in the calculation of this maximum value because it was already introduced in determining the steel area A_{vf} by which the shear force is applied. Accordingly,

$$V_n \le 800 \times 16 \times 24 = 308 \text{ kips}$$

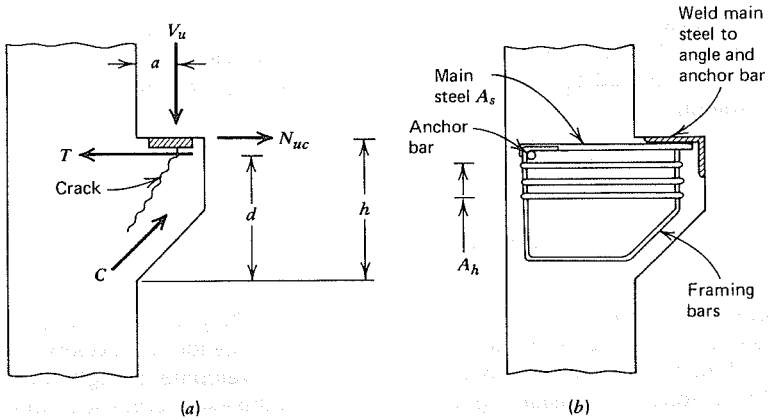

FIGURE 12.16 Typical reinforced concrete bracket.

The maximum shear force that could be applied in the given instance is

$$V_n = 1.76 \times 60 \cos 15° = 102 \text{ kips}$$

well below the specified maximum.

Additional confinement steel is recommended in Ref. 12.1, in the amount $V_u/8f_y$, to be placed in the form of hoops or hairpin bars confining the concrete near the bottom and end faces of a precast beam at the reaction. In the present case,

$$A_{cv} = A_{ch} = \frac{125}{8 \times 60}$$

$$= 0.26 \text{ in.}^2 \ (168 \text{ mm}^2)$$

One additional No. 4 hoop will be placed as near as possible to the end face, and two U-shaped No. 3 bars will be added parallel to the bottom of the beam as shown in Fig. 12.15*c* and 12.15*d*. Also shown in Fig. 12.15*d* are four No. 5 corner bars that will provide anchorage for the hoop steel.

12.5 BRACKETS AND CORBELS

Brackets such as shown in Fig. 12.16 are widely used in precast construction for supporting beams at the columns. When they project from a wall rather than from a column, they are properly called corbels. In either case, they are designed mainly to provide for the vertical reaction V_u at the end of the beam but, unless special precautions are taken to avoid horizontal forces due to restrained shrinkage, creep (in the case of prestressed beams), or temperature change, they must also resist a horizontal force N_{uc}. Such tensile force is to be regarded as live load, and a load factor of 1.7 applied. According to the ACI Code, unless special precautions are taken, a tensile force not less than 20 percent of the vertical reaction will be assumed to act.

Steel bearing plates or angles are generally used at the top surface of brackets to provide a uniform contact surface and to distribute the reaction. A corresponding steel bearing plate or angle is usually provided at the lower corner of the supported beam. If the two plates are welded together, as is commonly done, horizontally forces clearly must be allowed for in the design. However, they may be avoided by use of Teflon or elastomeric bearing pads.

The structural performance of a bracket is fairly complex, but may be visualized from Fig. 12.16. A correctly designed bracket, if overloaded, is likely to develop a diagonal crack such as shown in Fig. 12.16*a*. The applied forces V_u and N_{uc} (if present) are then equilibrated in a trusslike fashion by the tension force T in the main bars having area A_s (see Fig. 12.16*b*) and the diagonal force C in the concrete compression strut outside of the crack. A second possible mode of failure is by direct shear along a plane more or less flush with the vertical face of the main part of the column. Shear friction reinforcement crossing such a crack would include the area A_s previously determined and the area A_h below it. The bars providing A_h are placed in the form of closed hoops, and also serve to confine the diagonal crack shown in Fig. 12.16*a*. The framing bars of Fig. 12.16*b* are usually of about the same diameter as the stirrups, and serve mainly to improve stirrup anchorage at the outer end of the bracket.

Because bracket dimensions are small, special attention must be paid to providing proper anchorage for all bars. The main tensile bars of area A_s must develop their full yield strength directly under the load V_u, and for this reason are usually anchored by welding to the bearing plate or angle.

Present ACI Code provisions for the design of brackets and corbels have been developed, mainly based on tests (Refs. 12.11–12.13). They apply to brackets and corbels with a shear span ratio a/d of 1.0 or less (see Fig. 12.16*a*). The distance d is measured at the column face, and the depth at the outside edge of the bearing area must not be less than $0.5d$. The usual design basis is employed, that is, $M_u \le \phi M_n$ and $V_u \le \phi V_n$, and for brackets and corbels (for which shear dominates the design) ϕ is to be taken equal to 0.85 for all strength calculations.

The section at the face of the support must resist simultaneously the shear V_u, the moment $M_u = [V_u a + N_{uc}(h - d)]$, and the horizontal tension N_{uc}. Design for shear is based on the shear friction method of Section 12.4, and the total shear friction reinforcement A_{vf} is found by Eq. (12.4). The usual limitations that V_n must not exceed the smaller of $0.2f_c'A_c$ or $800A_c$ apply to the critical section at the support face. (For brackets, A_c is to be taken equal to the area bd according to the ACI Code.) Special ACI Code provisions introduce modifications for lightweight concrete.

An amount of steel A_f to resist the moment M_u can be found by the usual methods for flexural design. Thus

$$A_f = \frac{M_u}{\phi f_y (d - a/2)} \tag{12.6}$$

where $a = A_f f_y / 0.85 f_c' b$. An additional area of steel A_n must be provided to

resist the tensile component of force:

$$A_n = \frac{N_{uc}}{\phi f_y} \tag{12.7}$$

Thus, the total area required at the top of the bracket is

$$A_s = A_f + A_n \tag{12.8}$$

In addition, according to the ACI Code, the area A_s must not be less than

$$A_3 = \tfrac{2}{3}A_{vf} + A_n \tag{12.9}$$

An additional restriction, that A_s must not be less than $0.04(f_c'/f_y)bd$, is intended to avoid the possibility of sudden failure upon formation of a flexural tensile crack at the top of the bracket. Closed-hoop stirrups having area A_h (see Fig. 12.16*b*) not less than $0.5(A_s - A_n)$ must be provided, uniformly distributed within two-thirds of the effective depth adjacent to and parallel to A_s.

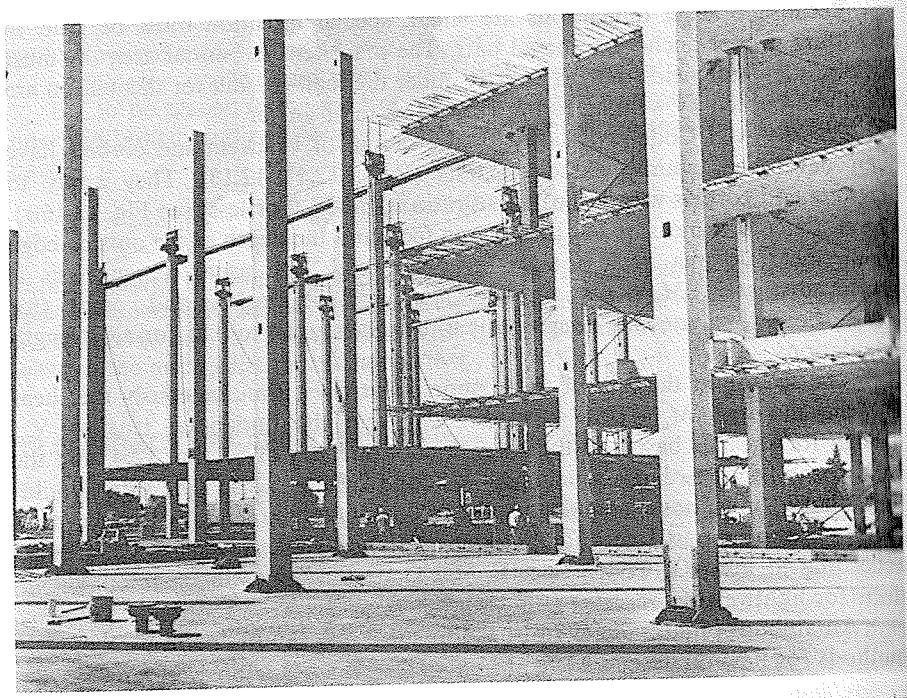

FIGURE 12.17 Construction of office building for Douglas Aircraft Company in Long Beach, California using lift-slab method. To facilitate lifting, each floor was divided into eight sections of about 12,000 ft^2 each. Courtesy of Post-Tensioning Institute.

12.6 LIFT-SLAB CONSTRUCTION

A form of on-site precast construction that has been widely exploited employs what is known as the lift-slab technique. An example is shown in Fig. 12.17. A casting bed, often doubling as the ground floor slab, is poured, columns are erected and braced, and at ground level successive slabs, which will later become upper floors, are cast. A membrane or sprayed parting agent is laid down between successive pours so that each slab can be lifted in its turn. Jacks placed atop the columns are connected to threaded rods extending down the faces of the columns and connecting, in turn, to lifting collars embedded in the slabs.

Columns may be steel or concrete. Often tubular steel sections are used. When a slab is in its final position, shear keys are welded to the column to transfer vertical reactions from the slab.

Lift-slab construction almost invariably implies flat plate construction (see Section 10.9) with no beams, dropped panels, or column capitals, for obvious reasons. The slabs are normally post-tensioned using unbonded strand encased in plastic tubing.

Typically, slab-to-column connections in lift-slab buildings can transfer little moment, and so frame stability against lateral loads causing sway must be provided by other resisting elements. Stairwells, elevator shafts, and utility shafts may be used for this purpose.

12.7 STANDARD PRECAST BRIDGE SECTIONS

The precasting of bridge beams and girders is particularly advantageous because it permits the rapid erection of a bridge superstructure with little or no interference with the traffic passing below. For spans up to about 140 ft, it is common to cast the main structural elements in one piece, either in a precasting plant or in a temporary casting yard established at the construction site, then to lift these into position with truck cranes. Placed side-by-side, often with a deck slab cast in place and designed to act in a composite sense with the precast elements, such bridge girders provide low initial cost, minimum maintenance, and high quality through plant control of mixing, placing, and curing the concrete.

Figure 12.18 shows some of the precast beam sections that are used for pretensioned prestressed bridges with spans up to about 100 ft (Ref. 12.14).[1] The voided slabs of Fig. 12.18*a* are similar to solid slabs, but are cast with longitudinal cylindrical voids to reduce self-weight. The voids generally stop about 15 to 18 in. from the end of the spans. With depth h ranging from 15 to 21 in., and width b either 3 or 4 ft, these slabs can carry AASHTO HS20 loads on simple spans from about 20 to 50 ft. Side joints are formed to receive a grout that, when

[1]Section properties for these bridge sections will be found in Appendix A.

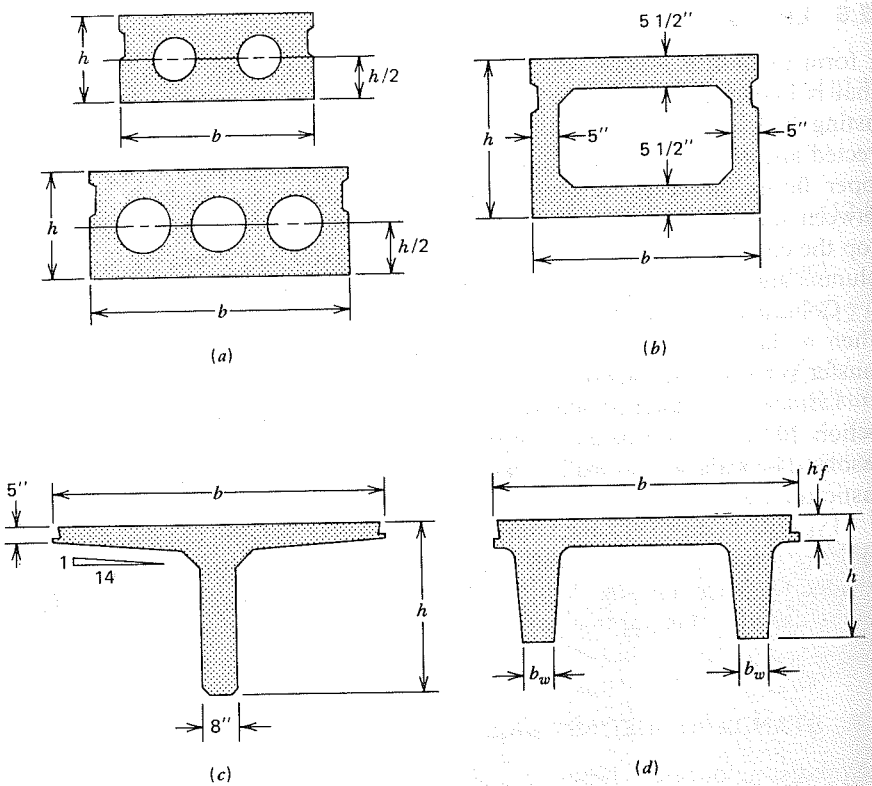

FIGURE 12.18 Typical cross sections used for precast prestressed short-span bridges. (*a*) Voided slabs. (*b*) Box beams. (*c*) Single-stemmed T-beams. (*d*) Double-stemmed channel beams.

hardened, locks adjacent slab sections together to prevent differential vertical movement.

The box beam section shown in Fig. 12.18*b* is widely used for spans from about 65 to 100 ft. The width is typically either 3 ft or 4 ft, and depth range from 27 to 42 in. Box sections are normally placed side-by-side, with side joints grouted, and often a composite slab is cast in place, bonding to the top surface of the precast units for composite action. Solid end blocks 18-in. long are used.

The single-stemmed T-beams of Fig. 12.18*c* are available with flange width *b* of 4, 5, or 6 ft, and in depths *h* from 24 to 51 in. They are normally placed side-by-side, with flange tips in contact, to form the roadway surface, usually with a slab cast in place over the T-beams. They are suitable, for simple spans, to carry AASHTO HS20 loads on spans to about 100 ft or more.

The double-stemmed channel beams shown in Fig. 12.18*d* are used for spans to about 60 ft. Standard widths are from 36 to 66 in., and depths range from 20

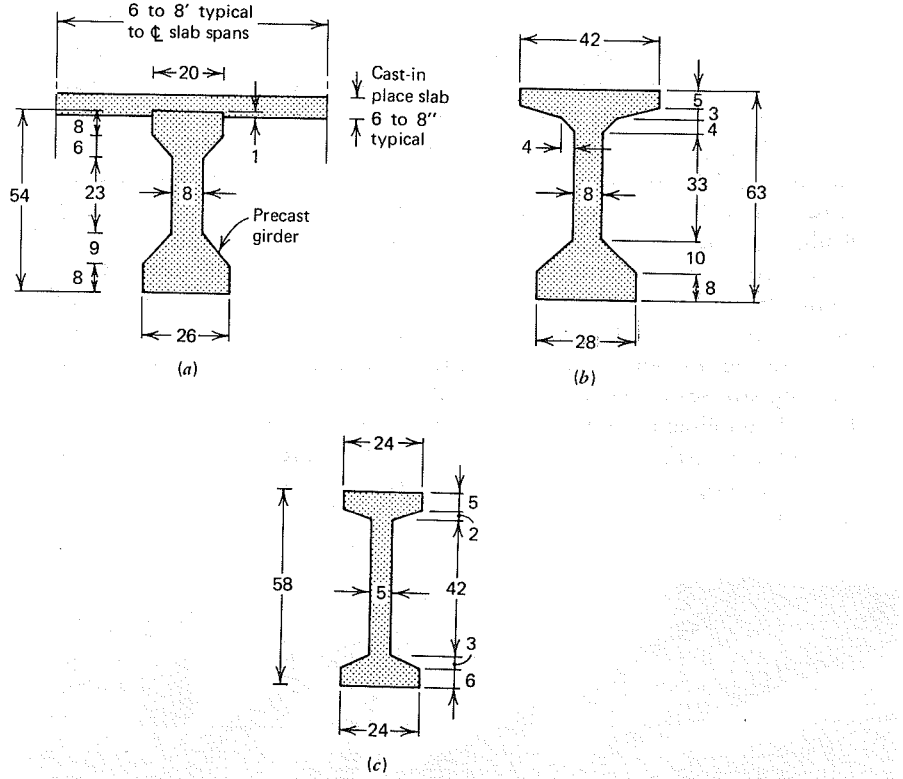

FIGURE 12.19 Precast bridge girder cross sections used on medium-span highway bridges (all dimensions inches or as noted). (*a*) AASHTO Type IV girder with slab. (*b*) AASHTO Type V girder. (*c*) Washington State standard bridge girder for 100-ft span.

to 35 in. in present practice. These sections, also, are generally used with a composite cast-in-place slab.

For longer spans, to about 140 ft, with HS20 loading, the AASHTO standard I-beams of Fig. 12.19*a* and 12.19*b* are widely used. Placed side-by-side at a spacing typically 6 to 10 ft, these beams provide support for temporary formwork to construct a cast-in-place deck slab 6 to 8-in. thick. The slab spans transversely, carrying wheel loads to the girders. In addition, composite action is developed in the main span direction between cast-in-place and precast section components, so that the slab provides the main part of the compression flange for the girders.

AASHTO girders of Types I, II, III, and IV have cross sections similar to the Type IV girder shown in Fig. 12.19*a*, with total depth respectively 28, 36, 45, and 54 in. They are best described as unsymmetrical I-beams. The large bottom flange

provides for heavy initial prestress force. They are suitable for spans from about 50 to 100 ft. For longer spans, to about 140 ft, the deeper sections of Type V and VI, similar to Fig. 12.19*b*, are more suitable. All six AASHTO sections represent somewhat inefficient sections with stocky proportions. They were developed some years ago when full prestressing (i.e., zero tensile stress at service load) was considered essential. Many states have now adopted more efficient members as standard, such as the I-beam of Fig. 12.19*c* adopted by the State of Washington.

Bridge girders may be pretensioned, with straight or deflected strands, post-tensioned, or prestressed using a combination of pretensioning and post-tensioning. When post-tensioning is used, a solid end block, of width equal to that of the narrower top flange and having length of three-quarters of the girder depth, is used to provide space for the end anchorages and to accommodate the high bearing stresses under the anchor plates.

Lateral diaphragms are used between bridge girders at the ends of the girders, and at midspan for spans to 80 ft or at the third points for spans above that. Section properties for standard AASHTO bridge girders are given in Appendix A.

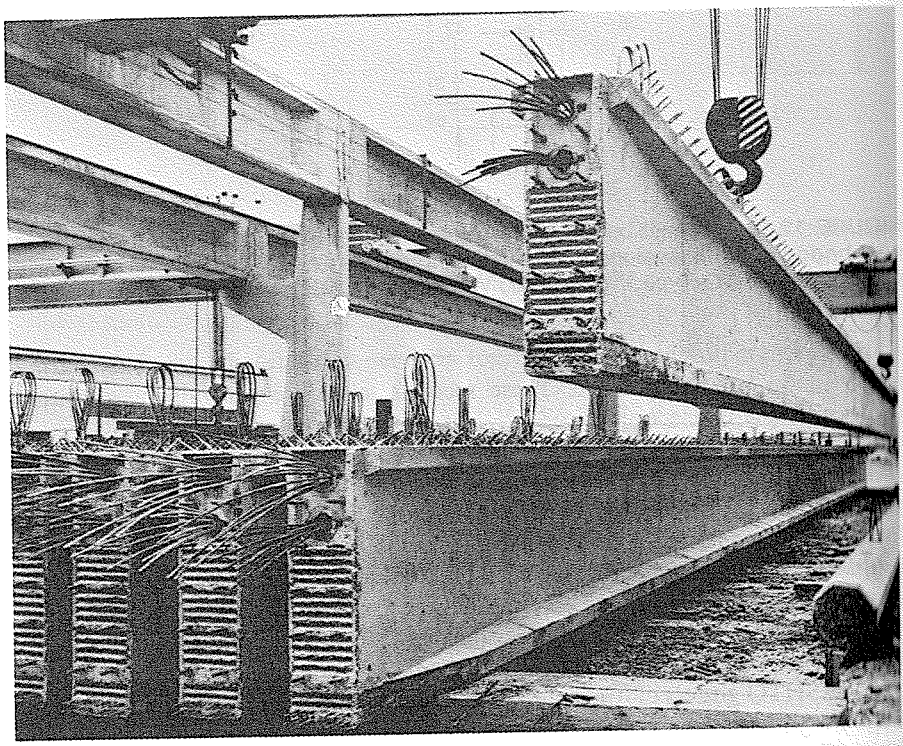

FIGURE 12.20 Standard highway girder, State of Washington. Courtesy of Concrete Technology Corporation, Tacoma, Washington.

Figure 12.20 shows a number of Washington State standard girders in a precasting yard. Note the reinforcing bar shear reinforcement extending upward for later embedment in the cast-in-place deck slab. The beam being lifted has one post-tensioning tendon stressed to facilitate handling the girder, and those on the ground to the left have both tendons stressed. In addition to the post-tensioning tendons, straight pretensioned strands were used in the bottom flanges. Note also the flared end block, used to provide room for the post-tensioning anchorages. The web width of the girders in the main part of the span is only 5 in., as shown in Fig. 12.19*c*.

12.8 SEGMENTALLY PRECAST BRIDGE CONSTRUCTION

One of the most important developments in structural concrete in the past two decades has been the use of prestressed box girders for medium and long span bridges. The Houston Ship Channel bridge shown in Fig. 12.21, opened to traffic in May 1982, is a fine example of this type of construction. The central span is 750 ft, and the side spans are 375 ft.

Such bridges are built segmentally, balanced cantilevers projecting from the piers and eventually meeting at midspan. The segments may be cast in place, or may be precast in a plant or casting yard and lifted into position. In either case, each segment is post-tensioned to the construction already in place, and after the midspan joint is made, continuous cables are stressed to provide full continuity.

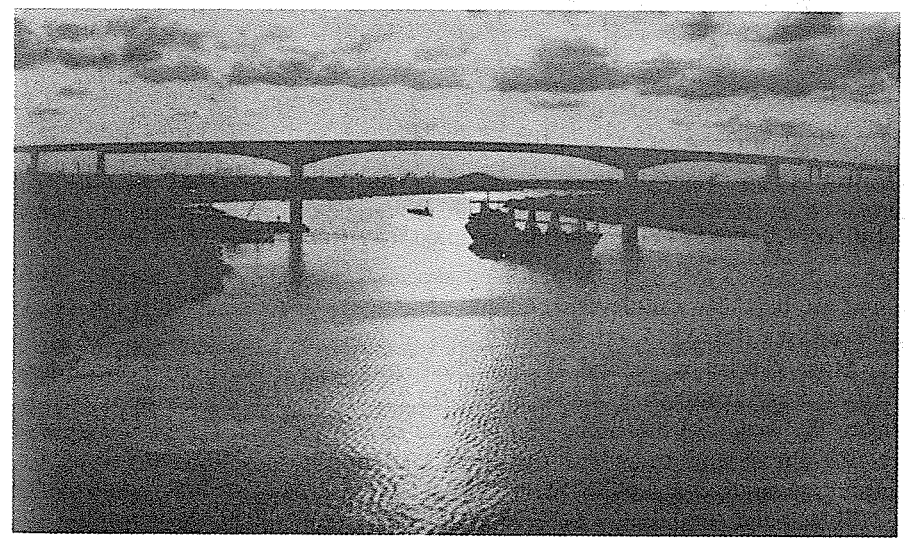

FIGURE 12.21 Houston Ship Channel bridge, with a 750-ft center span and 375-ft side spans. The box-girder depth varies from 47.5 ft at the piers to 15 ft at the centerline of the channel. Courtesy of Figg and Muller Engineers Inc.

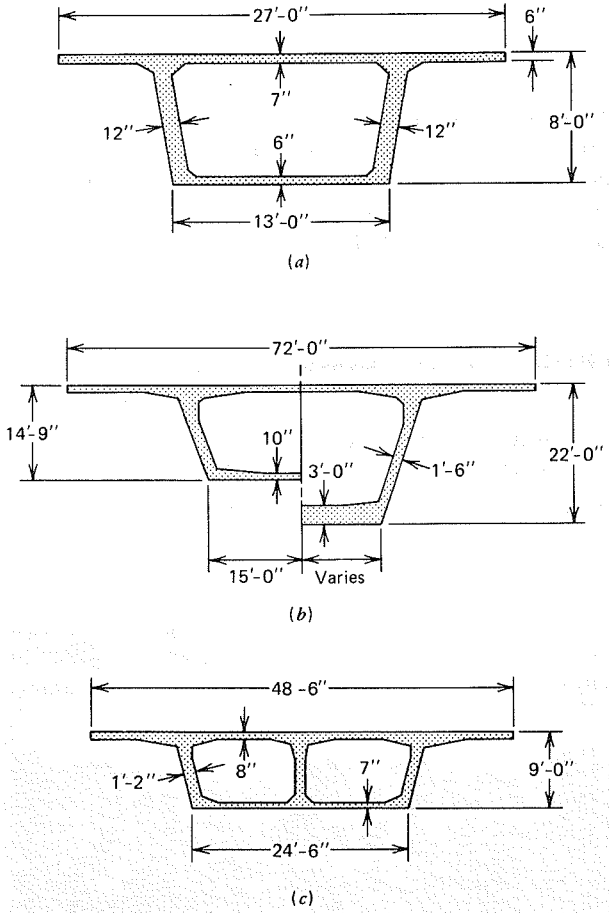

FIGURE 12.22 Typical cross sections of segmental concrete bridges. (*a*) Single-cell cross section of constant depth. (*b*) Single-cell cross section of variable depth. (*c*) Double-cell cross section. Adapted from Ref. 12.16.

Using the balanced cantilever technique, clear spans as long as 790 ft have been achieved (see Ref. 12.15, pp. 61–63).

Most precast segmental bridges have single or double-cell box girders. Typical cross sections are shown in Fig. 12.22. Cross sections are optimized to reduce the weight of individual segments, to reduce the cost of transporting and erecting them, and to reduce the dead load of the structure. Segments are normally from 6 to about 24-ft long (Ref. 12.16).

The use of prestressing for continuous box-girder bridges has extended the range of structural concrete far beyond what was thought possible just a few years ago. A technical description of some outstanding bridges of this type will be found in Ref. 12.17.

REFERENCES

12.1 *PCI Design Handbook*, 3rd edition, Prestressed Concrete Institute, Chicago, 1985.

12.2 Martin, L. D. and Korkosz, W. J., *Connections for Precast Prestressed Concrete Buildings*, Technical Report No. 2, Prestressed Concrete Institute, Chicago, March 1982.

12.3 Shemie, M., "Bolted Connections in Large Panel System Buildings," *J. PCI*, Vol. 18, No. 1, January–February 1973, pp. 27–33.

12.4 LaFraugh, R. W. and Magura, D. D., "Connections in Precast Concrete Structures —Column Base Plates," *J. PCI*, Vol. 11, No. 6, December 1966, pp. 18–39.

12.5 Raths, C. H., "Embedded Structural Steel Connections," *J. PCI*, Vol. 19, No. 3, May–June 1974, pp. 104–112.

12.6 Burns, N. H., "Development of Continuity Between Precast Prestressed Concrete Beams," *J. PCI*, Vol. 11, No. 3, June 1966, pp. 23–36.

12.7 Birkland, P. W. and Birkland, H. W., "Connections in Precast Concrete Construc tion," *J. ACI*, Vol. 63, No. 3, March 1966, pp. 345–368.

12.8 Mast, R. F., "Auxiliary Reinforcement in Precast Concrete Connections," *J. Structural Division, ASCE*, Vol. 94, No. ST6, June 1968, pp. 1485–1504.

12.9 Mattock, A. H. and Hawkins, N. M., "Shear Transfer in Reinforced Concrete—Recent Research," *J. PCI*, Vol. 17, No. 2, March–April 1972, pp. 55–75.

12.10 Mattock, A. H., "Shear Transfer in Concrete Having Reinforcement at an Angle to the Shear Plane," Special Publication SP-42, American Concrete Institute, Detroit, 1974, pp. 17–42.

12.11 Kriz, L. B. and Raths, C. H., "Connections in Precast Concrete Structures—Strength of Corbels," *J. PCI*, Vol. 10, No. 1, February 1965, pp. 16–47.

12.12 Mattock, A. H., Chen, K. C., and Soongswang, K., "The Behavior of Reinforced Concrete Corbels," *J. PCI*, Vol. 21, No. 2, March–April 1976, pp. 52–77.

12.13 Mattock, A. H., "Design Proposals for Reinforced Concrete Corbels," *J. PCI*, Vol. 21, No. 3, May–June 1976, pp. 18–24.

12.14 *Precast Prestressed Concrete Short Span Bridges—Spans to 100 Feet*, Prestressed Concrete Institute, Chicago, 1975.

12.15 Podolny, W. and Muller, J. M., *Prestressed Concrete Segmental Bridges*, John Wiley, 1982.

12.16 Wium, D. J. W. and Buyukozturk, O., *Behavior of Precast Segmental Concrete Bridges*. Research Report No. R84-06-766, Department of Civil Engineering, Massachusetts Institute of Technology, Boston, Massachusetts, May 1984.

12.17 Leonhardt, F., *Bridges*, Deutsche Verlags-Anstalt, Stuttgart, 1982.

THIRTEEN

APPLICATIONS

13.1 INTRODUCTION

Yves Guyon remarked many years ago that there is probably no structural problem to which prestress cannot provide a solution, and often a revolutionary one. The diverse applications of prestressed concrete described recently in the technical literature and in the general press confirm the truth of this observation. Prestressing is more than a technique; it is a general principle.

The members and structures that will be described in the following pages serve to illustrate the variety of engineering designs in which prestresssed concrete may be employed advantageously. Because of space limitations, specific applications will be described only in the most general terms. However, an extensive list of references is included, which will provide an entry into the literature for those seeking details.

13.2 BRIDGES

Prestressed concrete has proved to be technically advantageous, economically competitive, and esthetically superior for bridges, from very short span structures using precast standard components to cable-stayed girders and continuous box girders with clear spans of nearly 1,000 ft. Nearly all concrete bridges, even those of relatively short span, are now prestressed. Precasting, cast-in-place construction, or a combination of the two methods may be used. Both pretensioning and post-tensioning are employed, often on the same project.

In the United States, highway bridges generally must meet loading, design, and construction requirements of the AASHTO Specification (Ref. 13.1). A summary of the most important AASHTO provisions relating to loads on concrete bridge structures will be found in Ref. 13.2.

The design and construction of railway bridges are governed by provisions of the AREA Manual for Railway Engineering (Ref. 13.3). Design requirements for pedestrian crossings and bridges serving other purposes may be established by local, state, or regional codes. ACI Code provisions are often incorporated by reference, and in most cases, serve as model provisions for other governing documents.

A. SHORT SPAN BRIDGES

Bridge spans to about 100 ft often consist of precast integral-deck units such as described in Section 12.7 and shown in Fig. 12.18. Common cross sections include voided slabs, box beams, single-stemmed T-beams, and double-stemmed channel sections. These units offer low initial cost, and high-quality material and workmanship due to plant fabrication, fast and easy erection with little interference to traffic below, and very low maintenance. The pretensioned units are placed side-by-side, and are often post-tensioned laterally at intermediate diaphragms and at the ends of the span, after which shear keys between adjacent units are filled with nonshrinking mortar to insure that the completed structure will act in an integral sense under traffic. A cast-in-place topping slab is often placed over the precast units, bonding to their roughened top surface to provide for composite action in resisting live loads. An asphalt wearing surface may be applied directly to the top of the precast units, or, if a topping slab is used, over the cast-in-place slab.

Section properties for the precast units described in Chapter 12 will be found in Appendix A. In many cases, details and dimensions vary slightly depending on the precasting plant, and pretensioning is designed to suit the specific job requirements. Useful design information will be found in Ref. 13.4.

B. MEDIUM SPAN BRIDGES

For medium span (from about 80 to 140 ft) highway bridges some type of precast, pretensioned, I- or T-section girders have often proved to be most economical. The older standard AASHTO–PCI sections developed in the 1950s and early 1960s, as shown in Fig. 13.1*a* and Fig. 12.19, are still widely used, but have been shown to be inefficient compared with more slender sections (Ref. 13.5). Section properties for standard AASHTO–PCI girders of Types I through VI will be found in Appendix A. Many states have now adopted more slender, more efficient sections. Colorado uses the sections of Fig. 13.1*c*, and the State of Washington employs the four standard sections of Fig. 13.1*d*. The

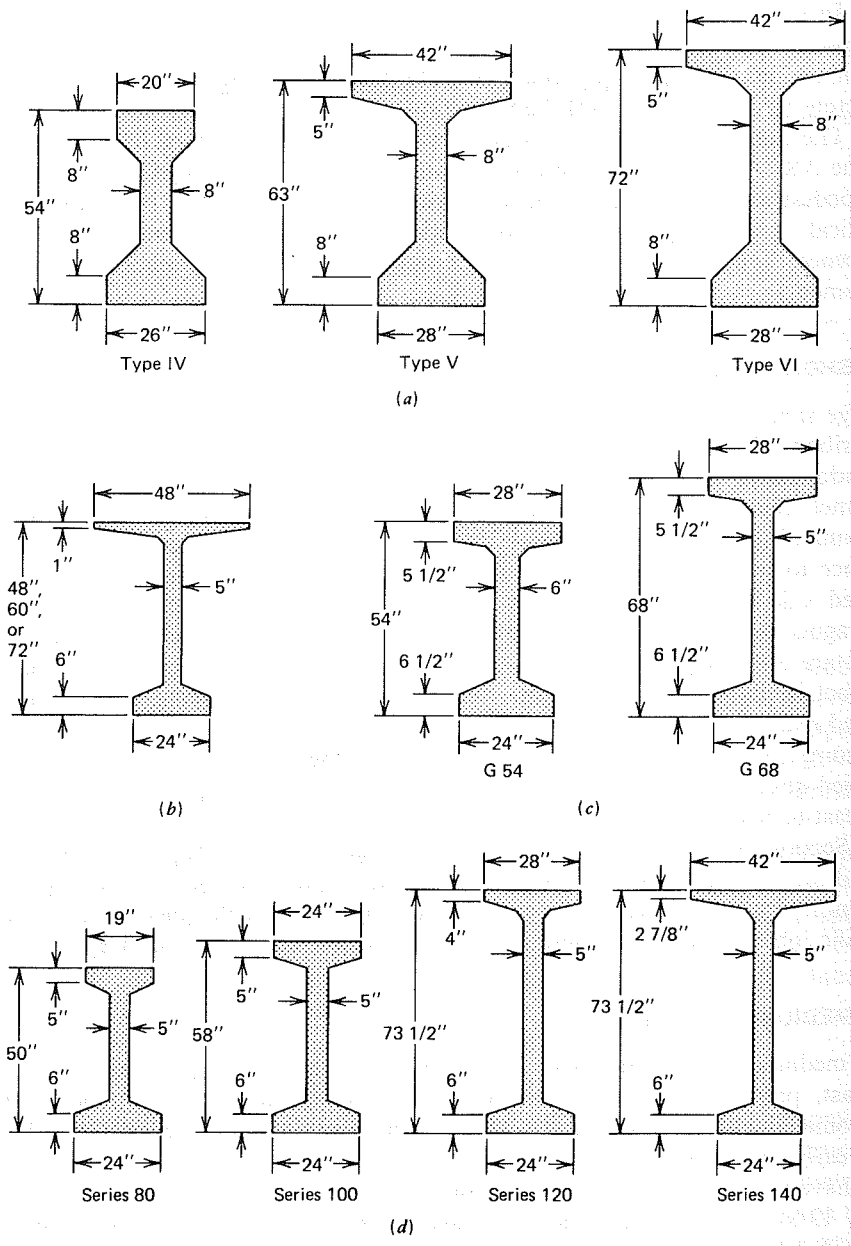

FIGURE 13.1 Standard sections for precast medium-span highway bridges. (*a*) AASHTO-PCI sections. (*b*) Bulb-T section. (*c*) State of Colorado standard girders. (*d*) State of Washington standard girders. All dimensions are in inches.

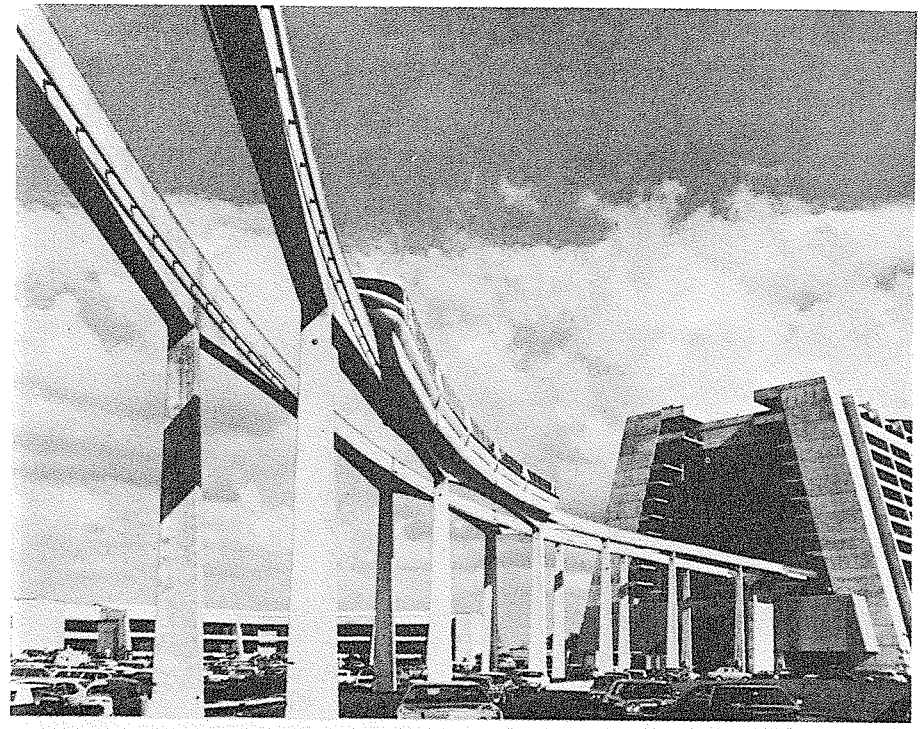

FIGURE 13.2 Walt Disney World Monorail. Courtesy of ABAM Engineers, Inc.

bulb-T of Fig. 13.1*b* is very efficient. Some modifications to further improve the girders shown in Fig. 13.1*b* through 13.1*d* are suggested in Ref. 13.5.

The precast girders shown in Fig. 13.1 are intended for use with a composite cast-in-place roadway slab, spanning laterally between parallel girders that are typically spaced at eight to ten ft. In some cases, these girders combine pretensioning of the precast girder, to carry self-weight and noncomposite dead load, with post-tensioning of the beam after the deck slab has hardened and composite action obtained.

The use of specially designed precast girders to carry a monorail transit system is illustrated in Fig. 13.2. The finished guideway features a series of segments, each consisting of six simply supported pretensioned precast beams, post-tensioned together to form a continuous structure. Typical spans are 100 to 110 ft. Approximately one-half of the 337 beams used have some combination of vertical and horizontal curvatures and variable superelevation. All beams are hollow, a feature achieved by inserting a styrofoam form inside the curved beams and using a moving mandrel in straight beam production.

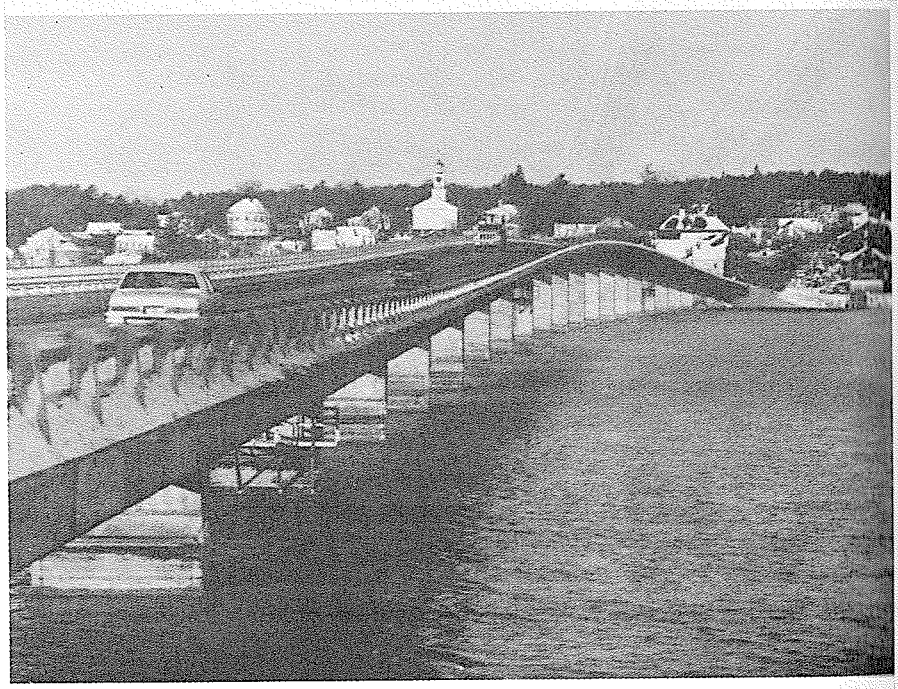

FIGURE 13.3 Continuous post-tensioned box girder bridge over the Sheepscot River at Wiscasset, Maine. Courtesy of the Maine Department of Transportation and Prestressed Concrete Institute.

Not all medium span bridges are precast in span-length girders. Figure 13.3 shows New England's first precast concrete segmental bridge. The award-winning design features 280 individual box-girder segments, weighing 38 tons each, cast in a plant 95 miles away and trucked to the site. After erection on temporary falsework, the segments were post-tensioned for continuity over the 2,719 ft total length.

Increasingly, to meet special requirements of alignment and grade, medium span crossings are cast-in-place, often using multiple-cell box section spans that are post-tensioned for full continuity. A particularly interesting structure of this type is shown in Fig. 13.4 and Fig. 13.5. No expansion joints were provided in the sharply curved structure. The deck is anchored at both abutments and is free to slide in any direction at all the intermediate piers, so that expansion or

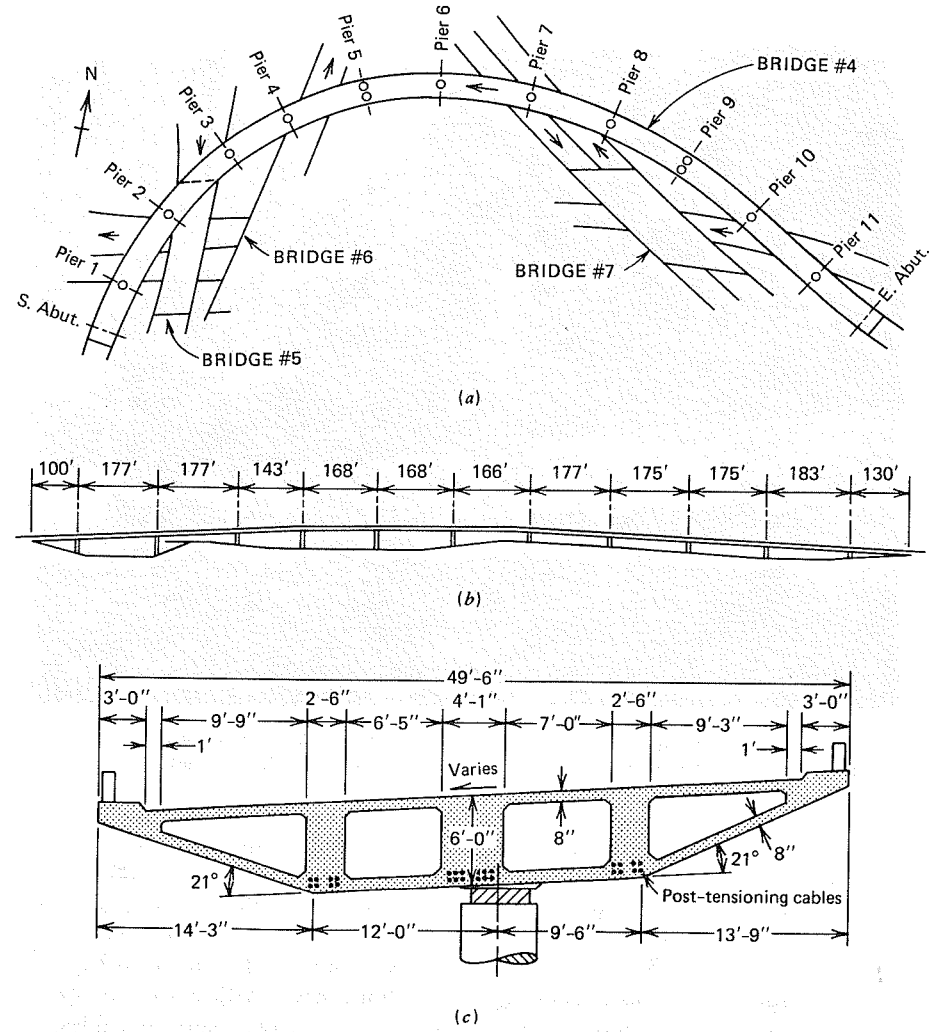

FIGURE 13.4 Highway 420/QEW interchange at Niagara Falls, Ontario. (*a*) Plan. (*b*) Elevation. (*c*) Deck cross section.

contraction is accommodated by flexing of the curved deck in the horizontal plane. Lateral forces due to wind, centrifugal, and earthquake loading can also be accommodated by bending of the deck and by compressive and tensile axial stresses similar to those in an arch. Only four torque-resisting supports are provided in the structure. These are located at each abutment and at two of the intermediate piers. Single-column supports are placed eccentrically with respect

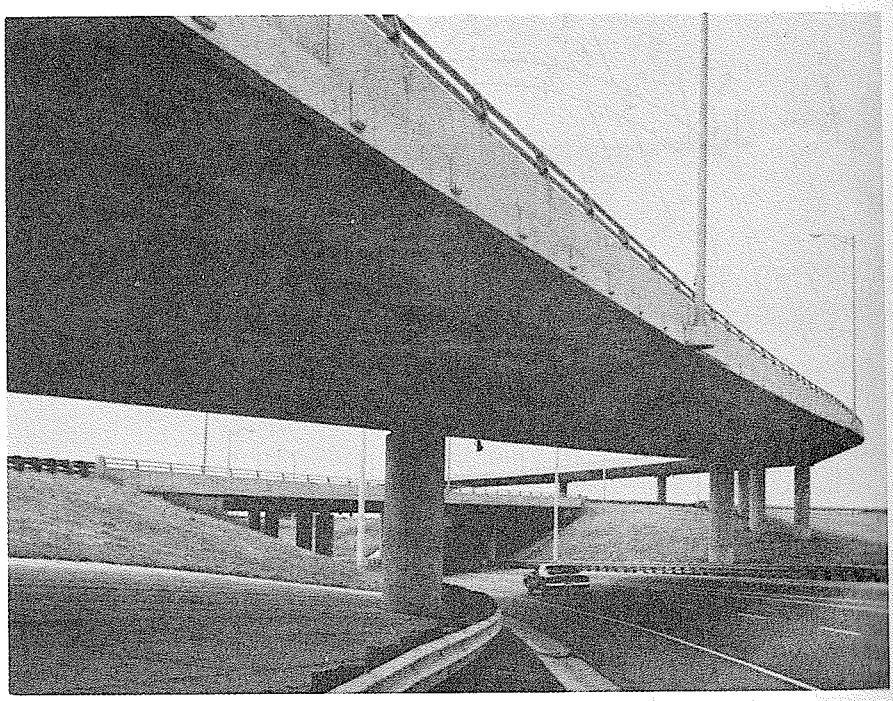

FIGURE 13.5 Highway 420/QEW interchange at Niagara Falls, Ontario. Courtesy of the Ministry of Transportation and Communications, Ontario, Canada.

to the longitudinal centerline of the deck to balance the torsional moments induced in the deck by the dead load and longitudinal prestressing (Ref. 13.6).

A type of bridge well-suited to light loads and medium to long spans is the stress-ribbon bridge, pioneered many years ago by the German engineer Ulrich Finsterwalder (Refs. 13.7 and 13.8). The stress-ribbon bridge shown in Fig. 13.6 carries a pipeline and pedestrians over the Rhone River with a span of 446 ft. The superstructure erection sequence was to (a) erect two pairs of cables, (b) place precast slabs forming a sidewalk deck and a U channel under each of the sets of cables, and (c) cast concrete in place in the two U's. The pipeline is placed off to one side atop supports at railing height, which greatly increases the critical wind speed of the structure (Ref. 13.9).

C. LONG SPAN BRIDGES

There is a clear trend toward the use of longer spans for bridges. Safety is improved by eliminating central piers for ordinary highway crossings, and by

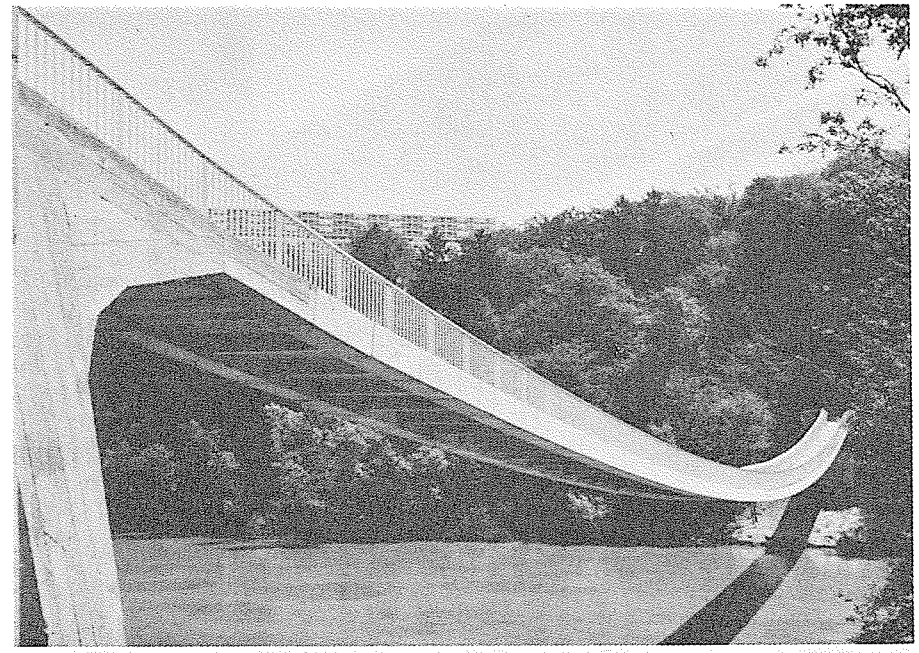

FIGURE 13.6 Stress-ribbon bridge of 446-ft span carrying pedestrian traffic and pipeline over the Rhone River near Lignon-Loex. Courtesy of *Civil Engineering*.

moving outer piers farther away from the edges of the roadway. Long spans facilitate traffic flow beneath elevated urban expressways and minimize obstruction to other activities. Concern for environmental damage led to the choice of elevated long spans for viaducts such as shown in Fig. 13.7. For river or ocean-bay crossings intermediate piers may be impossible because of water depths or navigational requirements, and very long spans may be required.

The need for such bridges led to the development in Europe, and further evolution in the United States, of two types of bridge structures that have dramatically increased the range of spans that can be attained with structural concrete. The first type is the segmental post-tensioned box girder bridge, and the second is the cable-stayed bridge.

Figure 13.8 shows the Houston Ship Channel Bridge under construction. Following the construction of the piers, the spans were cast segmentally using forms supported by the construction already completed. The construction proceeded in each direction by the balanced cantilever method, each segment being post-tensioned to the work already completed. Finally, after the closing joint was made in midspan, the structure was further post-tensioned for full continuity. The hollow-box cross section was prestressed transversely and vertically, in

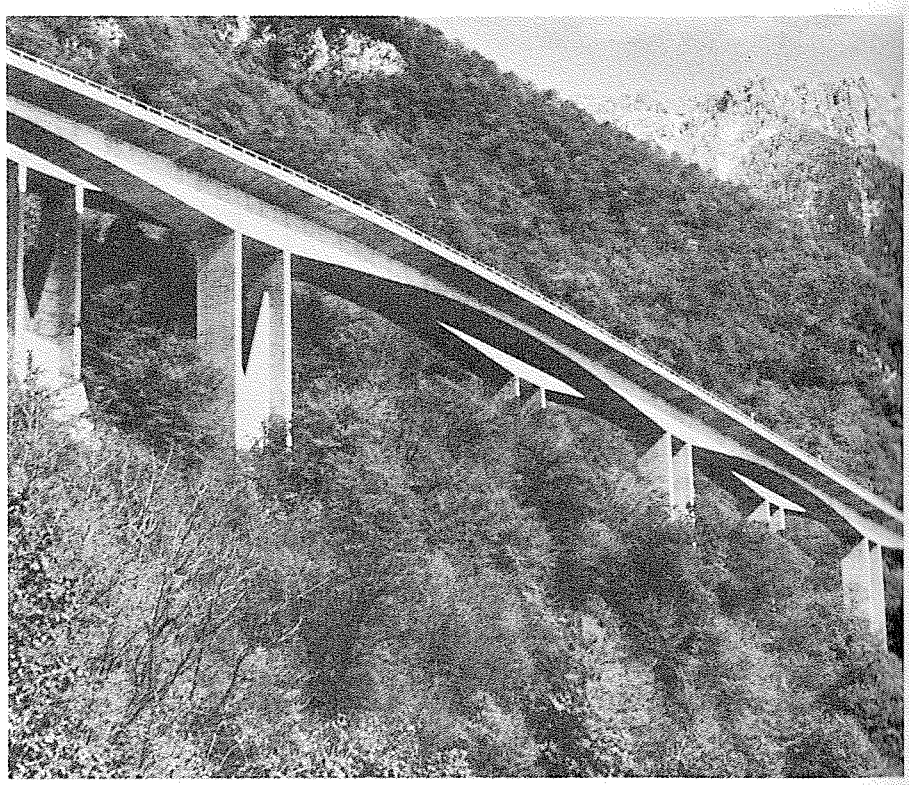

FIGURE 13.7 Chillon Viaduct at Lake of Geneva, Switzerland.

addition to the longitudinal post-tensioning. Figure 13.9 shows the completed structure, which presently (1986) holds the U.S. record with a clear span of 750 ft over the main channel. It ranks fifth in the world for clear span (Ref. 13.10).

The use of precast segments, up to about 20-ft long, is often seen in segmentally post-tensioned, long span bridges. A casting yard is established at the construction site or nearby, and the individual segments are transported to the bridge and lifted into position using cranes mounted on the already completed part of the structure. Special forms permit variable depth sections and variable wall thickness. Often, each unit is cast using the immediately preceding unit as an end form, thus ensuring near-perfect alignment. Shear keys may be used on the vertical faces between segments, and precast units are glued with epoxy to ensure proper transfer of vertical forces. (Refs. 13.11, 13.12, and 13.13).

The second type of prestressed concrete bridge used for very long spans is the cable-stayed girder bridge. An outstanding example is shown in Fig. 13.10. The Pasco–Kennewick Intercity Bridge has a clear span of 981 ft, flanked by two

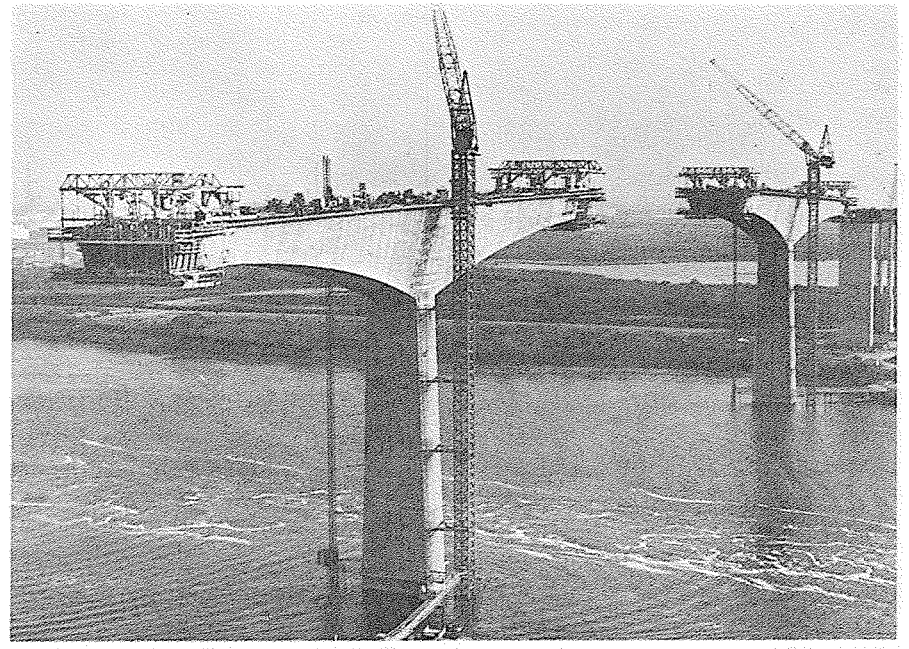

FIGURE 13.8 The Jesse H. Jones Memorial Bridge over the Houston Ship Channel, shown under construction using post-tensioned cast-in-place segments. Courtesy of Figg and Muller Engineers, Inc.

adjacent spans of 407 ft each. Typical precast girder elements were 80-ft wide and only 7-ft deep. The construction of bridges of this type is more complex than for the cantilever segmental bridges described previously, but they require less material and permit a shallower depth of construction below the roadway.

It is particularly appropriate in discussing bridge types and forms to mention the matter of structural esthetics. The time is past when structures could be designed solely on the basis of function, minimum cost, and technical advantages. Bridge structures, in particular, are exposed for all to see. To produce a structure that is visually offensive, as has occurred all too often in the past, must be considered an act of professional irresponsibility. Particularly for major spans, which may be in use for 100 years or more, architectural advice should be sought early in the conceptual stage of the design process, and close collaboration maintained throughout the work. To some extent, the judgment of what is esthetically pleasing and what is not must remain subjective. However, careful study of good bridges and bad can reveal certain principles that provide valuable guidance. Fritz Leonhardt, one of the world's leading designers of bridges of all

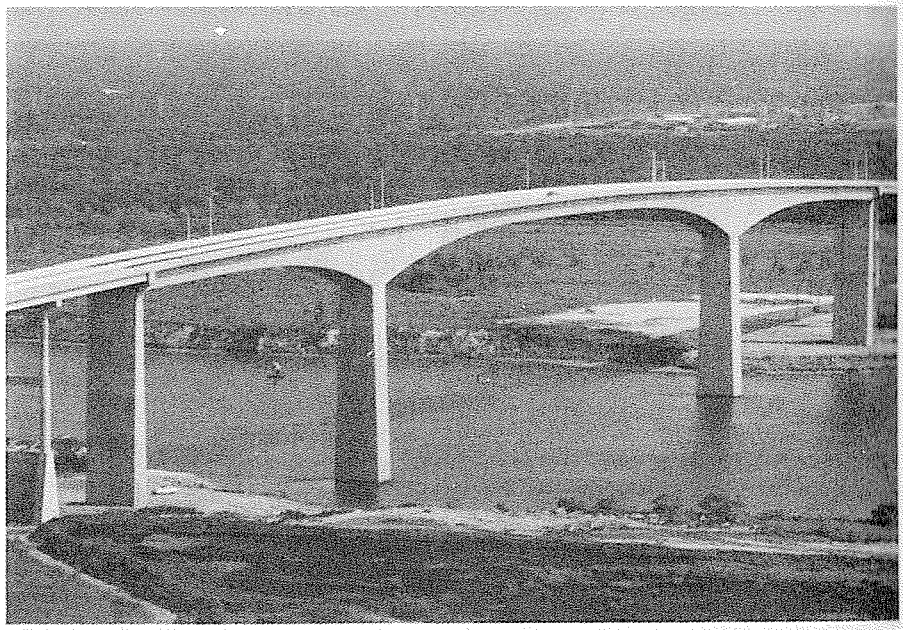

FIGURE 13.9 The completed Houston Ship Channel Bridge. The 750-ft main span is the longest for a segmentally constructed concrete bridge in the United States. Courtesy of Howard, Needles, Tammen and Bergendoff.

types, has published his views in the book *Bridges* (Ref. 13.14), a unique treatment of the subject of bridge esthetics that should be required reading for anyone contemplating work in this field.

13.3 SHELLS AND FOLDED PLATES

In a well-designed shell structure, the loads are for the most part resisted by membrane forces acting in the plane tangent to the shell surface at any point. Principal tensile stresses, where they exist, are likely to cause cracking in the concrete shell, and may adversely affect its performance. It is an obvious idea to cancel these tensile stresses by prestressing, and the optimum arrangement of the tendons is along the lines of the principal tensile stress trajectories.

Advantages of shell prestressing are important. By avoiding cracking at the service load stage, the shell more nearly satisfies the assumption usually made in analysis that the structure is uncracked and elastic. By prestressing, deflections may be minimized with the result that secondary stresses are avoided. Required steel is more conveniently placed in the form of high-tensile tendons than ordinary bar reinforcement. Not only are steel areas smaller, and thus more easily

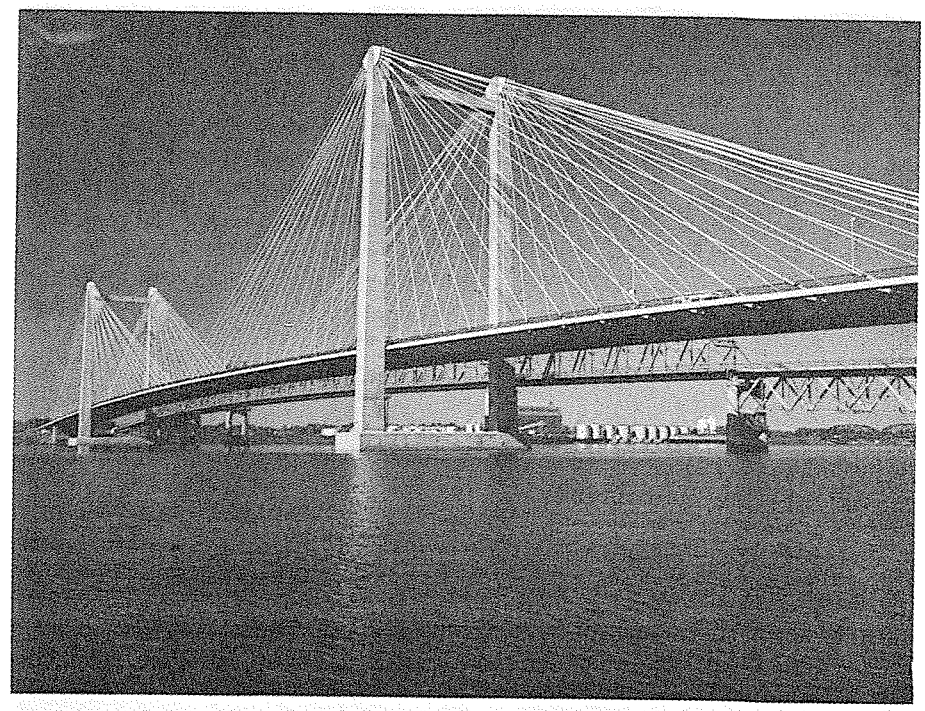

FIGURE 13.10 The Pasco–Kennewick Intercity Bridge, Pasco, Washington. Courtesy of Arvid Grant and Associates, Inc.

accommodated within the usually small thickness of the shell, but full-length reinforcement is possible without the need for bar splices, which are often a source of trouble when heavy reinforcing bars are used.

Concrete shells such as the hyperbolic paraboloids shown in Fig. 13.11 resist their loads mainly by membrane stresses, although in certain regions, such as near the projecting tips and near the edge beams, bending moments are significant. Prestressing tendons are used to cancel the membrane tensile stresses that act in the direction of the concave-upward parabolic curvature and serve to minimize deformation of the loaded shell, thus reducing the secondary bending of the shell surface.

Concrete folded plate roofs, which may be regarded as prismatic shells, have also been prestressed to good advantage. The folded plate roof shown in Fig. 13.12 spans 125 ft between end frames and carries the second floor from a system of cable hangers, as well as ordinary roof loads. Much longer spans are possible (Ref. 13.15). In folded plate roofs, the loads are first carried by the flat surface spanning laterally between fold lines. Ordinary bar reinforcement is normally provided in this direction. Longitudinally, the plates span as deep girders

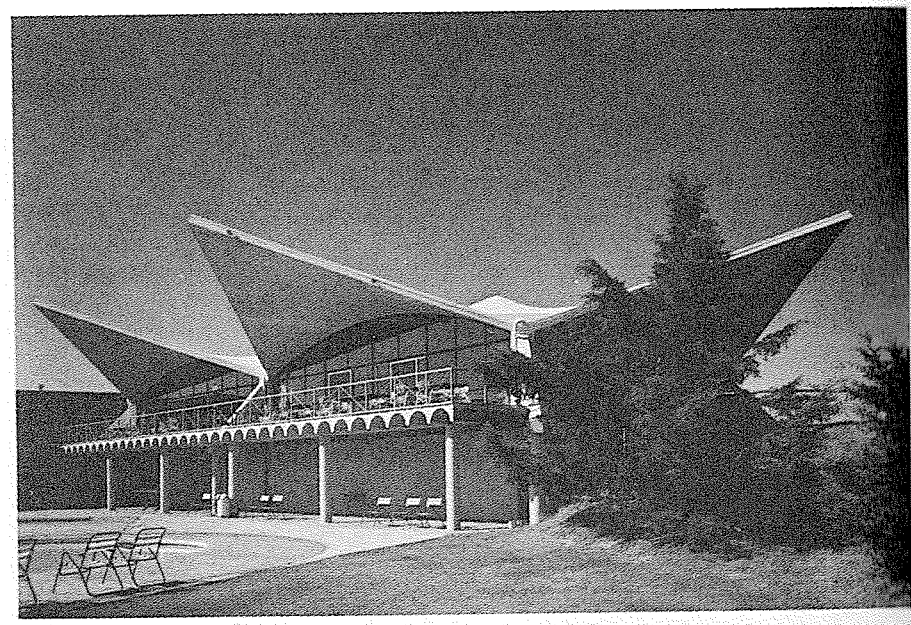

FIGURE 13.11 Concrete hyperbolic paraboloid shells.

FIGURE 13.12 Concrete folded plate roof structure.

between end walls or frames (see Fig. 13.12), and in this direction, draped post-tensioning strands may be used.

13.4 TRUSSES AND SPACE FRAMES

Prestressed concrete has not often been used for truss-type structures, but a few strikingly successful designs have been produced. The prestressing of axial tension members has been discussed in Chapter 11, and it was pointed out that not only can tensile stresses and cracking be avoided at service load, but the elongation when the member is loaded is very small compared with the elongation that would result if a steel member had been used. This great increase in stiffness has been used to good advantage for long span roof trusses.

Perhaps the most remarkable structure of this type is the aircraft service depot designed by A. J. and J. D. Harris Engineers for Transair, Ltd. at Gatwick, near London. A view of a part of the roof structure is shown in Fig. 13.13. Secondary "triangulated beams," or space trusses span 105 ft front-to-back of the hanger, and are carried across the front of the structure by a main beam, also triangulated, continuous on two 140-ft spans. Precast components making up the secondary trusses were assembled at ground level, then post-tensioned and hoisted into position. The main carrying beam was then made up in place by installing precast elements between the end frames of the secondary beams, after which the parabolic main cables were positioned and post-tensioned. Connections were detailed to be virtually free from bending to eliminate secondary stresses. The resulting structure is an inspiring example of the strength and elegance that can be achieved by a combination of precasting and prestressing (Ref. 13.16).

13.5 WATER STORAGE TOWERS

Elevated water storage tanks are a common feature of the skylines of both large and small communities. Too often they are designed solely based on utility and economics. Besides performing its function, a well-designed water tower can be an esthetic asset for any region. This fact is widely recognized in European countries, especially Sweden, Finland, and France (Refs. 13.17 and 13.18). A dramatic tower may become the symbol of a city and the source of great community pride.

It has been estimated that the exceptional esthetics of Finnish water towers, for example, add about 15 to 20 percent to their cost (Ref. 13.18). In many instances, the incremental expense may be at least partially recovered through the income from restaurants and observation decks incorporated in the design.

A fine example of the merging of function and esthetics is the 58-m high tower at Orebro in Sweden, seen in the photograph of Fig. 13.14 and shown in section in Fig. 13.15. The structure consists of a conical shell of 46 m external

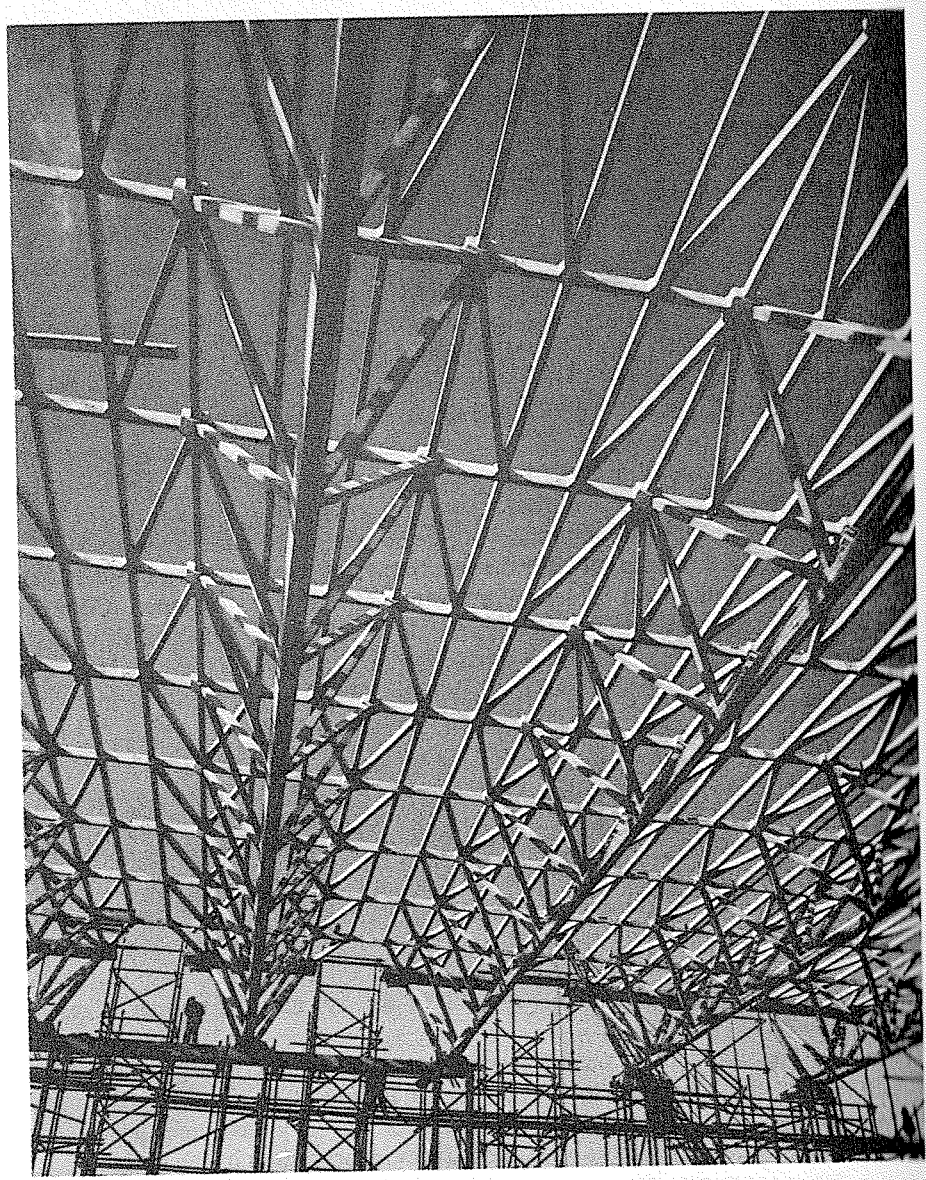

FIGURE 13.13 Prestressed concrete space frames for aircraft service depot at Gatwick, England. Courtesy of A. J. Harris, P. W. Abeles, and the Cement and Concrete Association.

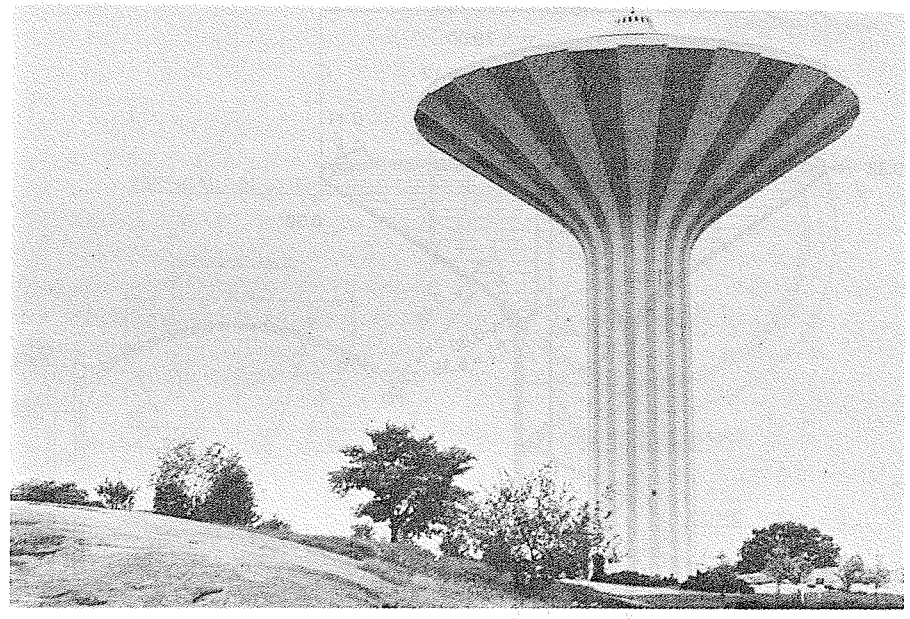

FIGURE 13.14 Water tower of 9,000 m^3 capacity at Orebro, Sweden.

diameter, supported on a tall shaft. Atop the tank itself is an observation platform covered by an umbrellalike conical shell. The shell of the main tank is circumferentially prestressed using 206 Freyssinet cables, each containing 12 wires of 7-mm diameter. Sixteen vertical ribs were provided for architectural reasons, and also serve to anchor the prestressing cables, each one of which extends halfway around the tank circumference. Typical of many such structures, the tank was cast at ground level and raised to its final position by hydraulic jacks placed on the circumference of the tower and fixed to the bottom face of the tank base ring. Construction of the tower proceeded as the tank was raised.

13.6 NUCLEAR CONTAINMENT VESSELS

The development of nuclear energy for electric-power generation has resulted in new applications for prestressed concrete. Two types of post-tensioned prestressed concrete reactor structures are used. In the first type, the complete pressure circuit embracing reactor and heat exchangers is placed within a prestressed concrete reactor vessel, always with massive concrete walls, placed in triaxial compression through post-tensioning. The second type of reactor structure is a containment vessel, designed to protect the environment from radioactive release in case in an accident to the plant. In this type of design, the reactor

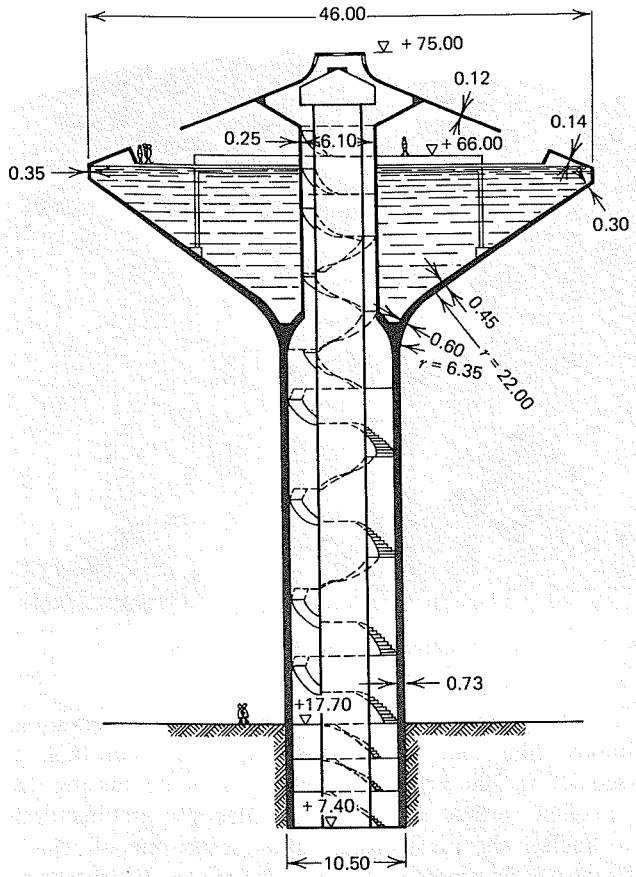

FIGURE 13.15 Section through the Orebro tower. Adapted from Ref. 13.17.

is contained in a steel pressure vessel connected by external ducts to heat exchangers. The complete system is then surrounded by the larger containment structure (Ref. 13.19).

A typical nuclear containment vessel of 40-m diameter and 54-m height is shown in Fig. 13.16. The shell is prestressed vertically and circumferentially in the cylindrical wall, and the dome is prestressed by tendons arranged at 120 degrees.

The circumferential or hoop prestressing force required for a typical secondary vessel is about 700 kips per foot. To apply this large force economically, post-tensioning tendons of much larger capacity than normal have been developed (Ref. 13.20).

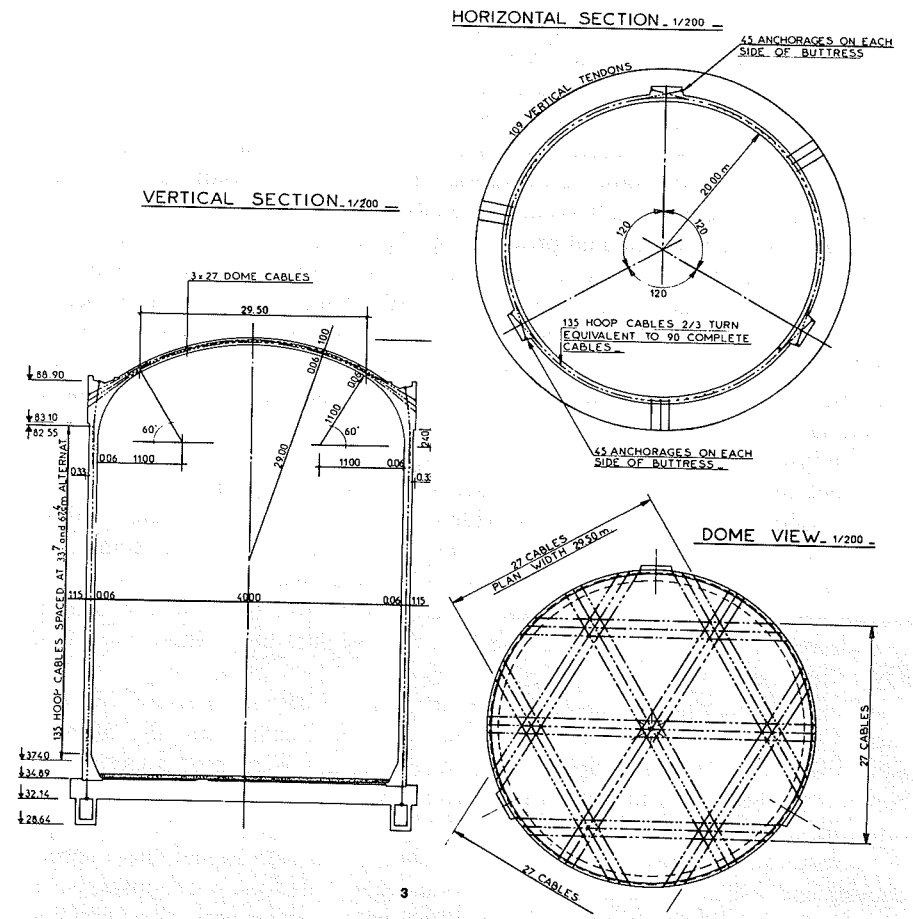

FIGURE 13.16 Nuclear containment vessel in Asco, Spain. Courtesy of Freyssinet International.

13.7 PAVEMENTS AND SLABS ON GRADE

Constantly increasing traffic volume and weight on concrete pavement slabs, both for highways and airports, call for improvement in pavement design and construction. Conventional pavements are designed on the basis of the concrete's low modulus of rupture; thus, the high compressive strength of the material cannot be utilized. When steel is included, it is intended to control and distribute cracking of the concrete, but not to eliminate it. On the other hand, experience indicates that pavement deterioration always starts at the cracks and transverse joints.

In longitudinally prestressed concrete pavements, fluctuating stresses resulting from passing wheel loads remain in the compressive range. Cracking is eliminated and transverse joints are decreased in number or eliminated completely, resulting in longer pavement life and smoother riding characteristics. In addition, costs may be reduced through reduction in slab thickness. Experience with experimental and prototype prestressed pavements has confirmed that they are practical and economically competitive (Refs. 13.21–13.27).

Techniques for longitudinal prestressing of pavements vary, but some details of a project in Pennsylvania are of interest (Ref. 13.23). Unbonded coated tendons of 0.68-in. diameter were used, placed 24 in. on centers and located slightly below the middle of the 6-in. thick slab. A slipform concrete paver was modified to feed the 12 tendons into the slab as it passed. Polyethelyne sheets were used on the base under the slab so the slab could contract during tensioning.

The typical length between transverse expansion joints was 600 ft. Four foot long blockouts at joint locations provided space for jacking the tendons, which were stressed to 46,000 lb each to provide compression in the concrete of about 320 psi. A typical joint detail, shown in Fig. 13.17, provides for the transfer of anchorage force from temporary anchors "A" to final anchors "B" after the 4-ft blockouts have been concreted. Anchors "C" provide for the dead end restraint of tendons in the next segment of slab. The expansion joint provided for a total movement of 3.5 in.

The resulting slab is expected to be virtually maintenance-free for 40 years, whereas conventional pavement requires heavy maintenance usually after 20 years. Compared with a competing design of ordinary reinforced concrete, the thickness of the pavement was reduced from 9 to 6 in., and the amount of steel was reduced 90 percent by weight.

Post-tensioning has been used for warehouse slabs on grade where special requirements call for a crack-free floor. Examples include food warehouses, where sanitary considerations require either filling of all cracks or their complete elimination, and storage warehouses subject to heavy traffic and large wheel

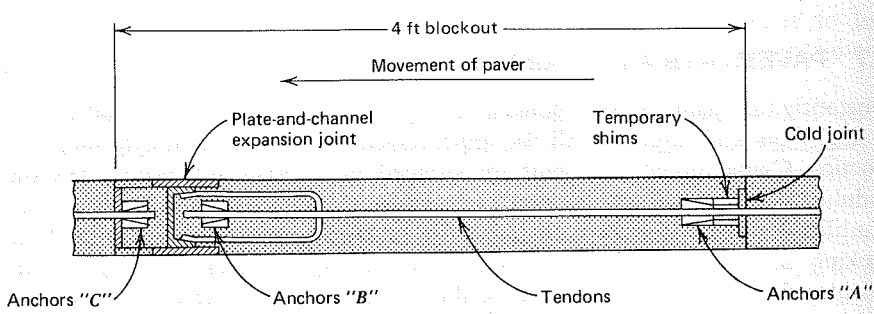

FIGURE 13.17 Prestressed concrete pavement. Adapted from Ref. 13.23.

loads, which can lead to progressive slab disintegration at cracks and joints. One prestressed slab was laid in strips about 15-ft wide and 300-ft long, with longitudinal prestressing using unbonded tendons in plastic sheathing and normal shrinkage steel in the perpendicular direction. Careful grading of the subbase was required, plus isolation of all slab penetrations and installation of a polyethylene slip sheet to reduce friction with the subbase. The end result was a slab entirely free of cracks. Two-dimensional post-tensioning has been used as well. In either case, the tendons are placed approximately at the middepth of the slab. Thickness up to 2 in. less than a normal reinforced slab has proved successful (Ref. 13.28).

13.8 MAT FOUNDATIONS

There are many instances where deep foundations such as concrete or steel piles, caissons, or large spread footings, may not be the best solution when coping with heavy loads on poor soils. Shallow post-tensioned concrete mats have been used successfully and economically under such conditions. Figure 13.18 shows a recent

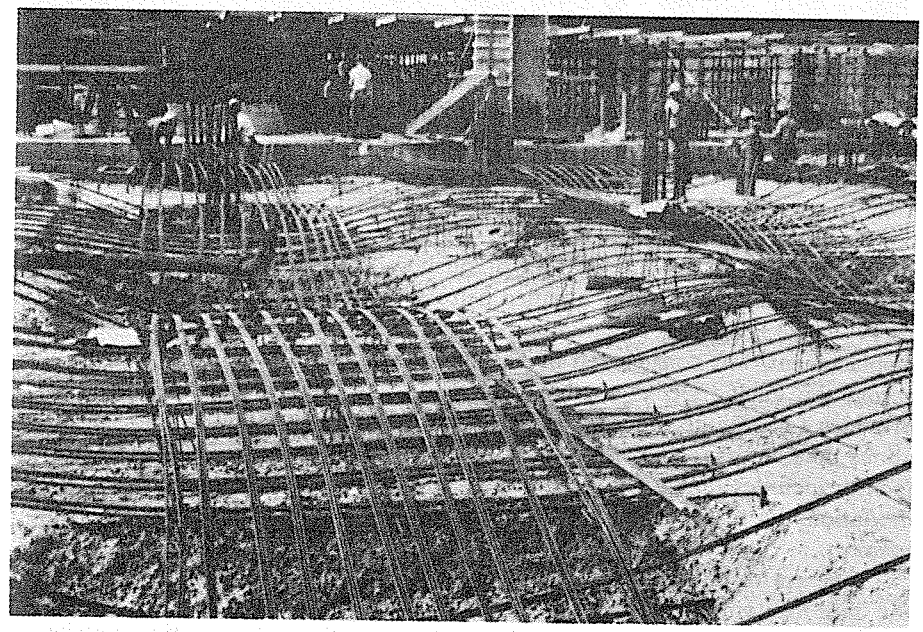

FIGURE 13.18 Post-tensioned foundation mat for the Executive Plaza in Springfield, Virginia. The tendon configuration is that of an inverted flat plate. Tendons are banded in one direction and distributed in the other. Courtesy of VSL Corporation.

example. The mat was designed according to the same methods used for flat plates and flat slabs (see Chapter 10). The mat had drop heads at the columns, formed by deepening the excavation slightly. The tendons used a parabolic shape, concave-downward, to provide a downward pressure between column locations to equilibrate the upward reaction of the soil. The design was based on load balancing. Tendons were banded along the column lines in one direction and distributed in the other (Ref. 13.29).

Advantages of this type of foundation include:

1. Low bearing pressure resulting from use of the total available bearing area.
2. Speed of construction achieved by eliminating all pile caps, grade beams, and so on.
3. Minimized differential deflection and avoidance of frame moments that might otherwise result.
4. Good resistance to hydrostatic uplift and water penetration.
5. Lower cost compared with alternative designs.

Such prestressed mats appear to be most suitable for foundations that have regular geometry (regular column grid and uniform elevation) on relatively soft soils, and for tall structures where column loads are large (Ref. 13.29).

13.9 MARINE STRUCTURES

Prestressed concrete has found frequent application in recent years in marine structures of all types. These range from routine seawall constructions to prestressed concrete tanker ships and the massive "Ekofisk" oil storage and tanker-loading caisson recently built in Norway and towed to its permanent location in the North Sea (Refs. 13.30, 13.31, and 13.32).

Indicative of the possibilities of offshore structures is the giant precast, prestressed concrete floating liquified petroleum gas (LPG) facility shown in Fig. 13.19 (Ref. 13.33). This remarkable structure of 461-ft total length and 65,000-ton displacement, was constructed in Tacoma, Washington, and towed 10,000 miles across the Pacific Ocean to the Ardjuna oil and gas field in the Java Sea. It provides for storage of liquified petroleum gas in 12 insulated steel tanks, six above deck and six below, having a total capacity of 375,000 barrels. The entire facility includes tanks, refrigeration machinery, an electric power plant, accommodations for a 50-person crew, crane service for maintenance, and lifeboats and heliport.

The entire hull structure was precast in segments. As shown in Fig. 13.20, the hull bottom is made of precast concrete shell segments (a), which are delivered to the graving dock (b). Vertical side shell and longitudinal bulkheads are cast in place (c). The partially completed hull is launched (d). When afloat, the lower six tanks are installed (e) and remaining hull concrete is cast in place

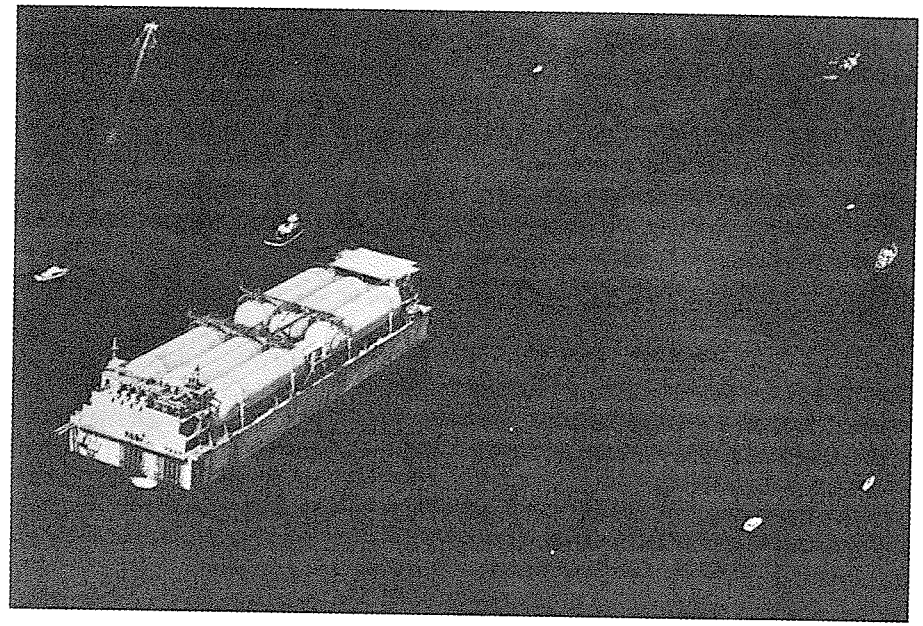

FIGURE 13.19 Floating liquified petroleum gas vessel being towed to its destination in Indonesia. Courtesy of ABAM Engineers and Concrete Technology Corporation.

(f). Finally, deck tank supports and tanks are installed (g). Precast elements were reinforced and provided with ducts for both longitudinal and transverse tendons. During assembly of the shell segments, each joint was coated with epoxy adhesive, after which the segment was promptly post-tensioned to its neighbor.

In comparing construction of prestressed concrete for the facility with an alternative design in steel, the following advantages were noted:

1. Lower initial construction cost.
2. Superior durability in sea water environment.
3. Ductile behavior when severely overloaded.
4. Freedom from damage under fatigue loading.
5. Excellent properties at extremely low temperatures.
6. Superior behavior when exposed to fire.
7. Ease of repair when damaged by collision.
8. Freedom from need for drydocking at regular intervals for inspection, repair, and maintenance.

Based on this pioneering venture, prospects for future development of offshore facilities using prestressed concrete are most favorable.

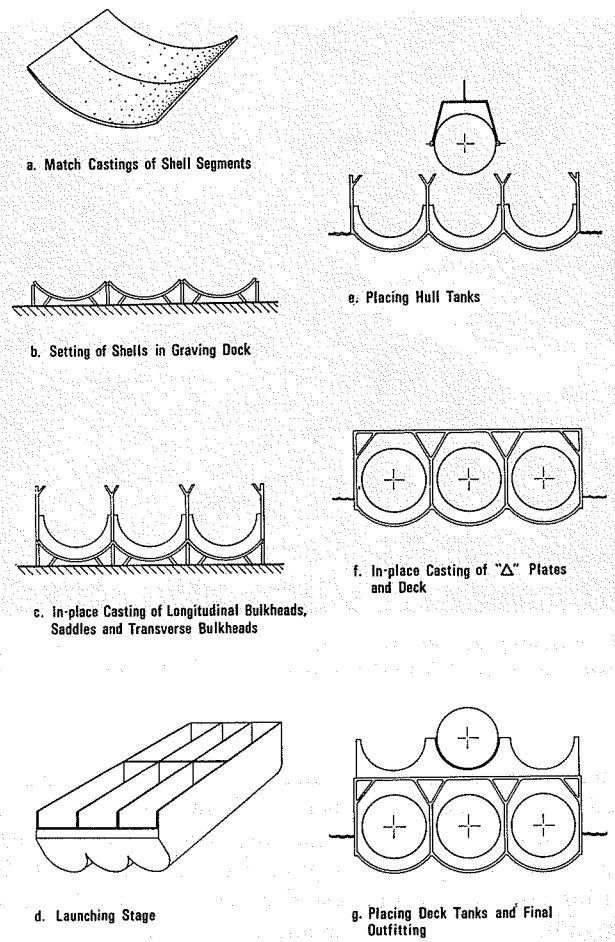

FIGURE 13.20 Construction sequence of floating LPG terminal. From Ref. 13.33.

13.10 MISCELLANEOUS STRUCTURAL ELEMENTS

A. PILING

Prestressed concrete has been used extensively for bearing and friction piles as well as for sheet piling, and offers the advantages of low cost and a high degree of permanence. Although they are primarily compression members, piles are subjected to tensile stresses caused by bending during lifting and placing, as well as in service and, in addition, must withstand tensile forces during driving. A prestress force producing axial compression of about 700 psi in the concrete is often used, almost always produced by pretensioning (Refs. 13.34, 13.35, 13.36).

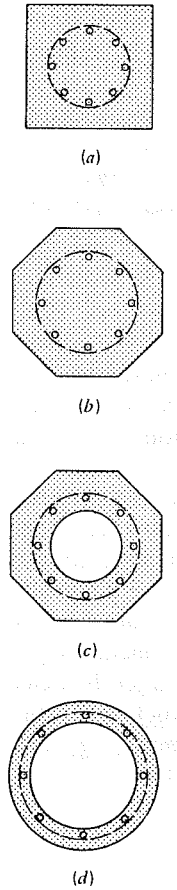

FIGURE 13.21 Typical prestressed concrete piling sections. (*a*) Square solid section. (*b*) Octagonal solid section. (*c*) Voided octagonal section. (*d*) Cylindrical section.

Typical foundation pile cross sections are shown in Fig. 13.21. The square solid section of Fig. 13.21*a* is economical for load ranges between about 60 and 80 tons. For loads to about 125 tons the octagonal pile of Fig. 13.21*b*, of 14 to 18-in. flat dimension, is more suitable. The voided octagonal pile of Fig. 13.21*c*, usually of 24 in. dimension, has been widely used for waterfront construction. Very large size cylindrical piles (Fig. 13.21*d*) of diameters 36, 54, and 60 in. have been employed for the supports for major bridge piers, and may develop capacities in excess of 800 tons.

When length requirements dictate, prestressed concrete piles may be spliced using non-prestressed reinforcing bars cast into the end of the upper section and thrust into grout-filled sockets provided in the next section.

Sheet piling (Ref. 13.37) is used to resist earth pressure or hydrostatic pressure through flexural resistance, and may also carry vertical loads. Water-

tightness, if required, is achieved through specially designed interlocking joints. The complete installation of such piling may also include horizontal support beams, backstays, and anchorages.

Prestressed concrete piles may be subjected to large bending and shearing forces as a result of seismic action, and they must possess sufficient strength and ductility to resist such effects. Recent analytical and experimental information has led to specific recommendations for prestressed, non-prestressed, and confinement reinforcement (Refs. 13.38 and 13.39).

B. ROCK AND SOIL ANCHORS

Where sheet pile walls or unstable rock formations must be anchored to firm subsoil or rock, prestressed anchors are suitable. The restraining force provided by the highly stressed ties places the exposed material in compression, preventing lateral displacement and slides.

A typical installation is shown in Fig. 13.22. The hole to receive the stressing rod is drilled in rock or augered into the soil, after which the prestressing rod, containing a core hole, is placed to full depth. High-strength grout is forced into the top under pressure, flowing out the base of the stressing rod and filling the drilled hole to a sufficient length to develop the tensile strength of the steel by bond. Deformed bars may be used to reduce the required development length, and in some cases, the base of the drilled hole may be belled to a larger diameter to further insure against pullout. After the wall has been constructed and the grout has achieved sufficient strength, the rod is stressed by post-tensioning jacks, and wedge anchorages or nuts placed at the bearing plate (Ref. 13.40).

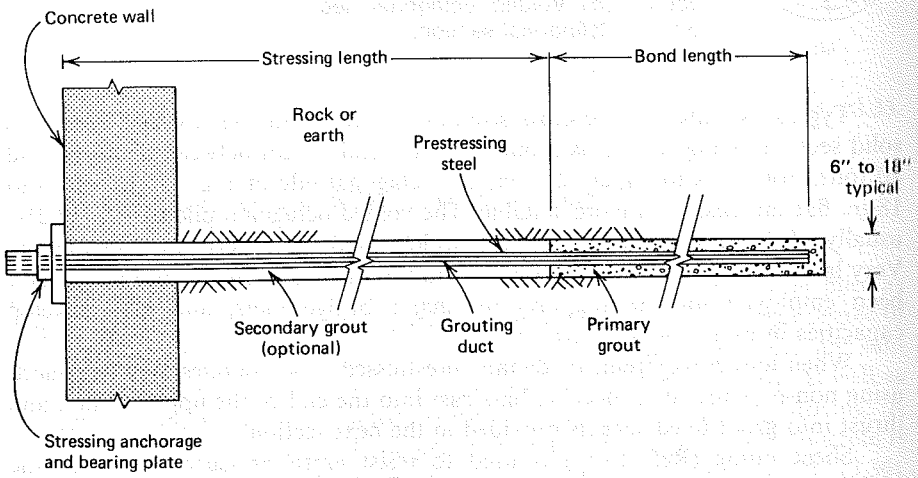

FIGURE 13.22 Prestressed rock anchor in drilled hole. Adapted from Ref. 13.41.

C. RAILROAD TIES

With the long-delayed, but much-needed reconstruction of the United States railroads, there appears to be a promising opportunity to rebuild substandard track using prestressed concrete ties or sleepers. These have been in use in Europe for several decades, and have proved both economical and practical (Refs. 13.41 to 13.44). Well over four million prestressed concrete ties are already in use in North America.

The design of such ties has been standardized by the Association of American Railroads. Although there are several alternative designs, the AAR Type I ties shown in Fig. 13.23 has been used most widely in United States construction. The top surface of the tie is flat to accept the indirect fixation rail

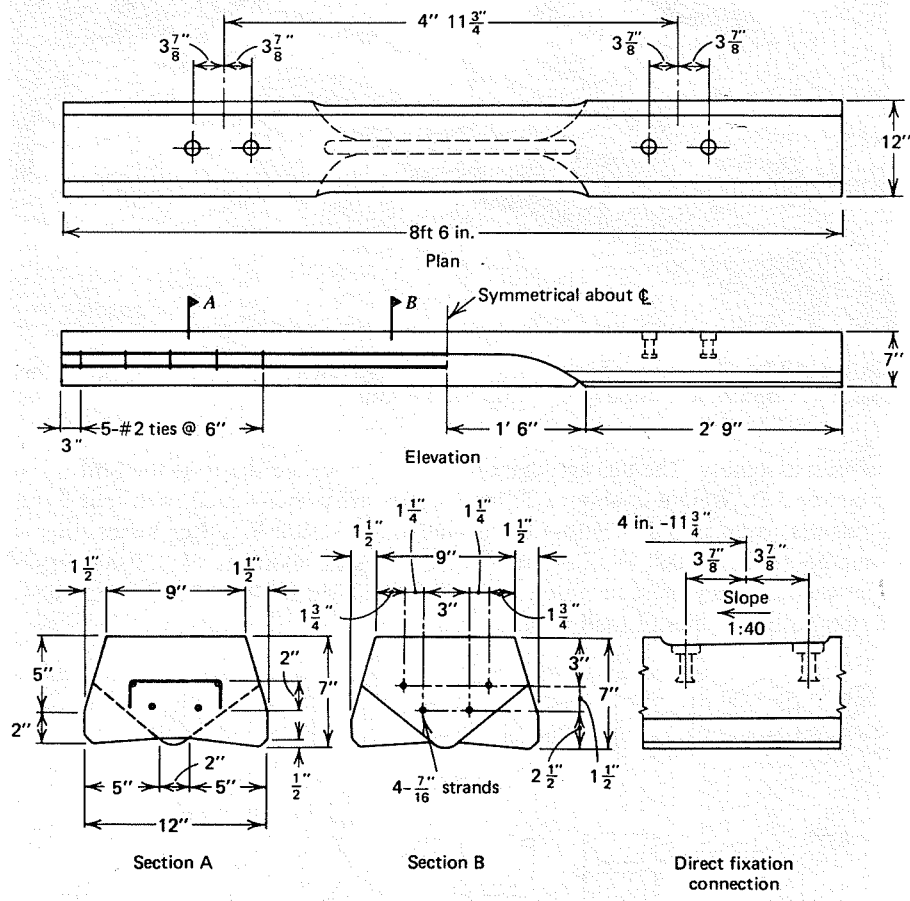

FIGURE 13.23 Prestressed concrete railroad tie, AAR Type E, Association of American Railroads.

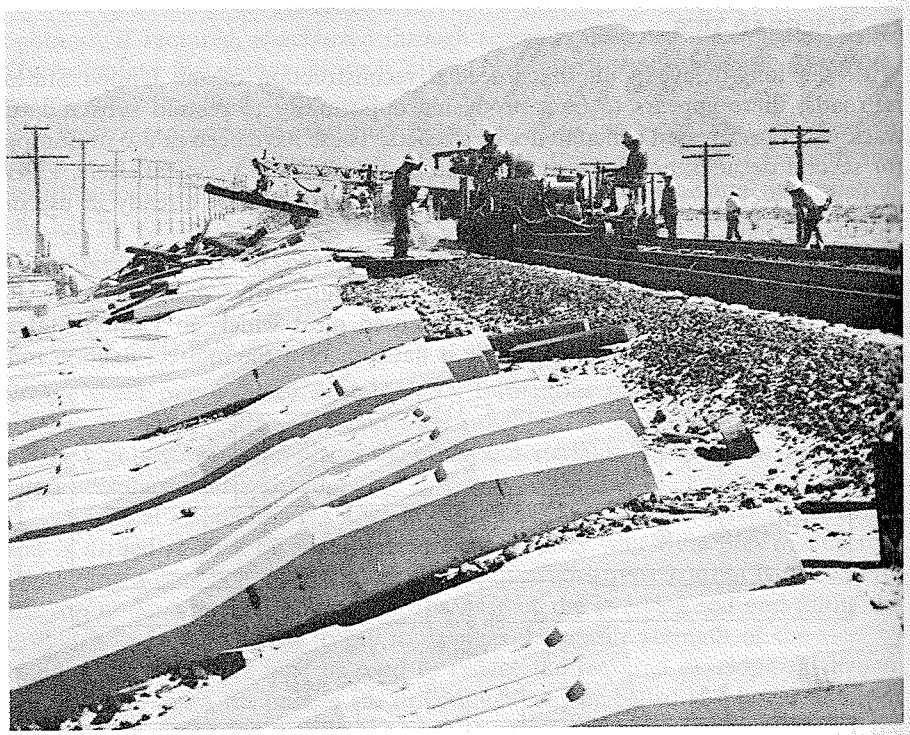

FIGURE 13.24 Prestressed concrete railway ties awaiting installation in a test project in California. Courtesy of Santa Fe Railway.

fastening assembly. The ties are characterized by a wedge shape at the bottom of the center 3 ft. Weight is about 620 lb. The ties are pretensioned with four 7/16 in. strands to an initial prestress force that totals 81,600 lb. After losses, this is estimated to be 69,000 lb. Designed for a cracking moment of 150,000 in.-lb under the rail, they must be able to withstand 200,000 in.-lb of bending moment for two million cycles of load without failure.

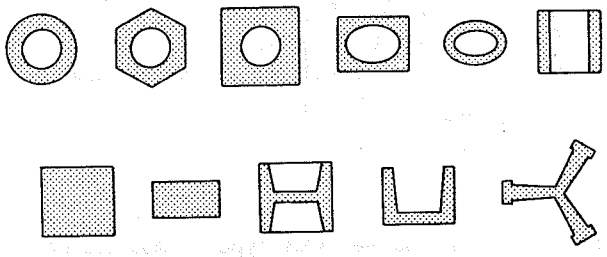

FIGURE 13.25 Typical cross sections of prestressed concrete poles. From Ref. 13.49.

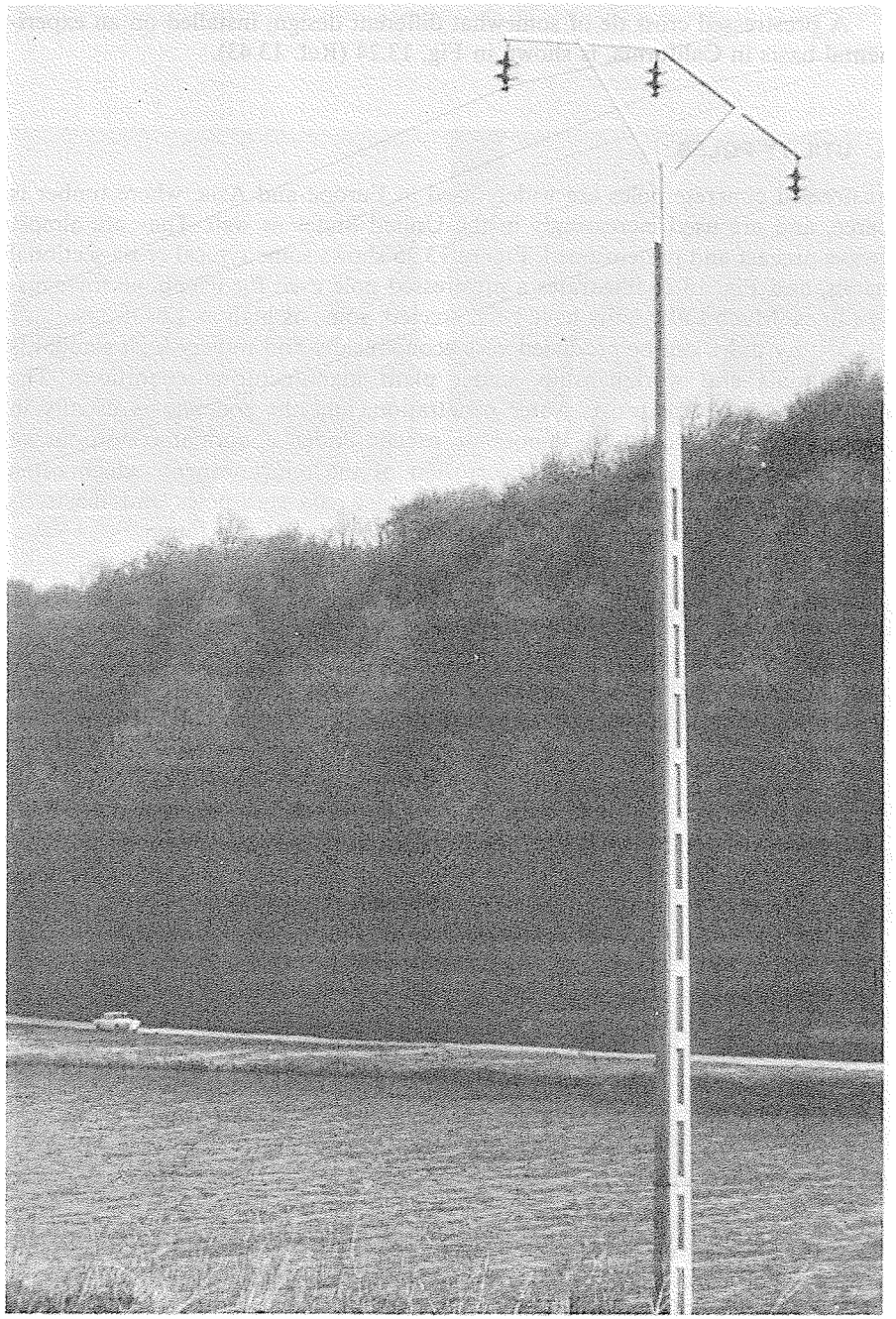

FIGURE 13.26 Prestressed concrete utility pole.

A prestressed cross tie of somewhat different design, installed on an experimental basis in California, is shown in Fig. 13.24 (Ref. 13.43).

D. UTILITY POLES

Prestressed concrete poles are widely used in Europe and Asia, where timber is scarce, and are used increasingly in the United States as well. They are almost always precast and pretensioned. Figure 13.25 shows some typical cross-sectional shapes, and Fig. 13.26 illustrates a prestressed pole used for telephone transmission lines. Much taller units have been erected, some as high as 120 ft.

Utility poles can be produced very economically and to very high standards of materials and workmanship, under plant manufacturing conditions. The high-quality concrete resists water penetration, and the concrete is usually in compression so cracking is impossible except under abnormal conditions of handling or service. As a result, corrosion of the reinforcement, which often causes spalling and disintegration of reinforced concrete poles and masts, is avoided. Prestressed poles are highly resistance to impact and fatigue.

FIGURE 13.27 CN Tower, Toronto, the world's tallest self-supporting structure at 1,815 ft. Courtesy of CN Tower Ltd.

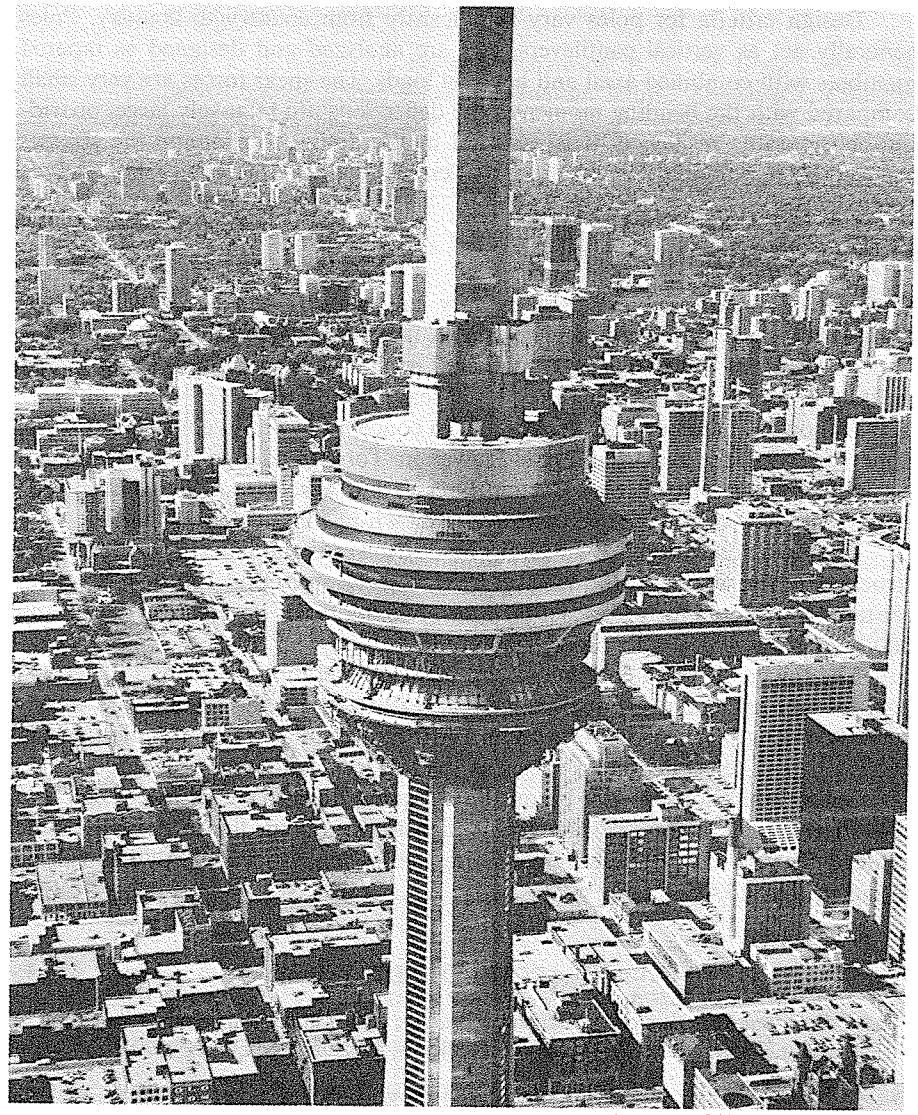

FIGURE 13.28 View of CN Tower at elevation 1,100 ft. The structure contains broadcast facilities, observation decks, and a revolving restaurant. Courtesy of CN Tower Ltd.

Pole elements must be designed to resist their own weight, dead loads from wire and attachments, ice, lateral forces from wind and from changes in alignment of wires, and longitudinal forces resulting from broken wires, stringing loads, unbalanced ice loading, loss of an adjacent structure, and unequal spans.

Design criteria for poles vary significantly from country to country. Poles generally act as vertical cantilevers, and are analyzed and designed as tapered members with combined axial and bending loads. The shear forces are very small compared with the bending moments; the deflections are relatively large, providing considerable resilience. It is essential in the design to examine the stresses induced by handling, transportation, and erection (Refs. 13.45 to 13.48).

13.11 TOWERS AND MASTS

The use of prestressed concrete in very tall towers to support restaurants, observation decks, and radio and television facilities originated in 1953 with the famous Stuttgart Tower designed by Fritz Leonhardt. With a total height of 211 m, that structure features a high-level 170-seat restaurant.

Although a number of towers similar in concept have been constructed since, none can rival the remarkable CN Tower in Toronto, designed for Canadian National Railways by Nicolet, Carrier, Dressel and Associates, Ltd. of Montreal. An overall view of the completed tower is shown in Figs. 13.27 and 13.28.

Having a total height of 1,815 ft, the CN tower is the tallest self-supporting structure in the world. At the 1,100 ft level, a seven-story pod 140 ft in diameter contains four floors for broadcast facilities, two floors for observation decks, and one floor for a 400-seat revolving restaurant.

The tower, cast in a continuous slip-forming operation, contains 150 vertical post-tensioning tendons. Some individual 1/2-in. diameter strands are nearly 1,500 ft in length. The mast rests on an 18-ft thick cellular raft foundation, which was itself post-tensioned in 16 stages as the tower construction proceeded.

Space limitations do not permit an adequate description of the design and execution of this landmark structure, which ranks among the most remarkable achievements of the structural engineering profession. Additional details will be found in Ref. 13.49.

REFERENCES

13.1 *Standard Specifications for Highway Bridges*, 13th edition, American Association of State Highway and Transportation Officials, Washington, D.C., 1983.

13.2 Nilson, A. H. and Winter, G., *Design of Concrete Structures*, 10th edition, McGraw-Hill, New York, 1986.

13.3 *Manual for Railway Engineering*, American Railway Engineering Association, Washington, D.C., 1978.

13.4 *Short Span Bridges: Spans to 100 Feet*, Prestressed Concrete Institute, Chicago, 1975.

13.5 Rabbat, B. G. and Russell, H. G., "Optimized Sections for Precast, Prestressed Bridge Girders," *Res. Develop. Bulletin RD080.01E*, Portland Cement Association, Skokie, Illinois, 1983.

13.6 Campbell, T. I., Francis, L. N., and Richardson, B. S., "A Long Curved Post-Tensioned Concrete Bridge Without Expansion Joints," *Canadian J. Civil Eng.*, Vol. 2, No. 3, 1975, pp. 262–269.

13.7 Finsterwalder, U., "Prestressed Concrete Bridge Construction," *J. ACI*, Vol. 62, No. 9, September 1965, pp. 1037–1046.

13.8 Wilson, A. J. and Wheen, R. J., "Direct Design of Taut Cables Under Uniform Loading," *J. Struct. Division, ASCE*, Vol. 100, No. ST3, March 1974, pp. 565–578.

13.9 "World's Top Prestressed Structures—1970 to 1974", *Civil Engineering*, Vol. 44, No. 8, August 1974, pp. 68–71.

13.10 "Concrete Box Girder Span Establishes U.S. Record," *Engineering News-Record*, January 7, 1982, pp. 22–25.

13.11 Podolny, W. and Muller, J. M., *Construction and Design of Prestressed Concrete Segmental Bridges*, Wiley, New York, 1982, 561 pp.

13.12 Schlaich, J. and Scheef, H., *Concrete Box Girder Bridges*, International Association for Bridge and Structural Engineering, Zurich, 1982.

13.13 Libby, J. R. and Perkins, N. D., *Modern Prestressed Concrete Highway Bridge Superstructures*, Grantville Publishing Co., San Diego, 1976.

13.14 Leonhardt, F., *Bridges*, Deutsche Verlags-Anstalt, Stuttgart, 1982.

13.15 Firnkas, S., "Prestressed Folded Plate Hanger for Allegheny Airlines—Design and Construction," *J. PCI*, Vol. 16, No. 2, March–April 1971, pp. 43–62.

13.16 Haines, W. J. M. and Harris, A. J., "Structure of Aircraft Service Depot at Gatwick for Transair Ltd." *J. PCI*, Vol. 4, No. 3, December 1959, pp. 46–60.

13.17 Leonhardt, F., *Prestressed Concrete Design and Construction*, 2nd edition, Wilhelm Ernst and Son, Berlin, 1964.

13.18 Klus, J. P. and Wortley, C. A., "Finns Emphasize Esthetics in Water Towers," *Civil Engineering*, Vol. 43, No. 9, September 1973, pp. 84–87.

13.19 *Prestressed Concrete in Nuclear Power*, Europe Etudes, Boulogne, France, 1974.

13.20 Schupack, M., "Large Post-Tensioning Tendons," *J. PCI*, Vol. 17, No. 3, May–June 1972, pp. 14–28.

13.21 Sargious, M. and Wang, S. K., "Economical Design of Prestressed Concrete Pavements," *J. PCI*, Vol. 16, No. 4, July–August 1971, pp. 64–79.

13.22 Huyghe, G. and Celis, R., "Joint-Free Experimental Prestressed Pavement," *J. PCI*, Vol. 17, No. 1, January–February 1972, pp. 58–72.

13.23 "Prestressed Concrete Pavement No Longer Seen as Experimental," *Engineering News-Record*, May 23, 1974, pp. 16–17.

13.24 "Prestressed Paving Design Advances," *Engineering News-Record*, September 24, 1981, pp. 16–17.

13.25 "Prestressing Gets and Chance," *Engineering News-Record*, October 27, 1983, p. 38.

13.26 "Prestressed Concrete Pavement: Status Report," *Civil Engineering*, Vol. 54, No. 12, December 1984, pp. 53–55.

13.27 *Prestressed Pavement*, Vols. 1, 2, and 3, Federal Highway Administration, Reports FHWA/RD-82/090, FHWA/RD-82/091, and FHWA/RD-82/092, June 1983.

13.28 Garber, G., "Post-Tensioning for Crack Free Superflat Floors," *Concrete Construction*, May 1983, pp. 396–400.

13.29 Cronin, H. J., "Post-Tensioned Foundations as Economical Alternative," *Civil Engineering*, Vol. 50, No. 3, March 1980, pp. 62–65.

13.30 Gerwick, Jr., B. C., "Concrete Structures: Key to Development of the Oceans," *J. ACI*, Vol. 71, No. 12, December 1974, pp. 611–616.

13.31 Moe, J., "Feasibility Study of Prestressed Concrete Tanker Ships," *J. ACI*, Vol. 71, No. 12, December 1974, pp. 617–626.

13.32 *Ekofisk Prestressed Concrete Oil Storage Caisson*, Europe Etudes, Boulogne, France, 1972.

13.33 Anderson, A. R., "World's Largest Prestressed LPG Floating Vessel," *J. PCI*, Vol. 22, No. 1, January–February 1977, pp. 12–31.

13.34 *PCI Design Handbook*, 3rd edition, Prestressed Concrete Institute, Chicago, 1985.

13.35 Goble, G. G., Fricke, K., and Likens, G. E., Jr., "Driving Stresses in Concrete Piles," *J. PCI*, Vol. 21, No. 1, January–February, 1976, pp. 70–88.

13.36 Anderson, A. R. and Moustafa, S. E., "Dynamic Driving Stresses in Prestressed Concrete Piles," *Civil Engineering*, Vol. 41, No. 8, August 1971, pp. 55–58.

13.37 Li, S. T. and Ramakrishnan, V., "Optimum Prestress, Analysis, and Ultimate Strength Design of Prestressed Concrete Sheet Piles," *J. PCI*, Vol. 16, No. 3, May–June 1971, pp. 60–81.

13.38 Sheppard, D. A., "Seismic Design of Prestressed Concrete Piling," *J. PCI*, Vol. 28, No. 2, March–April 1983, pp. 20–49.

13.39 Park, R. and Falconer, T. J., "Ductility of Prestressed Concrete Piles Subjected to Simulated Seismic Loading," *J. PCI*, Vol. 28, No. 5, September–October 1983, pp. 112–144.

13.40 *Recommendations for Prestressed Rock and Soil Anchors*, Post-Tensioning Institute, Phoenix, Arizona, 1980.

13.41 Weber, J. W., "Concrete Crossties in the United States," *J. PCI*, Vol. 14, No. 1, February 1969, pp. 46–61.

13.42 Kaar, P. H. and Hanson, N. W., "Bond Fatigue Tests of Beams Simulating Pretensioned Concrete Crossties," *J. PCI*, Vol. 20, No. 5, September–October 1975, pp. 65–80.

13.43 "Concrete Railway Ties Tested in California," *J. ACI*, Vol. 69, No. 3, March 1972, p. N5.

13.44 Hanna, A. N., "Prestressed Concrete Ties for North American Railroads," *J. PCI*, Vol. 24, No. 5, September–October 1979, pp. 32–61.

13.45 Rodgers, T. E., "A Utility's Development and Use of Prestressed Concrete Poles," *J. PCI*, Vol. 17, No. 3, May–June 1972, pp. 8–13.

13.46 "Guide Specification for Prestressed Concrete Poles," PCI Committee on Prestressed Concrete Poles, *J. PCI*, Vol. 27, No. 3, May–June 1982, pp. 18–29.

13.47 "Guide for Design of Prestressed Concrete Poles," PCI Committee on Prestressed Concrete Poles, *J. PCI*, Vol. 28, No. 3, May–June 1983, pp. 22–87.

13.48 Rodgers, T. E., "Prestressed Concrete Poles: State-of-the-Art," *J. PCI*, Vol. 29, No. 5, September–October 1984, pp. 52–103.

13.49 "Slipformed Tower Post-Tensioned to Record Height of 1,805 Ft," *Engineering News-Record*, May 23, 1974, pp. 18–20.

APPENDIX A

DESIGN AIDS

Table A.1 Properties of Prestressing Steels[a]

Seven-Wire Strand, $f_{pu} = 270$ ksi

Nominal Diameter (in.)	Area (sq in.)	Weight (plf)	$0.7\,f_{pu}A_p$ (kips)	$0.75\,f_{pu}A_p$ (kips)	$0.8\,f_{pu}A_p$ (kips)	$f_{pu}A_p$ (kips)
$\frac{3}{8}$(0.375)	0.085	0.29	16.1	17.2	18.4	23.0
$\frac{7}{16}$(0.438)	0.115	0.40	21.7	23.3	24.8	31.0
$\frac{1}{2}$(0.500)	0.153	0.53	28.9	31.0	33.0	41.3
$\frac{9}{16}$(0.563)	0.192	0.65	36.3	38.9	41.4	51.8
(0.600)	0.215	0.74	40.7	43.5	46.5	58.1

Seven-wire strand, $f_{pu} = 250$ ksi

Nominal Diameter (in.)	Area (sq in.)	Weight (plf)	$0.7\,f_{pu}A_p$ (kips)	$0.8\,f_{pu}A_p$ (kips)	$f_{pu}A_p$ (kips)
$\frac{1}{4}$(0.250)	0.036	0.12	6.3	7.2	9.0
$\frac{5}{16}$(0.313)	0.058	0.20	10.2	11.6	14.5
$\frac{3}{8}$(0.375)	0.080	0.27	14.0	16.0	20.0
$\frac{7}{16}$(0.438)	0.108	0.37	18.9	21.6	27.0
$\frac{1}{2}$(0.500)	0.144	0.49	25.2	28.8	36.0
(0.600)	0.215	0.74	37.6	43.0	53.8

Table A.1 (*Continued*)

Three- and Four-wire Strand, $f_{pu} = 250$ ksi

Nominal Diameter (in.)	Number of wires	Area (sq in.)	Weight (plf)	$0.7\,f_{pu}A_p$ (kips)	$0.8\,f_{pu}A_p$ (kips)	$f_{pu}A_p$ (kips)
$\frac{1}{4}$(0.250)	3	0.036	0.13	6.3	7.2	9.0
$\frac{5}{16}$(0.313)	3	0.058	0.20	10.2	11.6	14.5
$\frac{3}{8}$(0.375)	3	0.075	0.26	13.2	15.0	18.8
$\frac{7}{16}$(0.438)	4	0.106	0.36	18.6	21.2	26.5

Prestressing Wire

Diameter	Area (sq in.)	Weight (plf)	Ult. strength f_{pu}, (ksi)	$0.7\,f_{pu}A_p$ (kips)	$0.8\,f_{pu}A_p$ (kips)	$f_{pu}A_p$ (kips)
0.105	0.0087	0.030	279	1.70	1.94	2.43
0.120	0.0114	0.039	273	2.18	2.49	3.11
0.135	0.0143	0.049	268	2.68	3.06	3.83
0.148	0.0173	0.059	263	3.18	3.64	4.55
0.162	0.0206	0.070	259	3.73	4.26	5.33
0.177	0.0246	0.083	255	4.39	5.02	6.27
0.192	0.0289	0.098	250	5.05	5.78	7.22
0.196	0.0302	0.100	250	5.28	6.04	7.55
0.250	0.0491	0.170	240	8.25	9.42	11.78
0.276	0.0598	0.200	235	9.84	11.24	14.05

Smooth Prestressing Bars, $f_{pu} = 145$ ksi[b]

Nominal Diameter (in.)	Area (sq in.)	Weight (plf)	$0.7\,f_{pu}A_p$ (kips)	$0.8\,f_{pu}A_p$ (kips)	$f_{pu}A_p$ (kips)
$\frac{3}{4}$(0.750)	0.442	1.50	44.9	51.3	64.1
$\frac{7}{8}$(0.875)	0.601	2.04	61.0	69.7	87.1
1(1.000)	0.785	2.67	79.7	91.0	113.8
$1\frac{1}{8}$(1.125)	0.994	3.38	100.9	115.3	144.1
$1\frac{1}{4}$(1.250)	1.227	4.17	124.5	142.3	177.9
$1\frac{3}{8}$(1.375)	1.485	5.05	150.7	172.2	215.3

Table A.1 (*Continued*)

Smooth Prestressing Bars, $f_{pu} = 160$ ksi[b]					
Nominal Diameter (in.)	Area (sq in.)	Weight (plf)	$0.7 f_{pu} A_p$ (kips)	$0.8 f_{pu} A_p$ (kips)	$f_{pu} A_p$ (kips)
$\frac{3}{4}$(0.750)	0.442	1.50	49.5	56.6	70.7
$\frac{7}{8}$(0.875)	0.601	2.04	67.3	77.0	96.2
1(1.000)	0.785	2.67	87.9	100.5	125.6
$1\frac{1}{8}$(1.125)	0.994	3.38	111.3	127.2	159.0
$1\frac{1}{4}$(1.250)	1.227	4.17	137.4	157.0	196.3
$1\frac{3}{8}$(1.375)	1.485	5.05	166.3	190.1	237.6

Deformed Prestressing Bars						
Nominal Diameter (in.)	Area (sq in.)	Weight (plf)	Ult. strength, f_{pu} (ksi)	$0.7 f_{pu} A_p$ (kips)	$0.8 f_{pu} A_p$ (kips)	$f_{pu} A_p$ (kips)
$\frac{5}{8}$(0.625)	0.28	0.98	157	30.5	34.8	43.5
1(1.000)	0.85	3.01	150	89.3	102.0	127.5
1(1.000)	0.85	3.01	160	95.2	108.8	136.0
$1\frac{1}{4}$(1.250)	1.25	4.39	150	131.3	150.0	187.5
$1\frac{1}{4}$(1.250)	1.25	4.39	160	140.0	160.0	200.0
$1\frac{3}{8}$(1.375)	1.58	5.56	150	165.9	189.6	237.0

[a]Adapted from *PCI Design Handbook*, 3rd ed., Prestressed Concrete Institute, Chicago, 1985.
[b]Verify availability before specifying.

Table A.2 Designations, Areas, Perimeters, and Weights of Standard Reinforcing Bars

Bar No.[a]	Diameter (in.)	Cross-sectional area (in.^{2})	Perimeter (in.)	Unit weight per foot (lb)
3	$\frac{3}{8}$(0.375)	0.11	1.18	0.376
4	$\frac{1}{2}$(0.500)	0.20	1.57	0.668
5	$\frac{5}{8}$(0.625)	0.31	1.96	1.043
6	$\frac{3}{4}$(0.750)	0.44	2.36	1.502
7	$\frac{7}{8}$(0.875)	0.60	2.75	2.044
8	1(1.000)	0.79	3.14	2.670
9	$1\frac{1}{8}$(1.128)[b]	1.00	3.54	3.400
10	$1\frac{1}{4}$(1.270)[b]	1.27	3.99	4.303
11	$1\frac{3}{8}$(1.410)[b]	1.56	4.43	5.313
14	$1\frac{3}{4}$(1.693)[b]	2.25	5.32	7.650
18	$2\frac{1}{4}$(2.257)[b]	4.00	7.09	13.600

[a]Based on the number of eighths of an inch included in the nominal diameter of the bars. The nominal diameter of a deformed bar is equivalent to the diameter of a plain bar having the same weight per foot as the deformed bar.
[b]Approximate to the nearest 1/8 in.

Table A.3 Areas of Groups of Standard Reinforcing Bars (in.^{2})

Bar No.	Number of bars											
	1	2	3	4	5	6	7	8	9	10	11	12
4	0.20	0.39	0.58	0.78	0.98	1.18	1.37	1.57	1.77	1.96	2.16	2.36
5	0.31	0.61	0.91	1.23	1.53	1.84	2.15	2.45	2.76	3.07	3.37	3.68
6	0.44	0.88	1.32	1.77	2.21	2.65	3.09	3.53	3.98	4.42	4.86	5.30
7	0.60	1.20	1.80	2.41	3.01	3.61	4.21	4.81	5.41	6.01	6.61	7.22
8	0.79	1.57	2.35	3.14	3.93	4.71	5.50	6.28	7.07	7.85	8.64	9.43
9	1.00	2.00	3.00	4.00	5.00	6.00	7.00	8.00	9.00	10.00	11.00	12.00
10	1.27	2.53	3.79	5.06	6.33	7.59	8.86	10.12	11.39	12.66	13.92	15.19
11	1.56	3.12	4.68	6.25	7.81	9.37	10.94	12.50	14.06	15.62	17.19	18.75
14	2.25	4.50	6.75	9.00	11.25	13.50	15.75	18.00	20.25	22.50	24.75	27.00
18	4.00	8.00	12.00	16.00	20.00	24.00	28.00	32.00	36.00	40.00	44.00	48.00

Table A.4 Perimeters of Groups of Standard Reinforcing Bars (in.)

Bar No.	Number of bars											
	1	2	3	4	5	6	7	8	9	10	11	12
4	1.6	3.1	4.7	6.2	7.8	9.4	11.0	12.6	14.1	15.7	17.3	18.8
5	2.0	3.9	5.9	7.8	9.8	11.8	13.7	15.7	17.7	19.5	21.6	23.6
6	2.4	4.7	7.1	9.4	11.8	14.1	16.5	18.8	21.2	23.6	25.9	28.3
7	2.8	5.5	8.2	11.0	13.7	16.5	19.2	22.0	24.7	27.5	30.2	33.0
8	3.1	6.3	9.4	12.6	15.7	18.9	22.0	25.1	28.3	31.4	34.6	37.7
9	3.5	7.1	10.6	14.2	17.7	21.3	24.8	28.4	31.9	35.4	39.0	42.5
10	4.0	8.0	12.0	16.0	20.0	23.9	27.9	31.9	35.9	39.9	43.9	47.9
11	4.4	8.9	13.3	17.7	22.2	26.6	31.0	35.4	39.9	44.3	48.7	53.2
14	5.3	10.6	16.0	21.3	26.6	31.9	37.2	42.6	47.9	53.2	58.5	63.8
18	7.1	14.2	21.3	28.4	35.5	42.5	49.6	56.7	63.8	70.9	78.0	85.1

Table A.5 Areas of Reinforcing Bars in Slabs ($in.^2/ft$)

Spacing (in.)	Bar No.								
	3	4	5	6	7	8	9	10	11
3	0.44	0.78	1.23	1.77	2.40	3.14	4.00	5.06	6.25
$3\frac{1}{2}$	0.38	0.67	1.05	1.51	2.06	2.69	3.43	4.34	5.36
4	0.33	0.59	0.92	1.32	1.80	2.36	3.00	3.80	4.68
$4\frac{1}{2}$	0.29	0.52	0.82	1.18	1.60	2.09	2.67	3.37	4.17
5	0.26	0.47	0.74	1.06	1.44	1.88	2.40	3.04	3.75
$5\frac{1}{2}$	0.24	0.43	0.67	0.96	1.31	1.71	2.18	2.76	3.41
6	0.22	0.39	0.61	0.88	1.20	1.57	2.00	2.53	3.12
$6\frac{1}{2}$	0.20	0.36	0.57	0.82	1.11	1.45	1.85	2.34	2.89
7	0.19	0.34	0.53	0.76	1.03	1.35	1.71	2.17	2.68
$7\frac{1}{2}$	0.18	0.31	0.49	0.71	0.96	1.26	1.60	2.02	2.50
8	0.17	0.29	0.46	0.66	0.90	1.18	1.50	1.89	2.34
9	0.15	0.26	0.41	0.59	0.80	1.05	1.33	1.69	2.08
10	0.13	0.24	0.37	0.53	0.72	0.94	1.20	1.52	1.87
12	0.11	0.20	0.31	0.44	0.60	0.78	1.00	1.27	1.56

Table A.6 Development Length in Tension (in.)

For No. 11 bars or smaller: $l_{db} = 0.04A_b f_y / \sqrt{f'_c}$, but $\geq 0.0004 d_b f_y$

For No. 14 bars: $l_{db} = 0.085 f_y / \sqrt{f'_c}$

For No. 18 bars: $l_{db} = 0.11 f_y / \sqrt{f'_c}$

(Minimum length 12 in. in all cases.)

Bar No.	f_y	f'_c = 3,000		f'_c = 4,000		f'_c = 5,000		f'_c = 6,000	
		Basic l_{db}	Top bars $1.4l_{db}$	Basic l_{db}	Top bars $1.4l_{db}$	Basic l_{db}	Top bars $1.4l_{db}$	Basic l_{db}	Top bars $1.4l_{db}$
3	40	12	12	12	12	12	12	12	12
	50	12	12	12	12	12	12	12	12
	60	12	13	12	13	12	13	12	13
4	40	12	12	12	12	12	12	12	12
	50	12	14	12	14	12	14	12	14
	60	12	17	12	17	12	17	12	17
5	40	12	14	12	14	12	14	12	14
	50	13	18	13	18	13	18	13	18
	60	15	21	15	21	15	21	15	21
6	40	13	18	12	17	12	17	12	17
	50	16	22	15	21	15	21	15	21
	60	19	27	18	25	18	25	18	25
7	40	18	25	15	21	14	20	14	20
	50	22	31	19	27	18	25	18	25
	60	26	37	23	32	21	29	21	29
8	40	23	32	20	28	18	25	16	23
	50	29	40	25	35	22	31	20	29
	60	35	48	30	42	27	38	24	34
9	40	29	41	25	35	23	32	21	29
	50	37	51	32	44	28	40	26	36
	60	44	61	38	53	34	48	31	43
10	40	37	52	32	45	29	40	26	37
	50	46	65	40	56	36	50	33	46
	60	56	78	48	67	43	60	39	55
11	40	46	64	39	55	35	49	32	45
	50	57	80	49	69	44	62	40	56
	60	68	96	59	83	53	74	48	68
14	40	62	87	54	75	48	67	44	61
	50	78	109	67	94	60	84	55	77
	60	93	130	81	113	72	101	66	92
18	40	80	113	70	97	62	87	57	80
	50	100	141	87	122	78	109	71	99
	60	121	169	104	146	93	131	85	119

Table A.7 Common Stock Styles of Welded Wire Fabric

Steel designation		Steel area, $(in.^2/ft)^a$		Weight (approximate), lb per 100 ft^{2b}
New designation (by W number)	Old designation (by steel wire gage)	Londitudinal	Transverse	
Rolls				
6×6-W1.4×W1.4	6×6-10×10	0.029	0.029	21
6×6-W2.0×W2.0	6×6-8×8[c]	0.041	0.041	30
6×6-W2.9×W2.9	6×6-6×6	0.058	0.058	42
6×6-W4.0×W4.0	6×6-4×4	0.080	0.080	58
4×4-W1.4×W1.4	4×4-10×10	0.043	0.043	31
4×4-W2.0×W2.0	4×4-8×8[c]	0.062	0.062	44
4×4-W2.9×W2.9	4×4-6×6	0.087	0.087	62
4×4-W4.0×W4.0	4×4-4×4	0.120	0.120	85
Sheets				
6×6-W2.9×W2.9	6×6-6×6	0.058	0.058	42
6×6-W4.0×W4.0	6×6-4×4	0.080	0.080	58
6×6-W5.5×W5.5	6×6-2×2[d]	0.110	0.110	80
4×4-W4.0×W4.0	4×4-4×4	0.120	0.120	85

[a] 0.01 in^2/ft = 21.17 mm^2/m.
[b] 1 $lb/100\ ft^2$ = 4.88 $kgf/100\ m^2$.
[c] Exact W-number size for 8 gage is W2.1.
[d] Exact W-number size for 2 gage is W5.4.

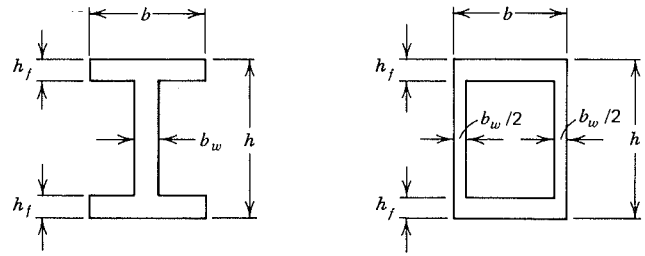

Table A.8 Section Properties of Symmetrical I-and Box Beams

b_w/b	h_f/h	A_c	I_c	c_1	c_2	r^2
0.1	0.1	$0.280bh$	$0.0449bh^3$	$0.500h$	$0.500h$	$0.160h^2$
0.1	0.2	0.460	0.0671	0.500	0.500	0.146
0.1	0.3	0.640	0.0785	0.500	0.500	0.123
0.2	0.1	0.360	0.0492	0.500	0.500	0.137
0.2	0.2	0.520	0.0689	0.500	0.500	0.132
0.2	0.3	0.680	0.0791	0.500	0.500	0.117
0.3	0.1	0.440	0.0535	0.500	0.500	0.121
0.3	0.2	0.580	0.0707	0.500	0.500	0.122
0.3	0.3	0.720	0.0796	0.500	0.500	0.111
0.4	0.1	0.520	0.0577	0.500	0.500	0.111
0.4	0.2	0.640	0.0725	0.500	0.500	0.113
0.4	0.3	0.760	0.0801	0.500	0.500	0.105

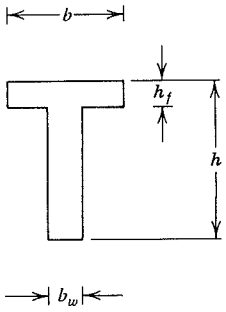

Table A.9 Section Properties of T-Beams

b_w/b	h_f/h	A_c	I_c	c_1	c_2	r^2
0.1	0.1	$0.190bh$	$0.0179bh^3$	$0.286h$	$0.714h$	$0.0945h^2$
0.1	0.2	0.280	0.0192	0.244	0.756	0.0688
0.1	0.3	0.370	0.0193	0.245	0.755	0.0520
0.2	0.1	0.280	0.0283	0.371	0.629	0.1010
0.2	0.2	0.360	0.0315	0.322	0.678	0.0875
0.2	0.3	0.440	0.0319	0.309	0.691	0.0725
0.3	0.1	0.370	0.0365	0.415	0.585	0.0985
0.3	0.2	0.440	0.0408	0.374	0.626	0.0928
0.3	0.3	0.510	0.0417	0.355	0.645	0.0819
0.4	0.1	0.460	0.0440	0.441	0.559	0.0954
0.4	0.2	0.520	0.0486	0.408	0.592	0.0935
0.4	0.3	0.580	0.0499	0.391	0.609	0.0860

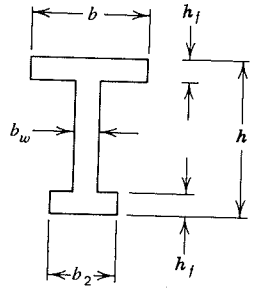

Table A.10 Section Properties of Unsymmetrical I-Beams

b_w/b	h_f/h	A_c	I_c	c_1	c_2	r^2
			$b_2/b = 0.30$			
0.1	0.1	$0.210bh$	$0.0260bh^3$	$0.350h$	$0.650h$	$0.1236h^2$
0.1	0.2	0.320	0.0345	0.325	0.675	0.1080
0.1	0.3	0.430	0.0387	0.328	0.672	0.0900
0.2	0.1	0.290	0.0316	0.390	0.610	0.1090
0.2	0.2	0.380	0.0378	0.353	0.647	0.0994
0.2	0.3	0.470	0.0402	0.345	0.655	0.0856
			$b_2/b = 0.50$			
0.1	0.1	$0.230bh$	$0.0326bh^3$	$0.403h$	$0.597h$	$0.1420h^2$
0.1	0.2	0.360	0.0464	0.389	0.611	0.1288
0.1	0.3	0.490	0.0535	0.394	0.606	0.1090
0.2	0.1	0.310	0.0373	0.428	0.572	0.1204
0.2	0.2	0.420	0.0488	0.405	0.595	0.1160
0.2	0.3	0.530	0.0540	0.401	0.599	0.1020
0.3	0.1	0.390	0.0430	0.443	0.557	0.1103
0.3	0.2	0.480	0.0510	0.418	0.582	0.1065
0.3	0.3	0.570	0.0553	0.408	0.592	0.0970
			$b_2/b = 0.70$			
0.1	0.1	$0.250bh$	$0.0381bh^3$	$0.446h$	$0.554h$	$0.1525h^2$
0.1	0.2	0.400	0.0560	0.440	0.560	0.1391
0.1	0.3	0.550	0.0651	0.443	0.557	0.1182
0.2	0.1	0.330	0.0425	0.460	0.540	0.1290
0.2	0.2	0.460	0.0578	0.448	0.552	0.1258
0.2	0.3	0.590	0.0657	0.447	0.553	0.1113
0.3	0.1	0.410	0.0467	0.466	0.534	0.1140
0.3	0.2	0.520	0.0598	0.454	0.546	0.1150
0.3	0.3	0.630	0.0663	0.450	0.550	0.1051

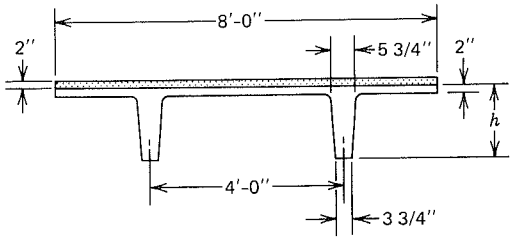

Table A.11 Section Properties of Double-T Beams[a]

	Untopped					Topped		
h	A_c (in.^{2})	I_g (in.^{4})	c_1 (in.)	c_2 (in.)	r^2 (in.^{2})	I_g (in.^{4})	c_1 (in.)	c_2 (in.)
12	287	2,872	2.87	9.13	10.01	4,389	3.55	10.45
14	306	4,508	3.49	10.51	14.74	6,539	4.03	11.97
16	325	6,634	4.07	11.93	20.41	9,306	4.48	13.52
18	344	9,300	4.73	13.27	27.03	12,749	5.00	15.00
20	363	12,551	5.41	14.59	34.58	16,935	5.55	16.45
24	401	20,985	6.85	17.15	52.33	27,720	6.73	19.27

[a]Adapted from *PCI Design Handbook*, Ref. 4.6. 1985.

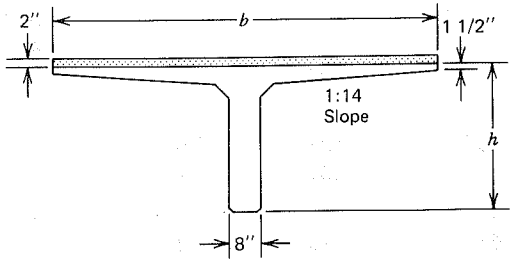

Table A.12 Section Properties of Single-T Beams[a]

		Untopped					Topped		
h	b	A_c (in.^{2})	I_g (in.^{4})	c_1 (in.)	c_2 (in.)	r^2 (in.^{2})	I_g (in.^{4})	c_1 (in.)	c_2 (in.)
36	96	570	68,917	9.99	26.01	120.91	83,212	9.72	28.28
36	120	686	74,607	8.72	27.28	108.76	—	—	—
48	120	782	169,020	12.81	35.19	216.14	—	—	—

[a]Adapted from *PCI Design Handbook*, Ref. 4.6.

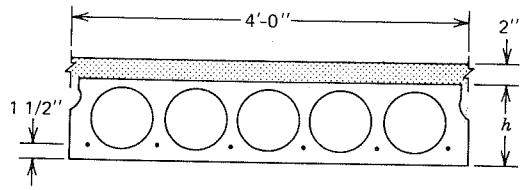

Table A.13 Section Properties of Hollowcore Slabs[a]

		Untopped						Topped		
h	Number of voids	A_c (in.^{2})	I_g (in.^{4})	c_1 (in.)	c_2 (in.)	b_w (in.)	r^2 (in.^{2})	I_g (in.^{4})	c_1 (in.)	c_2 (in.)
6	8	187	763	3.00	3.00	16.00	4.08	1,640	3.86	4.14
8	6	215	1,666	4.00	4.00	12.00	7.75	3,071	4.71	5.29
10	5	259	3,223	5.00	5.00	10.50	12.44	5,328	5.66	6.34
12	4	262	4,949	6.00	6.00	8.00	18.89	7,811	6.45	7.55

[a]Adapted from *PCI Design Handbook*, Ref. 4.6.

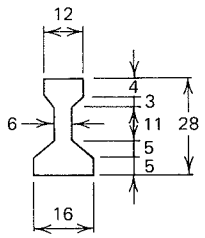

Type I
35 to 45 ft

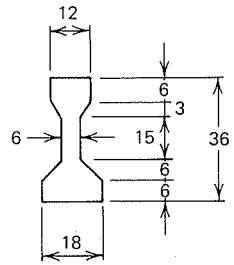

Type II
40 to 50 ft

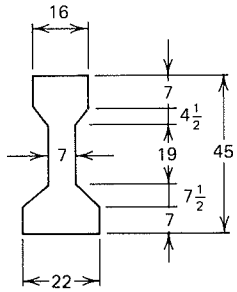

Type III
55 to 80 ft

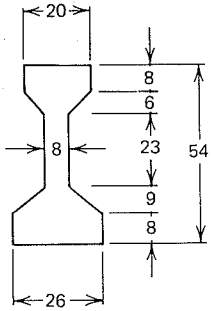

Type IV
70 to 100 ft

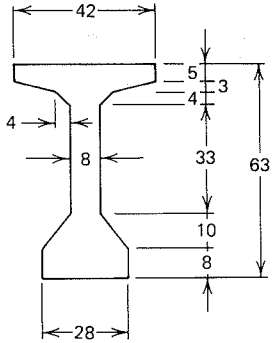

Type V
90 to 120 ft

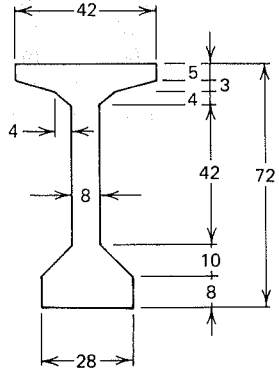

Type VI
110 to 140 ft

Table A.14 Section Properties of AASHTO Bridge Girders

Type	h (in.)	A_c (in.^{2})	I_g (in.^{4})	c_1 (in.)	c_2 (in.)	r^2 (in.^{2})	w_o (plf)
I	28	276	22,750	15.41	12.59	82	288
II	36	369	50,979	20.17	15.83	138	384
III	45	560	125,390	24.73	20.27	224	583
IV	54	789	260,741	29.27	24.73	330	822
V	63	1,013	521,180	31.04	31.96	514	1055
VI	72	1,085	733,320	35.62	36.38	676	1130

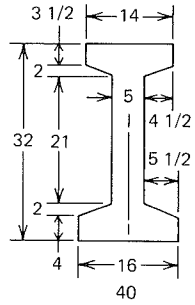

40

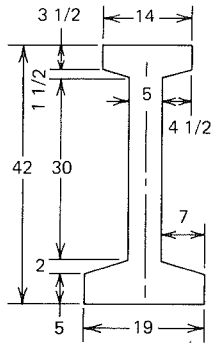

60

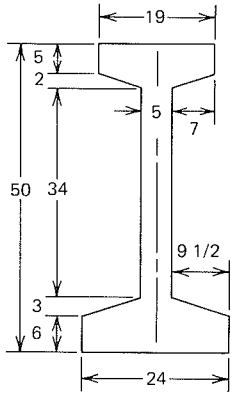

80

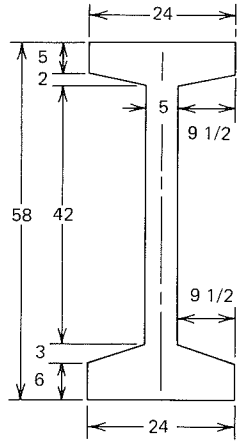

100

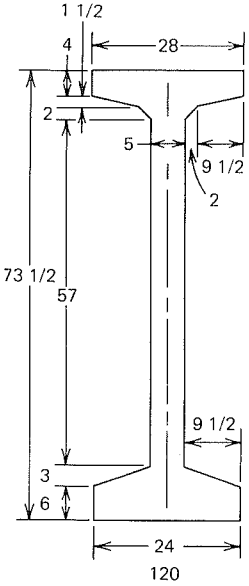

120

Table A.15 Section Properties of State of Washington Bridge Girders

Type	h (in.)	A_c (in.^{2})	I_g (in.^{4})	c_1 (in.)	c_2 (in.)	r^2 (in.^{2})	w_o (plf)
40	32	253	31,000	16.84	15.16	123	264
60	42	332	70,100	23.37	18.63	211	346
80	50	476	154,900	27.47	22.53	325	496
100	58	546	249,000	30.10	27.90	456	569
120	73.5	626	456,000	37.90	35.60	728	652

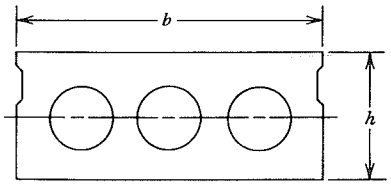

Table A.16 Section Properties of Voided Bridge Slabs[a]

h (in.)	b (in.)	Number of voids	A_c (in.^{2})	I_g (in.^{4})	c_1 (in.)	c_2 (in.)	r^2 (in.^{2})	w_o (plf)
15	36	2	439	9,725	7.50	7.50	22.16	457
18	36	2	491	16,514	9.00	9.00	33.63	511
21	36	2	530	25,747	10.50	10.50	48.58	552
15	48	3	569	12,897	7.50	7.50	22.67	593
18	48	3	628	21,855	9.00	9.00	34.80	654
21	48	3	703	34,517	10.50	10.50	49.10	733

[a]Adapted from *Short Span Bridges: Spans to 100 Feet*, Ref. 13.4.

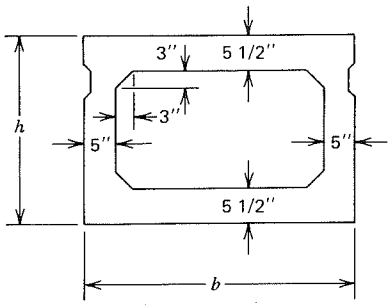

Table A.17 Section Properties of Box Bridge Beams[a]

Type	h (in.)	b (in.)	A_c (in.^{2})	I_g (in.^{4})	c_1 (in.)	c_2 (in.)	r^2 (in.^{2})	w_o (plf)
B I-36	27	36	561	50,334	13.65	13.35	89.7	584
B II-36	33	36	621	85,153	16.71	16.29	137.1	647
B III-36	39	36	681	131,145	19.75	19.25	192.6	709
B IV-36	42	36	711	158,644	21.27	20.73	223.1	740
B I-48	27	48	693	65,941	13.63	13.37	95.2	722
B II-48	33	48	753	110,499	16.67	16.33	146.7	784
B III-48	39	48	813	168,367	19.71	19.29	207.1	847
B IV-48	42	48	843	203,088	21.22	20.78	240.9	878

[a]Adapted from *Short Span Bridges: Spans to 100 Feet*, Ref. 13.4.

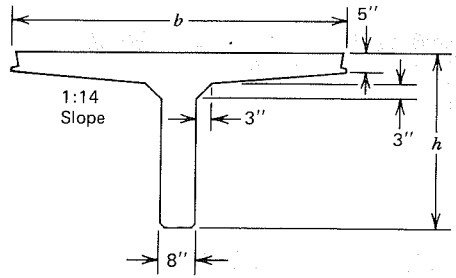

Table A.18 Section Properties of Single-T Bridge Beams[a]

h (in.)	b (in.)	A_c (in.^{2})	I_g (in.^{4})	c_1 (in.)	c_2 (in.)	r^2 (in.^{2})	w_o (plf)
24	48	430	18,555	7.04	16.96	43.2	448
36	48	526	61,058	11.24	24.76	116.1	548
48	48	622	139,038	15.99	32.01	223.5	648
24	60	510	19,788	6.47	17.53	38.8	531
36	60	606	65,673	10.20	25.80	108.4	631
48	60	702	150,643	14.55	33.45	214.6	731
24	72	595	20,782	6.06	17.94	34.9	620
36	72	691	69,323	9.38	26.62	100.3	720
48	72	787	160,146	13.36	34.64	203.5	820

[a]Adapted from *Short Span Bridges: Spans to 100 Feet*, Ref. 13.4.

APPENDIX B

POST-TENSIONING HARDWARE

Inryco CONA Single-Strand Post Tensioning System

Inland-Ryerson single strand tendons use the Cona wedge anchor system developed by the designers of the BBRV system. Tendons employ cold drawn, stress relieved, seven-wire strands of 0.5″ or 0.6″ diameter, conforming to ASTM A-416.

Cona Single strand tendons are normally used in unbonded construction, but may be used as bonded tendons where specifications require. The small diameter strand bundle is particularly suited for use in thin, one-way slabs, two-way flat plates and flat slabs and topping slabs.

Differentiae of the Cona single-strand system are:

- Very small tendon diameter allows optimum eccentricities, hence efficient use of P-T steel.
- Small anchor plate meets edge-size restrictions of thin slabs and light structural shapes. (0.5″ Anchors require only 3½″ concrete thickness; 0.6″ Anchor require 4¼″ concrete thickness.)
- Oversize anchor plates are available to accommodate stressing at low concrete strengths.
- Like all wedge-grip, strand systems, anchorage develops slightly less than ultimate capacity of the tendon, but two-piece wedge design reduces seating losses to a minimum.
- Design of anchor components and stressing equipment allows accurate overstress and back-off to lock-off force without premature, uncontrolled seating of wedges.
- Coupling is never necessary. There are essentially no length restrictions, and tension can be applied separately to successive sections of total length by stressing at any intermediate point, and then continuing the same strand.
- No large pockets to form and patch. Re-usable pocket-former comes with anchor hardware; attaches to formwork for quick positioning of anchor, and creates small, clean, stressing void that's easily patched.
- Tendons are "built" at the job site from pre-assembled anchor components and wrapped lengths of strand. (Excess can be burned off.) So special accuracy in cutting to length and fabricating is not required.
- Stressing equipment is small and light—easily handled by one man.

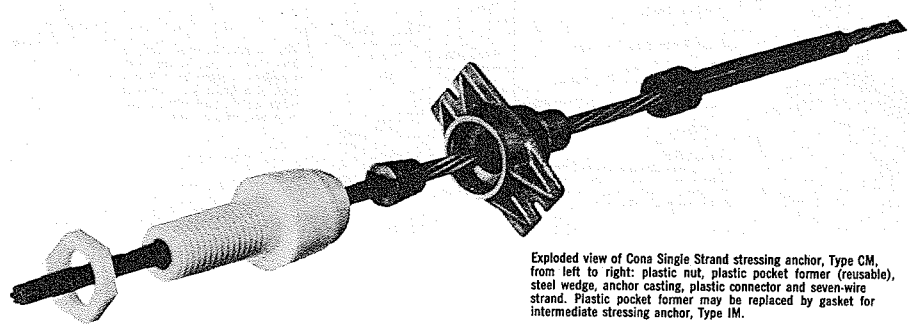

Exploded view of Cona Single Strand stressing anchor, Type CM, from left to right: plastic nut, plastic pocket former (reusable), steel wedge, anchor casting, plastic connector and seven-wire strand. Plastic pocket former may be replaced by gasket for intermediate stressing anchor, Type IM.

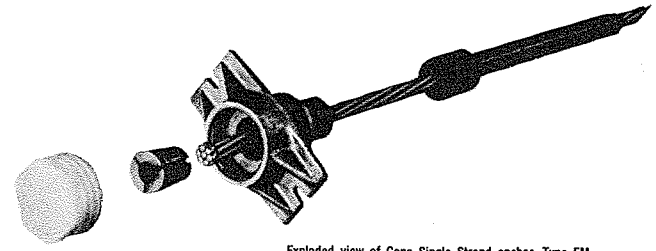

Exploded view of Cona Single Strand anchor, Type EM, from left to right: plastic cap, steel wedges, anchor casting, plastic connector and button-headed seven-wire strand.

CONA SINGLE STRAND ANCHOR

INLAND-RYERSON POST TENSIONING SYSTEMS

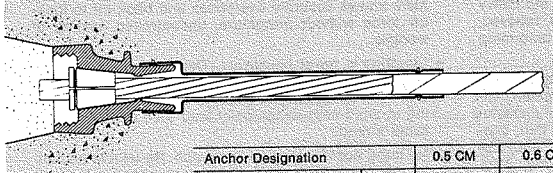

Type CM (stressing)

Anchor Designation		0.5 CM	0.6 CM
Base Plate Size (inches)	(A)	4½ x 2¼	5⅜ x 2¾
	(B)	6¼ x 2¼	7⅛ x 2¾
Pocket Former O.D. (inches)		2¼	2¾
Pocket Former Length (inches)		1⅜	1⅝
Bundle O.D. (inches)		0.5	0.6

The fixed Cona anchors, Types EM and EG, are identical in basic design and size to the stressing anchors. The end of the strand is button-headed. Wedges are hydraulically power seated, providing a positive non-slip, fixed-end anchorage.

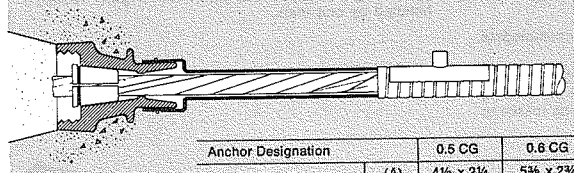

Type CG (stressing)

Anchor Designation		0.5 CG	0.6 CG
Base Plate Size (inches)	(A)	4½ x 2¼	5⅜ x 2¾
	(B)	6¼ x 2¼	7⅛ x 2¾
Pocket Former O.D. (inches)		2¼	2¾
Pocket Former Length (inches)		1⅜	1⅝
Conduit O.D. (inches)		1	1⅛

Bearing plate "A" is designed to accommodate stressing at a concrete compressive strength of 2,500 to 3,000 psi, depending on the geometry of the concrete and tendon spacing. Bearing plate "B" designed to accommodate stressing at concrete strength of 1,500 to 2,000 psi, depending on geometry of concrete and tendon spacing.

Also available on special order is Type LM anchorage for special applications or repair work. It consists of a wedge grip contained within a short steel collar, backed by a steel bearing plate.

TYPICAL CONA SINGLE STRAND TENDON INSTALLATION

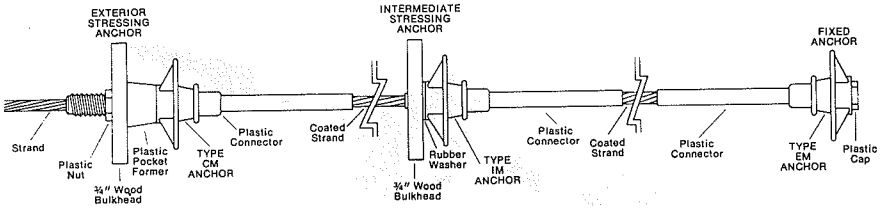

Inryco CONA Multi-Strand Post Tensioning System

The Cona Multi-Strand anchor system was developed by the Swiss engineers who created the BBRV wire system (pp. 16-20) and introduced to the U.S. market by Inland-Ryerson in 1970. It is most applicable to heavy beams or to structures requiring large-capacity tendons — cases where a structure's irregularity dictates the use of post-tensioning tendons of varying size and length, or where accurate determination of length is not possible.

The system is made up of multiple units of seven-wire strands, each 0.5″ or 0.6″ in diameter. Steel wedges anchor each strand and all strands of a given tendon are stressed simultaneously.

An important feature of the system is the capability to hydraulically power-seat all wedges of the stressing anchor (WG) to assume a uniform initial force and to control seating loss.

Cona Multi-Strand tendons are usually grouted and are especially suited for the pass-through method of tendon installation. In this procedure, only empty rigid ducts are placed in forms prior to concreting. Site-fabricated tendons are pulled through the ducts, and are stressed and grouted in one continuous operation. Tendons can also be shop-fabricated.

Anchorages using 0.5″ dia. strands are available in 7, 12, 19, 31 and 55 strand units. Tendons using 0.6″ dia. strands, are available in 4, 7, 12, 19 and 31 strand units.

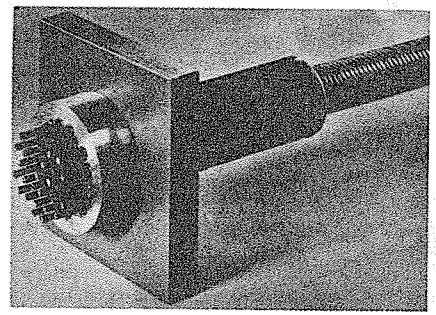

Type WG stressing anchor.

CONA MULTI-STRAND ANCHORS

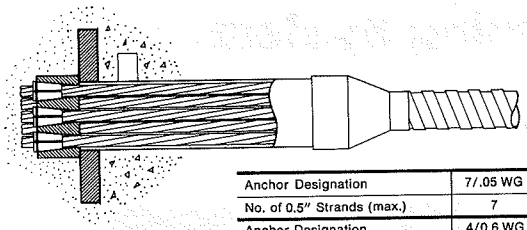

Type WG (stressing)

Anchor Designation		7/.05 WG	12/0.5 WG	19/0.5 WG	31/0.5 WG	55/0.5 WG
No. of 0.5" Strands (max.)		7	12	19	31	55
Anchor Designation		4/0.6 WG	7/0.6 WG	12/0.6 WG	19/0.6 WG	31/0.6 WG
No. of 0.6" Strands (max.)		4	7	12	19	31
Bearing Plate Size (inches)		8½ x 8½	11 x 11	14 x 14	17½ x 17½	24 x 24
Trumpet O.D. (inches)		3¼	4½	5¾	7½	10
Trumpet Length (inches)		8	16	20	26	36
Conduit O.D. (inches)	Pull-through	2⅜	2¾	3⅜	4⅜	5¾
	Assembled	2	2⅜	3	3¾	5¼

Type WG used as fixed anchorage for pull through tendon installations. Wedges are pressed into anchorhead by special retaining plate.

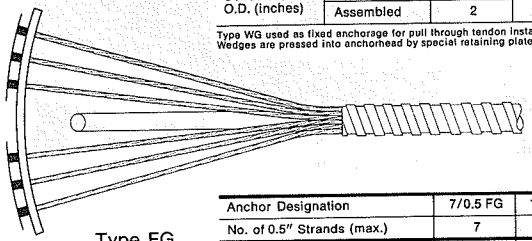

Type FG (fixed)

Anchor Designation		7/0.5 FG	12/0.5 FG	19/0.5 FG	31/0.5 FG	55/0.5 FG
No. of 0.5" Strands (max.)		7	12	19	31	55
Anchor Designation		4/0.6 FG	7/0.6 FG	12/0.6 FG	19/0.6 FG	31/0.6 FG
No. of 0.6" Strands (max.)		4	7	12	19	31
Bearing Plate Size (inches)	(A)	6 x 6	10½ x 10½	13½ x 13½	17 x 17	22½ x 22½
	(B)	4¾ x 14¼	6¼ x 18¾	8 x 24	9⅞ x 29½	13 x 39

Type FG anchorage used for fixed anchorage where tendon is plant fabricated and is cast in concrete. Strand ends are buttonheaded.

BBRV tendons and anchors

BBRV post tensioning was developed in 1949 by four Swiss engineers, Birkenmeier, Brandestini, Ros and Vogt, whose initials give the system its name. Use of the BBRV system has spread rapidly throughout the free world, and in the United States it is now probably the most widely used method of post tensioning.

A BBRV tendon consists of several (or many) parallel lengths of ¼" high-strength wire with each end of each wire terminating in a cold-formed buttonhead, after the wire passes separately through a machined anchorage fixture. The system provides for the simultaneous stressing of all the wires in a tendon and the buttonheads allow development of ultimate tendon forces.

Tendons are produced for either bonded or unbonded installation. They can be furnished in practically any length and in a range of sizes and force capacities from 8 to 52 wires for building construction. For heavy construction, such as nuclear containment vessels, tendons with 90-170 wires are commonly used. Engineering data for such sizes is available on request.

In the bonded or grout-type tendons, the wires are encased in flexible metal conduit. The unbonded BBRV tendons are generally mastic-coated and wrapped in heavy paper but in certain applications conduit-encased tendons are also used ungrouted. In these instances the conduit is filled with grease after the tendon has been installed and stressed.

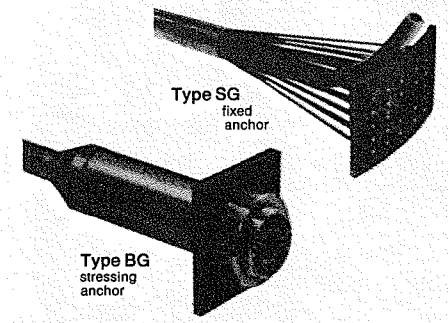

Differentiae of the BBRV system are:

- Button-head terminals for every wire give positive, no-slip anchorage and eliminate seating losses, making it possible to develop the full potential force of every tendon.
- Tendons are precisely engineered and completely shop fabricated which minimizes field labor and allows more exact control of quality and accuracy. This feature may result in a higher *initial* cost-per-lb. of tendon than with other systems, but not necessarily in a higher *installed* cost. And often the highest initial cost may yield the *lowest cost-per-lb. of force delivered.*
- Tendons may be fabricated in long lengths when desirable (we have supplied them over 400 ft. long).
- Long tendons present no problems in fabrication or in shipping since they are furnished coiled on "lazy susan" racks 6 ft. in diameter. This method of shipment also reduces job-site storage requirements, makes on-the-job handling of any length tendon easy and minimizes exposure to transit damage.
- Coupling of BBRV tendons is easily accomplished, with no loss of forces.
- Curved or draped positioning of tendons within a structural member, often desirable from a design standpoint, is readily achieved because of the small diameter (¼") of the steel elements. For the same reason, however, BBRV tendons positioned vertically require substantial support.
- Developed force can be closely matched to design requirements with no waste of prestress steel because BBRV tendons are available in a wide range of size-force units — with each single-wire increment adding 7 kips of force.
- BBRV can provide much the greatest force from single tendons because of multi-wire, high-strength steel construction. But take into account the fact that large-capacity tendons require large, less-easily-handled field equipment. Also remember that this type of tendon and anchor requires relatively large blockouts.

The BBRV anchorages illustrated here are the standard types. But special types can be developed to meet unusual requirements and any anchorage can be produced with any number of wires (up to the hardware's maximum capacity) needed to produce a specified prestressing force.

POST TENSIONING SYSTEMS

STRESSING ANCHORS FOR BBRV TENDONS

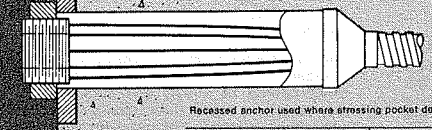

Type BG

Recessed anchor used where stressing pocket depth is limited. Type BM also available.

Anchor Designation		18 BG	24 BG	30 BG	38 BG	46 BG	52 BG
No. of Wires (max.)		18	24	30	38	46	52
Bearing Plate Size (inches)	A	7½ x 7½	8½ x 8½	9½ x 9½	10½ x 10½	11½ x 11½	12¼ x 12¼
	B	6 x 9½	7 x 10½	8 x 11½	9 x 12¼	10 x 13½	11 x 13½
Trumpet O.D. (inches)		3¼	4½	5	5¼	5½	5¾
Conduit O.D. (inches)		1⅝	1⅞	2	2⅜	2⅝	2¾

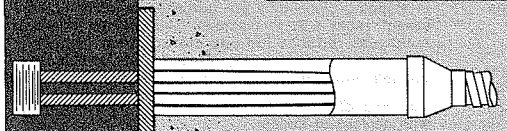

Type MG

Non-recessed type, preferred where there is no limitation on depth of stressing pocket.

Anchor Designation		8 MG	12 MG	18 MG	24 MG	30 MG	38 MG	46 MG
No. of Wires (max.)		8	12	18	24	30	38	46
Bearing Plate Size (inches)	A	3½ x 8¼	4 x 8½	5 x 10	6 x 11½	7 x 12½	8 x 13¾	9 x 14¾
	B	3½ x 10	5 x 7¾	6 x 9¾	7 x 11¼	8 x 12¼	9 x 14	10 x 15
Trumpet O.D. (inches)		1½	3	3	4	4½	5	5½
Conduit O.D. (inches)		1¼	1⅜	1⅝	1⅞	2	2⅜	2¾

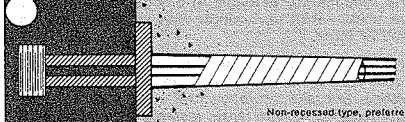

Type MM

Non-recessed type, preferred where there is no limitation on depth of stressing pocket.

Anchor Designation		8 MM	12 MM	18 MM	24 MM	30 MM	38 MM	46 MM
No. of Wires (max.)		8	12	18	24	30	38	46
Bearing Plate Size (inches)	A	3½ x 8¼	4 x 8½	5 x 10	6 x 11½	7 x 12½	8 x 13¾	9 x 14¾
	B	3½ x 10	5 x 7¾	6 x 9¾	7 x 11¼	8 x 12¼	9 x 14	10 x 15
Bundle O.D. (inches)		1	1¼	1½	1¾	2	2⅛	2¼

FIXED ANCHORS FOR BBRV TENDONS

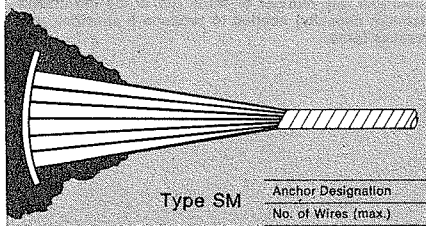

Type SM

Anchor Designation	8 SM	12 SM	18 SM	24 SM	30 SM	38 SM	46 SM	52 SM
No. of Wires (max.)	8	12	18	24	30	38	46	52
Bearing Plate Size (inches)	3½ x 8	5 x 8	5 x 10	6 x 11½	7 x 12½	8 x 13¾	9 x 15	10 x 15

Engineering data on BBRV tendon systems for heavy construction, with 170 wire capacity, available on request.

Type SG anchor for grouted installations is similar to Type SM.

STRESSTEEL

Post-Tensioning

STRESSTEEL BAR SYSTEM

The choice of anchorages and couplers offered by Stressteel Bar System provides wide latitude in design options. Ask Stressteel engineers for design information, specific details and quotations based on the advantages of this system.

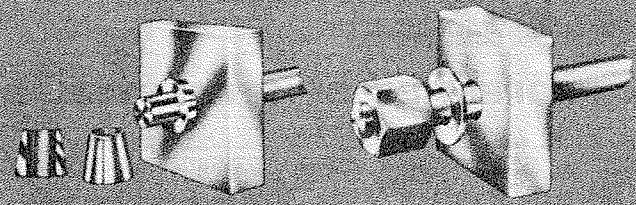

Wedge Anchorage
A Stressteel Bar, Wedge Anchor and Wedge Plate.

Nut and Thread Anchorage
A threaded Stressteel Bar, Nut, load distributing Washer and Plate.

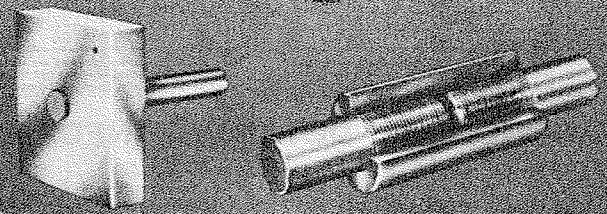

Threaded Plate Anchorage
A threaded Stressteel Bar and Threaded Plate (for use on non-precast end only).

Threaded Coupler
Threaded Stressteel Bars and Coupler.

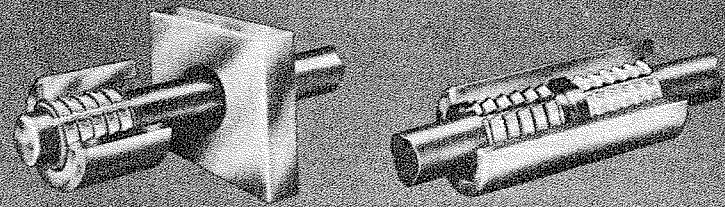

HOWLETT Grip Nut Anchorage
A Stressteel Bar, Howlett Grip Nut and Sleeve, and Plate.

HOWLETT Grip Coupler
Stressteel Bars, a Howlett Grip Coupler and two Sleeves.

Separate manuals describe STRESSTEEL Systems for post-tensioning strand tendons — STRESSTEEL S/H Wedge Anchorage System for monostrand and multistrand systems. Copies sent upon request.

STRESSTEEL CORPORATION
221 Canyonlands Avenue, Wilkes-Barre, Penna. 18702
Phone (717) 823-7181

WESTERN DIVISION
32420 Central Avenue, Union City, California 94587
Phone (415) 471-6610

SALES OFFICES:
New York • St. Petersburg • Memphis • San Francisco
Seattle • Portland

STRESSTEEL BARS

STRESSTEEL Bars are available in diameters from ¾" to 1⅜", in increments of ⅛".* Bars can be ordered in any length to 100'. Lengths greater than 100' are obtained by use of couplers.

These bars are manufactured from specially selected hot rolled alloy steels. Each bar is cold stretched, which uniformly cold works the cross section and develops high yield strength. The bar is then stress relieved in a gas fired furnace, insuring ductility and uniform stress-strain characteristics. This carefully controlled process provides high strength bars ideal for prestressing.

The cold stretching process, in addition, proof stresses each bar to 100% of its minimum guaranteed yield stress. Proof stressing eliminates all bars with surface imperfections or metallurgical defects detrimental to the strength of the steel. It guarantees that every bar possesses the necessary properties to perform as required.

STRESSTEEL Bars are manufactured in two grades: REGULAR STRESSTEEL with a guaranteed minimum ultimate strength of 145,000 psi, and SPECIAL STRESSTEEL with a guaranteed minimum ultimate strength of 160,000 psi.

* Smaller and larger bars are available on special order. Ultimate strengths and physical properties of these bars vary from those indicated. Inquire for specific information.

DESIGN PROPERTIES OF STRESSTEEL BARS

Nominal Bar Size Ø"	Nominal Weight Pounds Lin/Ft.	Nominal Area Square Inches	Ultimate Strength Guaranteed Minimum		Recommended Initial Tensioning Load—0.7 f'st†		Maximum Recommended Final Design Load—0.6 f'st†	
			REGULAR 145 ksi	SPECIAL 160 ksi	REGULAR 101.5 ksi	SPECIAL 112 ksi	REGULAR 87 ksi	SPECIAL 96 ksi
			(All units in values of 1000 pounds)					
¾	1.50	.442	64	71	45	50	39	42
⅞	2.04	.601	87	96	61	67	52	58
1	2.67	.785	114	126	80	88	68	75
1⅛	3.38	.994	144	159	101	111	87	95
1¼	4.17	1.227	178	196	125	137	107	118
1⅜	5.05	1.485	215	238	151	166	129	143

† Design properties indicated are in accordance with ACI Building Code 318-63, Sections 2606 and 2607. Temporary jacking stresses up to 0.8f's are permitted to overcome losses due to tendon friction, anchorage seating and elastic shortening. Losses due to creep, shrinking and steel relaxation should be deducted from the recommended initial tensioning load to obtain actual final design load. Actual final design load, after losses are accounted for, may be less than 0.6f's.

BAR ANCHORAGE DETAILING INFORMATION

Wedges and Nuts

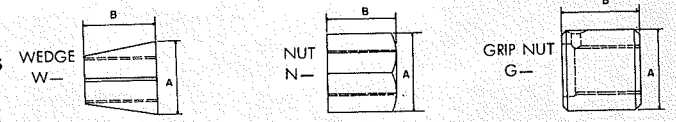

BAR Ø"	WEDGES Part No.	A	B	Wt. # Ea.	NUTS* Part No.	A	B	Wt. # Ea.	GRIP NUTS Part No.	A	B	Wt. # Ea.
¾	W6	1⅜	1¼	.2	N6	1⅜	1¼	.5	G6	1⅞	1¼	1.0
⅞	W7	1¾	1½	.3	N7	1⅝	1 7/16	.7	G7	2 1/16	2	1.5
1	W8	1¾	1½	.5	N8	1⅞	1⅝	1.0	G8	2¼	2¼	2.5
1⅛	W9	2	1¾	.7	N9	2⅛	1 13/16	1.5	G9	2½	2½	2.7
1¼	W10	2¼	2	.8	N10	2¼	2	2.0	G10	2¾	2⅜	3.2
1⅜	W11	2⅜	2 3/16	1.1	N11	2⅜	2	2.0	G11	3	2⅞	4.2

All data subject to revision as new developments are made.

* 3/16" washer shipped with each nut.

All dimensions in inches

Couplers

BAR Ø"	THREADED COUPLERS Part No.	A	B	C	D	I.D." Coupler Shield	Wt. # Ea.	GRIP COUPLERS Part No.	A	B	C	D	I.D." Coupler Shield	Wt. # Ea.
¾	TC6	1¼	3	1⅜	¼	1½	1.1	GC6	1⅞	3⅜	1 7/16	⅜	2¼	2.0
⅞	TC7	1½	3½	1⅝	¼	2	1.8	GC7	2⅛	3⅞	1¾	⅜	2¼	3.0
1	TC8	1¾	3¾	1¾	¼	2	1.9	GC8	2¼	4¼	1 13/16	⅜	2¾	3.5
1⅛	TC9	2	4¼	1⅞	½	2½	2.5	GC9	2½	4⅝	2⅛	⅜	3	4.9
1¼	TC10	2¼	4¾	2⅛	½	2½	3.7	GC10	2¾	5⅛	2⅜	⅜	3	6.2
1⅜	TC11	2¼	5	2¼	½	2½	3.5	GC11	3	5⅝	2⅝	⅜	3½	8.1

All data subject to revision as new developments are made.

All dimensions in inches

Bar Anchorage Detailing Information (cont'd)

Plates

BAR Ø"	Part No. WP.-TP. or P.*	No. of Holes	DIMENSIONS IN INCHES A	B	C	D	E	T	Wt. Lbs. Ea.
¾	6	1	4	4	2	—	2	1	4.5
⅞	7	1	5	4½	2½	—	2¼	1½	9.5
1	8	1	5½	5	2¾	—	2½	1½	11.9
1⅛	9	1	6	6	3	—	3	1¾	17.8
1¼	10	1	7	6	3½	—	3	1¾	20.8
1⅜	11	1	7½	7	3¾	—	3½	2	29.7
2 @ 1	8-2	2	11	5	3	5	2½	1½	23.4
2 @ 1⅛	9-2	2	11½	6	3¼	5	3	1¾	32.2
2 @ 1¼	10-2	2	12	7	3½	5	3½	1¾	41.6
2 @ 1⅜	11-2	2	14½	7	4¼	6	3½	2	57.5

* Precede part number by using appropriate letter designation: WP=Wedge Plate; TP=Threaded Plate; EP=Plate with Drilled Hole; Hole ¼" larger than bar Ø.

NOTES:

1. Standard Plate sizes shown, when used with regular grade bars, conform to allowable bearing stresses of ACI Building Code 318-63, Section 2605, assuming that f'c=5000 psi and Ab'/Ab=1.0. For lower strength concrete a larger bearing area should be provided. For higher strength concrete, or where Ab'/Ab exceeds 1.0, smaller plates may be used. Consult our Engineering Department for recommendations on plate design.
2. Standard Plates are fabricated from AISI C-1040 Steel.
3. Plates to anchor a larger number of bars, plates to anchor bars of different diameters, or plates of non-rectangular shape may be designed to meet the specific needs of the engineer.

JACKS

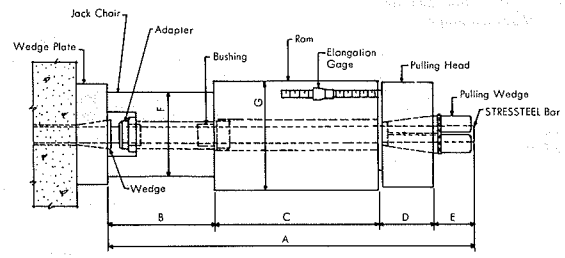

TYPE	DIMENSIONS IN INCHES *A	B	C	D Closed	E	F	G	Wt. of Heaviest Part (lbs.)
30 Ton — 6" Travel	21½	6¼	9¾	3¼	2¼	5	6½	36
60 Ton — 3" Travel	21⅜	6¼	9⅝	3¼	2¼	5	6½	63
60 Ton — 10" Travel	30¼	6¼	18½	3¼	2¼	5	6½	120
100 Ton — 3" Travel	23½	6¼	10½	3¾	2¾	5**	7½	95
100 Ton — 6" Travel	25¼	6¼	12¼	3¾	2¾	5**	7½	114
100 Ton — 10" Travel	29½	6¼	16½	3¾	2¾	5**	7½	145

* Minimum Bar Length Necessary for Jacking, outside of plate.
** 6½" for 1⅜" Ø bars.
NOTE 1. Special adaptations can be made to fit unusual applications. Consult Sales Department for special design jacking components.
NOTE 2. Bushings are provided to center pulling head and rams. 6" and 10" Travel Rams have hydraulic return; 3" Travel Rams have spring return.

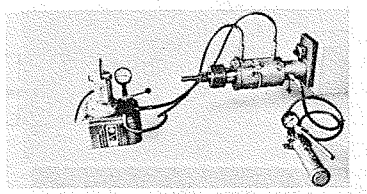

General Arrangement of Hydraulic Components

6" Travel, 100-ton STRESSTEEL Hydraulic Jacking Unit with electric pump. Note jack chair and wedge seating ram with connection to hand operated hydraulic pump.

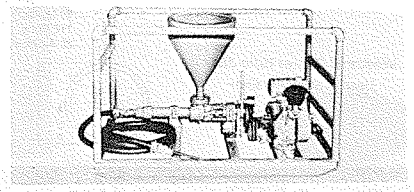

Grouting

Grouting is done through previously formed openings. The grout mix should be specified by the engineer and grouting performed at his direction. For grout mix and method recommendations see PCI Recommended Practice on Grouting.

Standard STRESSTEEL Grout Pump with gas or electric motor will develop 150 psi grout pressure.

The Westrand Mono-System

Tendons and Anchors

Mono-System tendons use ½" diameter seven-wire strand in single or multiple groups. The strand is stress relieved and conforms to ASTM A-416. Features of the Mono-System are:

- Rectangular anchor plate provides flexibility to meet the restrictions of thin slabs or narrow beams.
- Fixed end anchorages are attached and pre-set at factory to reduce field labor and prevent strand slippage at the fixed end.
- Coupling is never necessary since tension can be applied separately to successive sections of total length by stressing at any intermediate point, and then continuing the same strand.
- No large pockets to form and patch. Re-usable pocket former comes with anchor. The entire assembly attaches to form work and when removed after concreting, leaves a small, clean stressing pocket that is easily patched.
- Stressing equipment is small and light-weight, easily handled by one man. Operation is semi-automatic and fast.

The advantages of the Westrand Mono-System of post-tensioning place the flexibility of prestressing within the scope of any project. With this flexibility long spans, cantilevers and heavy loading are no longer a problem.

Design Data

Strand Area	.153	in²
Maximum Jacking Force 0.80 f's	33.0	Kips
Maximum Anchoring Force 0.70 f's	28.9	Kips
Maximum Effective Force 0.60 f's	24.8	Kips

Anchor Castings are 2¼" x 5"

Short Form Specification

1.0 Material

1.1 Strand used in post-tensioning shall conform to ASTM A416 (Specification for uncoated seven-wire stress relieved strand for prestressed concrete.)

1.2 Strand anchorages shall develop at least 95% of the minimum specified ultimate strength of the prestressing steel without exceeding anticipated set.

1.3 Sheathing shall have sufficient strength to resist damage during transport, storage at jobsite, and during installation. It shall prevent the intrusion of cement paste and the escape of coating material.

2.0 Placing

2.1 Anchorage assemblies shall be securely fastened to the edge forms and shall be perpendicular to the longitudinal axis of the tendon.

2.2 Post-Tensioning tendons shall be secured at regular intervals to prevent vertical or lateral movement during the placement of the concrete.

3.0 Stressing

3.1 Post-Tensioning shall not be started until the concrete has attained a minimum strength of 3,000 psi.

3.2 The strand may be temporarily stressed up to 80% of f's to overcome friction.

3.3 The anchor force shall not exceed 70% of f's.

3.4 The effective force shall be assumed to be 60% of f's assuming losses of 10%, unless there is data to prove otherwise.

Stressing Equipment

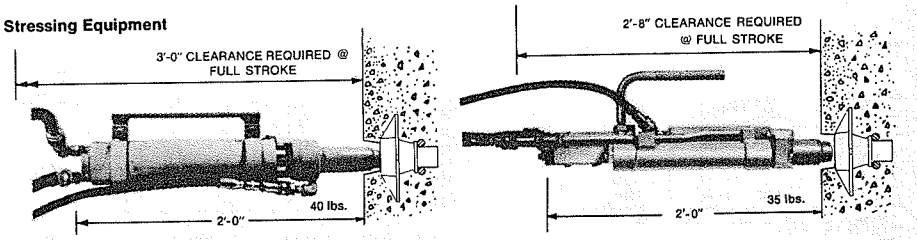

ELECTRICAL POWER REQUIREMENTS
60 Hertz
110 Volts
20 Amps per jack

Westrand Center Hole Jack
Used at Stressing End

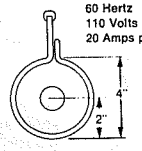

Westrand Open-Throat Jack
Used at Intermediate Stressing End and at Stressing End

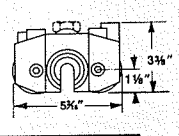

Mono-System Installation

1. All Westrand Mono-System tendons are fabricated and coiled in multiples whenever possible to facilitate field placement; by this method up to 4 tendons are placed in a single operation.
2. Intermediate and fixed end anchors are attached to the tendon in the factory so that only the required portion of a particular tendon need be uncoiled for each pour.
3. The stressing anchor is attached to the edge form by means of a pocket former, spindle and hex nut. The anchor is now ready to receive the stressing end of the tendon which is easily pushed through the entire assembly.
4. Once the concrete sets, the hex nuts, spindles, edge form and pocket formers are removed. Upon reaching the required strength, generally about 5 days, stressing proceeds.
5. The stressing ram is placed over the tendon and set against the anchor. The tendon is then gripped and pulled to the specified elongation and force. As the hydraulic pressure is released the ram automatically seats the wedges and then retracts. The stressing time is approximately 30 seconds per tendon.

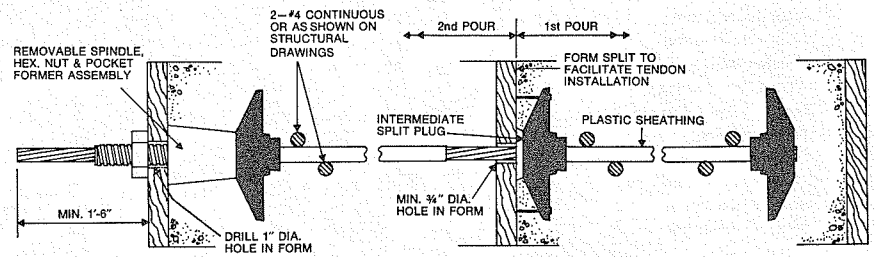

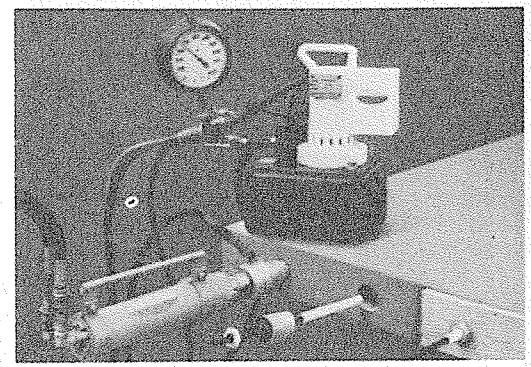

Phases of the stressing operation

The Westrand Multi-System

The Westrand Multi-System provides post-tensioning for a wide range of force requirements from the 99K four strand system to the 1189K forty eight strand system. This system, commonly used with grouted tendons, has many applications.

- Cast-in-place and precast, continuous, long span bridges.
- Transverse deck post-tensioning in cast-in-place or precast bridge construction
- Beams or girders in commercial structures where grouted tendons are advantageous or desirable.
- Tanks or containment structures as either circumferential or vertical tendons.
- Tension rings used to support domes or arches of any type of construction.

Anchorage Assembly		4s	12s	16s	20s	24s	28s	48s
Number of ½" Dia. 270^k Strands		4	12	16	20	24	28	48
Strand Area (Based on 0.153 in²)		.612	1.836	2.448	3.060	3.672	4.284	7.344
Maximum Jacking Force 0.80 f's	(Kips)	132	396	529	661	793	925	1586
Maximum Anchoring Force 0.70 f's	(Kips)	116	347	463	578	694	810	1388
Maximum Effective Force 0.60 f's	(Kips)	99	297	396	496	595	694	1189
Rigid Duct Diameter	O.D. (In)	1¾	2⅜	3	3⅜	3⅝	3⅞	5⅛
Square Bearing Plate	A (In)	6¾	10⅞	13	14¼	15¼	16⅜	21¾
Square Wedge Plate	B (In)	3¾	6	8	8	8	8	13
Wedge Plate Thickness	C (In)	1¾	2¾	3	4	4	4	5
Bearing Plate Thickness	D (In)	1	1½	1¾	2	2½	2¾	3
Transition Length	E (In)	12	22	35	35	35	31	54
Maximum Transition Diameter	F (In)	2¾	4⅜	6¾	6¾	6¾	6¾	9¾
Stressing Clearance	G (Ft)	3'-0"	8'-0"	8'-0"	8'-0"	8'-0"	8'-0"	8'-0"
Stressing Clearance	H (In)	4	12	12	12	12	12	16
Stressing Equipment		30^T	200^T	500^T	500^T	500^T	500^T	1000^T

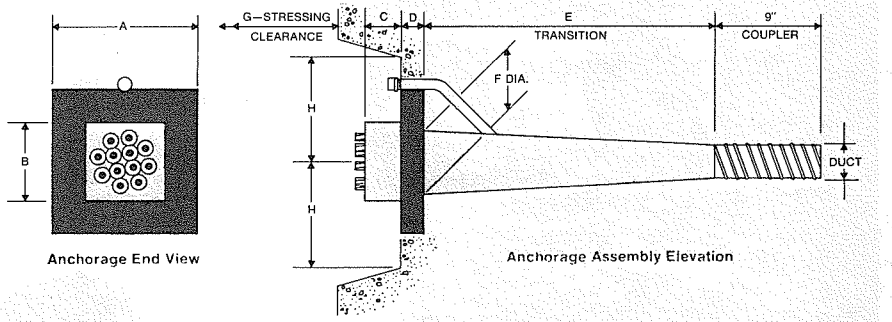

Anchorage End View

Anchorage Assembly Elevation

VSL POST-TENSIONING For Circular Structures

Horizontal Stressing Locations

1. Each tendon stressed at three locations simultaneously

2. 3. 4. Stressing location rotates on succeeding tendons to equalize post-tensioning force in wall

Typical Wall Section

Details shown are for hinged base condition. Sliding, partially fixed or fully fixed condition may be provided at the option of the designer.

Bonded tendon details are illustrated. Preplaced and/or unbonded tendons are available. Unbonded tendons are not recommended for liquid storage.

Mild steel reinforcing is not shown for clarity.

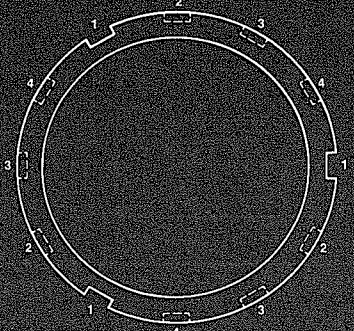

Horizontal Stressing Locations

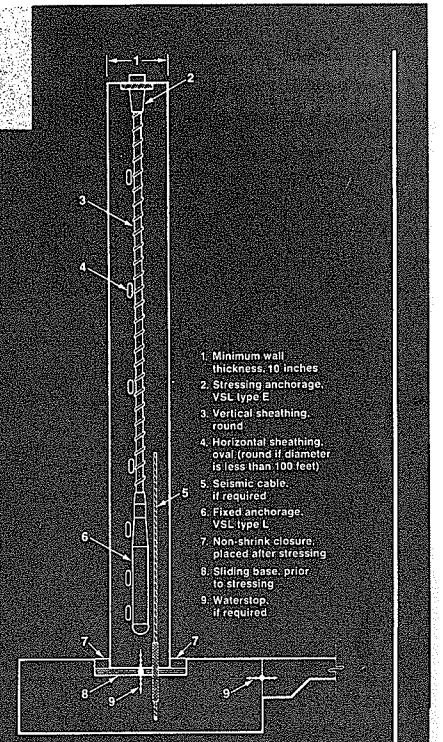

Typical Wall Section

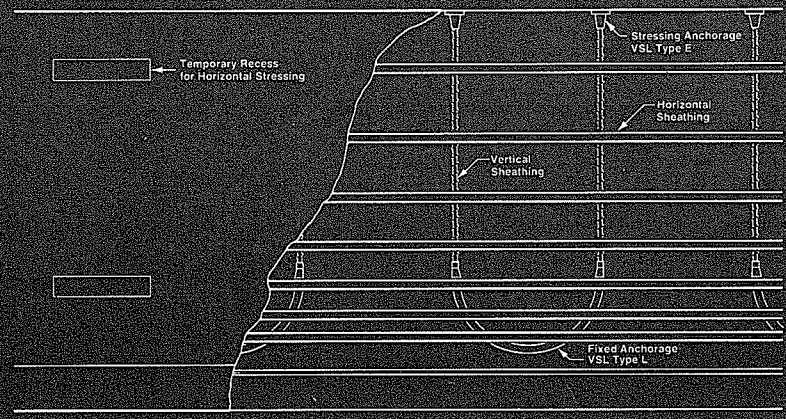

Typical Wall Elevation

Horizontal Prestressing

Stressing Anchorage VSL Type Z

This anchorage allows seating of grippers in two directions, thus providing a continuous, self-anchored horizontal tendon. To reduce friction loss, normally three anchorages are provided for each 360° tendon. Stressing points for succeeding tendons are rotated to equalize the circumferential force at any vertical section. The VSL Z5 anchorage produces compression in the wall without concentrated bearing. Cost of additional formwork, concrete, and mild steel reinforcing, associated with external pilasters, is eliminated. If pilasters are desired, the VSL E5 anchorage is used.

Applicable Dimensions — Inches

Unit	H	D	W	h	d	w
Z5-4	6¼	3½	2⅞	7	5¼	30
Z5-6	7⅞	5¼	3½	8½	6⅞	42
Z5-12	11	5½	5½	12½	7¼	60

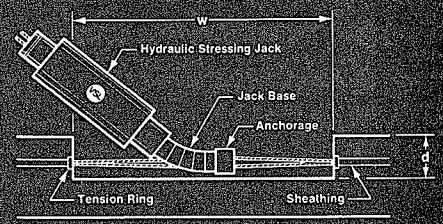

Plan - Temporary Recess

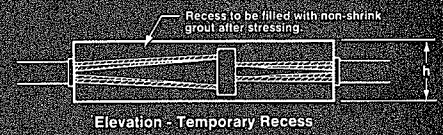

Elevation - Temporary Recess

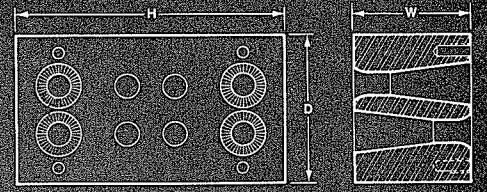

VSL Type Z

Vertical Prestressing

Fixed Anchorage VSL Type L

The advantage of this anchorage is that tendon sheathing can be embedded in concrete prior to the installation of prestressing steel. Prestressing steel can be installed in an "inaccessible" or "dead-end" location using the "pull-through" method. Prestressing force is transferred to the concrete along the pre-flattened intrados of the loop.

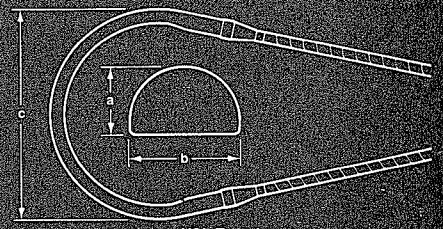

VSL Type L

Stressing Anchorage VSL Type E

The stressing anchorage, a VSL type E, consists of an anchor head, VSL grippers, bearing plate and sleeve. Bearing plates shown are standard and are based on a bearing stress of 3,000 psi at working force. Compressive strength of concrete at the time of initial prestress $f'_c = 3{,}500$ psi.

Applicable Dimensions — Inches

Unit	a	b	c
L5-3	2½	3	48
L5-4	2½	3	48
L5-7	2½	3	48
E5-3	5¼ x 5¼	3½	4
E5-4	6⅛ x 6⅛	3½	4½
E5-7	8 x 8	3½	8

Other sizes are available.

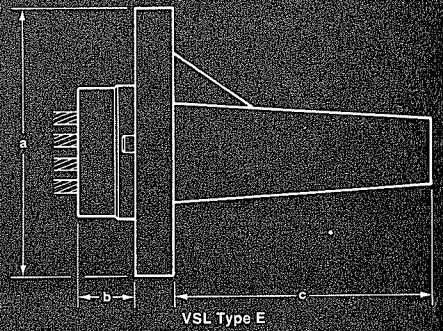

VSL Type E

FREYSSINET
post tensioning

Description

Most Freyssinet strand tendons are composed of twelve strands, but fewer strands — six, eight or nine — are also used. Available strand diameters are limited to ½″ and 0.6″. All Freyssinet strand tendons conform to ASTM A-416, latest edition.

Each Freyssinet strand tendon is coded to indicate the number of strands in the tendon, strand diameter, and steel quality.

Tendon Sizes

250 KSI Grade	270 KSI Grade
Half-Inch Diameter Tendons	
6/500 = 6 strands	6/500K = 6 strands
8/500 = 8 strands	8/500K = 8 strands
9/500 = 9 strands	9/500K = 9 strands
12/500 = 12 strands	12/500K = 12 strands
0.6-Inch Diameter Tendons	
6/600 = 6 strands	6/600K = 6 strands
8/600 = 8 strands	8/600K = 8 strands
9/600 = 9 strands	9/600K = 9 strands
12/600 = 12 strands	12/600K = 12 strands

The largest ultimate capacity tendons currently available are 12/500K (495.6 kips) and 12/600K (703.2 kips).

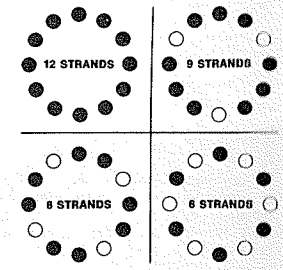

Tensioning

A variety of techniques are available to meet all possible site needs. The Freyssinet system accommodates almost any construction technique and provides safe and effective recovery procedures from unexpected site conditions.

The load in the tendon is easily controllable to any required level by relaxing, partial tensioning, retensioning, or detensioning. Freyssinet tendons may be tensioned to 80% of the guaranteed steel strength to overcome friction.

Recovering anchorage set. If the anchorage set affects the final required prestressing force, the set may be adjusted with a jacking chair and shims. External anchorages with bearing plates are used to do this (see illustrations).

Detensioning. Freyssinet strand tendons may be detensioned at any stage either to remove entirely the prestressing force in the tendon or to reduce the force to meet some special need of the project.

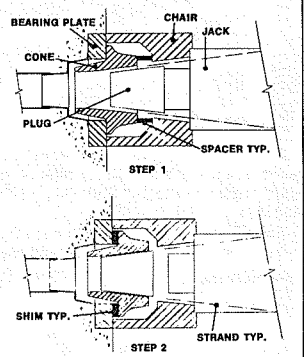

Upswept tendons. Tendons may be anchored in the top surface of a member. The minimum angle of rise, 25°, and the recess dimensioned at the right is for internal half-inch strand anchorages. However, all Freyssinet anchorages may be used in this manner.

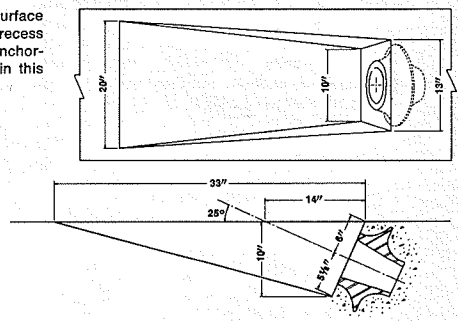

Cast-in-Place anchorages. Anchorages that have been cast into a structure and are completely inaccessible thereafter are called "Dead End Anchorages." The illustration to the right shows a typical standard detail for a Dead End Anchorage.

The Freyssinet engineering staff should be consulted when any special situation is encountered.

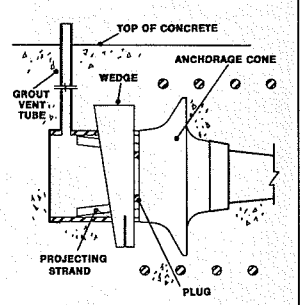

Table A—Tendon Characteristics

STRAND SIZE		½″ DIAMETER				0.6″ DIAMETER			
Ultimate Strength of One Strand		41,300 lbs.				58,600 lbs.			
Nominal Steel Area of One Strand		0.1531 in².				0.217 in².			
Number of Strands in Tendon		6	8	9	12	6	8	9	12
Nominal Steel Area (In²)		0.92	1.22	1.38	1.84	1.30	1.74	1.95	2.60
Ultimate Tendon Strength (Kips)		247.8	330.4	371.7	495.6	351.6	468.8	527.4	703.2
Maximum Jacking Force — 80% f'_s (Kips)		198.2	264.3	297.4	396.5	281.3	375.0	421.9	562.6
Maximum Force After Anchoring — 70% f'_s (Kips)		173.5	231.3	260.2	346.9	246.1	328.2	369.2	492.2
Maximum Effective Force — 60% f'_s (Kips)		148.7	198.2	223.0	297.4	211.0	281.3	316.4	421.9
Tendon Weight — Without Sheath (lbs/ft)		3.15	4.20	4.73	6.30	4.38	5.84	6.57	8.76
Sheath Diameter — I.D. (In)		1⅞	2¼	2¼	2⅝	2¼	2⅝	2⅝	3
	A (IN)	9	9½	10	10	10	10	10	12
	B (IN)	9	10½	11	13½	10	13	14½	15
	C (IN)	1	1¼	1¼	1½	1¼	1½	1½	1¾
	D (IN)	6½	7	7	8	—	—	—	—
	E (IN)	9	9	10	11	—	—	—	—
	F (No.)	5	6	6	7	—	—	—	—
	G (IN)	2	1¾	1¾	1½	—	—	—	—

Notes

- Will not be equally strand of ½" or 0.6" diameter may be used when required.
- The dimensions A & B have been calculated using A-36 steel or equal and a bearing stress in accordance with current ACI Building Code Specifications.
- The dimensions A & B may be varied to suit concrete strength and bond dimensions providing the minimum plate areas of 9" and 10" for ½" and 0.6" strand tendons, respectively, are maintained.
- Two or more anchorages may be placed on a common bearing plate. Bearing plates may assume special shapes to meet unique site conditions.
- Our engineering staff is available at all times to adapt the Freyssinet system to your particular needs.
- For external anchorage applications, minimum concrete cover shall be two inches.

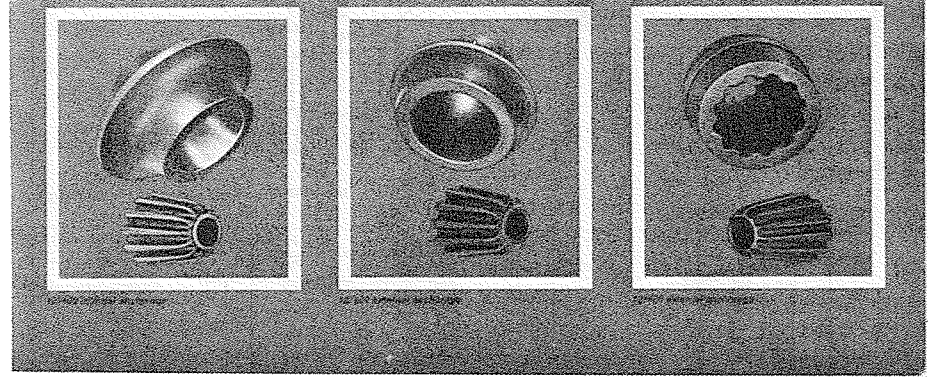

Anchorage Details

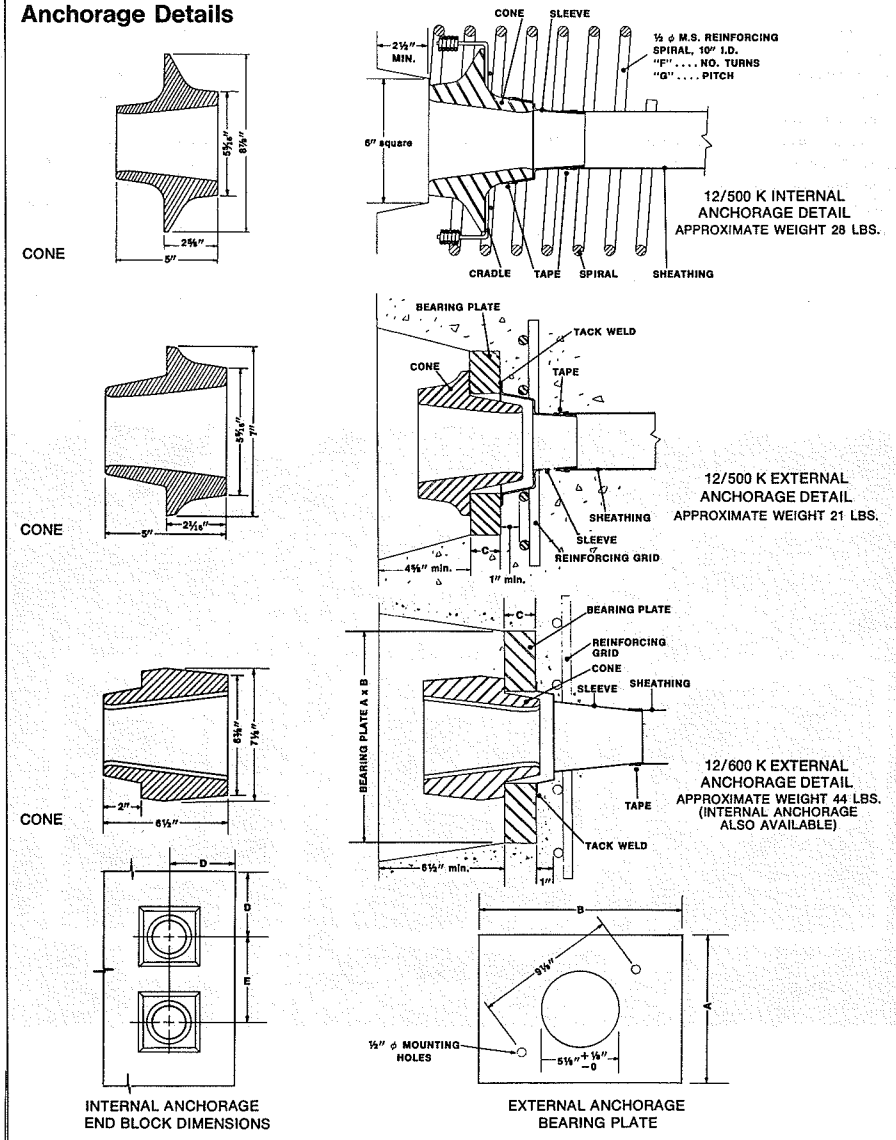

DYWIDAG Single-bar tendon

Bell Anchorage

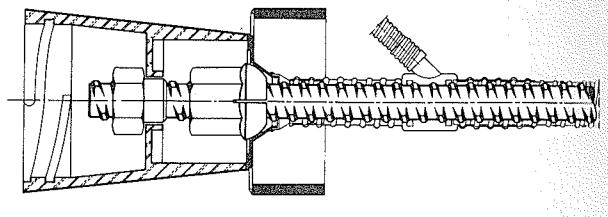

Anchorage with Solid Plate
(square or rectangular)

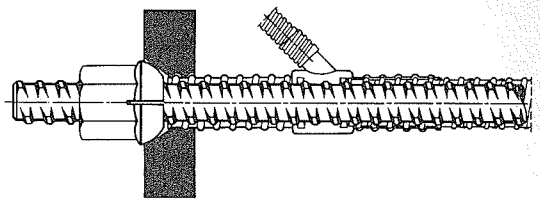

Tendon Characteristics

Nominal Diam.	in.	3/8"	5/8" S	1"	1"	1 1/4"	1 1/4"	1 3/8"
Actual Diam.	mm.	15.0	16.0	26.5	26.5	32.0	32.0	36.0
Ultimate Strength	KSI	157	230	150	160	150	160	150
Area	sq. in.	0.28	0.31	0.85	0.85	1.25	1.25	1.58
Ultimate load f_{pu}	KIP	43.5	70.5	127.5	136.0	187.5	200.0	237.0
0.8 f_{pu}	KIP	34.8	56.5	102.0	108.8	150.0	160.0	189.6
0.7 f_{pu}	KIP	30.5	49.5	89.3	95.2	131.0	140.0	165.9
0.6 f_{pu}	KIP	26.1	42.3	76.5	81.6	112.5	120.0	142.2
Weight	lbs/ft	0.98	1.09	3.01	3.01	4.39	4.39	5.56
Min. elastic bending radius*	ft	26	15	52	49	64	60	72

* For smaller radii bars are cold prebent

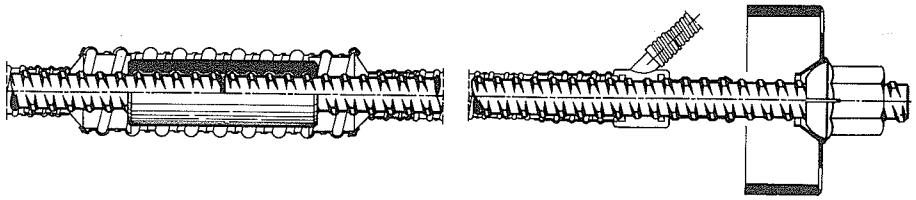

Anchorage Details

Bar Diameter	5/8	5/8 S'	1	1 1/4	1 3/8
Bell Inchor O. D. in	3 1/4 ϕ × 1 1/2	4 ϕ × 2 1/4	5 1/2 ϕ × 2 5/8	6 3/4 ϕ × 2 3/8	7 3/4 ϕ × 3 1/8
Plate Anchor Solid	3×3×3/4 2×5×1	4×4×1 3×5×1	5×5 1/2×1 1/4 4×6 1/2×1 1/4	6×7×1 1/2 5×8×1 1/2	7×7 1/2×1 3/4 5×9 1/2×1 3/4
Nut Extension	1	1 5/8	1 7/8	2 1/2	2 3/4
Bar Protrusion	2	3	2 1/2	3	3 1/2

Pocket Former

Height in.	4 3/8	4 3/8	7	8	8 5/8
Max. O. D. in	3 1/8	3 1/8	5 1/8	6 1/2	6 1/2

Coupling Details

Length in.	3 1/2	5 1/2	5 1/2	6 3/4	8 5/8
Diameter O. D. in.	1 1/8	1 1/4	2	2 3/8	2 5/8

Sheathing

Bar Sheathing O. D. in	1	1	1 1/2	1 3/4	2
I. D. in	3/4	3/4	1 1/4	1 1/2	1 3/4
Coupling Sheathing O. C. in	1 3/4	1 3/4	2 3/4	3 1/4	3 3/4
I. D. in.	1 3/8	1 3/8	2 3/8	2 7/8	3 3/8

APPENDIX C

SI CONVERSION FACTORS[a]

CONVERSION FACTORS — U.S. CUSTOMARY UNITS TO SI METRIC UNITS

OVERALL GEOMETRY

Spans	1 ft = 0.3048 m
Displacements	1 in. = 25.4 mm
Surface area	1 ft^2 = 0.0929 m^2
Volume	1 ft^3 = 0.0283 m^3
	1 yd^3 = 0.765 m^3

STRUCTURAL PROPERTIES

Cross-sectional dimensions	1 in. = 25.4 mm
Area	1 $in.^2$ = 645.2 mm^2
Section modulus	1 $in.^3$ = 16.39 × 10^3 mm^3
Moment of inertia	1 $in.^4$ = 0.4162 × 10^6 mm^4

MATERIAL PROPERTIES

Density	1 lb/ft^3 = 16.03 kg/m^3
Modulus and stress	1 $lb/in.^2$ = 0.006895 MPa
	1 $kip/in.^2$ = 6.895 MPa

LOADINGS

Concentrated loads	1 lb = 4.448 N
	1 kip = 4.448 kN
Density	1 lb/ft^3 = 0.1571 kN/m^3
Linear loads	1 kip/ft = 14.59 kN/m
Surface loads	1 lb/ft^2 = 0.0479 kN/m^2
	1 kip/ft^2 = 47.9 kN/m^2

STRESSES AND MOMENTS

Stress	1 lb/in.^{2} = 0.006895 MPa
	1 kip/in.^{2} = 6.895 MPa
Moment or torque	1 ft-lb = 1.356 N-m
	1 ft-kip = 1.356 kN-m

SI METRIC EQUIVALENTS OF LIMITING VALUES

UNITS

	U.S. Customary	*S.I. Metric*
Area	in.^{2}	mm^2
	ft^2	m^2
Density	lb/ft^3	kg/m^3
Load	lb	N
Size	in.	mm
	ft	m
Stress	lb/in.^{2}	MPa = N/mm^2

STRESS

U.S. Customary	*S.I. Metric*
$\sqrt{f'_c}$	$0.08\sqrt{f'_c}$
$0.5\sqrt{f'_c}$	$0.04\sqrt{f'_c}$
$0.6\sqrt{f'_c}$	$0.05\sqrt{f'_c}$
$2/3\sqrt{f'_c}$	$0.06\sqrt{f'_c}$
$1.1\sqrt{f'_c}$	$0.091\sqrt{f'_c}$
$1.2\sqrt{f'_c}$	$0.10\sqrt{f'_c}$
$1.25\sqrt{f'_c}$	$0.10\sqrt{f'_c}$
$1.5\sqrt{f'_c}$	$0.13\sqrt{f'_c}$
$1.6\sqrt{f'_c}$	$0.13\sqrt{f'_c}$
$1.7\sqrt{f'_c}$	$0.14\sqrt{f'_c}$
$1.9\sqrt{f'_c}$	$0.16\sqrt{f'_c}$
$2.0\sqrt{f'_c}$	$0.17\sqrt{f'_c}$
$2.4\sqrt{f'_c}$	$0.20\sqrt{f'_c}$
$3.0\sqrt{f'_c}$	$0.25\sqrt{f'_c}$
$3.3\sqrt{f'_c}$	$0.27\sqrt{f'_c}$
$3.5\sqrt{f'_c}$	$0.29\sqrt{f'_c}$
$4.0\sqrt{f'_c}$	$0.33\sqrt{f'_c}$
$4.4\sqrt{f'_c}$	$0.37\sqrt{f'_c}$
$5.0\sqrt{f'_c}$	$0.42\sqrt{f'_c}$
$5.5\sqrt{f'_c}$	$0.46\sqrt{f'_c}$
$6.0\sqrt{f'_c}$	$0.50\sqrt{f'_c}$
$6.3\sqrt{f'_c}$	$0.52\sqrt{f'_c}$
$6.5\sqrt{f'_c}$	$0.54\sqrt{f'_c}$
$7.0\sqrt{f'_c}$	$0.58\sqrt{f'_c}$
$7.5\sqrt{f'_c}$	$0.62\sqrt{f'_c}$
$8.0\sqrt{f'_c}$	$0.67\sqrt{f'_c}$
$10.0\sqrt{f'_c}$	$0.83\sqrt{f'_c}$
$12.0\sqrt{f'_c}$	$1.00\sqrt{f'_c}$

METAL REINFORCEMENT

Reinforcing Bars

Bar size	U.S. Customary			Metric		
	Nominal diameter (in.)	Nominal area ($in.^2$)	Nominal weight (lb/ft)	Nominal diameter (mm)	Nominal area (mm^2)	Nominal mass (kg/m)
3	0.375	0.11	0.376	9.525	71	0.560
4	0.500	0.20	0.668	12.700	129	0.994
5	0.625	0.31	1.043	15.875	200	1.552
6	0.750	0.44	1.502	19.050	284	2.235
7	0.875	0.60	2.044	22.225	387	3.042
8	1.000	0.79	2.670	25.400	510	3.973
9	1.128	1.00	3.400	28.651	645	5.060
10	1.270	1.27	4.303	32.258	819	6.404
11	1.410	1.56	5.313	35.814	1,006	7.907
14	1.693	2.25	7.650	43.002	1,452	11.385
18	2.257	4.00	13.600	57.328	2,581	20.240

Wire Reinforcement

W and *D* Size		U.S. Customary			Metric		
Smooth	Deformed	Nominal diameter (in.)	Nominal area ($in.^2$)	Nominal weight (lb/ft)	Nominal diameter (mm)	Nominal area (mm^2)	Nominal mass (kg/m)
W31	D31	0.628	0.310	1.054	15.951	200.0	1.569
W30	D30	0.618	0.300	1.020	15.697	193.6	1.518
W28	D28	0.597	0.280	0.952	15.164	180.7	1.417
W26	D26	0.575	0.260	0.934	14.605	167.7	1.390
W24	D24	0.553	0.240	0.816	14.046	154.8	1.214
W22	D22	0.529	0.220	0.748	13.437	141.9	1.113
W20	D20	0.504	0.200	0.680	12.802	129.0	1.012
W18	D18	0.478	0.180	0.612	12.141	116.1	0.911
W16	D16	0.451	0.160	0.544	11.455	103.2	0.810
W14	D14	0.422	0.140	0.476	10.719	90.3	0.708
W12	D12	0.390	0.120	0.408	9.906	77.4	0.607
W11	D11	0.374	0.110	0.374	9.500	71.0	0.557
W10.5		0.366	0.105	0.357	9.296	67.7	0.531
W10	D10	0.356	0.100	0.340	9.042	64.5	0.506
W9.5		0.348	0.095	0.323	8.839	61.3	0.481
W9	D9	0.338	0.090	0.306	8.585	58.1	0.455
W8.5		0.329	0.085	0.289	8.357	54.8	0.430
W8	D8	0.319	0.080	0.272	8.103	51.6	0.405
W7.5		0.309	0.075	0.255	7.849	48.4	0.380
W7	D7	0.298	0.070	0.238	7.569	45.2	0.354
W6.5		0.288	0.065	0.221	7.315	41.9	0.329
W6	D6	0.276	0.060	0.204	7.010	38.7	0.304
W5.5		0.264	0.055	0.187	6.706	35.5	0.278
W5	D5	0.252	0.050	0.170	6.401	32.3	0.253
W4.5		0.240	0.045	0.153	6.096	29.0	0.228
W4	D4	0.225	0.040	0.136	5.715	25.8	0.202
W3.5		0.211	0.035	0.119	5.359	22.6	0.177
W3		0.195	0.030	0.102	4.953	19.4	0.152
W2.9		0.192	0.029	0.098	4.877	18.7	0.146
W2.5		0.178	0.025	0.085	4.521	16.1	0.127
W2		0.159	0.020	0.068	4.039	12.9	0.101
W1.4		0.135	0.014	0.049	3.429	9.0	0.073

Prestressing Tendons

Type	U.S. Customary			Metric		
	Nominal diameter (in.)	Nominal area (in.^{2})	Nominal weight (lb/ft)	Nominal diameter (mm)	Nominal area (mm^2)	Nominal mass (kg/m)
Seven-wire strand (Grade 250)	$\frac{1}{4}$(0.250)	0.036	0.12	6.350	23.2	0.179
	$\frac{5}{16}$(0.313)	0.058	0.20	7.950	37.4	0.298
	$\frac{3}{8}$(0.375)	0.080	0.27	9.525	51.6	0.402
	$\frac{7}{16}$(0.438)	0.108	0.37	11.125	69.7	0.551
	$\frac{1}{2}$(0.500)	0.144	0.49	12.700	92.9	0.729
	(0.600)	0.216	0.74	15.240	139.4	1.101
Seven-wire strand (Grade 270)	$\frac{3}{8}$(0.375)	0.085	0.29	9.525	54.8	0.432
	$\frac{7}{16}$(0.438)	0.115	0.40	11.125	74.2	0.595
	$\frac{1}{2}$(0.500)	0.153	0.53	12.700	98.7	0.789
	(0.600)	0.215	0.74	15.240	138.7	1.101
Prestressing wire	0.192	0.029	0.098	4.877	18.7	0.146
	0.196	0.030	0.10	4.978	19.4	0.149
	0.250	0.049	0.17	6.350	31.6	0.253
	0.276	0.060	0.20	7.010	38.7	0.298
Prestressing bars (smooth)	$\frac{3}{4}$(0.750)	0.44	1.50	19.050	283.9	2.232
	$\frac{7}{8}$(0.875)	0.60	2.04	22.225	387.1	3.036
	1(1.000)	0.78	2.67	25.400	503.2	3.973
	$1\frac{1}{8}$(1.125)	0.99	3.38	28.575	638.7	5.030
	$1\frac{1}{4}$(1.250)	1.23	4.17	31.750	793.5	6.206
	$1\frac{3}{8}$(1.375)	1.48	5.05	34.925	954.8	7.515
Prestressing bars (deformed)	$\frac{5}{8}$(0.625)	0.28	0.98	15.875	180.6	1.458
	$\frac{3}{4}$(0.750)	0.42	1.49	19.050	271.0	2.217
	1(1.000)	0.85	3.01	25.400	548.4	4.480
	$1\frac{1}{4}$(1.250)	1.25	4.39	31.750	806.5	6.535
	$1\frac{3}{8}$(1.375)	1.56	5.56	34.925	1006.5	8.274

[a]SI equivalents of all design equations will be found in "Building Code Requirements for Reinforced Concrete," (ACI 318M-83), American Concrete Institute, Detroit, 1983.

INDEX

Printed by Kim Hup Lee Printing Co. Pte Ltd — Singapore